

**SMU EE 6392**  
**Photonic Waveguides**  
**Fall 1997**

**Instructor:** Gary Evans  
[gae@seas.smu.edu](mailto:gae@seas.smu.edu); 214-768-3032 (voice); 214-768-3573 (fax)

**Handout #1: September 22, 1997**

**Students:**      Michael Marley  
                        Danielle Perry

**EE 6392**  
**Photonic Waveguides**  
**Fall 1997**

**Time:** Tuesday: 9:00 AM  
**Location:** Caruth 319  
**Instructor:** Gary Evans 319 Caruth Hall 768-3032 (o) 768-3573 (fax)  
**Office Hours:** M W F 11:00:00-noon or by appointment  
**Text:** Required: Optoelectronics by Pollock

**References:**

1. An Introduction to Optical Waveguides, M. J. Adams, John Wiley & Sons, 1981
2. Optical Waveguides, N. S. Kapany and J. J. Burke, Academic Press, 1972
3. Integrated Optics, T. Tamir, editor, Springer-Verlag, 1975
4. Light Transmission Optics, D. Marcuse, Van Nostrand Reinhold, 1972
5. Dielectric Optical Waveguides, D. Marcuse, Van Nostrand Reinhold, 1978?
6. Optical Waveguide Theory, A. W. Snyder and J. D. Love, Chapman and Hall, 1983
7. Semiconductor Lasers and Heterojunction LEDs, H. Kressel and J. K. Butler, Academic Press, 1977

<b>Week</b>	<b>Course Topics</b>
1	course overview, electromagnetics overview,
2	1D planar dielectric waveguides
3	1D planar dielectric waveguides (cont'd)
4	1D planar dielectric waveguides (cont'd)
5	far-field distributions
6	1D QW laser structures (MODEIG)
7	2D planar dielectric waveguides:
8	effective index method,
9	CSP, ridge-guides
10	complex dielectric waveguides
11	circular (fiber) waveguides
12	coupled mode theory
13	photonic devices: lasers
14	modulators and switches
15	detectors

**Projects:**

we will do two or more of the following:

1. Measure near- and far-field patterns of semiconductor lasers and compare with theoretical predictions.
2. Write a computer program to calculate near-field intensities and mode charts for circular fibers.
3. Analyse  $1.55 \mu\text{m}$  InGaAsP laser structures
4. Analyse  $0.65 \mu\text{m}$  AlGaInP laser structures

**Grade:** the course grade will be determined based on class discussions and the projects.

**EE 6392**  
**Photonic Waveguides**  
**Spring 1993**  
**(revised 1/26/93)**

**Time:** MW F 11:00 am -11:50 am

**Location:** Lectures Caruth Hall 128

**Instructor:** Gary Evans 319 Caruth Hall 768-3032 (o) 768-3883 (fax)

**Office Hours:** M W F 2:00-3:00 pm or by appointment

**Text: Required:**

Guided-Wave Photonics, by A. Bruce Buckman, Saunders College Publishing, 1992

**References:**

An Introduction to Optical Waveguides, M. J. Adams, John Wiley & Sons, 1981

Optical Waveguides, N. S. Kapany and J. J. Burke, Academic Press, 1972

Integrated Optics, T. Tamir, editor, Springer-Verlag, 1975

Light Transmission Optics, D. Marcuse, Van Nostrand Reinhold, 1972

Dielectric Optical Waveguides, D. Marcuse, Van Nostrand Reinhold, 1978?

Optical Waveguide Theory, A. W. Snyder and J. D. Love, Chapman and Hall, 1983

Semiconductor Lasers and Heterojunction LEDs, H. Kressel and J. K. Butler, Academic Press, 1977

<b>Week</b>	<b>Date</b>	<b>Course Topics</b>
1	1/8H, 1/20, 1/22	course overview, electromagnetics overview, semiconductor laser "overview"
2	1/25, 1/27, 1/29	1D planar dielectric waveguides, MODEIG, ((discuss first mini-project))
3	2/1, 2/3, 2/5	2D planar dielectric waveguides ((NSF 2/5))
4	2/8, 2/10, 2/12	circular dielectric waveguides
5	2/15, 2/17, 2/19	effective index method, applications
6	2/22, 2/24, 2/26	"complex" or "real" dielectric waveguides
7	3/1, 3/3, 3/5	((discuss second mini-project)), "complex" or "real" dielectric waveguides, cont'd
8	3/8, 3/10, 3/12	"complex" or "real" dielectric waveguides, cont'd, <b>MIDTERM</b>
9	3/15, 3/17, 3/19	<b>SPRING BREAK</b>
10	3/22, 3/24, 3/26	mode coupling, coupled mode theory
11	3/29, 3/31, 4/2	fiber coupling
12	4/5, 4/7, 4/9H	passive guided wave devices
13	4/12, 4/14, 4/16	modulators and switches
14	4/19, 4/21, 4/23	sources, basic and advanced
15	4/26, 4/28, 4/30	sources, advanced
16	5/3, 5/5, 5/7	sensors, prepare manuscript from minireport #2
17	5/13	<b>FINAL EXAM</b> (Thursday 11:30 am - 2:30 pm)

### **Grade Composition:**

midterm exam:	25%
miniproject #1:	25%
homework	20%
miniproject #2:	30%
final exam:	no final exam

### **Mini Projects**

- **study of existing problems in optoelectronics**
- **experience in writing up research work\***
- **experience in critiquing other research work**
- **become a published author**

#1. Minimizing the far-field beam divergence while maintaining a minimum active layer confinement factor.

#2. Analyzing a new waveguide configuration for visible (red) semiconductor lasers.

\* See R. T. Compton, Jr., "Fourteen Steps to a Clearly Written Technical Paper", appearing in article by K. Werner "Technical Communications", IEEE Circuits and Devices, p. 54-56. September, 1992.

### **Minireport #1**

- Outline of the approach for minireport #1 is due Monday, February 15.
- Minireport #1 is due Monday, March 1
  - submit an original plus 2 copies
  - each manuscript is sent to 2 (in class) reviewers on March 1
- Reviewer's comments on minireport #1 are due back March 8
- Final revised minireport #1 is due Monday, March 12.

### **Minireport #2**

- Outline of the approach for minireport #2 is due Friday, March 26.
- Minireport #2 is due Monday, April 19.
  - submit an original plus 2 copies
  - each manuscript is sent to 2 (in class) reviewers on April 19
- Reviewer's comments on minireport #2 are due back April 23
- Final revised minireport #2 is due Monday, April 30.

### **COURSE GOALS**

- understand photonic waveguides and related concepts and devices
- improve technical writing and submit a (group) manuscript for publication

## Review of E & M

### Maxwell's Equations (differential form)

$$\nabla \times \vec{E} = -\frac{\partial \vec{B}}{\partial t} \quad \text{Faraday's Law}$$

$$\nabla \times \vec{H} = \vec{J} + \frac{\partial \vec{D}}{\partial t} \quad \text{Amperes' Law}$$

$$\nabla \cdot \vec{B} = 0 \quad \text{Gauss' Law (magnetic field)}$$

$$\nabla \cdot \vec{D} = \rho \quad \text{" " " (electric field)}$$

where:

$\vec{E}$  — the electric field

intensity vector

(volts/meter)

(2)

$\vec{H}$  - magnetic field  
intensity vector  
(amperes/meter)

$\vec{B}$  - magnetic flux density  
vector  
(gauss =  $10^{-4}$  webers/m<sup>2</sup>)

$\vec{D}$  - electric displacement  
vector  
(Amperes/m<sup>2</sup>)

$\vec{J}$  - Current density  
vector  
(Amperes/m<sup>2</sup>)

(3)

$\rho$  = charge density  
 $(\text{coulombs/m}^3)$

$$\vec{E}, \vec{B}, \vec{H}, \vec{D} = f(\vec{F}, t)$$

$\vec{r}$  - position vector (m)

$t$  - time (seconds)

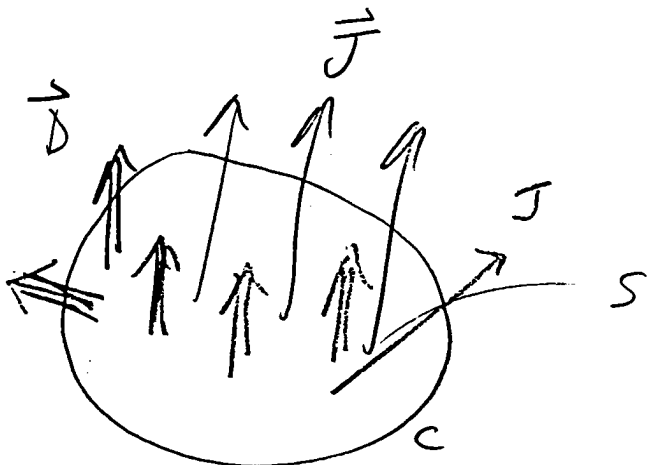
(integral form)

$$\oint_C \vec{E} \cdot d\vec{l} = -\frac{\partial}{\partial t} \int_S \vec{B} \cdot d\vec{S}$$

Faradays Law

(4)

$$\oint \vec{H} \cdot d\vec{l} = \int \vec{J} \cdot d\vec{s} + \frac{\partial}{\partial t} \int \vec{D} \cdot d\vec{s}$$

Ampere's  
Law

$$\oint \vec{D} \cdot d\vec{s} = \iiint_V \rho dV$$

Gauss'  
Law

$$\oint_S \vec{B} \cdot d\vec{s} = 0$$

" "

(5)

## Auxiliary Equations

• dependent on medium

$$\vec{D} = \tilde{\epsilon} \cdot \vec{E}$$

electric  
permittivity

$$\vec{B} = \tilde{\mu} \cdot \vec{H}$$

magnetic  
permeability

In general,  $\tilde{\epsilon}$  &  $\tilde{\mu}$   
are tensors

$\tilde{\epsilon}$  &  $\tilde{\mu}$  are the defining  
constants of the medium

(6)

- If  $\tilde{\epsilon}$  &  $\tilde{\mu}$  are not functions of position in the material, the medium is homogeneous
  - otherwise, the medium is inhomogeneous
- If  $\tilde{\mu}$  and  $\tilde{\epsilon}$  are scalar quantities (not tensors), the material is isotropic,
  - otherwise, the medium is anisotropic

The most general medium is inhomogeneous, anisotropic, + time varying!

(7)

$$\vec{D} = \epsilon \vec{E} = \underline{\epsilon_0 \epsilon_{\text{ref}}} \vec{E}$$

$\epsilon_0$  - the permittivity  
of free space

$$\epsilon_0 = 8.854 \times 10^{-12} \text{ farads/m}$$

$\epsilon_{\text{ref}}$  = relative permittivity  
 $= n^2$ ,  $n$  = index  
of refraction

example: for Silicon,

$$\epsilon_{\text{ref}} \approx 11.7 \Rightarrow n = 3.42$$

for  $\text{SiO}_2$

$$\epsilon_{\text{ref}} \approx 3.9 \Rightarrow n = 1.97$$

for GaAs ( $\lambda \sim 0.9 \mu\text{m}$ )

$$n = 3.64 \Rightarrow \epsilon_{\text{ref}} \approx 13.25.$$

$\Rightarrow \epsilon_{\text{rel}}$  is a property of the material

- \*  $\epsilon_{\text{rel}}$  can be complex

$$\epsilon_{\text{rel}} = (\epsilon_{\text{rel}})_{\text{real}} + j(\epsilon_{\text{rel}})_{\text{imag}}$$

$$\Rightarrow n = n_{\text{real}} + j n_{\text{imag}} \\ = n_{\text{real}} + j k$$

imaginary parts are associated with loss (or gain)

- \*  $\epsilon_{\text{rel}}$  depends on frequency ( $\omega$ ) [or wavelength,  $\lambda$ ]
- $\rightarrow$  The frequency dependence of  $\epsilon_{\text{rel}}$  is called material dispersion

Dispersion - Waves with different frequencies (or wavelengths) travel with different velocities in the same media

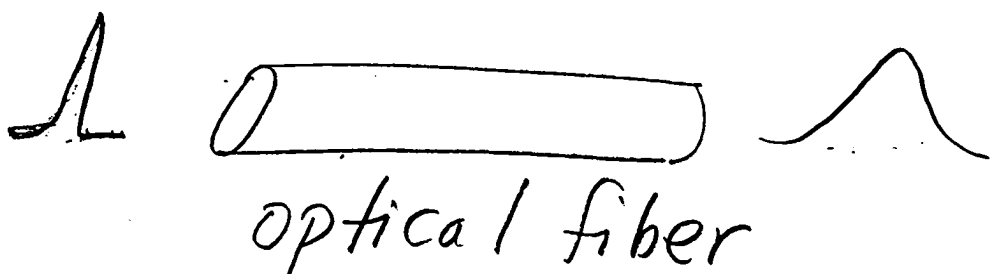
→ different runners on the same track (different wavelength photons in the same material)

$\epsilon_{nl}$  - causes the same wavelength photons to have different velocities in different media

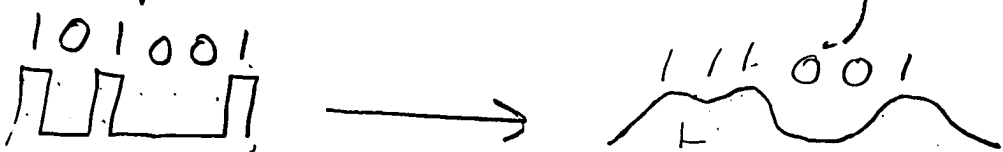
→ the same runner has different velocities on grass, pavement, or mud

→ waveguides (photonic or otherwise) have dispersion (waveguide dispersion)

Generally, dispersion is not "good"



- pulse broadening



- bit errors

Generally, loss is not "good"

- high fiber losses  $\Rightarrow$  more repeaters
- high losses in semiconductor laser waveguide  $\Rightarrow$  high threshold, low efficiency

There are exceptions -  
instances where dispersion  
and/or loss are desirable

loss & dispersion determine  
the wavelength of laser sources  
for optical fiber systems:

$\lambda = 1.3\mu\text{m}$  - minimum<sup>fiber</sup> dispersion

$\lambda = 1.5\mu\text{m}$  - minimum<sup>fiber</sup> loss

Going back to  $\vec{E}$ :

In general,

$$\nabla \cdot \vec{D} = \tilde{\epsilon} \cdot \vec{E} \quad \text{where}$$

$\tilde{\epsilon}$  is a tensor

$$\vec{D} = \begin{bmatrix} \epsilon_{xx} & \epsilon_{xy} & \epsilon_{xz} \\ \epsilon_{yx} & \epsilon_{yy} & \epsilon_{yz} \\ \epsilon_{zx} & \epsilon_{zy} & \epsilon_{zz} \end{bmatrix} \cdot \vec{E}$$

$\Rightarrow$  the permittivity (refractive index) depends on the direction of the applied  $\vec{E}$  field

$\Rightarrow \vec{D}$  and  $\vec{E}$  not parallel

\*  $\epsilon$  can depend on  $\vec{E}$ :  $\epsilon = \epsilon(\vec{E})$

$\Rightarrow$  2<sup>nd</sup> harmonic generation  
frequency doubling  
electro-optic effect

(Gats, LiNbO<sub>3</sub>, ADP, KDP, ...)

\*  $\epsilon$  can depend on the environment

$\Rightarrow \epsilon = f(\text{Temperature, pressure, stress, } \vec{E}, \vec{H})$

→ fiber-optic sensors

→ electro-optic sensors



Magnetic permeability  
similar relationships

$$\vec{B} = \mu \vec{H} = \mu_0 \mu_r \vec{H}$$

$\mu_0$  = permeability of free space  
 $= 1.2566 \times 10^{-6}$  henrys/meter

$\mu_r$  = relative permeability

→ for most photonic waveguides,

$$\mu_r = 1$$

## Additional Auxiliary Equations

- Force Law:

$$\vec{F} = q [\vec{E} + \vec{v} \times \vec{B}]$$

(Lorentz Eq.)

- Conduction current:

$$\vec{J} = \sigma \vec{E} \quad (\text{Ohm's law})$$

conductivity in  $\frac{1}{\text{ohm} \cdot \text{meter}}$

- Convection current

$$\vec{J} = \rho(\vec{r}, t) \vec{v}(\vec{r}, t)$$

charge density moving  
with velocity  $\vec{v}$

• The Equation of Continuity  
recall,

$$\nabla \times \vec{H} = \vec{J} + \frac{\partial \vec{D}}{\partial t}$$

take  $\nabla \cdot$  to both sides:

$$\nabla \cdot \nabla \times \vec{H} = \nabla \cdot \vec{J} + \frac{\partial}{\partial t} (\nabla \cdot \vec{D})$$

$$(\nabla \cdot \nabla \times \vec{A} \equiv 0), \quad \text{so}$$

$$\nabla \cdot \vec{J} = - \frac{\partial \rho}{\partial t}$$

since

$$\nabla \cdot \vec{D} = \rho$$

Useful vector identities:

$$\nabla \times (\phi \vec{A}) = \phi \nabla \times \vec{A} + \nabla \phi \times \vec{A}$$

(16)

$$\nabla \times \nabla \times \vec{A} = \nabla(\nabla \cdot \vec{A}) - \nabla^2 \vec{A}$$

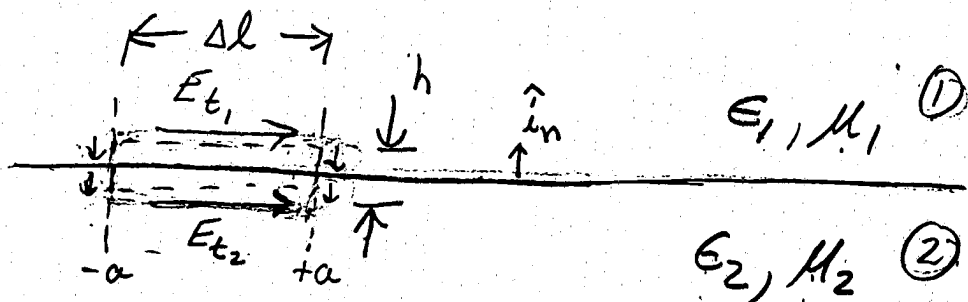
$$\nabla \cdot \phi \vec{A} = \phi \nabla \cdot \vec{A} + \vec{A} \cdot \nabla \phi$$

Boundary Conditions

- deduce from Maxwell's Equations:

A Consider Faradays Law

$$\oint_C \vec{E} \cdot d\vec{l} = -\frac{\partial}{\partial t} \int_S \vec{B} \cdot d\vec{S}$$



$$\oint_C \rightarrow E_{t_1} \Delta l + E_{n_1} \frac{h}{2} + E_{n_3} \frac{h}{2} - E_{t_2} \Delta l - E_{n_2} \frac{h}{2} - E_{n_1} \frac{h}{2}$$

(17)

$$-\frac{\partial}{\partial t} \int_S \vec{B} \cdot d\vec{S} = -\frac{\partial \vec{B}}{\partial t} \cdot h d\ell$$

as  $h \rightarrow 0$ , (assuming  $\frac{\partial \vec{B}}{\partial t}$  is finite)

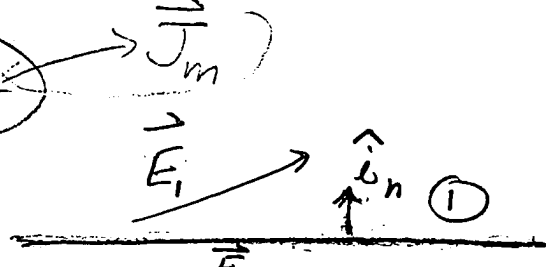
$$(E_{t_1} - E_{t_2}) d\ell = 0$$

$$\therefore \underbrace{E_{t_1} = E_{t_2}}$$

"Tangential  $\vec{E}$  is continuous"

$$\hat{i}_n \times (\vec{E}_1 - \vec{E}_2) = 0$$

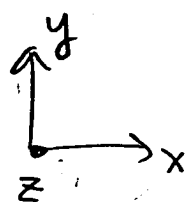
Example:



$$\vec{E}_1 = E_A \hat{i}_x + E_B \hat{i}_y + E_C \hat{i}_z$$

$$\vec{E}_2 = E_D \hat{i}_x + E_E \hat{i}_y + E_F \hat{i}_z$$

$$\text{choose } \hat{i}_n = \hat{i}_y$$



Then,

(18)

$$\hat{i}_y \times \vec{E}_1 = \begin{vmatrix} i_x & i_y & i_z \\ 0 & 1 & 0 \\ E_A & E_B & E_C \end{vmatrix}$$

$$= E_C \hat{i}_x + 0 \hat{i}_y - E_A \hat{i}_z$$

and

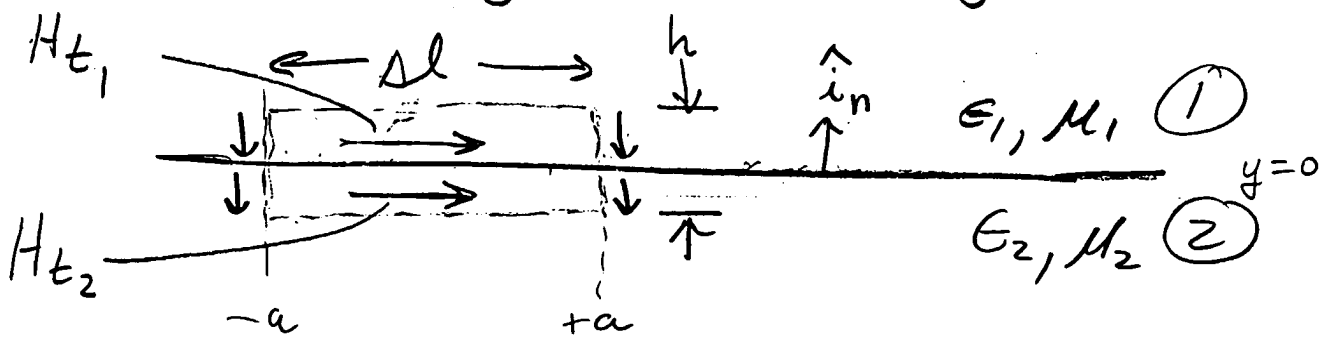
$$\hat{i}_y \times \vec{E}_2 = E_F \hat{i}_x + 0 \hat{i}_y - E_D \hat{i}_z$$

so,

$$\hat{i}_n \times (\vec{E}_1 - \vec{E}_2) \Rightarrow \underbrace{E_C = E_F}_{\boxed{E_A = E_D}}$$

B Consider Amperes Law:

$$\oint_C \vec{H} \cdot d\vec{l} = \int_S \vec{J} \cdot d\vec{S} + \frac{\partial}{\partial t} \int_S \vec{D} \cdot d\vec{S}$$



(19)

$$\oint_C \phi = H_{t_1} \Delta l + H_{h_1} \Big| \frac{h}{2} + H_{n_2} \Big| \frac{h}{2} \\ - H_{t_2} \Delta l - H_{n_2} \Big| \frac{h}{2} - H_{n_1} \Big| \frac{h}{2}$$

$$\int_S \vec{J} \cdot d\vec{S} = J \cdot h \Delta l$$

$$\frac{\partial}{\partial t} \int_S \vec{D} \cdot d\vec{S} = \frac{\partial \vec{D}}{\partial t} \cdot h \Delta l \rightarrow 0$$

as  $h \rightarrow 0$ ,

$$\oint_C \phi \rightarrow (H_{t_1} - H_{t_2}) \Delta l$$

$$\int_S \vec{J} \cdot d\vec{S} \rightarrow 0 \text{ if } J \text{ is finite}$$

↓

$$\int_S J_s \Delta l \text{ if } J = J_s \delta(y)$$

perfect conductor

super conductor

"grating" at interface

(20)

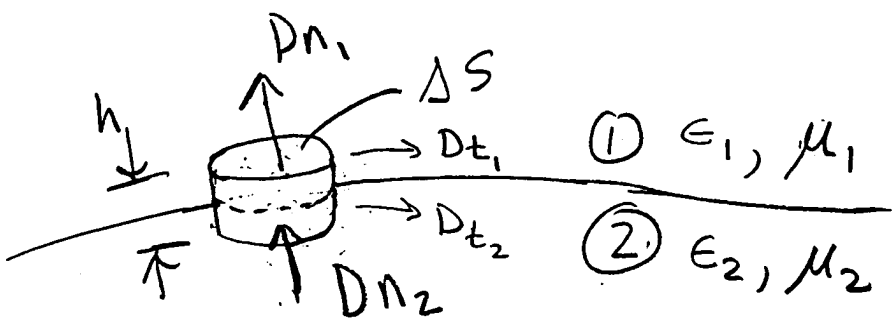
So,

$$H_{1t} - H_{2t} = \vec{J}_S \quad \text{or,}$$

$$\hat{\lambda}_n \times (\vec{H}_1 - \vec{H}_2) = \vec{J}_S$$

C. Consider Gauss' Law

$$\oint_S \vec{D} \cdot d\vec{S} = \int_V \rho dV$$



$$\oint_S = D_{n_1} \Delta S - D_{n_2} \Delta S$$

if  $\rho$  is finite ( $\rho_v$ )

$$\int_V \rho dV = h \Delta S \rho \rightarrow \oint_S \rho \Delta S \text{ if }$$

$$\rho = \rho_s \delta(y)$$

(21)

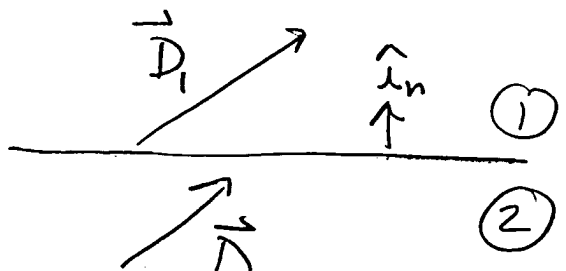
$$(D_{n_1} - D_{n_2}) \Delta S = \int_S \Delta S$$

$$\left\{ D_{n_1} - D_{n_2} = \rho \right.$$

Note: if  $\rho_s = 0$  stop here

$$\epsilon_1 E_{n_1} = \epsilon_2 E_{n_2}$$

$$\left\{ \hat{i}_n \cdot (\vec{D}_1 - \vec{D}_2) = \rho \right.$$



$$\vec{D}_1 = D_A \hat{i}_x + D_B \hat{i}_y + D_C \hat{i}_z$$

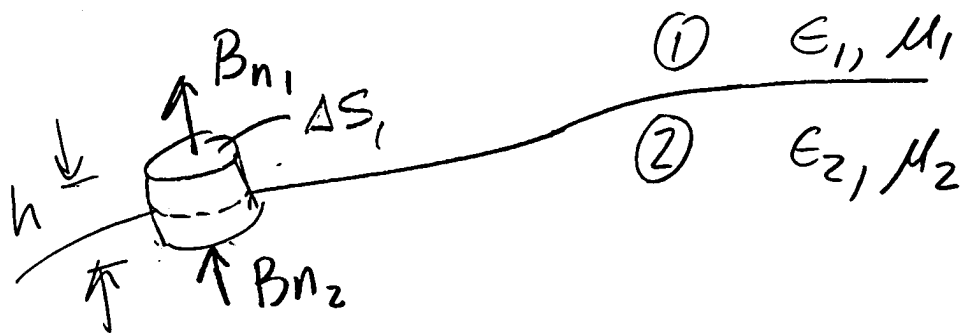
$$\vec{D}_2 = D_D \hat{i}_x + D_E \hat{i}_y + D_F \hat{i}_z$$

$$\text{let } \hat{i}_n = \hat{i}_y$$

$$\hat{i}_y \cdot (\vec{D}_1 - \vec{D}_2) = D_B - D_E = \rho$$

D. Consider Gauss' Law

$$\oint_S \vec{B} \cdot d\vec{S} = 0$$



$$\oint_S \rightarrow B_{n_1} \Delta S - B_{n_2} \Delta S = 0$$

$$B_{n_1} = B_{n_2}$$

$$\hat{n} \cdot (\vec{B}_1 - \vec{B}_2) = 0$$

# Wave Equation

$$(1) \nabla \times \vec{E} = -\frac{\partial \vec{B}}{\partial t} \quad \text{Faraday's Law}$$

$$(2) \nabla \times \vec{H} = \vec{J}_e + \frac{\partial \vec{D}}{\partial t} \quad \text{Ampere's Law}$$

$$(3) \nabla \cdot \vec{B} = 0 \quad \text{Gauss' Law}$$

$$(4) \nabla \cdot \vec{D} = \rho \quad " \quad "$$

$$(5) \vec{D} = \epsilon \vec{E}, \quad \vec{B} = \mu \vec{H}$$

Consider a homogeneous, isotropic, time independent media:

$$(6) \begin{aligned} \nabla \times (\nabla \times \vec{E}) &= -\mu \frac{\partial}{\partial t} (\nabla \times \vec{H}) \\ &= -\mu \frac{\partial}{\partial t} (\vec{J}_e + \frac{\partial \vec{D}}{\partial t}) \end{aligned}$$

(24)

Use the vector identity

$$(7) \nabla \times \nabla \times \vec{A} = \nabla(\nabla \cdot \vec{A}) - \nabla^2 \vec{A}$$

The lhs of (6) becomes

$$(8) \nabla(\nabla \cdot \vec{E}) - \nabla^2 \vec{E}$$

but from (5),

$$\nabla \cdot (\epsilon \vec{E}) = \rho, \text{ so (6)} \rightarrow$$

$$\nabla(\rho_\epsilon) - \nabla^2 \vec{E} = -\mu \frac{\partial \vec{J}}{\partial t} - \mu \epsilon \frac{\partial^2 \vec{E}}{\partial t^2}$$

or

$$(9) \nabla^2 \vec{E} - \mu \epsilon \frac{\partial^2 \vec{E}}{\partial t^2} = \frac{1}{\epsilon} \nabla(\rho) + \mu \frac{\partial \vec{J}}{\partial t}$$

if  $\vec{J} = \sigma \vec{E}$ ,  $\mu \frac{\partial \vec{J}}{\partial t} = \mu \sigma \frac{\partial \vec{E}}{\partial t}$

For many cases,

$\rho = \vec{\tau} = 0$ , and (8)  $\rightarrow$

$$\left\{ \nabla^2 \vec{E} - \mu \epsilon \frac{\partial^2 \vec{E}}{\partial t^2} = 0 \quad (9) \right.$$

Consider a simple case:

$$\vec{E} = E_x(z, t) \hat{i}_x, \quad (9) \rightarrow$$

$$(\nabla^2 \vec{A} = \nabla^2 A_x \hat{i}_x + \nabla^2 A_y \hat{i}_y + \nabla^2 A_z \hat{i}_z)$$

$$\frac{\partial^2 E_x(z, t)}{\partial z^2} - \mu \epsilon \frac{\partial^2 E_x(z, t)}{\partial t^2} = 0 \quad (10)$$

Let  $\xi = \sqrt{\mu \epsilon} z$ , Then (10)  $\rightarrow$

$$\frac{\partial^2 E_x}{\partial \xi^2} - \frac{\partial^2 E_x}{\partial t^2} = 0 \quad (11)$$

Or,

$$(12) \quad \left( \frac{\partial}{\partial \xi} + \frac{\partial}{\partial t} \right) \left( \frac{\partial}{\partial \xi} - \frac{\partial}{\partial t} \right) E_x = 0$$

which is satisfied if

$$\frac{\partial E_x}{\partial \xi} + \frac{\partial E_x}{\partial t} = 0 \quad (13a)$$

or

$$\frac{\partial E_x}{\partial \xi} - \frac{\partial E_x}{\partial t} = 0 \quad (13b)$$

Consider (13a);

$$\frac{\partial E_x}{\partial \xi} = - \frac{\partial E_x}{\partial t} \quad (14)$$

Note: any arbitrary fcn  
 $f(t-\xi)$  is a solution  
 to (13a) or (14)

let  $u = t - \xi$

$$\frac{\partial f}{\partial t} = \frac{\partial f}{\partial u} \frac{\partial u}{\partial t} = f' \stackrel{+1}{=} f'$$

$$\frac{\partial f}{\partial \xi} = \frac{\partial f}{\partial u} \frac{\partial u}{\partial \xi} = -f' \stackrel{-1}{=} -f'$$

Similarly, the solution to (13b) is

$$g(t + \xi)$$

So, the general solution to (10) is

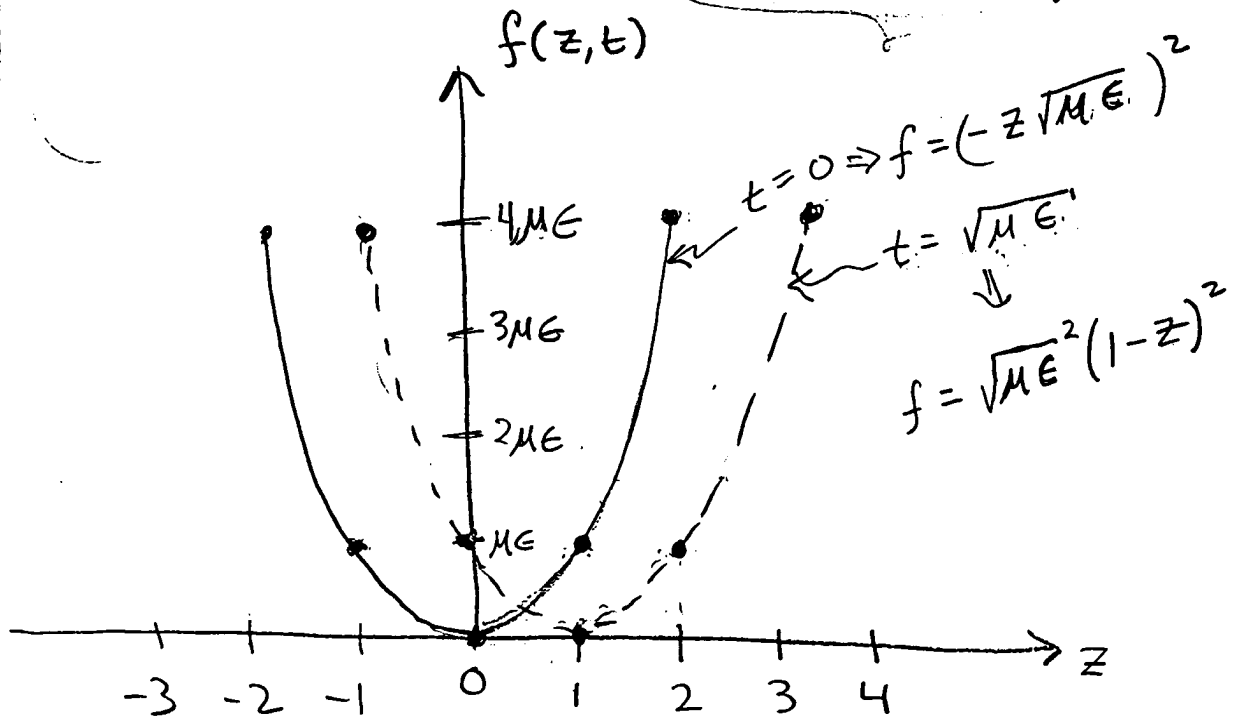
$$E_x(z, t) = A_n f(t - \sqrt{\mu\epsilon} z) \quad (15)$$

$$+ B_n g(t + \sqrt{\mu\epsilon} z)$$

28

What are  $f$  and  $g$ ?

let  $f(z, t) = \underbrace{(t - z\sqrt{\mu\epsilon})^2}_{f(z, t)}$



A given value of the function moves forward in  $z$  with increasing time -- So we have

Wave propagating  
in the  $+z$  direction!

We can calculate  
the velocity:

$$t - z \sqrt{\mu, \epsilon} = \text{constant}$$

$$V = \frac{dz}{dt} = \frac{1}{\sqrt{\mu, \epsilon}}, \text{ if } \mu = \mu_0, \epsilon = \epsilon_0$$

$$= \frac{1}{[(1.256 \times 10^{-6})(8.854 \times 10^{-12})]^{1/2}} = 2.9979 \times 10^8 \text{ m/sec}$$

Similarly,  $g(t + \sqrt{\mu \epsilon} z)$

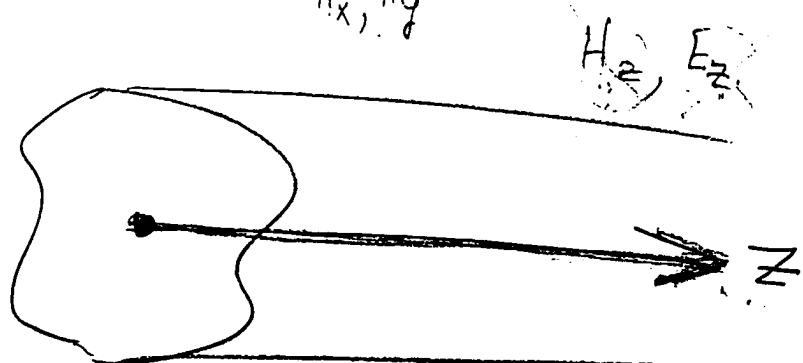
is a wave propagating  
in the  $-z$  direction.

Basic Equations for  
Steady state waves

propagating along a  
uniform (photonic,  
dielectric--even metallic)

Waveguide :

$$\begin{matrix} E_x, E_z \\ H_x, H_y \end{matrix}$$



Assume a complex  
propagation factor

(31)

$$e^{(j\omega t - \gamma z)}$$

where  $\gamma = \alpha + j\beta$

if there are no losses  
(or gain),

$$\alpha = 0, \text{ and}$$

$$e^{j(\omega t - \beta z)} + z \text{ wave}$$

The physical field is given by

$$\vec{A}_t = \operatorname{Re} [\vec{A}(x, y) e^{(j\omega t - \gamma z)}]$$

From  $\nabla \times \vec{E} = - \frac{\partial \vec{B}}{\partial t}$ ,

$$\rightarrow \nabla \times \vec{E} = -j\omega \mu_0 \vec{H}$$

to here  
1/25/93

Similarly,

$$\nabla \times \vec{H} = \vec{J} + \frac{\partial \vec{D}}{\partial t}$$

(let  $\vec{J} = 0$ ),  $\Rightarrow$

$$\nabla \times \vec{H} = j\omega \epsilon \vec{E}$$

$$\nabla \times \vec{E} = \begin{vmatrix} i_x & i_y & i_z \\ \frac{\partial}{\partial x} & \frac{\partial}{\partial y} & \frac{\partial}{\partial z} \\ E_x & E_y & E_z \end{vmatrix} = -j\omega \mu \vec{H}$$

$$= \left( \frac{\partial E_z}{\partial y} - \frac{\partial E_y}{\partial z} \right) \hat{i}_x$$

$$- \left( \frac{\partial E_z}{\partial x} - \frac{\partial E_x}{\partial z} \right) \hat{i}_y$$

$$+ \left( \frac{\partial E_y}{\partial x} - \frac{\partial E_x}{\partial y} \right) \hat{i}_z$$

$$= -j\omega \mu H_x \hat{i}_x - j\omega \mu H_y \hat{i}_y - j\omega \mu H_z \hat{i}_z$$

so

$$\frac{\partial E_z}{\partial y} + \gamma E_y = -j\omega\mu H_x \quad (16)$$

$$-\gamma E_x - \frac{\partial E_z}{\partial x} = -j\omega\mu H_y \quad (17) \checkmark$$

$$\frac{\partial E_y}{\partial x} - \frac{\partial E_x}{\partial y} = -j\omega\mu H_z \quad (18)$$

Similarly,

$$\frac{\partial H_z}{\partial y} + \gamma H_y = j\omega\epsilon E_x \quad (19) \checkmark$$

$$-\gamma H_x - \frac{\partial H_z}{\partial x} = j\omega\epsilon E_y \quad (20) \checkmark$$

$$\frac{\partial H_y}{\partial x} - \frac{\partial H_x}{\partial y} = j\omega\epsilon E_z \quad (21)$$

(34)

Combining (16) & (20):

$$\frac{\partial E_z}{\partial y} + \frac{\gamma}{j\omega\epsilon} \left[ -\gamma H_x - \frac{\partial H_z}{\partial x} \right] = -j\omega\mu H_x$$

$$\frac{\partial E_z}{\partial y} - \frac{\gamma^2}{j\omega\epsilon} H_x - \frac{\gamma}{j\omega\epsilon} \frac{\partial H_z}{\partial x} = -j\omega\mu H_x$$

$$j\omega\epsilon \frac{\partial E_z}{\partial y} - j \frac{\partial H_z}{\partial x} = \left( \gamma^2 + \underbrace{\omega^2 \mu \epsilon}_{k^2} \right) H_x$$

So,

PDS<sup>20</sup>

$$\boxed{H_x = \frac{1}{\gamma^2 + k^2} \left[ j\omega \epsilon \frac{\partial E_z}{\partial y} - \gamma \frac{\partial H_z}{\partial x} \right]} \quad (22)$$

Combining (17) &amp; (19) :

$$\frac{-\gamma}{j\omega \epsilon} \left[ \frac{\partial H_z}{\partial y} + \gamma H_y \right] - \frac{\partial E_z}{\partial x} = -j\omega \mu H_y \quad (17)$$

$$-\gamma \frac{\partial H_z}{\partial y} - \gamma^2 H_y - j\omega \epsilon \frac{\partial E_z}{\partial x} = +\underbrace{\omega^2 \mu \epsilon}_k H_y$$

$$\boxed{H_y = \frac{-1}{\gamma^2 + k^2} \left[ j\omega \epsilon \frac{\partial E_z}{\partial x} + \gamma \frac{\partial H_z}{\partial y} \right]} \quad (23)$$

Combining (19) &amp; (17) :

$$\frac{\partial H_z}{\partial y} + \frac{\gamma}{-j\omega \mu} \left[ -\gamma E_x - \frac{\partial E_z}{\partial x} \right] = j\omega \epsilon \underline{E_x}$$

$$j\omega\mu \frac{\partial H_2}{\partial y} + \gamma^2 E_x + \gamma \frac{\partial E_2}{\partial x} = -\underbrace{\omega^2 \mu \epsilon}_{k^2} E_x$$

$$E_x = \frac{-1}{(\gamma^2 + k^2)} \left[ \gamma \frac{\partial E_2}{\partial x} + j\omega\mu \frac{\partial H_2}{\partial y} \right] \quad (24)$$

Combining (17) & (20):

$$\frac{\gamma}{j\omega\mu} \left[ \frac{\partial E_2}{\partial y} + \gamma E_y \right] - \frac{\partial H_2}{\partial x} = j\omega\epsilon E_y$$

$$\gamma \frac{\partial E_2}{\partial y} + \gamma^2 E_y - j\omega\mu \frac{\partial H_2}{\partial x} = -\underbrace{\omega^2 \mu \epsilon}_{k^2} E_y$$

$$E_y = \frac{-1}{\gamma^2 + k^2} \left[ \gamma \frac{\partial E_2}{\partial y} - j\omega\mu \frac{\partial H_2}{\partial x} \right] \quad (25)$$

~~$\cancel{k^2} = R^2$~~ 

$$R = \omega^2 \mu \epsilon$$

$$\gamma = \alpha + j\beta$$

## Classification of Wave Solutions

- 1) TEM-waves that contain neither an electric nor a magnetic field component in the direction of propagation  
"Transverse Electro Magnetic"
- 2) TE-waves that contain a magnetic field component in the direction of propagation (but no  $\vec{E}$  component idp)
- 3) TM-waves that contain an electric field component

in the direction of propagation  
 (but no  $\vec{H}$  component idp)

4) Hybrid - waves that contain both an electric and a magnetic field in the direction of propagation

"TEM modes" "TM modes"

"TE modes" "Hybrid modes"

from (22), (23), (24), + (25)

(see 1/22 p(13), (14)):

$$\text{if } E_z = 0 \Rightarrow H_x \propto \frac{\partial H_z}{\partial x}$$

(TE mode)

$$H_y \propto \frac{\partial H_z}{\partial y}$$

$$E_x \propto \frac{\partial H_z}{\partial y}$$

$$E_y \propto \frac{\partial H_z}{\partial x}$$

If  $H_z = 0$  (TM mode)

$$H_x \propto \frac{\partial E_z}{\partial y}$$

$$H_y \propto \frac{\partial E_z}{\partial x}$$

$$E_x \propto \frac{\partial E_z}{\partial x}$$

$$E_y \propto \frac{\partial E_z}{\partial y}$$

## Phase & Group Velocity

Consider a positive travelling wave:

$$A^+ \cos(\omega t - \beta z + \phi) \underbrace{\quad}_{\bar{\Phi}(z,t)}$$

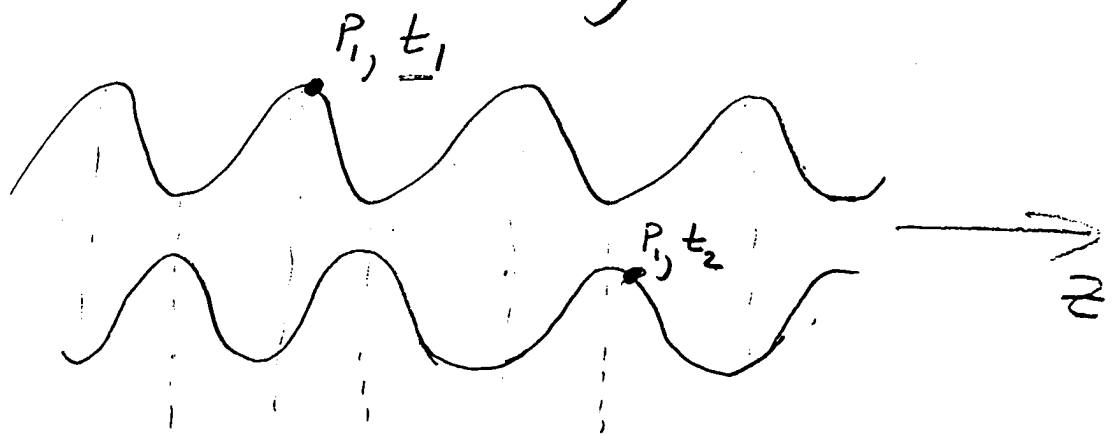
The phase of the wave  $\bar{\Phi}(z,t)$  in general varies with time  
 varies with time

Consider a point on the wave of fixed phase:

$$(1) \bar{\Phi}(z,t) = \omega t - \beta z + \phi = \text{const}$$

(41)

We can find the velocity of the point (phase front) by differentiating wrt time:



$$\omega dt - \beta dz = 0$$

$$v_{\text{phase}} = \frac{dz}{dt} = \frac{\omega}{\beta}$$

$v_{\text{phase}}$  ≡ the velocity with which a phase front moves past a point.

## Group Velocity

- Unusual to have a wave with a single frequency
- Invariably, many waves of different frequencies compose a wave packet

For simplicity, consider two simple sinusoidal waves with only slightly different frequencies and propagation constants

- both propagating in the  $+z$  direction
- both have equal amplitudes:

(43)

$$U_1(z, t) = \cos(\omega t - \beta z)$$

$$U_2(z, t) = \cos[(\omega + \Delta\omega)t - (\beta + \Delta\beta)z]$$

$$\Delta\omega \ll \omega, \quad \Delta\beta \ll \beta$$

The total wave is

$$U_T(z, t) = U_1(z, t) + U_2(z, t)$$

Recall:

$$\cos(X_1) + \cos(X_2) = 2\cos\left(\frac{X_1 - X_2}{2}\right)\cos\left(\frac{X_1 + X_2}{2}\right)$$

so,

slow variation

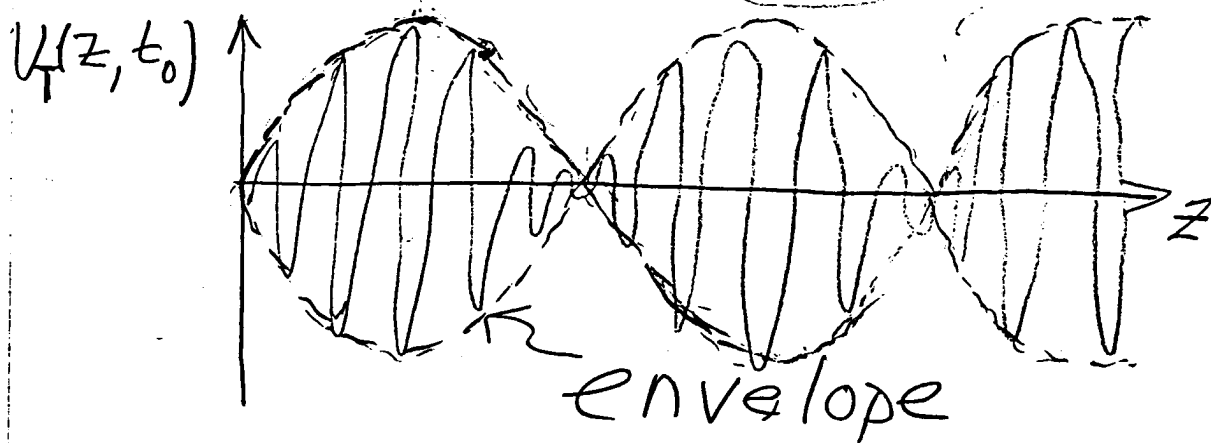
$$U_T(z, t) = 2\cos\left[-\frac{\Delta\omega}{2}t - \left(-\frac{\Delta\beta}{2}\right)z\right]$$

$$\times \cos\left[\left(\omega + \frac{\Delta\omega}{2}\right)t - \left(\beta + \frac{\Delta\beta}{2}\right)z\right]$$

rapid variation

$U_T(z, t)$  is a wave of carrier frequency  $\omega + \Delta\omega/2$  and propagation constant  $\beta + \Delta\beta/2$ , with a slowly varying amplitude

$$A = 2 \cos\left(\frac{\Delta\omega}{2}t - \frac{\Delta\beta}{2}z\right)$$



The envelope forms "groups" or "packets"

What is the velocity of

a "group"?

A constant phase of the envelope is given

by  $\frac{\Delta\omega}{2}t - \frac{\Delta\beta}{2}z = \text{const}$

So differentiating wrt time:

$$\frac{\Delta\omega}{2} - \frac{\Delta\beta}{2} \frac{dz}{dt} = 0$$

$$v_g = \frac{dz}{dt} = \frac{\Delta\omega}{\Delta\beta} \rightarrow \frac{d\omega}{d\beta}$$

for a pulse or signal composed of frequencies

IN A NARROW SPECTRUM

- group velocity  $v_g$  is commonly considered to be the velocity with which energy travels -- but this is only true sometimes (ideal transmission lines, ideal waveguides -- not true for transmission lines & waveguides with losses)

## Dispersion

The relation between  $\omega$  and  $\beta$  is called the dispersion relation

$$\omega = f(\omega)\beta$$

if  $f(\omega) = \text{const} (= \frac{1}{\sqrt{\mu_0 \epsilon_0}})$

for plane wave ( $\propto -\theta^{1/2}$ )

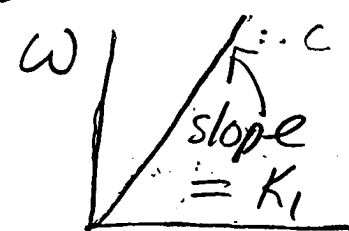
then

$$\omega = c\beta$$

$$V_{ph} = \frac{\omega}{\beta} = k_1, \quad V_g = \frac{d\omega}{d\beta} = k_1$$

and

$$V_{ph} = V_g = k_1 \Rightarrow$$



$\Leftarrow \omega - \beta$  relation  
for a photonic tube

# 3-layer Dielectric

## Waveguide (infinite slab)

Recall, Eq(9), p.③ on 1/22:

$$\nabla^2 \vec{E} - \mu\epsilon \frac{\partial^2 \vec{E}}{\partial t^2} = 0 \quad (1)$$

Assume (p⑨, 1/22)

$$\vec{E}_r = \text{Re} \left[ \vec{E}(x, y) e^{(j\omega t - \gamma z)} \right]$$

Let's consider (1):

$$\nabla^2 \vec{E} = \left( \frac{\partial^2}{\partial x^2} + \frac{\partial^2}{\partial y^2} + \frac{\partial^2}{\partial z^2} \right) \vec{E}$$

$$\vec{E} = E_x(x, y, z) \hat{i}_x + E_y(x, y, z) \hat{i}_y + E_z(x, y, z) \hat{i}_z$$

$$\text{so } \frac{\partial^2}{\partial z^2} \vec{E} = \gamma^2 \vec{E}$$

also;

$$\frac{\partial^2 \vec{E}}{\partial t^2} = (j\omega)^2 \vec{E} = -\omega^2 \vec{E}$$

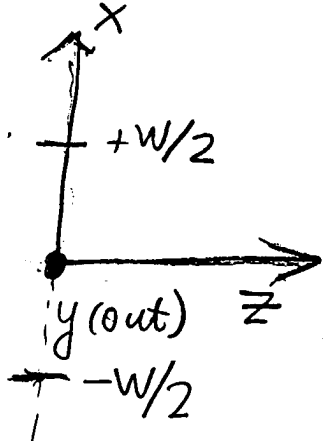
so (1) becomes

$$\left( \text{let } \nabla_t^2 = \frac{\partial^2}{\partial x^2} + \frac{\partial^2}{\partial y^2} \right)$$

$$\nabla_t^2 \vec{E}(x, y) + \gamma^2 \vec{E}(x, y) + \underbrace{\omega^2 \mu_0 \epsilon_0}_{k^2} \vec{E} = 0$$

$$\gamma = \alpha + j\beta; \text{ let } \alpha = 0$$

- ①  $\mu_1 = \sqrt{\epsilon_1} M_0$
- ②  $w$   $\mu_2 = \sqrt{\epsilon_2} M_0$
- ③  $\mu_3 = \sqrt{\epsilon_3} M_0$



(50)

Infinite slab in  $y \neq z$  direction

$$\Rightarrow \frac{\partial}{\partial y} = 0$$

The wave equation becomes

$$(\text{let } k^2 = \omega^2 \mu \epsilon)$$

$$k_0^2 = \omega^2 \mu_0 \epsilon_0$$

$$k_i^2 = \omega^2 \mu_0 \epsilon_0 \epsilon_i = \epsilon_i k_0^2$$

$i = i_{th}$  layer,  $\epsilon_i = \text{relative permittivity of } i_{th} \text{ layer}$

In region ①:

$$(2) \quad \frac{\partial^2 \vec{E}(x)}{\partial x^2} + (\epsilon_1 k_0^2 - \beta^2) \vec{E}_x = 0$$

In region ②:

$$(3) \quad \frac{\partial^2 \vec{E}(x)}{\partial x^2} + (\epsilon_2 k_0^2 - \beta^2) \vec{E} = 0$$

in region ③:

$$(4) \frac{\partial^2 \vec{E}_x(x)}{\partial x^2} + (\epsilon_3 k_0^2 - \beta^2) \vec{E}_x(x) = 0$$

(Note: each vector equation is three scalar equations)

Assume that  $\underline{\epsilon_2 > \epsilon_3 > \epsilon_1}$

why  
↓  
tir!

case 1 Consider  $\beta^2 > \epsilon_2 k_0^2$

$$\Rightarrow \beta^2 > \epsilon_1 k_0^2 \text{ and } \beta^2 > \epsilon_3 k_0^2$$

so,

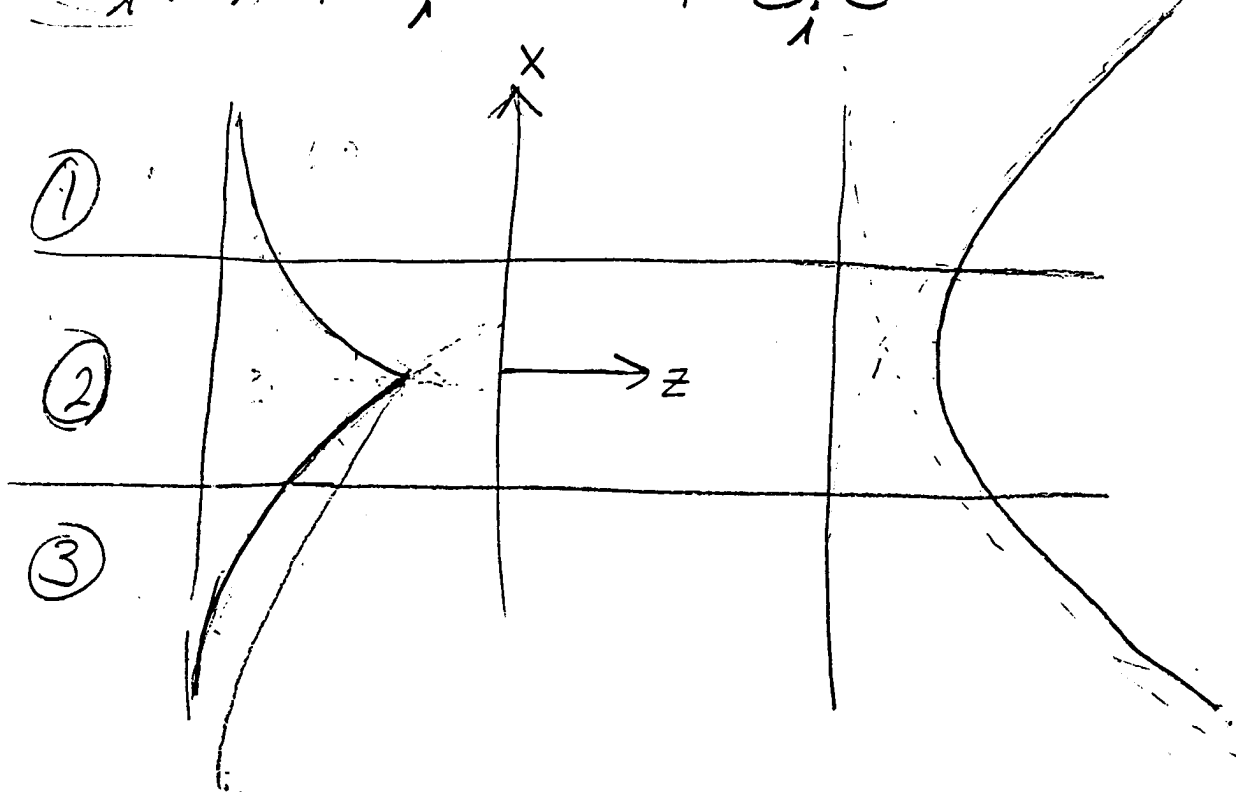
$$(5) \quad \frac{\partial^2 E_i(x)}{\partial x^2} = + c_i^2 E_i(x)$$

where  $c_i^2$  is positive and real

( $i = \text{layer ①, ②, or ③}$ )

the solution to (5):  $\beta^2 > \epsilon_i k_0^2$

$$\underline{E_i(x)} = A_i e^{-c_i x} + B_i e^{+c_i x}$$



solutions in all 3 regions  
are exponential — and  
not physical

case 2 Consider

$$\epsilon_1 k_0^2 < \epsilon_3 k_0^2 < \beta^2 < \epsilon_2 k_0^2$$

In Region ②,

$$\frac{\partial^2 E_2(x)}{\partial x^2} = -c_i^2 E_2(x)$$

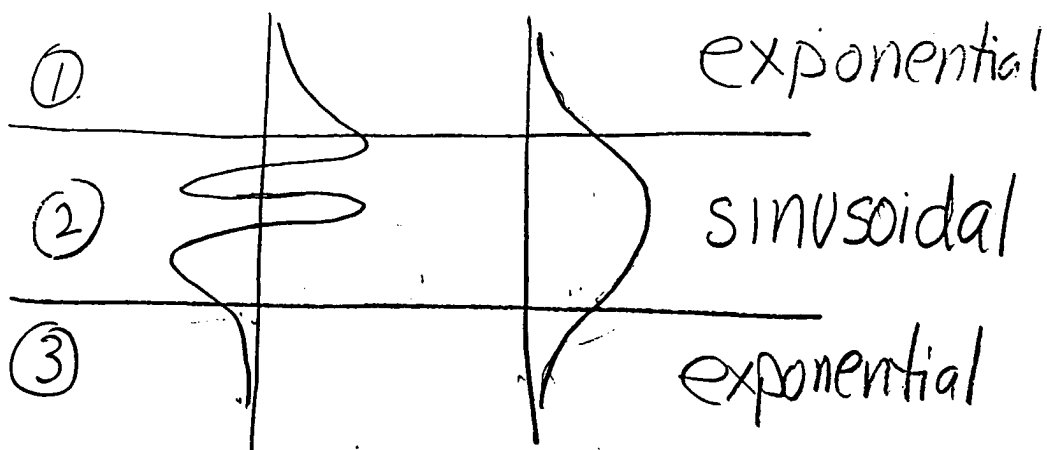
positive, real

so

$$E_2(x) = A_2 e^{-j\zeta_2 x} + B_2 e^{-j\zeta_2 x}$$

or, equivalently

$$E_2(x) = A'_2 \sin(\zeta_2 x) + B'_2 \cos(\zeta_2 x)$$

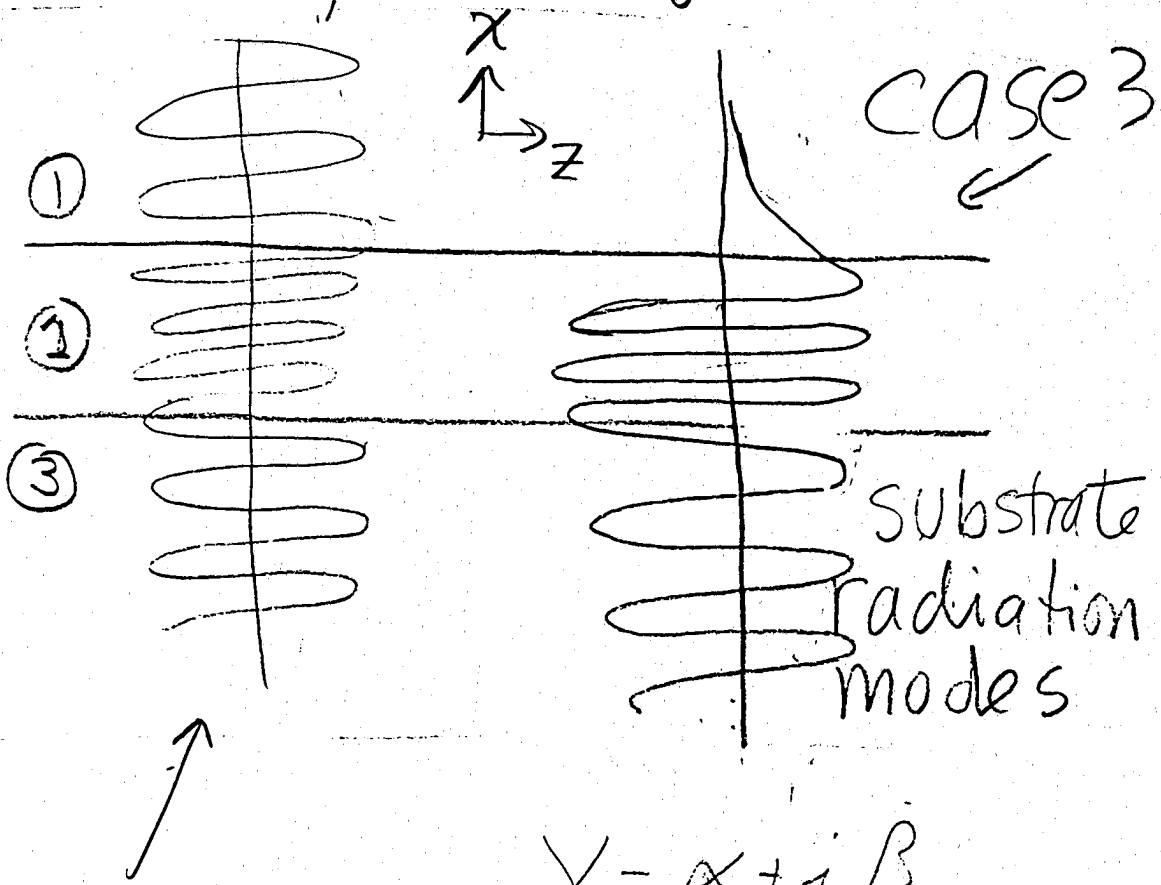


"confined," "guided" or

"bound" modes

Case 3: Consider

$$\epsilon_1 k_0^2 < \beta^2 < \epsilon_3 k_0^2 < \epsilon_2 k_0^2$$

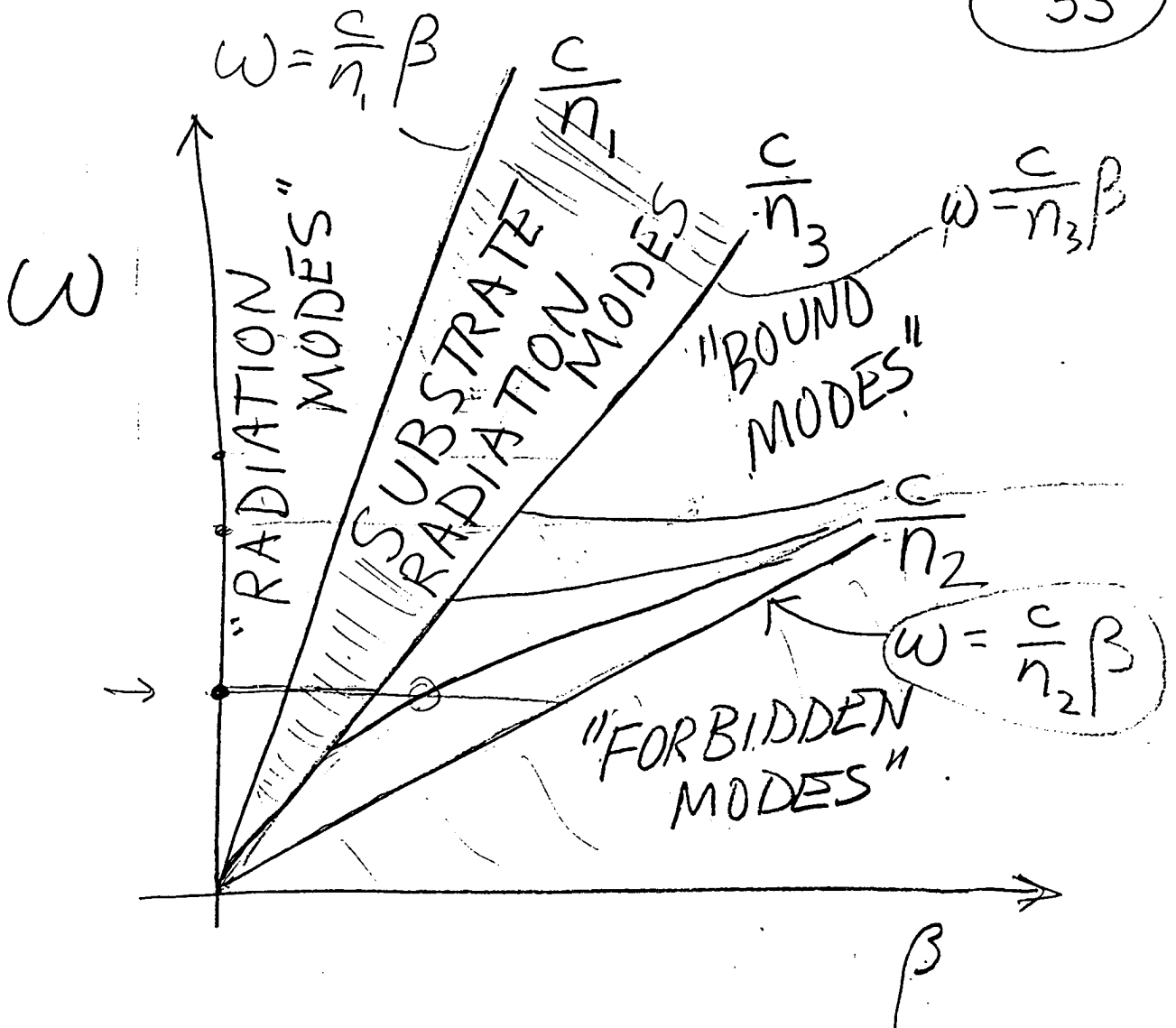


Case 4:

$$\beta^2 < \epsilon_1 k_0^2 < \epsilon_3 k_0^2 < \epsilon_2 k_0^2$$

$\Rightarrow$  radiation modes

to here  
11/27



$$y = mx$$

$$\beta$$

$$k_i^2 = \omega^2 \mu_0 \epsilon_0 \epsilon_i; \text{ boundaries}$$

$$\beta = \omega \sqrt{\mu_0 \epsilon_0 \epsilon_i} = \omega \frac{n_i}{c}$$

$$y = m \\ w = m^2$$

Case 1:  $\beta > k_2$  ( $\epsilon_2 > \epsilon_3 > \epsilon_1$ )

Case 2:  $\beta > k_3$  ( $< k_2$ )

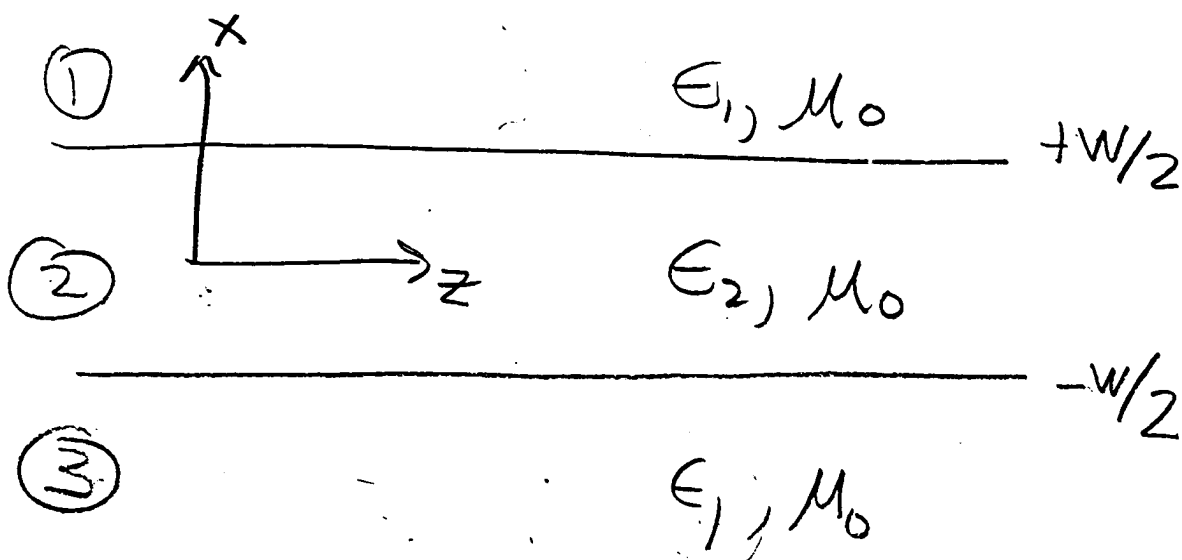
Case 3:  $\beta > k_1$  ( $< k_3, < k_2$ )

Case 4:  $\beta < k_1$  ( $< k_3, k_2$ )

# 3-layer Dielectric Waveguide, cont'd

## I Special Case

(Symmetric  $\rightarrow \epsilon_1 = \epsilon_3$ )



From 1/22 p. 13, 14

(Recall  $\frac{\partial}{\partial y} = 0$ )

Consider 22, 23, 24 & 25:

$$(22) \Rightarrow H_x = \frac{+j\beta}{k_i^2 - \beta^2} \frac{\partial H_z}{\partial x}$$

$$(23) \Rightarrow H_y = \frac{-j\omega\epsilon}{k_i^2 - \beta^2} \frac{\partial E_z}{\partial x}$$

$$(24) \Rightarrow E_x = \frac{-j\beta}{k_i^2 - \beta^2} \frac{\partial E_z}{\partial x}$$

$$(25) \Rightarrow E_y = \frac{j\omega\mu}{k_i^2 - \beta^2} \frac{\partial H_z}{\partial x}$$

Note: • only  $H_z$  or  $E_z$   
 (not both)

• (22)+(25)  $\Rightarrow E_y, H_x, H_z$   
 (TE modes)

• (23)+(24)  $\Rightarrow H_y, E_x, E_z$   
 (TM modes)

Lets solve for TE

2 (at least) choices:

- Solve a wave equation for  $H_z$  (homework)

and  $H_z \Rightarrow E_y, H_x$

Or,

- Solve a wave equation for  $E_y$  (Okay!)

From p 1/27 ⑪:

$$\frac{\partial^2 \vec{E}(x)}{\partial x^2} + (\epsilon_i k_0^2 - \beta^2) \vec{E} = 0$$

$$\vec{E} = E_x(x) \hat{i}_x + E_y(x) \hat{i}_y + E_z(z) \hat{i}_z$$

TE modes  $\Rightarrow E_z \equiv 0$

Eq (22) & (25)  $\Rightarrow E_x = 0$

So, for  $|x| \leq W/2$ ,

$$(1) \frac{\partial^2 E_y(x)}{\partial x^2} + (\epsilon_2 k_0^2 - \beta^2) E_y(x) = 0$$

$- \delta^2 E_y$  for  $|x| \geq W/2$ ,

$$(2) \frac{\partial^2 E_y(x)}{\partial x^2} + (\epsilon_1 k_0^2 - \beta^2) E_y(x) = 0$$

Bound modes  $\Rightarrow$

$$\epsilon_1 k_0^2 < \beta < \epsilon_2 k_0^2$$

(60)

For  $|X| \leq W/2$ ,

Solution is sinusoidal

For  $|X| \geq W/2$ ,

Solution is exponential:

$$E_y(x) = \begin{cases} A e^{-\delta x} + B e^{\delta x} \\ \quad \downarrow \text{(for } x > W/2) \\ C e^{-\delta x} + D e^{\delta x} \\ \quad \text{for } x < -W/2 \end{cases}$$

$$E_y(x) = F \cos(\delta x) \quad \text{for } |x| < \frac{W}{2}$$

$$+ G \sin(\delta x)$$

(61)

Eq (1)  $\Rightarrow$ 

$$-\gamma^2 + \epsilon_2 k_0^2 - \beta^2 = O(3)$$

Eq (2)  $\Rightarrow$ 

$$+\gamma^2 + \epsilon_1 k_0^2 - \beta^2 = O(4)$$

Consider even & odd  
modes

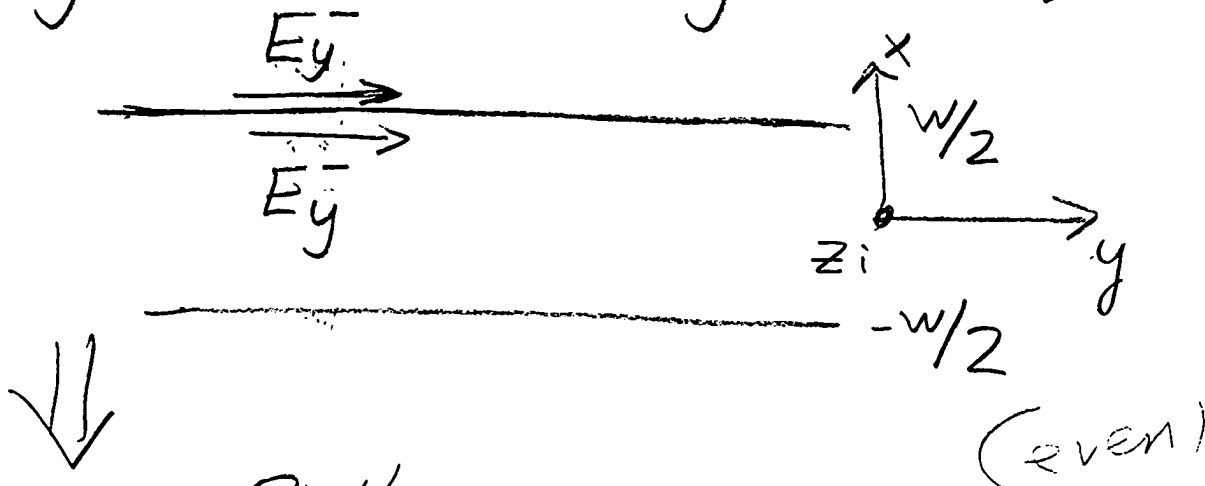
$$E_y(x) = \begin{cases} F \cos(sx) & (\text{even}) \\ G \sin(sx) & (\text{odd}) \end{cases}$$

Boundary conditions

(62)

Tangential  $\vec{E}$  continuous:

$$E_y(x=w/2^+) = E_y(x=w/2^-)$$



$$\underline{A} \vec{e}^{-sw/2} = F \cos(sw/2) (5)$$

Tangential  $\vec{H}$  continuous:

From  $\nabla \times \vec{H} = j\omega \epsilon \vec{E} (\vec{J} \equiv 0)$

$$\underline{H}_2 = -\frac{1}{j\omega \mu_0} \left( \frac{\partial E_y}{\partial x} \right).$$

[also see '22 p. 11, Eq (18)]

(63)

$$H_3 = \frac{s}{j\omega\mu_0} A e^{-sx} \quad (5)$$

$x \geq w/2$

$$H_3 = \frac{s}{j\omega\mu_0} F \sin(sx) \quad (6)$$

$|x| \leq w/2$

@  $x = w/2$

$$\frac{s}{j\omega\mu_0} A e^{-sw/2} = \frac{s}{j\omega\mu_0} F \sin\left(\frac{sw}{2}\right) \quad (7)$$

From (5)  $\leftarrow$  PT

$$\underline{A} = e^{sw/2} F \cos\left(\frac{sw}{2}\right)$$

SO (7)  $\Rightarrow$

$$\cancel{Se^{\frac{sw}{2}} F e^{-\frac{sw}{2}}} \cos\left(\frac{sw}{2}\right)$$

$$= SF \sin\left(\frac{sw}{2}\right)$$

OR,

$$\frac{sw}{2} = \frac{sw}{2} \tan\left(\frac{sw}{2}\right) \quad (8a)$$

(even modes)

Similarly, for odd modes:

$$\frac{sw}{2} = -\frac{sw}{2} \cotan\left(\frac{sw}{2}\right) \quad (8b)$$

Note: 2 Eq's, 2 Unk's

$$Eq(4) - Eq(3) \Rightarrow k_0 = \frac{2\pi}{\lambda_0}$$

$$(9) \left(\frac{\delta w}{2}\right)^2 + \left(\frac{s w}{2}\right)^2 = (\epsilon_2 - \epsilon_1) \left(\frac{k w}{2}\right)^2 = r^2$$

$$(10) \left(\frac{sw}{2}\right) = \left(\frac{sw}{2}\right) \begin{cases} \tan\left(\frac{sw}{2}\right) & (\text{even}) \\ -\cot\left(\frac{sw}{2}\right) & (\text{odd}) \end{cases}$$

$$(3), (4) \Rightarrow \beta = f(s) \text{ or } f(\delta)$$

$$E_y(x, z, t) = A f(x) e^{j(\omega t - \beta z)}$$

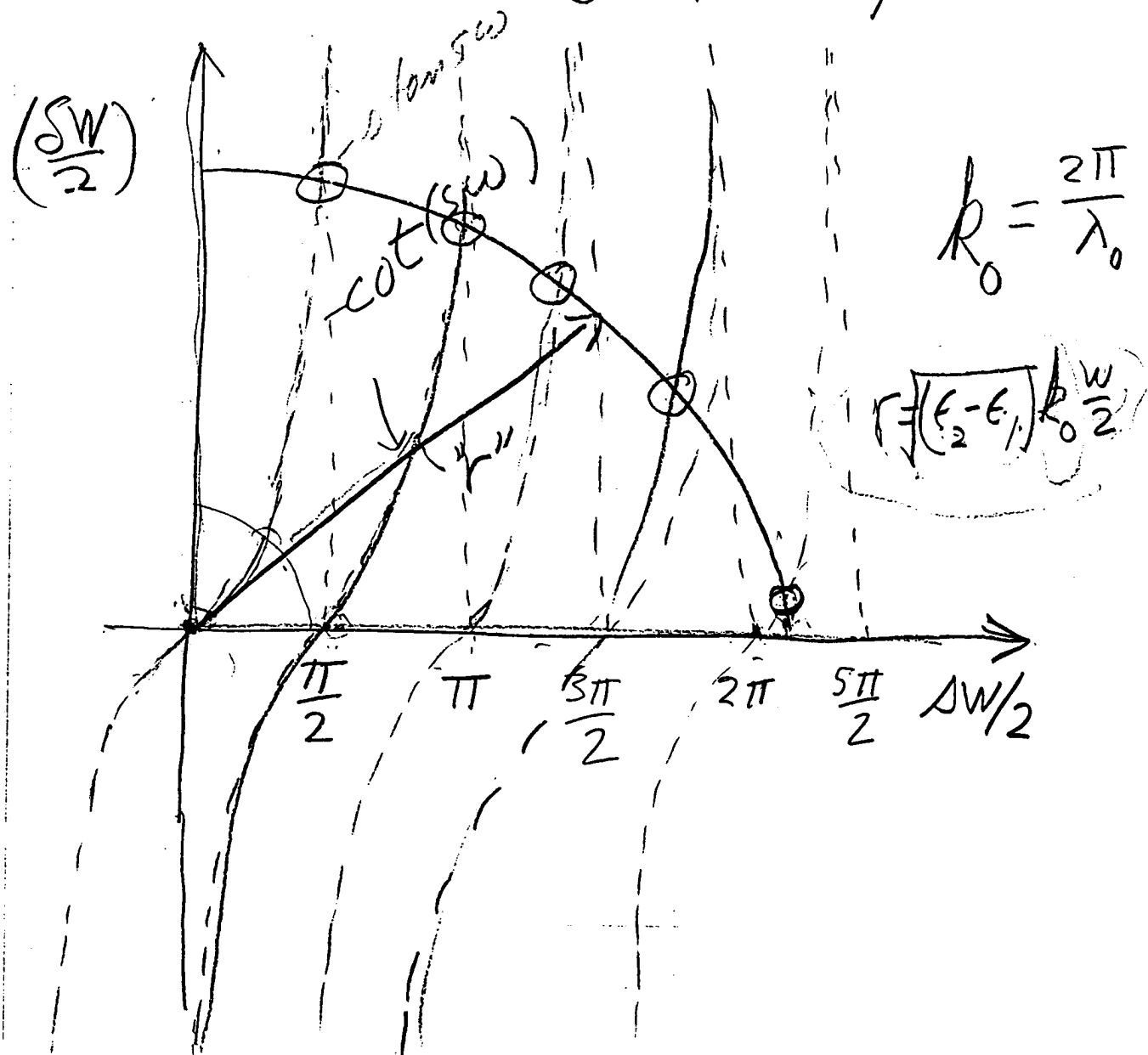
$$f(x) = \begin{cases} \frac{\cos(sx)}{\cos(sw/2)} & \text{even} \\ \frac{\sin(sx)}{\sin(sw/2)} & |x| \leq \frac{w}{2} \\ & \text{odd} \end{cases}$$

(66)

$$f(x) = \begin{cases} \exp(SW_2 - S|x|) & (\text{even}) \\ \text{sign}(x) \exp(SW_2 - S|x|) & (\text{odd}) \end{cases}$$

*for here*

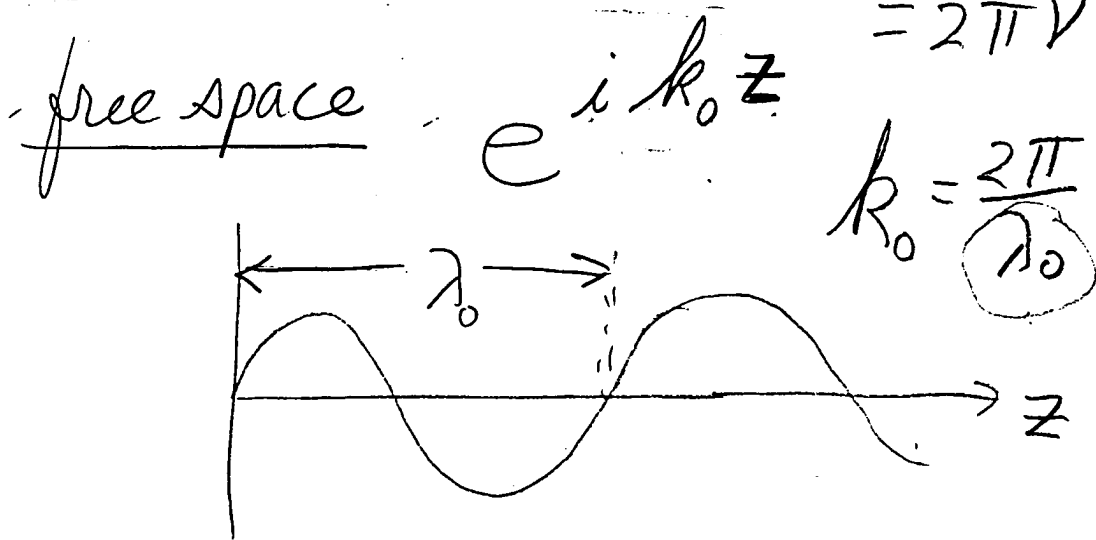
(9) + (10), graphically:



$$k_0^2 = \omega^2 \mu_0 \epsilon_0$$

$$\omega = 2\pi f$$

$$= 2\pi v$$



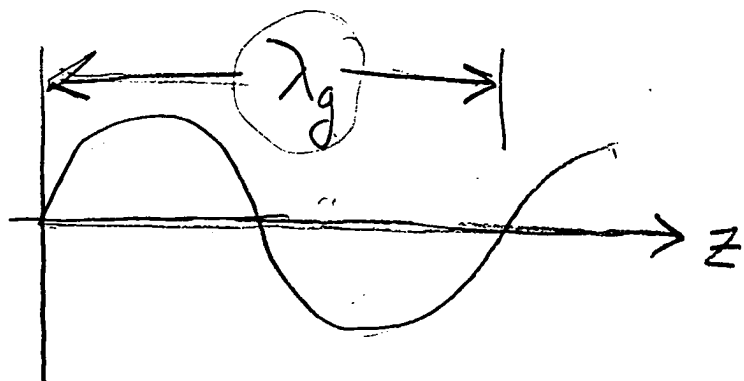
$$k_0 = \frac{2\pi}{\lambda_0}$$

$$\frac{\beta}{k_0} = n_{\text{eff}}$$

waveguide

$$e^{i\beta z}$$

$$n_{\text{eff}} = \frac{\beta}{k_0}$$



$$\beta = \frac{2\pi}{\lambda_g}$$

$$\omega = k_0 \sqrt{\mu_0 \epsilon_0} = \frac{2\pi}{\lambda_0} \sqrt{\mu_0 \epsilon_0}$$

We Know

$$\underline{\epsilon_1, \epsilon_2, \mu_0, \epsilon_0, w}$$

and  $\lambda_0$  (generally)  $\Rightarrow k_0, \omega$

solve (9) & (10)

(several ways)

$\Rightarrow \delta, s$

from (3)

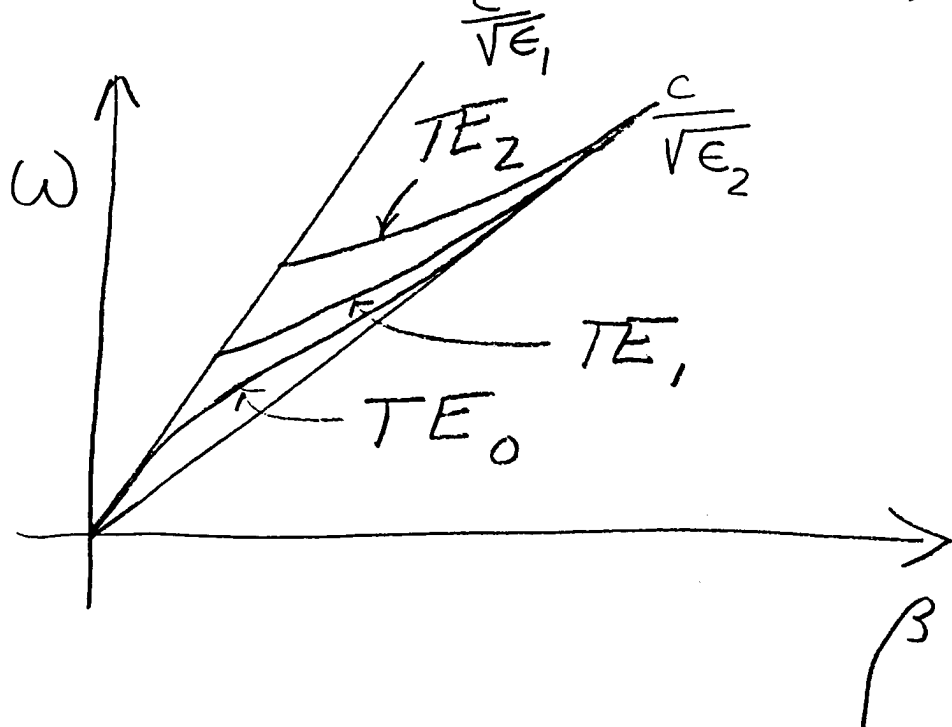
$$\beta^2 = \epsilon_2 k_0^2 - s^2 \quad (11)$$

or from (4)

$$\beta^2 = s^2 + \epsilon_1 k_0^2 \quad (12)$$

Now we have the dispersion relation,

$$\beta = f(\omega, \epsilon_1, \epsilon_2, \mu_0, \epsilon_0, n)$$



What about  $H_x$  &  $H_z$ ?

See Eq(16), (18) on 11 of 1/22

Or,

$$\nabla_x \vec{E} = -j\omega \mu \vec{H}$$

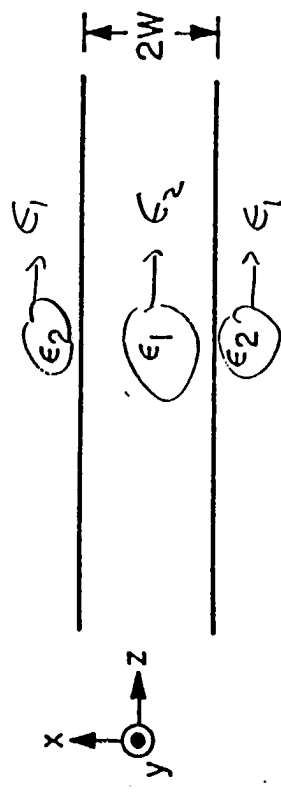


Fig. A.1 Thin film waveguide geometry.

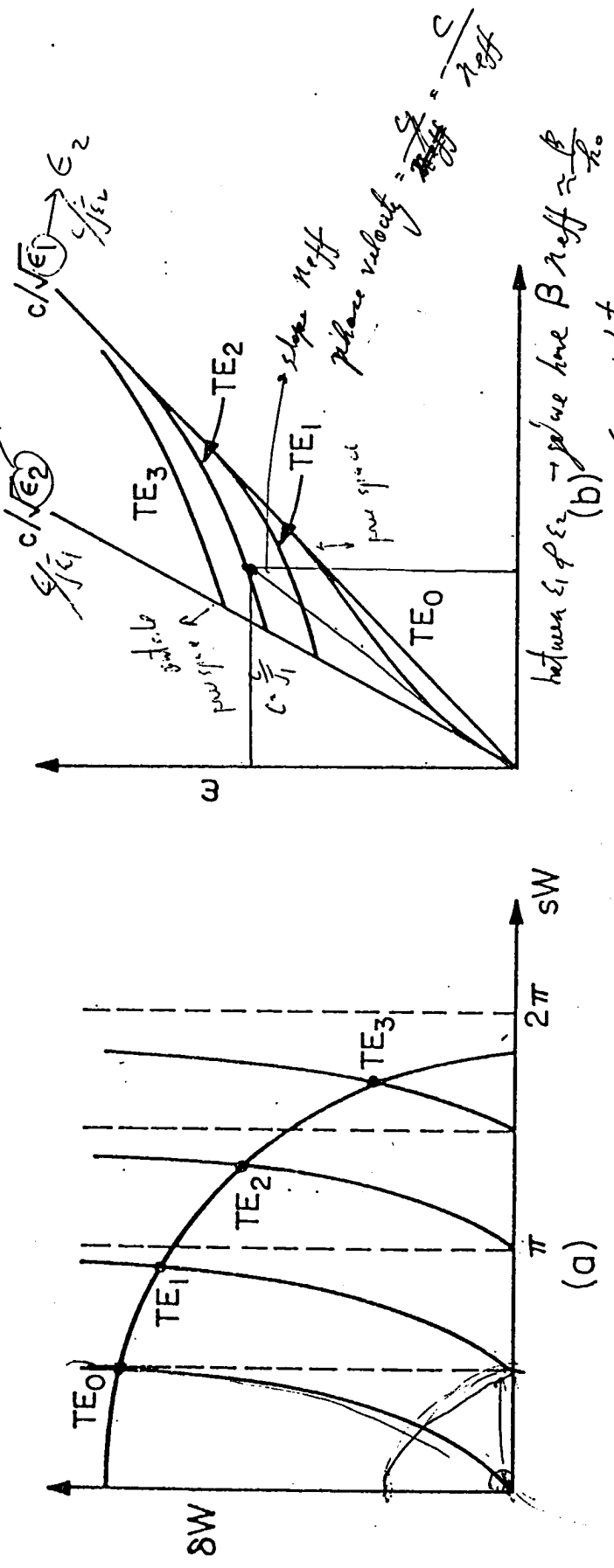


Fig. A.2 (a) graphical solution of equations (A.6) and (A.7);  
 (b)  $\omega$ - $\beta$  diagram for TE modes of a thin film waveguide.

$n_{eff}$

$\beta$

$c$

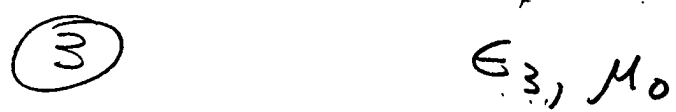
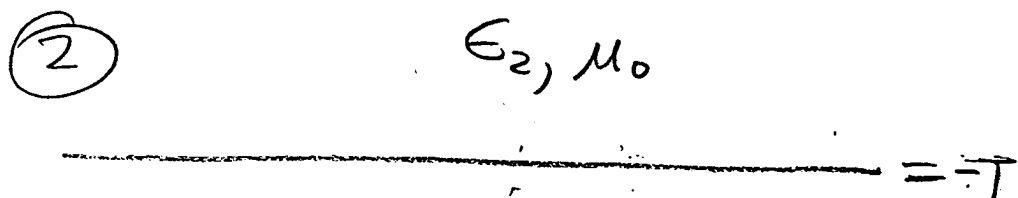
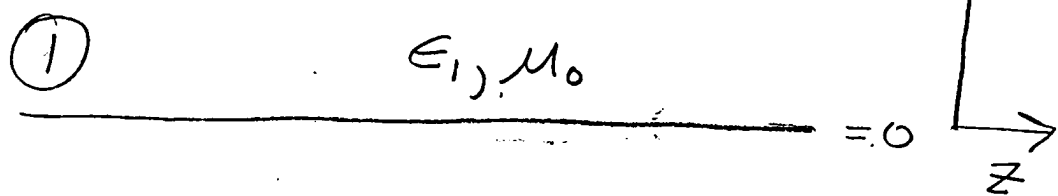
$\omega$

70

# 3-layer Dielectric } Waveguide, cont'd }

## II General Case

$$\epsilon_2 > \epsilon_3 > \epsilon_1$$



As before, we have

TE + TM modes

Same form of solutions  
to

$$(1) \frac{\partial^2 E_y(x)}{\partial x^2} + (\epsilon_i k_0^2 - \beta^2) E_y(x) = 0$$

$$i = 1, 2, 3$$

Want to find "bound"

Modes  $\Rightarrow$

$$\frac{\epsilon_1 k^2}{k_0^2} < \frac{\epsilon_3 k^2}{k_0^2} < \frac{\beta^2}{k_0^2} < \frac{\epsilon_2 k^2}{k_0^2}$$

Process:

- find solutions in all 3 regions
- find  $E_y + H_z$  (TE) +  $H_y + E_z$  (TM)
- Require  $\vec{E}(x = \pm\infty) \rightarrow 0$   
 $\vec{H}(x = \pm\infty) \rightarrow 0$

$\pi$  (radiation condition)

• Apply boundary conditions at

$$x=0, -T$$

$$\xrightarrow{\text{1...}} \rho$$

In ② (TE Modes):

$s$ : transverse ray vector  
units of  $\frac{1}{x}$ .

$$(2) E_y(x) = A \cos sx + B \sin sx \quad (0 \leq x \leq T)$$

In ①

$$(3) E_y(x) = C e^{-sx} + D e^{sx}, \quad (x > 0)$$

In ③

$$(4) E_y(x) = D e^{\xi(x+T)} + D e^{-\xi(x+T)} \quad (x < -T)$$

assuming we know  
the coeff.

From (1),

$$\delta^2 + \epsilon_1 k_0^2 - \beta^2 = 0 \quad (5)$$

$$-\delta^2 + \epsilon_2 k_0^2 - \beta^2 = 0 \quad (6)$$

$$\gamma^2 + \epsilon_3 k_0^2 - \beta^2 = 0 \quad (7)$$

BC on  $E_y(x=0) \Rightarrow$

$$A = C \quad (8)$$

BC on  $E_y(x=-T) \Rightarrow$

$$A \cos(\omega T) - B \sin(\omega T) = D \quad (9)$$

From

$$H_z = -\frac{1}{j\omega \mu_0} \frac{\partial E_y}{\partial x}$$

We find

in ①,  $H_z = +\frac{8C}{j\omega M_0} e^{-sx}$ ,  $x \geq 0$  (10)

in ②,  $H_z = +\frac{1}{j\omega M_0} (A \sin(sx) - B \cos(sx))$ ,  $0 \geq x \geq -T$  (11)

in ③,  $H_z = -\frac{\xi D}{j\omega M_0} e^{\xi(x+T)}$ ,  $x < -T$ ,

or (Eq(9)),

$$H_z = -\frac{\xi}{j\omega M_0} (A \cos(\omega T) - B \sin(\omega T)) * e^{\xi(x+T)}, \quad (12)$$

$(x < -T)$

BC on  $H_z @ x=0$ :

$$\delta A = -\delta B \quad (13)$$

(76)

BC on  $H_2 @ x = -T$ :

$$\begin{aligned} & S[A \sin(ST) - B \cos(ST)] \quad (14) \\ &= -\xi [A \cos(ST) - B \sin(ST)] \end{aligned}$$

(13), (14)  $\Rightarrow$  2 Eq's, 2 Unks.

Solution if det vanishes:

$$SA + SB = 0 \quad (13')$$

$$[S \sin(ST) - \xi \cos(ST)]A \quad (14')$$

$$\begin{aligned} &+ [S \cos(ST) + \xi \sin(ST)]B \\ &= 0 \end{aligned}$$

i.e.,

$$a_{11}x_1 + a_{12}x_2 = 0$$

$$a_{21}x_1 + a_{22}x_2 = 0$$

has a solution if

$$a_{11}a_{22} - a_{21}a_{12} = 0$$

so:

$$\delta[s \cos(\omega T) + \ell \sin(\omega T)]$$

$$-s[s \sin(\omega T) - \ell \cos(\omega T)] = 0.$$

or,

$$(\delta s + \ell \omega) \cos(\omega T) \quad (15)$$

$$+ (\delta \ell - s^2) \sin(\omega T) = 0$$

or (15)  $\rightarrow$

$$\frac{\sin(ST)}{\cos(ST)} = -\frac{S(\delta + \xi)}{(\xi S - S^2)} =$$

!!

$$\tan(ST) = F(ST) \quad (16)$$

Really  $F(ST)$  only?

Recall (5, 6, 7), p④ 3/3:

$$(5) \Rightarrow \delta = (\beta^2 - \epsilon_1 k_0^2)^{1/2}$$

$$(7) \Rightarrow \xi = (\beta^2 - \epsilon_3 k_0^2)^{1/2}$$

$$(6) \Rightarrow \beta^2 = \sqrt{-S^2 + \epsilon_2 k_0^2}$$

so,

$$\delta = \left[ (\epsilon_2 - \epsilon_1) k_0^2 - s^2 \right]^{1/2}$$

$$\zeta = \left[ (\epsilon_2 - \epsilon_3) k_0^2 - s^2 \right]^{1/2}$$

so,  $F(ST) =$

$$\frac{ST \left\{ \left[ (\epsilon_2 - \epsilon_1) (k_0 T)^2 - (ST)^2 \right]^{1/2} + \left[ (\epsilon_2 - \epsilon_3) (k_0 T)^2 - (ST)^2 \right]^{1/2} \right\}}{(ST)^2 - \left[ (\epsilon_2 - \epsilon_1) (k_0 T)^2 - (ST)^2 \right]^{1/2} \left[ (\epsilon_2 - \epsilon_3) (k_0 T)^2 - (ST)^2 \right]^{1/2}}$$

(Eq. 16)

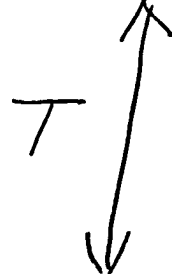
Example: AlGaAs/GaAs

Dielectric Waveguide

①  $\text{Al}_{0.1} \text{Ga}_{0.9} \text{As} \dots \infty$

$x=0$  —————

②  $\text{GaAs}$



③  $\text{Al}_{0.3} \text{Ga}_{0.7} \text{As} \dots \infty$

≈



④  $\text{GaAs}$  (substrate)  
negligible

Assume  $\lambda_0 = 1\mu\text{m}$

$$T = 3.22825\mu\text{m}$$

$$D = 10\mu\text{m}$$

$$F(ST) = \frac{ST [24^2 (ST)^2]^{1/2} + [11^2 - (ST)^2]^{1/2}}{(ST)^2 - [24^2 - (ST)^2]^{1/2} [11^2 - (ST)^2]^{1/2}}$$

(81)

$$\lambda_0 = 1.0 \mu m,$$

$$10\% AlAs \Rightarrow n_1 = 3.315177$$

$$\Rightarrow \underline{\epsilon_1 = 10.9904} \quad (1)$$

$$0\% AlAs (GaAs) \Rightarrow n_2 = 3.52$$

$$\Rightarrow \underline{\epsilon_2 = 12.3904} \quad (2)$$

$$30\% AlAs \Rightarrow n_3 = 3.478562$$

$$\Rightarrow \underline{\epsilon_3 = 12.1004} \quad \frac{2\pi}{\lambda_0}$$

so

$$(\epsilon_2 - \epsilon_1)^2 k_0 T = \underline{2.4} = \cancel{\lambda_0} a$$

$$(1.1832) (6.28)(3.228)$$

$$(\epsilon_2 - \epsilon_3)^2 k_0 T = \underline{11} = \cancel{\lambda_0} b$$

$$0.538$$

$$20.28$$

2/3

82

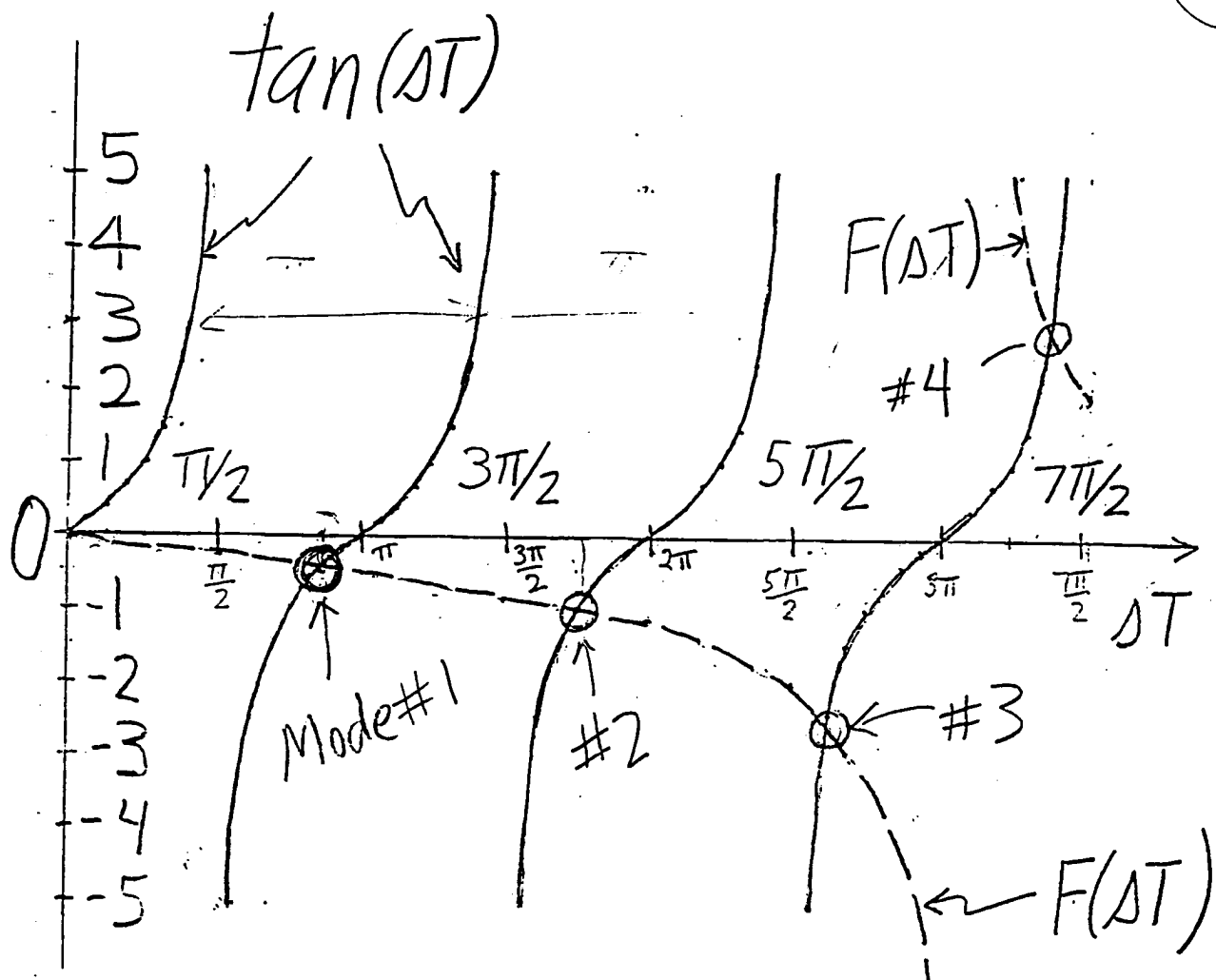


Fig. 1

Graphical solution  
of Eq.(16) for asymmetrical  
slab with

$$(\epsilon_2 - \epsilon_3)^{1/2} k_b T = 11 = \delta$$

$$(\epsilon_2 - \epsilon_1)^{1/2} k_b T = 24 = \delta$$

Fig. 1  $\Rightarrow$

$$(ST)_1 \approx 2.7 \Rightarrow S_1 = 0.84$$

$$(ST)_2 \approx 5.5 \Rightarrow S_2 = 1.7$$

$$(ST)_3 \approx 8.2 \Rightarrow S_3 = 2.54$$

$$(ST)_4 \approx 10.6 \Rightarrow S_4 = 3.28$$

Can find  $\delta$ ,  $\xi$ , and  $\beta$

from (5), (6), & (7)

P⑧, 2/3  $\epsilon_{\text{r}} \text{ (P5 73) } (2)(3), (4)$

$\Rightarrow$  know  $(E_y, H_x, H_z)$

Asymmetric 3 layer WG

• How many modes?

$$F(ST) =$$

$\boxed{\text{see p. 9, 2/3}}$

$$(1) \frac{ST \left\{ \left[ (\epsilon_2 - \epsilon_1)(k_0 T)^2 - (ST) \right]^2 + \left[ (\epsilon_2 - \epsilon_3)(k_0 T)^2 - (ST) \right]^2 \right\}^{\frac{1}{2}}}{(ST)^2 - \left[ (\epsilon_2 - \epsilon_1)(k_0 T)^2 - (ST)^2 \right]^{\frac{1}{2}} \left[ (\epsilon_2 - \epsilon_3)(k_0 T)^2 - (ST)^2 \right]^{\frac{1}{2}}}$$

$F(ST)$  becomes complex

if we take  $\sqrt{\text{neg \#}}$

$$(2) \Rightarrow \text{if } (\epsilon_2 - \epsilon_3)(k_0 T)^2 > ST$$

$\Rightarrow F(ST)$  is complex!

Define a parameter

$$V_w = (\epsilon_2 - \epsilon_3)^{1/2} k_b T \quad (3)$$

Consider "V" for the cutoff of the  $n^{th}$  waveguide mode =  $V_{n,c}$

How can we find  $V_{n,c}$ ?

- at cutoff,

$$\xi_{n,c} = 0 \quad (4)$$

from (7) p ⑧, 2/3,

$$\xi = (\beta^2 - \epsilon_3 k_b^2)^{1/2}$$

SO,

$$\beta_{n,c}^2 = \epsilon_3 k_0^2 \quad (5)$$

from (6), p ⑧

$$\beta^2 = -S^2 + \epsilon_2 k_0^2$$

SO,

$$S_{n,c}^2 T^2 = (\epsilon_2 - \epsilon_3) k_0^2 T \quad (6)$$

$$SO \quad F(S_{c,n} T) = \dots$$

$$\frac{A_{n,c} T \{(\epsilon_2 - \epsilon_1) - (\epsilon_2 - \epsilon_3)\}^{1/2} k_0 T}{(S_{n,c} T)^2} \quad (7)$$

By definition, [Eq(3)]

$$\underline{V_w} = (\epsilon_2 - \epsilon_3)^{1/2} k_b T,$$

so

$$\underline{V_{n,c}} = S_{n,c} T \quad (8)$$

since  $\tan(S_{n,c} T) = F(S_{n,c} T)$

$$F(V_{n,c}) = \frac{(\epsilon_3 - \epsilon_1)^{1/2} k_b T}{(\epsilon_2 - \epsilon_3)^{1/2} k_b T}$$

$$= \tan(V_{n,c}) \quad (9)$$

So,

$$\boxed{V_{n,c}} = \tan^{-1} \left[ \frac{\epsilon_3 - \epsilon_1}{\epsilon_2 - \epsilon_3} \right]^{1/2} + n\pi \quad n=0,1,2,\dots$$

if  $0 < \tan^{-1}(x) < \pi/2$  (10)

$n=0 \Rightarrow$  mode 1

$n=1 \Rightarrow$  mode 2

$\vdots$

$\vdots$

$n=N \Rightarrow$  mode  $N+1$

For a given Waveguide,

$$V_w = (\epsilon_2 - \epsilon_3)^{1/2} k_b T$$

and

$$V_{c,N} < V_w < V_{c,N+1} \quad (11)$$

$N$  = highest order guided mode

$N+1$  = 1<sup>st</sup> unguided mode

(12)  $V_w < (N\pi)^{1/2} + \tan^{-1} \left( \frac{\epsilon_3 - \epsilon_1}{\epsilon_2 - \epsilon_3} \right)^{1/2}$

$$\text{Int}[2.06] = 3$$

(89)

$$N_{TE} = \text{Int} \left\{ \frac{1}{\pi} \left[ V_W - \tan^{-1} \left( \frac{\epsilon_3 - \epsilon_1}{\epsilon_2 - \epsilon_3} \right)^2 \right] \right\} + 1$$

$$(V_W > \frac{\pi}{2}, \text{ if } V_W < \frac{\pi}{2}, N_{TE} = 0) \quad (13)$$

Can show for TM modes:

$$N_{TM} = \text{Int} \left\{ \frac{1}{\pi} \left[ V_W - \tan^{-1} \left( \frac{\epsilon_2}{\epsilon_1} \sqrt{\frac{\epsilon_3 - \epsilon_1}{\epsilon_2 - \epsilon_3}} \right) \right] \right\} + 1 \quad (14)$$

check Eq (13) with Fig. 1:

$$(\epsilon_2 - \epsilon_3)(k_0 T)^2 = (11)^2; (\epsilon_2 - \epsilon_1)(k_0 T)^2 = (24)^2$$

$$\cancel{V_W} = (\epsilon_3 - \epsilon_1)^{1/2} k_0 T = \left[ (24)^2 - (11)^2 \right]^{1/2} = 21.33$$

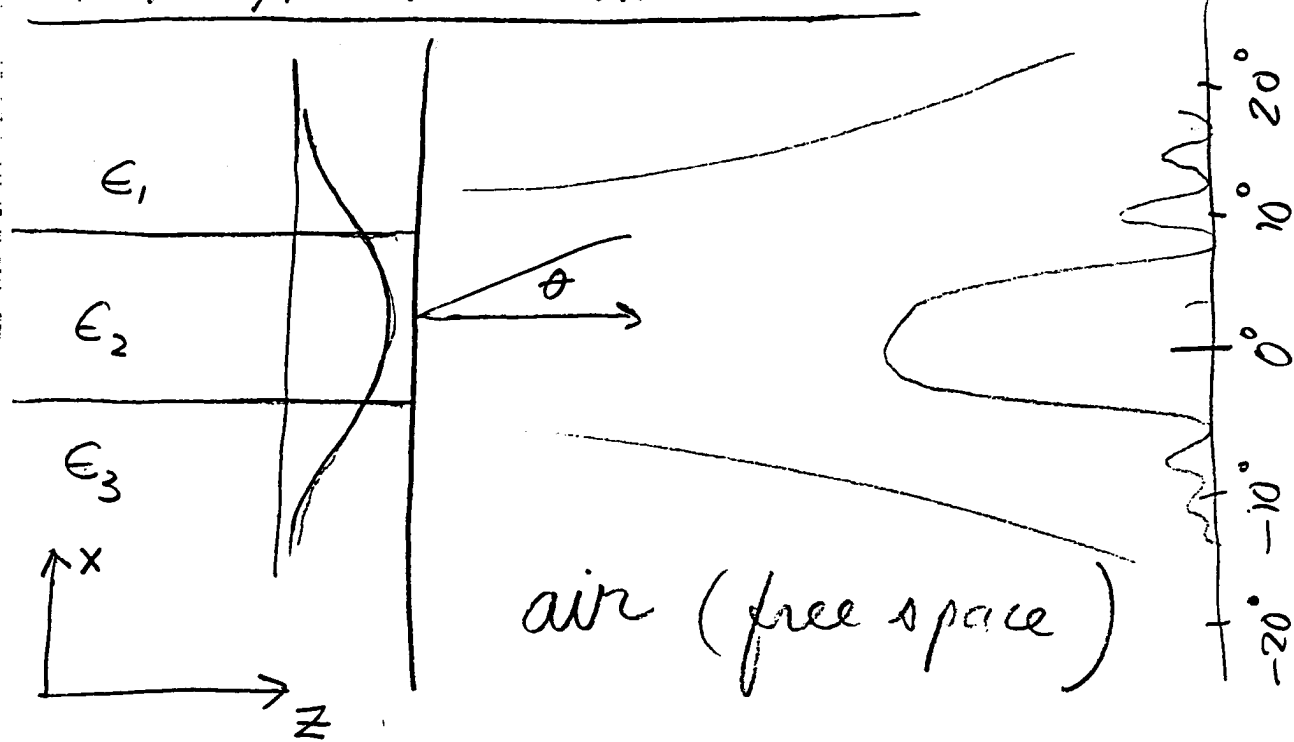
$$N_{TE} = \text{Int} \left\{ \frac{1}{\pi} \left[ 11 - \tan \left( \frac{21.33}{11} \right) \right] \right\}^{1.09} + 1$$

$$N_{TE} = \text{Int} \left[ \frac{9.91}{\pi} \right] + 1 = \underline{\underline{4}}$$

previously assuming  $\infty$  length

$$\theta \sim \frac{1}{D} \left\{ \begin{array}{l} 53^{\circ} 0' \\ 53^{\circ} 12' \\ 53^{\circ} 11' \end{array} \right\} \quad (90)$$

## Far-field Patterns



- for a given modal distribution  $E_y(x)$  in the WG, what is the resulting radiation pattern "far away" from the waveguide termination?  
exact calculation is fairly complicated

• first-order approximation:

$$\text{far field} = \text{FT}(\text{near field})$$

$\downarrow \{\text{near field}\}$

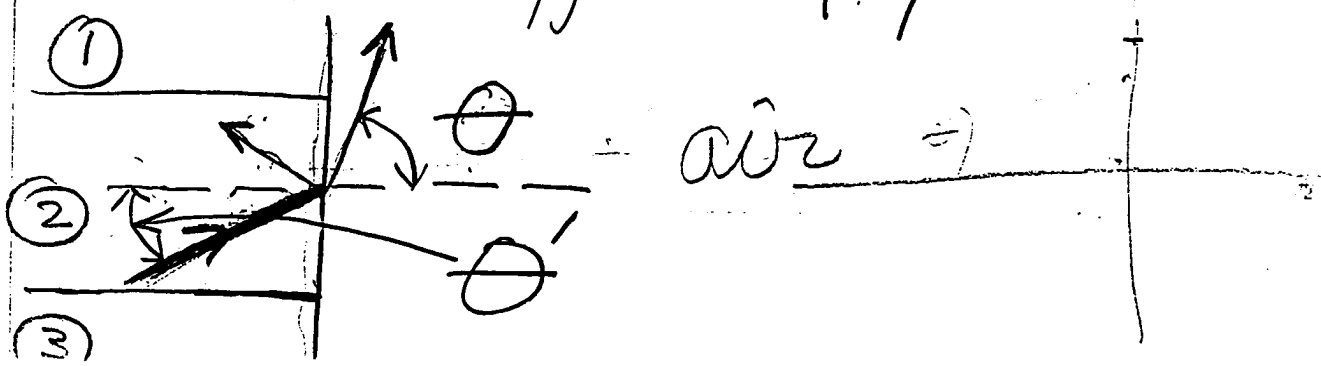
- antenna patterns +  
antenna apertures

- method not quite  
accurate for dielectric  
waveguides

• Our method:

$$\text{ff} \underset{\text{far field}}{\approx} [\text{FT}(nf)] \cos\theta$$

-  $\cos\theta$  = Huygens obliquity factor



$$n_{\text{eff}} \sin \theta' = n_{\text{air}} \sin \theta \quad (1)$$

(Snell's Law)

let  $n_{\text{eff}} \sim 3.4$

$$n_{\text{air}} = 1.0$$

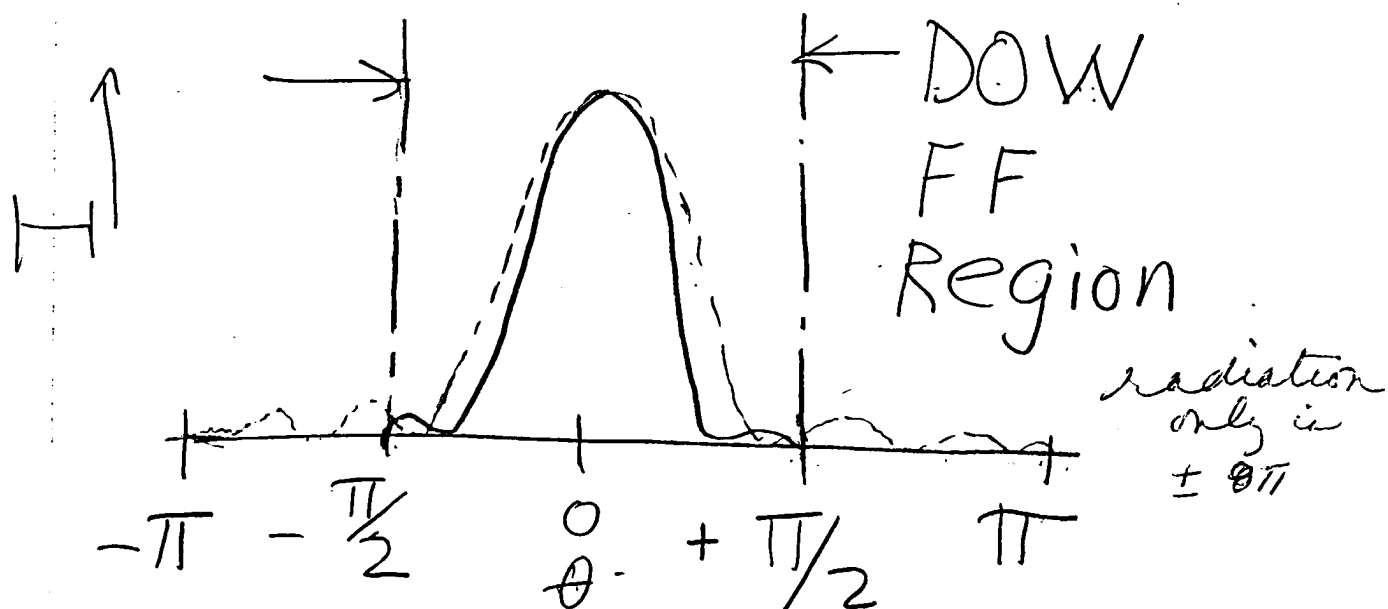
We have TIR when

$$\theta = \frac{\pi}{2}, \text{ or}$$

$$(2) \quad \theta' = \sin^{-1} \left( \frac{n_{\text{air}}}{n_{\text{eff}}} \right)$$

$$\theta' = 17.1^\circ \text{ for}$$

typical values for  
a GaAs/AlGaAs WG



- TIR  $\Rightarrow$  DOW has as opposed to metal
- FF with  $-\frac{\pi}{2} \leq \theta \leq \frac{\pi}{2}$

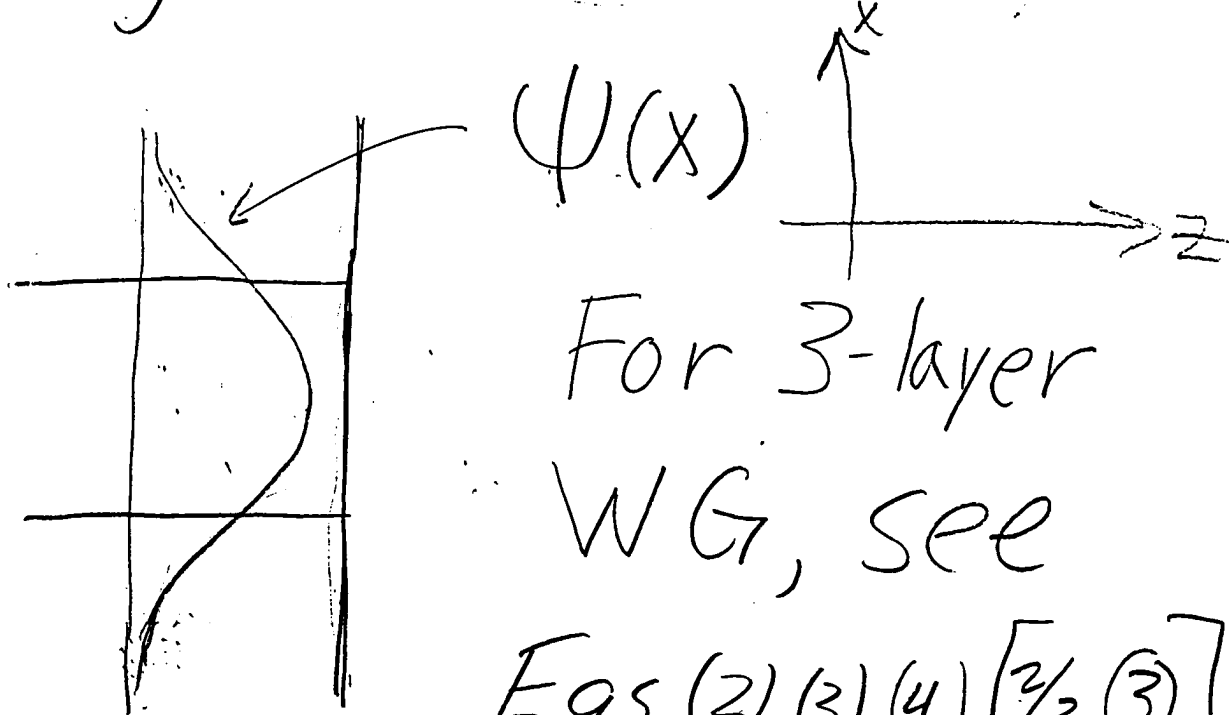
- Antenna  $\Rightarrow$  FF with  $-\pi \leq \theta \leq \pi$

- TIR  $\Rightarrow$  Obliquity Factor

# General DOW FF

For TE waves, ( $\frac{t_0}{2/10}$ )

$$(0) E_y(x) = A \Psi(x) \exp(i[\omega t - \beta z])$$



For 3-layer

WG, see

Eqs (2), (3), (4) [2/3 ③]

and (5), (6), (7) [2/3 ④] and

Eg (16) [2/3 ⑧]

Can we write  $\psi(x)$   
in terms of plane waves?  
Yes [Recall Eq(15), 1/22 p5]

Let

$$(2) \psi(x) = \frac{1}{\sqrt{2\pi}} \int_{-\infty}^{\infty} \bar{\Psi}(p) e^{-ipx} dp$$

by FT theory:

$$(3) \bar{\Psi}(p) = \frac{1}{\sqrt{2\pi}} \int_{-\infty}^{\infty} \psi(x) e^{ipx} dx$$

What is  $\bar{\Psi}(p)$ ?

- an infinite distribution  
of plane waves

- each plane wave has a (generally) different amplitude and propagation direction.

Recall:-

$\psi(x)$  is the modal distribution and propagates in the  $+z$  direction only.

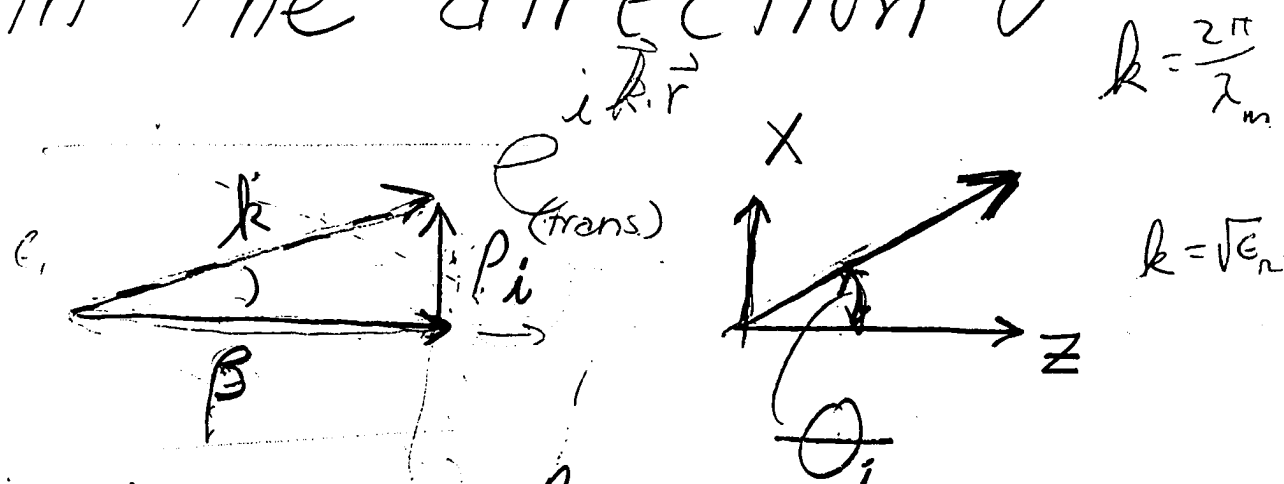
The plane wave form of  $E_y(x)$  can be

written as  $(\text{see}(0), p(5)\%$ )

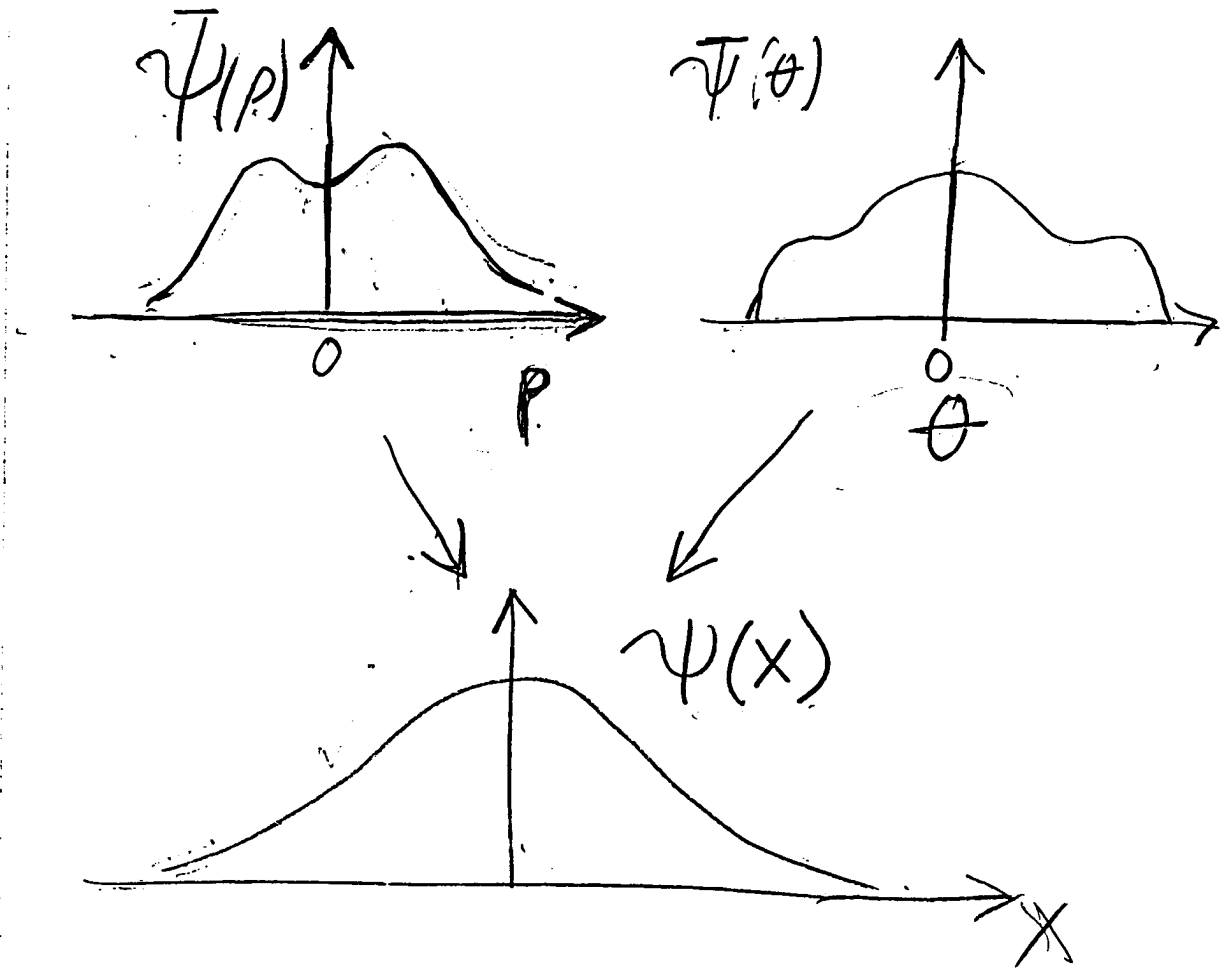
$$\bar{E}_y(\vec{p}) = \dots \quad (4)$$

$$A \int_{-\infty}^{\infty} \psi(p) e^{i(wt - px - \beta z)} dp$$

For a given value of  $p$ ,  
 $p = p_i$ , the plane  
wave propagates  
in the direction  $\theta$



$$\tan \theta_i = \frac{p_i}{\beta} \quad (5)$$



A plane wave component  
of (4) is

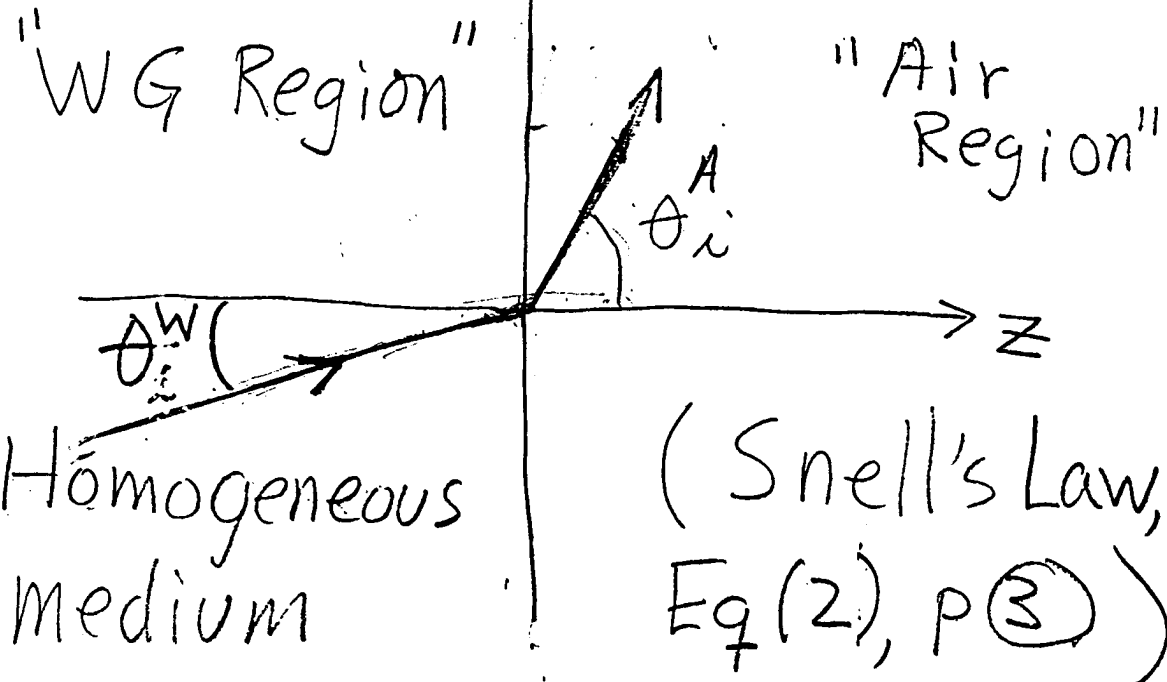
$$E_y(\vec{r}) = A \bar{\psi}(ρ) e^{i(wt - px - βz)} \quad (6)$$

This is a plane wave,  
propagating in a  
homogeneous medium

with a propagation constant

$$k_i = \sqrt{P_i^2 + \beta^2} \quad (7)$$

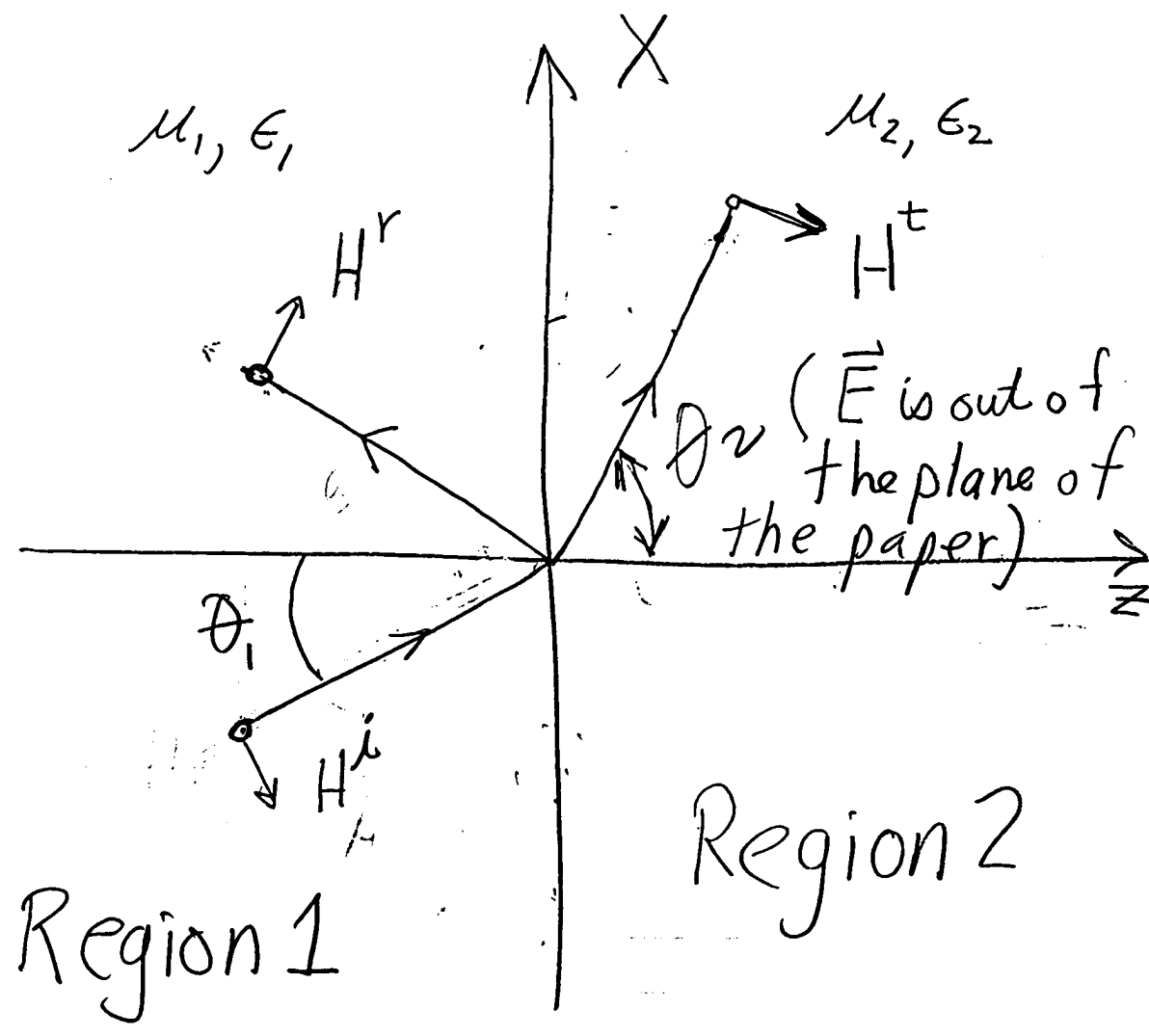
in the direction  $\theta_i^W$  [Eq(5)]  
in the "waveguide  
region".



but in the direction  $\theta_i^A$   
in air.

## Reflection and Transmission at Plane Boundaries

From the next homework assignment we will find that



the field reflection coefficient  $\rho$  and the field transmission coefficient  $\tau$  are:

$$\rho_{12} = \frac{Z_2 - Z_1}{Z_2 + Z_1} \quad \begin{matrix} \text{reflection and} \\ \text{transmission as} \\ \text{function of} \\ \text{incidence} \\ \text{angle} \end{matrix} \quad (1)$$

$$\tau_{12} = \frac{2 Z_2}{Z_2 + Z_1} \quad (2)$$

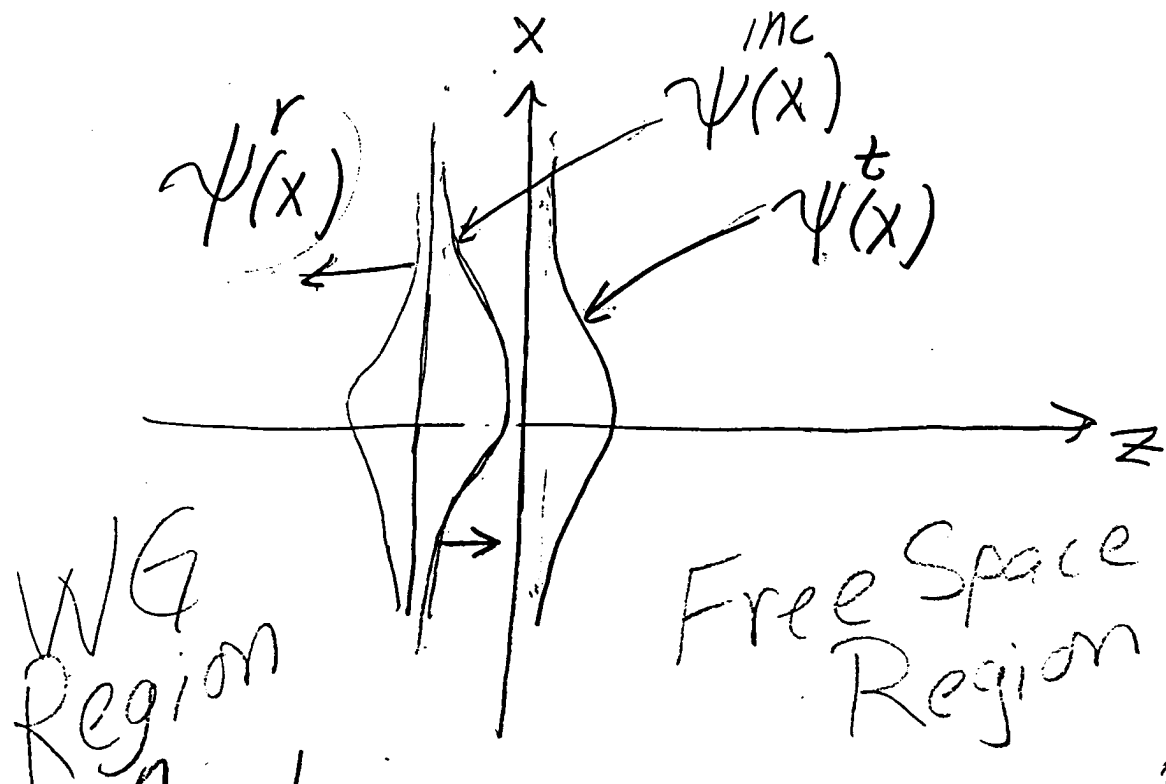
(TE modes)

where  $(\gamma_0 = \sqrt{\frac{\mu_0}{\epsilon_0}})$

$$Z_1 = -\frac{\gamma_0 k_0}{\beta} \quad (3)$$

$$Z_2 = -\frac{\gamma_0 k_0}{(\beta^2 - \rho^2)^{1/2}} \quad (4)$$

Now, back to the FF:



A plane wave component of the transmitted field is

$$\underline{\Psi^t(p)} = \tau_{12} \Psi^{inc}(p) \quad (5)$$

$$= \tau_i A \Psi(p) e^{i(wt - p_i x - q_i z)}$$

[by Eq (6) p⑦, 2/8]

Why  $q_i$  in (5)?

$$e^{i(wt - p_i x - q_i z)}$$

In region I we have

$$e^{i(wt - p_i x - \beta z)} \quad \begin{matrix} \text{no constraint or} \\ q \text{ outside of WG} \end{matrix}$$

but there is a waveguide  
in region I

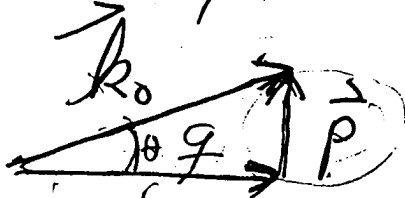
In region II, no WG;

just plane waves  $\frac{2\pi}{\lambda_0}$

and  $p^2 + q^2 = k_0^2$  (6)

$$\cos \theta = \frac{r}{k_0}$$

$$\sin \theta = \frac{P}{k_0}$$



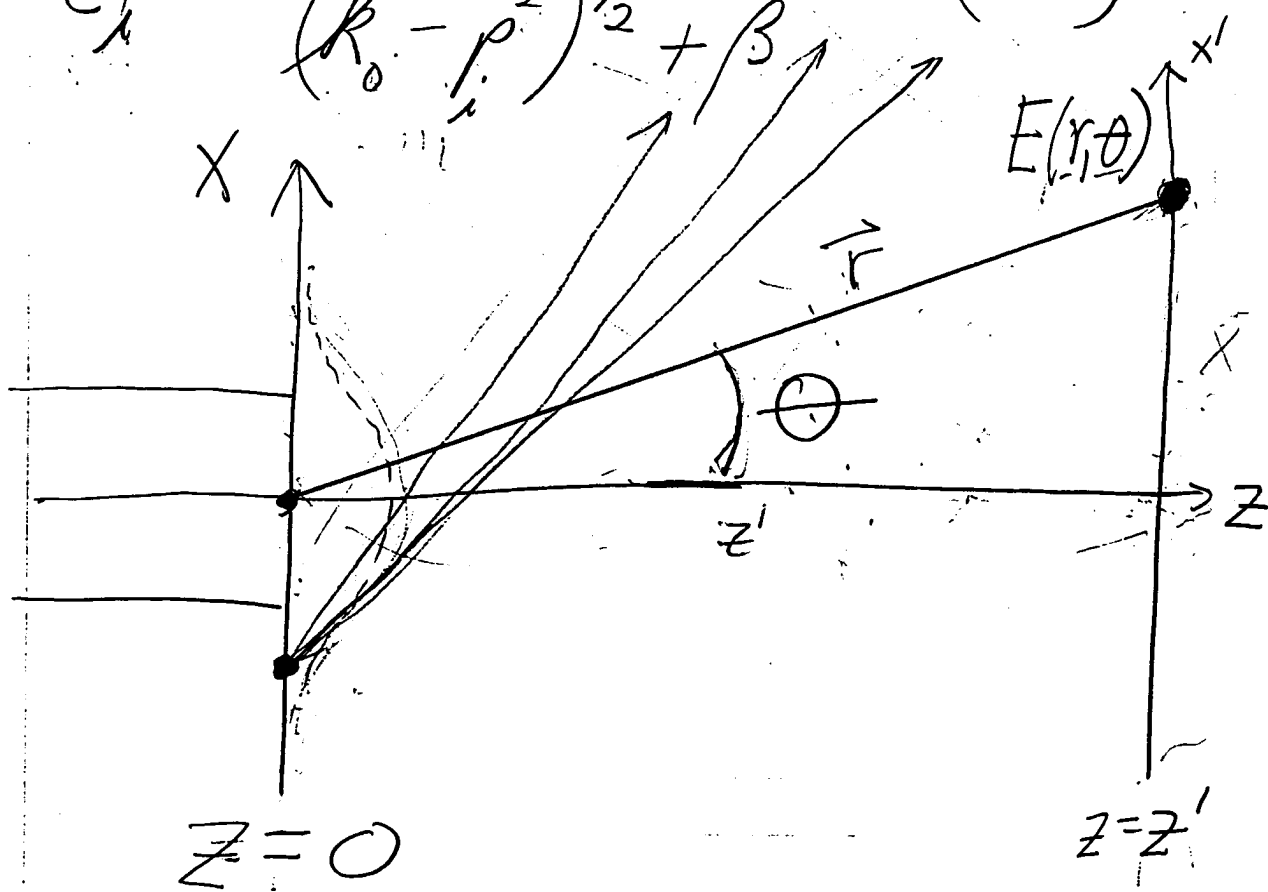
$$\cos \theta = \frac{q}{k_0} \quad \sin \theta = \frac{p}{k_0}$$

$Eg (2), (3), + (4) \Rightarrow$

amount of  
field  
transmitted.

$$\overline{T}_i = \frac{-2\pi_0 k_0}{(R_0^2 - P_i^2)^{1/2}} - \pi_0 k_0 \left[ \frac{1}{(R_0^2 - P_i^2)^{1/2}} + \frac{1}{\beta} \right]$$

$$\overline{T}_i = \frac{2\beta}{(R_0^2 - P_i^2)^{1/2} + \beta} \quad (7)$$



The total field intensity at  $(r, \theta)$  due to all of  $E_y(x, z=0^+)$  is ~~Stephan~~<sub>1/2</sub>

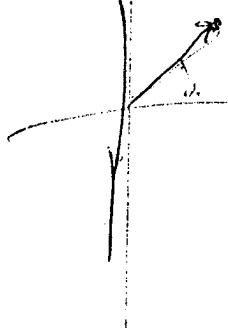
$$E_{(r,\theta)}^{ff} = \int_{-\infty}^{+\infty} \bar{\zeta} A \bar{\Psi}(p) e^{i(wt - px' - qz')} dp \quad (8)$$

where  $x' = r \frac{\sin \theta}{\cos \theta}$  (9a)  
 $z' = r \frac{\sin \theta}{\cos \theta}$  (9b)

So (8) becomes

over for explanation!

$$E_{(r,\theta)}^{ff} = 2\beta A \int_{-\infty}^{\infty} \frac{1}{q + \beta} \bar{\Psi}(p) \exp(i(p x' + q z')) dp \quad (10)$$



$$\exp(-i(px' + qz'))]$$

have suppressed  $e^{i\omega t}$ ,  
and used  $(k_0^2 - p^2)/2 = q^2$ .

Now, trick #1:

$$\text{let } p = k_0 \sin(\omega) \quad (11)$$

$$\text{since } p^2 + q^2 = k_0^2$$

$$q = k_0 \cos(\omega) \quad (12)$$

also, use  $z' = r \cos(\theta)$

$$x' = r \sin \theta$$

$$\therefore dp = (k_0 \cos(\omega)) d\omega$$

and rewrite (10):

$$E(k, \theta) = 2 \beta A k_0 \times$$

$$\int_{-\infty}^{\infty} \frac{\cos(w) \bar{V}(k_0 \sin(w)) \exp[]}{k_0 \cos(w) + \beta} dw \quad (13)$$

where  $[ ] = [ik_0 r \cos(\theta - w)]$

is from

$$px' + qz' = k_0 \sin w r \sin \theta$$

$$+ k_0 \cos w r \cos \theta$$

$$= k_0 r (\sin w \sin \theta - \cos w \cos \theta)$$

$$= k_0 r \cos(\theta - w)$$

Eq (13) can be approximated by the Saddle point method for large  $k_0 r$  - (which is the definition of the "far-field")

The "saddle point" technique:

$$I = \int_{-\infty}^{\infty} g(x) e^{k h(x)} dx$$

$$\approx g(a) e^{k h(a)} \sqrt{\frac{-2\pi}{k h''(a)}}$$

$x=a$  where  $a$  is from  $h'(x)=0$

$$h'(a) = 0, \text{ or}$$

$$-\sin(\theta - w) = 0 \Rightarrow$$

$$w = \theta$$

so, (13)  $\Rightarrow E^{ff}(r, \theta)$

$$= \frac{-i k_0 \beta A 2\sqrt{2\pi} \cos\theta \psi(k_0 \sin\theta)}{\sqrt{k \cdot r} (k_0 \cos\theta + \beta)} \quad (14)$$

$\times e^{ik_0 r}$  Intensity

$$(14) \Rightarrow I^{ff}(\theta) = |E^{ff}(r, \theta)|^2$$

$$I^{ff}(\theta) = I_0 \frac{\cos^2 \theta |\psi(k_0 \sin\theta)|^2}{|k_0 \cos\theta + \beta|^2} \quad (15)$$

(see pages 9-11), 2/10

110

Correction + additional detail:

Eg 113) + the saddle point technique:

$$g(x) = \frac{\cos w}{k_0 \cos w + \beta} \tilde{\Psi}(k_0 \sin w)$$

$$h(x) = \cos(\theta - w)$$

$$h'(x) = -\sin(\theta - w) \left( \frac{d\psi}{dw} \right) = \sin(\theta - w)$$

$$h''(x) = -\cos(\theta - w)$$

$$h'(a) = 0 \Rightarrow w = \theta$$

$$h''(a) = -\cos(0) = -1,$$

$$\sqrt{\frac{-2\pi}{k_0 h''(a)}} = \sqrt{\frac{-2\pi}{ik_0 r(-1)}} = \frac{\sqrt{2\pi}}{\sqrt{k_0 r}}$$

(111)

# Saddle Point Technique

## THE FOURIER INTEGRAL AND ITS APPLICATIONS

*ATHANASIOS PAPOULIS*

Professor of Electrical Engineering  
Polytechnic Institute of Brooklyn

McGRAW-HILL BOOK COMPANY, INC. 1962

New York      San Francisco      London      Toronto

$r \rightarrow \infty$ . But for  $r_0$  small enough, we have

$$\int_{\Gamma_0} \frac{e^z}{z} dz \simeq \int_{\Gamma_0} \frac{dz}{z} = -j\pi$$

and since  $e^z/z$  is analytic in  $C$ , we conclude that

$$\int_{-r}^{-r_0} \frac{e^{jy}}{jy} j dy + \int_{r_0}^r \frac{e^{jy}}{jy} j dy - j\pi \rightarrow 0 \quad \text{for } r_0 \rightarrow 0, r \rightarrow \infty$$

Hence

$$\int_0^\infty \frac{e^{jy} - e^{-jy}}{y} dy - j\pi = 0$$

and finally

$$\int_0^\infty \frac{\sin y}{y} dy = \frac{\pi}{2} \quad (\text{II-57})$$

#### II-4. Saddle-point Method of Integration†

In this section we shall evaluate integrals of the form

$$\int_C g(z)e^{kh(z)} dz \quad (\text{II-58})$$

for large values of the parameter  $k$ . This will be done by modifying the path of integration in such a way that only a small portion of the new path will contribute significantly to the value of the integral. As a preparation, we shall first assume that  $C$  is the real axis.

Method of Laplace.‡ Consider the real integral

$$I = \int_{-\infty}^{\infty} g(x)e^{kh(x)} dx \quad (\text{II-59})$$

We assume that the second derivative  $h''(x)$  of  $h(x)$  exists, that  $h(x)$  has only a single maximum  $x = a$  on the entire real axis

$$h'(a) = 0 \quad h''(a) < 0 \quad (\text{II-60})$$

and that  $g(x)$  is continuous, at least near  $x = a$ . We shall show that, under these assumptions,  $I$  is given by

$$\int_{-\infty}^{\infty} g(x)e^{kh(x)} dx \sim g(a)e^{kh(a)} \sqrt{\frac{-2\pi}{kh''(a)}} \quad (\text{II-61})$$

for large values of  $k$ .

† This is only a short introduction of the method; for a detailed discussion see:  
L. B. Felsen and N. Marcuvitz, "Modal Analysis and Synthesis of Electromagnetic Fields," AFCRC-TN-59-991, Microwave Research Institute, Polytechnic Institute of Brooklyn; A. Erdelyi, "Asymptotic Expansions," Dover Publications, New York, 1956; N. G. De Bruijn, "Asymptotic Methods in Analysis," North-Holland Publishing Company, Amsterdam, 1958.

‡ D. V. Widder, "The Laplace Transform," Princeton University Press, Princeton, N.J., 1941.

*Proof.* The given integral can be written in the form

$$I = e^{kh(a)} \int_{-\infty}^{\infty} g(x) e^{k[h(x)-h(a)]} dx \quad (\text{II-62})$$

From (II-60) we have,

$$h(x) - h(a) < 0 \quad \text{for } x \neq a$$

(Fig. II-19a); hence, for sufficiently large  $k$ , the quantity

(II-57)

$$e^{k[h(x)-h(a)]}$$

is close to zero everywhere except near the point  $x = a$ . Therefore only the integration in an interval close to  $a$  determines the value of  $I$ . But in such an interval we have

$$g(x) \simeq g(a)$$

$$h(x) - h(a) \simeq \frac{h''(a)}{2} (x - a)^2$$

Hence

$$I \sim e^{kh(a)} g(a) \int_{-\infty}^{\infty} e^{k\frac{h''(a)}{2}(x-a)^2} dx$$

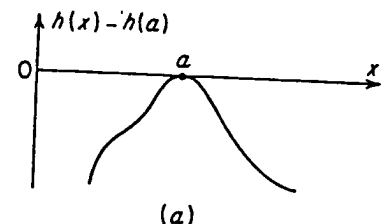
The last integral is given by [see (2-65)]

$$\int_{-\infty}^{\infty} e^{k\frac{h''(a)}{2}(x-a)^2} dx = \sqrt{\frac{-2}{kh''(a)}} \int_{-\infty}^{\infty} e^{-y^2} dy = \sqrt{\frac{-2\pi}{kh''(a)}}$$

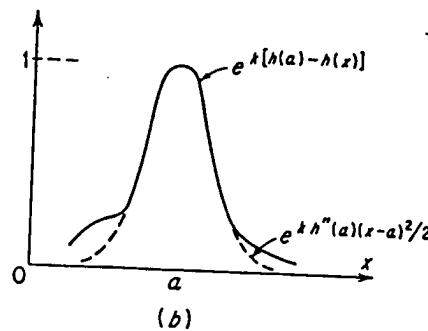
and (II-61) is proved.

From the above proof we easily conclude that, if  $g(x)$  is discontinuous at  $x = a$  but the limits  $g(a^+)$  and  $g(a^-)$  exist, then (II-61) is still valid provided  $g(a)$  is replaced by  $[g(a^+) + g(a^-)]/2$ . We also see that, since only the value of the integrand in the vicinity of  $x = a$  matters, (II-61) holds even if the integration is performed over a finite or semi-infinite interval as long as  $x = a$  is an interior point of this interval. If  $x = a$  coincides with one of the end points, then the right-hand side of (II-61) must be divided by 2.

*Comment.* The method of Laplace reminds us of the stationary-phase method discussed in Sec. 7-7. In (7-89) the integration away from the stationary point  $\omega_0$  was negligible because of the rapid oscillation of the integrand; in (II-61) this is so because the integrand tends to zero for  $x \neq a$ .



(a)



(b)

FIGURE II-19

**Example II-5.** We shall apply (II-61) to determine the value of  $n!$  for large  $n$ . We have from (9-5)

$$\int_0^\infty e^{-pt} t^n dt = \frac{n!}{p^{n+1}}$$

and with  $p = 1$ ,  $t = nx$ ,

$$n! = n^{n+1} \int_0^\infty e^{n(-x + \ln x)} dx \quad (\text{II-63})$$

The above integral is of the form (II-59) with  $k = n$ ,  $h(x) = -x + \ln x$ , and  $g(x) = 1$ . Since

$$h'(x) = -1 + \frac{1}{x}$$

we have  $a = 1$      $h(a) = -1$      $h''(a) = -1$

Therefore [see (II-61)]

$$n! \sim n^{n+1} e^{-n} \sqrt{\frac{2\pi}{n}} = \sqrt{2\pi n^{n+\frac{1}{2}}} e^{-n} \quad (\text{II-64})$$

This result is known as *Stirling's formula*.

**Example II-6.** Using (II-61), we shall show that

$$\lim_{k \rightarrow \infty} \left[ \int_c^d |f(x)|^k dx \right]^{1/k} = |f|_{\max}$$

where  $|f|_{\max} = |f(a)|$  is the maximum of  $|f(x)|$  in the interval  $(c, d)$ , with zero slope at  $x = a$ . The result holds even if  $a$  is an end point of the above interval, provided  $f'(a)$  is zero. We can assume  $f(x) \geq 0$ . From (II-61) we have

$$\int_c^d f^k(x) dx = \int_c^d e^{k \ln f(x)} dx \underset{k \rightarrow \infty}{\sim} e^{k \ln f(a)} \sqrt{\frac{-2\pi}{kh''(a)}} = f_{\max}^k \frac{A}{\sqrt{k}}$$

where the constant  $A = \sqrt{-2\pi/h''(a)}$  is independent of  $k$  and  $h(x) = \ln f(x)$ .

$$\text{Thus } \left[ \int_c^d f^k(x) dx \right]^{1/k} \underset{k \rightarrow \infty}{\sim} f_{\max} \left( \frac{A}{\sqrt{k}} \right)^{1/k}$$

It is easy to see that  $\lim (A/\sqrt{k})^{1/k} = 1$  for  $k \rightarrow \infty$ , and the desired result follows. If  $a$  equals  $c$  or  $d$ , then the constant  $A$  will be reduced by a factor of 2; however, the value of the limit will not be affected.

We now return to the integral (II-58) and we assume, without loss of generality, that  $k$  is real. Suppose that the derivative of  $h(z)$  has a simple zero at a point  $z = z_0$  of the plane

$$h'(z_0) = 0$$

[saddle point of  $h(z)$ ]. We attempt to find a path  $C_1$  with the property that the imaginary part of  $h(z)$  is constant everywhere on  $C_1$

This is  
value  
gratio  
one pa  
necess  
point  
exam  
details

If t  
and C  
knowi  
be eva

Con  
of La  
station  
path (

then 1

rapidl

simila

Exa

Bessel

[see (6

as in

(path of steepest descent), its real part is maximum at  $z_0$

$$\operatorname{Im} h(z) = \operatorname{Im} h(z_0) \quad \operatorname{Re} h(z) \leq \operatorname{Re} h(z_0) \quad z \text{ on } C_1 \quad (\text{II-65})$$

and such that

$$\int_C g(z)e^{kh(z)} dz = \int_{C_1} g(z)e^{kh(z)} dz \quad (\text{II-66})$$

Because of (II-65), the last integral above is essentially of the form (II-59); therefore the estimate (II-61) can be used. We thus have for large  $k$

$$\int_{C_1} g(z)e^{kh(z)} dz \sim e^{kh(z_0)} g(z_0) \sqrt{\frac{2\pi}{-kh''(z_0)}} \quad (\text{II-67})$$

This is the saddle-point method of integration. The choice of the value of the square root in (II-67) depends on the direction of integration along  $C_1$ . Often it is necessary to integrate along more than one path of steepest descent, in order to satisfy (II-66). It is then necessary to add the contributions to the integral from each saddle point on  $C_1$ , in the estimate (II-67). This will be shown in the next example, where we shall also explicitly specify  $C_1$  and will clarify the details of the method and the choice of the radical sign.

If the function  $g(z)e^{kh(z)}$  is not analytic in the region between  $C$  and  $C_1$ , then (II-66) is not true; however, if its singularities are known poles, then the difference of the two integrals in (II-66) can be evaluated.

*Comment.* The saddle-point method of integration is an extension of Laplace's real integral (II-61) to a contour integration. The stationary-phase method of Sec. 7-7 can be similarly extended. If a path  $C'_1$  is found such that for  $z$  on  $C'_1$  the real part of  $h(z)$  is constant, then the amplitude of  $e^{kh(z)}$  remains constant but its phase varies rapidly as we move away from  $z_0$ . We thus obtain an integral similar to (7-89) and the estimate (7-90) can be used.

**Example II-7.** We shall use the saddle-point method to evaluate the Bessel function

$$J_n(t) = \frac{1}{2\pi} \int_0^{2\pi} e^{j(t \sin \phi - n\phi)} d\phi \quad (\text{II-68})$$

[see (6-91)] for large values of  $t$ . With

$$z = e^{j\phi}$$

as in (II-45), the above becomes a contour integral

$$J_n(t) = \frac{1}{2\pi j} \int_C \frac{e^{(z-z^{-1})t/2}}{z^{n+1}} dz \quad (\text{II-69})$$

along the unit circle  $|z| = 1$  (Fig. II-20a). It is of the form (II-58) with

$$h(z) = \frac{1}{2}(z - z^{-1}) \quad g(z) = \frac{1}{z^{n+1}}$$

The saddle points of  $h(z)$  are given by

$$h'(z) = \frac{1}{2} \left( 1 + \frac{1}{z^2} \right) = 0 \quad z = \pm j$$

The path  $C_1$  of steepest descent passing through  $j$  is shown in Fig. II-20b. As we shall presently explain, it starts from the origin tangent to the real axis, crosses the imaginary line at a  $3\pi/4$  angle, and extends to infinity, with the line  $z = j2$  as its asymptote. The path  $C_2$  through  $-j$  is the conjugate of

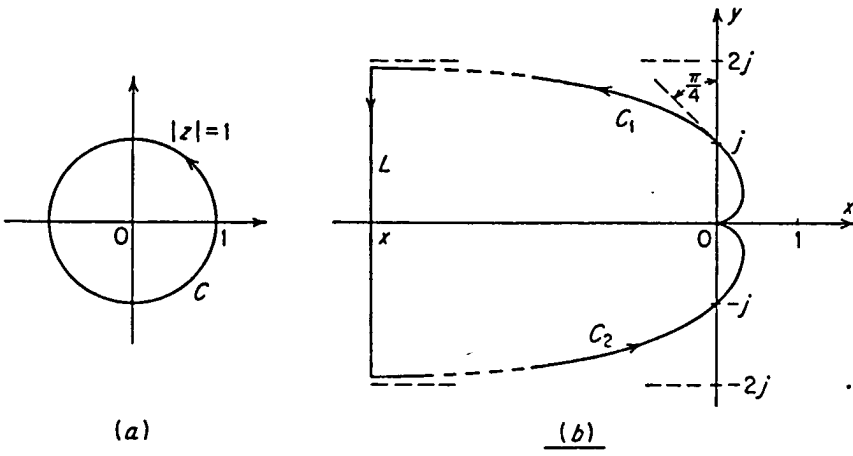


FIGURE II-20

$C_1$ . We now form a closed contour as in Fig. II-20b, consisting of  $C_1$ ,  $C_2$ , and the vertical segment  $L$ . This contour encloses in its interior the only singularity  $z = 0$  of the integrand in (II-69); and since the same is true for the unit circle, we conclude from Cauchy's theorem that

$$\int_C \frac{e^{(z-z^{-1})t/2}}{z^{n+1}} dz = \int_{C_1+C_2+L} \frac{e^{(z-z^{-1})t/2}}{z^{n+1}} dz \quad (\text{II-70})$$

The length of  $L$  is less than 4 and the integrand for  $z$  on  $L$  tends to zero with  $x \rightarrow -\infty$ ; therefore the integration along  $L$  tends also to zero. From (II-67) we have for large  $t$

$$\int_{C_1} \frac{e^{(z-z^{-1})t/2}}{z^{n+1}} dz \sim e^{jt} \frac{1}{j^{n+1}} \sqrt{\frac{2\pi}{-tj}} \quad (\text{II-71})$$

since

$$h(j) = j \quad h''(j) = -j \quad g(j) = \frac{1}{j^{n+1}}$$

Similarly

$$\int_{C_2} \frac{e^{(z-z^{-1})t/2}}{z^{n+1}} dz \sim e^{-jt} \frac{1}{(-j)^{n+1}} \sqrt{\frac{2\pi}{tj}} \quad (\text{II-72})$$

SEC. II

From ()

$J_n(t) \sim$

The ch  
clear, b

we have

Hence if

subject

Thus th  
of the r.

Since  $h''$

where  $r$

Hence

and for

Thus th  
we simil

II-5. F

We s  
that ar  
of linea

† W. C  
German)

From (II-69) and the above equations we finally obtain for large  $t$

$$J_n(t) \sim \frac{1}{2\pi j} \left[ \frac{e^{jt}}{j^{n+1}} e^{j3\pi/4} + \frac{e^{-jt}}{(-j)^{n+1}} e^{-j\pi/4} \right] \sqrt{\frac{2\pi}{t}} = \sqrt{\frac{2}{\pi t}} \cos \left( t - \frac{2n+1}{4}\pi \right) \quad (\text{II-73})$$

The choice in the selection of the value of the radical will presently become clear, but first the equation of the curves  $C_1$  and  $C_2$ : with

$$h(z) = u + jv$$

we have  $h(x + jy) = \frac{1}{2} \left( x - \frac{x}{x^2 + y^2} \right) + \frac{j}{2} \left( y + \frac{y}{x^2 + y^2} \right)$

Hence for (II-65) to be true, we must have

$$y + \frac{y}{x^2 + y^2} = \pm 2 \quad (\text{II-74})$$

subject to the condition

$$x - \frac{x}{x^2 + y^2} = u \leq 0 \quad (\text{II-75})$$

Thus the two curves  $C_1$  and  $C_2$  of Fig. II-20b result. We now come to the sign of the radical. Near the stationary point  $z = j$ , we have

$$h(z) \simeq h(j) + \frac{h''(j)}{2} (z - j)^2$$

Since  $h''(j) = -j$ , and  $h(z) - h(j) < 0$  [see (II-65)], we obtain with

$$z - j = re^{j\delta} \quad \delta \text{ constant}$$

where  $r$  is positive in the direction of integration,

$$r^2 e^{j2\delta} j < 0$$

Hence

$$\delta = 3\pi/4$$

and for large  $t$

$$\int_{C_1} e^{h''(j)(z-z_0)^2 t/2} dz \simeq e^{j3\pi/4} \int_{-\infty}^{\infty} e^{-r^2 t/2} dr = \sqrt{\frac{2\pi}{-tj}}$$

Thus the first term in (II-73) is justified. For the integration near  $z = -j$  we similarly obtain  $\delta = -\pi/4$ .

## II-5. Positive Real Functions†

We shall now discuss the properties of a class of analytic functions that are used in network theory to characterize the input impedance of linear passive systems. They are unilateral Laplace transforms of

† W. Cauer, "Synthesis of Linear Communication Networks" (translated from German), 2d ed., McGraw-Hill Book Company, Inc., New York, 1958.

redefining  $I_0'$  divided  
out  $k_0$

$$I(\theta) = I_0'' \frac{\cos^2 \theta / \psi(k_0 \sin \theta)}{\left( \cos \theta + \beta/k_0 \right)^2} \quad (16)$$

since  $\beta/k_0 = n_{\text{eff}} \approx n_2$

$$\cos \theta + \frac{\beta}{k_0} \underset{\sim 1}{\approx} \underset{\sim 3}{\approx} \underset{\sim 3}{\approx} \frac{\beta}{k_0}$$

gross approximation

and

$$I(\theta) \approx I_0 \left( \cos^2 \theta / \psi(k_0 \sin \theta) \right)^2 \quad (17)$$

Intensity Obliquity  
Factor

(119)

"FT tactic  
most plane  
intensity & see how they  
are sorted up"

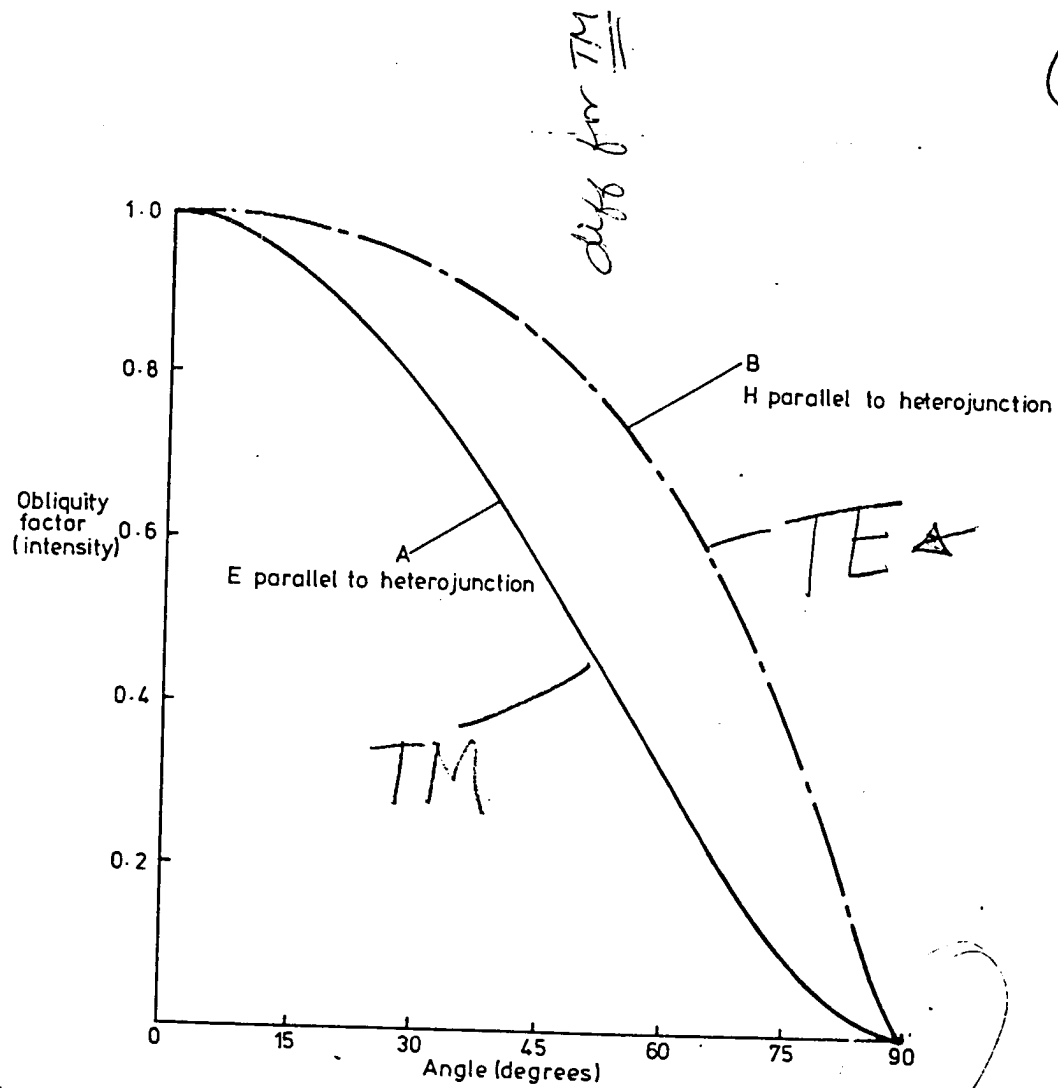
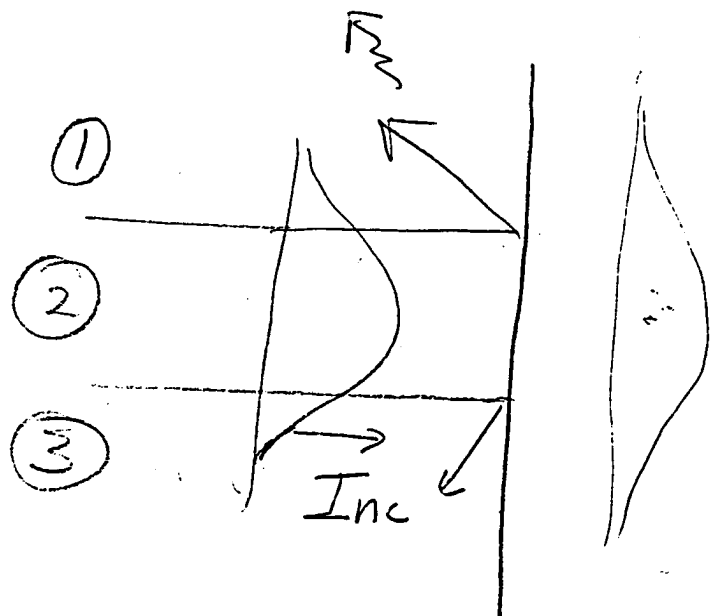


Figure 4.12 Obliquity factor as a function of emission angle for optical intensity of radiated wave from source with (a) electric vector parallel to heterojunctions and (b) magnetic vector parallel to heterojunctions

P. 186, Thompson

Physics of Semiconductor  
Lasers; J. Wiley  
1980

We ignored mode conversion upon reflection at the interface:



mode conversion < 1%

On the waveguide side, the mode is converted to other bound modes (if the waveguide is multimode) and to radiation modes.

In general, radiation modes are required to match the boundary conditions at the interface (Davies and Walpole, IEEE JQE, Vol.12, p.291, 1976)

The wave equation is a Sturm-Liouville equation  $\Rightarrow$

- eigenvalues form a complete orthonormal basis set
- for dielectric waveguides, the basis set is the bound modes and the radiation modes

Theoretically, expect far-fields of DOWs to be symmetric:

$$I(\theta) = F(\theta) / |\bar{\Psi}(k_0 \sin \theta)|^2$$

- Obliquity Factor  $\approx \cos(\theta)$ 
  - $\cos(\theta)$  is symmetric
- $\bar{\Psi}$  is the Fourier Transform of the near field distribution
  - nf of a DOW is a real function (....)
  - FT of any real function is symmetric

Experimentally - FFs  
are usually symmetric  
(not always)

- maybe 10% are not

\* Could the obliquity  
factor be asymmetric?  
(don't know !!)

\* Could the near field  
be complex  
(possible--especially  
"CSP" lasers)

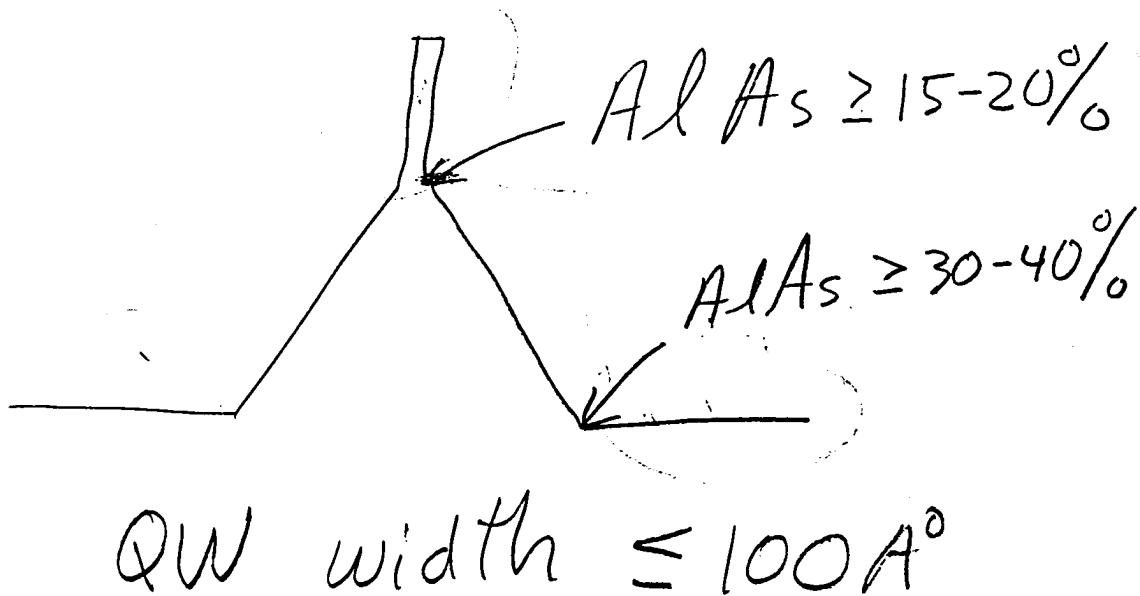
\* Radiation modes in layer  
① and in layer ③ may not  
be symmetric  
(don't know!)

(124)

# MODEIG DEMO

Additional Mini Project

#1 Constraints



(125)

```

CASE      KASE=LINCOLN LABS (LDI806)
CASE      EPS1=1E-7      GAMEPS=1E-3          QZMR=10.89      QZMI=0.0
CASE      PRINTF=0      INITGS=0      AUTOQW=0          NFPLT=1      FFPLT=1

MODCON   KPOL=1      APB1=0.25      APB2=0.25

STRUCT   NQW=3.6      WVL=.806
STRUCT   GRW=.15      QW=.0100
STRUCT   ALPERC1=.7    ALPERC2=0.7

LAYER    ALPERC=.00      !GaAs substr
LAYER    ALPERC=.25      TL=0.05      !1st trans.
LAYER    ALPERC=.50      TL=0.05      !"
LAYER    ALPERC=^1      TL=1.1      ! n-Clad
LAYER    ALPERC=^1      ! 1st (n) GRINSCH
LAYER    NSLC=10      !"
LAYER    ALPERC=.25      !"
!LAYER   ALPERC=.00      TL=.0075      ! 1st (n) Barrier
LAYER    QWS=1      !QW GaIn(.14)As-LAYER
!LAYER   ALPERC=.00      TL=.0075      !2nd (p) Barrier
LAYER    ALPERC=.25      !2nd (p) GRINSCH
LAYER    NSLC=10      !"
LAYER    ALPERC=^2      !"
!LAYER   ALPERC=^2      TL=.1      !1st p-Clad-Layer28
!LAYER   ALPERC=.5      TL=.005      !1st etch stop trans.
!LAYER   ALPERC=.25      TL=.005      !"
!LAYER   ALPERC=0.1      TL=0.00      !Etch stop AlGaAs-sub-Grating -layer
!LAYER   NREAL=3.38066    TL=0.15      !Etch stop AlGaAs-Grating -layer
!LAYER   ALPERC=.2      TL=.005      !2nd etch stop trans.
!LAYER   ALPERC=.3      TL=.005      !"
LAYER    ALPERC=^2      TL=1.1      !2nd p-Clad
!LAYER   NREAL=1.9      TL=.12      !SiN3 insulator!
!LAYER   ALPERC=.08      TL=0.05      !"
LAYER    ALPERC=.00      TL=0.12      !GaAs Cap
!LAYER   NREAL=1      !Air

OUTPUT   PHMO=1      GAMMAO=1      WZRO=1      WZIO=1      QZRO=1      QZIO=0
OUTPUT   FWHPNO=1      FWHPFO=1      KMO=1      ITO=1
OUTPUT   SPLTF1=1      MODOUT=0      LYROUT=1
GAMOUT  LAYGAM=16      COMPGAM=0      GAMALL=0

!LOOPX1 ILX='TL'      FINV=0.0      XINC=-0.05      LAYCH=30
LOOPZ1  ILZ='GRW'      FINV=.4      ZINC=.01
!LOOPZ2  ILZ='WVL'      FINV=0.955     ZINC=-0.005

!LOOPZ1 ILZ='QZMR'      FINV=10.9      ZINC=-.05!THIS LOOPS TO FIND INITIAL GUESS
!LOOPZ1 ILZ='GRW'      FINV=.202      ZINC=.001
!LOOPZ1 ILZ='ALPERC1'    FINV=.401      ZINC=.0005
!LOOPX1 ILX='TL'      FINV=.15      XINC=.01      LAYCH=33
!LOOPX1 ILX='TL'      FINV=.0      XINC=-.01      LAYCH=34
END

```

126

CASE KASE=MINIPROJECT (1)  
CASE EPS1=1E-7 GAMEPS=1E-3 QZMR=11.0206 QZMI=0.0  
CASE PRINTF=0 INITGS=0 AUTOQW=0 NFPLT=1 FFPLT=1

MODCON KPOL=1 APB1=0.25 APB2=0.25

STRUCT NQW=3.64 WVL=.808  
STRUCT GRW=.15 QW=.0070  
STRUCT ALPERC1=.6 ALPERC2=0.3

LAYER ALPERC=.00 !GaAs substr  
LAYER ALPERC=^1 TL=1.3 ! n-Clad  
LAYER ALPERC=^1 ! 1st (n) GRINSCH  
LAYER NSLC=10 !"  
LAYER ALPERC=^2 !"  
LAYER QWS=1 !OW GaAs-LAYER  
LAYER ALPERC=^2 !2nd (p) GRINSCH  
LAYER NSLC=10 !"  
LAYER ALPERC=^1 !"  
LAYER ALPERC=^1 TL=1.2 !2nd p-Clad  
LAYER ALPERC=.00 TL=0.5 !GaAs Cap  
!LAYER NREAL=1 !Air

OUTPUT PHMO=1 GAMMAO=1 WZRO=1 WZIO=1 QZRO=1 QZIO=0  
OUTPUT FWHPNO=1 FWHPFO=1 KMO=1 ITO=1  
OUTPUT SPLTFL=1 MODOUT=0 LYROUT=1  
GAMOUT LAYGAM=16 COMPGAM=0 GAMALL=0

!LOOPX1 ILX='TL' FINV=0.0 XINC=-0.05 LAYCH=30  
!LOOPZ1 ILZ='GRW' FINV=.4 ZINC=.01  
!LOOPZ2 ILZ='WVL' FINV=0.955 ZINC=-0.005

!LOOPZ1 ILZ='QZMR' FINV=10.9 ZINC=-.1 !THIS LOOPS TO FIND INITIAL GUESS  
!LOOPZ1 ILZ='GRW' FINV=.202 ZINC=.001  
!LOOPZ1 ILZ='ALPERC1' FINV=.401 ZINC=.0005  
!LOOPX1 ILX='TL' FINV=.15 XINC=.01 LAYCH=33  
!LOOPX1 ILX='TL' FINV=.0 XINC=-.01 LAYCH=34

END

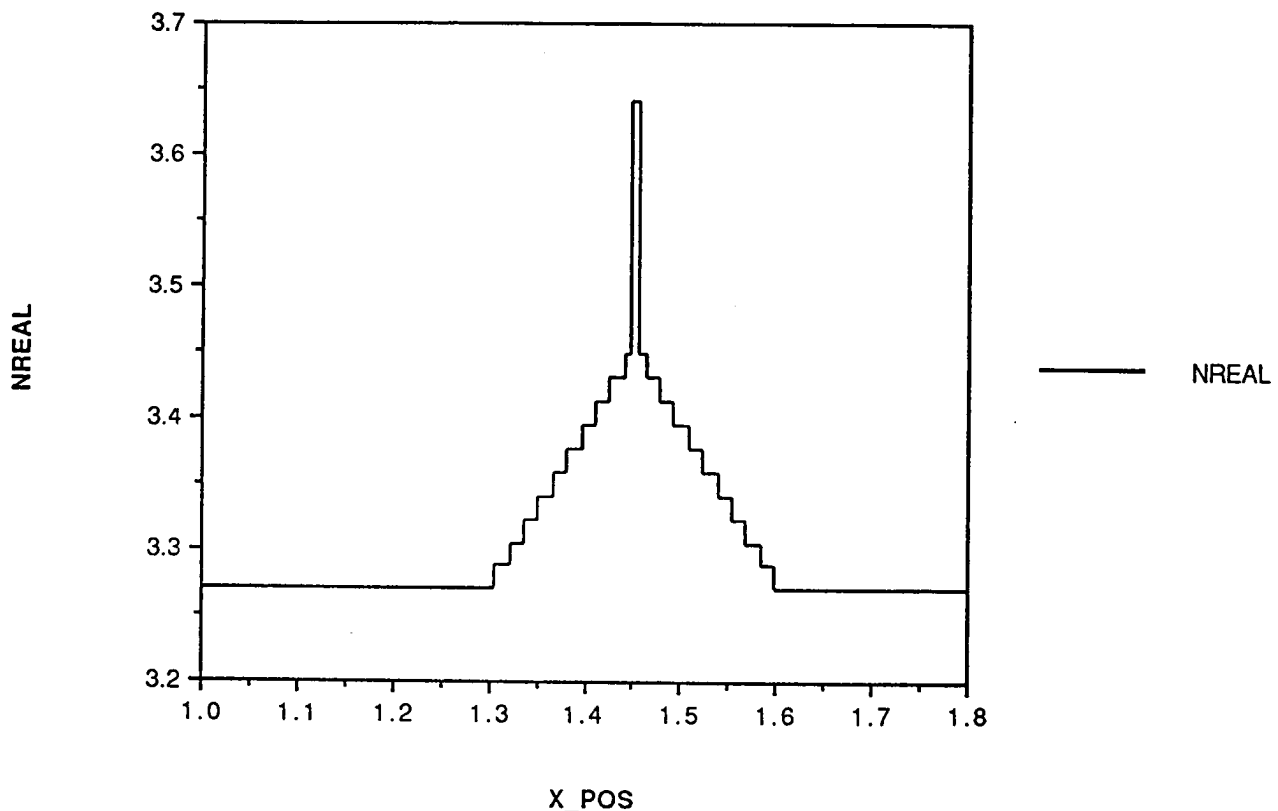
# of layers = 27

LAYER01	NLOSS= .00000	NREAL= 3.67329	TL= .00000
LAYER02	NLOSS= .00000	NREAL= 3.26943	TL= 1.30000
LAYER03	NLOSS= .00000	NREAL= 3.26943	TL= .00750
LAYER04	NLOSS= .00000	NREAL= 3.28719	TL= .01500
LAYER05	NLOSS= .00000	NREAL= 3.30496	TL= .01500
LAYER06	NLOSS= .00000	NREAL= 3.32272	TL= .01500
LAYER07	NLOSS= .00000	NREAL= 3.34048	TL= .01500
LAYER08	NLOSS= .00000	NREAL= 3.35824	TL= .01500
LAYER09	NLOSS= .00000	NREAL= 3.37601	TL= .01500
LAYER10	NLOSS= .00000	NREAL= 3.39377	TL= .01500
LAYER11	NLOSS= .00000	NREAL= 3.41153	TL= .01500
LAYER12	NLOSS= .00000	NREAL= 3.42929	TL= .01500
LAYER13	NLOSS= .00000	NREAL= 3.44705	TL= .00750
LAYER14	NLOSS= .00000	NREAL= 3.64000	TL= .00700
LAYER15	NLOSS= .00000	NREAL= 3.44705	TL= .00750
LAYER16	NLOSS= .00000	NREAL= 3.42929	TL= .01500
LAYER17	NLOSS= .00000	NREAL= 3.41153	TL= .01500
LAYER18	NLOSS= .00000	NREAL= 3.39377	TL= .01500
LAYER19	NLOSS= .00000	NREAL= 3.37601	TL= .01500
LAYER20	NLOSS= .00000	NREAL= 3.35824	TL= .01500
LAYER21	NLOSS= .00000	NREAL= 3.34048	TL= .01500
LAYER22	NLOSS= .00000	NREAL= 3.32272	TL= .01500
LAYER23	NLOSS= .00000	NREAL= 3.30496	TL= .01500
LAYER24	NLOSS= .00000	NREAL= 3.28719	TL= .01500
LAYER25	NLOSS= .00000	NREAL= 3.26943	TL= .00750
LAYER26	NLOSS= .00000	NREAL= 3.26943	TL= 1.20000
LAYER27	NLOSS= .00000	NREAL= 3.67329	TL= .00000

\*\*\*\*\*  
\*\*

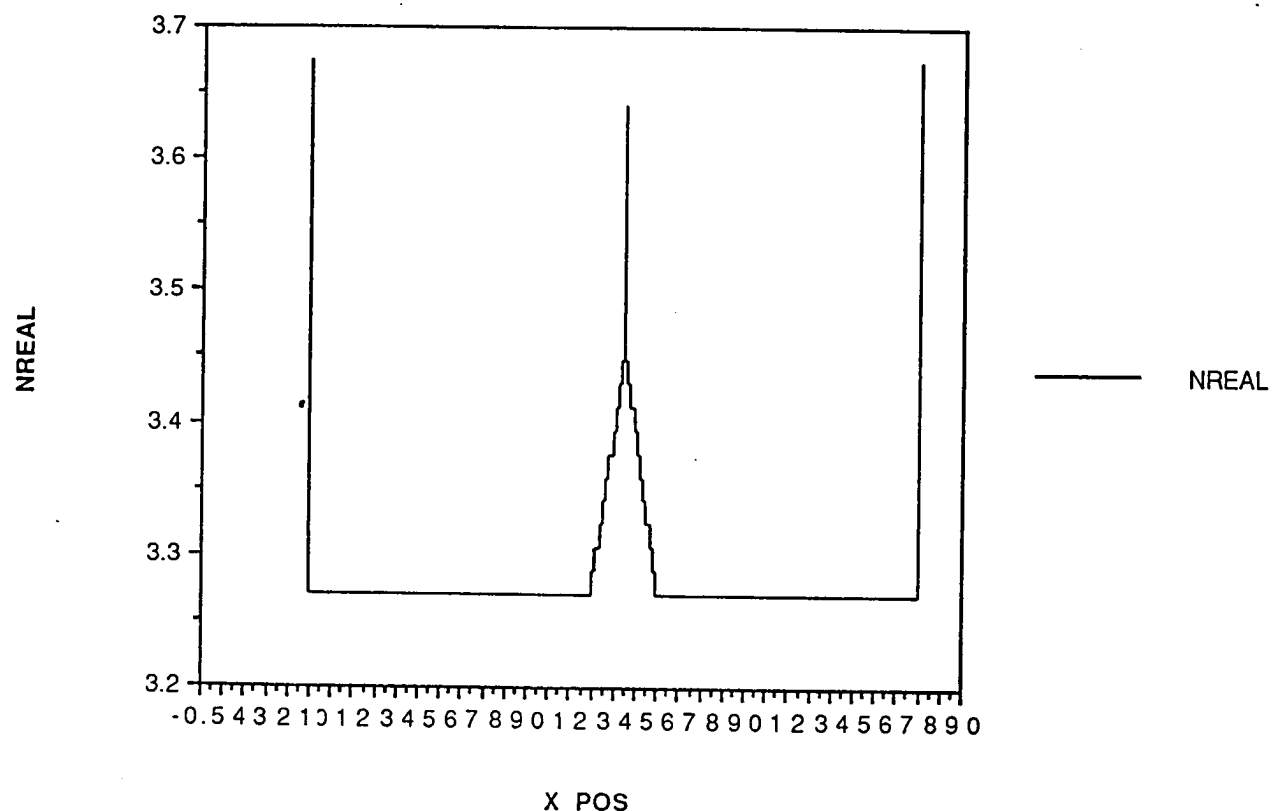
128

Data from "IndexPlot\_out"



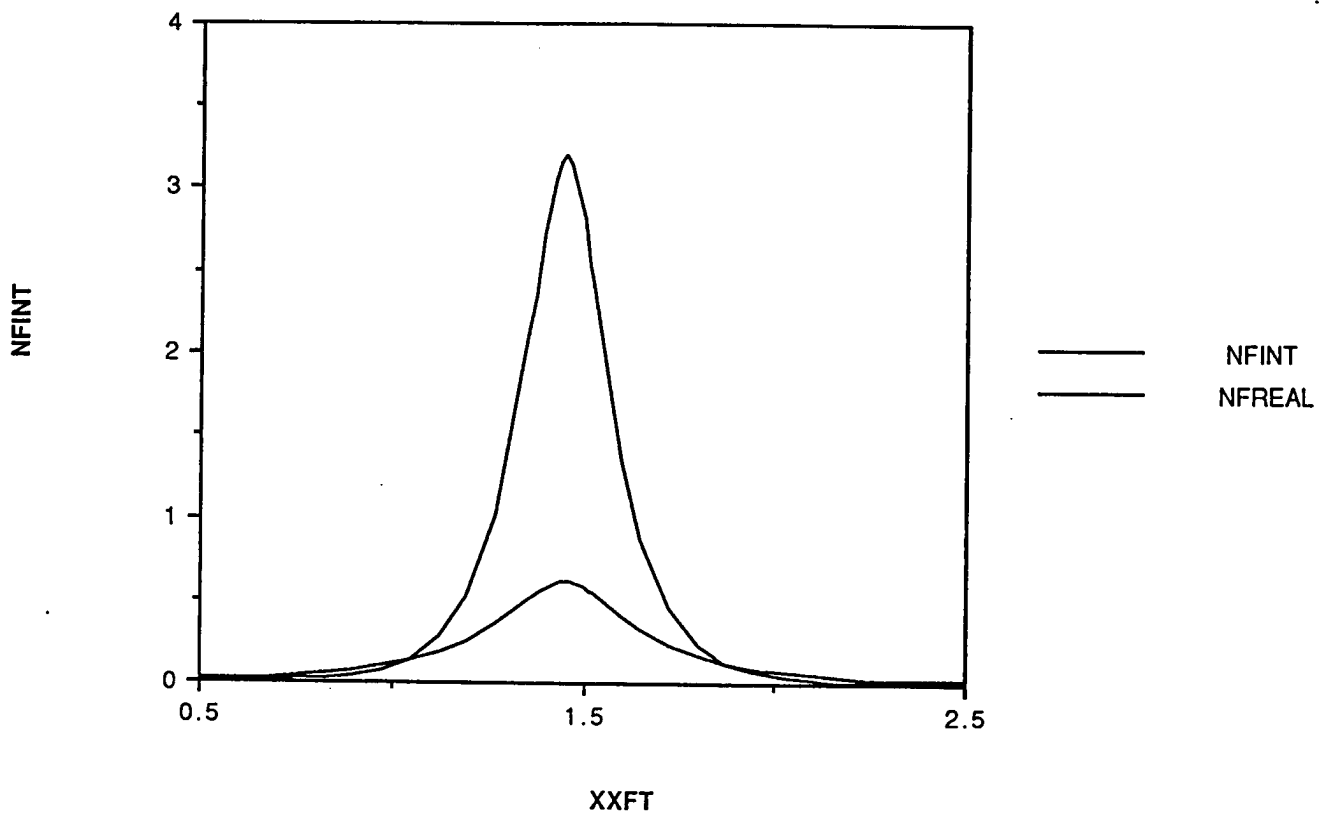
129

Data from "IndexPlot\_out"



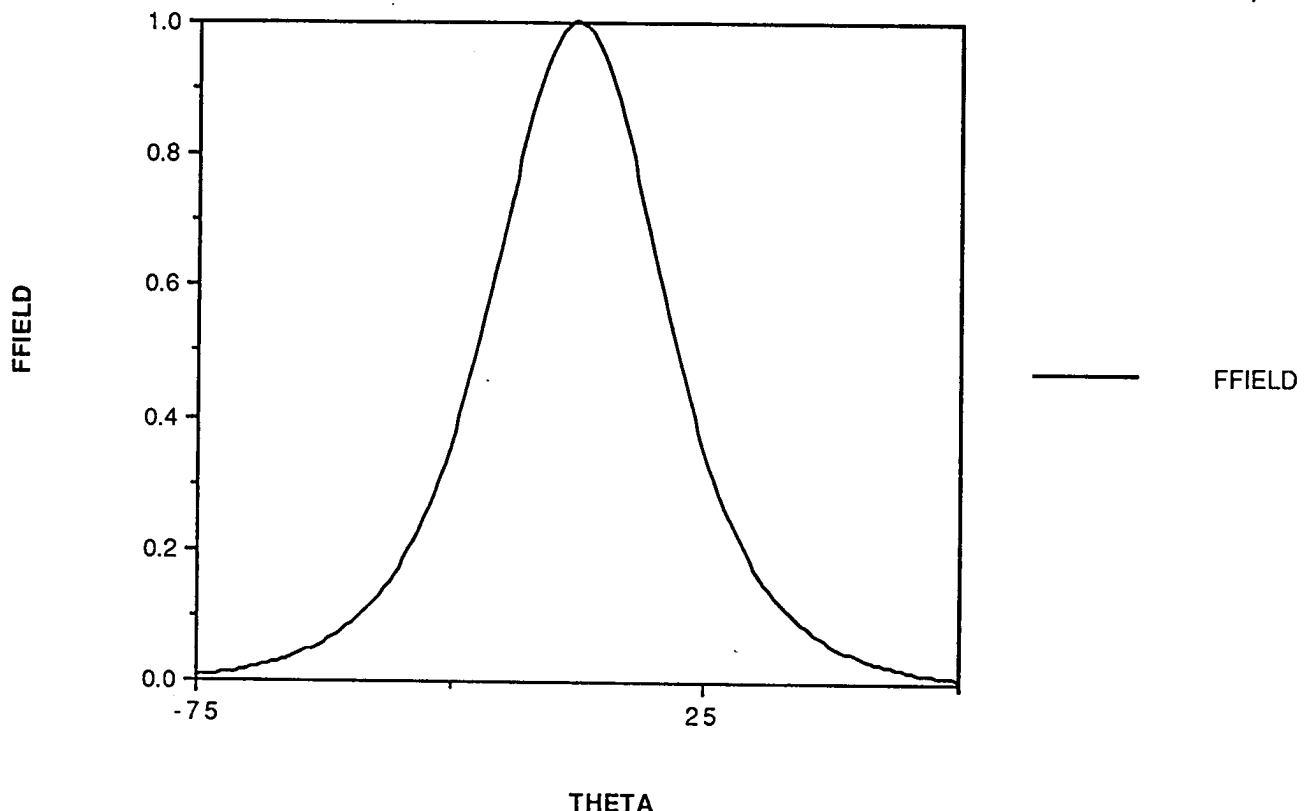
130

Data from "6392nf"



131

Data from "6392ff"



CASE KASE=MINIPROJECT (1)

CASE EPS1=1E-7 GAMEPS=1E-3 QZMR=11.0206 QZMI=0.0  
CASE PRINTF=0 INITGS=0 AUTOQW=0 NFPLT=1 FFPLT=1

MODCON KPOL=1 APB1=0.25 APB2=0.25

STRUCT NQW=3.64 WVL=.808  
STRUCT GRW=.15 QW=.0070  
STRUCT ALPERC1=.6 ALPERC2=0.3

LAYER ALPERC=.00 !GaAs substr  
LAYER ALPERC=<sup>1</sup> TL=1.3 !n-Clad  
LAYER ALPERC=<sup>1</sup> ! 1st (n)GRINSCH  
LAYER NSLC=10 !"  
LAYER ALPERC=<sup>2</sup> !"  
LAYER QWS=1 !QW GaAs-LAYER  
LAYER ALPERC=<sup>2</sup> !2nd (p) GRINSCH  
LAYER NSLC=10 !"  
LAYER ALPERC=<sup>1</sup> !"  
LAYER ALPERC=<sup>1</sup> TL=1.2 !2nd p-Clad  
LAYER ALPERC=.00 TL=0.5 !GaAs Cap  
!LAYER NREAL=1 !Air

OUTPUT PHMO=1 GAMMAO=1 WZRO=1 WZIO=1 QZRO=1 QZIO=0  
OUTPUT FWHPNO=1 FWHPFO=1 KMO=1 ITO=1  
OUTPUT SPLTF=1 MODOUT=0 LYROUT=1  
GAMOUT LAYGAM=14 COMPGAM=0 GAMALL=0

!LOOPX1 ILX='TL' FINV=0.0 XINC=-0.05 LAYCH=30  
!LOOPZ1 ILZ='GRW' FINV=.4 ZINC=.01  
!LOOPZ2 ILZ='WVL' FINV=0.955 ZINC=-0.005

!LOOPZ1 ILZ='QZMR' FINV=10.9 ZINC=-.1!THIS LOOPS TO FIND INITIAL GUESS  
!LOOPZ1 ILZ='GRW' FINV=.202 ZINC=.001  
LOOPZ1 ILZ='ALPERC1' FINV=.4 ZINC=-.005  
!LOOPX1 ILX='TL' FINV=.15 XINC=.01 LAYCH=33  
!LOOPX1 ILX='TL' FINV=.0 XINC=-.01 LAYCH=34  
END

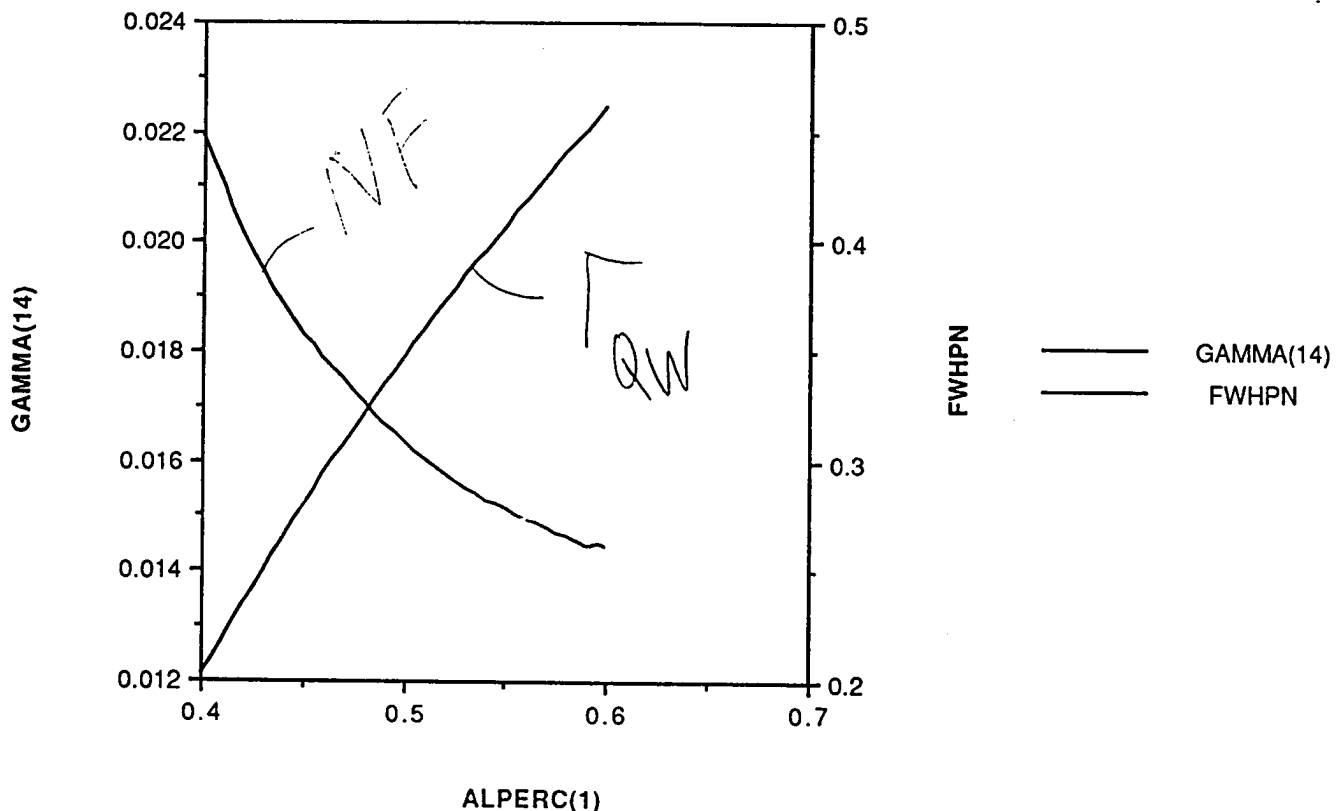
# DBASE

	PHM	GAMMA(14)	WZR	WZI	QZR	FWHPN	FWHPF	KM	T
*	ALPERC(1)	3.561981E-01	2.246067E-02	3.319740E+00	5.538958E-07	1.102067E+01	2.615820E-01	3.946414E+01	2
	6.000000E-01	3.552210E-01	2.225529E-02	3.321511E+00	6.246880E-07	1.103243E+01	2.620690E-01	3.908882E+01	3
	5.950000E-01	3.541592E-01	2.204785E-02	3.323287E+00	7.045802E-07	1.104424E+01	2.615387E-01	3.870946E+01	3
	5.900000E-01	3.530197E-01	2.183829E-02	3.325068E+00	7.946993E-07	1.105608E+01	2.634545E-01	3.833140E+01	3
	5.850000E-01	3.518072E-01	2.162657E-02	3.326855E+00	8.963552E-07	1.106796E+01	2.654001E-01	3.795132E+01	3
	5.800000E-01	3.505255E-01	2.141261E-02	3.328647E+00	1.011009E-06	1.107989E+01	2.674055E-01	3.757964E+01	3
	5.750000E-01	3.491773E-01	2.119638E-02	3.330444E+00	1.140327E-06	1.109186E+01	2.694642E-01	3.720509E+01	3
	5.700000E-01	3.477646E-01	2.097781E-02	3.332248E+00	1.286170E-06	1.110388E+01	2.715789E-01	3.682759E+01	3
	5.650000E-01	3.462889E-01	2.075684E-02	3.334058E+00	1.450639E-06	1.111594E+01	2.737527E-01	3.644704E+01	3
	5.600000E-01	3.447510E-01	2.053340E-02	3.335874E+00	1.636093E-06	1.112805E+01	2.759889E-01	3.606332E+01	3
	5.550000E-01	3.431517E-01	2.030744E-02	3.337697E+00	1.845188E-06	1.114022E+01	2.782909E-01	3.568828E+01	3
	5.500000E-01	3.414914E-01	2.007890E-02	3.339526E+00	2.080906E-06	1.115244E+01	2.806625E-01	3.531335E+01	3
	5.450000E-01	3.397702E-01	1.984770E-02	3.341363E+00	2.346599E-06	1.116471E+01	2.821472E-01	3.493593E+01	3
	5.400000E-01	3.379880E-01	1.961378E-02	3.343207E+00	2.646027E-06	1.117704E+01	2.847959E-01	3.456341E+01	3
	5.350000E-01	3.361444E-01	1.937707E-02	3.345059E+00	2.983410E-06	1.118942E+01	2.875257E-01	3.418221E+01	3
	5.300000E-01	3.342392E-01	1.913751E-02	3.346919E+00	3.363477E-06	1.120187E+01	2.902406E-01	3.380427E+01	3
	5.250000E-01	3.322718E-01	1.889502E-02	3.348787E+00	3.791523E-06	1.121438E+01	2.932473E-01	3.343855E+01	3
	5.200000E-01	3.302414E-01	1.864955E-02	3.350664E+00	4.273475E-06	1.122695E+01	2.967436E-01	3.306696E+01	3
	5.100000E-01	3.281472E-01	1.840101E-02	3.352549E+00	4.815956E-06	1.123959E+01	3.003422E-01	3.269417E+01	3
	5.050000E-01	3.259885E-01	1.814934E-02	3.354444E+00	5.426362E-06	1.125229E+01	3.040437E-01	3.232017E+01	3
	5.000000E-01	3.237643E-01	1.789448E-02	3.356348E+00	6.112940E-06	1.126507E+01	3.082466E-01	3.194709E+01	3
	4.950000E-01	3.214736E-01	1.763636E-02	3.358262E+00	6.884875E-06	1.127792E+01	3.124595E-01	3.158633E+01	3
	4.900000E-01	3.191153E-01	1.737492E-02	3.360186E+00	7.752381E-06	1.129085E+01	3.167701E-01	3.122406E+01	3
	4.850000E-01	3.1668885E-01	1.711009E-02	3.362120E+00	8.726798E-06	1.130385E+01	3.212290E-01	3.086181E+01	3
	4.800000E-01	3.141923E-01	1.684183E-02	3.364066E+00	9.820693E-06	1.131694E+01	3.258330E-01	3.049990E+01	3
	4.750000E-01	3.116263E-01	1.657008E-02	3.366023E+00	1.104797E-05	1.133011E+01	3.305388E-01	3.013775E+01	3
	4.700000E-01	3.089905E-01	1.629479E-02	3.367919E+00	1.242397E-05	1.134336E+01	3.368398E-01	2.978565E+01	3
	4.650000E-01	3.062886E-01	1.601593E-02	3.369972E+00	1.396560E-05	1.135671E+01	3.416333E-01	2.943774E+01	4
	4.600000E-01	3.035460E-01	1.573347E-02	3.371964E+00	1.569142E-05	1.137014E+01	3.466296E-01	2.909122E+01	4
	4.550000E-01	3.028986E-01	1.544739E-02	3.371970E+00	1.762326E-05	1.138368E+01	3.518464E-01	2.874594E+01	4
	4.500000E-01	3.017411E-01	1.515769E-02	3.375989E+00	1.978062E-05	1.139730E+01	3.573031E-01	2.978536E+01	4
	4.450000E-01	2.998833E-01	1.486436E-02	3.378022E+00	2.218896E-05	1.141104E+01	3.639796E-01	2.943774E+01	4
	4.400000E-01	2.976851E-01	1.456745E-02	3.380069E+00	2.487450E-05	1.142487E+01	3.711420E-01	2.774256E+01	4
	4.350000E-01	2.952482E-01	1.426698E-02	3.382131E+00	2.786562E-05	1.143881E+01	3.786032E-01	2.741752E+01	4
	4.300000E-01	2.926191E-01	1.396301E-02	3.384208E+00	3.119279E-05	1.145287E+01	3.863936E-01	2.840236E+01	4
	4.250000E-01	2.898237E-01	1.365564E-02	3.386301E+00	3.488869E-05	1.146703E+01	3.945477E-01	2.678747E+01	4
	4.200000E-01	2.8687789E-01	1.334497E-02	3.388410E+00	3.898810E-05	1.148132E+01	4.041371E-01	2.647211E+01	4
	4.150000E-01	2.837968E-01	1.303114E-02	3.390535E+00	4.352790E-05	1.149573E+01	4.145330E-01	2.613659E+01	4
	4.100000E-01	2.805873E-01	1.271431E-02	3.392678E+00	4.854690E-05	1.151026E+01	4.250444E-01	2.585186E+01	4
	4.050000E-01	2.772596E-01	1.239469E-02	3.394838E+00	5.408570E-05	1.152492E+01	4.362680E-01	2.555693E+01	4

133

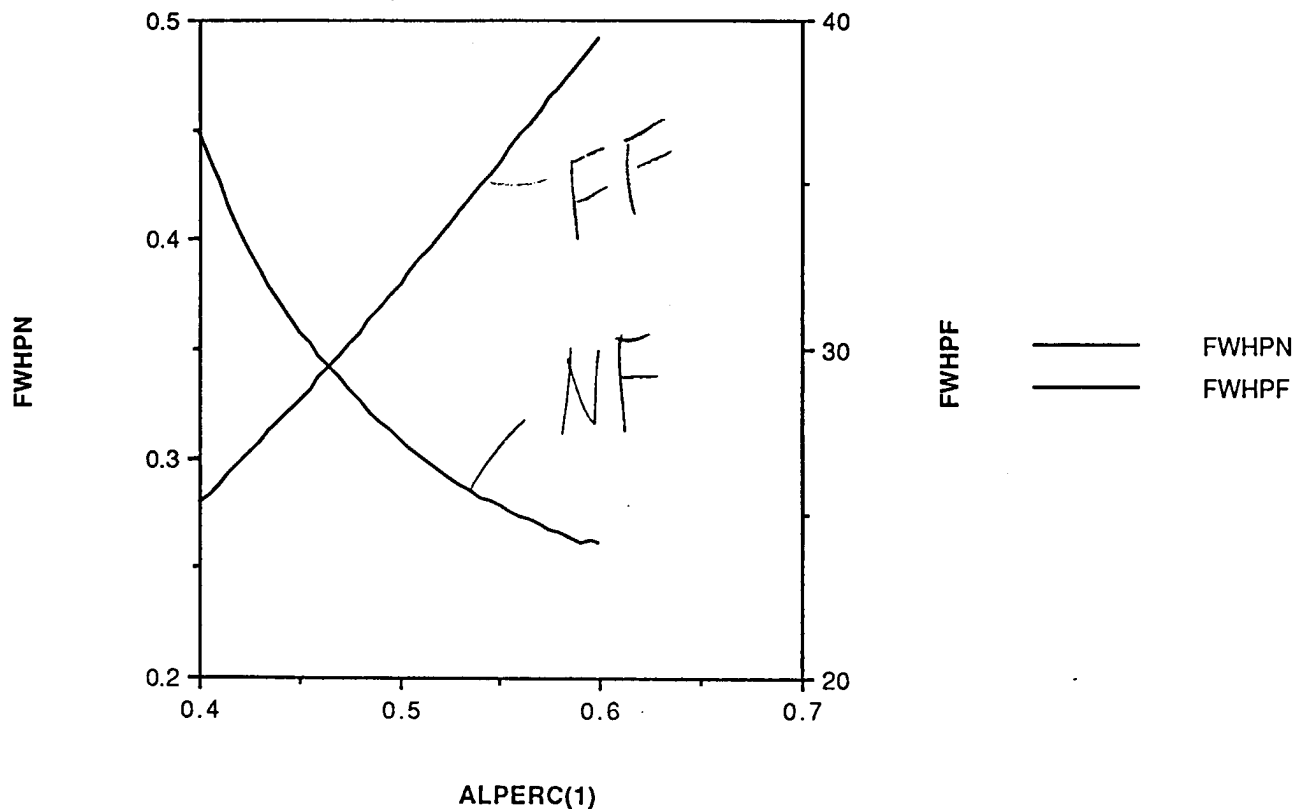
134

Data from "6392ldiv\_DBASE\_"



(135)

Data from "6392ldiv\_DBASE\_"



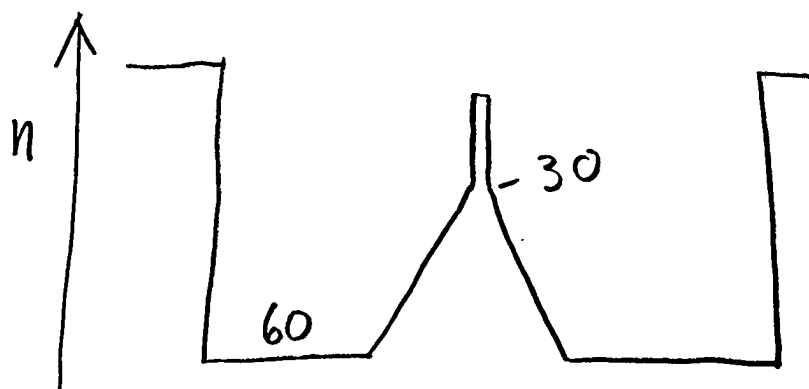
(Kamino - Fri)

136

- Outline of MR#1 due today
- MR#1 due March 8 Monday
  - sent to (in class) reviewers
  - comments due back March 12
- Final revised report due March 22

Last Wednesday & Friday:

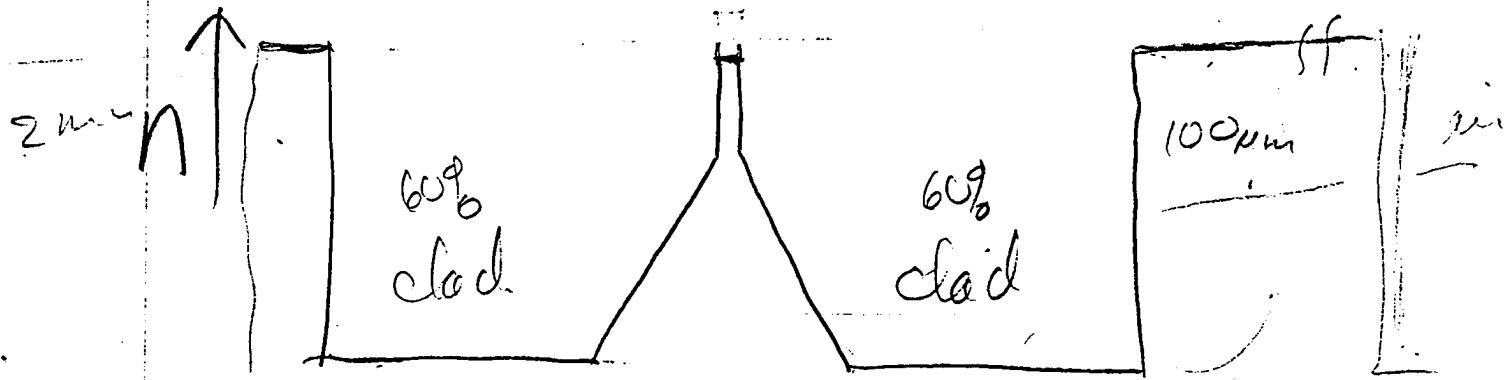
Solved LDI structure

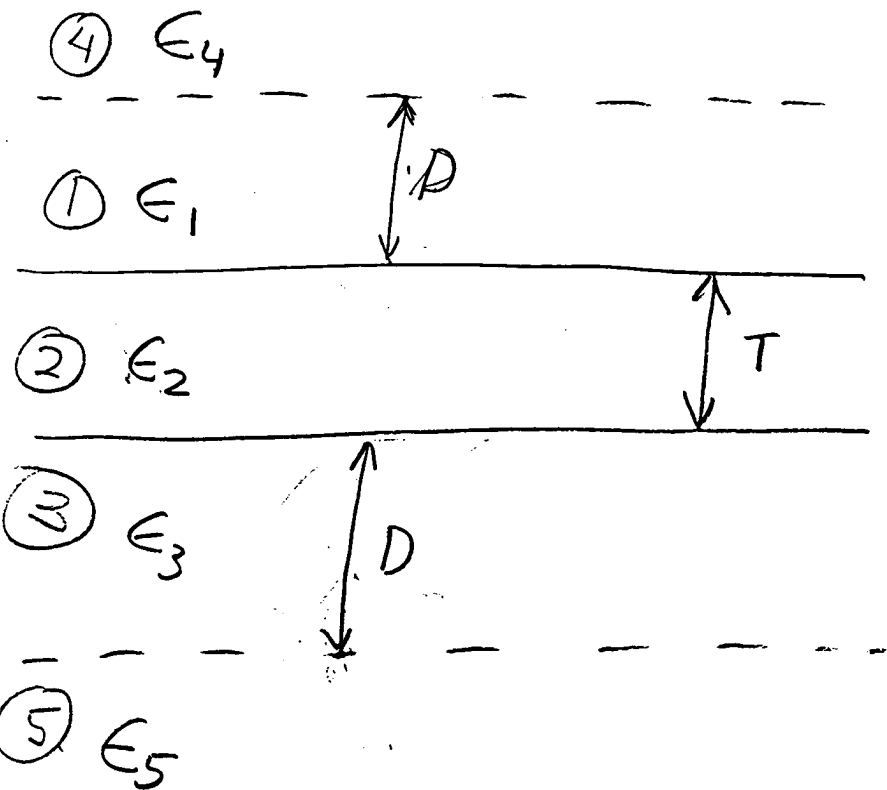


- found near-field )
- " far- field )
- found  $\Gamma_{QW} = 2.25\%$
- plotted  $\Gamma_{QW}$  FWHP<sub>nf</sub>)  
for clad = 60% → 35%
- also plotted FWHP<sub>ff</sub>)

## Question on Solution

to WG profile:

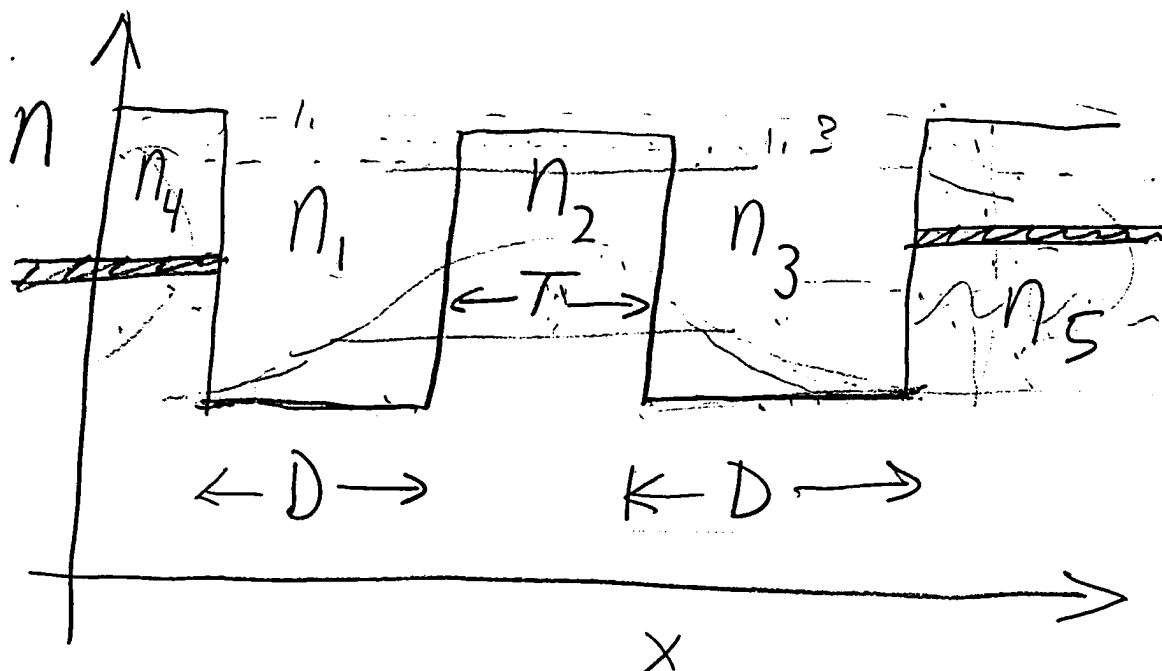




Let  $E_2 > E_1, E_3$

$E_4, E_5 > E_1, E_3$

$E_4, E_5 \approx E_2$



From the wave equation:

$$\frac{\partial^2 E_y}{\partial x^2} + (\epsilon_2 k_0^2 - \beta^2) E_y = 0 \quad (1)$$

For  $D = \infty$ , bound modes occur for

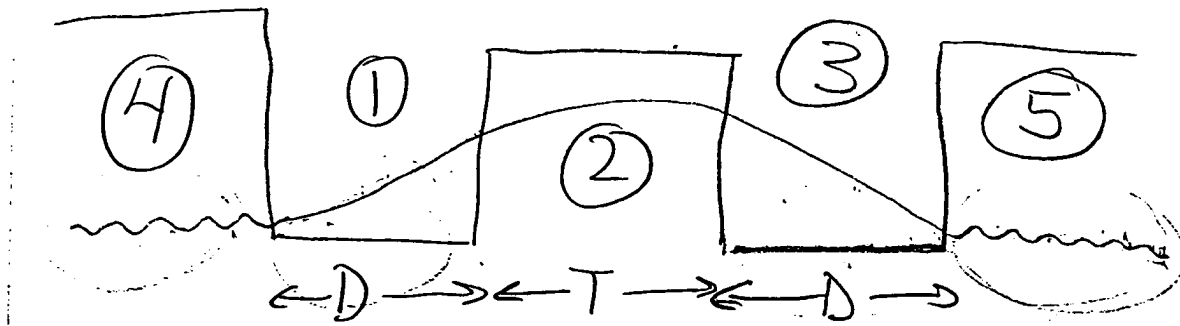
$$\epsilon_2 k_0^2 < \beta^2 < \epsilon_1 k_0^2$$

For  $D$  finite and  $D \gg \lambda_m$

(say  $D = 10 \lambda_m$  or  $100 \lambda_m$ )

We can ignore layers  
 ④ and ⑤ !!

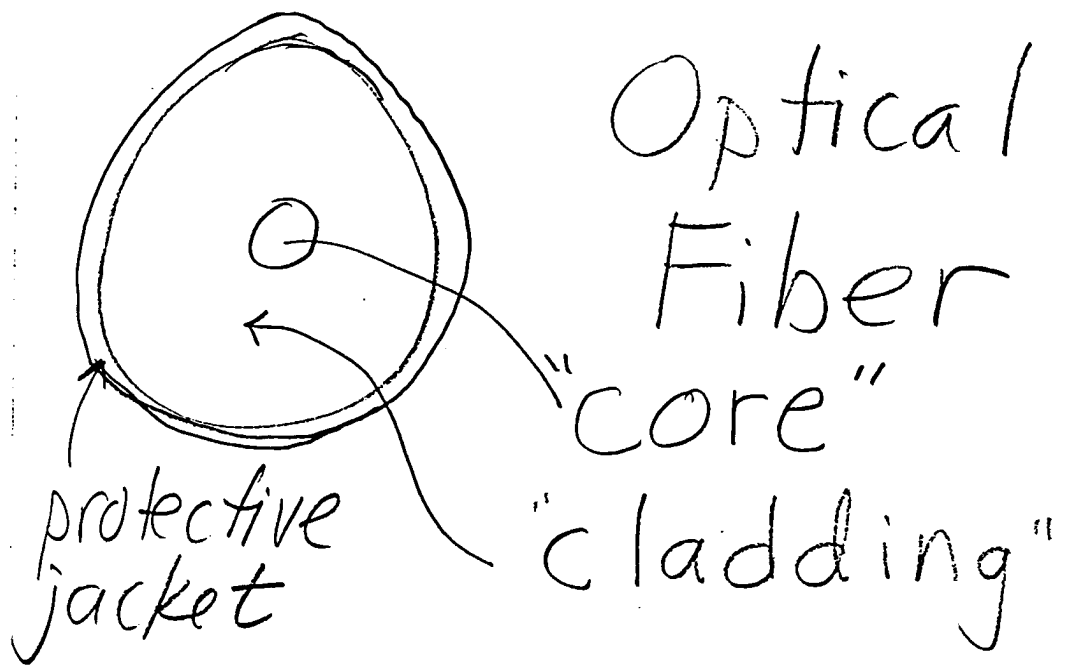
In principle,



the solutions to (1) are oscillatory in ④ and ⑤

But if  $D$  is large,  
the fraction of mode  
energy in ④ & ⑤ is  
negligible -- we just  
have a 3-layer WG.

\* This is the concept  
of a "cladding" or  
"isolation" layer



The purpose of a cladding layer is optical isolation

- optical fibers can lay on metal, be immersed in liquid, ....
- semiconductor lasers can be mounted on copper blocks

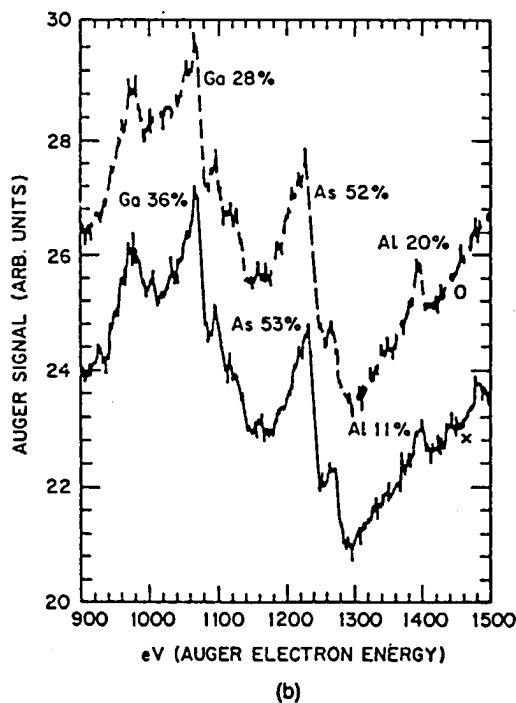
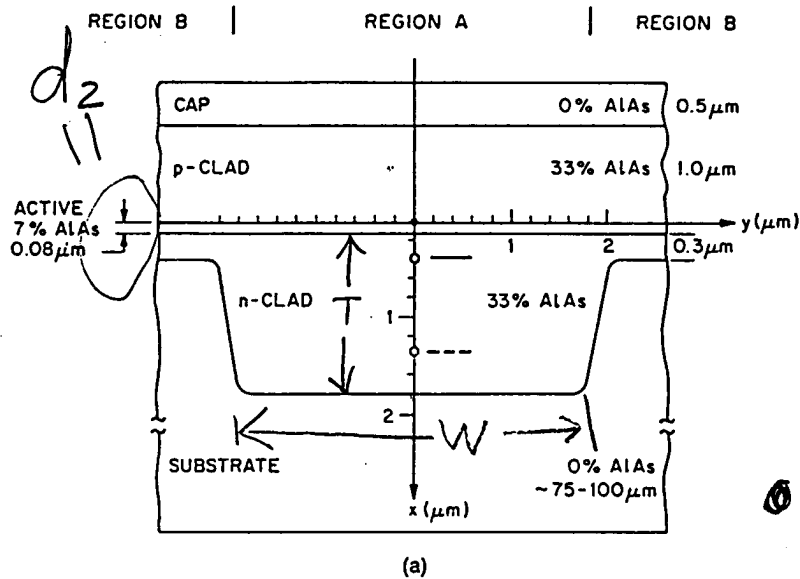


FIGURE 4.14. (a) Geometry of a typical CSP-type laser;  $x = 0$  is the top of the active layer and  $x = 1.8 \mu\text{m}$  is the bottom of the channel. (b) Auger analysis of a cleaved facet of a CSP-type laser showing a higher Al composition near the bottom of the channel ( $x = 1.4 \mu\text{m}$ , dashed line) than near the top of the channel ( $x = 0.4 \mu\text{m}$ , solid line).

CSP  
Laser

• What happens as  $T \rightarrow 0$ ?

• Assume 1D problem

•  $W = \infty$

$$\alpha_s \approx 5,000 \text{ cm}^{-1}$$

Figs. from Evans & Butler, "Analysis of CSP,..." appearing in Recent Advances in Electromagnetic Theory Springer-Verlag 1990 11Y

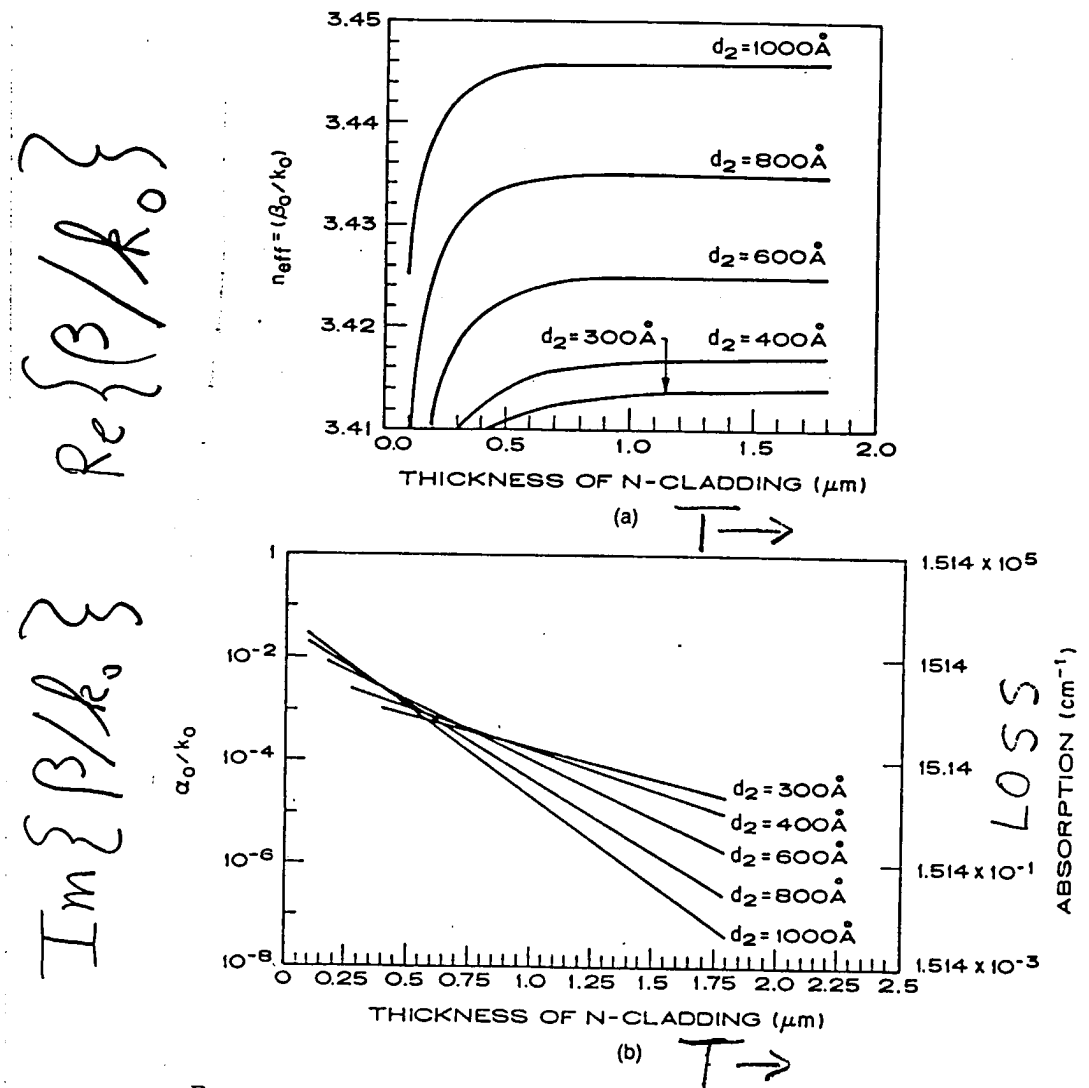
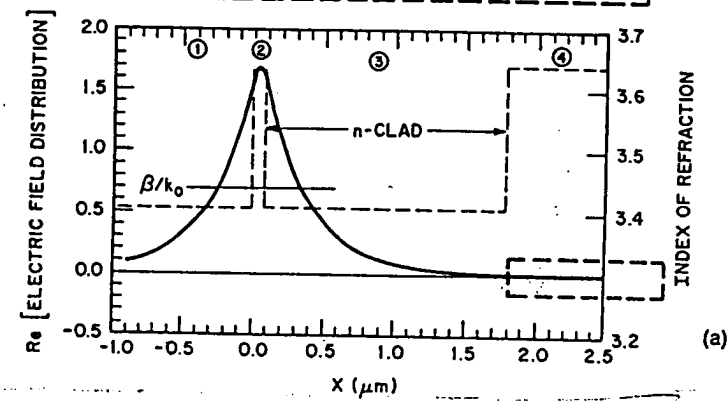


FIGURE 4.7. (a) The real part of the effective index and (b) the imaginary part of the effective index as a function of the  $n$ -clad thickness for active layer thicknesses of 400, 600, 800, and 1000  $\text{\AA}$  of a conventional CSP laser.

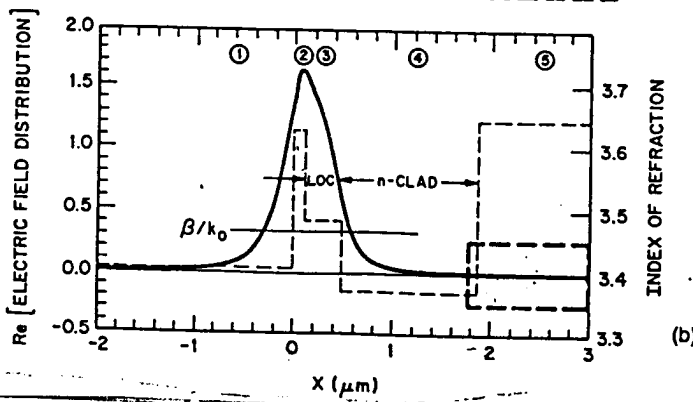
- For  $T \geq 1.0 \mu\text{m}$ 
  - no change in  $\text{Re}\{\beta/k_0\}$
  - negligible change in  $\text{Im}\{\beta/k_0\}$

# Re[Electric Field Distribution]



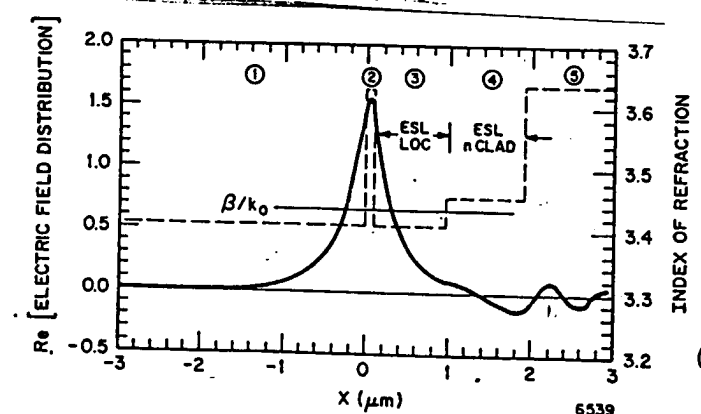
(a)

$$\boxed{4} \approx 3 \times 10^{-6}$$



(b)

$$\boxed{5} \approx 3 \times 10^{-9}$$



(c)

$$\boxed{5} \approx 8 \times 10^{-2}$$

FIGURE 4.16 (continued)

FIGURE 4.16. Index profiles (---) and corresponding electric field distributions (—) for (a) a conventional CSP laser; (b) a CSP-LOC laser; and (c) an ESL-CSP laser. The layer compositions, thicknesses, and effective index for each structure are listed in Tables 4.5–4.7. The dashed rectangles in (a) and (b) show the field distributions on expanded scales for  $x > 1.8 \mu\text{m}$ .

# Structure Details

TABLE 4.5. CSP structure.

Layer	Thickness ( $\mu\text{m}$ )	% AlAs	Index ( $\lambda = 0.83 \mu\text{m}$ )	$\Gamma_{\text{layer}}$	$\text{Re}\{n_{\text{eff}}^*\}$	$\text{Re}\{n_e''\}$
1. <i>p</i> -Clad	> 1.0	33	3.40657	0.389		
2. Active	0.08	7	3.62805	0.222	3.43401	
3. <i>n</i> -Clad	1.8	33	3.40657	0.389		$6.6 \times 10^{-5}$
4. Substrate	~75	0	3.64			$3.4 \times 10^{-6}$

14

TABLE 4.6. CSP-LOC structure.

Layer	Thickness ( $\mu\text{m}$ )	% AlAs	Index ( $\lambda = 0.83 \mu\text{m}$ )	$\Gamma_{\text{layer}}$	$\text{Re}\{n_{\text{eff}}^*\}$	$\text{Im}\{n_{\text{eff}}^*\}$
1. <i>p</i> -Clad	> 1.0	33	3.40657	0.19043		
2. Active	0.08	7	3.62805	0.19205	3.43401	
3. LOC	0.4	22	3.48276	0.59205	3.46932	
4. <i>n</i> -Clad	1.8	40	3.364	0.02546		$6.6 \times 10^{-5}$
5. Substrate	~75	0	3.64			$2.9 \times 10^{-9}$

15

TABLE 4.7. ESL-CSP structure.

Layer	Thickness ( $\mu\text{m}$ )	% AlAs	Index ( $\lambda = 0.83 \mu\text{m}$ )	$\Gamma_{\text{layer}}$	$\text{Re}\{n_{\text{eff}}^*\}$	$\text{Im}\{n_{\text{eff}}^*\}$
1. <i>p</i> -Clad	> 1.0	33	3.40657	0.331		
2. Active	0.08	7	3.62805	0.190		
3. LOC	0.9	33	3.40657	0.346	3.43405	
4. <i>n</i> -Clad	1.8	26.3	3.45245	0.125		$5.11 \times 10^{-4}$
5. Substrate	~75	0	3.64			0.008

15

$$\alpha_i = 10 \text{ cm}^{-1} \quad i=1,2,3(4)$$

$$\alpha_{\text{sub}} = 5000 - 10,000 \text{ cm}^{-1}$$

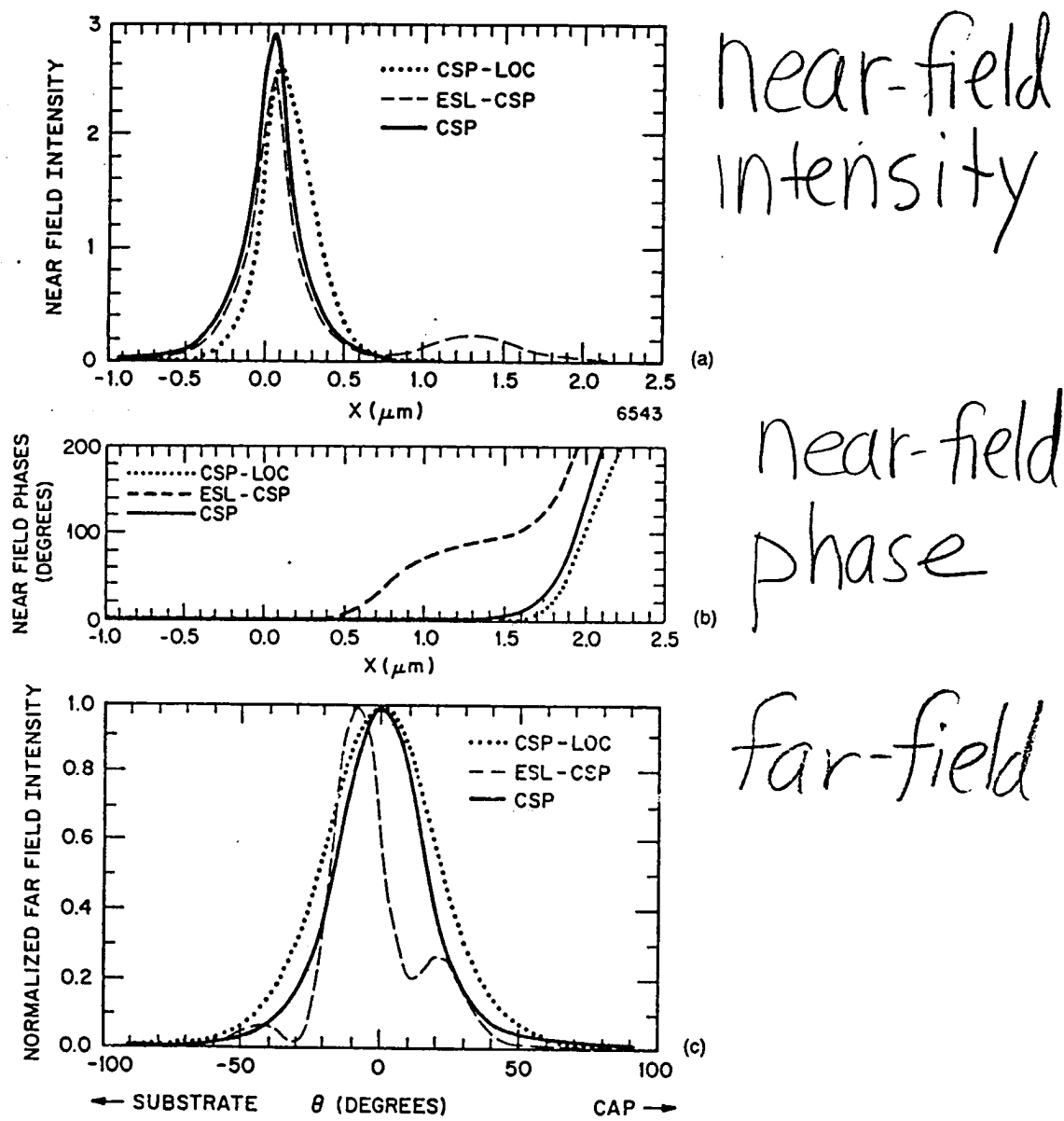


FIGURE 4.20. Calculated (a) near-field intensities, (b) near-field phases, and (c) far-field intensities  $I_{\text{ch}}(\theta)$  perpendicular to the junction for a conventional CSP laser (—), a CSP-LOC laser (...), and an ESL-CSP laser (---) for the parameters listed in Tables 4.4-4.7.

- ESL-CSP: Far-Field is not symmetric

### CSP & CSP-LOC:

- phase is flat when near field  $I \neq 0$   
 $\Rightarrow$  field distribution is real  
 $\Rightarrow$  far-field is symmetric

$$I_{ff}(\theta) = \cos\theta [FT(n_f)]$$

### CSP-ESL:

- phase varies when near field  $I \neq 0$   
 $\Rightarrow$  field distribution is complex  
 $\Rightarrow$  far-field is asymmetric

So, Ignore ① & ⑦ LDI structure  
(most times)

$$\begin{array}{c} \text{---} \\ \text{I} \\ \text{---} \end{array} \rightarrow z$$

(148)

## 2 D DOW WG

Rectangular Cross section

- exact analytical treatment not possible

⇒ approximate analytic technique:

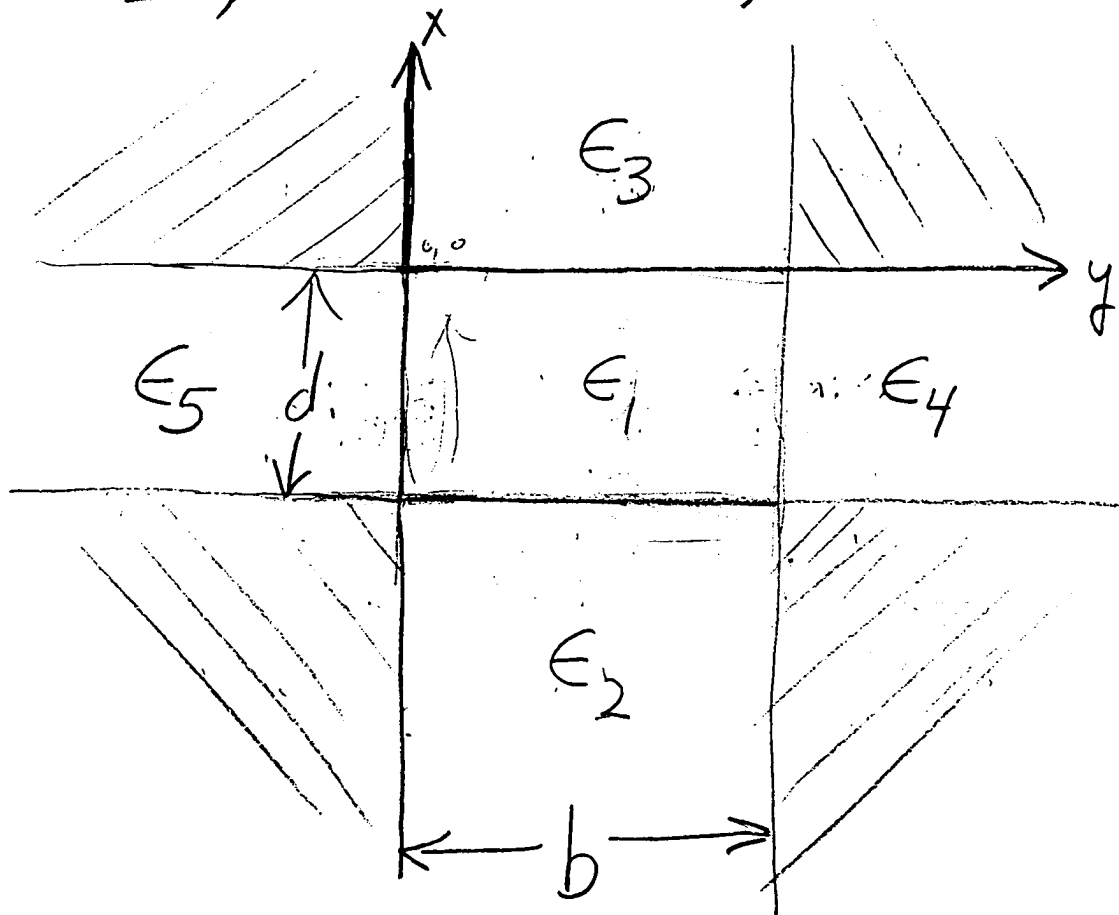
(E.A.J. Marcatili "Dielectric Rectangular Waveguide and directional coupler for integrated optics," Bell Syst. Tech. J., 48, 2071-2102, 1969.)

⇒ "exact" numerical method  
J. E. Goell, "A circular-

and found in 20  
and prop in the third

(149)

harmonic computer analysis  
of rectangular dielectric  
waveguides," Bell Syst. Tech.  
J., 51, 2133-2160, (1969).

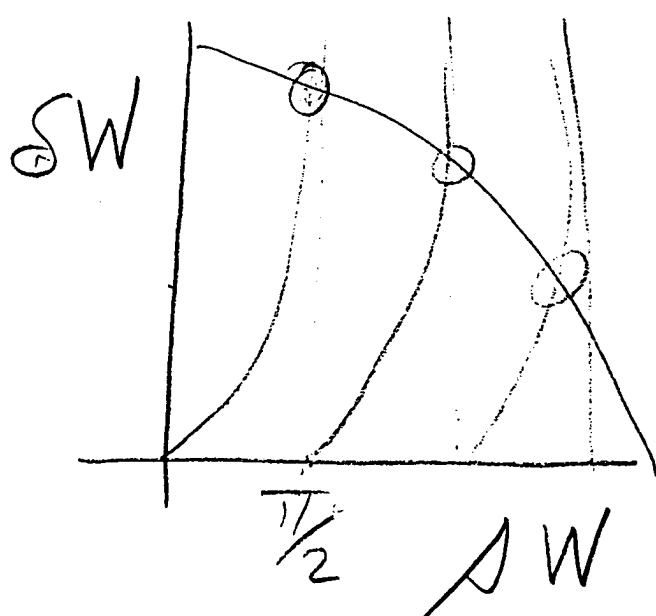


- ignore fields in shaded regions
- assume  $\epsilon_1 > (\epsilon_2, \epsilon_3, \epsilon_4, \epsilon_5)$

assume far from  
cutoff

$$\Rightarrow \beta \approx \sqrt{\epsilon_1} k_0$$

$$\delta \gg s$$



$$\begin{aligned} SW &= jw \tan(Sw) \\ (Sw)^2 - (Sw)^2 &= (\epsilon_1 - \epsilon_2) k_0^2 \end{aligned}$$

$\Rightarrow$  field almost all  
confined to "core" ( $\epsilon_1$  Region)

Longitudinal  $E$  &  $H$   
components satisfy

$$\frac{\partial^2 \psi}{\partial x^2} + \frac{\partial^2 \psi}{\partial y^2} + (k_0^2 \epsilon_i - \beta^2) \psi = 0 \quad (1)$$

$$i=1, 2, 3, 4, 5; \quad \psi = \begin{cases} E_z \\ H_z \end{cases}$$

• Solve (1) for  $E_z, H_z \Rightarrow$

$$H_x, H_y, E_x, E_y : Eq(22) - (25)/22 \quad (3)$$

The  $\approx$  solution separates into 2 polarizations (Preview)

$E_{pq}^x$  : polarized predominantly along the  $x$  direction

$E_{pq}^y$  : polarized predominantly along the  $y$  direction

$E_{pq}^x$  corresponds to choosing

$$H_x = 0$$

$E_{pq}^y$  corresponds to choosing

$$H_y = 0$$

Consider the  $E_{pq}^x$  modes:

In region ① ( $\epsilon_1$ ), assume

$$E_z^{(1)}(x,y) = A \cos S_x(x+\xi) \cos S_y(y+\eta) e^{-j\beta z} \quad (2)$$

(suppressed)

(2) into (1)  $\Rightarrow \lambda_0$

$$-S_x^2 - S_y^2 + k_0^2 \epsilon_1 - \beta^2 = 0 \quad (3)$$

Or,  $S_x^2 + S_y^2 = k_0^2 \epsilon_1 - \beta^2 \quad (4)$

Now,  $H_x = 0$  (see 1/22, p(13), Eq(22))

$$\Rightarrow \omega \epsilon_0 \epsilon_1 \frac{\partial E_z}{\partial y} = \beta \frac{\partial H_z}{\partial x}$$

so (Eq 2)  $\Rightarrow$

$$\frac{\partial H_z}{\partial x} = \frac{\omega \epsilon_0 \epsilon_1}{\beta} (-S_y A) \cos S_x(x+\xi) \\ \times (\sin S_y(y+\eta))$$

or,

$$H_z = -\frac{S_y}{S_x} A \frac{\omega \epsilon_1 \epsilon_0}{\beta} \sin S_x(x+\xi) \sin S_y(y+\eta)$$

Note:

$$\frac{\omega \epsilon_1 \epsilon_0}{\beta} = \frac{\epsilon_1 \omega \sqrt{\mu_0 \epsilon_0}}{\beta} \sqrt{\frac{\epsilon_0}{\mu_0}} = \frac{\epsilon_1 k_0}{\beta} \sqrt{\frac{\epsilon_0}{\mu_0}}$$

so

$$H_2^{(1)} = -A \sqrt{\frac{\epsilon_0}{\mu_0}} \epsilon_1 \left( \frac{S_y}{S_x} \right) \frac{k_0}{\beta} \sin S_x(x+\xi) \\ \times (\sin S_y(y+\eta)) \quad (5)$$

From Eq's 22-25,  $\gamma_{22}$ , P(3):  
 (left as an exercise:)

$$E_x^{(1)} = \frac{jA}{S_x \beta} \left( \epsilon_1 k_0^2 S_x^2 \right) \sin S_x(x+\xi) \\ \times (\cos S_y(y+\eta)) \quad (6)$$

$$E_y^{(1)} = -jA \left( \frac{S_x}{\beta} \right) \cos S_x(x+\xi) \sin S_y(y+\eta) \quad (7)$$

$$H_x^{(1)} = 0. \quad (8)$$

$$H_y^{(1)} = jA \sqrt{\frac{\epsilon_0}{\mu_0}} \epsilon_1 \left( \frac{k_0}{S_x} \right) \sin S_x(x+\xi) \cos S_y(y+\eta) \quad (9)$$

$$\frac{\epsilon_1}{\epsilon_2} \quad \cancel{\beta}$$

(155)

Recall, far from cutoff,

$\beta \approx \sqrt{\epsilon_1} k_0$ , and from (4),

$$S_x^2 + S_y^2 = \epsilon_1 k_0^2 - \beta^2 \approx 0$$

so

$$S_x \ll \beta, \quad S_y \ll \beta$$

Now by (2), (6), & (7),

$$|E_z| = |A| \quad ?? \quad (10)$$

$$|E_x| = |A| \left( \frac{\beta}{S_x} - \frac{S_x}{\beta} \right) \quad (11)$$

$$|E_y| = |A| \frac{S_x}{\beta} \approx 0 \quad (12)$$

$$|E_y| \ll |E_z| \ll |E_x| \quad (13)$$

$\Rightarrow$  ignore  $E_y$  ( $2^{nd}$  order term)

In Regions ②-⑤,  
the fields must vanish  
as  $x \rightarrow \pm\infty, y \rightarrow \pm\infty$

So, at  $x = -d$ , (Eq 2)

$$\textcircled{2} \quad E_z = A \cos \delta_x (\xi - d) \cos \delta_y (y + \eta) \\ \times \left\{ \exp [\delta_2 (x + d)] \right\} \quad (14)$$

(Requiring  $E_z$  continuous @

$x = -d$ )  
From  $H_x = 0 \Rightarrow$  in Region ②:

$$\omega \epsilon_0 \epsilon_2 \frac{\partial E_z}{\partial y} = \beta \frac{\partial H_z}{\partial x}$$

So

$$\frac{\partial H_z^{(2)}}{\partial x} = \frac{\omega \epsilon_0 \epsilon_2}{\beta} s_y A \cos(\gamma) \cdot \sin(\gamma) \exp[S_2(x+d)]$$

↓

$$H_z^{(2)} = -\frac{A k_0}{\beta} \sqrt{\frac{\epsilon_0}{\mu_0}} \epsilon_2 \left( \frac{s_y}{S_2} \right) \cos \Delta_x (\ell-d) \quad (15)$$

$$\cdot \sin \Delta_y (y+\gamma) \exp[S_2(x+d)]$$

from Eq's (22-25) / 22, P(13):

$$E_x^{(2)} = jA \left[ (S^2 + \epsilon_2 k_0^2) / S_2 \beta \right] \cos \Delta_x (\ell-d) \cdot \cos \Delta_y (y+\gamma) \exp[S_2(x+d)] \quad (16)$$

$$E_y \approx 0 \quad (\text{from (13)}) \quad (17)$$

$$H_x = 0 \quad (18)$$

$$\textcircled{2} \quad H_y = jA \sqrt{\frac{\epsilon_0}{M_0}} \epsilon_2 \left( \frac{k_0}{\delta_2} \right) \cos S_x (\xi - d)$$

(19)  $\cos S_y (y + \eta) \exp [\delta_2 (x + d)]$

Note: I have used the relationship from Eq(1)  
applied to region  $\textcircled{2}$ :

$$\delta_2^2 - S_y^2 + k_0^2 \epsilon_2 - \beta^2 = 0$$

or

$$S_y^2 - \delta_2^2 = k_0^2 \epsilon_2 - \beta^2 \quad (20)$$

Similarly, in  $\textcircled{3}$ , ( $x \geq 0$ ),

$$E_z^{\textcircled{3}} = A \cos S_x (\xi) \quad (19)$$

$$\cos S_y (y + \eta) \exp [-\delta_3 x]$$

Requiring  $H_x = 0$ ,

$$\frac{\partial H_z}{\partial x} = \omega \epsilon_0 \epsilon_3 \frac{\partial E_z}{\partial y}$$

$$= (-\omega \epsilon_3 \epsilon_0 A \cos \delta_x \xi) \sin S_y(y + \eta) \exp[-\delta_3 x]$$

$$\sin S_y(y + \eta) \exp[-\delta_3 x] \Big) S_y$$

so

$$H_z^{(3)} = A \left( \frac{\epsilon_0}{\mu_0} \epsilon_3 \left( \frac{S_y}{\delta_3} \right) k_0 \beta \right) \cos \delta_x \xi$$

$$(20) \quad \cdot \sin S_y(y + \eta) \exp[-\delta_3 x]$$

and from Eqs (22-25) 1/2 p 13:

$$E_x = -jA \left[ (\delta_3^2 + \epsilon_3 k_0^2) / (\delta_3 \beta) \right] (21)$$

$$\cdot \cos \delta_x \xi \sin S_y(y + \eta) \exp[-\delta_3 x]$$

$$E_y \approx 0$$

$$H_x = 0$$

$$H_y = -jA\sqrt{\frac{\epsilon_0}{\mu_0}}\epsilon_3 \left(\frac{k_0}{\delta_3}\right) \cos \delta_x \xi \quad (22)$$

$$\cdot \cos \delta_y(y+\eta) \exp[-\delta_3 x]$$

and from (1),

$$\delta_y^2 - \delta_3^2 = k_0^2 \epsilon_3 - \beta^2 \quad (23)$$

In region ④, require  
that  $E_x$  be continuous

since  $E_x \gg E_z \gg E_y$   
by (13)

(161)

$$E_z^{(4)} = \left(\frac{\epsilon_1}{\epsilon_4}\right) A \cos \delta_y(b+\eta) \cos \delta_x(x+\xi) \cdot \{ \exp[-\delta_y(y-b)] \} \quad (24)$$

$$H_z^{(4)} = -\left(\frac{\epsilon_1}{\epsilon_4}\right) A \sqrt{\frac{\epsilon_0}{\mu_0}} \epsilon_4 \left(\frac{\delta_4}{\delta_x}\right) \frac{k_0}{\beta} \cos \delta_y(b+\eta) \cdot \{ \sin \delta_x(x+\xi) \exp[-\delta_y(y-b)] \} \quad (25)$$

and from Eq(1) p. ④ 2/24;

$$-\delta_x^2 + \delta_y^2 + k_0^2 \epsilon_4 - \beta^2 = 0$$

or

$$\delta_x^2 - \delta_y^2 = k_0^2 \epsilon_4 - \beta^2 \quad (26)$$

From Eqs (22)-(25), 1/22 p ⑬:

$$E_x^{(4)} = \left(\frac{\epsilon_1}{\epsilon_4}\right) j A \left[ (\epsilon_4 k_0^2 - \delta_x^2) / (\delta_x \beta) \right] \quad (27)$$

$$(\cos \delta_y(b+\eta) \sin \delta_x(x+\xi) \exp[-\delta_y(y-b)])$$

$$H_y = \left( \frac{E_1}{E_4} \right) j A \sqrt{\frac{\epsilon_0}{\mu_0}} \epsilon_4 \left( \frac{k_0}{s_x} \right) \cos s_y (b + \gamma) \\ \cdot \sin s_x (x + \delta) \exp[-s_y (y - b)] \quad (28)$$

@  $y = b$ , want  $E_x^{(1)}(x, b) = E_x^{(2)}(x, b)$

SINCE

$$E_x^{(1)}(x, b) = \frac{jA}{s_x \beta} (\epsilon_1 k_0^2 - s_x^2) \cos \sim$$

$$E_x^{(2)}(x, b) = \frac{jA}{s_x \beta} (\epsilon_4 k_0^2 - s_x^2) \cos \sim$$

to make  $E_x$  continuous,  
multiply  $E_x^{(1)} \left( \frac{\epsilon_1}{\epsilon_4} \right)$

• neglect  $s_x^2$  term<sup>2</sup>

Similarly, & finally, in ⑤  
( $y=0$ )

$$\underline{E}_z^{(5)} = \left(\frac{\epsilon_1}{\epsilon_5}\right) A \cos \delta_y \eta \cos S_x(x+\xi) \cdot \exp(\delta_5 y) \quad (29)$$

$$\underline{H}_z^{(5)} = \left(\frac{\epsilon_1}{\epsilon_5}\right) A \sqrt{\frac{\epsilon_0}{\mu_0}} \epsilon_5 \left(\frac{\delta_5}{\Delta_x}\right) \left(\frac{k_0}{\beta}\right) \cos \delta_y \eta \sin S_x(x+\xi) \exp(\delta_5 y) \quad (30)$$

$$\underline{E}_x^{(5)} = jA \left(\frac{\epsilon_1}{\epsilon_5}\right) \left[\left(\epsilon_5 k_0^2 - S_x^2\right) S_x \beta\right] \cos \delta_y \eta \times \sin S_x(x+\xi) \exp(\delta_5 y) \quad (31)$$

$$\underline{H}_y^{(5)} = \left(\frac{\epsilon_1}{\epsilon_5}\right) jA \sqrt{\frac{\epsilon_0}{\mu_0}} \epsilon_5 \left(\frac{k_0}{\Delta_x}\right) \cos \delta_y \eta \sin S_x(x+\xi) \exp(\delta_5 y) \quad (32)$$

where (by (1), p. 4, 2/24):

$$S_x^2 - S_5^2 = \epsilon_5 k_0^2 - \beta^2 \quad (33)$$

Now, match the remaining boundaries:

(so far,  $E_x$  is continuous if we neglect  $S_x^2$  terms  
 $E_y \approx 0$ , so  $E_y \approx$  continuous)

$E_z$  is already continuous, so require that  $H_z$  be continuous at  $x=0$ , and  $x=-d$ :

$$H_z^{(1)}(x=0, y) = H_z^{(3)}(x=0, y) \Rightarrow$$

$$-A\sqrt{\frac{\epsilon_0}{M_0}} \epsilon_1 \left(\frac{S_y}{S_x}\right) \left(\frac{k_0}{\beta}\right) \sin S_x \xi \cdot \sin S_y (4+n)$$

$$= A \sqrt{\frac{\epsilon_0}{\mu_0}} \epsilon_3 \left( \frac{S_y}{\delta_3} \right) \frac{k_0}{\beta} \cos S_x \xi \sin S_y (y + \eta)$$

or,

$$\frac{\epsilon_1}{S_x} \sin S_x \xi + \frac{\epsilon_3}{\delta_3} \cos S_x \xi = 0 \quad (34)$$

and from  $H_z^{(1)}(x = -d, y) = H_z^{(2)}(x = -d, y)$ :

$$-A \sqrt{\frac{\epsilon_0}{\mu_0}} \epsilon_1 \frac{S_y}{S_x} \left( \frac{k_0}{\beta} \right) \sin S_x (\xi - d) \cdot \sin S_y (y + \eta)$$

$$= -A \sqrt{\frac{\epsilon_0}{\mu_0}} \epsilon_2 \left( \frac{S_y}{\delta_2} \right) \frac{k_0}{\beta} \cos S_x (\xi - d)$$

$\cdot \sin S_y (y + \eta)$ , or

$$\frac{\epsilon_1}{S_x} \sin S_x (\xi - d) - \frac{\epsilon_2}{\delta_2} \cos S_x (\xi - d) = 0 \quad (35)$$

(166)

from:

$$\begin{aligned}\sin(z_1 + z_2) &= \sin z_1 \cos z_2 \\ &\quad + \cos z_1 \sin z_2\end{aligned}$$

$$\begin{aligned}\cos(z_1 + z_2) &= \cos z_1 \cos z_2 \\ &\quad - \sin z_1 \sin z_2\end{aligned}$$

we can write:

$$\begin{aligned}\sin s_x(\ell-d) &= \sin s_x \ell \cos s_x d \\ &\quad - \cos s_x \ell \sin s_x d\end{aligned}$$

$$\begin{aligned}\cos s_x(\ell-d) &= \cos s_x \ell \cos s_x d \\ &\quad + \sin s_x \ell \sin s_x d\end{aligned}$$

so we can write (35) as

$$\frac{\epsilon_1}{s_x} [\sin s_x \ell \cos s_x d - \cos s_x \ell \sin s_x d]$$

$$\begin{aligned}-\frac{\epsilon_2}{s_2} [\cos s_x \ell \cos s_x d + \sin s_x \ell \sin s_x d] \\ = 0 \quad (36)\end{aligned}$$

(167)

which can be written as

$$\left[ \frac{\epsilon_1}{S_x} \cos S_x d - \frac{\epsilon_2}{\delta_2} \sin S_x d \right] \sin S_x \} \quad (37)$$

$$-\left[ \frac{\epsilon_1}{S_x} \sin S_x d + \frac{\epsilon_2}{\delta_2} \cos S_x d \right] \cos S_x \} = 0$$

so (34)(35) can be written:

$$A \sin S_x \} - B \cos S_x \} = 0 \quad (37)$$

$$\frac{\epsilon_1}{S_x} \sin S_x \} + \frac{\epsilon_3}{\delta_3} \cos S_x \} = 0 \quad (34)$$

solution exists if  $\det = 0$

$$\Rightarrow \frac{\epsilon_3}{\delta_3} \left[ \frac{\epsilon_1}{S_x} \cos S_x d - \frac{\epsilon_2}{\delta_2} \sin S_x d \right] \quad (38)$$

$$+ \frac{\epsilon_1}{S_x} \left[ \frac{\epsilon_1}{S_x} \sin S_x d + \frac{\epsilon_2}{\delta_2} \cos S_x d \right] = 0$$

(168)

expanding,

$$\frac{\epsilon_3}{\delta_3} \frac{\epsilon_1}{\delta_1} \cos \delta_x d - \frac{\epsilon_3 \epsilon_2}{\delta_3 \delta_2} \sin \delta_x d$$

$$+ \frac{\epsilon_1^2}{\delta_x^2} \sin \delta_x d + \frac{\epsilon_1 \epsilon_2}{\delta_x \delta_2} \cos \delta_x d = 0$$

recombining,

$$\frac{\epsilon_1}{\delta_x} \left( \frac{\epsilon_3}{\delta_3} + \frac{\epsilon_2}{\delta_2} \right) \cos \delta_x d$$

$$- \left( \frac{\epsilon_3 \epsilon_2}{\delta_3 \delta_2} - \frac{\epsilon_1^2}{\delta_x^2} \right) \sin \delta_x d = 0$$

results in:

$$\tan(\delta_x d) = G(\delta_x d) \quad (39)$$

(169)

where  $G(S_x d) =$ 

$$\frac{\frac{\epsilon_1}{A_x} \left( \frac{\epsilon_3}{\delta_3} + \frac{\epsilon_2}{\delta_2} \right) \cdot \left( \frac{S_x^2 \delta_3 \delta_2}{A_x^2 \delta_3 \delta_2} \right)}{\left( \frac{\epsilon_3 \epsilon_2}{\delta_3 \delta_2} - \frac{\epsilon_1^2}{A_x^2} \right)} \quad // G(S_x d)$$

$$= \frac{A_x \epsilon_1 (\epsilon_3 \delta_2 + \epsilon_2 \delta_3)}{(\epsilon_3 \epsilon_2 A_x^2 - \epsilon_1^2 \delta_3 \delta_2)} \quad (40)$$

where

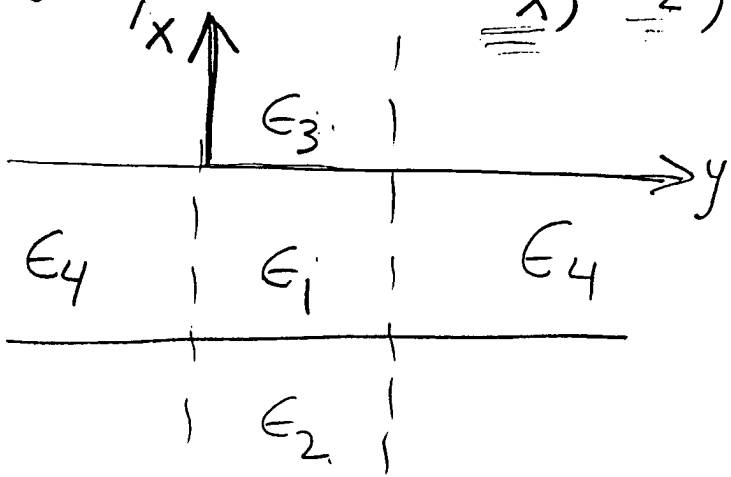
$$\delta_2 = [( \epsilon_1 - \epsilon_2 ) k_0^2 - A_x^2]^{1/2}$$

$$\delta_3 = [( \epsilon_1 - \epsilon_3 ) k_0^2 - A_x^2]^{1/2}$$

$$k_0 = \frac{2\pi}{\lambda_0} \leftarrow | \textcircled{d} \textcircled{s} \rightarrow$$

(170)

Note, we have the field components  $E_x, E_z, H_y, H_z$



From the point of view of

this guide,  
we have a

"TM" mode:  $E_x$  is  $\perp$  to the boundary.

The phase parameter} is determined from (34):

$$\frac{\epsilon_1}{S_x} \sin S_x \xi + \frac{\epsilon_3}{S_2} \cos S_x \xi = 0$$

why  $H_2$  instead of  $E_2$ ?  
because  $H_2 \rightarrow E_2$  satisfies eggs for  $E_2$ ,  $H_2 \in \{1, 5\}$ :  
Note:  $E_2$  satisfies as  $n_1, n_3, n_4, n_5 \rightarrow n_1 - 1$   
so approx improves for

OR,

$$\tan S_x \{ = - \frac{\epsilon_3}{\epsilon_1} \frac{S_x}{S_y} \quad (41)$$

Finally, require  $H_2$  continuous  
at  $y=0$ , D:

$$H_2^{(1)}(x, 0^+) = H_2^{(5)}(x, 0^-) \Rightarrow$$

$$H_2^{(1)} = -A \sqrt{\frac{\epsilon_0}{\mu_0}} \epsilon_1 \left( \frac{S_y}{S_x} \right) \left( \frac{k_0}{\beta} \right) \sin S_x (x + \{ )$$

$$y=0^+ \cdot \sin S_y \eta \quad (p(7), 2/24, E_g(5))$$

$$H_2^{(5)} = A \sqrt{\frac{\epsilon_0}{\mu_0}} \epsilon_1 \left( \frac{S_y}{S_x} \right) \left( \frac{k_0}{\beta} \right) \sin S_x (x + \{ )$$

$$y=0^- \cdot \cos S_y \eta \cdot 1 \quad (p(3), 3/1, E_g(30))$$

SO:

$$-\frac{S_y}{S_x} \sin S_y \eta = \frac{S_y}{S_x} \cos S_y \eta$$

OR,

$$(42) \quad S_5 \cos S_y \eta + S_y \sin S_y \eta = 0$$

at  $y = b$ ,

$$H_2^{(1)} = -A\sqrt{\frac{\epsilon_0}{\mu_0}} \epsilon_i \left( \frac{S_y}{S_x} \right) \frac{k_0}{\beta} \sin S_x(x+\xi)$$

$y=b$

$$\cdot \sin S_y(b+\eta) \quad (p\textcircled{1}, \textcircled{2}/4, \textcircled{5})$$

$$H_2^{(2)} = -A\sqrt{\frac{\epsilon_0}{\mu_0}} \epsilon_i \left( \frac{S_y}{S_x} \right) \frac{k_0}{\beta} \sin S_x(x+\xi)$$

$y=b^+$

$$\cdot \cos S_y(b+\eta) \quad (1) \quad (p\textcircled{3}, \textcircled{3}/1, \epsilon_9\textcircled{30})$$

so

$$-S_y \sin S_y(b+\eta)$$

$$= -S_y \cos S_y(b+\eta), \text{ or}$$

$$S_y \cos S_y(b+\eta) - S_y \sin S_y(b+\eta) = 0$$

(43)

since

$$\cos S_y(b+\eta) = \cos S_y b \cdot \cos S_y \eta - \sin S_y b \cdot \sin S_y \eta, \text{ and}$$

$$\begin{aligned} \sin S_y(b+\eta) &= \sin S_y b \cdot \cos S_y \eta \\ &\quad + \cos S_y b \cdot \sin S_y \eta \end{aligned}$$

(43)  $\Rightarrow$

$$\begin{aligned} S_y [\cos S_y b \cdot \cos S_y \eta] \\ - \sin S_y b \cdot \underline{\sin S_y \eta} \end{aligned}$$

$$\begin{aligned} -S_y [\sin S_y b \cdot \cos S_y \eta] \\ + \cos S_y b \cdot \underline{\sin S_y \eta}] = 0 \end{aligned}$$

and rearranging (43')

(174)

$$\begin{aligned}
 & \underbrace{\left\{ \delta_4 \cos \delta_y b - \delta_y \sin \delta_y b \right\} \cos \delta_y \eta}_{\text{``A''}} \\
 & - \underbrace{\left\{ \delta_4 \sin \delta_y b + \delta_y \cos \delta_y b \right\} \sin \delta_y \eta} \\
 & = 0 \quad \text{``B''} \quad (43'')
 \end{aligned}$$

we can write: (43'' + 42)

$$A \cos \delta_y \eta - B \sin \delta_y \eta = 0$$

$$\delta_5 \cos \delta_y \eta + \delta_y \sin \delta_y \eta = 0$$

which has a solution if

$$\det t = 0 \Rightarrow,$$

$$\begin{aligned}
 & \delta_y \left\{ \delta_4 \cos \delta_y b - \delta_y \sin \delta_y b \right\} \\
 & + \delta_5 \left\{ \delta_4 \sin \delta_y b + \delta_y \cos \delta_y b \right\} \\
 & = 0 \quad (44)
 \end{aligned}$$

$$s_y(\delta_4 + \delta_5) \cos s_y b$$

$$-(s_y^2 - \delta_4 \delta_5) \sin s_y b = 0$$

$$\tan(s_y b) = \frac{s_y(\delta_4 + \delta_5)}{(s_y^2 - \delta_4 \delta_5)} \quad (45)$$

Remember Eq(16) on 2/3 p.⑧?

$$\tan(s_y b) = F(s_y b)$$

TE modes!!

$$\delta_4 = [(\epsilon_1 - \epsilon_4) k_y^2 - s_y^2]^{1/2}$$

$$\delta_5 = [(\epsilon_1 - \epsilon_5) k_y^2 - s_y^2]^{1/2}$$

and we can find  $\eta$  from (42):

$$\tan(s_y \eta) = -\frac{\delta_5}{\delta_4} \quad (46)$$

Note that we have completely determined the  $E_{pq}^x$  modes:

① solve (39) [3/1, p⑧]  
for  $\lambda_x$

② solve (41) [3/3, p①]  
for  $\xi$

$$\lambda_x \Rightarrow \xi_3, \xi_2$$

③ solve (45) [3/3, p⑤]  
for  $\lambda_y$

④ solve (46) [3/3, p⑤]  
for  $\eta$

$$S_y \Rightarrow \delta_4, \delta_5$$

⑤  $S_y, S_x \Rightarrow \beta [(\beta), \frac{\beta^2}{24} p(5)]$

$$\beta^2 = E_1 k_s^2 - S_x^2 - S_y^2 \quad (47)$$

or use other formulas:

Eq (20), 2/24, p ⑪,

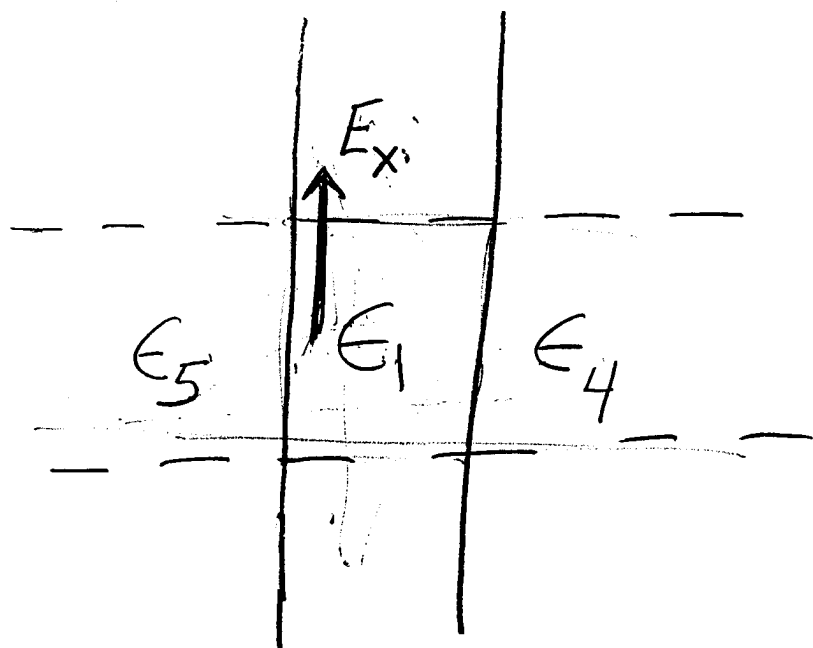
Eq (23), 2/24, p ⑬,

Eq (26), 3/1, p ⑩,

Eq (33), 3/1, p ⑭,

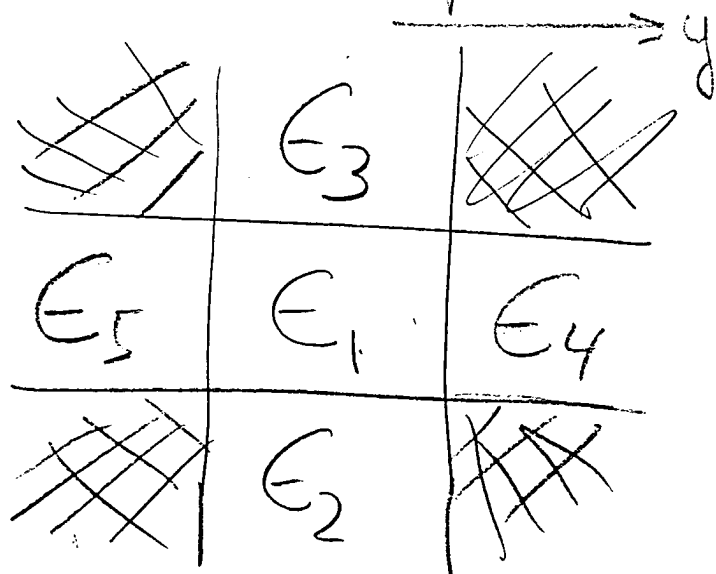
We can specify  $\vec{E}$  &  $\vec{H}$   
everywhere (approximately)

From the point of view  
of  $\epsilon_1, \epsilon_4, \epsilon_5$ , we have  
a TE mode --  $E_x$  is  
parallel to the boundary  
( $E_x$  is the dominant electric  
field)



$E_{pq}^x$ : P, q are mode #s  
indicating the number

of maxima of the field distribution in the  $x$  and  $y$  directions  $\uparrow^*$



- We have a field distribution for the core (0) and regions ②, ③, ④, + ⑤
- not for shaded regions
- solution not exact
- BC's not "exactly" matched in regions ①, ②, ③, ④, + ⑤

• BC match improves  
as  $\epsilon_2, \epsilon_3, \epsilon_4, \epsilon_5 \rightarrow \epsilon_1$   
(approximate solutions  
are best for small  $\Delta\epsilon$ )

• Theory assumed "far from  
cutoff"

• Marcatali's method  
led to the effective  
index method  $\rightarrow$  concept  
of treating a 2D WG  
as two 1D WGs

$$\Rightarrow n_{f_{2D}} \cong n_{f_{1D}} \cdot n_{f_{1D}}$$

$$\Rightarrow f_{f_{2D}} \cong f_{f_{1D}} \cdot f_{f_{1D}}$$

$$\frac{2b}{\lambda} (\epsilon_1 - \epsilon_4)^{\frac{1}{2}} \rightarrow$$

DIELECTRIC WAVEGUIDE

(#P)  
181

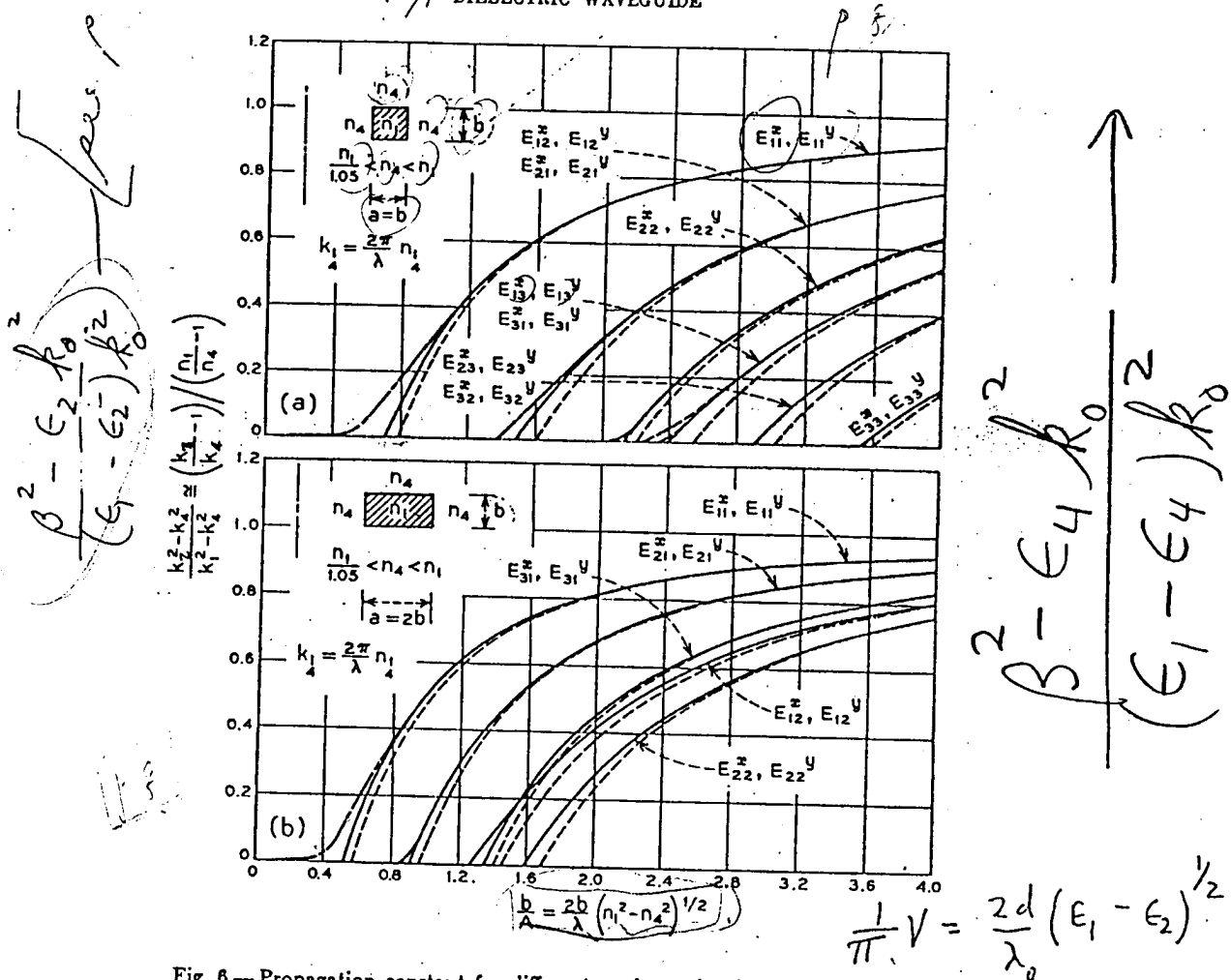


Fig. 6—Propagation constant for different modes and guides. — transcendental equation solutions; - - - closed form solutions; - · - Goell's computer solutions of the boundary value problem.

for several geometries and surrounding media.\* The ordinate in each of these figures is

$$\frac{k_s^2 - k_4^2}{k_1^2 - k_4^2};$$

it varies between 0 and 1. It is 0 when  $k_1 = k_2$ , that is, when the guide

\* In these figures we use the same symbol  $k_s$  for both the  $E_{p_1}$  and the  $E_{p_2}$  modes.

(12)  
(182)

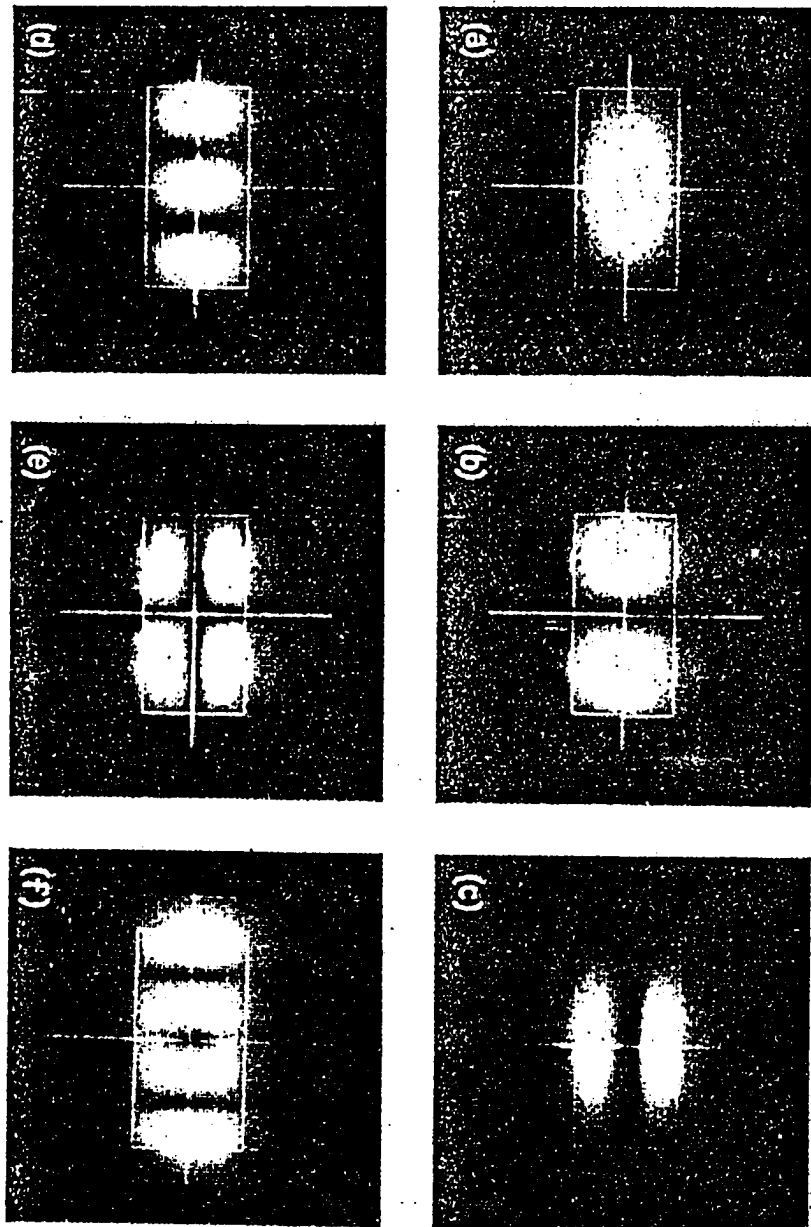


FIG. 6 — Intensity picture for some  $E'_{mn}$  modes with  $a/b = 2$ ,  $\mathfrak{R} = 2$ , and  $\Delta n_r = 0.01$ : (a)  $E'_{11}$ , (b)  $E'_{21}$ , (c)  $E'_{12}$ , (d)  $E'_{31}$ , (e)  $E'_{22}$ , and (f)  $E'_{41}$ .

THE BELL SYSTEM TECHNICAL JOURNAL, SEPTEMBER 1939

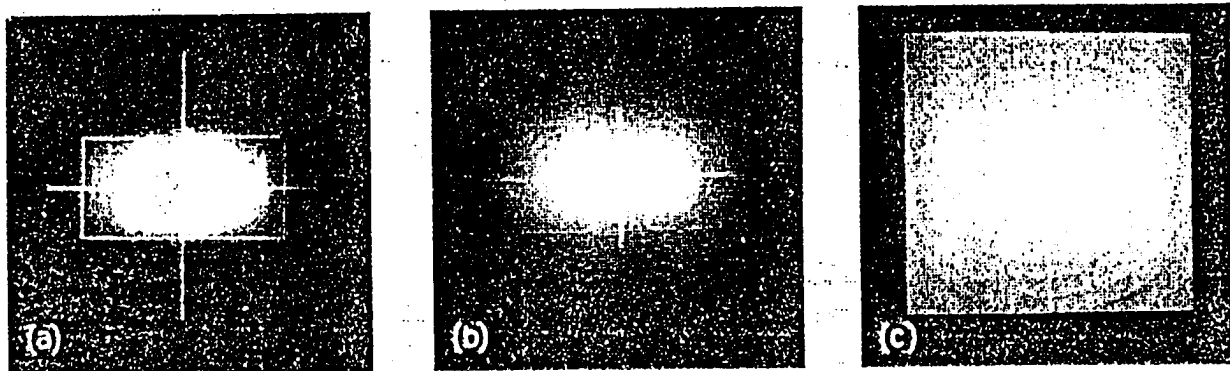


Fig. 14 — Intensity pictures of the  $E_{11}^*$  mode for (a)  $\Phi^2 = 0.81$ , (b)  $\Phi^2 = 0.50$ , and (c)  $\Phi^2 = 0.02$ .

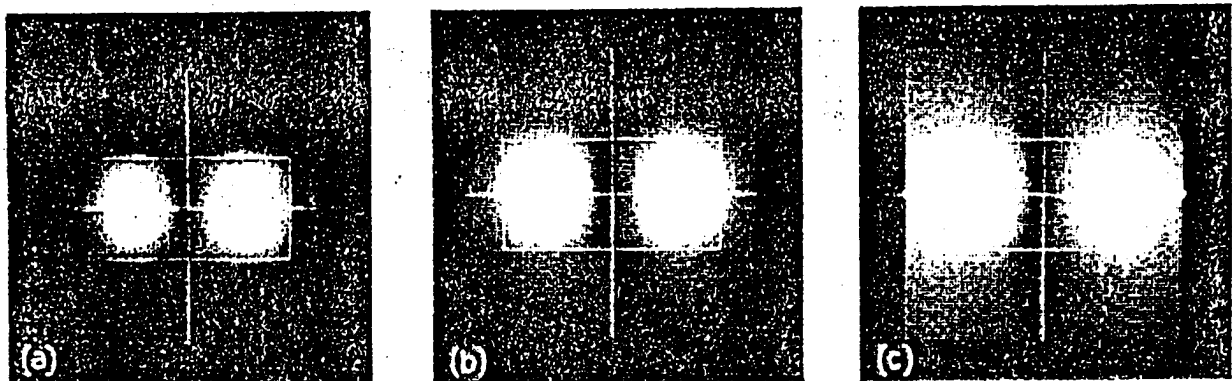


Fig. 15 — Intensity pictures of the  $E_{21}^*$  mode for (a)  $\Phi^2 = 0.76$ , (b)  $\Phi^2 = 0.31$ , and (c)  $\Phi^2 = 0.04$ .

(184)

text notation	class notation
$\rho^2 = \frac{(k_z/k_0)^2 - 1}{n_r^2 - 1}$	$\frac{(\beta/\epsilon_2 k_0)^2 - 1}{\epsilon_1/\epsilon_2 - 1}$

$$\beta = \frac{2b}{\lambda_0} (n_r^2 - 1) = \frac{2d}{\lambda_0} (\epsilon_1 - \epsilon_2)^{1/2}$$

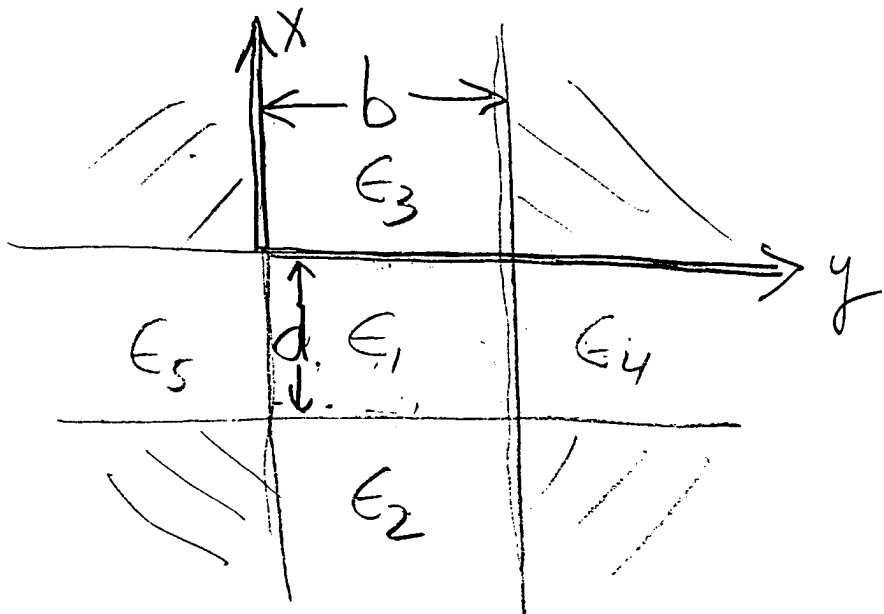
$$n_r = \frac{k_1}{k_0} = \sqrt{\frac{\epsilon_1}{\epsilon_2}}$$

also, can write

$$\rho^2 = \frac{\beta^2 - \epsilon_2 k_0^2}{(\epsilon_1 - \epsilon_2) k_0^2} \quad \text{in our class notation.}$$

Confusion arises because in Gloge's paper,  $k_0$  is the wavevector corresponding to a plane wave in the outside medium ( $\epsilon = \epsilon_0$ ,  $\epsilon_0 \neq$  free space value of  $\epsilon$ ). So Gloge's  $\lambda_0$  is not the free space wavelength, but  $\lambda_{f.s.}/\epsilon_{\text{medium}}$ .

Review:



- ① "solved Wave Eq. for  $E_z$
- ② chose  $E_{pq}^x$  polarization  
 $(H_x = 0 \Rightarrow H_z)$

$$E_z, H_z \Rightarrow E_x, E_y, H_x, H_y$$

$$|E_y| \ll |E_z| \ll |E_x|$$

$\Downarrow$   
 $\approx 0$

③  $|\vec{E}, \vec{H}| \rightarrow 0$  at  $x, y \rightarrow \infty$

④ Obtained  $\vec{E}, \vec{H}$  in

②, ③ ( $E_z$  cont')

$(E_y \approx 0)$

⑤ Obtained  $\vec{E}, \vec{H}$  in

④, ⑤ ( $E_x$  cont')

$(E_y \approx 0, E_z \ll E_x)$

$$\Rightarrow \left( \frac{\epsilon_1}{\epsilon_i} \right) \quad i = 4, 5$$

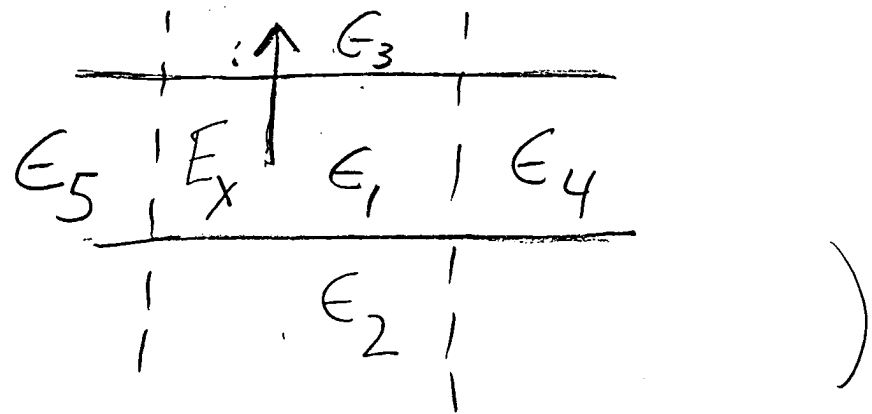
⑥ Req  $H_z$  cont' @ ②, ③

$(x=0, -d)$

⑦ obtained 2 Eq's,  
2 unknowns

$$\Rightarrow \tan(S_x d) = G(S_x d)$$

(TM modes of



⑧ require  $H_z$  cont'

@  $y=0, b$

$\Rightarrow$  2 Eqs, 2 unknowns

$\Rightarrow$  TE modes

The  $E_{pq}^y$  modes  
are derived similarly:

Require  $H_y = 0 \Rightarrow$

$$E_x \ll |E_z| \ll |E_y|$$

$$E_x \approx 0$$

$$\tan(s_x d) = F(s_x d)$$

$$\tan s_x \bar{\gamma} = \delta_3 / s_x$$

and

$$\tan(s_y b) = G(s_y b)$$

$$\tan s_y \bar{\gamma} = \frac{\epsilon_5}{\epsilon_1} \frac{s_y}{s_5}$$

- ④ {The Effective Index Method}
- difficult to derive
  - intuitively appealing
  - more accurate than expected

Rationale:

consider the scalar equation:

$$(1) \frac{\partial^2 \psi}{\partial x^2} + \frac{\partial^2 \psi}{\partial y^2} + (n^2 k_0 - \beta^2) \psi = 0$$

$n$  = refractive index of core region (or a suitable

constant average value).

The field in the core  
has the form (approx)

$$\Psi = A \cos(s_x x) \cos(s_y y) \cdot \exp(-i\beta z) \quad (2)$$

(2) into (1)  $\Rightarrow$

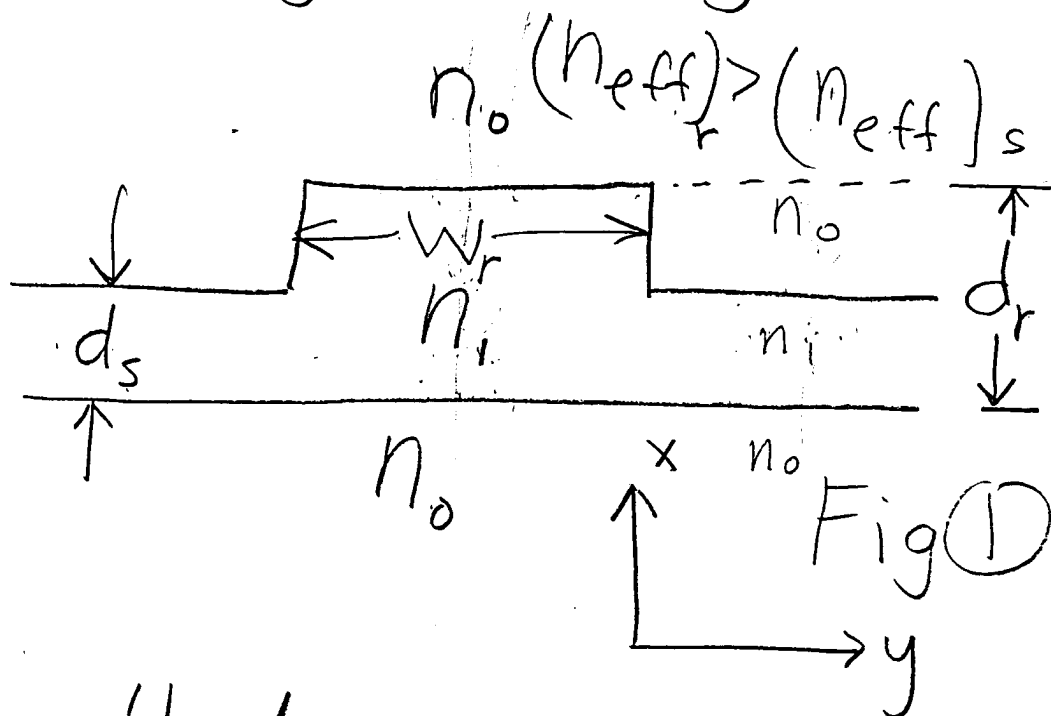
$$\beta = \sqrt{n^2 k_0^2 - s_x^2 - s_y^2} \quad (3)$$

$\Rightarrow$  if we know approx  
values of  $n$ ,  $s_x$ , and  $s_y$   
we can calculate  $\beta$ .

Illustration

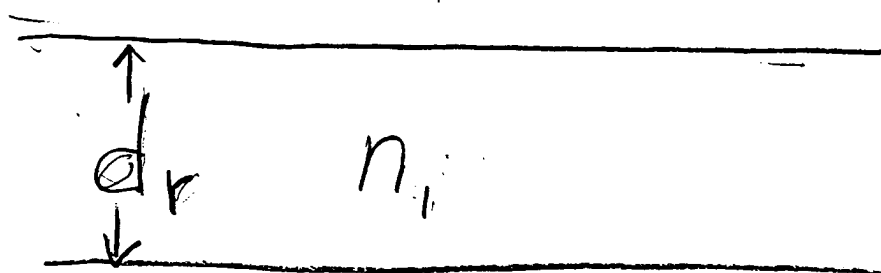
(191)

# ① Ridge Waveguide



method:

① ignore fact that  
 $W_r$  is finite  
 solve waveguide "A":  
 $n_o$



$n_o$  Fig(2)

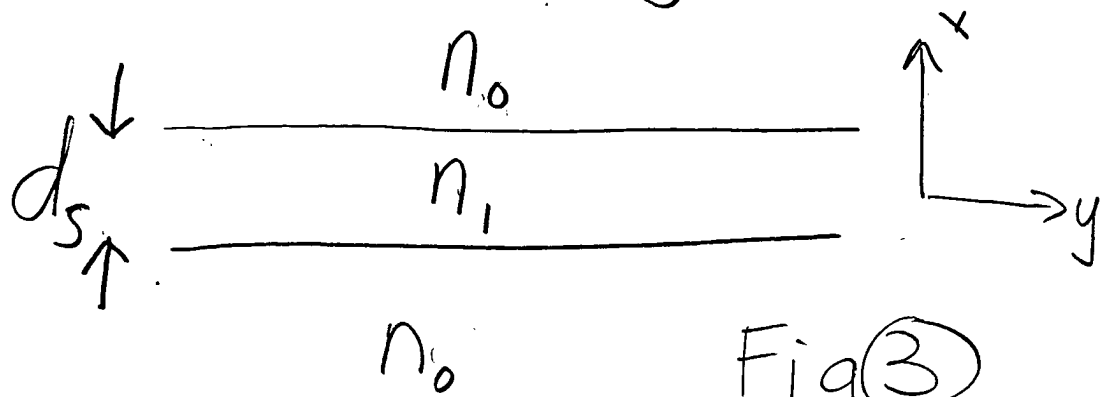
$$\tan(s_x d_r) = F(s_x d_r)$$

$\Rightarrow \beta_r$  the longitudinal propagation constant  
 for WG "A"  $\Rightarrow (n_{\text{eff}})_r = \frac{\beta_r}{k_0}$

Note:  $(n_{\text{eff}})_r$  is different

for every mode. For simplicity consider only fundamental mode

② solve waveguide "B"



$$\tan(s_x d_s) = F(s_x d_s)$$

$\Rightarrow \beta_s$  for WG "B"

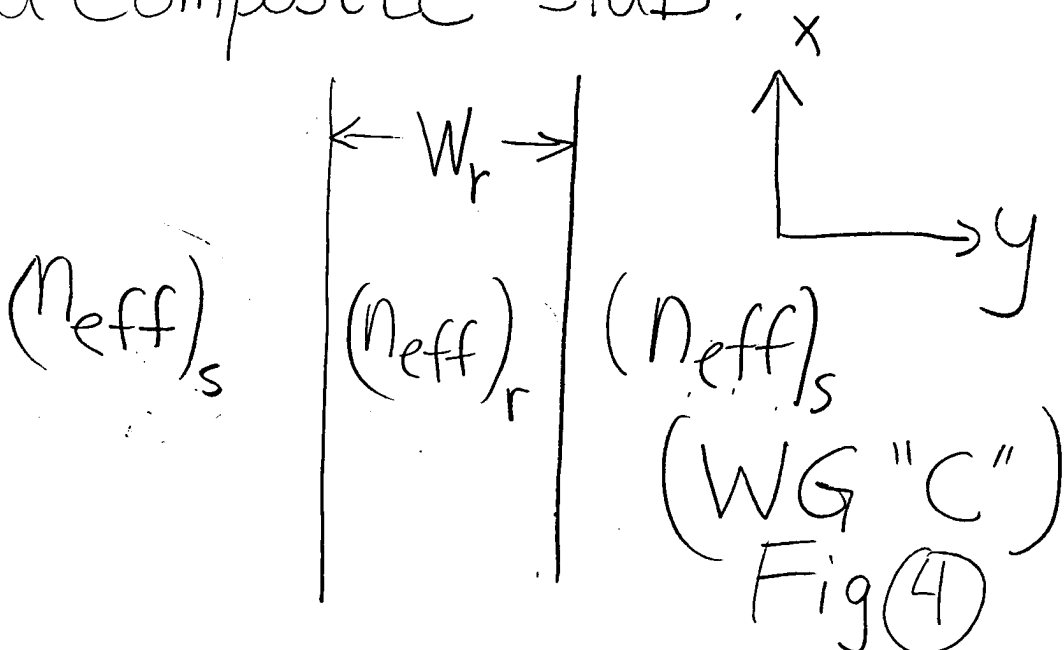
$$\Rightarrow (n_{\text{eff}})_s = \frac{\beta_s}{k_0}$$

note:

$$(n_{\text{eff}})_s < (n_{\text{eff}})_r$$

③

now consider Fig ① to be  
a composite slab:



④ Solve WG "C":

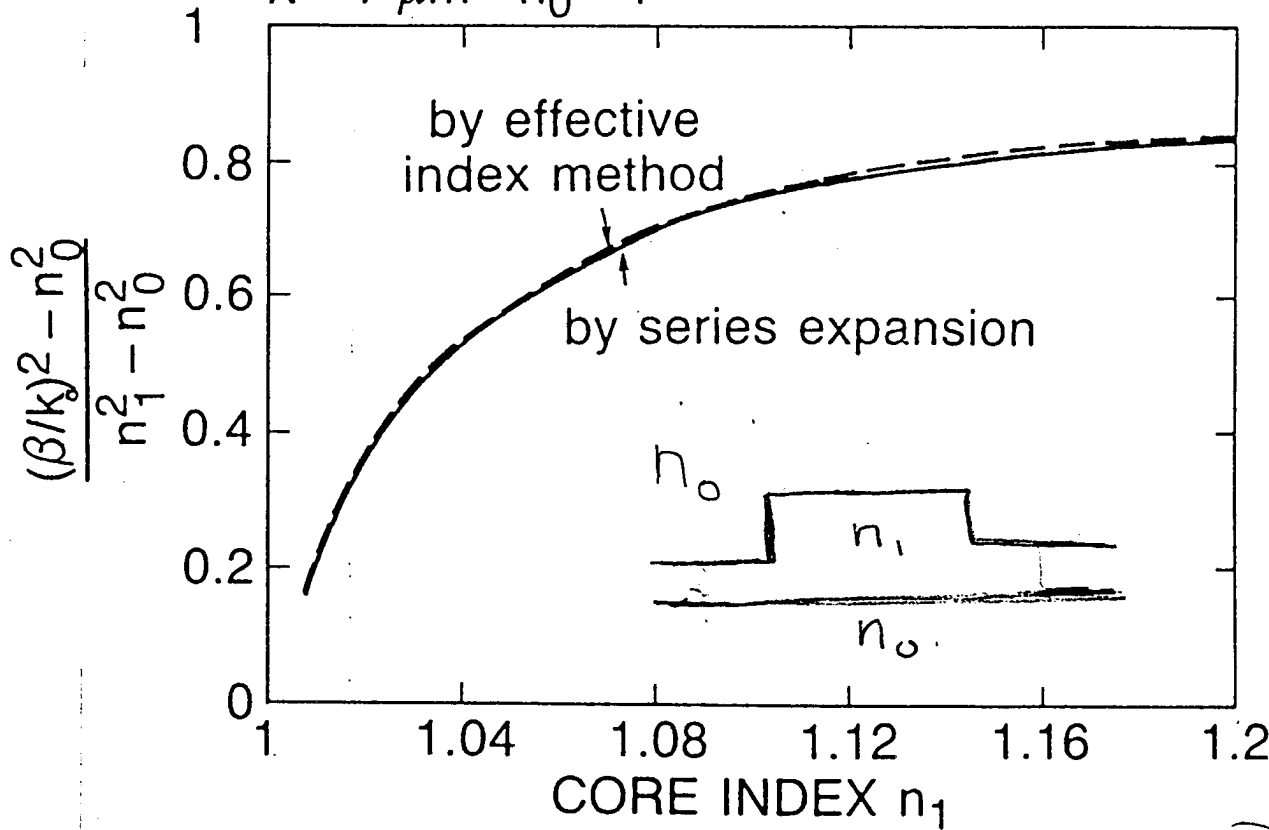
$$\tan(S_y W_r) = F(S_y W_r)$$

⑤ obtain  $\beta$  from(3):

$$\beta = \sqrt{n_1^2 k_0^2 - (S_x)_r^2 - (S_y)_r^2}$$

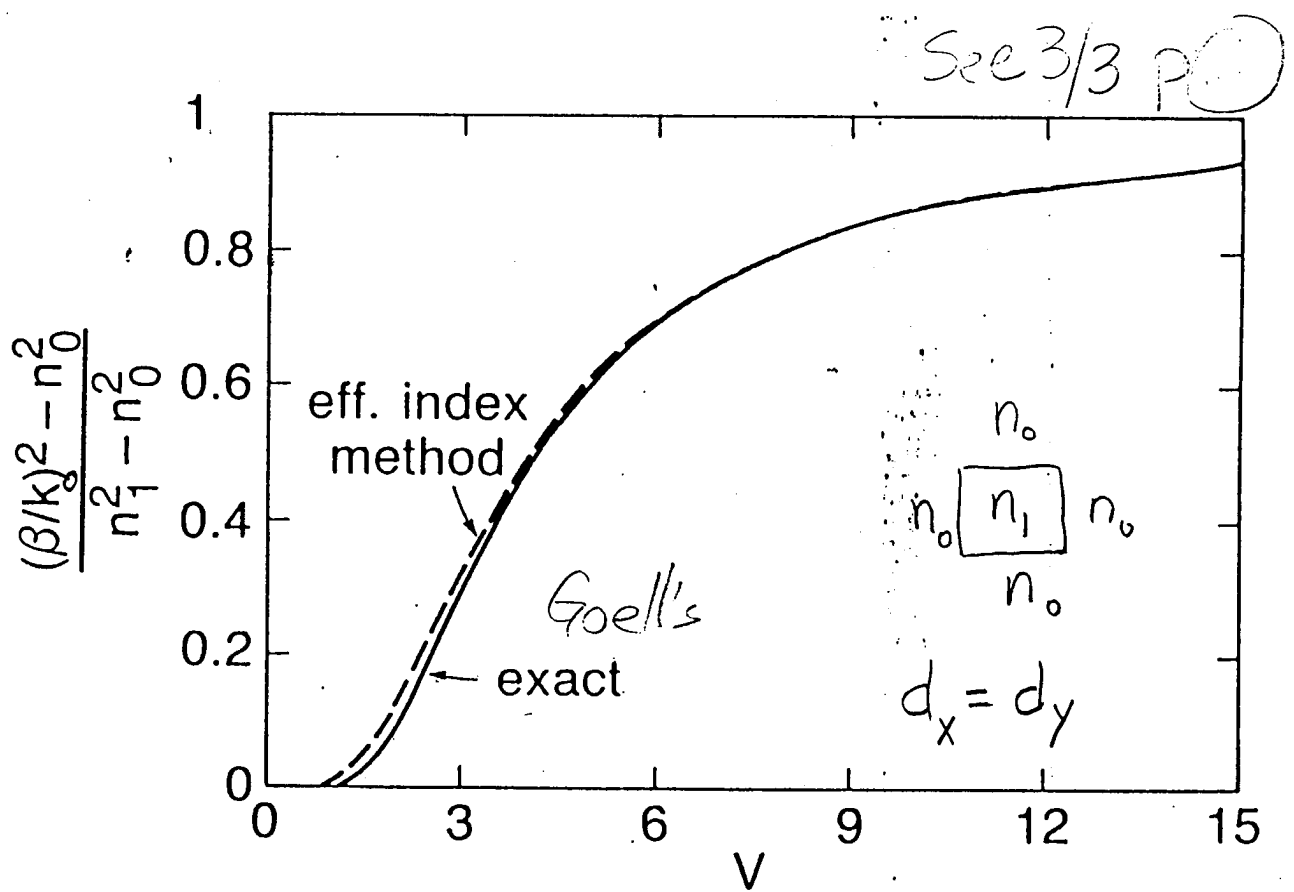
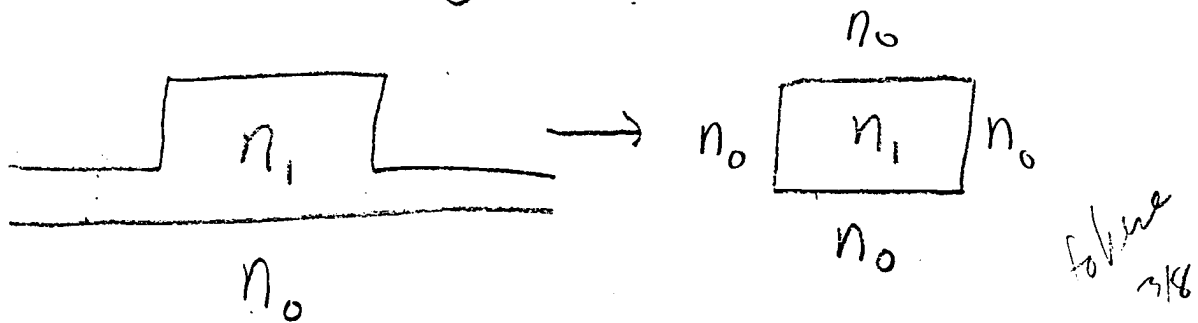
$$d_s = 1 \text{ } \mu\text{m}, d_r - d_s = 0.5 \text{ } \mu\text{m}, w = 5 \text{ } \mu\text{m}$$

$$\lambda = 1 \text{ } \mu\text{m} \quad n_0 = 1$$



Fia(5)

If  $d_s \rightarrow 0$ , ridge guide  
 $\rightarrow$  rectangular dielectric



$$V = \frac{2\pi d}{\lambda_0} \sqrt{n_1^2 - n_0^2}$$

Fig 6

• agreement between effective index method and numerical methods is remarkable (for  $\beta$ )

• effective index method works for any number of layers:

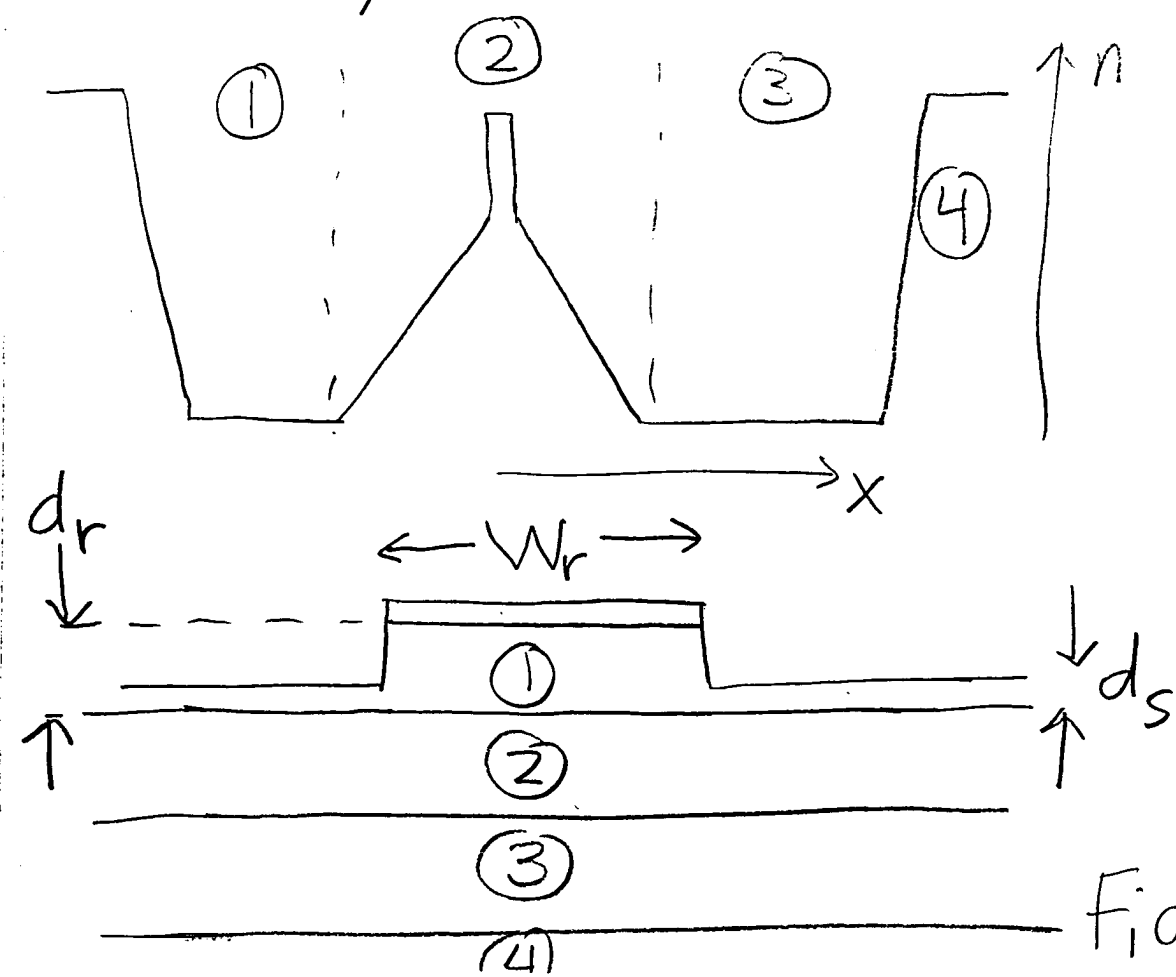
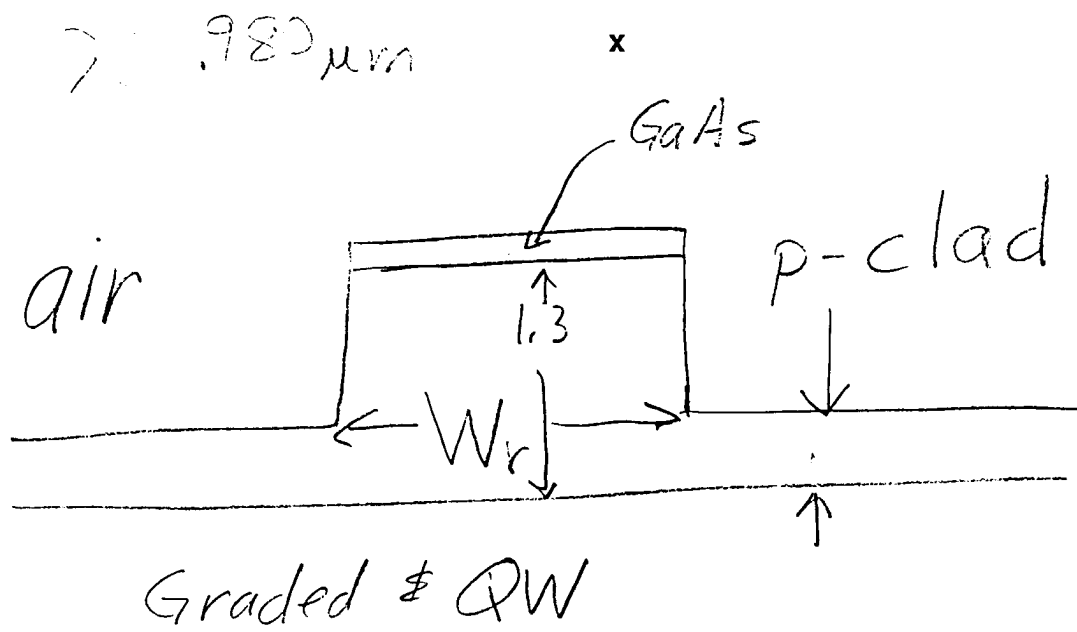
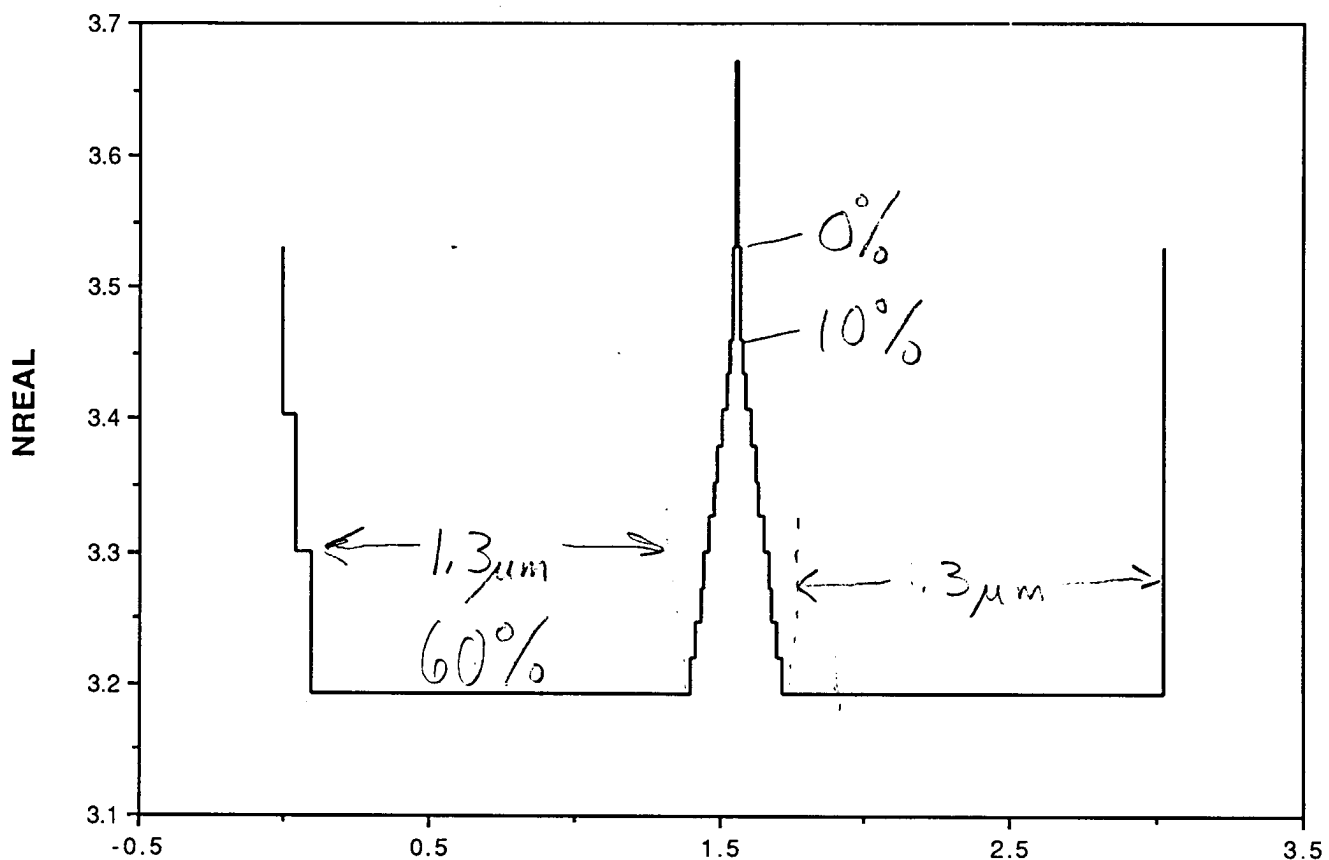


Fig ⑦

(197)

### Index Profile for GRIDGE-file



(198)

1

LL227

Tue, Jan 7, 1992

# Starting File (LL227)

CASE KASE=LINCOLN LABS (227)  
CASE EPS1=1E-7 GAMEPS=1E-3 QZMR=11.04 QZMI=0.0  
CASE PRINTF=0 INITG5=0 AUTOQW=0 NFPLT=0 FFPLT=0

MODCON KPOL=1 APB1=0.25 APB2=0.25

STRUCT NOW=3.67 WVL=.98  
STRUCT GRW=.15 QW=.0100  
STRUCT ALPERC1=.6 ALPERC2=0.4

LAYER ALPERC=.00 !GaAs substr  
LAYER ALPERC=.2 TL=0.05 !1st trans.  
LAYER ALPERC=.4 TL=0.05 !"  
LAYER ALPERC=^1 TL=1.3 ! n-Clad  
LAYER ALPERC=^1 ! 1st (n) GRINSCH  
LAYER NSLC=10 !"  
LAYER ALPERC=.1 !"  
LAYER ALPERC=.00 TL=.0075 ! 1st (n) Barrier  
LAYER QWS=1 ! QW GaIn(.14)As-LAYER  
LAYER ALPERC=.00 TL=.0075 !2nd (p) Barrier  
LAYER ALPERC=.1 !2nd (p) GRINSCH  
LAYER NSLC=10 !"  
LAYER ALPERC=^2 !"  
LAYER ALPERC=^2 TL=.1 !1st p-Clad-Layer28  
LAYER ALPERC=.3 TL=.005 !1st etch stop trans.  
LAYER ALPERC=.2 TL=.005 !"  
LAYER ALPERC=0.1 TL=0.00 !Etch stop AlGaAs-Grating -layer  
LAYER ALPERC=.2 TL=.005 !2nd etch stop trans.  
LAYER ALPERC=.3 TL=.005 !"  
LAYER ALPERC=^2 TL=1.0 !2nd p-Clad  
!LAYER NREAL=1.9 TL=.12 !SiN<sub>3</sub> insulator!  
!LAYER ALPERC=.08 TL=0.05 !"  
LAYER ALPERC=.00 TL=0.12 !GaAs Cap  
!LAYER NREAL=1 !Air

OUTPUT PHMO=1 GAMMAO=1 WZRO=1 WZIO=1 QZRO=1 QZIO=0  
OUTPUT FWHPNO=0 FWHPFO=0 KMO=1 ITO=1  
OUTPUT SPLTFL=1 MODOUT=0 LYROUT=1  
GAMOUT LAYGAM=17, 33 COMPGAM=0 GAMALL=0

!LOOPX1 ILX='TL' FINV=0.0 XINC=-0.05 LAYCH=30  
!LOOPZ1 ILZ='GRW' FINV=.15 ZINC=-.05  
!LOOPZ2 ILZ='WVL' FINV=0.955 ZINC=-0.005

!LOOPZ1 ILZ='QZMR' FINV=10.9 ZINC=-.05!THIS LOOPS TO FIND INITIAL GUESS  
!LOOPZ1 ILZ='GRW' FINV=.202 ZINC=.001  
!LOOPZ1 ILZ='ALPERC1' FINV=.401 ZINC=.0005  
LOOPX1 ILX='TL' FINV=.15 XINC=.001 LAYCH=33

END

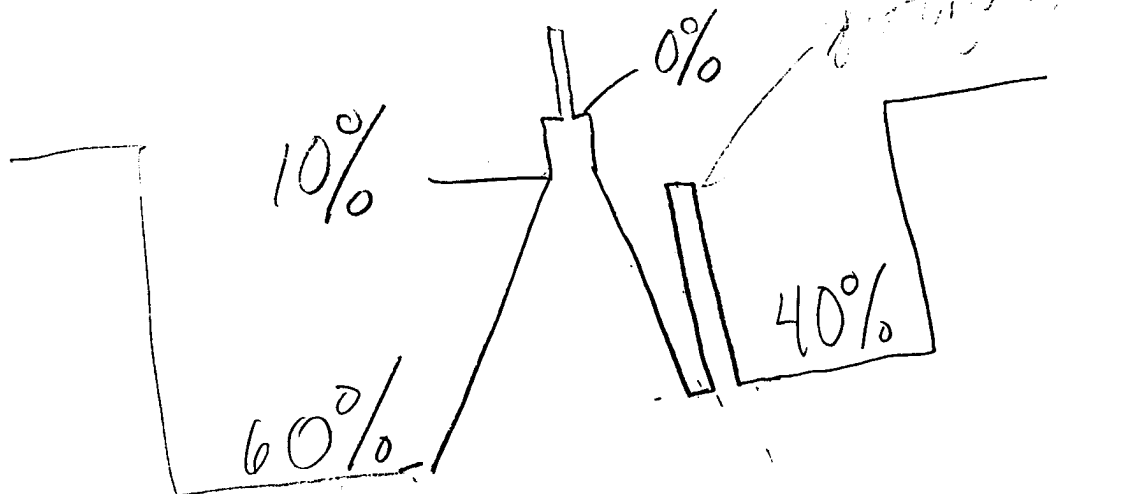
Strained QW  
@ 0.98 μm

# of layers = 31

LAYER01 NLOSS= .00000 NREAL= 3.52903 TL= .00000  
LAYER02 NLOSS= .00000 NREAL= 3.40297 TL= .05000  
LAYER03 NLOSS= .00000 NREAL= 3.29907 TL= .05000  
LAYER04 NLOSS= .00000 NREAL= 3.19192 TL= 1.30000  
LAYER05 NLOSS= .00000 NREAL= 3.19192 TL= .00750  
LAYER06 NLOSS= .00000 NREAL= 3.21877 TL= .01500  
LAYER07 NLOSS= .00000 NREAL= 3.24561 TL= .01500  
LAYER08 NLOSS= .00000 NREAL= 3.27245 TL= .01500  
LAYER09 NLOSS= .00000 NREAL= 3.29929 TL= .01500  
LAYER10 NLOSS= .00000 NREAL= 3.32613 TL= .01500  
LAYER11 NLOSS= .00000 NREAL= 3.35297 TL= .01500  
LAYER12 NLOSS= .00000 NREAL= 3.37981 TL= .01500  
LAYER13 NLOSS= .00000 NREAL= 3.40666 TL= .01500  
LAYER14 NLOSS= .00000 NREAL= 3.43350 TL= .01500  
LAYER15 NLOSS= .00000 NREAL= 3.46034 TL= .00750  
LAYER16 NLOSS= .00000 NREAL= 3.52903 TL= .00750  
LAYER17 NLOSS= .00000 NREAL= 3.67000 TL= .01000  
LAYER18 NLOSS= .00000 NREAL= 3.52903 TL= .00750  
LAYER19 NLOSS= .00000 NREAL= 3.46034 TL= .00750  
LAYER20 NLOSS= .00000 NREAL= 3.44421 TL= .01500  
LAYER21 NLOSS= .00000 NREAL= 3.42808 TL= .01500  
LAYER22 NLOSS= .00000 NREAL= 3.41196 TL= .01500  
LAYER23 NLOSS= .00000 NREAL= 3.39583 TL= .01500  
LAYER24 NLOSS= .00000 NREAL= 3.37970 TL= .01500  
LAYER25 NLOSS= .00000 NREAL= 3.36358 TL= .01500  
LAYER26 NLOSS= .00000 NREAL= 3.34745 TL= .01500  
LAYER27 NLOSS= .00000 NREAL= 3.33132 TL= .01500  
LAYER28 NLOSS= .00000 NREAL= 3.31519 TL= .01500  
LAYER29 NLOSS= .00000 NREAL= 3.29907 TL= .00750  
LAYER30 NLOSS= .00000 NREAL= 3.29907 TL= .10000  
LAYER31 NLOSS= .00000 NREAL= 3.52903 TL= .00000

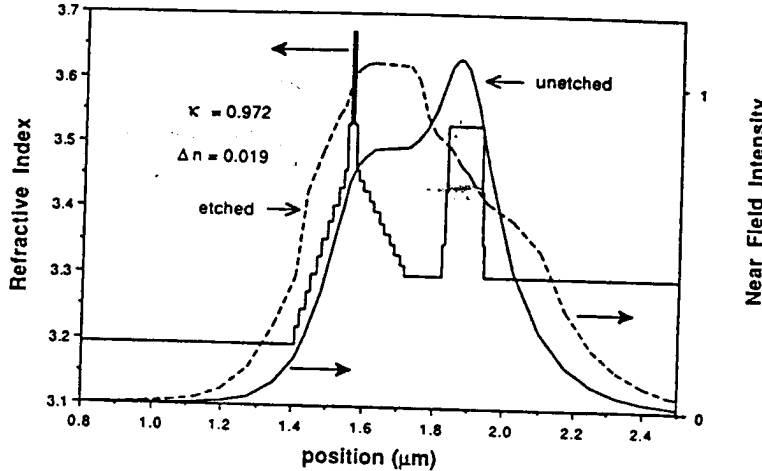
\*\*\*\*\*

LL 227 Layers



SQW  $\Rightarrow$  InGaAs

199

S:007  
S:008  
S:009  
S:010  
S:011  
S:012S:013  
S:014  
S:015  
S:016  
S:017  
S:018  
S:019  
S:020  
S:021  
S:022  
S:023

**Fig. 36.** Index profile for a buried grating MOPA and the near field distributions for a section of the device where the grating layer has been etched completely through with a 50% duty cycle and square wave profile, and a section of the device with the grating layer intact (not etched).

where the grating is not etched, reducing the effective index difference and increasing the mode overlap (Eq. 11) between the two regions.

Another source of reflections is from the terminations of the waveguide. If the ends are uncoated cleaved facets, reflections of 30% are expected (Eq. 24). These reflections can be greatly reduced by many techniques including sawing the ends at an angle or applying anti-reflection coatings. Another approach to minimizing reflections is to make the end sections of the waveguide highly lossy by implanting damage or by having an extended, passive grating outcoupling region. Most of these techniques can essentially eliminate end reflections.

S:024  
S:025  
S:026  
S:027  
S:028  
S:029  
S:030  
S:031  
S:038

## 2. Cascaded GSE-MOPA Arrays

To optimize power and efficiency from a chain of  $N$  identical cascaded power amplifiers and output coupler sections, the coupling strength of each grating coupler and the operating level of each amplifier must be selected so that the total losses of each grating section is balanced by the single-pass gain of each amplifier, as explained below (Mehuys et al., 1991b; Carlson et al., 1990a). Also, the transmission of each passive waveguide (with grating output coupler) must be sufficiently large so that the input power to each amplifier in the chain is high enough to saturate the gain to a level where

S:036 0252"01893"16252

(201)

7055 4 1 40 36 Galley 4

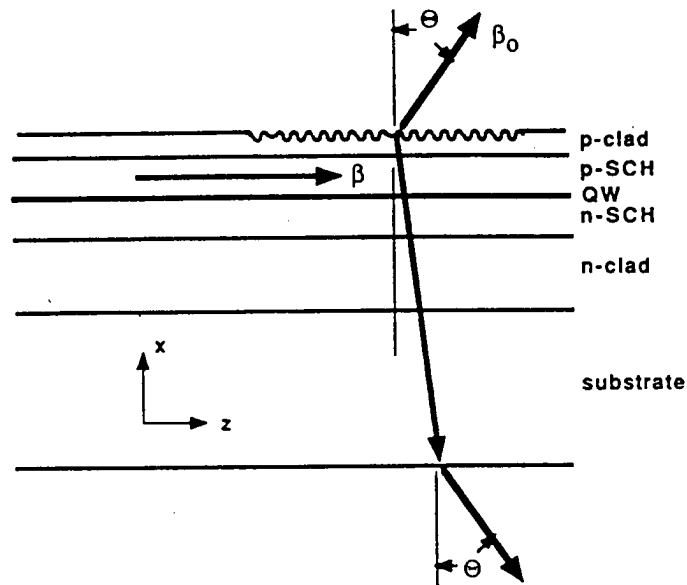


14001  
14003

122

G. A. Evans et al.

14004



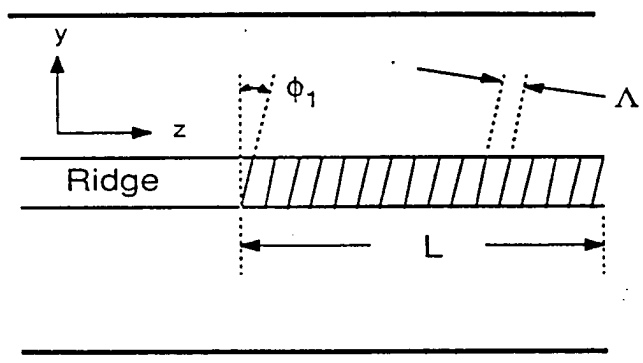
a)

14008  
14009  
14010  
14011

Fig. 2. (a) Sideview of a dielectric waveguide with a periodic surface corrugation; (b) top view showing the grating lines at an angle  $\Phi_1$  with respect to the direction of propagation.

14014

0042'''00359



b)

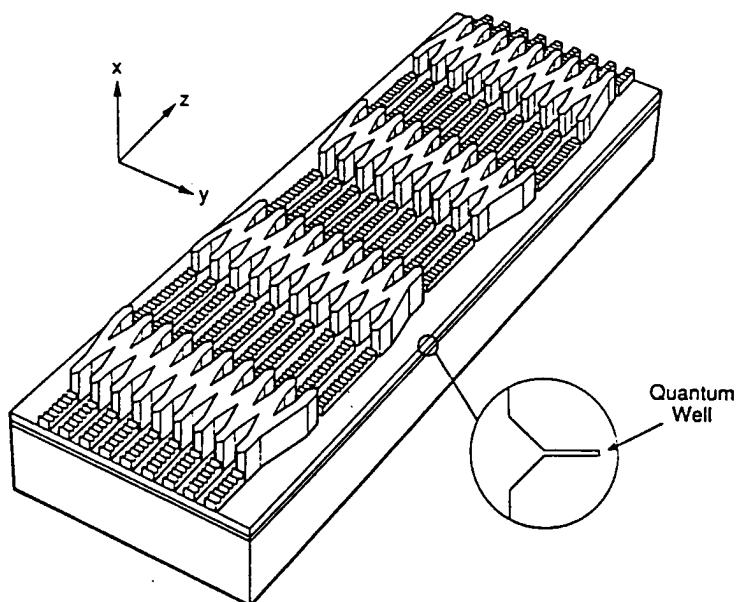
## 1002 Grating-Coupled Surface Emitting Semiconductor Lasers

129

1006 arrays (Liew *et al.*, 1991a). Single element arrays have achieved linewidths  
 1008 of less than 300 kHz (Carlson *et al.*, 1990b).

## 1010 D. Two-Dimensional GSE Arrays

1011 One approach to expand linear arrays into a two-dimensional array is by  
 1012 expanding each single gain section in the lateral direction as shown in Figs.  
 1013 5 and 6. As in one-dimensional arrays, the basic building block of two-  
 1014 dimensional arrays is the single-element GSE discussed above. Lateral  
 1015 coupling of the gain sections can be achieved using the methods discussed  
 1016 in Chapter 2 for edge-emitting arrays. Simple evanescent coupling of ridge-  
 1017 guided lasers has been mainly used for lateral coupling (Evans *et al.*, 1988b;  
 1018 Evans *et al.*, 1991), but Y-guide coupling (Streifer *et al.*, 1987; Welch *et al.*,  
 1019 1987) and 3-dB coupling has also been tried in GSE lasers (Evans *et al.*,  
 1020 1989). As in one-dimensional arrays, the grating performs several functions  
 1021 that are essential for phase-locked operation of the surface emitting array.  
 1022 The grating period is chosen so that the second diffraction order acts as a  
 1023 Bragg reflector in the waveguide plane, which provides the optical feedback



1024  
 1025 Fig. 5. Sketch of a  $10 \times N$  array showing four gain sections with Y-coupling. The  
 1026 quantum-well waveguide is common to both gain and grating regions.

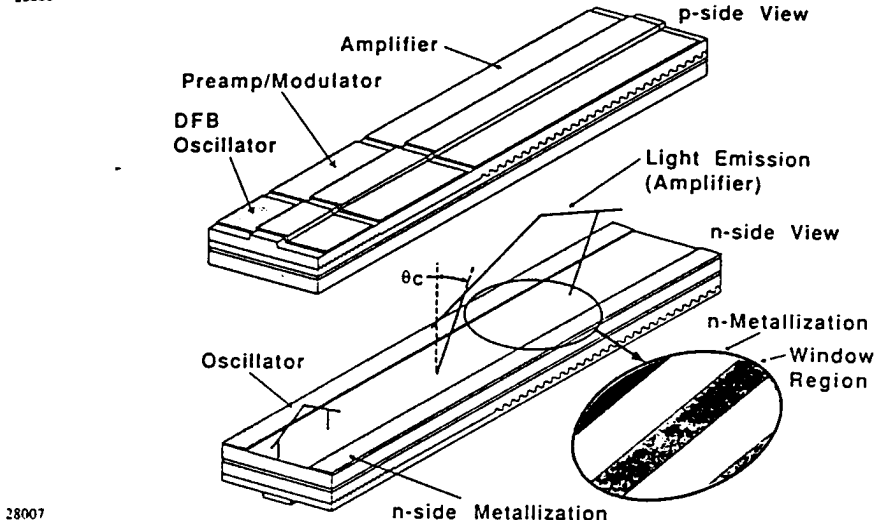
1027  
 1028  
 1029 0201'''01599



28003 136

G. A. Evans et al.

28004



28008 Fig. 13. Sketch of a continuous active grating GSE-MOPA device. Emission of  
28009 the grating output coupled light is in the "forward" direction. Inset shows the  
28010 window region for emission from the substrate side.

28011 aspect ratio using the simple external optics shown in Fig. 14 (Carlson et  
28012 al., 1990g; Liew et al., 1990).

28013 The continuous active-grating MOPA requires only two or three independent  
28014 electrodes, one for the oscillator, one for the amplifier, and possibly  
28015 one for a pre-amplifier. A pre-amplifier (without outcoupling) is useful to  
28016 match the output power of the oscillator to the saturation power of the  
28017 outcoupling amplifier region, resulting in the best far field pattern. Addi-  
28018 tional independent electrodes could be incorporated in the amplifier region  
28019 by fabricating segmented contacts, allowing some electronic control of the  
28020 beam pattern. The reduced number of independent electrodes is a significant  
28021 simplification over present GSE oscillator arrays and chained amplifiers.  
28022 and noise suppression.

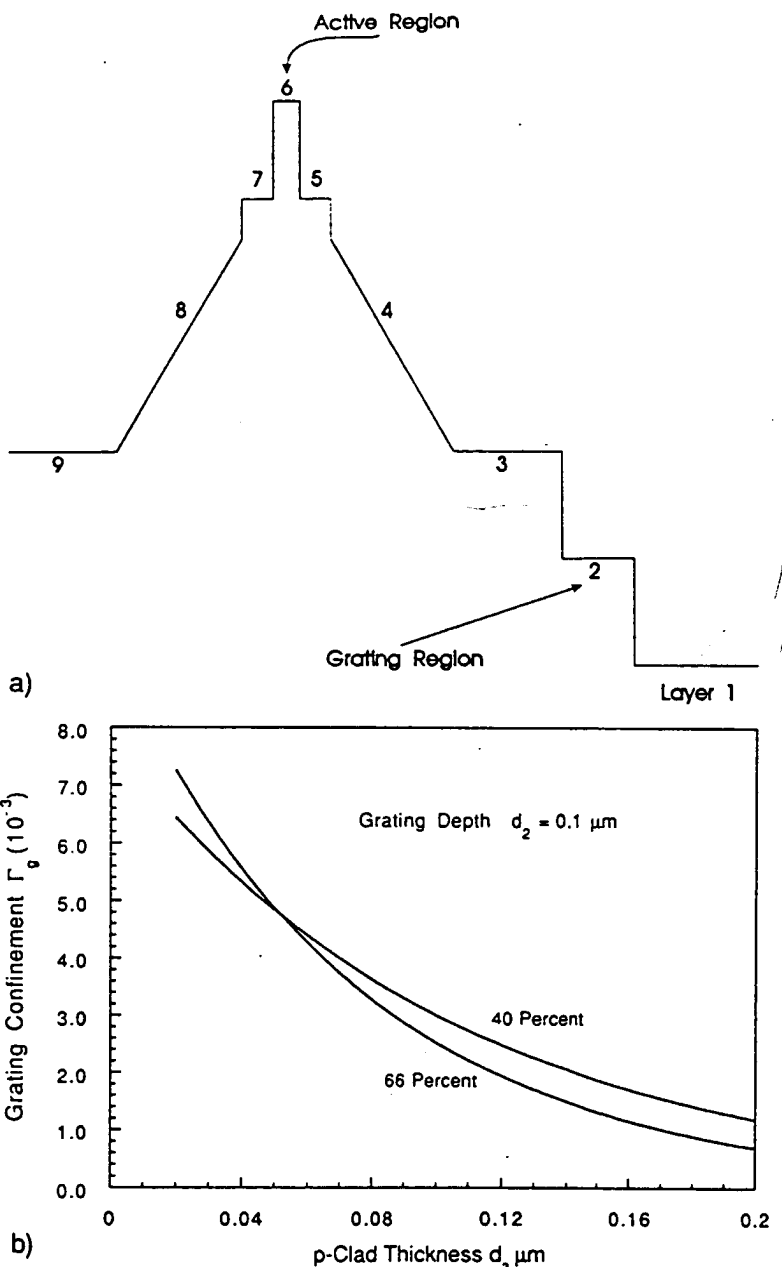
### 28025 III. DESIGN CONSIDERATIONS

#### 28026 A. GSE Oscillator Arrays

##### 28027 1. Structure Considerations

28028 As in most semiconductor lasers, GSE lasers require an active region  
28029 designed for efficiency and high power. The massive waveguide grating

28031 0176"01536



34008      Fig. 19. (a) Index profile of the GRINSCH-SCH structure shown in Fig. 15 with  
 34009      a grating at the p-clad/air interface, graded region thickness of  $0.15 \mu\text{m}$ , and 66% or 40%  
 34010      AlAs in the cladding regions; (b) the grating confinement factor for a  $1000 \text{ \AA}$  deep  
 34011      grating as a function of the p-clad thickness; (c) the grating confinement factor as  
 34012      a function of grating depth for a p-clad thickness of  $1000 \text{ \AA}$ .  
 34013  
 34014

34016      0074"00558

205

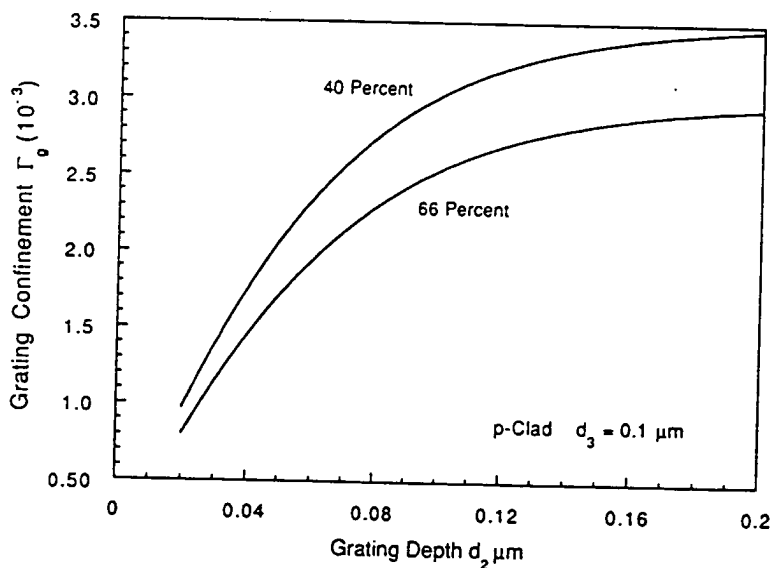
35001  
35002 Grating-Coupled Surface Emitting Semiconductor Lasers

35004  
35007 3. *Grating design*

35008 The etching required to produce a lateral index ridge exposes a surface  
 35009 in the region between the gain sections that is near the appropriate level  
 35010 for a grating to outcouple radiation. The fraction of the mode power  $\Gamma_{gr}$   
 35011 interacting with a grating formed at the *p*-clad/air interface (Fig. 19(a)) is  
 35012 given by

$$35013 \quad \Gamma_{gr} = \int_{gr} |E_w(x)|^2 dx / \int_{-\infty}^{\infty} |E_w(x)|^2 dx, \quad (10)$$

35014 where  $E_w(x)$  is the transverse field distribution in the waveguide section  
 35015 and the integral in the numerator is performed over the width of the grating  
 35016 region. The variation of  $\Gamma_{gr}$  (which is called the grating confinement factor)  
 35017 is shown in Fig. 19(b) as a function of the distance of the grating above  
 35018 the graded layer, for the laser structure described in Fig. 15 with a *p*-clad  
 35019 composition of 66% and a graded region thickness of 0.15  $\mu\text{m}$ . In these  
 35020 numerical calculations, the thickness of the grating region is the peak-to-



c)

35022

Fig. 19. Continued.

35024

35027 0167"01359

206

# of layers = 31

LAYER01	NLOSS= .00000	NREAL= 3.52903	TL= .00000
LAYER02	NLOSS= .00000	NREAL= 3.40297	TL= .05000
LAYER03	NLOSS= .00000	NREAL= 3.29907	TL= .05000
LAYER04	NLOSS= .00000	NREAL= 3.19192	TL= 1.30000
LAYER05	NLOSS= .00000	NREAL= 3.19192	TL= .00750
LAYER06	NLOSS= .00000	NREAL= 3.21877	TL= .01500
LAYER07	NLOSS= .00000	NREAL= 3.24561	TL= .01500
LAYER08	NLOSS= .00000	NREAL= 3.27245	TL= .01500
LAYER09	NLOSS= .00000	NREAL= 3.29929	TL= .01500
LAYER10	NLOSS= .00000	NREAL= 3.32613	TL= .01500
LAYER11	NLOSS= .00000	NREAL= 3.35297	TL= .01500
LAYER12	NLOSS= .00000	NREAL= 3.37981	TL= .01500
LAYER13	NLOSS= .00000	NREAL= 3.40666	TL= .01500
LAYER14	NLOSS= .00000	NREAL= 3.43350	TL= .01500
LAYER15	NLOSS= .00000	NREAL= 3.46034	TL= .00750
LAYER16	NLOSS= .00000	NREAL= 3.52903	TL= .00750
LAYER17	NLOSS= .00000	NREAL= 3.67000	TL= .01000
LAYER18	NLOSS= .00000	NREAL= 3.52903	TL= .00750
LAYER19	NLOSS= .00000	NREAL= 3.46034	TL= .00750
LAYER20	NLOSS= .00000	NREAL= 3.43350	TL= .01500
LAYER21	NLOSS= .00000	NREAL= 3.40666	TL= .01500
LAYER22	NLOSS= .00000	NREAL= 3.37981	TL= .01500
LAYER23	NLOSS= .00000	NREAL= 3.35297	TL= .01500
LAYER24	NLOSS= .00000	NREAL= 3.32613	TL= .01500
LAYER25	NLOSS= .00000	NREAL= 3.29929	TL= .01500
LAYER26	NLOSS= .00000	NREAL= 3.27245	TL= .01500
LAYER27	NLOSS= .00000	NREAL= 3.24561	TL= .01500
LAYER28	NLOSS= .00000	NREAL= 3.21877	TL= .01500
LAYER29	NLOSS= .00000	NREAL= 3.19192	TL= .00750
LAYER30	NLOSS= .00000	NREAL= 3.19192	TL= 1.30000
LAYER31	NLOSS= .00000	NREAL= 3.52903	TL= .00000

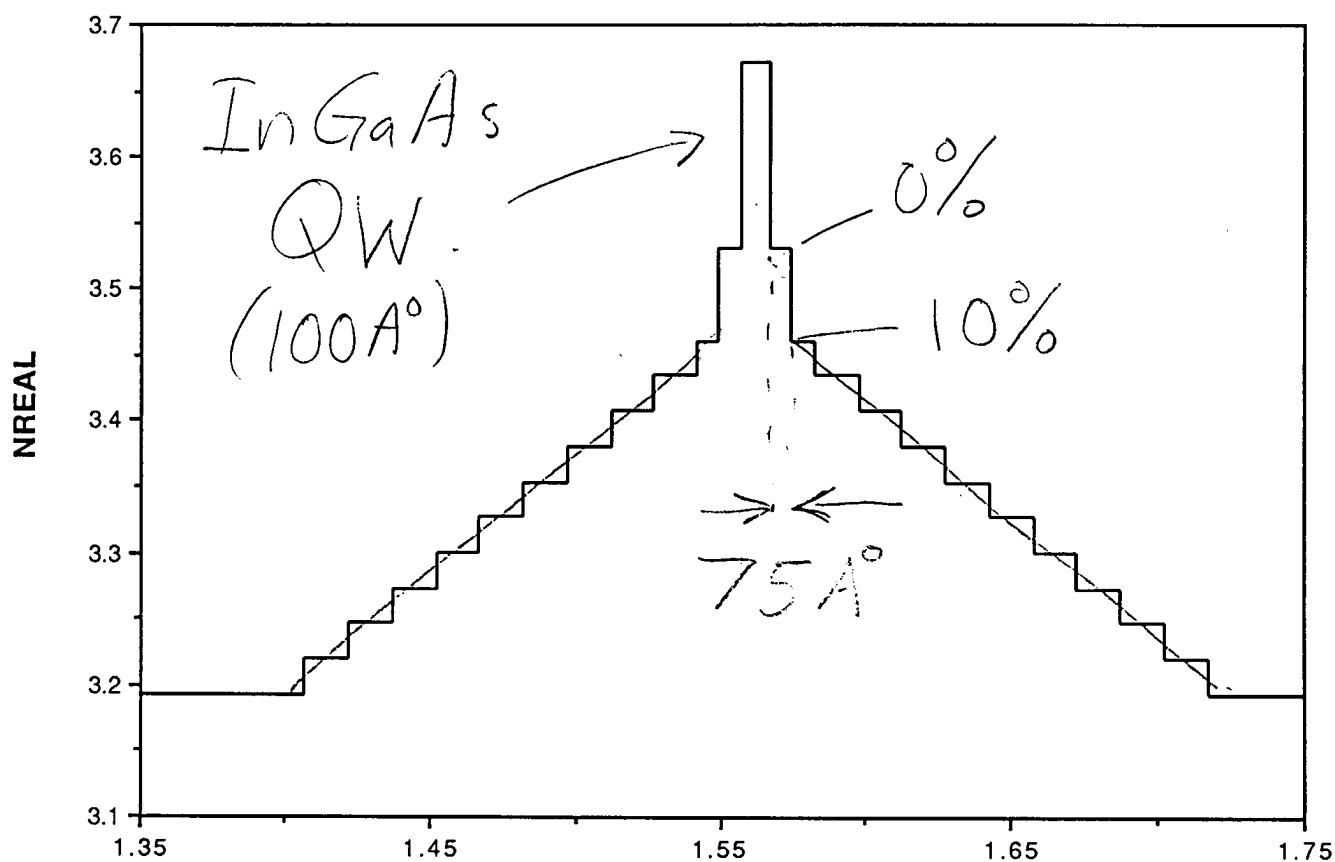
\*\*\*\*\*

LL 227 layers

- SQW → strained  
⇒ lattice constant of  
InGaAs  $\neq$  GaAs  
or AlGaAs

(207)

### Index Profile for GRIDGE-file-expanded



Why  $75 \text{ \AA}^\circ$  of GaAs?

- Best AlGaAs @  $T \sim 850^\circ\text{C}$
- Best InGaAs @  $T \sim 650^\circ\text{C}$
- GaAs good:  $650 - 850^\circ\text{C}$

gridge

Tue, Mar 9, 1993

1

```

CASE      KASE=LINCOLN LABS (227)
CASE      EPS1=1E-7      GAMEPS=1E-3          QZMR=10.8        QZMI=0.0
CASE      PRINTF=0      INITGS=0    AUTOQW=0      NFPLT=1        FFPLT=1

MODCON   KPOL=1      APB1=0.25    APB2=0.25

STRUCT   NQW=3.67      WVL=.98
STRUCT   GRW=.15       QW=.0100
STRUCT   ALPERC1=.6    ALPERC2=0.4

LAYER    ALPERC=.00      !GaAs substr
LAYER    ALPERC=.2       TL=0.05      !1st trans.
LAYER    ALPERC=.4       TL=0.05      !
LAYER    ALPERC=^1       TL=1.3      ! n-Clad
LAYER    ALPERC=^1       !           ! 1st (n) GRINSCH
LAYER    NSLC=10         !
LAYER    ALPERC=.1       !
LAYER    ALPERC=.00       TL=.0075     ! 1st (n) Barrier
LAYER    QWS=1            !QW GaIn(.14)As-LAYER
LAYER    ALPERC=.00       TL=.0075     !2nd (p) Barrier
LAYER    ALPERC=.1       !           !2nd (p) GRINSCH
LAYER    NSLC=10         !
LAYER    ALPERC=^1       !
LAYER    ALPERC=^1       TL=1.3      !1st p-Clad-Layer30
!LAYER   ALPERC=.00      TL=0.12      !GaAs Cap )
LAYER    NREAL=1          !Air

OUTPUT   PHMO=1      GAMMAO=1    WZRO=1      WZIO=1      QZRO=1      QZIO=0
OUTPUT   FWHPNO=1     FWHPFO=1    KMO=1       ITO=1
OUTPUT   SPLTFI=1      MODOUT=0     LYROUT=1
GAMOUT  LAYGAM=17     COMPGAM=0    GAMALL=0

!LOOPX1 ILX='TL'        FINV=0.0      XINC=-0.05    LAYCH=30
!LOOPZ1 ILZ='GRW'        FINV=.15      ZINC=-.05
!LOOPZ2 ILZ='WVL'        FINV=0.955   ZINC=-0.005

!LOOPZ1 ILZ='QZMR'       FINV=10.9    ZINC=-.05!THIS LOOPS TO FIND INITIAL GUESS
!LOOPZ1 ILZ='GRW'        FINV=.202    ZINC=.001
!LOOPZ1 ILZ='ALPERC1'   FINV=.401    ZINC=.0005
LOOPX1 ILX='TL'        FINV=0.0      XINC=-.1      LAYCH=30
END

```

gridgel

Tue, Mar 9, 1993

1

# of layers = 31

LAYER01	NLOSS= .00000	NREAL= 3.52903	TL= .00000
LAYER02	NLOSS= .00000	NREAL= 3.40297	TL= .05000
LAYER03	NLOSS= .00000	NREAL= 3.29907	TL= .05000
LAYER04	NLOSS= .00000	NREAL= 3.19192	TL= 1.30000
LAYER05	NLOSS= .00000	NREAL= 3.19192	TL= .00750
LAYER06	NLOSS= .00000	NREAL= 3.21877	TL= .01500
LAYER07	NLOSS= .00000	NREAL= 3.24561	TL= .01500
LAYER08	NLOSS= .00000	NREAL= 3.27245	TL= .01500
LAYER09	NLOSS= .00000	NREAL= 3.29929	TL= .01500
LAYER10	NLOSS= .00000	NREAL= 3.32613	TL= .01500
LAYER11	NLOSS= .00000	NREAL= 3.35297	TL= .01500
LAYER12	NLOSS= .00000	NREAL= 3.37981	TL= .01500
LAYER13	NLOSS= .00000	NREAL= 3.40666	TL= .01500
LAYER14	NLOSS= .00000	NREAL= 3.43350	TL= .01500
LAYER15	NLOSS= .00000	NREAL= 3.46034	TL= .00750
LAYER16	NLOSS= .00000	NREAL= 3.52903	TL= .00750
LAYER17	NLOSS= .00000	NREAL= 3.67000	TL= .01000
LAYER18	NLOSS= .00000	NREAL= 3.52903	TL= .00750
LAYER19	NLOSS= .00000	NREAL= 3.46034	TL= .00750
LAYER20	NLOSS= .00000	NREAL= 3.43350	TL= .01500
LAYER21	NLOSS= .00000	NREAL= 3.40666	TL= .01500
LAYER22	NLOSS= .00000	NREAL= 3.37981	TL= .01500
LAYER23	NLOSS= .00000	NREAL= 3.35297	TL= .01500
LAYER24	NLOSS= .00000	NREAL= 3.32613	TL= .01500
LAYER25	NLOSS= .00000	NREAL= 3.29929	TL= .01500
LAYER26	NLOSS= .00000	NREAL= 3.27245	TL= .01500
LAYER27	NLOSS= .00000	NREAL= 3.24561	TL= .01500
LAYER28	NLOSS= .00000	NREAL= 3.21877	TL= .01500
LAYER29	NLOSS= .00000	NREAL= 3.19192	TL= .00750
LAYER30	NLOSS= .00000	NREAL= 3.19192	TL= 1.30000
LAYER31	NLOSS= .00000	NREAL= 3.52903	TL= .00000 ← Ga As

\*\*\*\*\*

gridge\_LAYERS\_

Tue, Mar 9, 1993

1

TL(30) = 1.300

# of layers = 31

LAYER01	NLOSS= .00000	NREAL= 3.52903	TL= .00000
LAYER02	NLOSS= .00000	NREAL= 3.40297	TL= .05000
LAYER03	NLOSS= .00000	NREAL= 3.29907	TL= .05000
LAYER04	NLOSS= .00000	NREAL= 3.19192	TL= 1.30000
LAYER05	NLOSS= .00000	NREAL= 3.19192	TL= .00750
LAYER06	NLOSS= .00000	NREAL= 3.21877	TL= .01500
LAYER07	NLOSS= .00000	NREAL= 3.24561	TL= .01500
LAYER08	NLOSS= .00000	NREAL= 3.27245	TL= .01500
LAYER09	NLOSS= .00000	NREAL= 3.29929	TL= .01500
LAYER10	NLOSS= .00000	NREAL= 3.32613	TL= .01500
LAYER11	NLOSS= .00000	NREAL= 3.35297	TL= .01500
LAYER12	NLOSS= .00000	NREAL= 3.37981	TL= .01500
LAYER13	NLOSS= .00000	NREAL= 3.40666	TL= .01500
LAYER14	NLOSS= .00000	NREAL= 3.43350	TL= .01500
LAYER15	NLOSS= .00000	NREAL= 3.46034	TL= .00750
LAYER16	NLOSS= .00000	NREAL= 3.52903	TL= .00750
LAYER17	NLOSS= .00000	NREAL= 3.67000	TL= .01000
LAYER18	NLOSS= .00000	NREAL= 3.52903	TL= .00750
LAYER19	NLOSS= .00000	NREAL= 3.46034	TL= .00750
LAYER20	NLOSS= .00000	NREAL= 3.43350	TL= .01500
LAYER21	NLOSS= .00000	NREAL= 3.40666	TL= .01500
LAYER22	NLOSS= .00000	NREAL= 3.37981	TL= .01500
LAYER23	NLOSS= .00000	NREAL= 3.35297	TL= .01500
LAYER24	NLOSS= .00000	NREAL= 3.32613	TL= .01500
LAYER25	NLOSS= .00000	NREAL= 3.29929	TL= .01500
LAYER26	NLOSS= .00000	NREAL= 3.27245	TL= .01500
LAYER27	NLOSS= .00000	NREAL= 3.24561	TL= .01500
LAYER28	NLOSS= .00000	NREAL= 3.21877	TL= .01500
LAYER29	NLOSS= .00000	NREAL= 3.19192	TL= .00750
LAYER30	NLOSS= .00000	NREAL= 3.19192	TL= 1.30000
LAYER31	NLOSS= .00000	NREAL= 1.00000	TL= .00000

\*\*\*\*\*

TL(30) = 1.200

# of layers = 31

LAYER01	NLOSS= .00000	NREAL= 3.52903	TL= .00000
LAYER02	NLOSS= .00000	NREAL= 3.40297	TL= .05000
LAYER03	NLOSS= .00000	NREAL= 3.29907	TL= .05000
LAYER04	NLOSS= .00000	NREAL= 3.19192	TL= 1.30000
LAYER05	NLOSS= .00000	NREAL= 3.19192	TL= .00750
LAYER06	NLOSS= .00000	NREAL= 3.21877	TL= .01500
LAYER07	NLOSS= .00000	NREAL= 3.24561	TL= .01500
LAYER08	NLOSS= .00000	NREAL= 3.27245	TL= .01500
LAYER09	NLOSS= .00000	NREAL= 3.29929	TL= .01500
LAYER10	NLOSS= .00000	NREAL= 3.32613	TL= .01500
LAYER11	NLOSS= .00000	NREAL= 3.35297	TL= .01500
LAYER12	NLOSS= .00000	NREAL= 3.37981	TL= .01500
LAYER13	NLOSS= .00000	NREAL= 3.40666	TL= .01500
LAYER14	NLOSS= .00000	NREAL= 3.43350	TL= .01500
LAYER15	NLOSS= .00000	NREAL= 3.46034	TL= .00750
LAYER16	NLOSS= .00000	NREAL= 3.52903	TL= .00750
LAYER17	NLOSS= .00000	NREAL= 3.67000	TL= .01000

LAYER18	NLOSS=	.00000	NREAL=	3.52903	TL=	.00750
LAYER19	NLOSS=	.00000	NREAL=	3.46034	TL=	.00750
LAYER20	NLOSS=	.00000	NREAL=	3.43350	TL=	.01500
LAYER21	NLOSS=	.00000	NREAL=	3.40666	TL=	.01500
LAYER22	NLOSS=	.00000	NREAL=	3.37981	TL=	.01500
LAYER23	NLOSS=	.00000	NREAL=	3.35297	TL=	.01500
LAYER24	NLOSS=	.00000	NREAL=	3.32613	TL=	.01500
LAYER25	NLOSS=	.00000	NREAL=	3.29929	TL=	.01500
LAYER26	NLOSS=	.00000	NREAL=	3.27245	TL=	.01500
LAYER27	NLOSS=	.00000	NREAL=	3.24561	TL=	.01500
LAYER28	NLOSS=	.00000	NREAL=	3.21877	TL=	.01500
LAYER29	NLOSS=	.00000	NREAL=	3.19192	TL=	.00750
LAYER30	NLOSS=	.00000	NREAL=	3.19192	TL=	<b>1.20000</b>
LAYER31	NLOSS=	.00000	NREAL=	1.00000	TL=	.00000

\*\*\*\*\*

TL(30) = 1.100
----------------

# of layers = 31

LAYER01	NLOSS=	.00000	NREAL=	3.52903	TL=	.00000
LAYER02	NLOSS=	.00000	NREAL=	3.40297	TL=	.05000
LAYER03	NLOSS=	.00000	NREAL=	3.29907	TL=	.05000
LAYER04	NLOSS=	.00000	NREAL=	3.19192	TL=	1.30000
LAYER05	NLOSS=	.00000	NREAL=	3.19192	TL=	.00750
LAYER06	NLOSS=	.00000	NREAL=	3.21877	TL=	.01500
LAYER07	NLOSS=	.00000	NREAL=	3.24561	TL=	.01500
LAYER08	NLOSS=	.00000	NREAL=	3.27245	TL=	.01500
LAYER09	NLOSS=	.00000	NREAL=	3.29929	TL=	.01500
LAYER10	NLOSS=	.00000	NREAL=	3.32613	TL=	.01500
LAYER11	NLOSS=	.00000	NREAL=	3.35297	TL=	.01500
LAYER12	NLOSS=	.00000	NREAL=	3.37981	TL=	.01500
LAYER13	NLOSS=	.00000	NREAL=	3.40666	TL=	.01500
LAYER14	NLOSS=	.00000	NREAL=	3.43350	TL=	.01500
LAYER15	NLOSS=	.00000	NREAL=	3.46034	TL=	.00750
LAYER16	NLOSS=	.00000	NREAL=	3.52903	TL=	.00750
LAYER17	NLOSS=	.00000	NREAL=	3.67000	TL=	.01000
LAYER18	NLOSS=	.00000	NREAL=	3.52903	TL=	.00750
LAYER19	NLOSS=	.00000	NREAL=	3.46034	TL=	.00750
LAYER20	NLOSS=	.00000	NREAL=	3.43350	TL=	.01500
LAYER21	NLOSS=	.00000	NREAL=	3.40666	TL=	.01500
LAYER22	NLOSS=	.00000	NREAL=	3.37981	TL=	.01500
LAYER23	NLOSS=	.00000	NREAL=	3.35297	TL=	.01500
LAYER24	NLOSS=	.00000	NREAL=	3.32613	TL=	.01500
LAYER25	NLOSS=	.00000	NREAL=	3.29929	TL=	.01500
LAYER26	NLOSS=	.00000	NREAL=	3.27245	TL=	.01500
LAYER27	NLOSS=	.00000	NREAL=	3.24561	TL=	.01500
LAYER28	NLOSS=	.00000	NREAL=	3.21877	TL=	.01500
LAYER29	NLOSS=	.00000	NREAL=	3.19192	TL=	.00750
LAYER30	NLOSS=	.00000	NREAL=	3.19192	TL=	1.10000
LAYER31	NLOSS=	.00000	NREAL=	1.00000	TL=	.00000

\*\*\*\*\*

TL(30) = 1.000

# of layers = 31

skip to End

gridge\_LAYERS\_

Tue, Mar 9, 1993

8

LAYER27	NLOSS= .00000	NREAL= 3.24561	TL= .01500
LAYER28	NLOSS= .00000	NREAL= 3.21877	TL= .01500
LAYER29	NLOSS= .00000	NREAL= 3.19192	TL= .00750
LAYER30	NLOSS= .00000	NREAL= 3.19192	TL= .30000
LAYER31	NLOSS= .00000	NREAL= 1.00000	TL= .00000

\*\*\*\*\*

TL (30) = .2000

# of layers = 31

LAYER01	NLOSS= .00000	NREAL= 3.52903	TL= .00000
LAYER02	NLOSS= .00000	NREAL= 3.40297	TL= .05000
LAYER03	NLOSS= .00000	NREAL= 3.29907	TL= .05000
LAYER04	NLOSS= .00000	NREAL= 3.19192	TL= 1.30000
LAYER05	NLOSS= .00000	NREAL= 3.19192	TL= .00750
LAYER06	NLOSS= .00000	NREAL= 3.21877	TL= .01500
LAYER07	NLOSS= .00000	NREAL= 3.24561	TL= .01500
LAYER08	NLOSS= .00000	NREAL= 3.27245	TL= .01500
LAYER09	NLOSS= .00000	NREAL= 3.29929	TL= .01500
LAYER10	NLOSS= .00000	NREAL= 3.32613	TL= .01500
LAYER11	NLOSS= .00000	NREAL= 3.35297	TL= .01500
LAYER12	NLOSS= .00000	NREAL= 3.37981	TL= .01500
LAYER13	NLOSS= .00000	NREAL= 3.40666	TL= .01500
LAYER14	NLOSS= .00000	NREAL= 3.43350	TL= .01500
LAYER15	NLOSS= .00000	NREAL= 3.46034	TL= .00750
LAYER16	NLOSS= .00000	NREAL= 3.52903	TL= .00750
LAYER17	NLOSS= .00000	NREAL= 3.67000	TL= .01000
LAYER18	NLOSS= .00000	NREAL= 3.52903	TL= .00750
LAYER19	NLOSS= .00000	NREAL= 3.46034	TL= .00750
LAYER20	NLOSS= .00000	NREAL= 3.43350	TL= .01500
LAYER21	NLOSS= .00000	NREAL= 3.40666	TL= .01500
LAYER22	NLOSS= .00000	NREAL= 3.37981	TL= .01500
LAYER23	NLOSS= .00000	NREAL= 3.35297	TL= .01500
LAYER24	NLOSS= .00000	NREAL= 3.32613	TL= .01500
LAYER25	NLOSS= .00000	NREAL= 3.29929	TL= .01500
LAYER26	NLOSS= .00000	NREAL= 3.27245	TL= .01500
LAYER27	NLOSS= .00000	NREAL= 3.24561	TL= .01500
LAYER28	NLOSS= .00000	NREAL= 3.21877	TL= .01500
LAYER29	NLOSS= .00000	NREAL= 3.19192	TL= .00750
LAYER30	NLOSS= .00000	NREAL= 3.19192	TL= .20000
LAYER31	NLOSS= .00000	NREAL= 1.00000	TL= .00000

\*\*\*\*\*

TL (30) = .1000

# of layers = 31

LAYER01	NLOSS= .00000	NREAL= 3.52903	TL= .00000
LAYER02	NLOSS= .00000	NREAL= 3.40297	TL= .05000
LAYER03	NLOSS= .00000	NREAL= 3.29907	TL= .05000
LAYER04	NLOSS= .00000	NREAL= 3.19192	TL= 1.30000
LAYER05	NLOSS= .00000	NREAL= 3.19192	TL= .00750
LAYER06	NLOSS= .00000	NREAL= 3.21877	TL= .01500
LAYER07	NLOSS= .00000	NREAL= 3.24561	TL= .01500
LAYER08	NLOSS= .00000	NREAL= 3.27245	TL= .01500
LAYER09	NLOSS= .00000	NREAL= 3.29929	TL= .01500

(23)

LAYER10	NLOSS= .00000	NREAL= 3.32613	TL= .01500
LAYER11	NLOSS= .00000	NREAL= 3.35297	TL= .01500
LAYER12	NLOSS= .00000	NREAL= 3.37981	TL= .01500
LAYER13	NLOSS= .00000	NREAL= 3.40666	TL= .01500
LAYER14	NLOSS= .00000	NREAL= 3.43350	TL= .01500
LAYER15	NLOSS= .00000	NREAL= 3.46034	TL= .00750
LAYER16	NLOSS= .00000	NREAL= 3.52903	TL= .00750
LAYER17	NLOSS= .00000	NREAL= 3.67000	TL= .01000
LAYER18	NLOSS= .00000	NREAL= 3.52903	TL= .00750
LAYER19	NLOSS= .00000	NREAL= 3.46034	TL= .00750
LAYER20	NLOSS= .00000	NREAL= 3.43350	TL= .01500
LAYER21	NLOSS= .00000	NREAL= 3.40666	TL= .01500
LAYER22	NLOSS= .00000	NREAL= 3.37981	TL= .01500
LAYER23	NLOSS= .00000	NREAL= 3.35297	TL= .01500
LAYER24	NLOSS= .00000	NREAL= 3.32613	TL= .01500
LAYER25	NLOSS= .00000	NREAL= 3.29929	TL= .01500
LAYER26	NLOSS= .00000	NREAL= 3.27245	TL= .01500
LAYER27	NLOSS= .00000	NREAL= 3.24561	TL= .01500
LAYER28	NLOSS= .00000	NREAL= 3.21877	TL= .01500
LAYER29	NLOSS= .00000	NREAL= 3.19192	TL= .00750
LAYER30	NLOSS= .00000	NREAL= 3.19192	TL= 10000
LAYER31	NLOSS= .00000	NREAL= 1.00000	TL= .00000

\*\*\*\*\*

TL(30)=0.2776E-16

# of layers = 31

LAYER01	NLOSS= .00000	NREAL= 3.52903	TL= .00000
LAYER02	NLOSS= .00000	NREAL= 3.40297	TL= .05000
LAYER03	NLOSS= .00000	NREAL= 3.29907	TL= .05000
LAYER04	NLOSS= .00000	NREAL= 3.19192	TL= 1.30000
LAYER05	NLOSS= .00000	NREAL= 3.19192	TL= .00750
LAYER06	NLOSS= .00000	NREAL= 3.21877	TL= .01500
LAYER07	NLOSS= .00000	NREAL= 3.24561	TL= .01500
LAYER08	NLOSS= .00000	NREAL= 3.27245	TL= .01500
LAYER09	NLOSS= .00000	NREAL= 3.29929	TL= .01500
LAYER10	NLOSS= .00000	NREAL= 3.32613	TL= .01500
LAYER11	NLOSS= .00000	NREAL= 3.35297	TL= .01500
LAYER12	NLOSS= .00000	NREAL= 3.37981	TL= .01500
LAYER13	NLOSS= .00000	NREAL= 3.40666	TL= .01500
LAYER14	NLOSS= .00000	NREAL= 3.43350	TL= .01500
LAYER15	NLOSS= .00000	NREAL= 3.46034	TL= .00750
LAYER16	NLOSS= .00000	NREAL= 3.52903	TL= .00750
LAYER17	NLOSS= .00000	NREAL= 3.67000	TL= .01000
LAYER18	NLOSS= .00000	NREAL= 3.52903	TL= .00750
LAYER19	NLOSS= .00000	NREAL= 3.46034	TL= .00750
LAYER20	NLOSS= .00000	NREAL= 3.43350	TL= .01500
LAYER21	NLOSS= .00000	NREAL= 3.40666	TL= .01500
LAYER22	NLOSS= .00000	NREAL= 3.37981	TL= .01500
LAYER23	NLOSS= .00000	NREAL= 3.35297	TL= .01500
LAYER24	NLOSS= .00000	NREAL= 3.32613	TL= .01500
LAYER25	NLOSS= .00000	NREAL= 3.29929	TL= .01500
LAYER26	NLOSS= .00000	NREAL= 3.27245	TL= .01500
LAYER27	NLOSS= .00000	NREAL= 3.24561	TL= .01500
LAYER28	NLOSS= .00000	NREAL= 3.21877	TL= .01500
LAYER29	NLOSS= .00000	NREAL= 3.19192	TL= .00750

(214)

gridge\_LAYERS\_

Tue, Mar 9, 1993

10

LAYER30 NLOSS= .00000 NREAL= 3.19192 TL= 0.00000  
LAYER31 NLOSS= .00000 NREAL= 1.00000 TL= .00000

\*\*\*\*\*

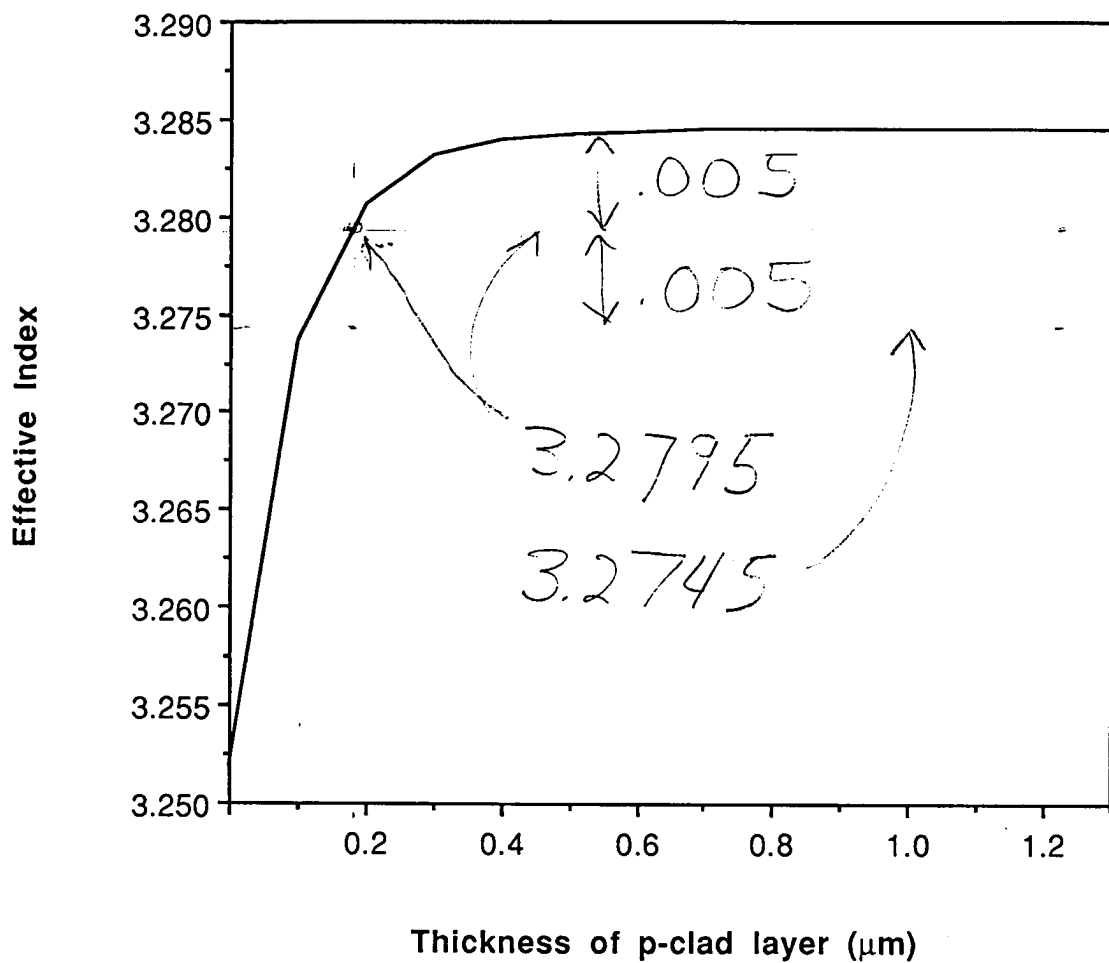
\*DBASE WITH CAP (final GaAs layer) INTACT AND P-CLAD (TL(30)) = 1.3  $\mu$ m:

PHM TL(30)	GAMMA(17) PHM	GAMMA(33) WZR	WZR WZI	QZR QZR	KM IT 3	IT
4.868978E-01	3.424811E-02	0.000000E-01	3.284418E+00	1.515883E-07	1.078740E+01	7
1.300000E+00	4.868956E-01	3.424375E-02	3.284418E+00	5.907478E-08	1.078740E+01	2.434824E-01
1.200000E+00	4.868959E-01	3.424188E-02	3.284418E+00	5.906744E-08	1.078740E+01	2.434823E-01
1.100000E+00	4.868969E-01	3.424178E-02	3.284418E+00	5.907111E-08	1.078740E+01	2.434820E-01
1.000000E+00	4.868998E-01	3.424007E-02	3.284417E+00	5.907478E-08	1.078739E+01	2.434812E-01
9.000000E-01	4.869074E-01	3.424687E-02	3.284415E+00	5.908946E-08	1.078738E+01	2.434790E-01
8.000000E-01	4.869283E-01	3.425819E-02	3.284409E+00	5.912982E-08	1.078734E+01	2.434729E-01
7.000000E-01	4.869846E-01	3.429525E-02	3.284394E+00	5.923241E-08	1.078724E+01	2.434567E-01
6.000000E-01	4.871368E-01	3.431799E-02	3.284352E+00	5.949176E-08	1.078697E+01	2.434129E-01
5.000000E-01	4.875488E-01	3.440822E-02	3.284240E+00	6.016589E-08	1.078623E+01	2.432947E-01
4.000000E-01	4.886674E-01	3.463182E-02	3.283932E+00	6.195220E-08	1.078421E+01	2.429764E-01
3.000000E-01	4.917211E-01	3.502373E-02	3.283085E+00	6.684794E-08	1.077865E+01	2.421272E-01
2.000000E-01	5.001126E-01	3.580989E-02	3.280691E+00	8.204101E-08	1.076293E+01	2.406360E-01
1.000000E-01	5.232213E-01	3.691358E-02	3.273634E+00	1.467550E-07	1.071668E+01	2.477919E-01
2.775558E-17	6.074230E-01	3.620565E-02	3.251833E+00	8.948663E-07	1.057455E+01	2.348841E-01

(615)

(216)

### Effective Index vs p-clad thickness

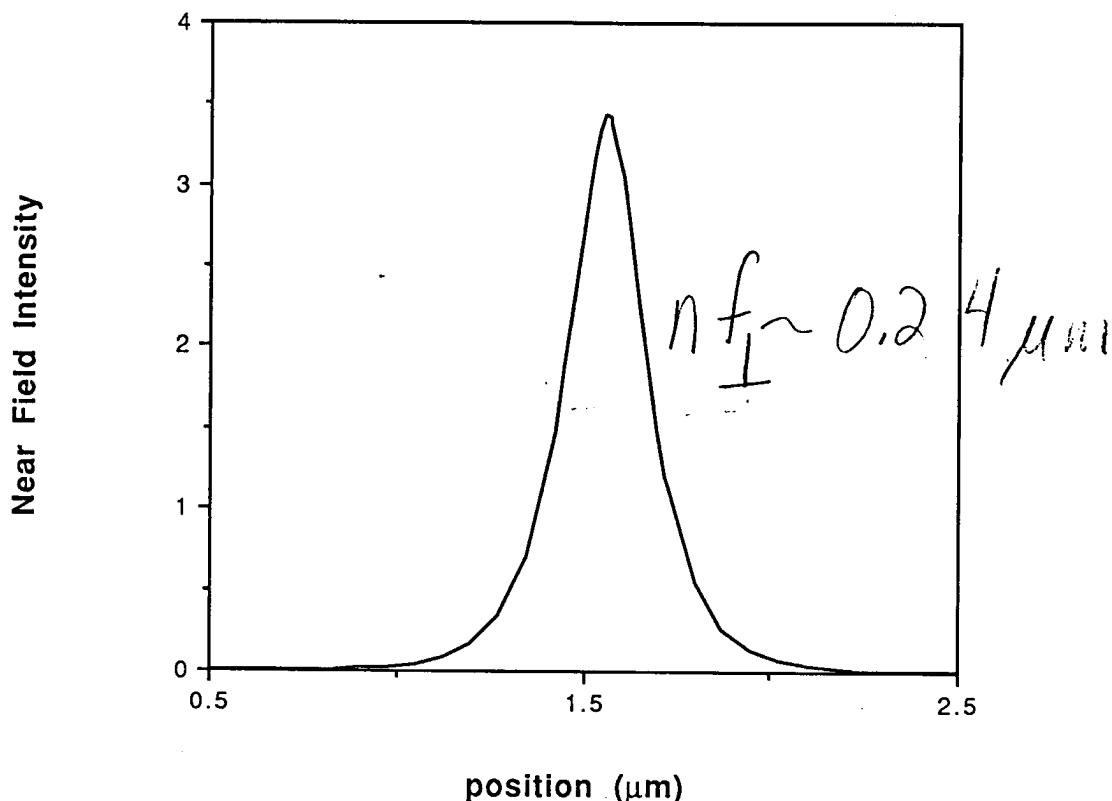


•  $\Delta n_{\text{lateral}} \sim 0.005 \text{ to } 0.01$

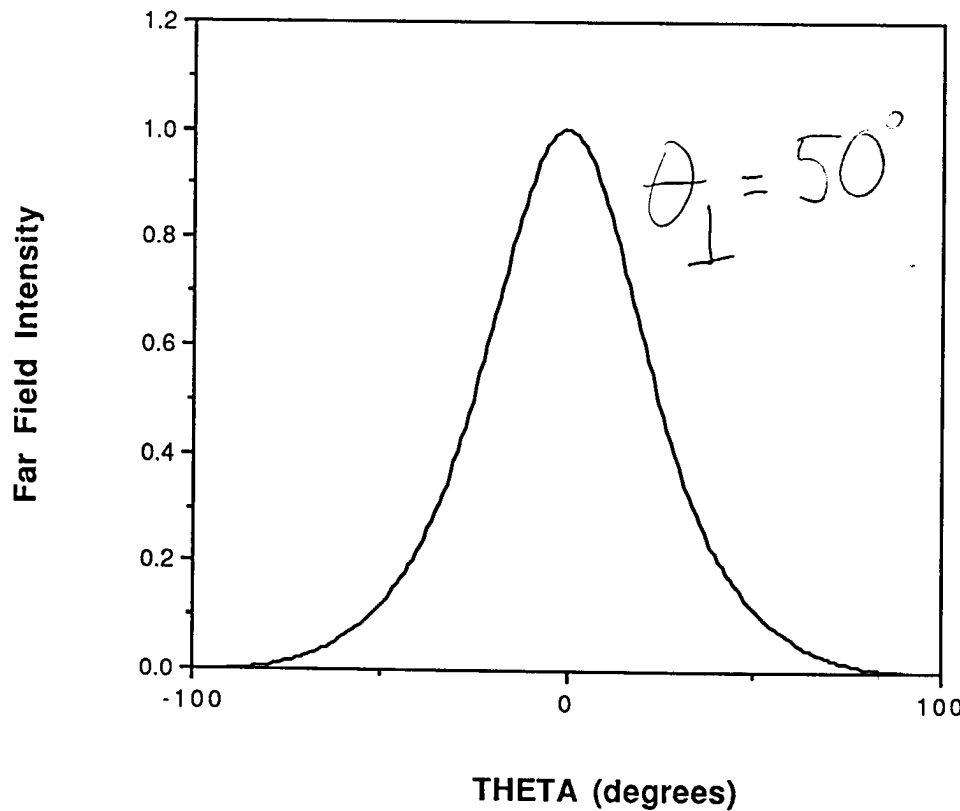
•  $\Delta X_{\text{p-clad}} \sim 0.18 \text{ to } 0.1 \mu\text{m}$

217

### Perpendicular Near Field for Graded Index Ridge Waveguide



### Perpendicular Far-Field For Graded Index Ridge Waveguide



$$\left( n_{\text{eff}} \right)_S \quad \left| \quad \left( n_{\text{eff}} \right)_r \quad \right| \quad \left( n_{\text{eff}} \right)_S$$

$$\begin{array}{c|c|c}
 & \xleftarrow{\quad W_r \quad} & \\
 3.2795 & 3.2844 & 3.2795 \\
 \downarrow n_S^2 & n_r^2 & \downarrow \\
 10.755 & & 10.787
 \end{array}$$

10.782

10.787

latridge

Tue, Mar 9, 1993

1

CASE KASE=lateral  
CASE EPS1=1E-7 GAMEPS=1E-3 QZMR=10.782 QZMI=0.001  
CASE PRINTF=0 INITGS=0 AUTOQW=0 NFPLT=1 FFPLT=1  
CASE IL=50

MODCON KPOL=1 APB1=0.25 APB2=0.25

STRUCT WV=.98

LAYER NREAL=3.2795 NLOSS=0.0 TL=0.  
LAYER NREAL=3.2844 NLOSS=0. TL=5.0  
LAYER NREAL=3.2795 NLOSS=0.0 TL=0.

OUTPUT PHMO=1 GAMMAO=1 WZRO=1 WZIO=1 QZRO=1 QZIO=0  
OUTPUT FWHPNO=0 FWHPFO=0  
OUTPUT SPLTFL=1 MODOUT=1 LYROUT=1  
OUTPUT FWHPNO=1 FWHPFO=1

GAMOUT LAYGAM=2 COMPGAM=0 GAMALL=0

!LOOPX1 ILX='NLOSS' FINV=0.2382 XINC=.05 LAYCH=1  
!LOOPX1 ILX='NLOSS' FINV=0.2382 XINC=.05 LAYCH=3  
!LOOPX1 ILX='TL' FINV=0.01 XINC=-0.01 LAYCH=2

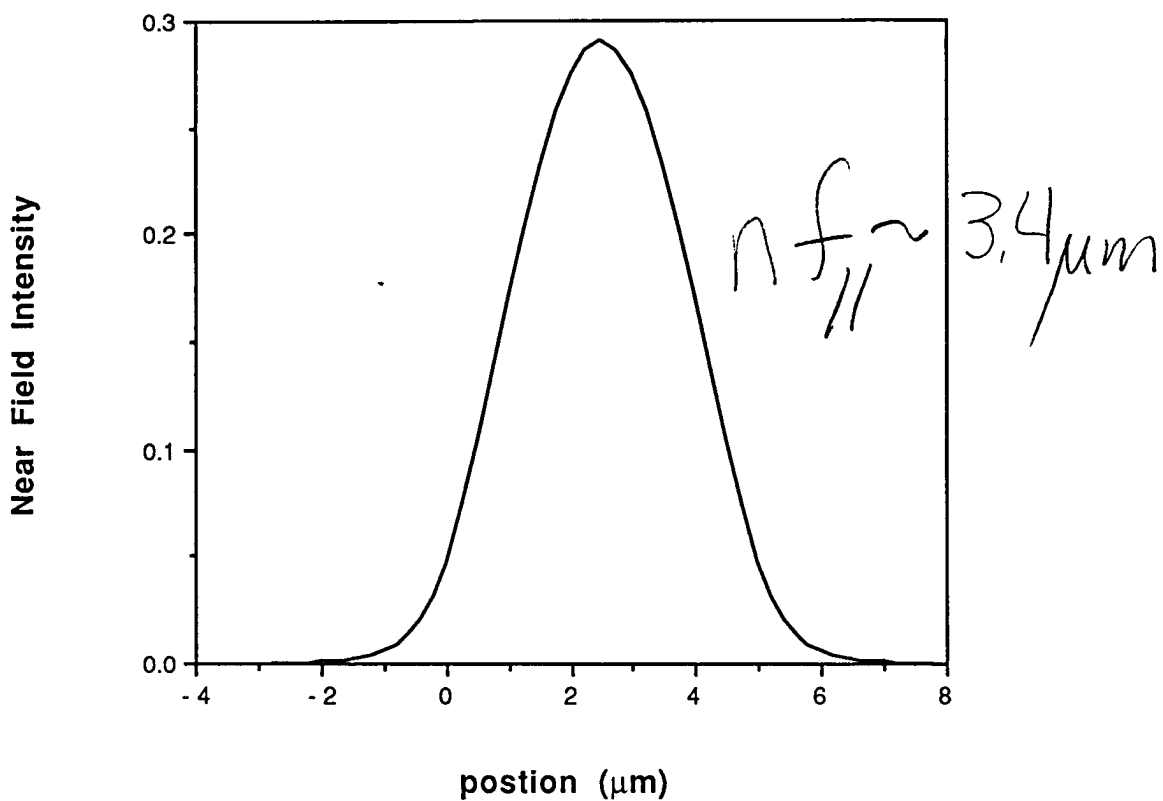
!LOOPZ1 ILZ='QZMR' FINV=10.7 ZINC=-.005

END

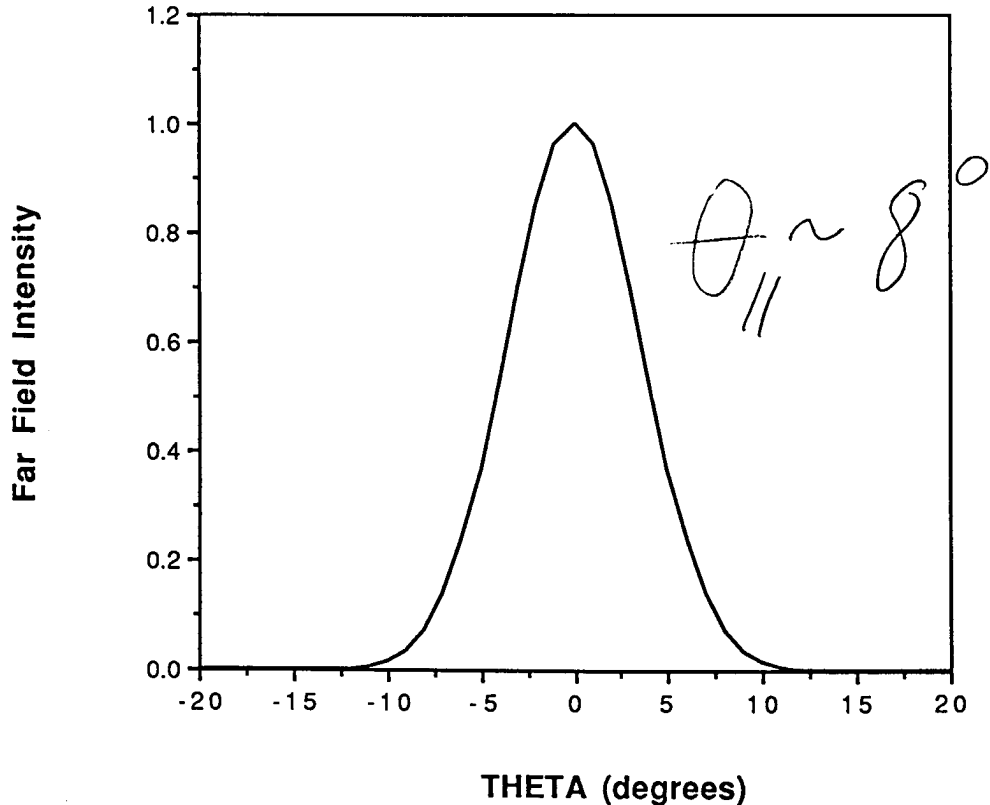
$5\mu m = \lambda_r$

Lateral Near Field for  
a Graded Ridge Waveguide

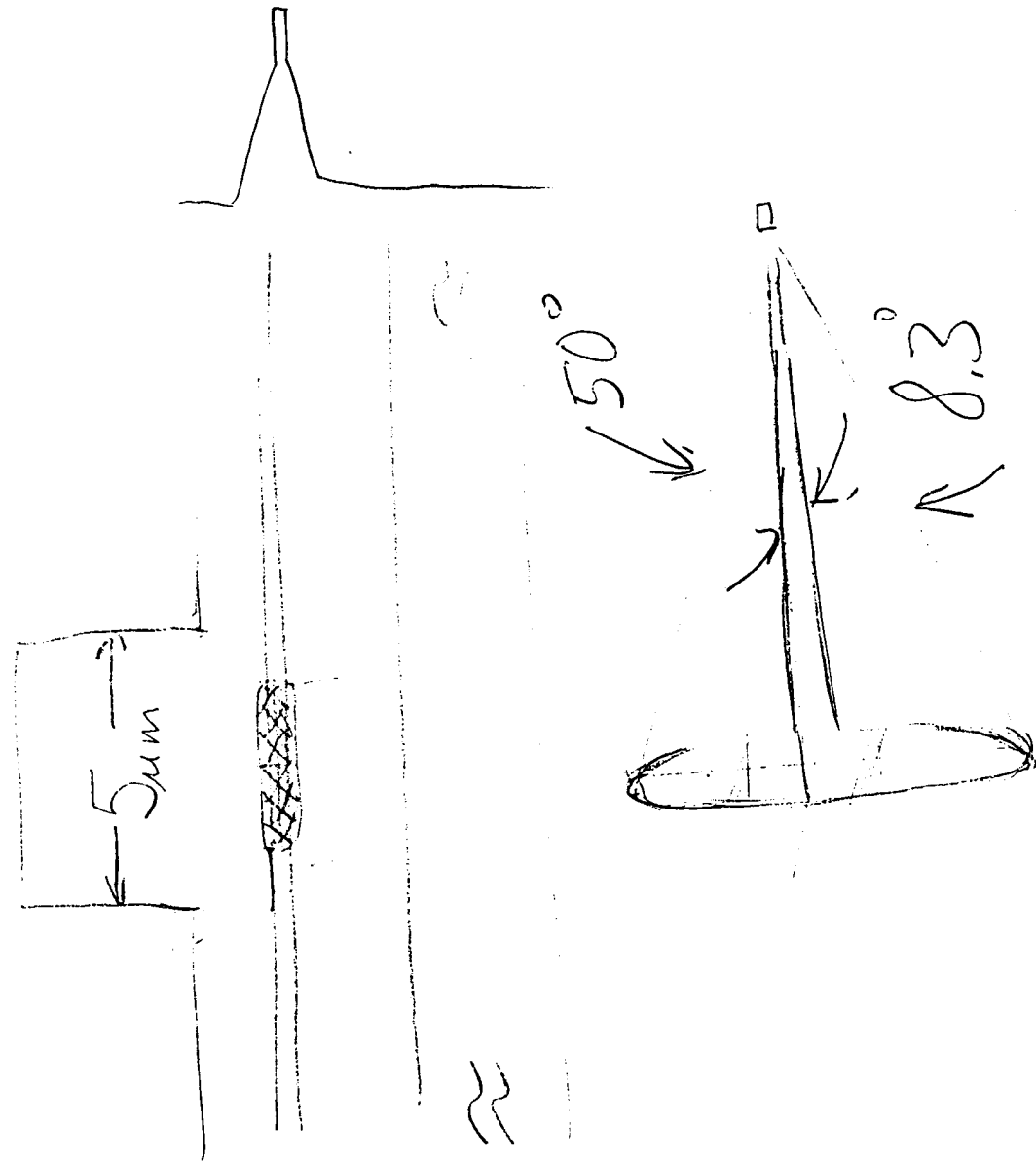
(220)



Lateral Far Field for  
a Graded Ridge Waveguide



$*$   
 PHM      GAMMA(2)      WZR      WZI      QZR      FWHPN      FWHPF  
 7.363655E-01    9.553500E-01    3.283607E+00    5.963374E-09    1.078208E+01    3.394623E+00    8.344343E+00



221



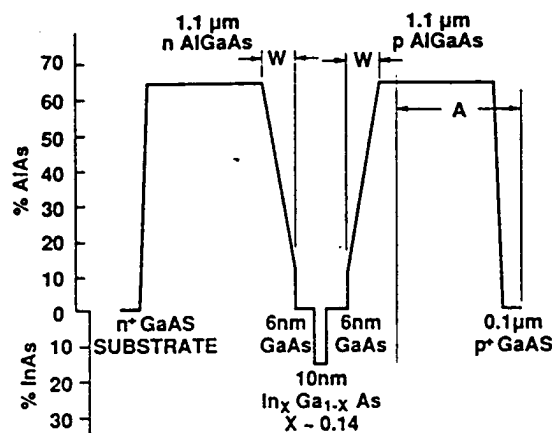
222

31002  
31003

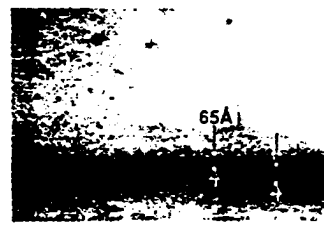
## Grating-Coupled Surface Emitting Semiconductor Lasers

31004

139



a)



b)

31008

Fig. 15. (a) The thickness and composition profile of a GRIN-SCH laser structure with 66% AlAs in the cladding layers (b) TEM of the quantum-well region.

31009

31010

31011

31012

31013

31014

31015

31016

31017

31018

31019

31020

31021

31022

31023

31024

31025

31026

31027

31028

31029

31030

31031

31032

31033

31034

31035

31036

31037

31038

31039

31040

31041

31042

31043

31044

31045

31046

31047

31048

31049

31050

31051

31052

31053

31054

31055

31056

31057

31058

31059

31060

31061

31062

31063

31064

31065

31066

31067

31068

31069

31070

31071

31072

31073

31074

31075

31076

31077

31078

31079

31080

31081

31082

31083

31084

31085

31086

31087

31088

31089

31090

31091

31092

31093

31094

31095

31096

31097

31098

31099

31100

31101

31102

31103

31104

31105

31106

31107

31108

31109

31110

31111

31112

31113

31114

31115

31116

31117

31118

31119

31120

31121

31122

31123

31124

31125

31126

31127

31128

31129

31130

31131

31132

31133

31134

31135

31136

31137

31138

31139

31140

31141

31142

31143

31144

31145

31146

31147

31148

31149

31150

31151

31152

31153

31154

31155

31156

31157

31158

31159

31160

31161

31162

31163

31164

31165

31166

31167

31168

31169

31170

31171

31172

31173

31174

31175

31176

31177

31178

31179

31180

31181

31182

31183

31184

31185

31186

31187

31188

31189

31190

31191

31192

31193

31194

31195

31196

31197

31198

31199

31200

31201

31202

31203

31204

31205

31206

31207

31208

31209

31210

31211

31212

31213

31214

31215

31216

31217

31218

31219

31220

31221

31222

31223

31224

31225

31226

31227

31228

31229

31230

31231

31232

31233

31234

31235

31236

31237

31238

31239

31240

31241

31242

31243

31244

31245

31246

31247

31248

31249

31250

31251

31252

31253

31254

31255

31256

31257

31258

31259

31260

31261

31262

31263

31264

31265

31266

31267

31268

31269

31270

31271

31272

31273

31274

31275

31276

31277

31278

31279

31280

31281

31282

31283

31284

31285

31286

31287

31288

31289

31290

31291

31292

31293

31294

31295

31296

31297

31298

31299

31300

31301

31302

31303

31304

31305

31306

31307

31308

31309

31310

31311

31312

31313

31314

31315

31316

31317

31318

31319

31320

31321

31322

31323

G. A. Evans et al.

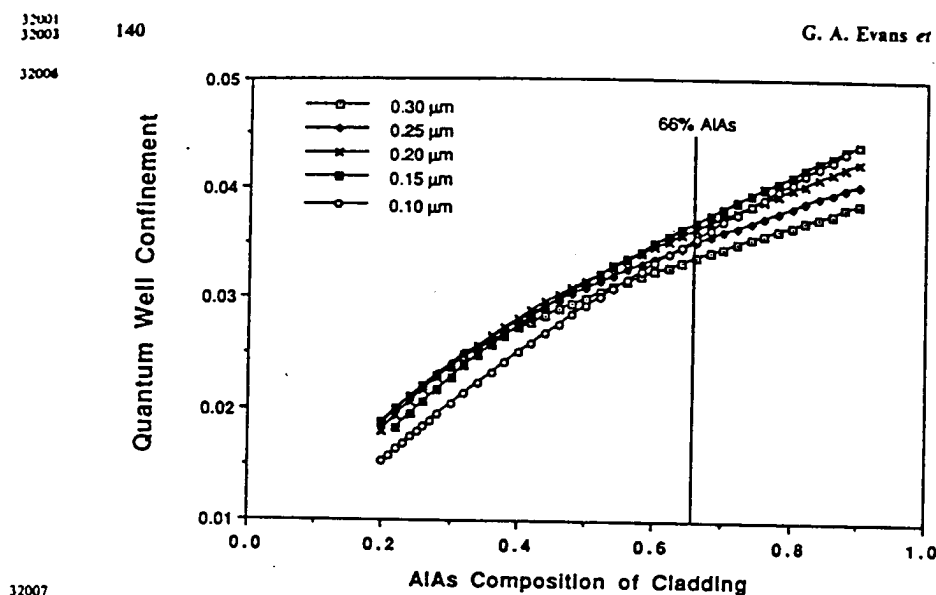


Fig. 16. The quantum-well confinement factor as a function of *p*-cladding composition for graded region thicknesses ranging from 0.1 to 0.3  $\mu\text{m}$ .

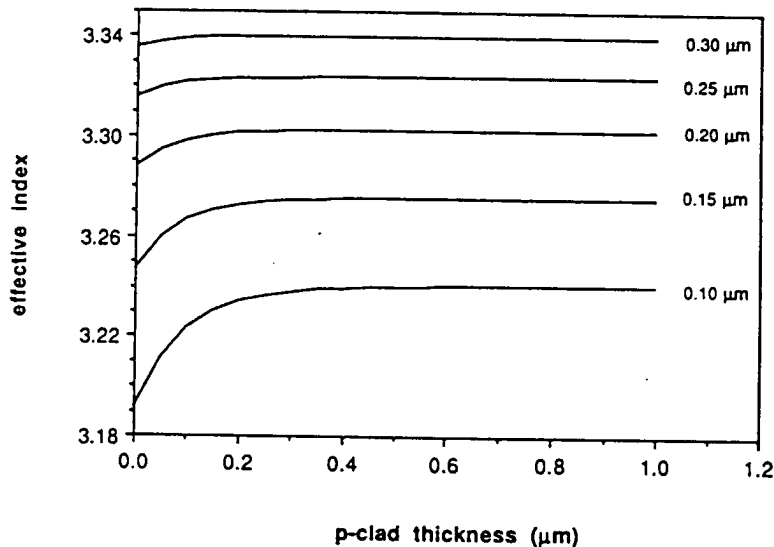
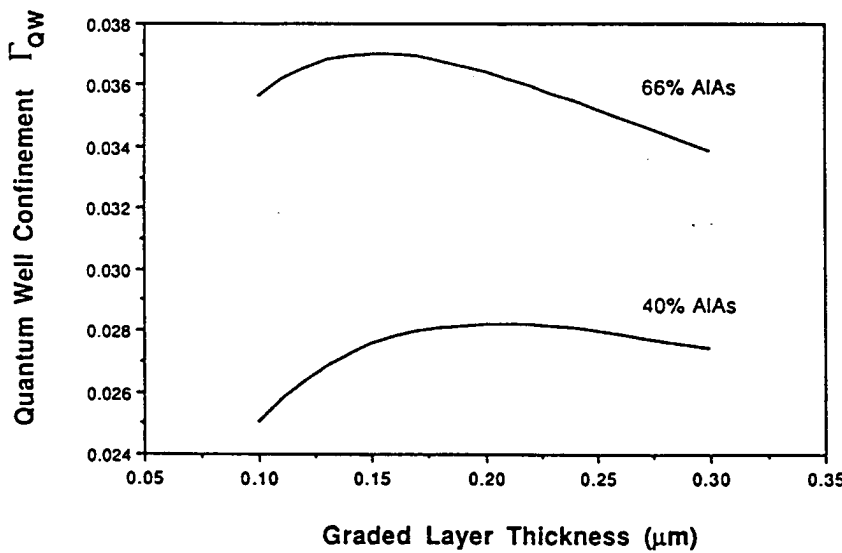


Fig. 17 The effective index of the fundamental waveguide mode for the laser structure shown in Fig. 15 with 60% AlAs in the clad regions for graded region thicknesses ranging from 0.1 to 0.3  $\mu\text{m}$  as a function of remaining *p*-cladding thickness.

0072"00649

33004  
 33007 1989; Thornton *et al.*, 1990; Zou *et al.*, 1990) and ridges formed by etching.  
 33008 Figure 17 shows the effective index of the fundamental transverse mode in  
 33009 the grating region as the *p*-clad thickness is etched away (after removal of  
 33010 the cap layer) for the graded-index separate confinement heterostructure  
 33011 (GRIN-SCH) single quantum-well geometry shown in Fig. 15. The different  
 33012 curves correspond to graded region widths of 0.1, 0.15, 0.2, 0.25, and 0.3  $\mu\text{m}$ .  
 33013 A lateral index step in the gain region can be achieved by etching away  
 33014 first the cap layer and then most of the *p*-clad material everywhere outside  
 33015 the ridges. The effective index remains almost constant for graded region  
 33016 thicknesses  $\geq 0.3 \mu\text{m}$ . In this case, there would be very little interaction of  
 33017 the optical field with a grating located at the *p*-clad-air interface. For  
 33018 a graded region thickness *W* of  $\leq 0.25 \mu\text{m}$ , substantial changes in the  
 33019 effective index occur as a function of *p*-clad thickness. For the case of  
 33020 a 0.15- $\mu\text{m}$ -thick graded layer, a lateral index step on the order of  
 33021  $3-8 \times 10^{-3}$  can be obtained by etching the *p*-clad to a thickness of about  
 33022 1500-800 Å.

33023 The dependence of the quantum-well confinement factor on graded layer  
 33024 thickness for cladding compositions of 66% AlAs and 40% AlAs is shown  
 33025 in Fig. 18.



33026 Fig. 18. The quantum-well confinement factor as a function of graded region  
 33027 thicknesses for cladding compositions of 40% and 66% AlAs.

33032 0233'''01652

## Mode Gain (or Loss)

- confinement factor
- gain or loss in a layer
- what happens if

$$\epsilon_l \rightarrow (\epsilon_l)_{\text{re}} + j(\epsilon_l)_{\text{mag.}}$$

( $l = \text{layer index}$ )

⇒ wavevectors are complex:

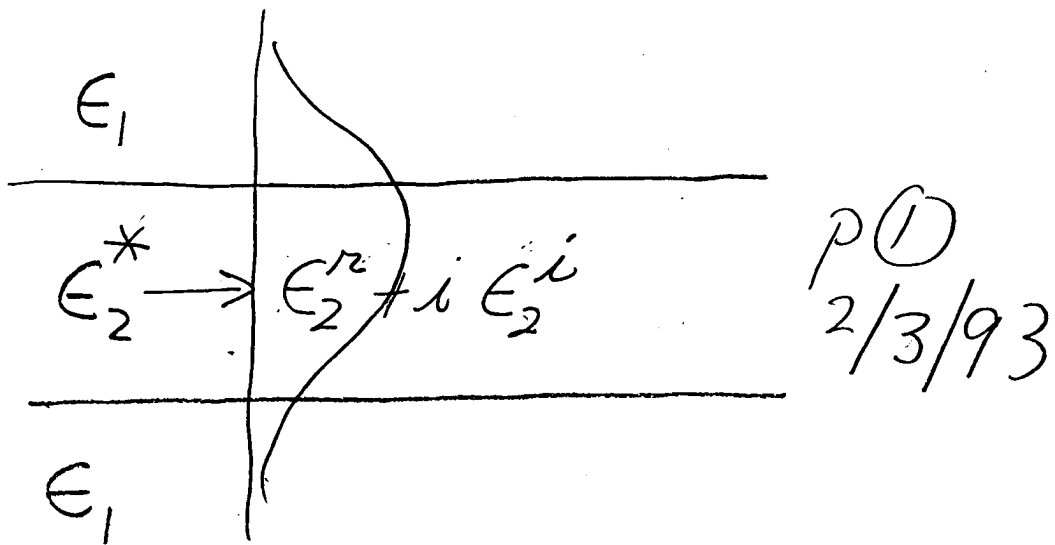
$$S \rightarrow S_{\text{re}} + j S_i$$

$$\delta \rightarrow \delta_{\text{re}} + j \delta_i$$

$$\beta \rightarrow \beta_{\text{re}} + j \beta_i$$

$(\gamma = \alpha + j\beta)$

I consider the 3 layer WG  
(symmetric)



Question: If there is gain\* in one layer, how does that effect the WG mode?

Sub-question: how does gain\* effect a plane wave in a homogeneous medium?

(\* or loss)

Subquestion answer:

a plane wave in a homogeneous, infinite media propagates as

$$\vec{E} = E_0 e^{j\omega t - j\sqrt{\epsilon_r} k_0 z} \hat{i}_n \quad (1)$$

if there is gain (or loss)

$$\epsilon \rightarrow \epsilon_{re} + j\epsilon_{im} \quad (2)$$

consider  $\epsilon_{mag} \ll \epsilon_{re}$

(almost always true), so

$$\sqrt{\epsilon_{re} + j\epsilon_{im}} \approx \sqrt{\epsilon_r} \left( 1 + j \frac{\epsilon_{im}}{\epsilon_r} \right)^{1/2}$$

$$(3) \qquad \approx \sqrt{\epsilon_r} \left( 1 + j \frac{\epsilon_{im}}{2\epsilon_r} \right)$$

so,

$$|\vec{E}| = E_0 e^{j\omega t - j\sqrt{\epsilon_r} k_0 z} e^{-j \frac{\epsilon_{im}}{2\epsilon_r} k_0 z}$$

$$= E_0 e^{+\alpha z} e^{j(\omega t - \sqrt{\epsilon_r} k_0 z)}$$

where  $\alpha = \frac{\epsilon_{im}}{2\epsilon_r} k_0$  (3.5)

so if  $\epsilon_{im}$  is +, the plane wave grows exp.  
 if  $\epsilon_{im}$  is -, the pw is exponentially damped

To see how a mode grows (gain) or decreases (loss), solve for  $\beta_i$

$$\beta^* \rightarrow \beta_r + j \beta_i$$

need to solve:

$$(4) \quad S = \begin{cases} \tan(\omega) & (e) \\ -\cot(\omega) & (o) \end{cases}$$

$$S^2 + \delta^2 = (\epsilon_2^* - \epsilon_1^*) R_0^2 \quad (5)$$

Since we are considering  
a perturbation: ( $\epsilon_i \ll \epsilon_r$ )

$$S \rightarrow S_r + j S_i, \quad S_i \ll S_r$$

$$\delta \rightarrow \delta_r + j \delta_i, \quad \delta_i \ll \delta_r$$

$$\beta \rightarrow \beta_r + j \beta_i \quad \beta_i \ll \beta_r$$

From (5),

$$(6) \quad S^2 = (S_r + j S_i)^2 = S_r^2 + 2j S_r S_i - \cancel{S_i^2}$$

$$(7) \quad \delta^2 = \delta_r^2 + 2j\delta_r\delta_i - \delta_i^2$$

$$\beta^2 = \beta_r^2 + 2j\beta_r\beta_i - \beta_i^2 \quad (8)$$

so (5)  $\Rightarrow$

$$\begin{aligned} & \delta_r^2 + 2j\delta_r\delta_i + \delta_r^2 + 2j\delta_r\delta_i \\ &= (\epsilon_2^r - \epsilon_1^r)k_0^2 + j(\epsilon_2^i - \epsilon_1^i)k_0^2 \end{aligned}$$

or  $\delta_r^2 + \delta_i^2 = (\epsilon_2^r - \epsilon_1^r)k_0^2 \quad (9a)$

$$\delta_r\delta_i + \delta_r\delta_i = (\epsilon_2^i - \epsilon_1^i)k_0^2 \quad (9b)$$

We also had Eq(3,4), 1/29, p⑥:

$$\delta^2 = \epsilon_2^* k_0^2 - \beta^2 \quad (10a)$$

$$-\delta^2 = \epsilon_1^* k_0^2 - \beta^2 \quad (10b)$$

$$SO \quad (10a) \Rightarrow$$

$$\delta_r^2 + 2j\delta_r s_i = (\epsilon_2^r + j\epsilon_2^i) k_0^2$$

$$\Rightarrow -(\beta_r^2 + 2j\beta_r \beta_i),$$

$$\delta_r^2 = \epsilon_2^r k_0^2 - \beta_r^2 \quad (11a)$$

$$\delta_r s_i = \frac{\epsilon_2^i k_0^2}{2} - \beta_r \beta_i \quad (11b)$$

$$(10b) \Rightarrow$$

$$-(\delta_r^2 + 2j\delta_r \delta_i) = (\epsilon_1^r + j\epsilon_1^i) k_0^2$$

$$-(\beta_r^2 + 2j\beta_r \beta_i)$$

$$\Rightarrow$$

$$-\delta_r^2 = \epsilon_1^r k_0^2 - \beta_r^2 \quad (12a)$$

$$-\delta_r \delta_i = \frac{\epsilon_1 k^2}{2} - \beta_r \beta_i \quad (12b)$$

Now look at (Eq(4)):

$$\mathcal{S}^* = \begin{cases} \tan(SW) & (e) \\ -\cot(SW) & (o) \end{cases}$$

Use a Taylor expansion

$$\underline{f(z)} = f(z_0) + (z - z_0)f'(z_0)$$

$$+ \left(\frac{z - z_0}{2}\right)^2 f''(z_0) + \dots$$

$$\dots + \frac{(z - z_0)^n}{n!} f^n(z_0)$$

so that

$$\tan(S_r W + j S_i W)$$

$$= \tan(S_r W) + j S_i W \sec^2(S_r W)$$

$+ O(S_i W)^2 + \dots$

$$\cot(S_r W + j S_i W) =$$

$$\cot(S_r W) - j S_i W \csc^2(S_r W)$$

$+ O(S_i W)^2 + \dots$

so (4)  $\Rightarrow$

$$(S_r + j S_i) = (S_r + j S_i)$$

$$x \begin{cases} \tan(S_r W) + j S_i W \sec^2(S_r W) \\ -\cot(S_r W) + j S_i W \csc^2(S_r W) \end{cases}$$

Equate real & imag:

$$(13a) S_r = s_r \begin{cases} \tan(s_r w) & (e) \\ -\cot(s_r w) & (o) \end{cases}$$

$$(13b) S_i = \begin{cases} s_i \tan(s_r w) + s_r s_i w \\ \cdot \sec^2(s_r w) & (e) \\ -s_i \cot(s_r w) + s_r (s_i w) \\ \cdot \csc^2(s_r w) & (o) \end{cases}$$

Recall, we want to

find  $\beta_{ij}$  so from

(12b):

$$\beta_r/\beta_i = \frac{\epsilon_1^i k_0^2}{2} + \delta_r \delta_i$$

or

$$\frac{\beta_i}{\beta} = \frac{\epsilon_1^i k_0^2}{2\beta^2} + \frac{\delta_r \delta_i}{\beta^2} \quad (14)$$

from (13a,b),  $\delta_r \delta_i = A_r A_i$

$$X \left\{ \begin{array}{l} \tan^2(A_r W) \left[ 1 + \frac{A_r W \sec^2(A_r W)}{\tan(A_r W)} \right] e \\ \cot^2(A_r W) \left[ 1 - \frac{A_r W \csc^2(A_r W)}{\cot(A_r W)} \right] o \end{array} \right.$$

(15)

III  
P<sub>2</sub>

From (11b),

$$\frac{S_R S_i}{\beta^2} = \frac{\epsilon_2^{ik^2}}{2\beta^2}, - \frac{\beta_i}{\beta^2} \quad (16)$$

so (14) →

$$\frac{\beta_i}{\beta} = \frac{\epsilon_1^{ik^2}}{2\beta^2} + \left( \frac{\epsilon_2^{ik^2}}{2\beta^2} - \frac{\beta_i}{\beta} \right) P_2$$

to here

or

$$\frac{\beta_i}{\beta_{re}} (1 + P_2) = \frac{\epsilon_1^{ik^2}}{2\beta^2} + \frac{\epsilon_2^{ik^2}}{2\beta^2} P_2$$

$$\beta_i = \frac{1}{2} \frac{k_0^2}{\beta_{re}} \left( \frac{\epsilon_1^i + \epsilon_2^i P_2}{1 + P_2} \right) \quad (17)$$

consider a semiconductor laser

$$\textcircled{1} \quad \epsilon_1 = \epsilon_1^{\text{re}}$$

$$\textcircled{2} \quad \epsilon_2^* = \epsilon_2^{\text{re}} + j\epsilon_2^i \quad P_{in}$$

$$\textcircled{1} \quad \epsilon_1 = \epsilon_1^{\text{re}}$$

$$\Rightarrow \beta_i = \frac{1}{2} \frac{k_0^2 \epsilon_2^i}{\beta} \left( \frac{P_2}{1+P_2} \right) \quad (18)$$

Physically,

$$\Gamma_2 = \frac{P_{in}}{P_{in} + P_{out}} \neq \frac{P_2}{1+P_2}$$

where

$$P_{in} = \text{const} \int_{-W}^W \frac{\cos^2(Sx) dx}{\cos^2(SW)}$$

(even modes)

$$P_{in} = \text{const} \int_{-W}^W \frac{\sin^2(SX) dx}{\sin^2(SW)} \quad (\text{odd modes})$$

$$P_{out} = 2 \text{ const} \int_W^\infty e^{-2Sx} e^{-2S.W} dx$$

so

$$P_{in} \propto \frac{1}{S} \left[ \frac{SW + \sin(SW)\cos(SW)}{\cos^2(SW)} \right] \quad (\text{even})$$

$$P_{in} \propto \frac{1}{S} \left[ \frac{SW - \sin(SW)\cos(SW)}{\sin^2(SW)} \right] \quad (\text{odd})$$

$$P_{out} \propto \frac{1}{S}, \quad \text{so}$$

$$\boxed{2} = \frac{A}{1+A}$$

where

$$A = \frac{\delta_n}{S_n} \left[ \frac{SW + \sin(SW)\cos(SW)}{\cos^2(SW)} \right]$$

(even)

$$A = \frac{\delta_n}{S_n} \left[ \frac{SW - \sin(SW)\cos(SW)}{\sin^2(SW)} \right]$$

(odd)

USING

$$\delta = \begin{cases} \tan(SW) & (e) \\ -\cot(SW) & (o) \end{cases}$$

we have  $A = P_2$

Result: (for gain in layer 2)

$$\underline{\underline{\beta_i}} = \frac{1}{2} \frac{k_0^2 \epsilon_2^{(i)}}{\beta} \Gamma_2 \quad (19)$$

$$e^{-j\beta z} - e^{-j(\beta_{20} + j\beta_i)z}$$

effective mode gain =  $C_{\text{eff}}$   
 $\equiv \frac{\text{gain of mode}}{\text{gain of plane wave}}$

gain of PW (Eq 3.5 p9):

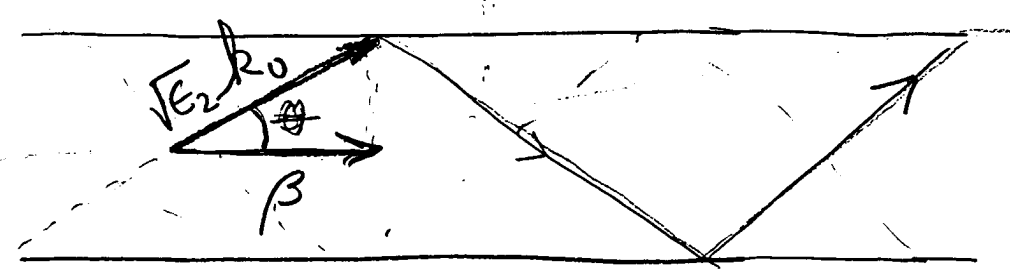
$$g_{\text{PW}} = \frac{\epsilon_2^i k_0}{2\Gamma\epsilon_2}$$

$$C_{\text{eff}} = \frac{\beta_i}{g_{\text{PW}}} = \frac{\left[ \frac{1}{2} k_0^2 \epsilon_2^i / \beta_{\text{re}} \right] \Gamma}{\left[ \frac{1}{2} k_0 \epsilon_2^i / \Gamma \epsilon_2 \right]}$$

$$C_{\text{eff}} = \frac{\sqrt{\epsilon_2^i} k_0}{\beta_{\text{re}}} \quad (20)$$

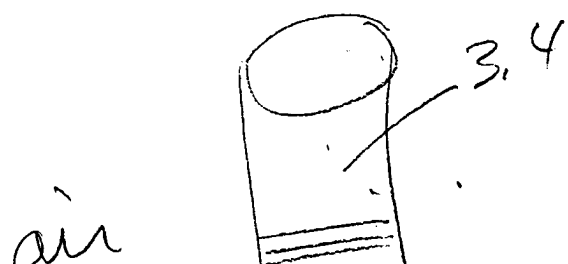
Can  $C_{\text{eff}}$  ever be  $> 1$ ?

(24)



$$\cos \theta = \frac{B_{re}}{\sqrt{\epsilon_2} k_0}$$

$$C_{eff} = \frac{1}{\cos \theta}$$

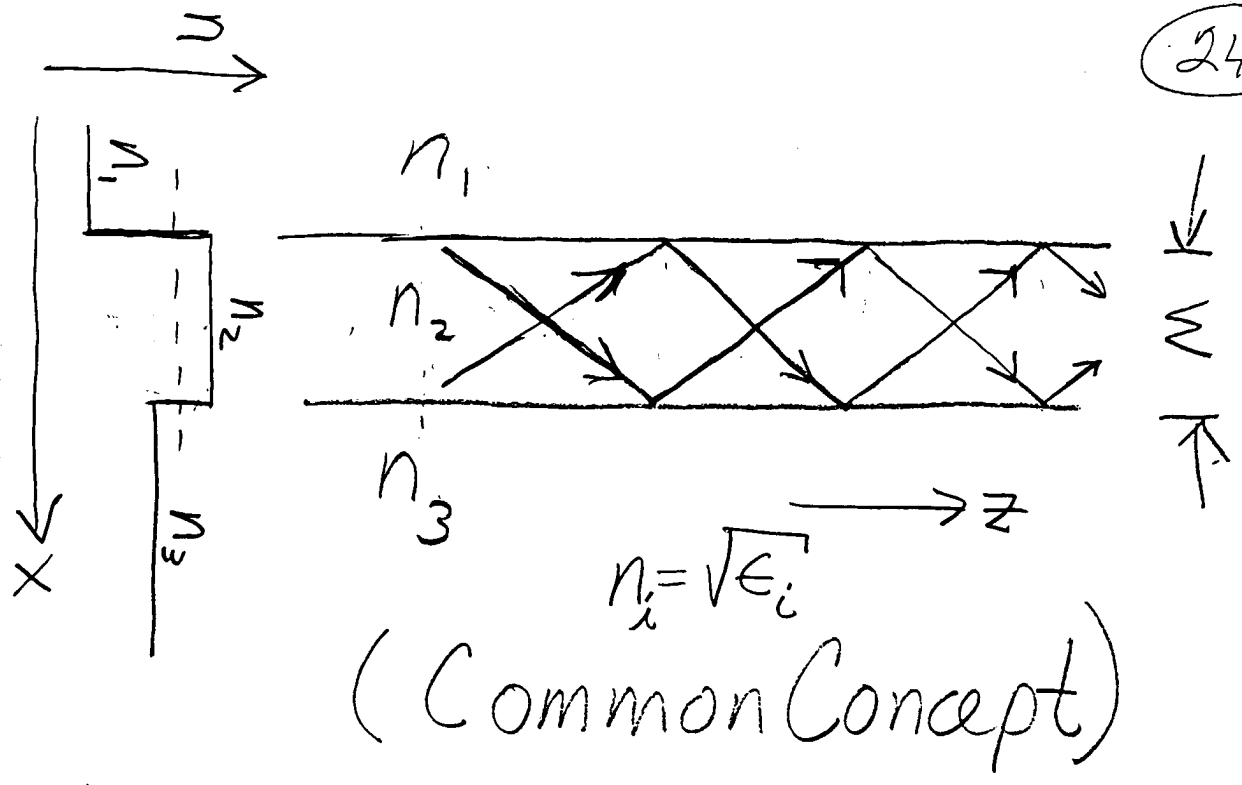


$$g_{mode} \approx (f_{material})^{1/2} \cos \theta$$

# Additional Waveguiding Concepts

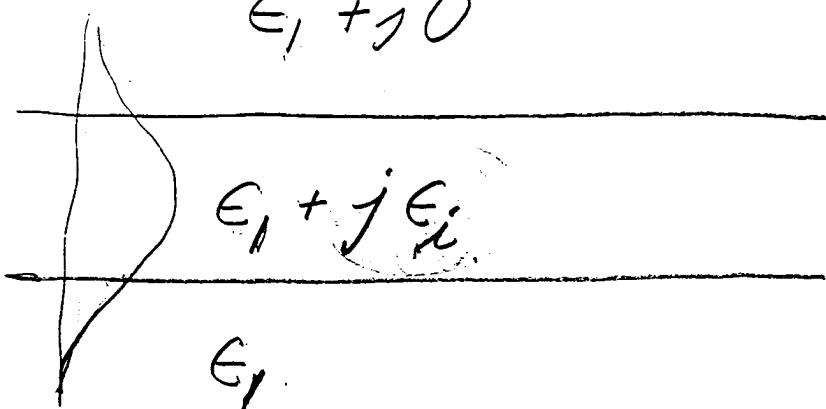
- Gain Guiding
- Loss Guiding
- "CSP" Geometry

Most common concept is that dielectric WGs have a positive index step, and total internal reflection causes the optical (or electromagnetic) energy to be confined near a "Core":



## 1) Gain Guiding

$$\epsilon_1 + j\epsilon_0$$



This waveguide supports modes

- Wavevectors are complex
- curved wavefronts,  
(astigmatism)

see W.O. Schlosser,  
 "Gain induced modes  
 in planar structures"  
 Bell System Tech. J.  
 Vol 52, p. 887, 1973.

In semiconductor lasers,  
 $\epsilon_i = \epsilon_i(x)$  is determined  
 by current spreading

- can be solved exactly  
 for certain forms of

$\epsilon_i(x)$  - parabolic  
 distribution  $\Rightarrow$  Hermite  
 Gaussian solutions

see Thompson, Physics  
of Semiconductor Lasers  
 WILEY 1980 D. 2000:

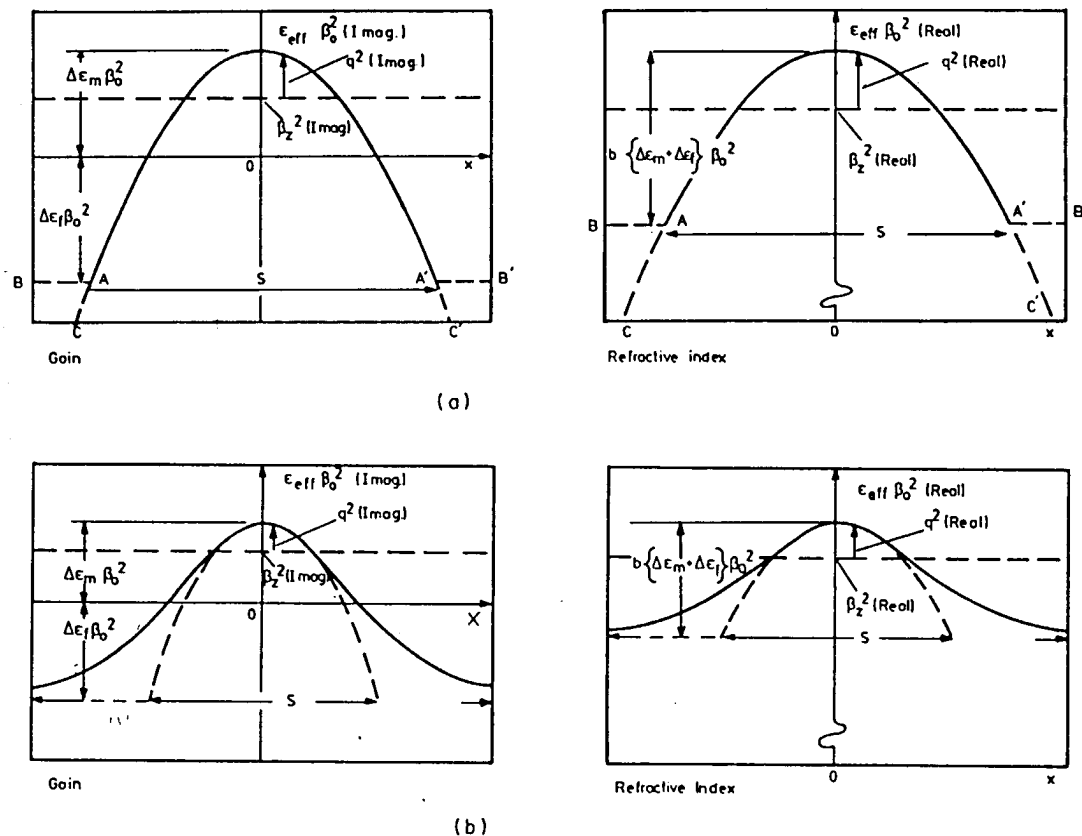
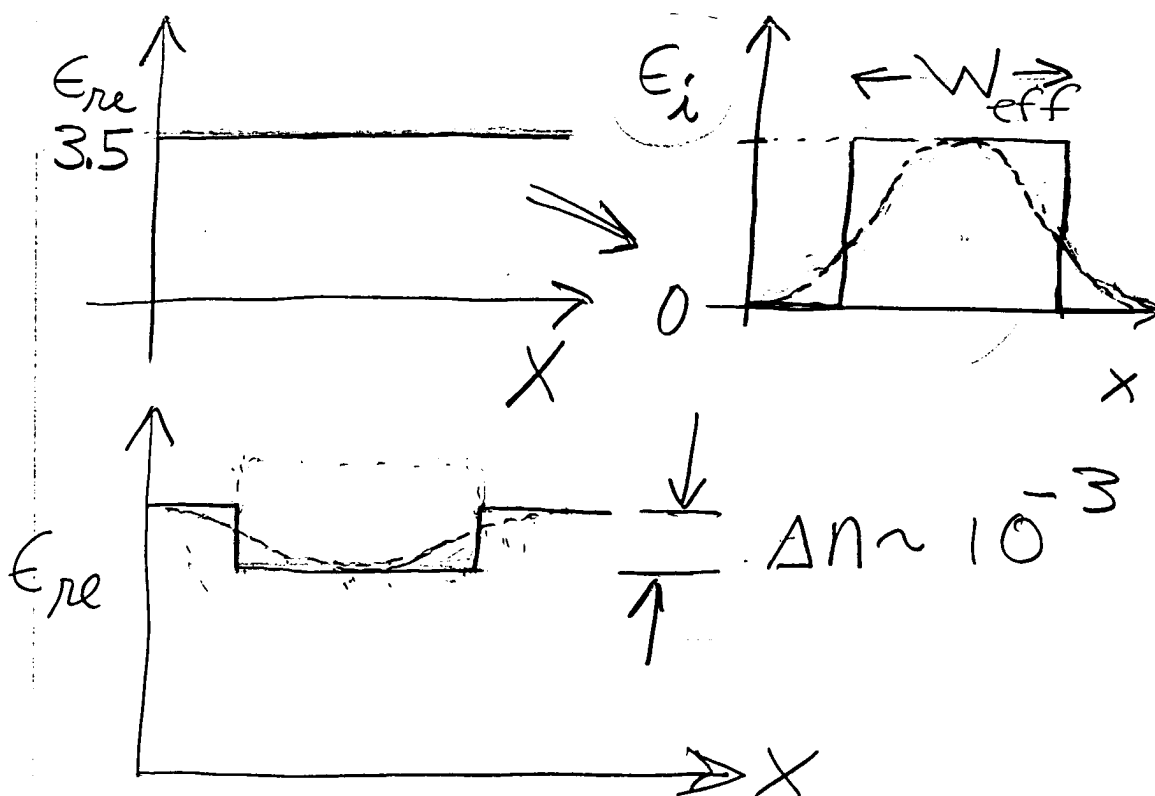
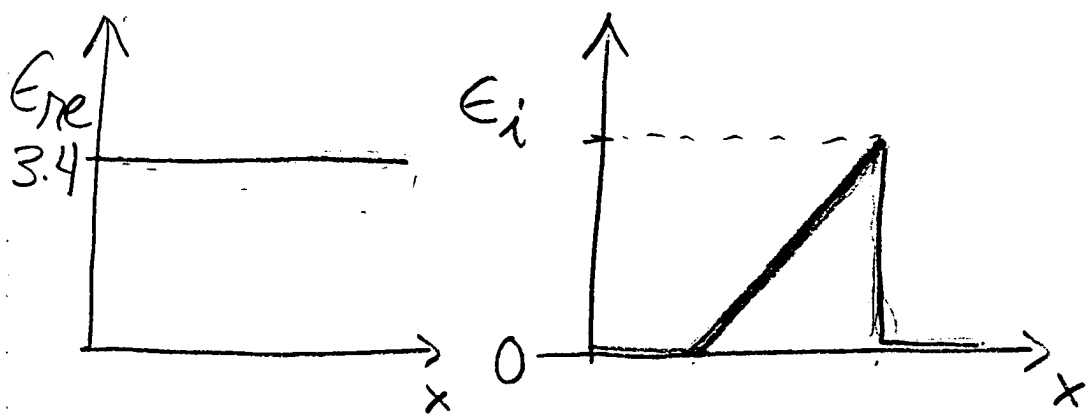


Figure 4.21 Two forms of continuous transverse distribution of dielectric constant for which exact mathematical solutions of the guided optical distribution may be found. (a) parabolic distribution, (b)  $\cosh^{-1}$  distribution. Left-hand diagrams represent gain, right-hand diagrams dielectric constant



Gain Induced Index Depression (J. Manning  
 [LaCourse] 82-83; see Ref 46 of CSP chapter)

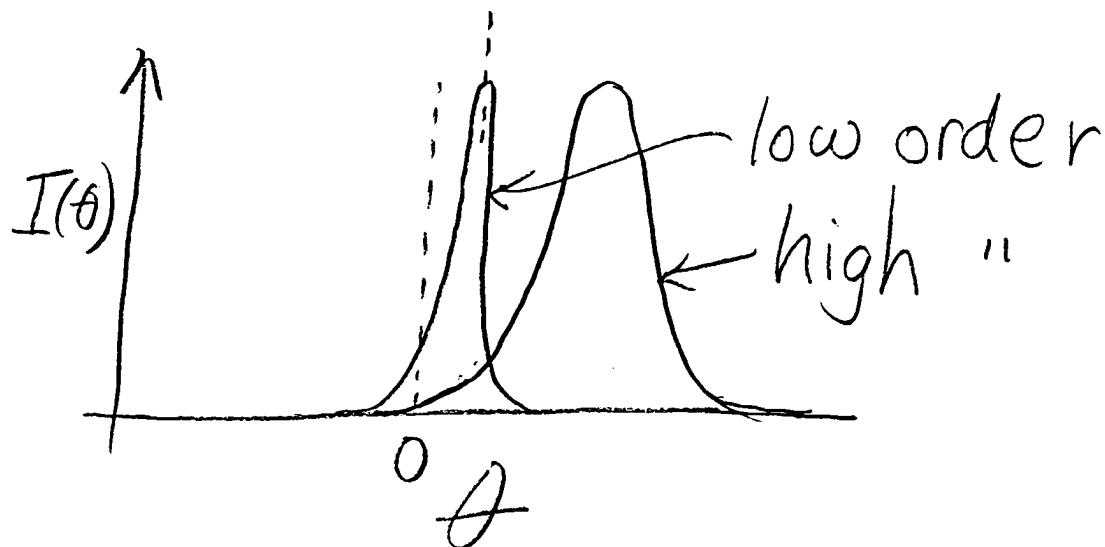
(a) "Ramped Gain" guide



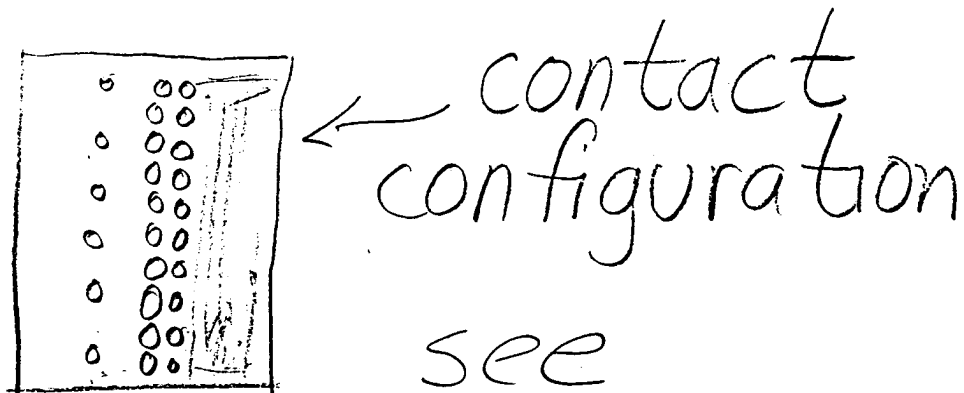
Interesting property:

⇒ ALL Far-Fields are Single-lobed !!?

(never proved)



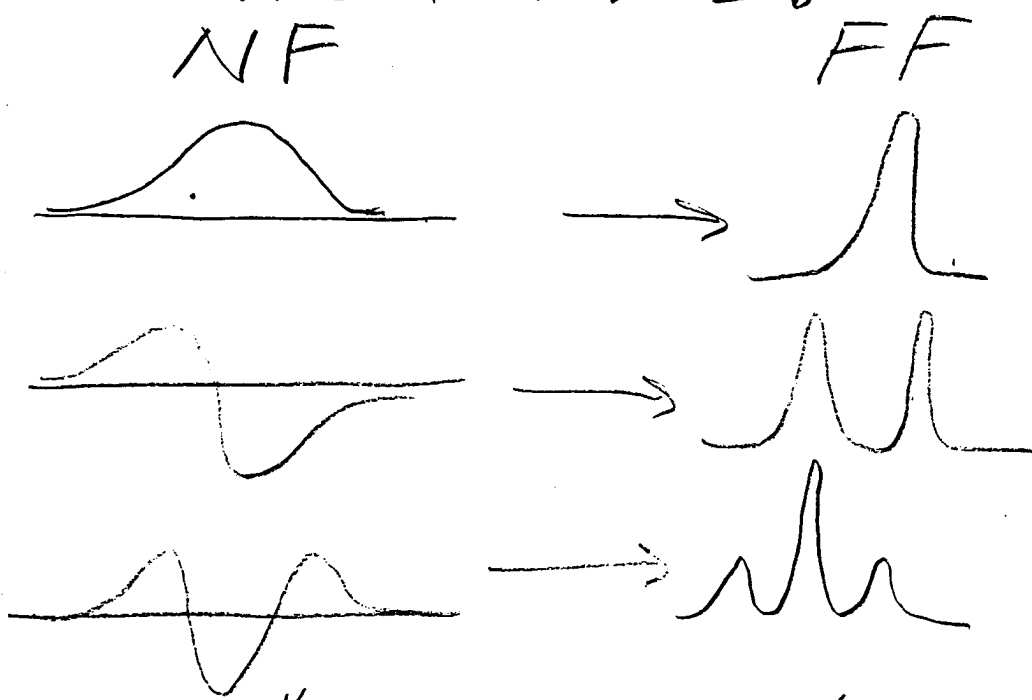
- pattern shifted from  $0^\circ$
- higher order modes shifted more



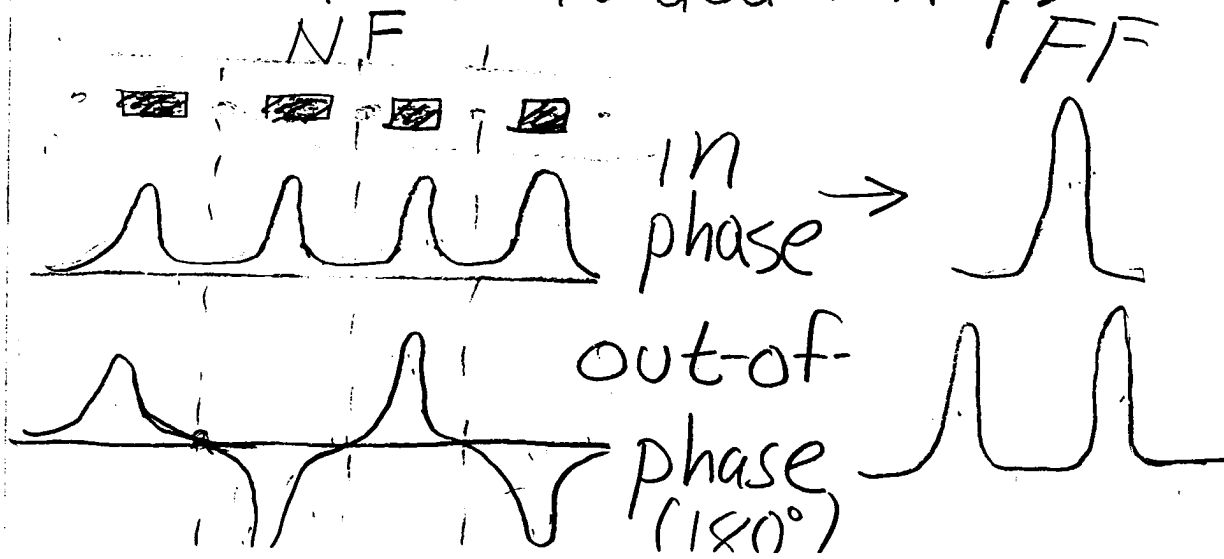
Lindsey, et al, IEEE JQE  
QE-23, 6, p.775-787, 1987.

- single lobe
- multiple transverse modes
- "broad far-field"

Note: different modes for index guided WG's have different # of far field lobes:



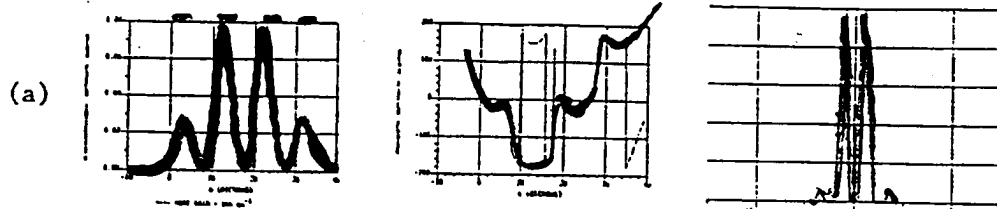
"Gain Guided" Arrays



249

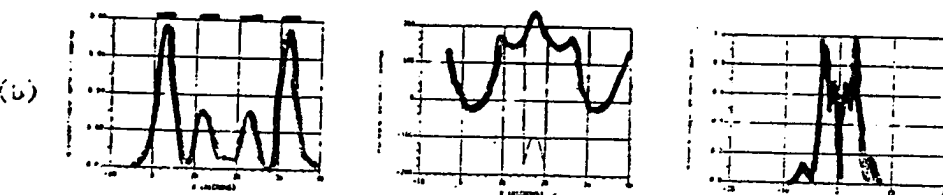
# Gain Guided Patterns

NF      NF Phase      FF



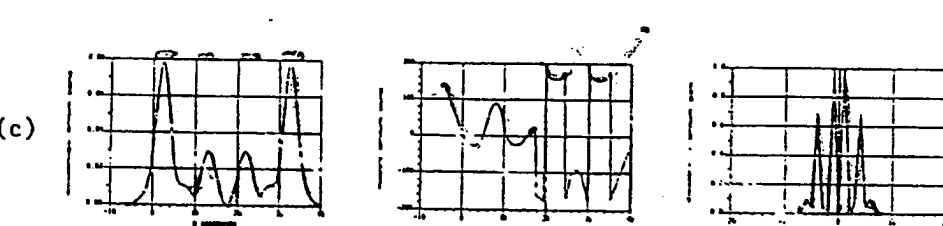
+ - + -

$$\beta_i \Rightarrow 167 \text{ cm}^{-1}$$



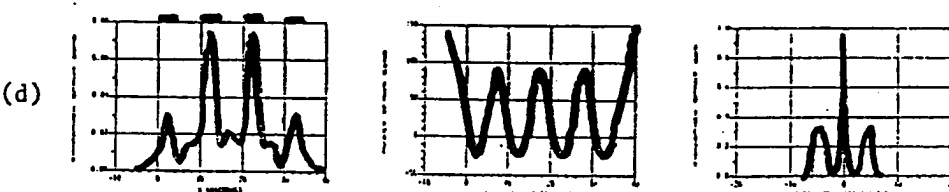
+ - - +

$$\beta_i \Rightarrow 163 \text{ cm}^{-1}$$



++ - -

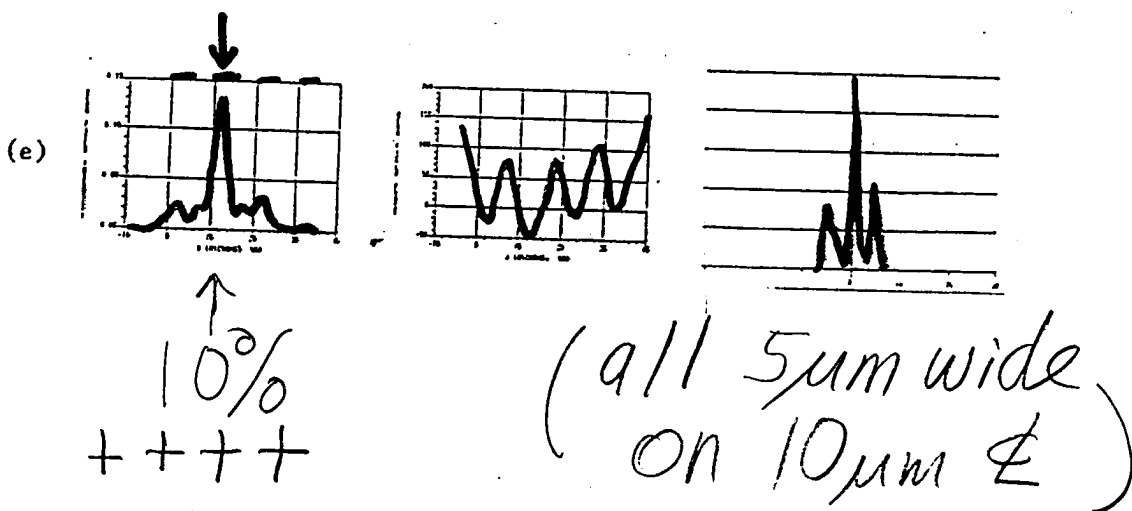
$$\beta_i \Rightarrow 157 \text{ cm}^{-1}$$



+++ +

$$\beta_i \Rightarrow 150 \text{ cm}^{-1}$$

Now, (reduce) the gain by 10% in element #2:



Note: NF collapses  
(FF hardly changes)

Key Points for GG Array:

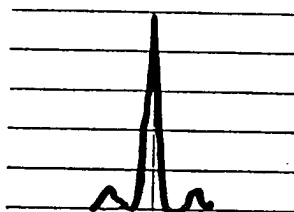
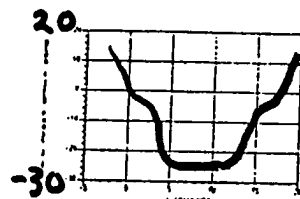
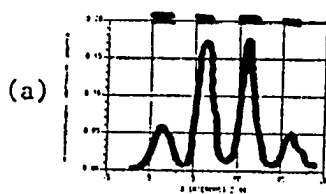
- Wants to oscillate in "out-of-phase" mode
- Very Sensitive
- Questionable Perf

# Index Guided Patterns

NF

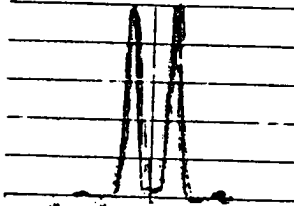
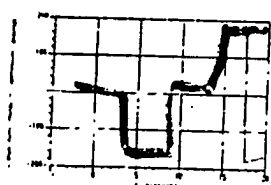
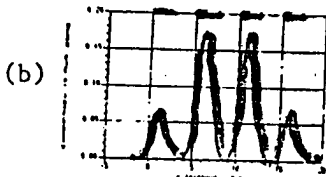
NFPhase

FF



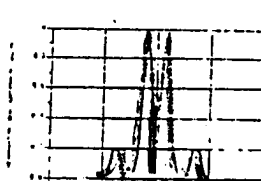
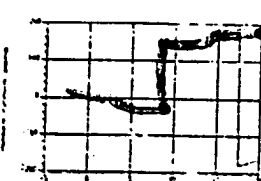
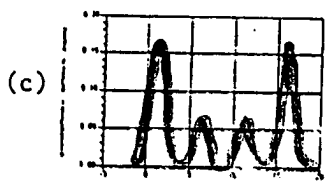
+++

$$\beta_i \Rightarrow 98.7 \text{ cm}^{-1}$$



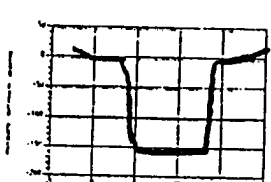
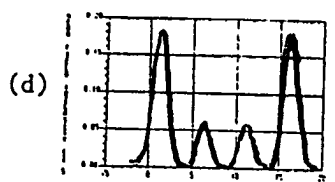
+--

$$\beta_i \Rightarrow 98.1 \text{ cm}^{-1}$$



++--

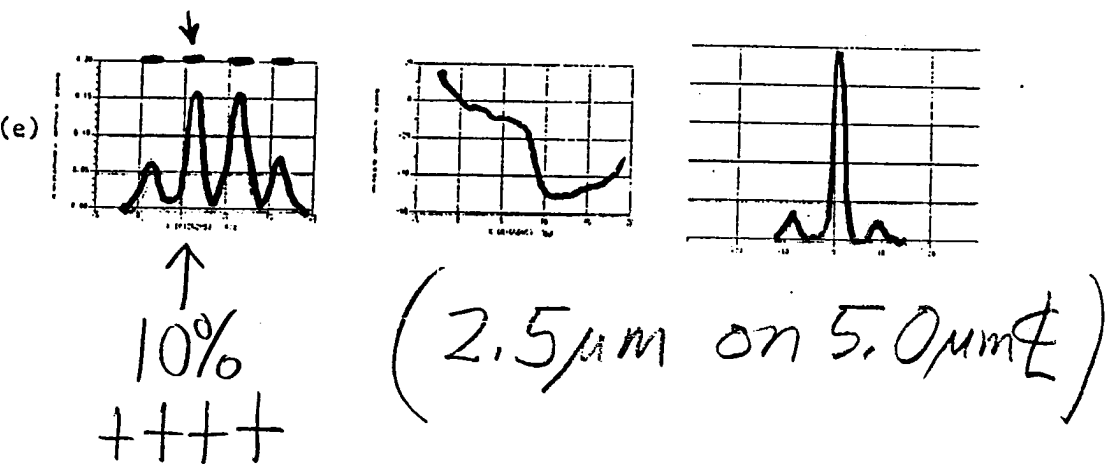
$$\beta_i \Rightarrow 95.7$$



+--+ +

$$\beta_i \Rightarrow 95.7$$

Now reduce the gain  
by 10% in element #2:



NF is insensitive.

Key Points, JG Array:

- can oscillate "in phase"

- less sensitive

- little mode discrimination

( $<1\%$  difference in

gain for +++,

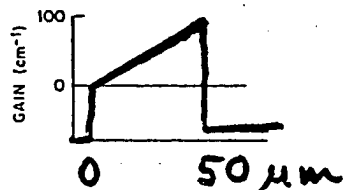
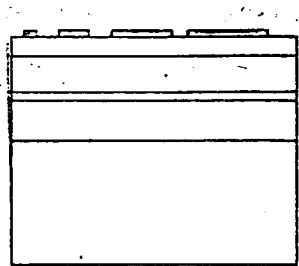
and +-+)

stopped  
3/31

(253)

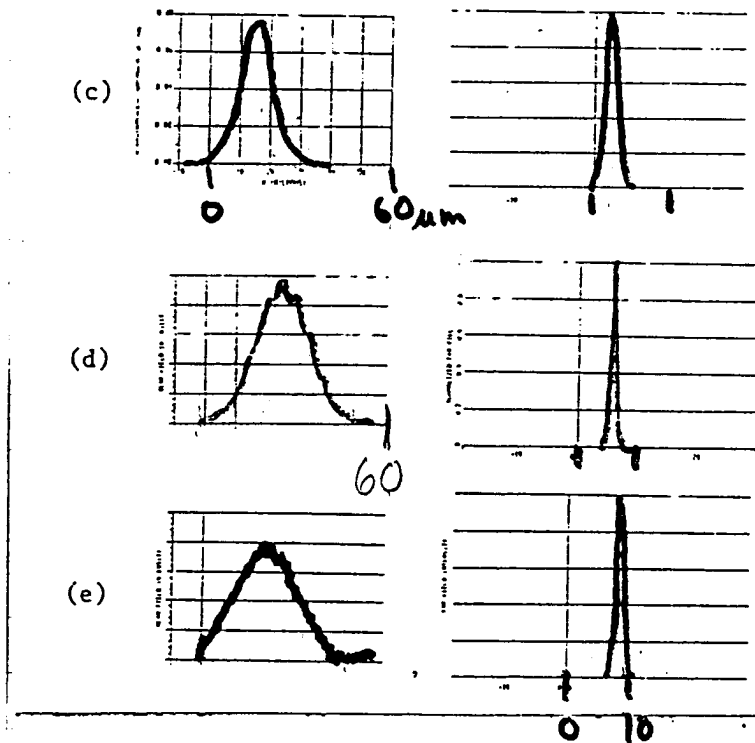
# Ramped Gain

$$W = 50 \mu\text{m}$$



NF

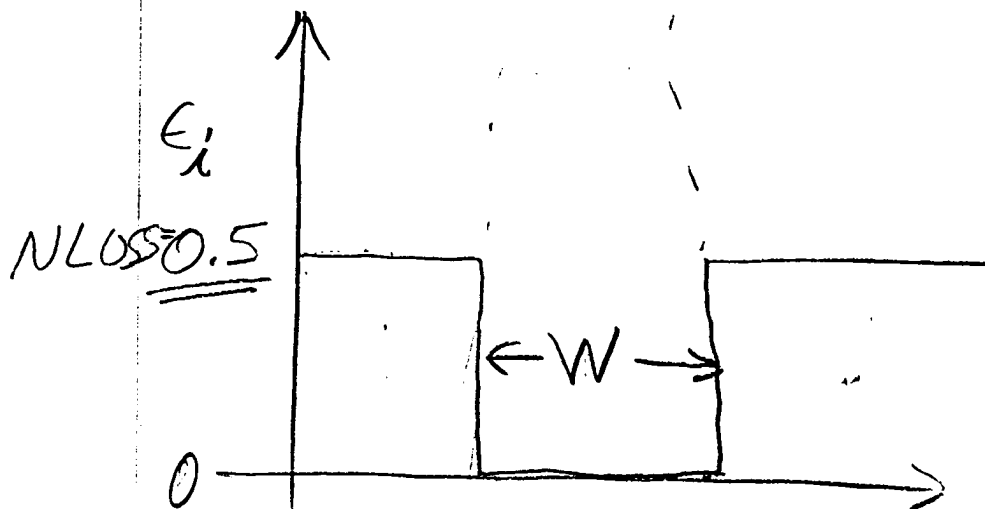
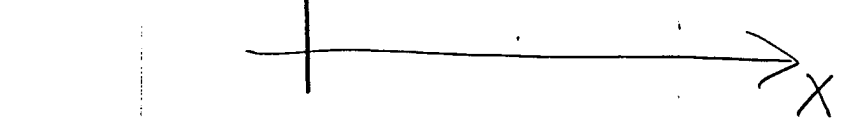
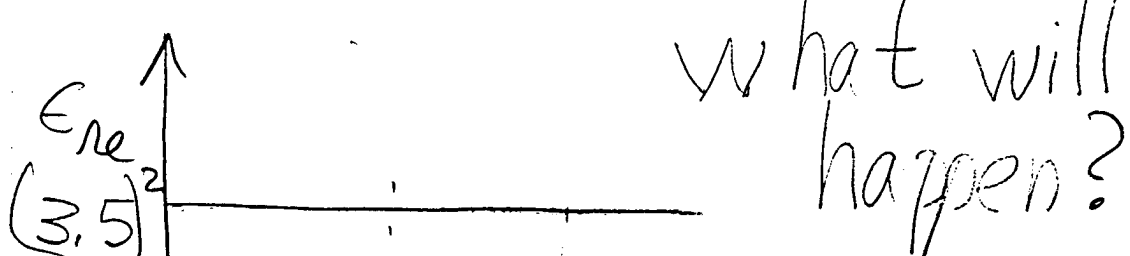
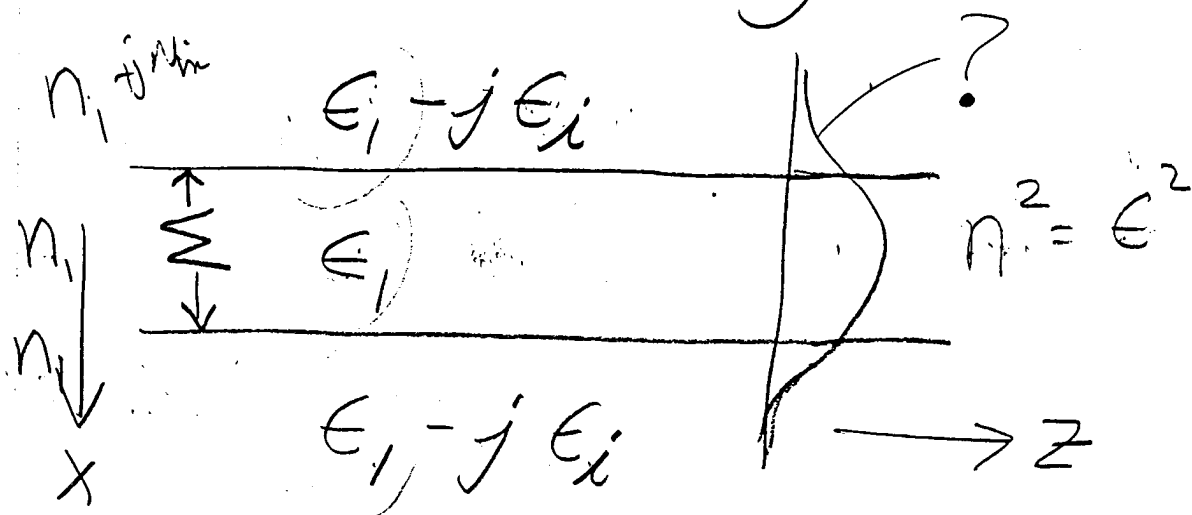
FF



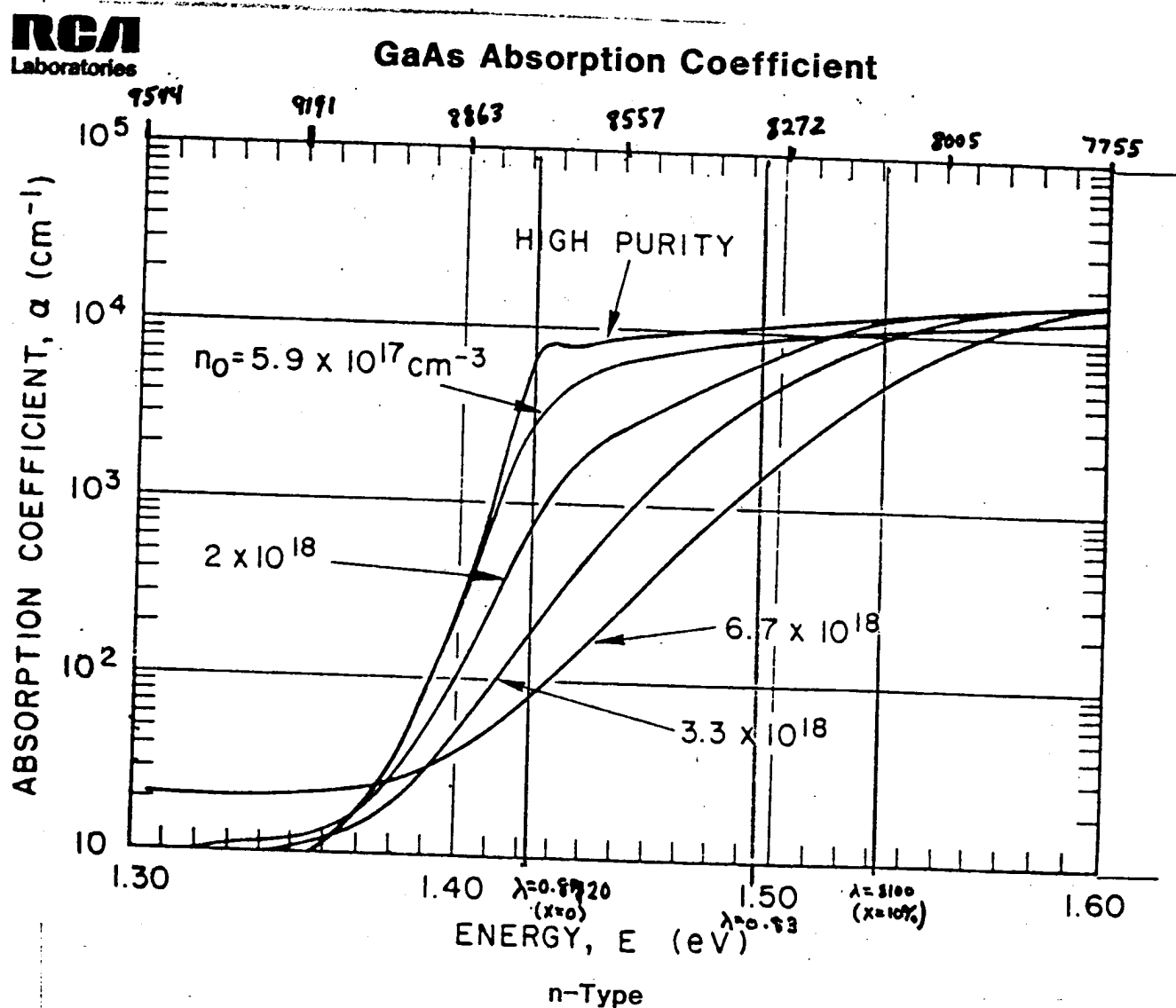
Step

Note relative use of  
gain medium

## 2) Loss Guiding



# Material Absorption VS $\lambda$ .



Energies  $< E_g$ ,  $\alpha \approx 10-20 \text{ cm}^{-1}$

$> E_g$ ,  $\alpha = 10,000 \text{ cm}^{-1}$

How do we put material loss or imaginary components of the index or permittivity in MODEIG?

We can specify

$$\left. \begin{aligned} (\epsilon)_{\text{real}} &= \text{PER} \\ (\epsilon)_{\text{mag}} &= \text{PEI} \end{aligned} \right) \text{ for each layer}$$

(original Modeig code)

Generally, we know the real part of the index of refraction for a material, and we may

know the absorption coefficient.

The absorption coefficient is also known as the "extinction coefficient" and describes the exponential decrease in power of a wave travelling in the media:

$$\text{Let } \tilde{n} = n_{\text{re}} + i n_{\text{imag}}$$

The field amplitude propagates as

$$A e^{i \tilde{n} k_0 z} \quad (1)$$

where  $k_0 = 2\pi/\lambda_0$

or,

$$A e^{i n_{\text{re}} k_0 z} e^{-n_{\text{imag}} k_0 z} \quad (2)$$

Since the mode power  $\propto (A \hat{e}^\dagger \hat{e})^2$ ,  
the power decays as

$$e^{-2 n_{\text{imag}} k_0 z} = e^{-\alpha_p z} \quad (3)$$

So the power absorption  
is

$$\boxed{\alpha_p = \frac{4\pi n_{\text{imag}}}{\lambda_0}} \quad (4)$$

From 3/26 p(14), the power absorption for GaAs at  $0.6\mu\text{m} < \lambda < 0.8\mu\text{m}$

$$15 \quad \alpha_p \approx 10,000 \text{ cm}^{-1}$$

Note: at  $\lambda = 0.65\mu\text{m}$

$$\begin{aligned} n_{\text{mag}} &= \frac{\alpha_p \lambda_0}{4\pi} \\ &= \frac{10^4 \text{ cm}^{-1} \cdot 65\mu\text{m} \frac{1\text{cm}}{10^4\mu\text{m}}}{4\pi} \\ &= 0.05 \end{aligned}$$

For historical reasons,  
MODEIG accepts loss  
directly -- BUT the  
loss term inputed to  
MODEIG (NLOSS) must be  
specified as

① Amplitude loss  
(not power)  
with

② Units of  $\mu\text{m}^{-1}$   
(not  $\text{cm}^{-1}$ )

(what could be simpler?)

(261)

Example: A layer has a real index of 3.5 and a power loss

$\alpha = 1 \times 10^4 \text{ cm}^{-1}$ . How is the layer specified in MODEIG?

Answer:

$$NLOSS = \frac{\alpha_p}{2} \\ = 5 \times 10^3 \frac{1}{\text{cm}} \frac{10^{-4} \text{ cm}}{\mu\text{m}}$$

$$\boxed{NLOSS = 0.5 \mu\text{m}^{-1}}$$

$$\overbrace{\text{LAYER NREAL}=3.5 \quad NLOSS=0.5}^{\overbrace{\text{TL}=1.7}}$$

This is also discussed  
in one of the MODEIG  
handouts:

"Reference Notes for  
the use of complex  
refractive indices with  
MODEIG" (Abeles & Evans)

Look in the back of  
Modeig/II Manual

```

CASE KASE=910101
CASE EPS1=1E-7 GAMEPS=1E-3 QZMR=12.25 QZMI=0.001
CASE PRINTF=0 INITGS=0 AUTOQW=0 NFPLT=1 FFPLT=1
CASE IL=50

```

```
MODCON KPOL=1 APB1=0.25 APB2=0.25
```

```
STRUCT WVLL=1.0
```

```
LAYER NREAL=3.5 NLLOSS=0.5 TL=0
LAYER NREAL=3.5 NLLOSS=0. TL=5.
LAYER NREAL=3.5 NLLOSS=0.5 TL=0.
```

```
OUTPUT PHMO=1 GAMMAO=1 WZRO=1 WZIO=1 QZRO=1 QZIO=0
OUTPUT FWHPNO=1 FWHPFO=1 KMO=1 IT0=1
OUTPUT SPLTFL=1 MODOUT=0 LYROUT=1
```

```
GAMOUT LAYGAM=2 COMPGAM=0 GAMALL=0
```

```
!LOOPX1 ILX='NLLOSS' FINV=0.2382 XINC=.05 LAYCH=1
!LOOPX1 ILX='NLLOSS' FINV=0.2382 XINC=.05 LAYCH=3
LOOPX1 ILX="TL" FINV=0.0 XINC=-0.1 LAYCH=2
```

```
!LOOPZ1 ILZ='QZMR' FINV=11.75 ZINC=-.05
```

```
END
```

0264

### Three Layer Loss Waveguide "Layer Data"

# of layers = 3  
LAYER01 NLOSS= .50000 NREAL= 3.50000 TL=.00000  
LAYER02 NLOSS= .00000 NREAL= 3.50000 TL= 5.00000  
LAYER03 NLOSS= .50000 NREAL= 3.50000 TL=.00000

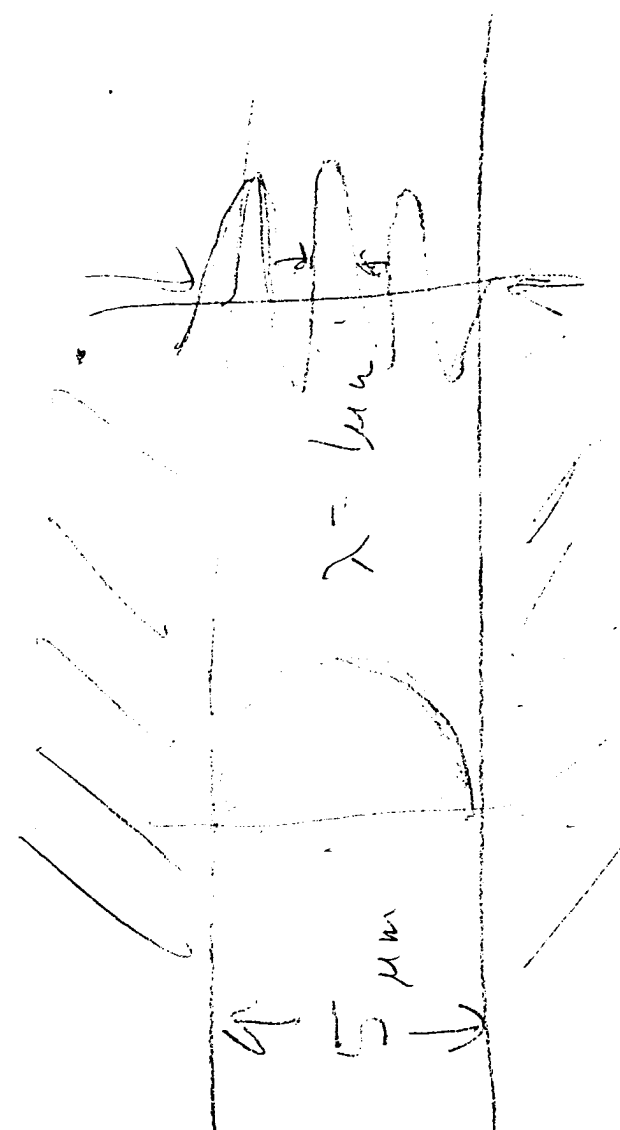
\*\*\*\*\*

(265)

$\rho_2(\beta)$   $f_m(\beta_{\mu_1})$   $k_0 \epsilon$

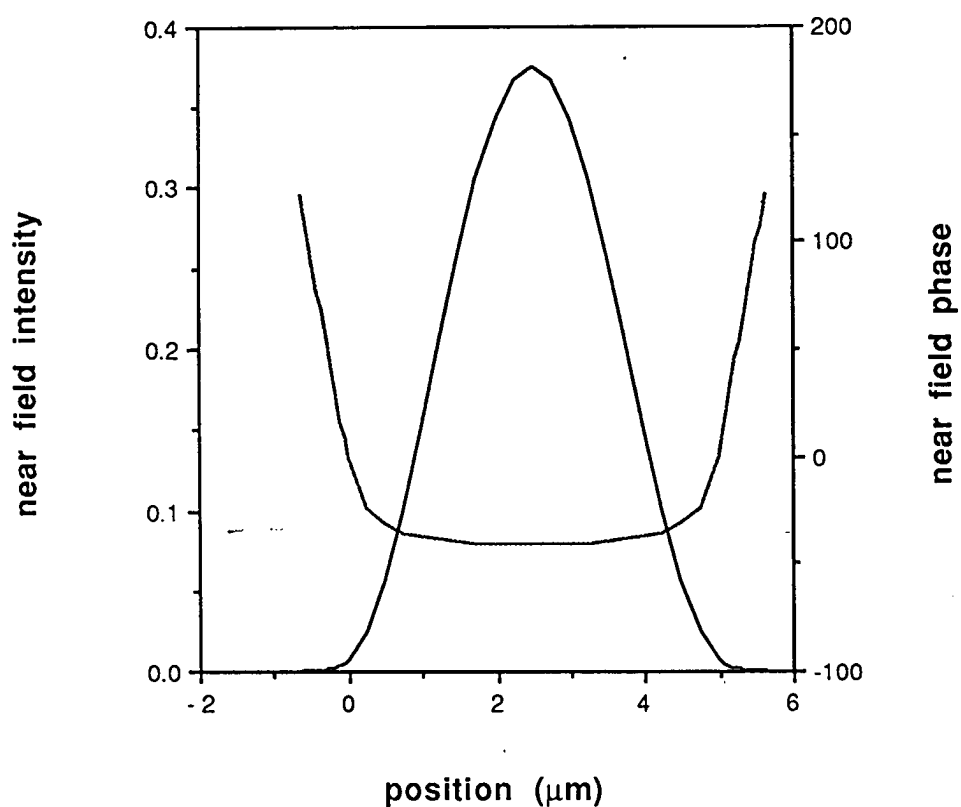
*	QZMR	PHM	GAMMA(2)	VZR	WZI	QZR	FWHPN	FWHPF
1.225000E+01	9.399147E-01	9.980289E-01	3.498742E+00	1.432068E-04	1.224119E+01	2.667237E+00	1.277766E+01	7
1.220000E+01	1.880487E+00	9.925312E-01	3.494961E+00	5.791037E-04	1.221475E+01	1.350117E+00	9.805452E+00	6
1.215000E+01	2.822521E+00	9.829607E-01	3.488639E+00	1.326075E-03	1.217060E+01	9.054465E-01	1.002601E+01	6
1.210000E+01	3.767083E+00	9.695480E-01	3.479740E+00	2.412659E-03	1.210859E+01	7.134691E-01	1.044847E+01	6
1.205000E+01	4.715524E+00	9.514015E-01	3.468208E+00	3.872527E-03	1.202845E+01	6.307239E-01	1.104359E+01	6
1.200000E+01	4.715524E+00	9.514015E-01	3.468208E+00	3.872527E-03	1.202845E+01	6.307239E-01	1.104359E+01	6
1.195000E+01	5.669333E+00	9.288295E-01	3.453960E+00	5.735302E-03	1.192981E+01	5.433983E-01	1.187500E+01	6
1.190000E+01	5.669333E+00	9.288295E-01	3.453960E+00	5.735302E-03	1.192981E+01	5.433983E-01	1.187500E+01	6
1.185000E+01	6.629631E+00	9.014714E-01	3.436898E+00	8.015651E-03	1.181221E+01	4.799959E-01	1.304118E+01	6
1.180000E+01	6.629631E+00	9.014714E-01	3.436898E+00	8.015651E-03	1.181221E+01	4.799959E-01	1.304118E+01	6
1.175000E+01	6.629631E+00	9.014714E-01	3.436898E+00	8.015651E-03	1.181221E+01	4.799959E-01	1.304118E+01	6

*	QZMR	PHM	GAMMA(2)	VZR	WZI	QZR	FWHPN	FWHPF
1.225000E+01	9.399147E-01	9.980289E-01	3.498742E+00	1.432068E-04	1.224119E+01	2.667237E+00	1.277766E+01	7
1.220000E+01	1.880487E+00	9.925312E-01	3.494961E+00	5.791037E-04	1.221475E+01	1.350117E+00	9.805452E+00	6
1.215000E+01	2.822521E+00	9.829607E-01	3.488639E+00	1.326075E-03	1.217060E+01	9.054465E-01	1.002601E+01	6
1.210000E+01	3.767083E+00	9.695480E-01	3.479740E+00	2.412659E-03	1.210859E+01	7.134691E-01	1.044847E+01	6
1.205000E+01	4.715524E+00	9.514015E-01	3.468208E+00	3.872527E-03	1.202845E+01	6.307239E-01	1.104359E+01	6
1.200000E+01	4.715524E+00	9.514015E-01	3.468208E+00	3.872527E-03	1.202845E+01	6.307239E-01	1.104359E+01	6
1.195000E+01	5.669333E+00	9.288295E-01	3.453960E+00	5.735302E-03	1.192981E+01	5.433983E-01	1.187500E+01	6
1.190000E+01	5.669333E+00	9.288295E-01	3.453960E+00	5.735302E-03	1.192981E+01	5.433983E-01	1.187500E+01	6
1.185000E+01	6.629631E+00	9.014714E-01	3.436898E+00	8.015651E-03	1.181221E+01	4.799959E-01	1.304118E+01	6
1.180000E+01	6.629631E+00	9.014714E-01	3.436898E+00	8.015651E-03	1.181221E+01	4.799959E-01	1.304118E+01	6
1.175000E+01	6.629631E+00	9.014714E-01	3.436898E+00	8.015651E-03	1.181221E+01	4.799959E-01	1.304118E+01	6



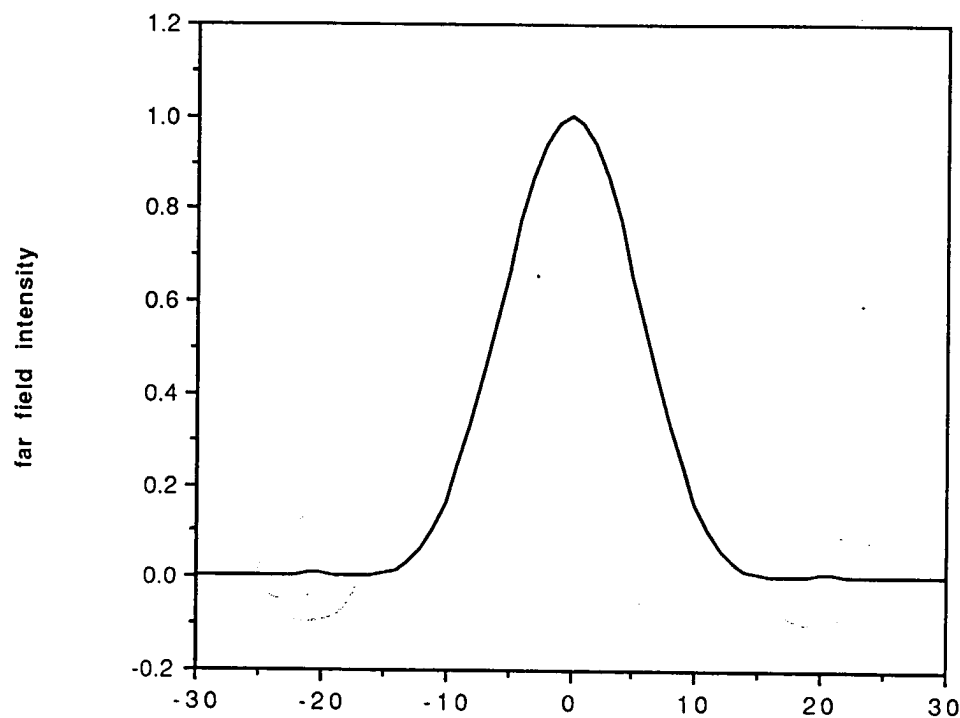
266

### Three layer loss waveguide



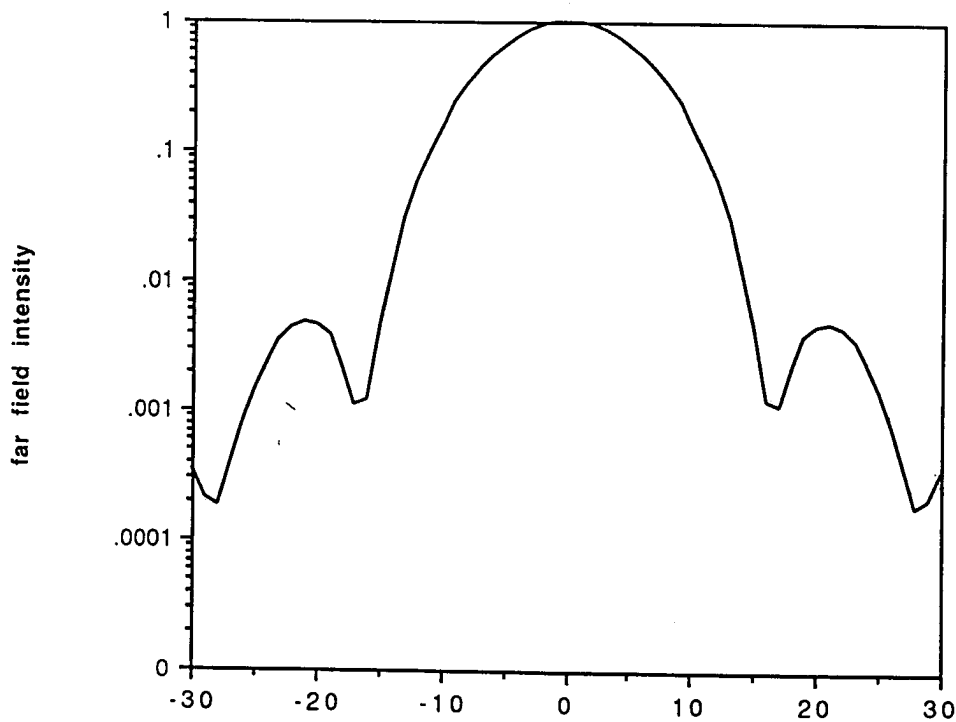
**Three layer loss waveguide**

3/30  
⑤  
267



**Theta**

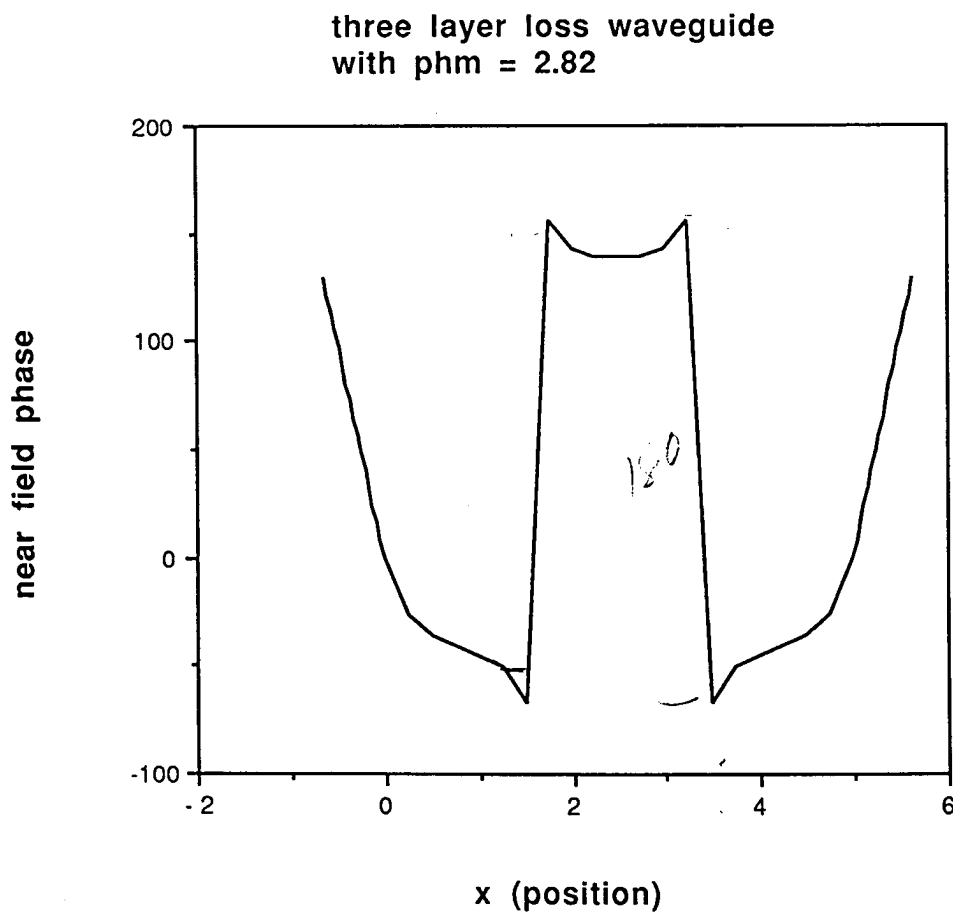
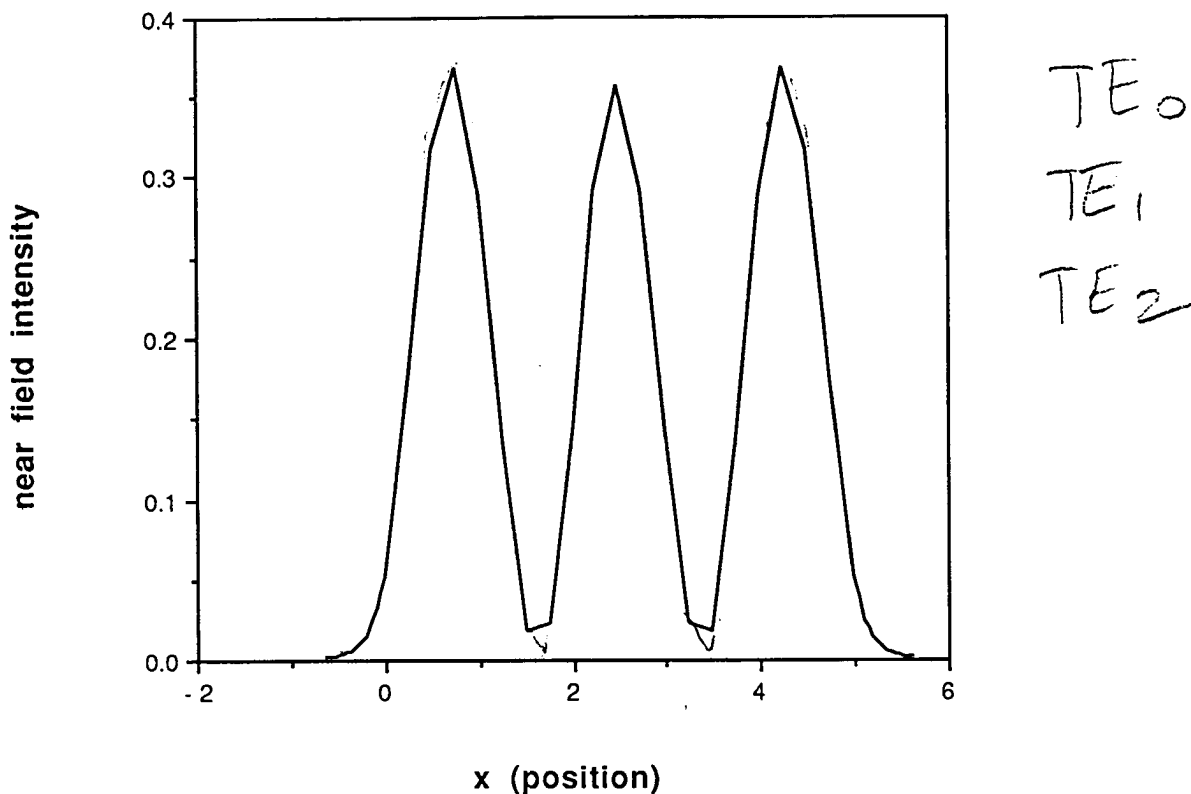
**Three layer loss waveguide**



**Theta**

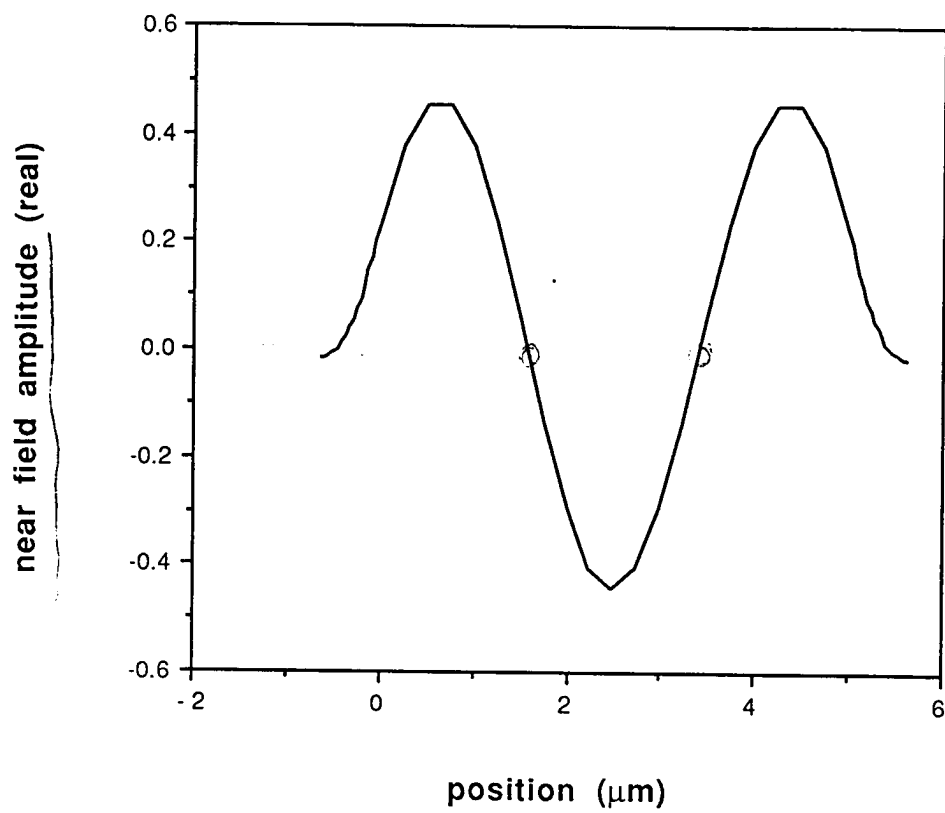
268

three layer loss waveguide  
with phm = 2.82

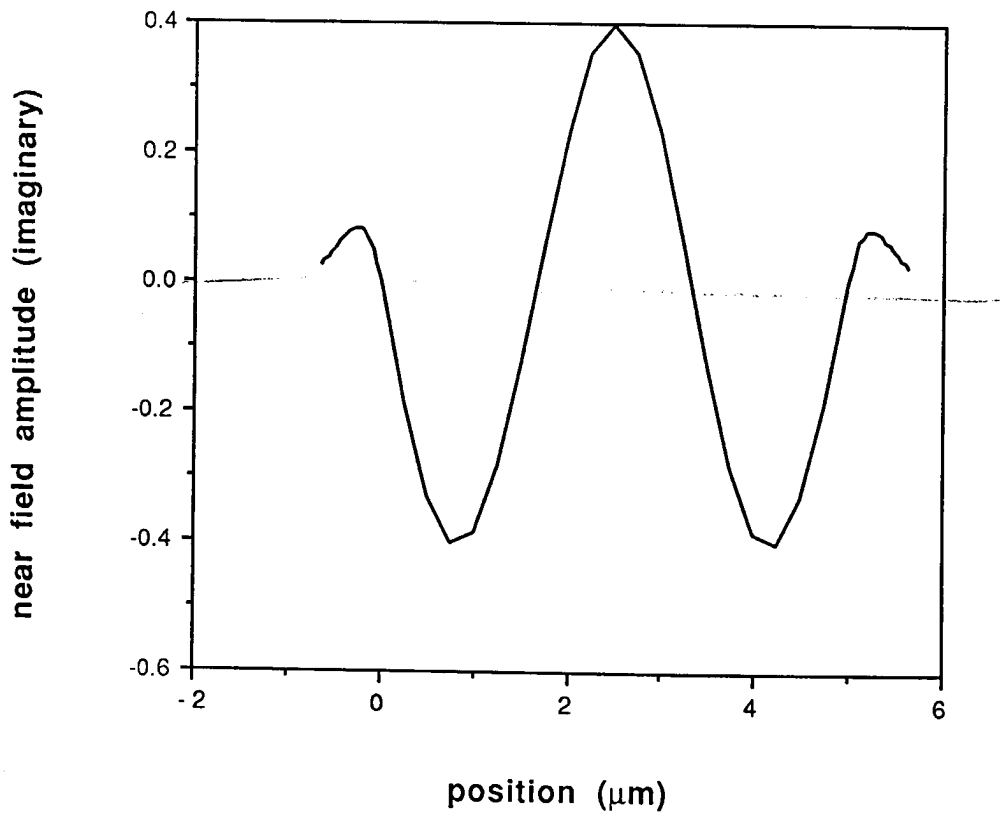


three layer loss waveguide  
with  $\text{phm} = 2.82$

(269)



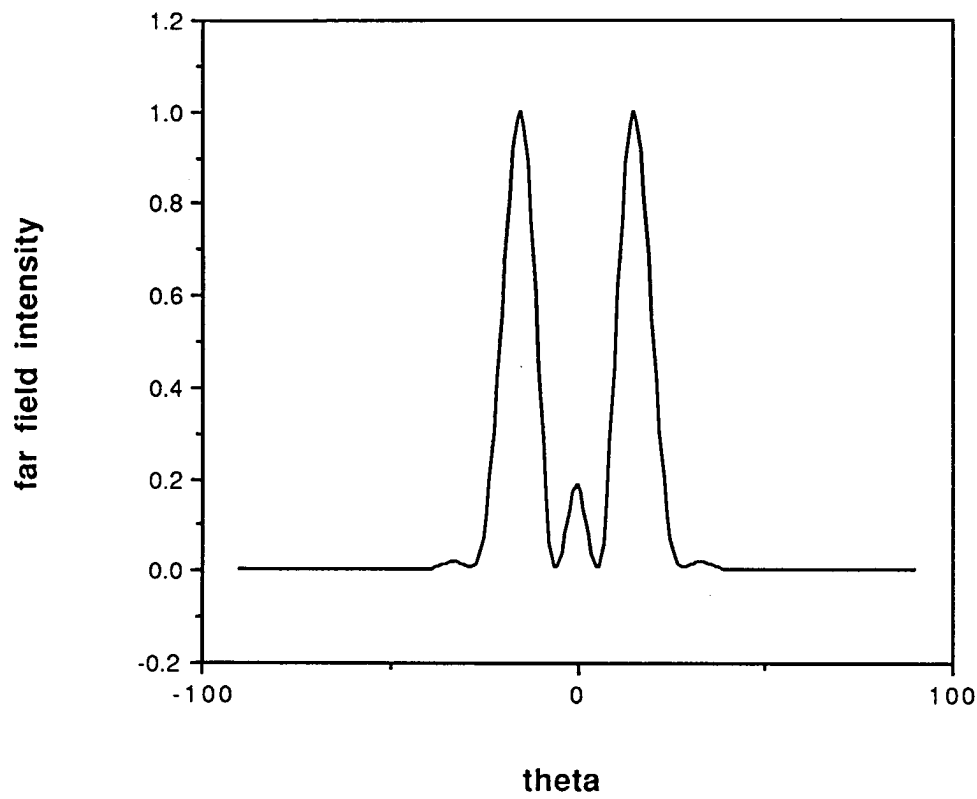
Three layer loss waveguide  
with  $\text{phm} = 2.28$



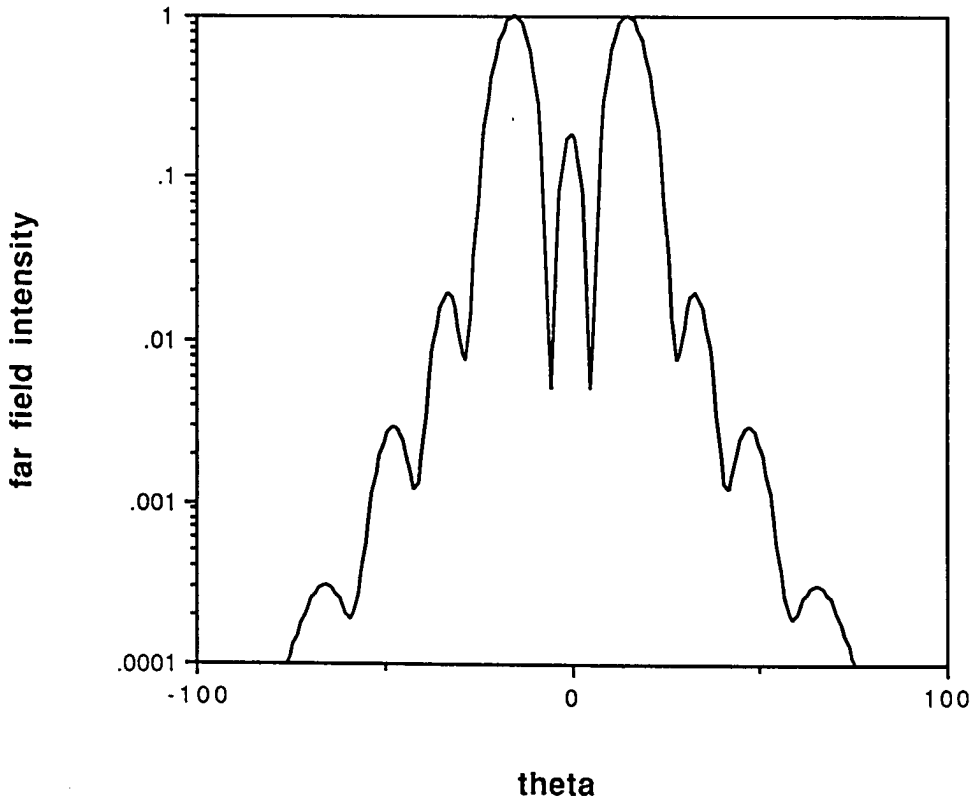
three layer loss waveguide  
with phm = 2.28

3/30

(8)  
270



three layer loss waveguide  
with phm = 2.28



To get the following data, set `MODOUT = 1`. After running `MODEIG`, the file `LOSS_OUTPUT` contains the following:

MODEIG/II  
version 1.4  
Revised: October 2, 1991

CASE NO. 910101, 1

SUMMARY OF LAYERED STRUCTURE, POLARIZATION, AND BOUNDARY CONDITIONS./  
 IMPLIED UNIT OF LENGTH XU= 0.10000D-05 METERS (BUT NOT USED EXPLICITLY). ALL QUANTITIES  
 NORMALIZED.

NOMINAL WAVELENGTH WVЛ= 1.00000 XU, AND FREE-SPACE KO= 2PI/WVЛ= 6.28319 RAD/XU.  
 COMPLEX FREQUENCY FACTOR KC=( 1.00000, .00000). EFFECTIVE-KO= KC\*KO=( 6.28319, .00000).  
 ALL PROPAGATION COEFFICIENTS ARE NORMALIZED TO EFFECTIVE-KO. (WAVE AND MATERIAL  
 REFRACTIVE INDICES, IF KF= UNITY)  
 WAVE ADMITTANCE(TE) AND IMPEDANCE(TM), YX AND YZ, ARE NORMALIZED TO THAT OF FREE SPACE.  
 NORMALIZED FREQUENCY KF=( 1.00000, .00000)= FREQ/C\*EFFE KО

POLARIZATION,  $K_{POL}=1$  ( $=1$  TE CASE,  $=2$  TM CASE), TRANSVERSE ELECTRIC CASE.  $\vec{E}_X=H_Y=0$ . TANGENTIAL  $F_Y=+E_Y$ ,  $F_Z=+H_Z$ . TRANSVERSE  $F_X=-H_X$ ,  $F_Y=+E_Y$ . LONGITUDINAL  $F_Z=+H_Z$ .  
 $Y_X=F_Z/F_Y=+H_Z/E_Y$ , AND  $Y_Z=F_X/F_Y=-H_X/E_Y$ , ARE WAVE ADMITTANCES. (IN THE POS X, Z, OR WAVE DIRECTION).

LAYERED STRUCTURE. 3 LAYERS TOTAL. 2 BOUNDARIES. 1 FINITE LAYERS.

L 1 SEMI-INFINITE QN=( 12.24367, .55704) PM=(-1.00000, .00000)  
RN=(-3.50000, .07958)

L1= 1---BOUNDARY FOR FIRST BOUNDARY CONDITION

-L 1---XL=.00000

PE=(-12.25000, .00000) PM=(-1.00000, .00000)  
TL= 5.00000 QN=( 12.25000, .00000) YN=(-1.00000, .00000)  
RN=( 3.50000, .00000) PH0=(109.95574, .00000)

-L 2---XL= 5.00000

L2= 2---BOUNDARY FOR SECOND BOUNDARY CONDITION  
PE=(-12.24367, .55704) PM=(-1.00000, .00000)  
PRINCIPAL BRANCH SPECIFICATION FOR WX. ANGLE APB=.250 PI, VECTOR VPB=( .707, .707),  
(WX\*DOT\*VPB.GE.0).  
EIGEN CONDITION. OUTWARD WAVE SOLUTION ONLY. (DIRECTION OF DECAY IF IM(WX).GT.0, OF PHASE  
PROPAGATION IF RE(WX).GT.0.)

FIRST BOUNDARY CONDITION. L1= 1, KBC1= 1, KBD1= 2.

OPEN BOUNDARY, SEMI-INFINITE ADJACENT LAYER.

PRINCIPAL BRANCH SPECIFICATION FOR WX. ANGLE APB=.250 PI, VECTOR VPB=( .707, .707),  
(WX\*DOT\*VPB.GE.0).

EIGEN CONDITION. OUTWARD WAVE SOLUTION ONLY. (DIRECTION OF DECAY IF IM(WX).GT.0, OF PHASE  
PROPAGATION IF RE(WX).GT.0.)

SECOND BOUNDARY CONDITION. L2= 2, KBC1= 1, KBD2= 2.

OPEN BOUNDARY, SEMI-INFINITE ADJACENT LAYER.

PRINCIPAL BRANCH SPECIFICATION FOR WX. ANGLE APB=.250 PI, VECTOR VPB=( .707, .707),  
(WX\*DOT\*VPB.GE.0).

EIGEN CONDITION. OUTWARD WAVE SOLUTION ONLY. (DIRECTION OF DECAY IF IM(WX).GT.0, OF PHASE  
PROPAGATION IF RE(WX).GT.0.)

END STRUCTURE DESCRIPTION.

\*\*\*\*SUBROUTINE SEARCH. KASE NO.=910101. 1, KDOS= 1, KOUS= 3.  
SEARCHING FOR MN= 1 EIGENVALUES. FOR INTENDED MODE INDICES FROM MM=MK= 0 TO MM=ML= 0.  
0. REPRESENTATIVE VALUES OF REAL QZ AND CORRESPONDING PHASE INTEGRAL  
QZR= .00000, 8.46667, 12.25000,  
PHM= 35.00000PI, 33.68976PI, 19.45079PI, .00000PI,

3/30/08  
21

KGSS= 1. INITIAL GUESSES FROM QZM OF MODSET, EITHER FROM INPUT OR RESULTS FROM PREV. CASE.  
KG CZ= 3

1 MM= 0 QZ=( 12.1500000, .00100000) PHM=( .3.162PI, .022DEC) KM= 5 IT= 0  
CALLING CZEROM FOR COMPLEX ROOT SEARCH. NN= 1 ROOTS, EPSZ= 0.10D-06, EPSF= 0.10D-07, II= 50,  
KOUT= 3, KEIF= 1.

SUBROUTINE CZEROM ITERATIONS.

NKR I DZ(I) Z(I) F(Z) F(Z)-REDUCED F-SQD  
1 7 4 (0.115D-05, 0.118D-05) (0.122D+02, 0.925D-02) (0.149D-08,-0.207D-07) (0.149D-08,-0.207D-07) 0.429E-15

RESULTS FROM EIGENVALUE ROOT SEARCH.

1 MM= 0 QZ=( 12.17060238, .00925239) PHM=( 2.823PI, .224DEC) KM= 7 IT= 4  
WZ=( 3.48863930, .00132607) PHR=( .8.867, -.515) PHI=(- .8.867, .515) ATQZ= 0.4840D-03PI/2.  
SM=(-0.2713D+01,-0.1250D+01)(0.1119D+01,0.9794D+00) DET(SM)= ( 0.2923D+00, 0.2191D+01)  
(-0.1119D+01,-0.9794D+00)(0.1492D-08,-0.2066D-07).  
CM=( 0.9635D+00, 0.2847D+00) (-0.1735D+01, 0.2028D+01) DET(CM)= ( 0.0000D+00, 0.0000D+00) + ( 1.0,0.0)  
(-0.1190D+00, 0.1771D+00) (-0.9635D+00, 0.2847D+00). DETNORM= ( 0.6948D+00,-0.1097D+01).  
L= 1 WX=( 0.5593D+00, 0.4897D+00) YX=( 0.5593D+00, 0.4897D+00) QX=( 0.7307D-01, 0.5478D+00) ATQX= .91558494PI/2.  
L= 3 WX=( 0.5593D+00, 0.4897D+00) YX=( 0.5593D+00, 0.4897D+00) QX=( 0.7307D-01, 0.5478D+00) ATQX= .91558494PI/2.

RE-STATE MODE SET IN TERMS OF NUMBER TRIED AND LOWEST ACTUALLY FOUND. NO. TRIED= 1.  
LOWEST FOUND= 0.  
NOW MM= 0, 0. FOR ANY MODE WITH PHMM NOT IN INTENDED RANGE, VALUE OF KM IS REDUCED BY 1.  
\*\*\*\*END SEARCH. RETURN.

\*\*\*\*\*SUBROUTINE FIELDS. KASE NO.=910101. 1, KDOF= 2, KOUF= 3.  
CALCULATE FIELD SOLUTIONS FOR EACH QZM(M), M= 1, 1. (NOT CALC FOR NON-CONVG, OR POOR QZ.  
SHOWN BY KM.LT.KMDO= 5.)  
CHECK SUBROUTINE FIELDS 1

M= 1, MM= 0, QZ=( 12.17060238, .00925239) ATQZ= 0.4840D-03PI/2 PHM=( .2.823, .224) KM= 6  
WZ=( 3.48863930, .00132607) ATWZ= 0.2420D-03PI/2 PHR=( 8.867, -.515) PHI=(- .8.867, .515).

3/30  
14  
2/21

TWO SOLN. FOR TANGENTIAL BDY. FIELDS, INDEPENDENTLY CALC., F(L) FROM BDY. COND. AT L1= 1  
, AND G(L) FROM BDY. COND. AT L2= 2.  
, NUMERICAL CHECKS, RECIPROCITY AND EIGEN CONDITIONS. USING POYNTING CROSS PRODUCTS F\*G.  
(F\*G-DIFF IS WRONSKIAN DET.)

EIG CHECK AT L2= 2, FY\*GZ = GY\*FZ,

DIFF=( 0.1922D-08,-0.2662D-07)=0.  
EIG CHECK AT L1= 1, FY\*GZ = GY\*FZ,  
(-0.7205D+00,-0.6308D+00)=(-0.7205D+00,-0.6308D+00).

DIFF=( 0.1922D-08,-0.2662D-07)=0.

RECIPROCITY CHECK. FG2-FG1=GF2-GF1,

( 0.1441D+01, 0.1262D+01)=( 0.1441D+01, 0.1262D+01).  
DIFF=( 0.0000D+00, 0.0000D+00)=0.

#### SOLUTION FOR TANGENTIAL FIELDS AT THE BOUNDARIES.

EIGEN-FUNCTION FIELD SOLUTION (AVG. OF SOLUTIONS BASED ON THE TWO BDY. COND. SEPARATELY.  
BDY. COND. CHECKS. AT L1, YX\*FY-FZ=(-0.847D-09, 0.117D-07). AT L2, YX\*FY-FZ=( 0.847D-09,-0.117D-07).  
TANGENTIAL BOUNDARY FIELDS AND TRANSVERSE AVG. POYNTING POWER.

1 X= .00000	FY=(- 1.134957, 0.000000)
FZ=(- .634819, -.555768)	PX=(-0.720492D+00, 0.630772D+00)
2 X= 5.00000	FY=(- 1.134957, 0.000000)
FZ=(- .634819, .555768)	PX=( 0.720492D+00, 0.630772D+00)

NET TIME-AVG POYNT. PWR. INTO STRUCTURE FROM OUTSIDE, PX(L1)-PX(L2)= (-0.144098D+01,  
0.126154D+01).

\*\*\*\*SUBROUTINE POWERS. KASE NO.=910101. 1, KDOP= 1, KOUP= 1.  
NO CALCULATION OF POWERS YET IMPLEMENTED.

3/30/12  
111

# CSP Waveguides

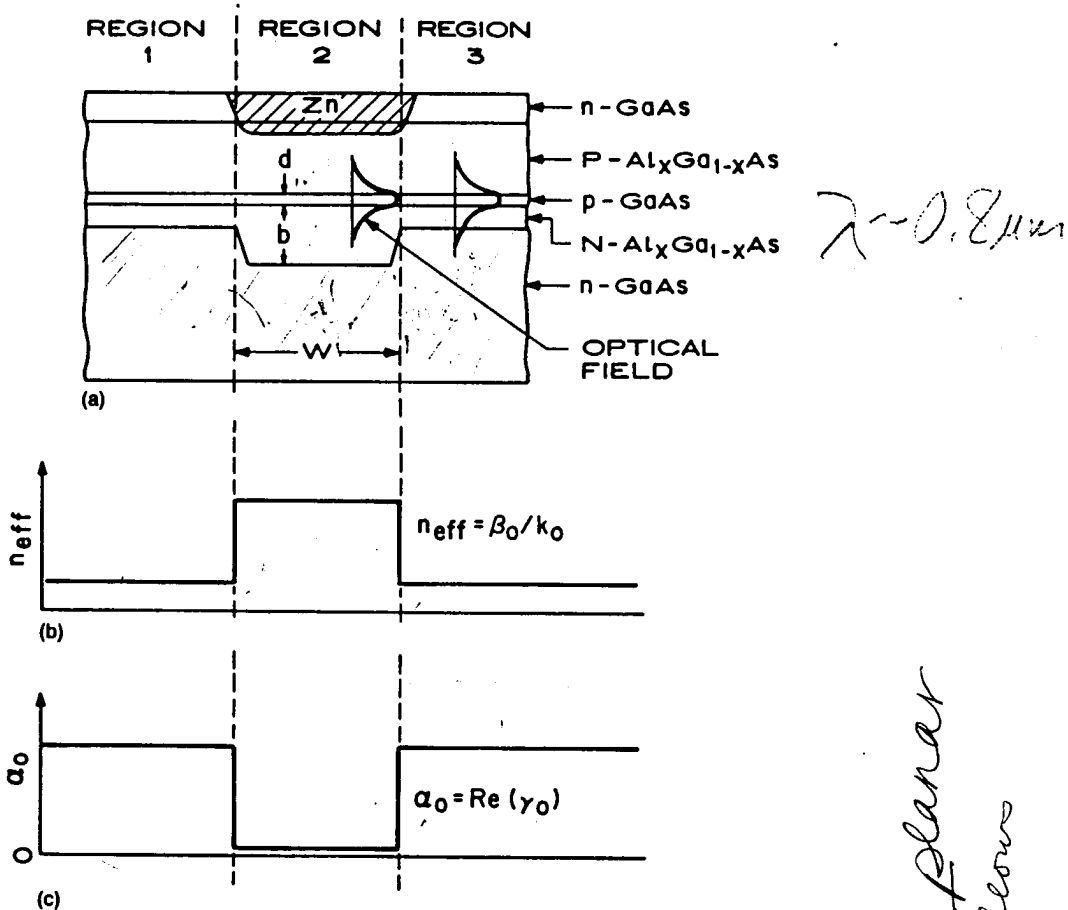


FIGURE 4.1. (a) Geometrical cross section of a CSP laser, (b) real part of the lateral effective index profile, and (c) imaginary part of the lateral effective index profile.

- Why does a CSP waveguide have a positive index step?

Channel substrate planar liquid phase epitaxy allows filling of ridges

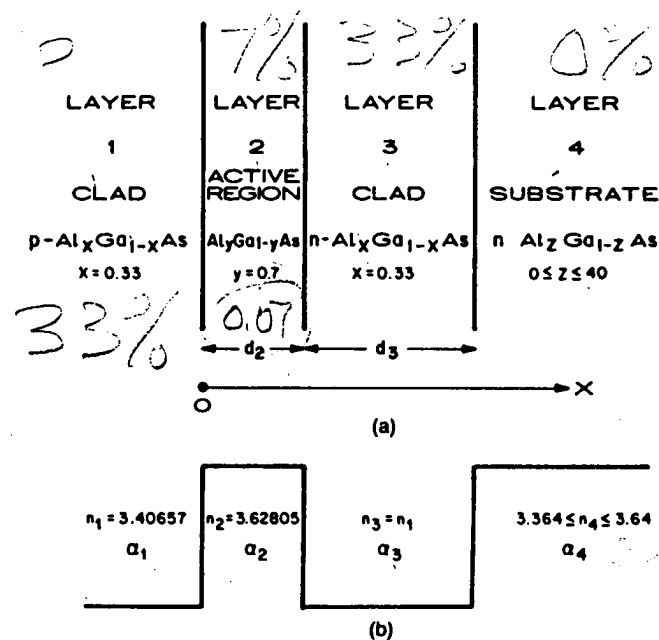
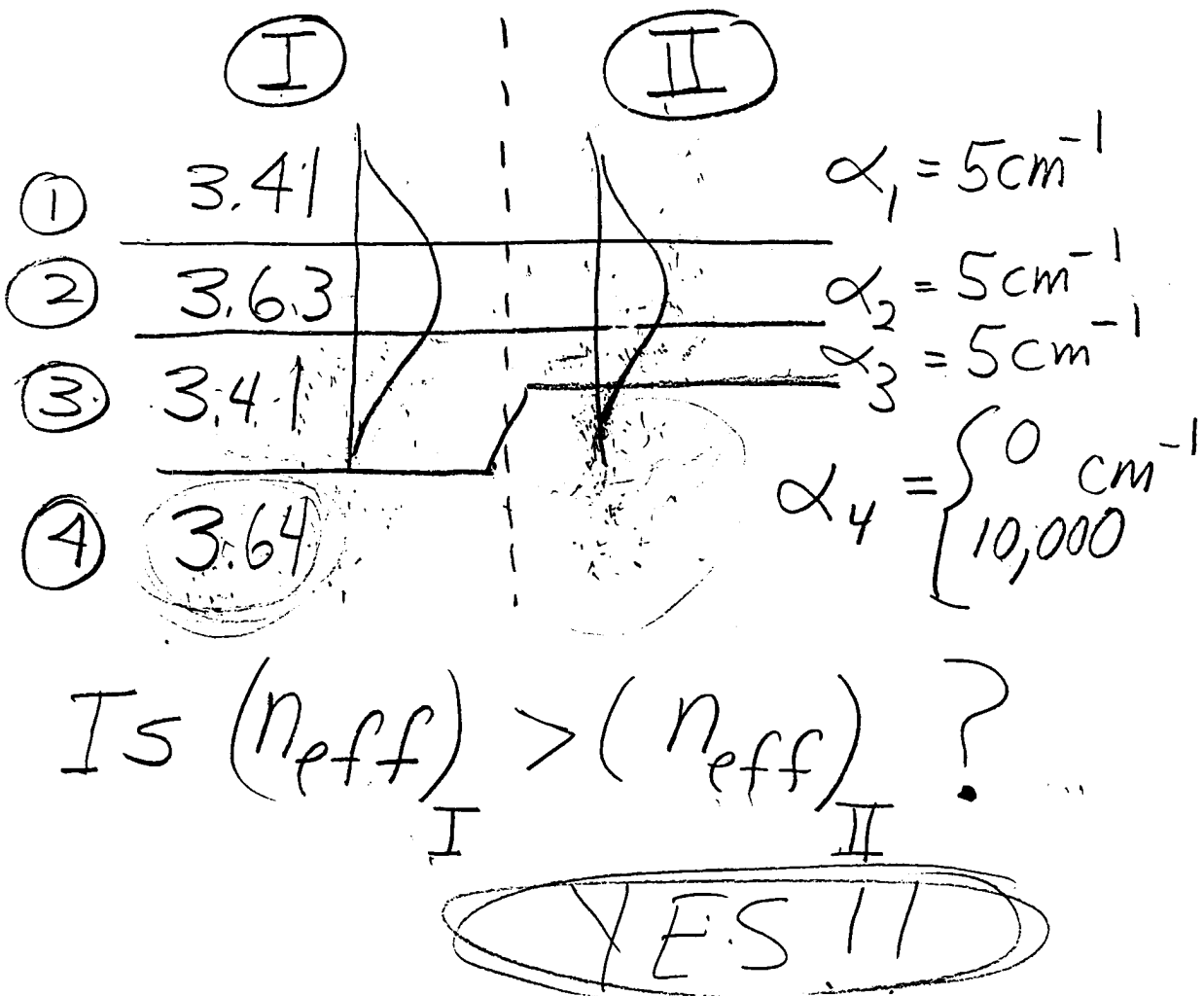


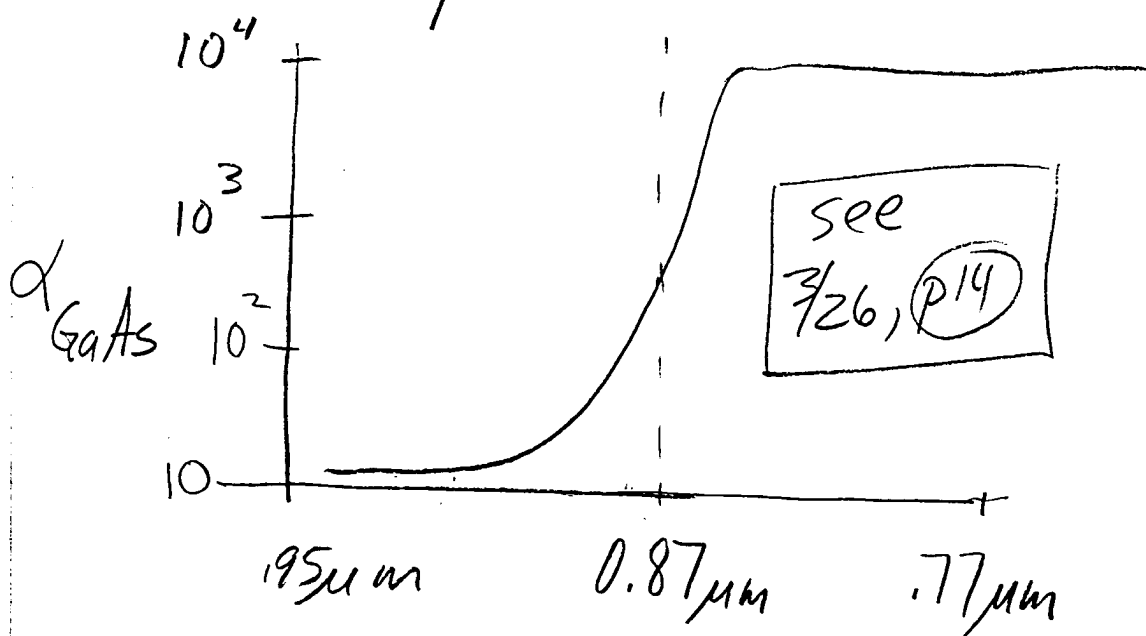
FIGURE 4.2. The four-layer waveguide structure with (a) the layer geometry and (b) the refractive index profile.



For  $0.8 < \lambda < 0.86 \mu\text{m}$ ,

$$\alpha_4 \approx 5,000 - 10,000 \text{ cm}^{-1}$$

A widely believed concept was that a CSP structure would only work for  $\lambda > 0.86 \mu\text{m}$



- NASA requirement for  $\lambda \sim 0.88 \mu\text{m}$

- CSP lasers worked,  
(i)  $\lambda \sim 0.89 \mu\text{m}$

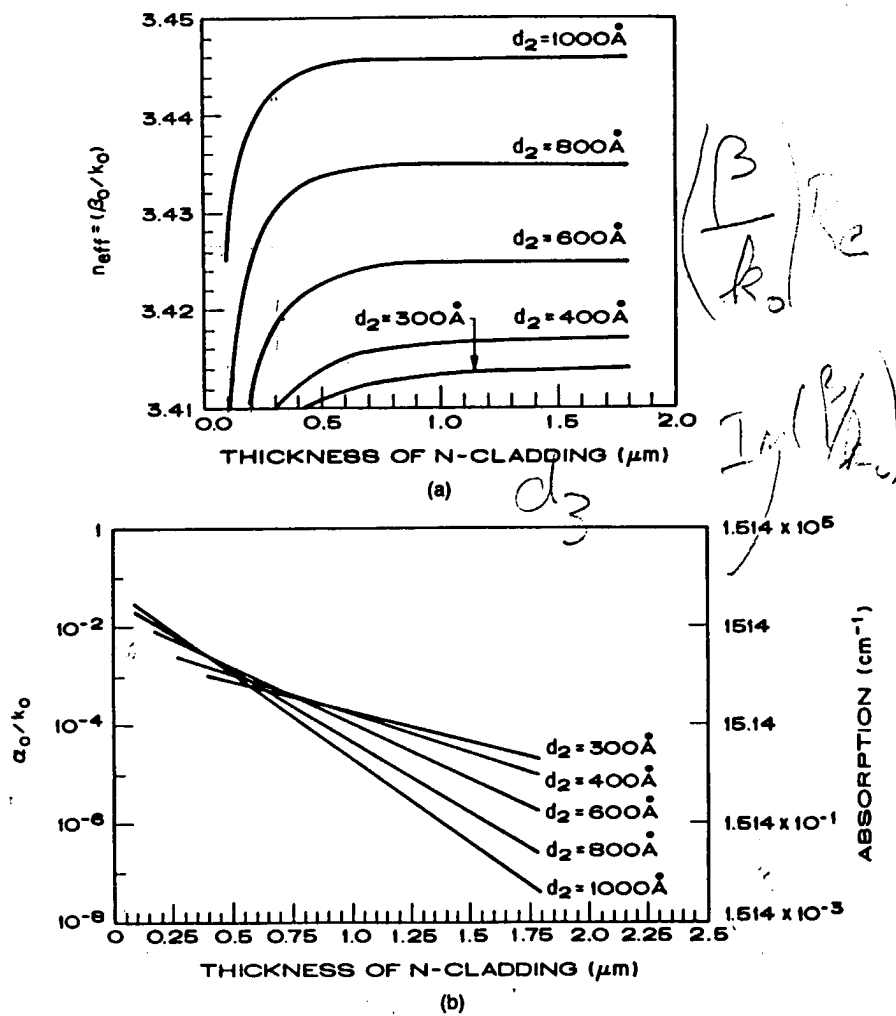
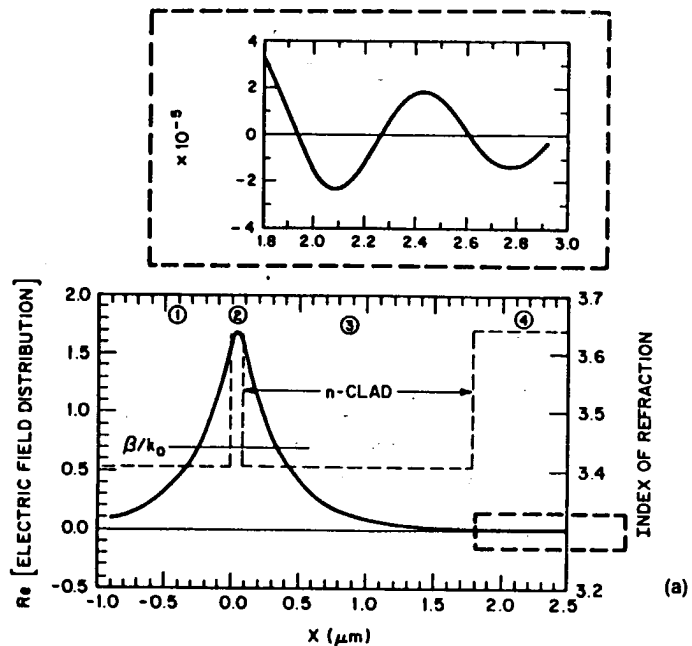


FIGURE 4.7. (a) The real part of the effective index and (b) the imaginary part of the effective index as a function of the  $n$ -clad thickness for active layer thicknesses of 400, 600, 800, and 1000 Å of a conventional CSP laser.

a) Why?

b) Seems reasonable



$$d_3 = 1.8 \mu\text{m}$$

$$\alpha_4 = 5000 \text{ cm}^{-1}$$

$$n_4 = 3.64$$

$$n_2 = 3.62805$$

$$n_{\text{eff}} = 3.43401 = \frac{\beta}{k_0}$$

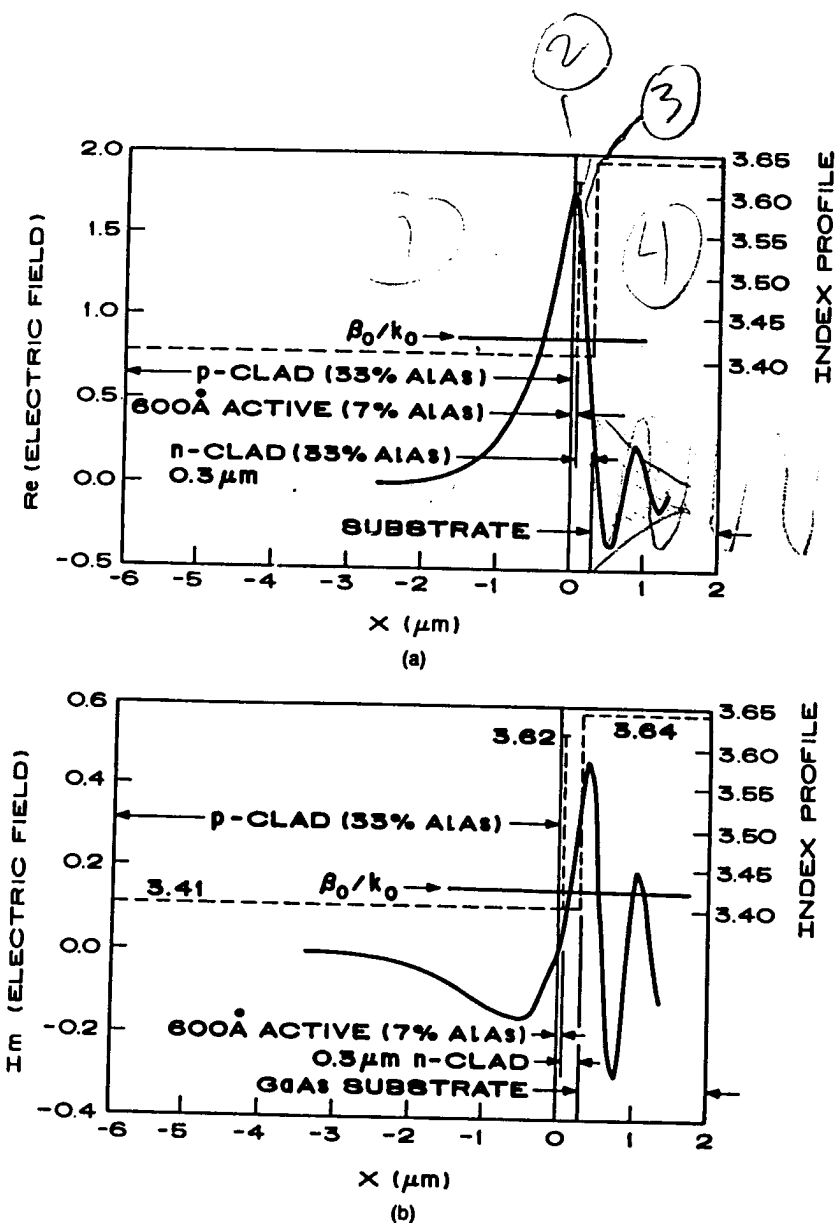


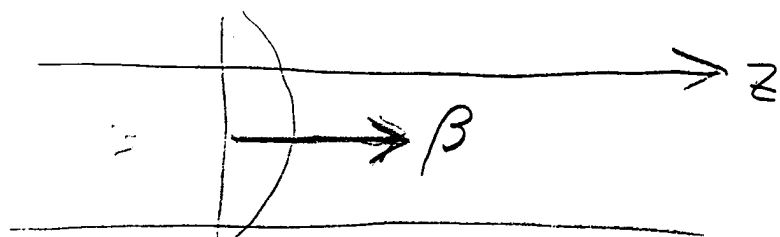
FIGURE 4.3. The (a) real and (b) imaginary part of the electric field distribution for the transverse profile shown in Figure 4.2 with  $d_2 = 600 \text{ \AA}$  and  $\alpha_s = 5000 \text{ cm}^{-1}$ .

$$d_3 = 0.3 \mu\text{m}$$

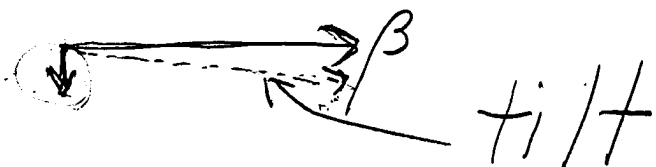
$$\Delta n_{\text{eff}} \approx 6.6 \times 10^{-3}$$

• What happens if  $\alpha_4$  changes?

- If  $\alpha_4 \uparrow$ , less field penetrates layer ④  
(If  $\alpha_4 \downarrow$ , more "...")
- What happens to the mode energy in layer ④?



④ radiating in  
the x direction!



(23)

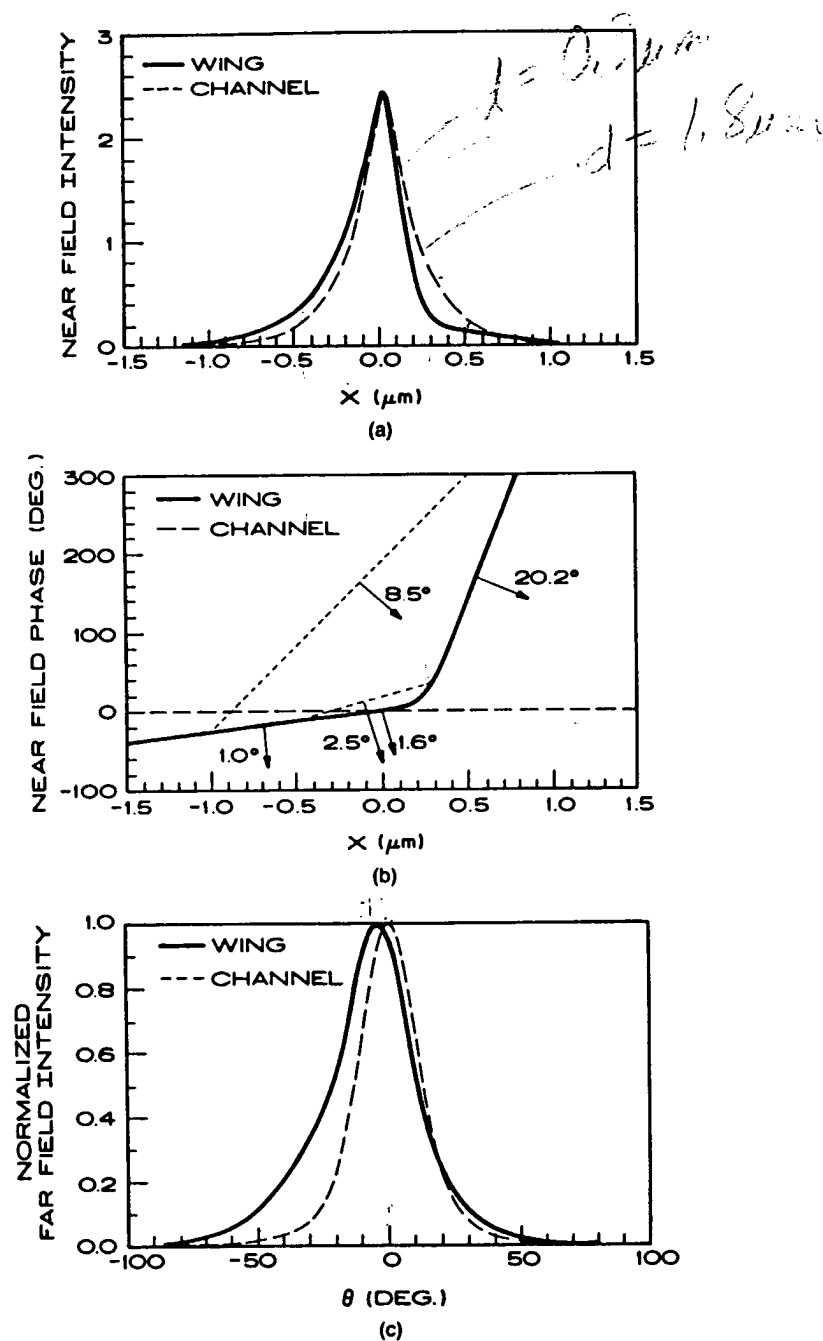


FIGURE 4.4. The transverse (a) near-field intensity, (b) near-field phase, and (c) far-field intensity  $I_{ch}(\theta)$  and  $I_w(\theta)$  for a conventional CSP laser with an active layer thickness of 600 Å in the region inside (---) and outside (—) the channel.

Note tilted wavefronts

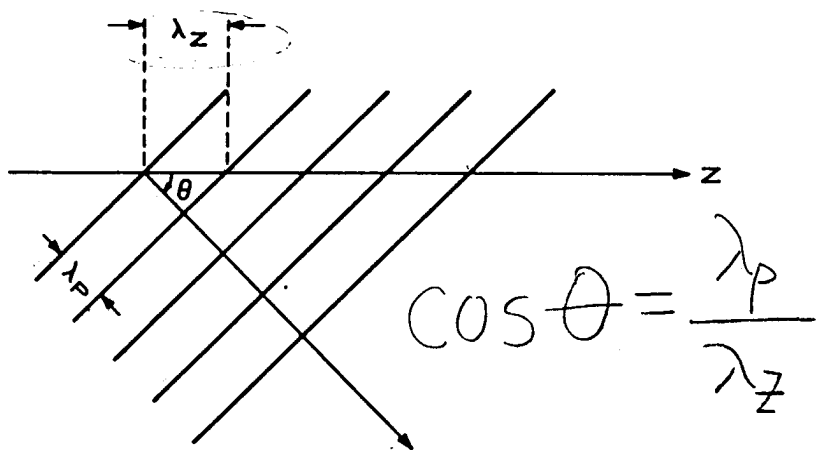


FIGURE 4.5. Relationship of the guide wavelength  $\lambda_z$  to the wavelength in the direction of propagation  $\lambda_p$  for a wave propagating at an angle  $\theta$  with respect to the guide axis.

What happens if  
the wavefront tilts?

$$N_{eff} = \beta/k_0 = \frac{2\pi/\lambda_z}{2\pi/\lambda_0}$$

$$= \frac{\lambda_0}{\lambda_z}$$

Note:  $\lambda_z$  increases  
as  $\theta$  increases!

$\Rightarrow$  tilt  $\Rightarrow N_{eff}$  decreases!

so:

{Wavelength tilt is the  
physical explanation  
of why a CSP waveguide  
has a positive index step}

What happens as  $\alpha_4 \downarrow$ ?

- more penetration

- into layer ④

- $\Rightarrow$  more tilt

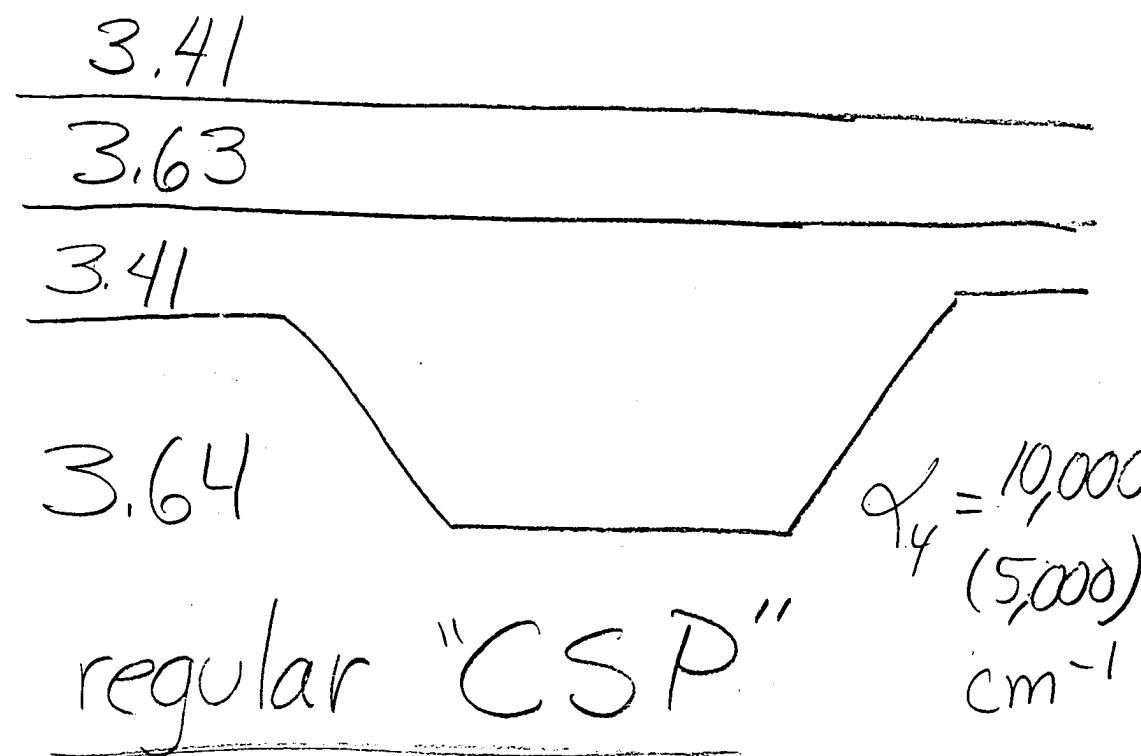
- $\Rightarrow$  more index step!

So CSP waveguides  
are "better" as  $\alpha_4 \rightarrow 0$

$\Rightarrow$  Also, the mode losses

Increase as the absorptm  
loss (in layer 4) decrease

Consider 3 structures



①

(286)

3.41

①

3.63

②

3.41

V  
③

3.64

 $\alpha_4 = 0$ 

"No Loss" CSP

② ((CSPNL))

3.41

3.63

3.41

3.41

 $\alpha_4 = 10,000$   
(5,000)cm<sup>-1</sup>"No Index  
Change"

③

CSP  
(CSPNIC)

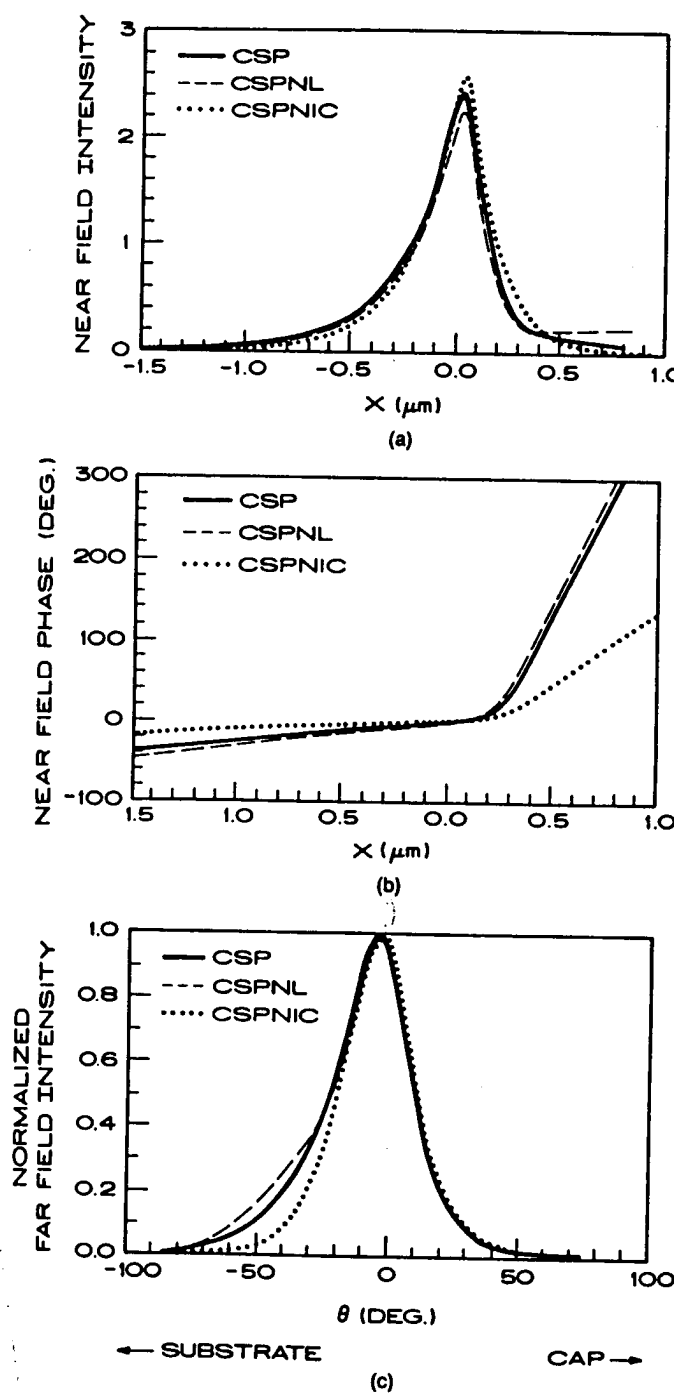
(287)

$$\begin{array}{lll} \text{CSP} & \text{CSPNL} & \text{CSPNTC} \\ 10,000 (5,000) \text{cm}^{-1} & 0 \text{cm}^{-1} & 10,000 (5,000) \text{cm}^{-1} \end{array}$$

$$\frac{\Delta n}{k_0} = \frac{6.59 \times 10^{-3}}{(5.07 \times 10^{-3})} = \frac{4.75 \times 10^{-3}}{5.37 \times 10^{-3}} = \frac{2.57 \times 10^{-3}}{(2.08 \times 10^{-3})} = \frac{2.55 \times 10^{-3}}{(2.57 \times 10^{-3})} = \frac{2.55 \times 10^{-3}}{(2.57 \times 10^{-3})} = \frac{2.55 \times 10^{-3}}{(2.57 \times 10^{-3})}$$

TABLE 4.1. Three models of CSP lasers.

	CSP	CSPNL	CSPNIC
$d_2$	600 Å	600 Å	600 Å
$a_4$	$10,000 \text{ cm}^{-1} (5000 \text{ cm}^{-1})$	$0 \text{ cm}^{-1}$	$10,000 \text{ cm}^{-1} (5000 \text{ cm}^{-1})$
$\Delta n$	$6.59 \times 10^{-3} (6.82 \times 10^{-3})$	$7.14 \times 10^{-3}$	$2.55 \times 10^{-3} (1.25 \times 10^{-1})$
$\Delta x/k_0$	$4.75 \times 10^{-3} (5.07 \times 10^{-3})$	$5.37 \times 10^{-3}$	$2.57 \times 10^{-3} (2.08 \times 10^{-1})$
$(\beta/k_0)^{1/2}$	$3.42315 (3.42315)$	$3.42315$	$3.42315 (3.42315)$
$(\beta/k_0)^2$	$3.41656 (3.41653)$	$3.41601$	$3.42061 (3.42190)$
FWHP of $I_{\text{ex}}(\theta)$	$25.18^\circ (25.17^\circ)$	$25.21^\circ$	$24.88^\circ (24.73^\circ)$
FWHP of $I_u(\theta)$	$32.12^\circ (32.21^\circ)$	$32.40^\circ$	$30.14^\circ (28.17^\circ)$

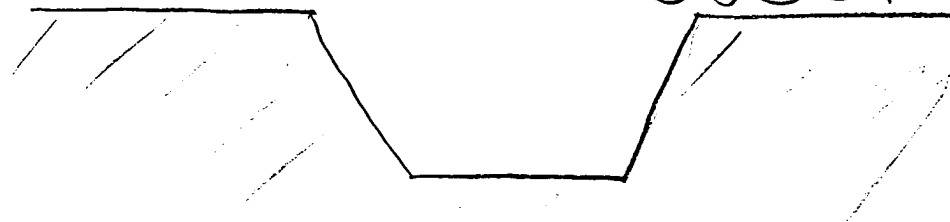


CSP  
CSPNL  
CSPNIC

$\Delta n$ ,  $\Delta x$  consistent  
w/ wavelength tilt!

# Liquid Phase Epitaxy

Channel in  
Substrate

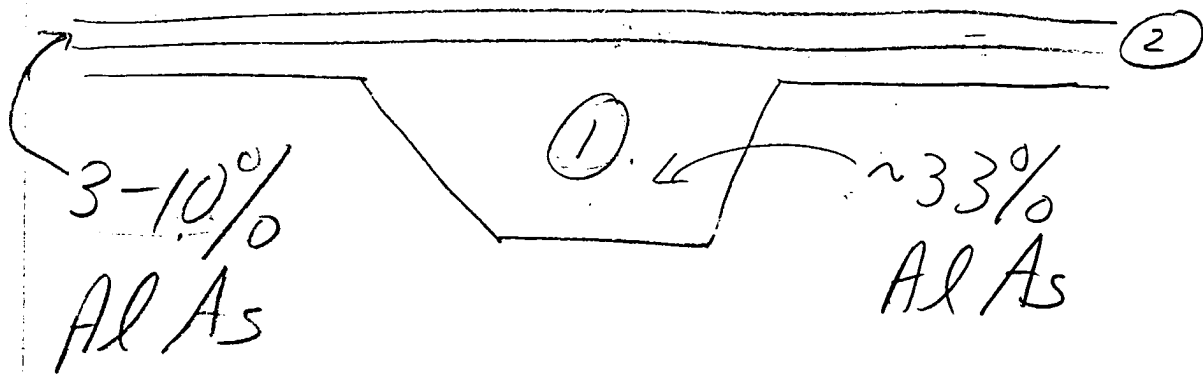


Ga As

GaAs "cap"

33% AlAs

(3)

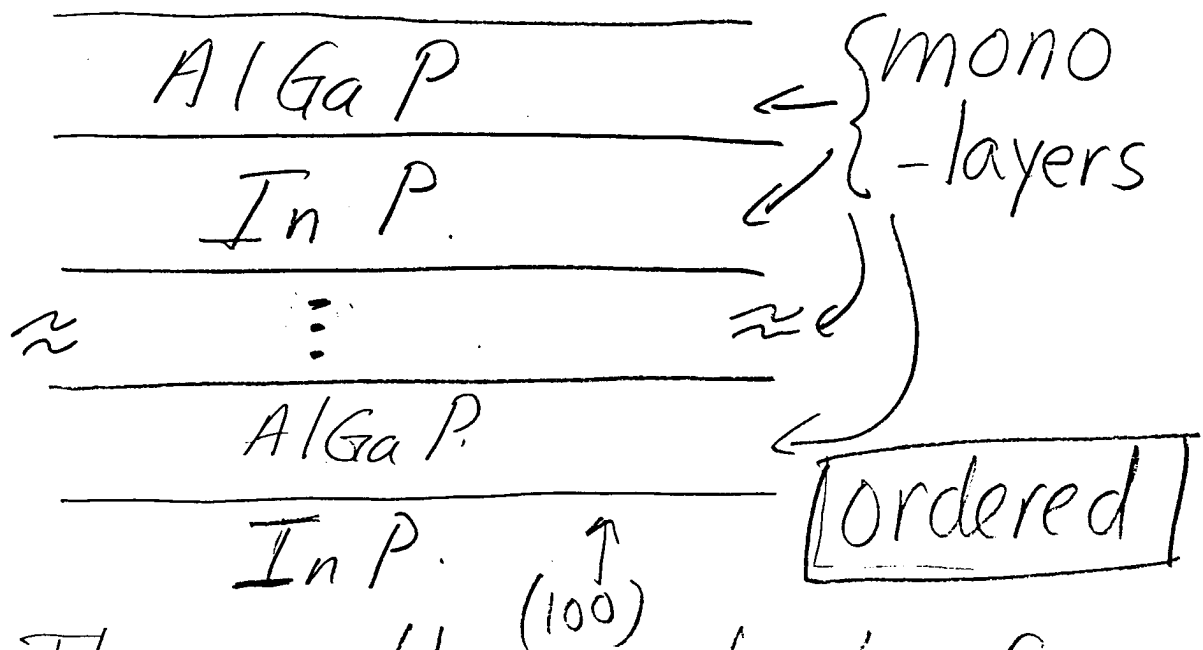


LPE tends to fill  
channels

## Ordered & Non-ordered (Dis-ordered) Growth of $(Al_xGa_{1-x})InP$

The quaternary material  
 $(Al_xGa_{1-x})InP$  is  
 $\sim 50\%$  AlGaP and  $\sim 50\%$  InP.

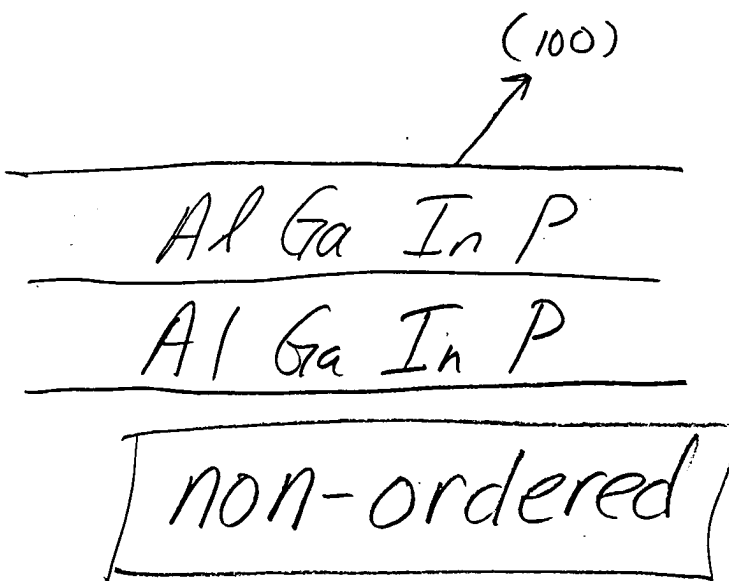
When  $AlGaInP$  is grown  
on a (100) surface, the  
material is "ordered"--  
a monolayer of AlGaP,  
a monolayer of InP,  
and so on:



The resulting stack of layers is called a

"SUPERLATTICE"

However, if AlGaInP is grown off-axis from (100), the "order" is lost—that is, within a layer, Al, Ga, In, and P are present:



The "randomizing" or loss of "order" increases as the growth surface is tilted away from (100)-- and by  $\sim 25^\circ$ , the randomness is complete (and at  $\sim 9^\circ - 10^\circ$ , the randomness is about  $\sim 90\%$  complete).

This ordering/non ordering was discovered in the late 80s, and was a "hot"

topic at the 1988 Semiconductor laser conference.

Ordering/non-ordering explained the "70 meV" mystery - which was that the same composition active layer lased at a wavelength about 70 meV shorter if the growth was on an "off-axis" ( $6^\circ$  off of 100) substrate.

The estimate for the energy shift ranges from 70 meV to as much as 150 meV.

In general (but not always),  
the index  $n$  decreases if the  
bandgap increases:

$\text{Al}_{0.3} \text{Ga}_{0.7} \text{As}$  has  $n \sim 3.41$

$$E_g \sim 1.75 \text{ eV}$$

$\text{GaAs}$  has  $n \sim 3.64$

$$E_g \sim 1.42 \text{ eV}$$

To estimate the difference in index between "ordered" and "non-ordered" material, we can use the index (see paper by Tanaka, et.al)

$$n^2 - 1 = E_0(E_d) \left( E_0^2 - E^2 \right)^{-1} \quad (1)$$

(225)

where

 $n = \text{refractive index}$  $E = \text{photon energy (eV)}$ 

$$E_0 = 3.39 + 0.62x \quad (\text{eV})$$

$$E_d = 28.07 + 1.72x \quad (\text{eV})$$

$$E = \frac{1.24}{\lambda (\mu\text{m})} \quad (\text{eV})$$

Example: (see fax from  
 D. Bour to G. Evans,  
 4/7/93) at  $\lambda = 0.645 \mu\text{m}$

$$\frac{n}{n_{\text{ordered}}} = 3.386 \quad (x=0.6)$$

$$E_g (\lambda = 0.645 \mu\text{m}) = 1.922 \text{ eV}$$

for non-ordered material at  $\lambda = 0.645 \mu\text{m}$ ,  
 (this is an approximation):

$$(E_g)_{\text{non-ordered}} = 1.922 \text{ eV} - 0.100 \text{ eV}$$

non-ordered

$$= 1.822 \text{ eV}$$

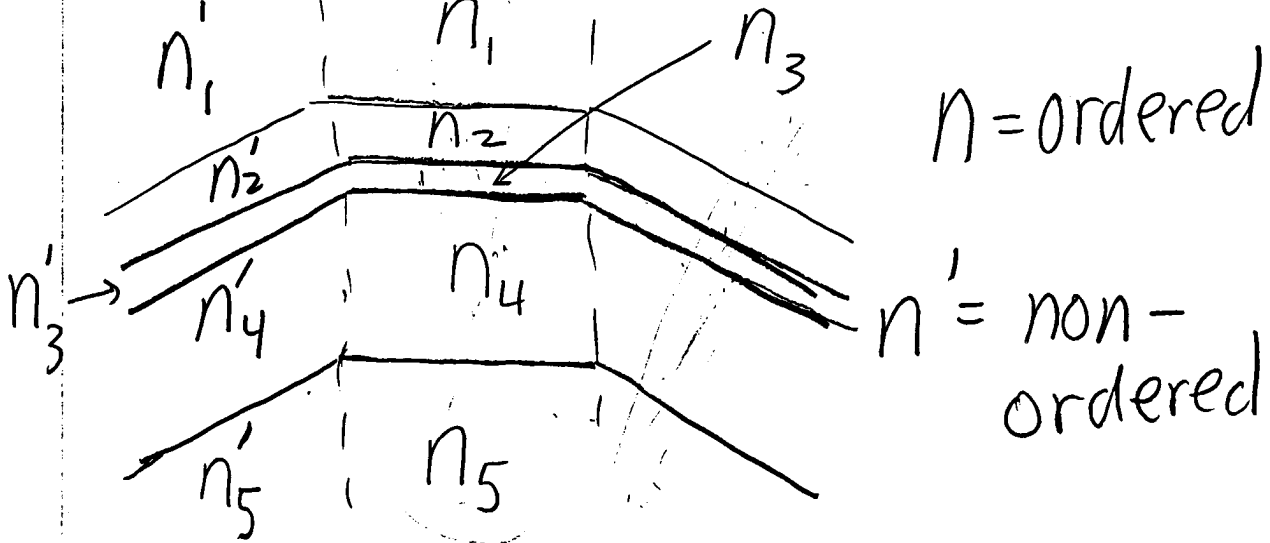
$$\Rightarrow n = 3.333$$

non-ordered

$$x =$$

$$60$$

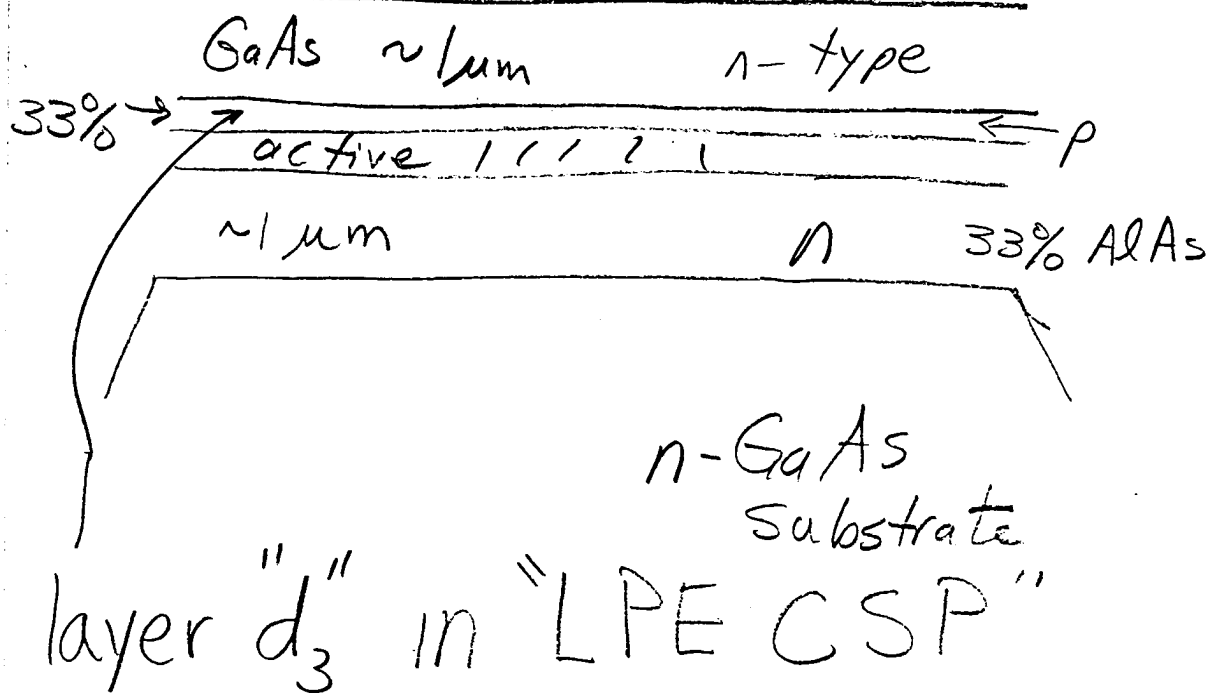
$$\text{So, } \Delta n = -0.053$$



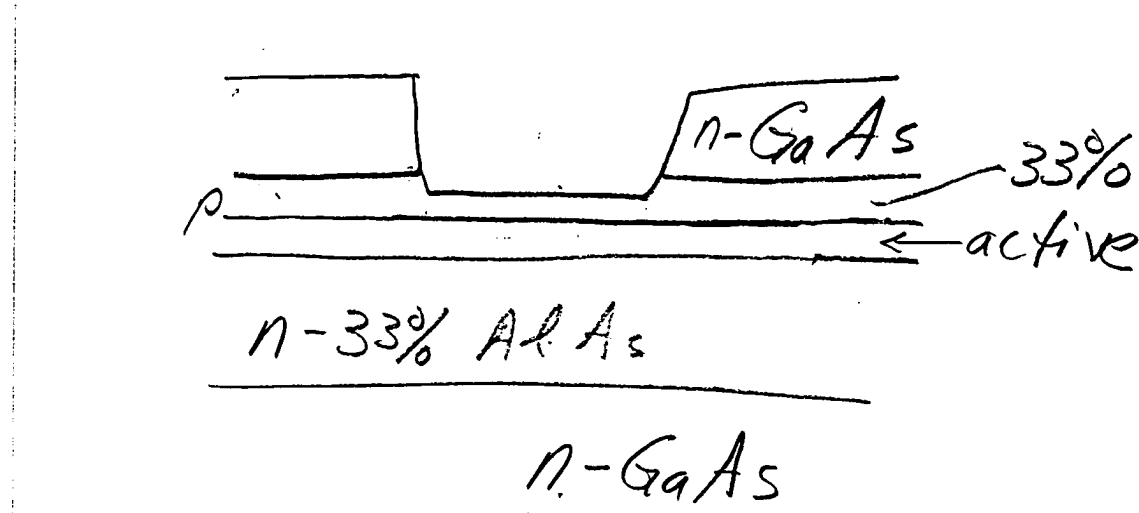
3.27

# Other "CSP" Waveguides

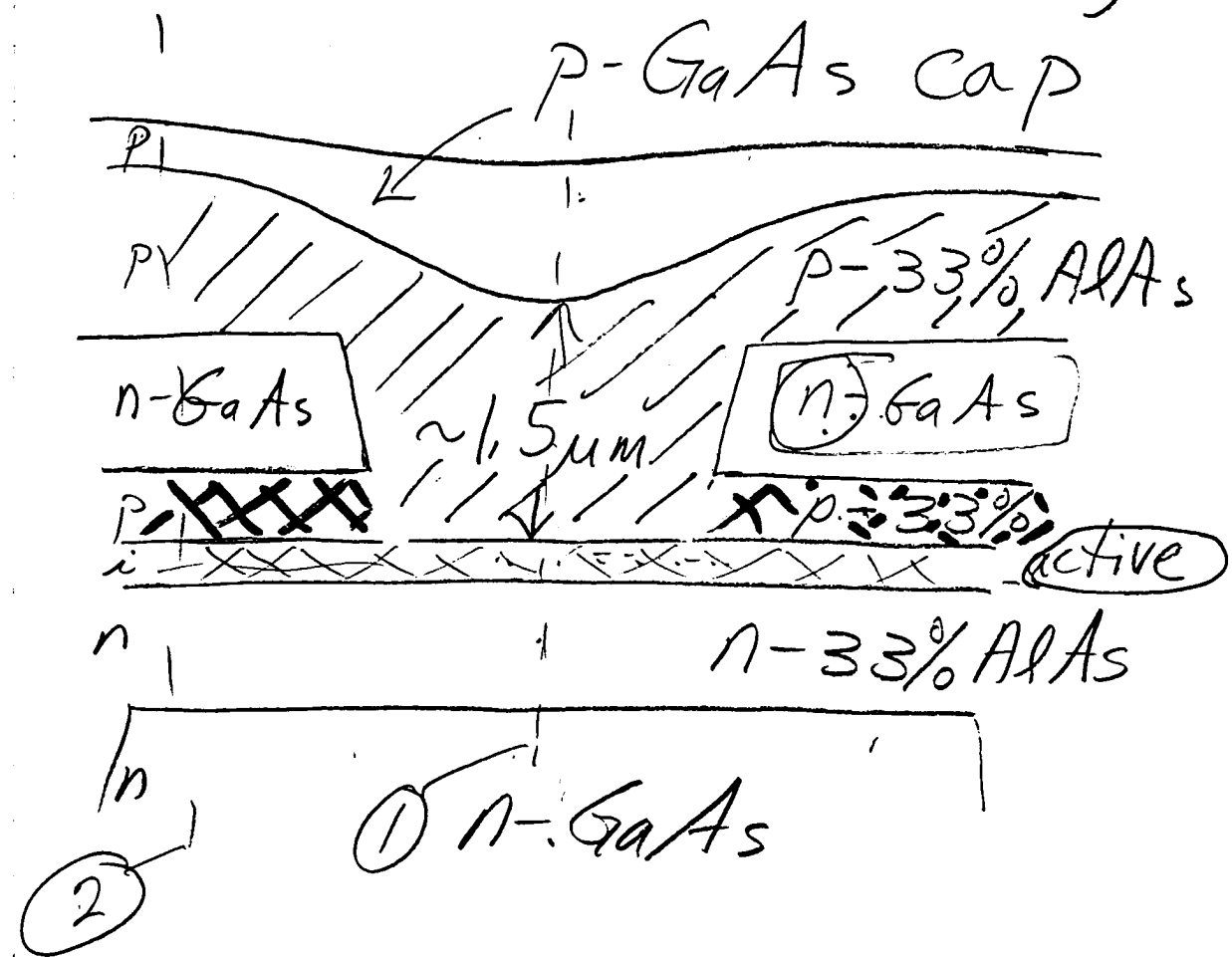
(A)  $\text{Al}^{st}$  Growth [AlGaAs/GaAs]



(B) Etch top GaAs layer:



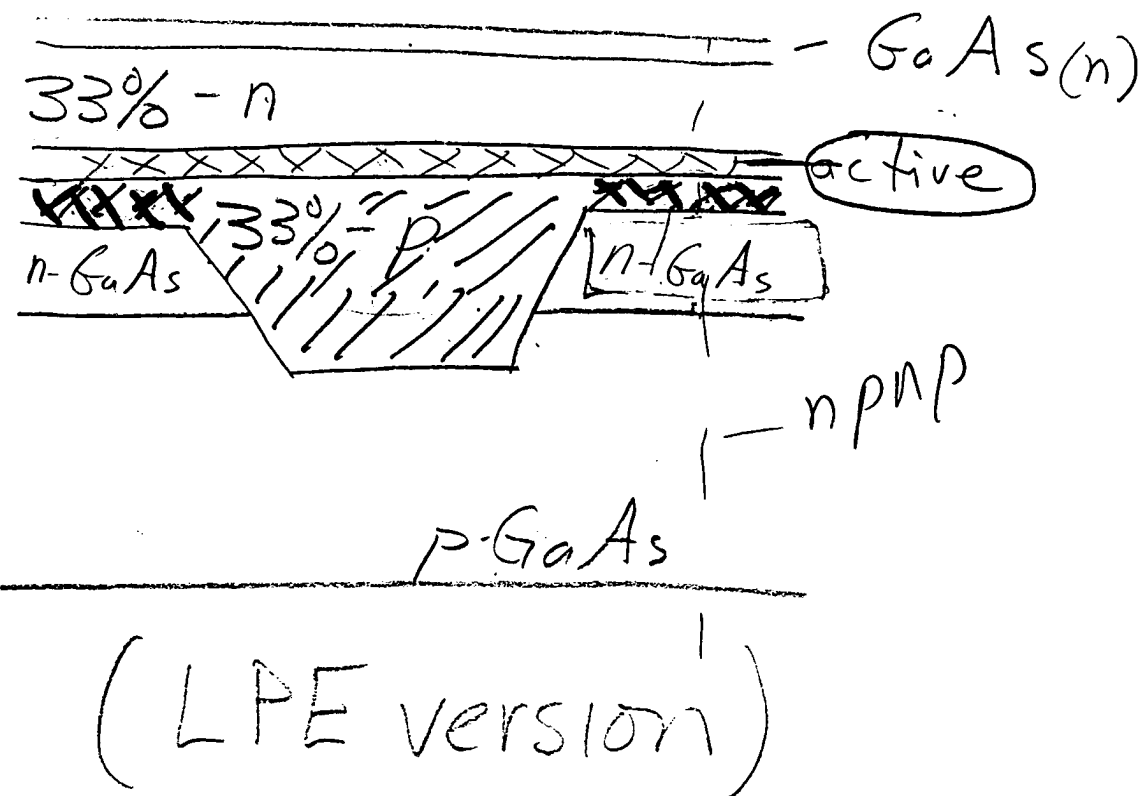
## ③ Regrowth (MBE, MOCVD)



"upside down" CSP

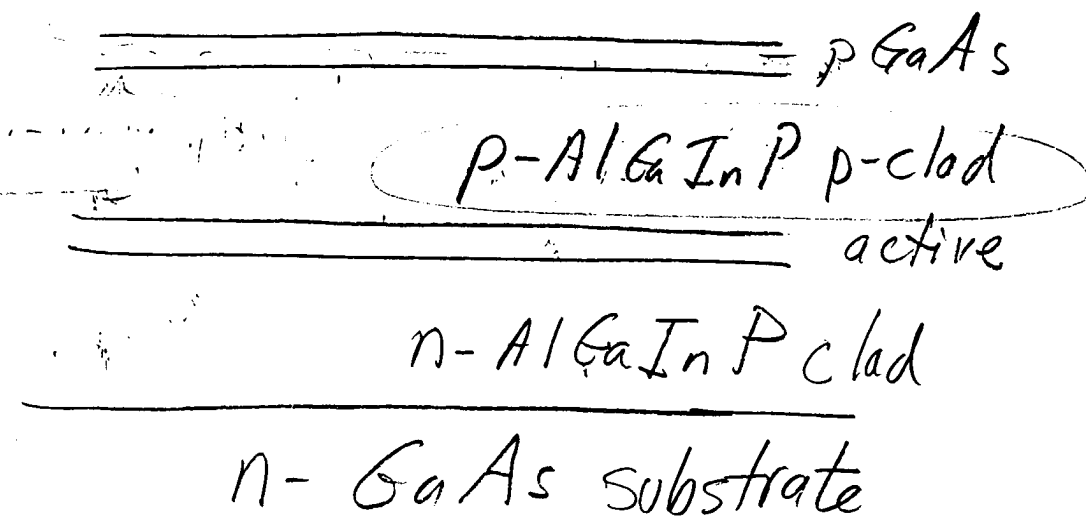
- ① On the channel: p-n junction
- ② Outside: p n p n  
⇒ current blocking

299



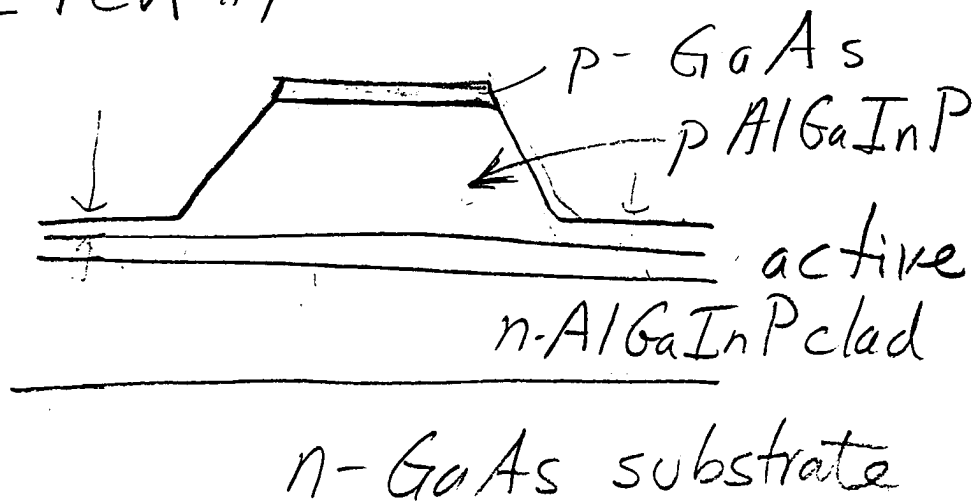
SBR (AlGaInP)

① 1<sup>st</sup> Growth

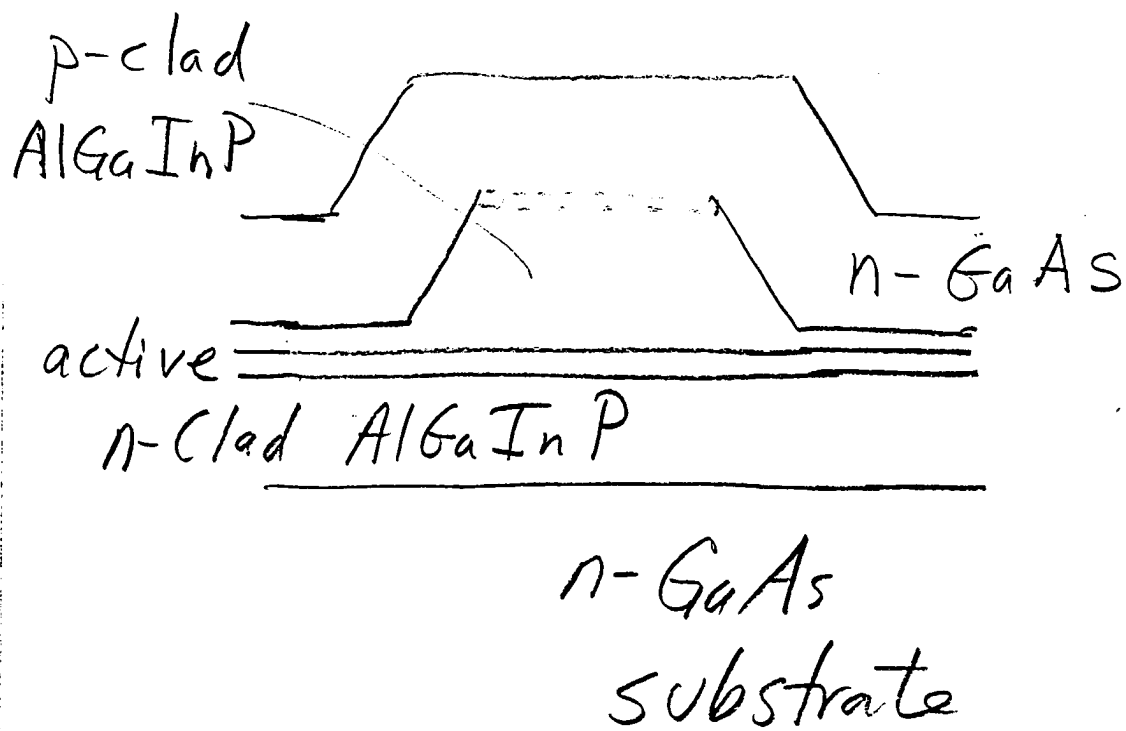


(300)

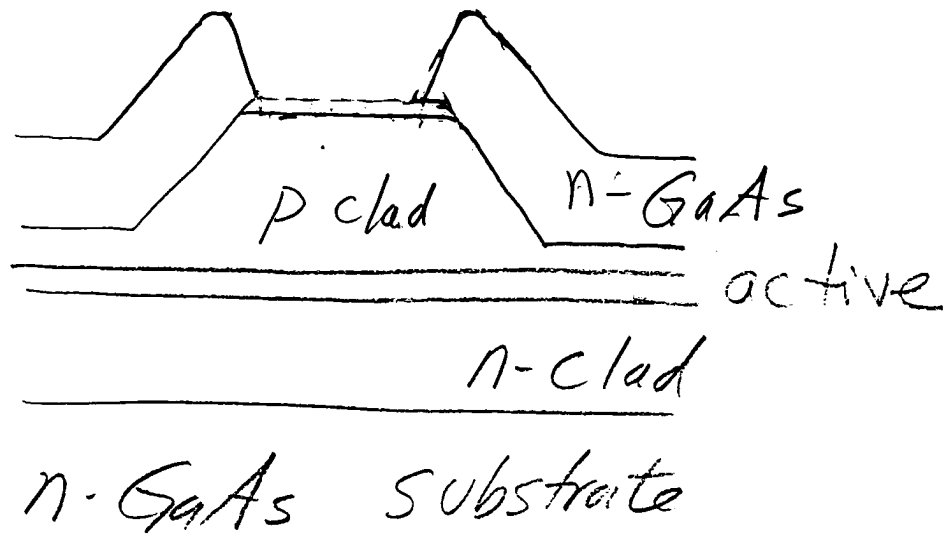
② Etch #1



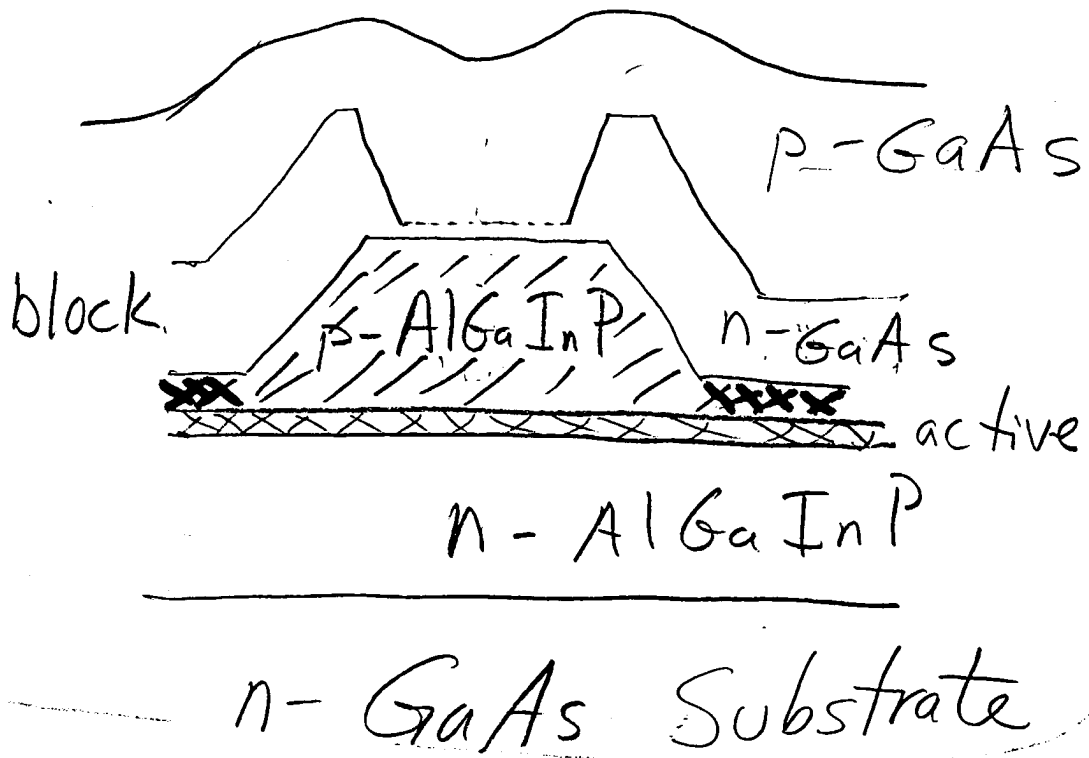
③ Regrowth #1



④ Etch #2



⑤ Regrowth #2



# Visible Ridge Guide $(\lambda \approx 630 - 680 \text{ nm})$

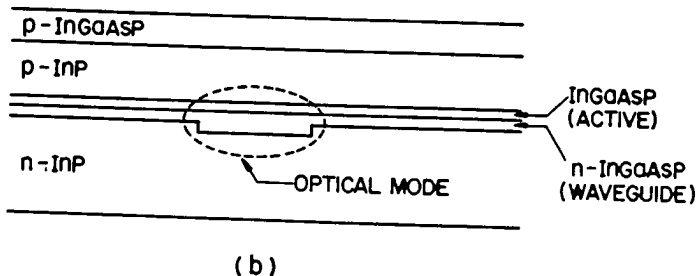
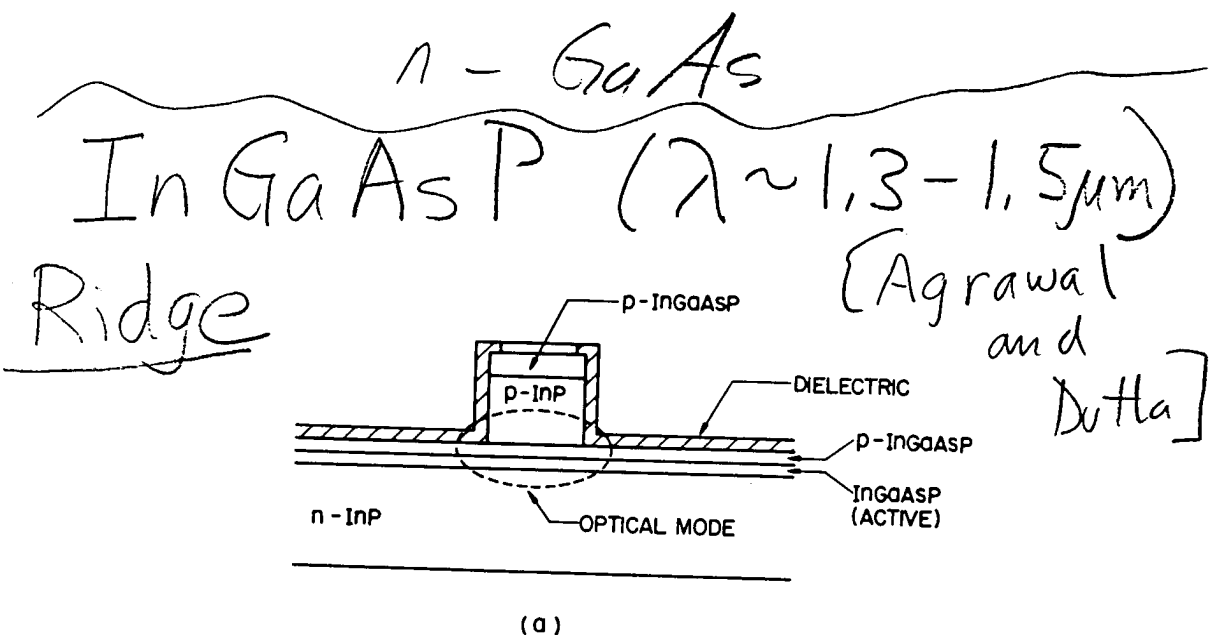
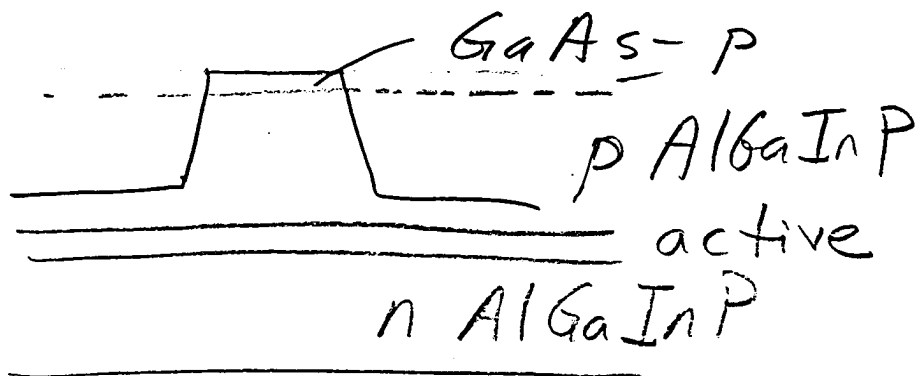


Fig. 5.17 Schematic representation of the optical mode in (a) ridge waveguide and (b) rib waveguide lasers. The dashed elliptical curve shows the spatial extent of the optical mode.

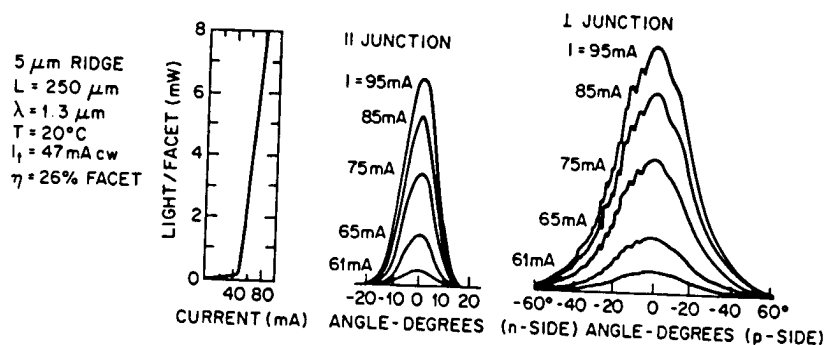


Fig. 5.16 Typical light-current (L-I) characteristics of a 1.3- $\mu\text{m}$  InGaAsP ridge waveguide laser. Far fields along and normal to the junction plane are also shown. (After Ref. 42 © 1983 IEEE)

## Buried Heterostructures

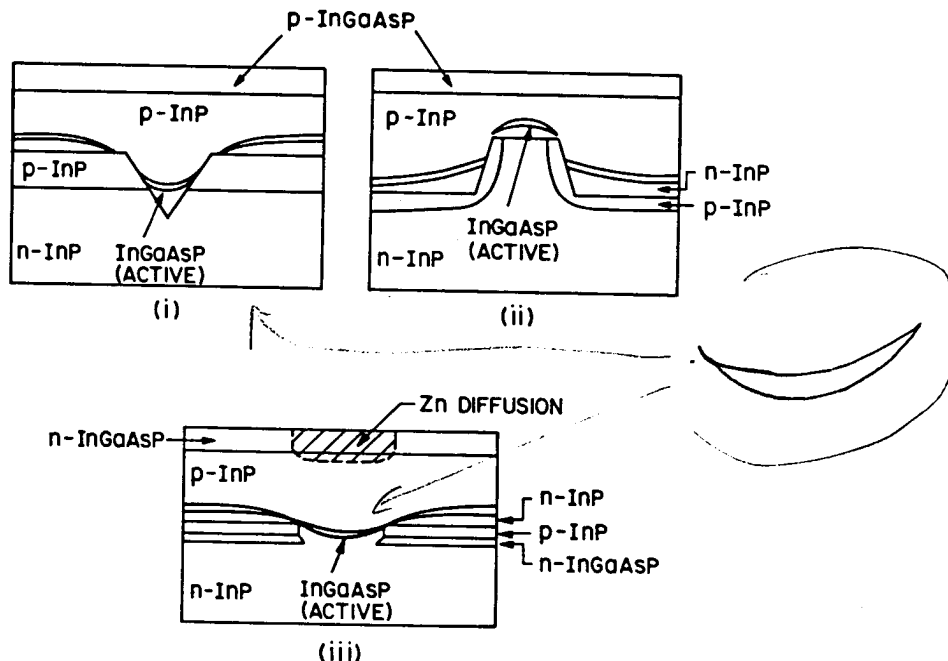


Fig. 5.19 Schematic cross section of different buried-heterostructure lasers with a nonplanar active layer: (i) V-grooved substrate or channelled-substrate buried heterostructure; (ii) mesa-substrate buried heterostructure; and (iii) buried crescent.

Crescent Active Layer

More BH at  $\lambda = 1.3, 1.5 \mu\text{m}$

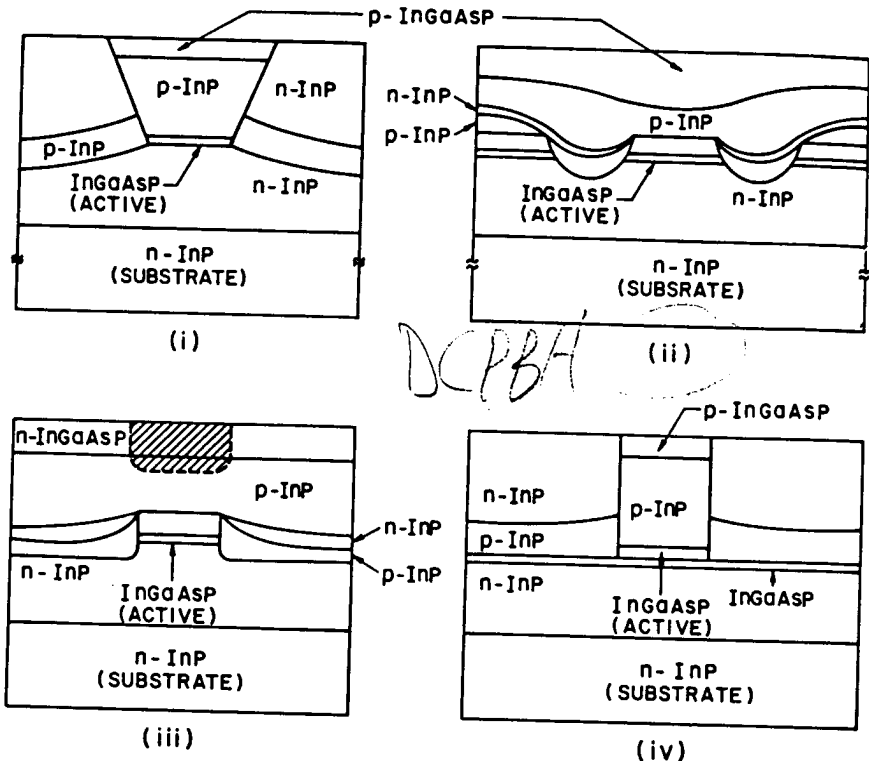
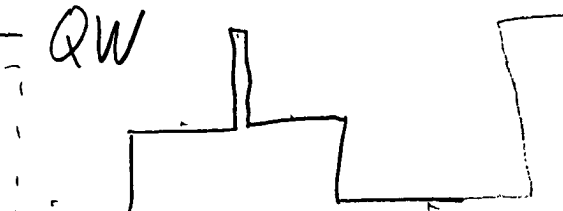
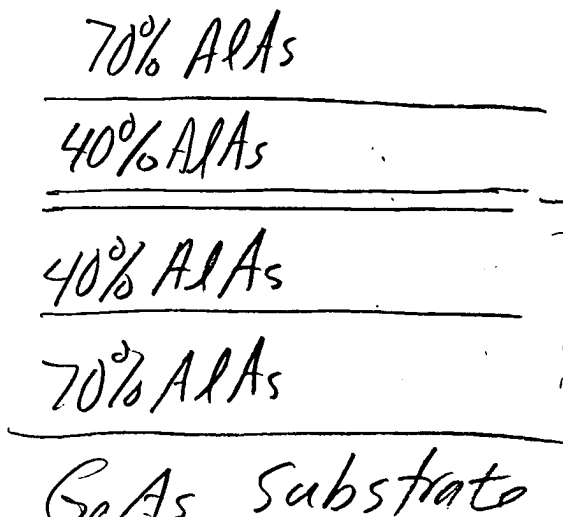
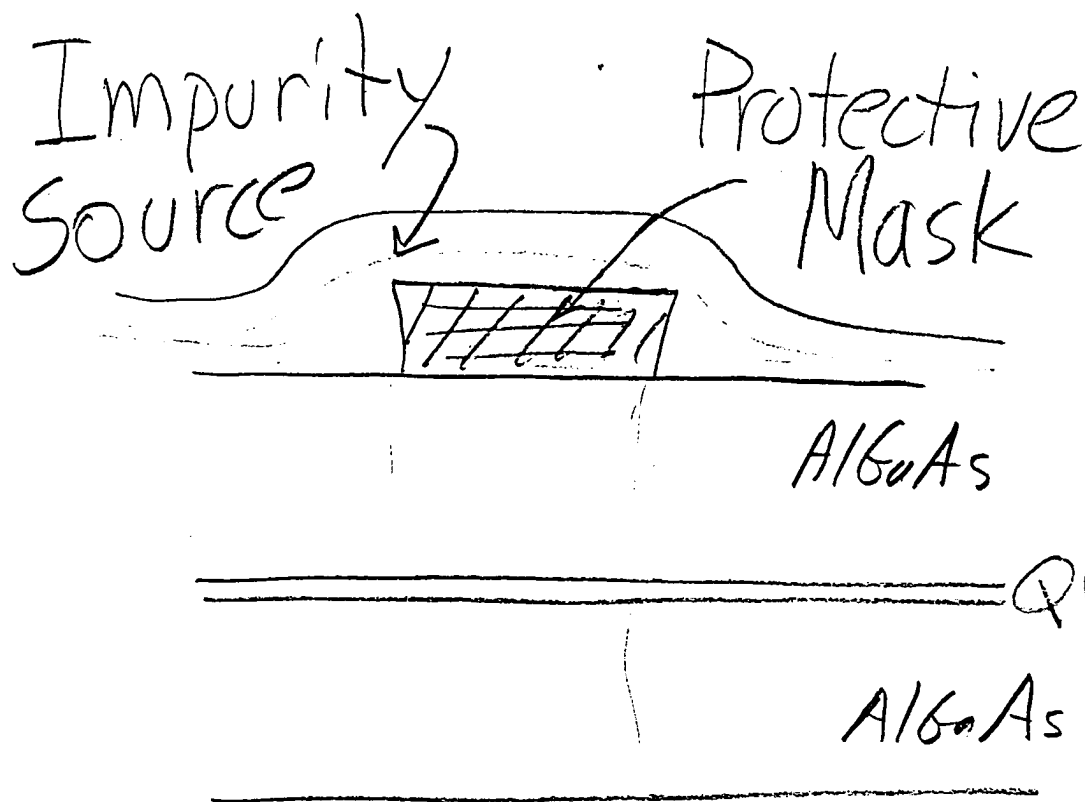


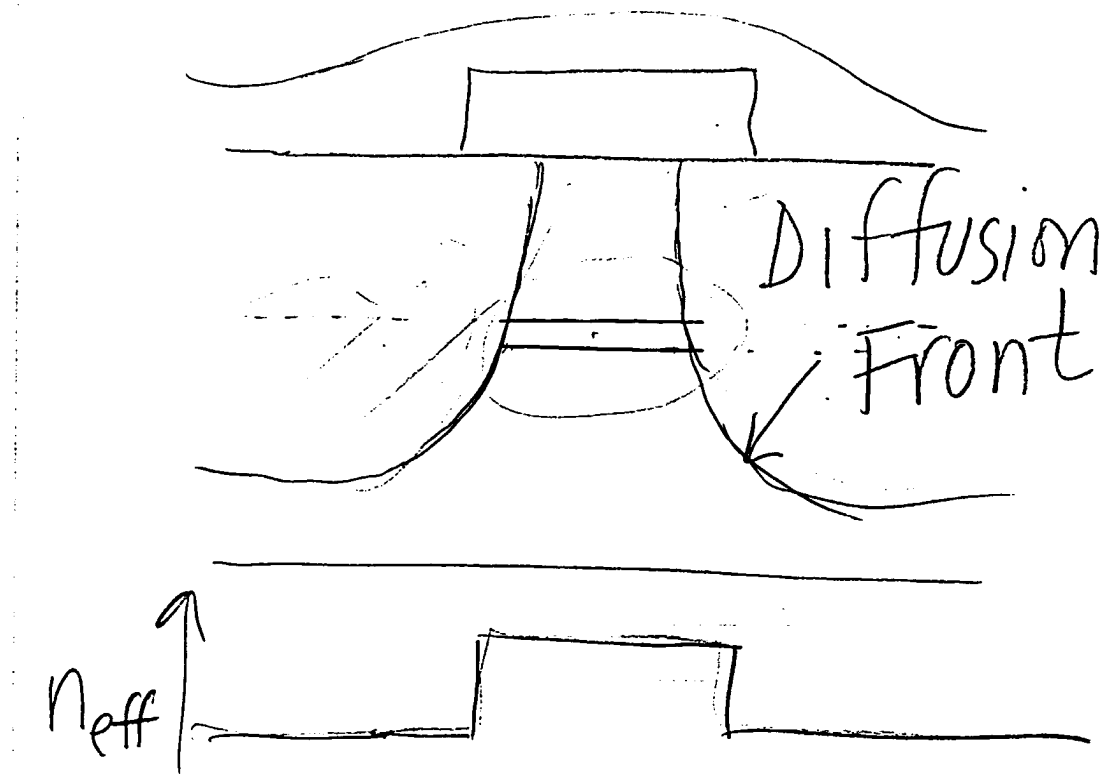
Fig. 5.18 Schematic cross section of different types of buried-heterostructure lasers with a planar active layer: (i) etched-mesa buried-heterostructure; (ii) double-channel planar buried heterostructure; (iii) planar buried heterostructure, and (iv) strip buried heterostructure.

Waveguides by Disordering





Add Heat & Time:



# Periodic Structures

## - coupled wave theory

- Floquet/Bloch (Keller)
  - (linear DE) (1928)
  - (partial DE) (1964)
  - (math of)

(Look at Ch 5, Buckman)

## Coupled Wave Theory

- Kogelnik & Shank, 1972, JAP  
 (John Pierce, 1950s)

### Assumptions

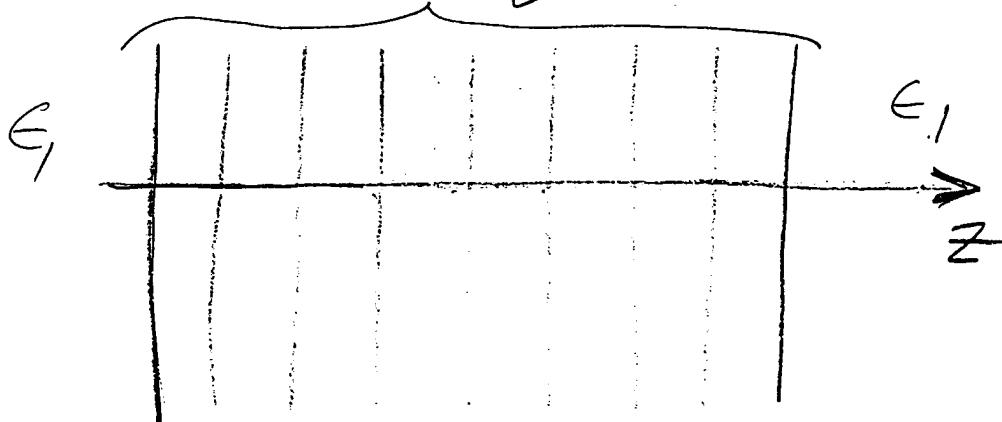
- 1) infinite media,  $(x, y)$
- 2) plane waves

Can be generalized to

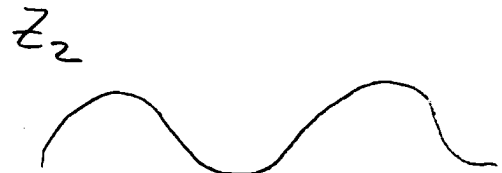
multi layer waveguides,  
 $TE$  &  $TM$  modes

$$\frac{\partial^2 E_y}{\partial z^2} + \epsilon_r(z) k_0^2 E_y = 0 \quad (1)$$

$$\epsilon_r(z) \downarrow$$

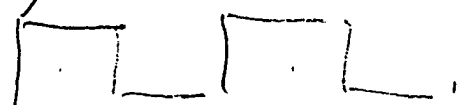


$$z_1 \rightarrow \leftarrow \Lambda$$



$$\epsilon_r(z) = \epsilon_1 (1 + \eta \cos kz)$$

$$k = \frac{2\pi}{\Lambda}$$



If  $\eta = 0$ , have  $+z$  &  $-z$

propagating plane waves:

$$F = R_0 e^{-j\beta_0 z} \quad (+z)$$

$$B = S_0 e^{j\beta_0 z} \quad (-z)$$

where  $\beta_0 = \sqrt{\epsilon_r} k_0$ ;  $k_0 = \frac{2\pi}{\lambda_0}$

If  $\eta$  is a slight perturbation,  
- expect little change.

Allow for perturbation  
by letting

$$R_0 \rightarrow R(z)$$

$$S_0 \rightarrow S(z)$$

$R(z)$ ,  $S(z)$  are slowly  
varying.

$$\beta = \beta_0 + \Delta\beta$$

The total perturbed electric field is:

$$E_y(z) = R(z)e^{-j\beta z} + S(z)e^{j\beta z} \quad (2)$$

Insert (2) into (1):

$$\frac{\partial E_y}{\partial z} = \overbrace{[ -j\beta R(z) + R'(z) ] e^{-j\beta z}}$$

$$+ [ j\beta S(z) + S'(z) ] e^{j\beta z} \quad (3)$$

$$\frac{\partial^2 E_y}{\partial z^2} = \left[ (-j\beta)^2 R(z) - j\beta R'(z) \right.$$

$$\left. - j\beta R'(z) + R''(z) \right] e^{-j\beta z}$$

+ (next page)

(310)

$$+ [(j\beta)^2 S(z) + j\beta S'(z) \\ + j\beta S'(z) + S''(z)] e^{j\beta z} \quad (4)$$

so (Recall (1))

$$\frac{\partial^2 E_y}{\partial z^2} + \epsilon_r(z) k_0^2 E_y = 0$$

$$\epsilon_r''(4)$$

$$\epsilon_r''(z) k_0^2 E_y(z) = \epsilon_1 (1 + \eta \cos kz) k_0^2 E_y$$

$$= \epsilon_1 k_0^2 E_y + \frac{\epsilon_1 k_0 \eta}{2} [e^{jkz} + e^{-jkz}] E_y$$

$\beta_0^2$  propagation

constant in unperturbed media

(5)

(311)

so

$$\underline{\epsilon_r(z) \beta_0^2 E_y} =$$

$$\beta_0^2 [R(z) e^{-j\beta z} + S(z) e^{+j\beta z}]$$

$$+ \frac{\eta}{2} \beta_0^2 [R(z) e^{-j(\beta-K)z}$$

$$+ S(z) e^{j(\beta+K)z}$$

$$+ R(z) e^{-j(\beta+K)z}$$

$$+ S(z) e^{j(\beta-K)z}]$$

$$e^{j(\beta z - \omega t)}$$

$$\begin{aligned} \beta - K &= -\beta \\ \beta &= -\beta + K \end{aligned}$$

The wave equation is of  
the form:

$$[\text{ } \text{ } \text{ } \text{ }] e^{-j\beta z} + [\text{ } \text{ } \text{ } \text{ }] e^{+j\beta z}$$

$$-\beta + K + \beta$$

$$(6) e^{+j\beta z}$$

$$= [\text{ } \text{ } \text{ } \text{ }] e^{-j(\beta-K)z} + [\text{ } \text{ } \text{ } \text{ }] e^{+j(\beta+K)z}$$

$$+ [\text{ } \text{ } \text{ } \text{ }] e^{-j(\beta+K)z} + [\text{ } \text{ } \text{ } \text{ }] e^{+j(\beta-K)z}$$

Note: if  $\beta$  and  $K$  satisfy

phase matching

$$\beta - K = -\beta \quad (7)$$

We can equate terms of equal exponential  $z$  dep.

What does (7) mean?

$$(7) \Rightarrow 2\beta = K$$

$$2 \frac{2\pi}{\lambda_0} \sqrt{E_1} = \frac{2\pi}{\lambda}$$

$$\begin{aligned} \beta + K &= \frac{\pi}{\lambda} \\ 2\beta &= \frac{\pi}{\lambda} \end{aligned}$$

$$\frac{2}{\lambda_m} = \frac{1}{\lambda} \quad \text{or}$$

$$\boxed{\lambda = \lambda_m = \frac{\lambda_0}{2 \text{neff}} \quad (8)}$$

which is the first-order Bragg condition

(313)

so require  $K = 2\beta$   
 and equate terms of  
 equal  $z$  dependence in (6):

$$\left\{ (-j\beta)^2 R(z) - 2j\beta R'(z) + R''(z) \right. \\ \left. + \beta_0^2 R(z) \right\} e^{-j\beta z} +$$

$$\left\{ (j\beta)^2 S(z) + 2j\beta S'(z) + S''(z) \right. \\ \left. + \beta_0^2 S(z) \right\} e^{j\beta z} = \\ -\frac{\eta\beta_0^2}{2} R(z) e^{-j(\beta-K)z} e^{-j\beta z} \\ -\frac{\eta\beta_0^2}{2} S(z) e^{j(\beta+K)z} e^{j\beta z} \quad (9) \\ -\frac{\eta\beta_0^2}{2} R(z) e^{-j(\beta+K)z} e^{-j\beta z} \\ -\frac{\eta\beta_0^2}{2} e^{j(\beta-K)z} S(z)$$

$$\omega / \kappa = 2\beta \text{ (or } \beta - \kappa = -\beta)$$

$$(j\beta)^2 S(z) + 2j\beta S'(z) + S''(z) \\ + \beta_0^2 S(z) = -\frac{\eta \beta_0^2}{2} R(z) \quad (10b)$$

and

$$(j\beta)^2 R(z) - 2j\beta R'(z) + R''(z) \\ + \beta_0^2 R(z) = -\frac{\eta \beta_0^2}{2} S(z) \quad (10a)$$

Recall,  $R(z)$  &  $S(z)$  are slowly varying, so can ignore

$R''(z)$  and  $S''(z)$  compared

to  $R'(z)$ ,  $R(z)$ ,  $S'(z)$ , &  $S(z)$ .

SO we can write (10) as:

$$-R'(z) + \frac{\beta_0^2 - \beta^2}{2j\beta} R(z) = -\frac{\eta \beta_0^2}{4j\beta} S(z) \quad (11a)$$

$$S'(z) + \frac{\beta_0^2 - \beta^2}{2j\beta} S(z) = -\frac{\eta \beta_0^2}{4j\beta} R(z) \quad (11b)$$

Note: if  $\epsilon_i \rightarrow \epsilon_i^* = \epsilon_i + j\epsilon_i'$   
 we would have:

$$-R'(z) + (\alpha - j\Delta\beta) R(z) = j\chi S(z) \quad (12a)$$

$$S'(z) + (\alpha + j\Delta\beta) S(z) = j\chi R(z) \quad (12b)$$

where:

$$\frac{\beta_0^2 - \beta^2}{2\beta} = \frac{(\beta_0 - \beta)(\beta_0 + \beta)}{2\beta} \approx \Delta\beta$$

$$\frac{(\Delta\beta)(2\beta_0 + \Delta\beta)}{2(\beta_0 + \Delta\beta)} \cdot \beta = \beta_0 + \Delta\beta$$

(316)

and

$$\alpha = \frac{\epsilon_0 k^2}{2\beta_0} = \dots \quad (13)$$

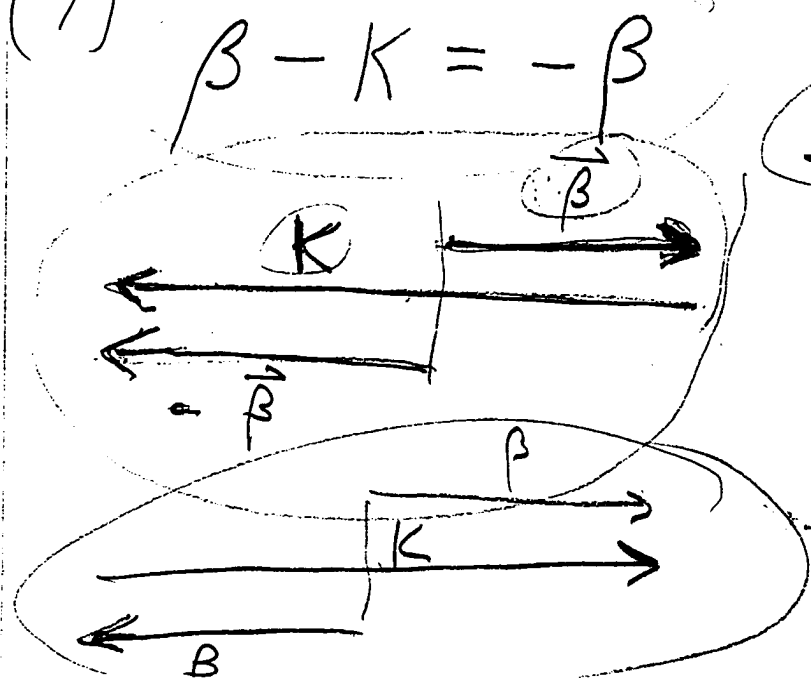
$$\chi = \frac{\gamma \beta_0^2}{4\beta} \approx \frac{\gamma \beta_0}{4} \quad (14)$$

$$\epsilon_n = \epsilon_1 (1 + \gamma \cos k z)$$

$$\epsilon_1^* \rightarrow \epsilon_1 + j\epsilon_2$$


---

(7)



$$\Lambda = \frac{2m}{2}$$

$$K = \frac{2\pi}{\Lambda}$$

$$\beta = \frac{2\pi}{2m}$$

(4/19)

(317)

Correction to 4/17 (14) &amp;

$$4/17 \quad (28) : \quad \epsilon_n(z) = \epsilon_i(1 + n \cos(kz))$$

if  $\epsilon_i^*$  is complex  $\rightarrow \epsilon_i + j\epsilon_{ii}$

and

$\eta^*$  is complex  $\rightarrow \eta + j\eta_{ii}$

$$\text{Then } \alpha = \frac{\epsilon_i k_0^2}{2\beta_0} \quad (13)$$

and

$$(14) \quad \chi = \frac{\eta^* \beta_0^2}{4\beta} = \frac{\eta \beta_0}{4} + j \frac{\eta_{ii} \beta_0}{4}$$

which compares to K-5

Eq (2):

$$n(z) = n + n_i \cos(Kz) \quad (2a)$$

$$\alpha(z) = \alpha + \alpha_i \cos(Kz) \quad (2b)$$

## Coupled Wave Equations

Eq 12a & 12b:

$$-R'(z) + (\alpha - j\Delta\beta) R(z) = j\chi S(z)$$

$$S'(z) + (\alpha - j\Delta\beta) S(z) = j\chi R(z)$$

General Form of Solution:

from 12a, taking  $\frac{d}{dz}$  (12a)  $\Rightarrow$

$$-R''(z) + (\alpha - j\Delta\beta) R'(z) = j\chi S'(z) \quad (15)$$

and using 12b,

$$\begin{aligned} -R''(z) + (\alpha - j\Delta\beta) R'(z) \\ = j\chi [j\chi R(z) - (\alpha - j\Delta\beta) S(z)] \end{aligned} \quad (16)$$

Use 12a to express  $S(z)$  in terms of  $R(z)$ :

$$-R''(z) + (\alpha - j\Delta\beta)R'(z) = \quad (17)$$

$$\begin{aligned} & j\chi \left[ j\chi R(z) - (\alpha - j\Delta\beta) \frac{1}{j\chi} \right] \left\{ -R'(z) \right. \\ & \left. + (\alpha - j\Delta\beta) R(z) \right\} \end{aligned} \quad = RHS$$

$$RHS = -\chi^2 R(z) + (\alpha - j\Delta\beta) R'(z)$$

$$- (\alpha - j\Delta\beta)^2 R(z)$$

$\frac{d^2y^{(n)}}{dx^2} + \sum g^{(k)} = 0$

so

$$-R''(z) + [\chi^2 + (\alpha - j\Delta\beta)^2] R(z) = 0 \quad (18)$$

which has solutions

$$R(z) = r_1 e^{\gamma z} + r_2 e^{-\gamma z} \quad (19)$$

where

$$\gamma^2 = \chi^2 + (\alpha - j\Delta\beta)^2 \quad (20)$$

Since

$$S(z) = \frac{1}{j\chi} [R'(z) + (\chi - j\Delta\beta)R(z)]$$

$$S(z) = s_1 e^{\gamma z} + s_2 e^{-\gamma z} \quad (21)$$

Recall

$$E_y(z) = R(z)e^{-j\beta_0 z} + S(z)e^{j\beta_0 z}$$

$$= [r_1 e^{\gamma z} + r_2 e^{-\gamma z}] e^{-j\beta_0 z} + [s_1 e^{\gamma z} + s_2 e^{-\gamma z}] e^{j\beta_0 z} \quad (22)$$

∴  $\gamma$  is the total correction to the periodic perturbation (index and/or gain).

From (20)

$$\gamma^2 = \chi^2 + (\alpha - j\Delta\beta)^2$$

-  $\Delta\beta = \beta - \beta_0$  (real)

CASE 1 (index-coupling)

If  $\gamma = 0$ ,  $\alpha = 0$ , (no gain or loss)

$$\chi^2 = \left(\frac{\gamma \beta_0}{4}\right)^2$$

and we can write (20)

$$\frac{\gamma^2}{\beta_0^2} = \left(\frac{\gamma}{4}\right)^2 - \left(\frac{\Delta\beta}{\beta_0}\right)^2 \quad (23)$$

$$\beta = \sqrt{\epsilon} k$$

$$\Delta \beta = \sqrt{\epsilon} \Delta k$$

$$\beta_0 = \sqrt{\epsilon_0} k_0$$

$$f\lambda = c$$

$$2\pi f \frac{\lambda}{2\pi} = v_{ph}$$

(322)

SINCE

$$\frac{\Delta \beta}{\beta_0} = \frac{\Delta \omega}{\omega_0}$$

$$\begin{aligned} \omega &= v_{ph} k \\ \Delta \omega &= v_{ph} \Delta k \\ \frac{\Delta k}{k} &= \frac{\Delta \omega}{\omega} \end{aligned}$$

$$\frac{\gamma^2}{\beta_0^2} = \left(\frac{\eta}{4}\right)^2 - \left(\frac{\Delta \omega}{\omega}\right)^2 \quad (23)$$

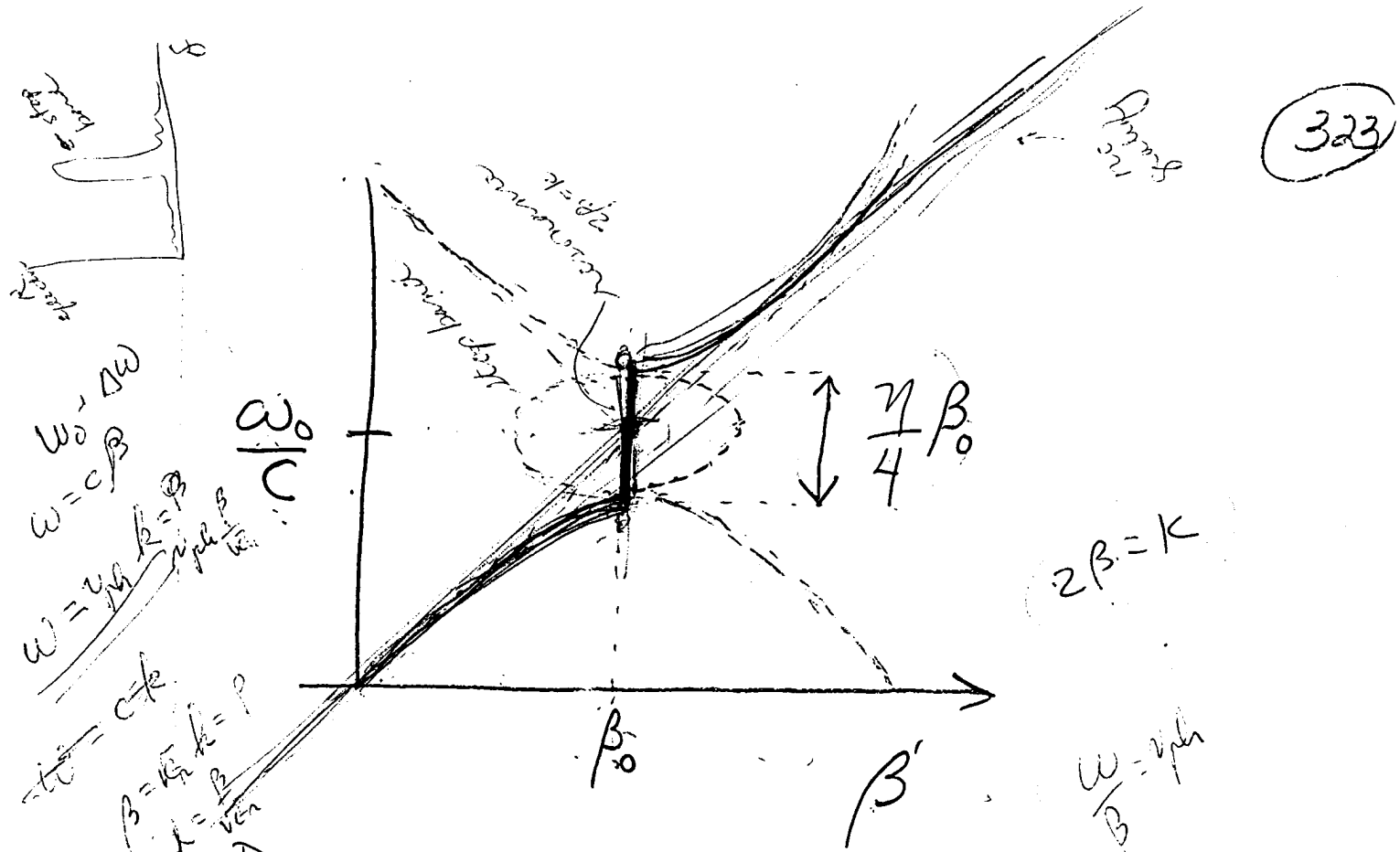
$$\frac{\gamma}{\beta_0} = \pm \sqrt{\left(\frac{\eta}{4}\right)^2 - \left(\frac{\Delta \omega}{\omega}\right)^2} \quad (24)$$

Recall:  $E_y \propto e^{(\gamma - j\beta)z}$

for  $\frac{\Delta \omega}{\omega} < \frac{\eta}{4}$

$\gamma$  is real

$\Rightarrow$  exponential decay  
(stop band)



Dispersion diagram  
for permittivity modulation  
with no loss or gain  
(compare Fig 2a, K-S).

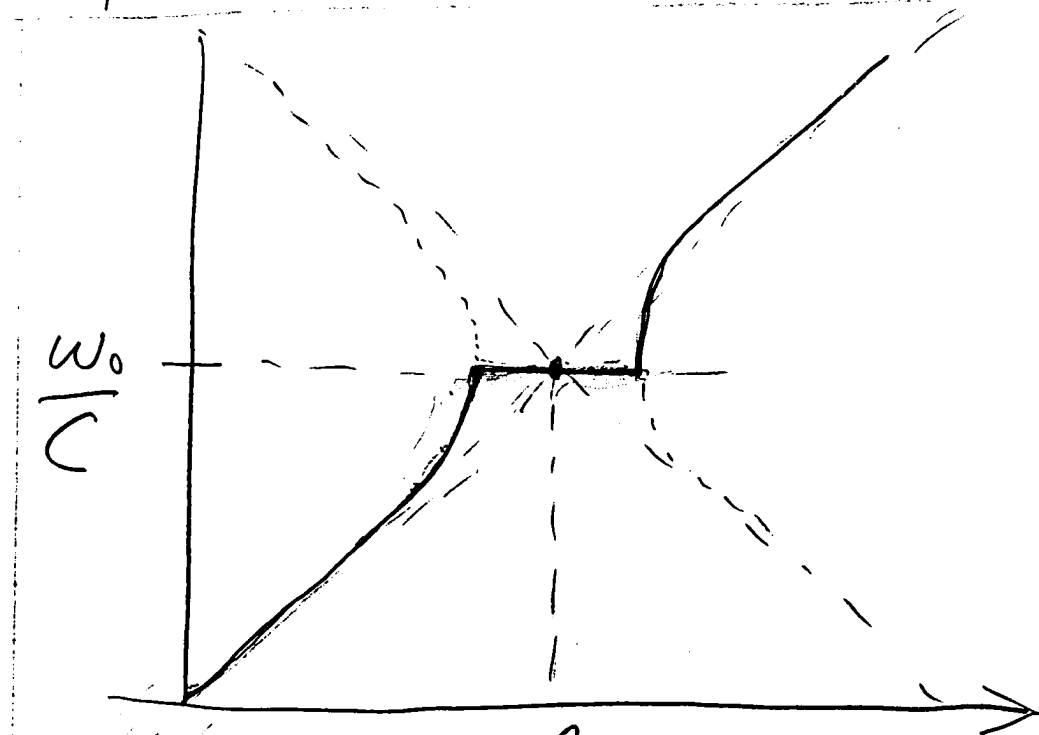
### Case 2 (gain coupling)

let  $\eta = 0, \eta_i \neq 0$        $\bar{\epsilon}_n \frac{\omega}{\beta} = \frac{1}{c}$   
 $\omega''$  and  $\alpha = 0 (\Rightarrow \text{no average loss or gain})$ .

20 becomes

$$\frac{\gamma^2}{\beta_0^2} = -\left(\frac{n_i \beta_0}{4}\right)^2 - \left(\frac{4\omega}{\omega}\right)^2$$

$$\frac{\gamma}{\beta_0} = \pm j \sqrt{\left(\frac{n_i \beta_0}{4}\right)^2 + \left(\frac{4\omega}{\omega}\right)^2} \quad (25)$$

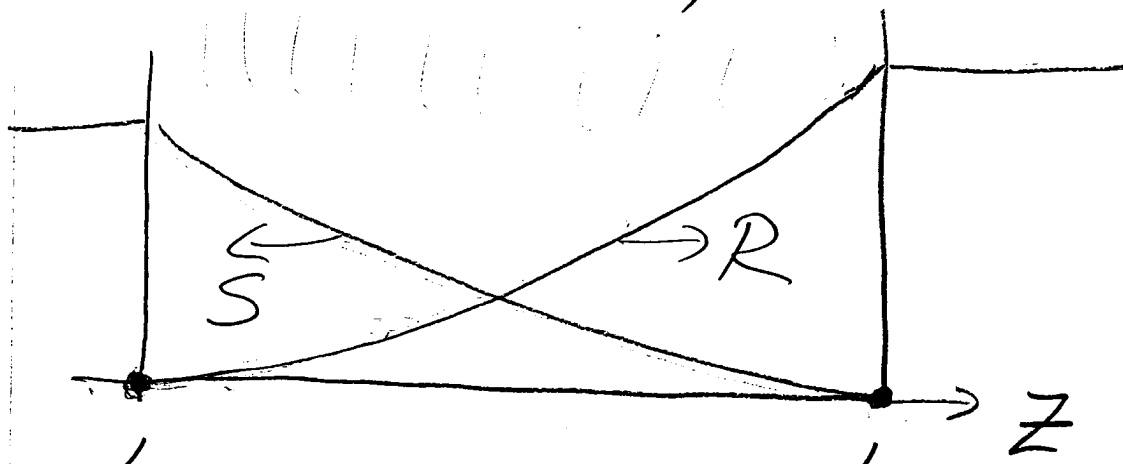


Dispersion diagram

for gain modulation  
with  $\alpha = 0$ .

For a DFB laser  
(distributed feedback)

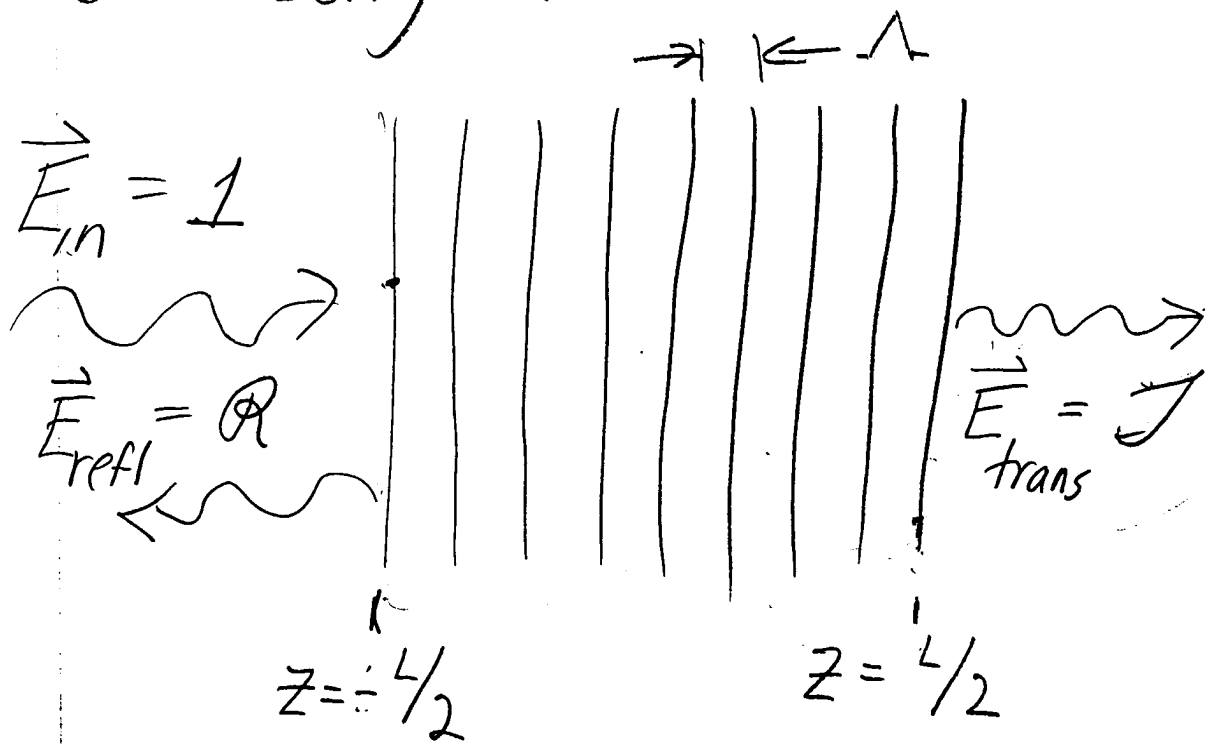
Kogelnik and Shank  
solve the coupled  
wave equations 12a+12b  
with boundary conditions



$$R(-\frac{L}{2}) = S(\frac{L}{2}) \equiv 0$$

Different Approach:

Consider an unbounded (in  $x \& y$ ) periodic medium of length  $L$ :



$R$  and  $T$  are amplitude reflection and transmission coefficients.

- use coupled wave theory

boundary conditions:

$$\underline{R(-L/2) = 1} \quad (a)$$

$$R(L/2) = J \quad (b)$$

$$S(-L/2) = Q \quad (c)$$

$$S(L/2) = 0 \quad (d)$$

from (19),  $R(\pm L/2)$

$$a \Rightarrow 1 = r_1 e^{-\delta L/2} + r_2 e^{\delta L/2} \quad (26)$$

$$b \Rightarrow J = r_1 e^{-\delta L/2} + r_2 e^{-\delta L/2} \quad (27)$$

$$c \Rightarrow Q = S_1 e^{-\delta L/2} + S_2 e^{\delta L/2} \quad (28)$$

$$d \Rightarrow 0 = S_1 e^{\delta L/2} + S_2 e^{-\delta L/2} \quad (29)$$

$$(26) \Rightarrow$$

$$r_1 e^{-\gamma L/2} = 1 - r_2 e^{\gamma L/2}$$

or

$$r_1 = e^{-\gamma L/2} - r_2 e^{\gamma L} \quad (30)$$

and

$$r_2 = e^{-\gamma L/2} - r_1 e^{-\gamma L} \quad (31)$$

$$\text{so } (27) \Rightarrow$$

$$J = r_1 e^{\gamma L/2} + \underbrace{(e^{-\gamma L/2} - r_1 e^{-\gamma L})}_{r_2} e^{-\gamma L/2}$$

$$r_1 (e^{\gamma L/2} - e^{-\gamma L/2}) = J - e^{-\gamma L} \quad (32)$$

$$r_1 = \frac{Je^{\gamma L/2} - e^{-\gamma L/2}}{e^{\gamma L} - e^{-\gamma L}} \quad (33)$$

similarly (again (27))

$$J = \left( e^{\gamma L/2} - r_2 e^{\gamma L} \right) e^{\gamma L/2} \\ \sim r_1 + r_2 e^{-\gamma L/2}$$

$$r_2(e^{-\gamma L/2} - e^{3\gamma L/2}) = J - e^{\gamma L} \quad (34)$$

$$\boxed{r_2 = \frac{J e^{-\gamma L/2} - e^{\gamma L/2}}{e^{-\gamma L} - e^{\gamma L}}} \quad (35)$$

by (29),

$$S_1 e^{\gamma L/2} = - S_2 e^{-\gamma L/2}$$

$$S_1 = - S_2 e^{-\gamma L} \quad (36a)$$

$$S_2 = - S_1 e^{\gamma L} \quad (36b)$$

by (28)

$$S_1 e^{-\delta L/2} + S_2 e^{\delta L/2} = R$$

$$S_1 e^{-\delta L/2} - S_1 e^{\delta L/2} e^{\delta L/2} = R$$

$$S_1 (e^{-\delta L} - e^{\delta L}) = R e^{-\delta L/2}$$

$$\boxed{S_1 = \frac{R e^{-\delta L/2}}{e^{-\delta L} - e^{\delta L}}} \quad (37)$$

finally,

$$-S_2 e^{-\delta L} e^{-\delta L/2} + S_2 e^{\delta L/2} = R$$

$$S_2 (e^{-\delta L/2} - e^{-3\delta L/2}) = R$$

$$\boxed{S_2 = \frac{R e^{\delta L/2}}{e^{\delta L} - e^{-\delta L}}} \quad (38)$$

returning to the CW Eqs:

$$-R'(z) + (\alpha - j\Delta\beta) R(z) = j\chi S(z) \quad (12a)$$

$$S'(z) + (\alpha - j\Delta\beta) S(z) = j\chi R(z) \quad (12b)$$

$$\begin{aligned} & -(\gamma r_1 e^{\gamma z} - \gamma r_2 e^{-\gamma z}) \\ & + (\alpha - j\Delta\beta)(r_1 e^{\gamma z} + r_2 e^{-\gamma z}) \\ & = j\chi (s_1 e^{\gamma z} + s_2 e^{-\gamma z}) \end{aligned} \quad (39a)$$

and

$$\begin{aligned} & (\gamma s_1 e^{\gamma z} - \gamma s_2 e^{-\gamma z}) \\ & + (\alpha - j\Delta\beta)(s_1 e^{\gamma z} + s_2 e^{-\gamma z}) \\ & = j\chi (r_1 e^{\gamma z} + r_2 e^{-\gamma z}) \end{aligned} \quad \text{where } 4/21 \quad (39b)$$

Equate terms of =  
exponential  $\neq$  dependence:  
(39a)  $\Rightarrow$

$$-\gamma r_1 + (\alpha - j\Delta\beta) r_1 = j\chi s_1 \quad (40a)$$

$$\gamma r_2 + (\alpha - j\Delta\beta) r_2 = j\chi s_2 \quad (40b)$$

$$\gamma s_1 + (\alpha - j\Delta\beta) s_1 = j\chi r_1 \quad (40c)$$

$$-\gamma s_2 + (\alpha - j\Delta\beta) s_2 = j\chi r_2 \quad (40d)$$

Eq (33) for  $r_1$ ; (37) for  $s$ ,  
in (40a)  $\Rightarrow$

$$[-\gamma + (\alpha - j\Delta\beta)] \frac{je^{\gamma L/2} - e^{-\gamma L/2}}{e^{\gamma L} - e^{-\gamma L}}$$

$$= j\chi \frac{Re^{-\gamma L/2}}{e^{-\gamma L} - e^{\gamma L}}$$

$$[-\gamma + (\alpha - j\Delta\beta)](je^{\gamma L/2} - e^{-\gamma L/2})$$

$$= -j\chi Re^{-\gamma L/2} \quad (41a)$$

Similarly, Eq (40b)  $\Rightarrow$

$$[\gamma + (\alpha - j\Delta\beta)] \frac{je^{-\gamma L/2} - e^{\gamma L/2}}{e^{-\gamma L} - e^{\gamma L}}$$

$$= j\chi Re^{\gamma L/2}$$

$$\frac{e^{\gamma L} - e^{-\gamma L}}{e^{\gamma L} - e^{-\gamma L}}$$

$$[\gamma + (\alpha - j\Delta\beta)](j e^{-\gamma L/2} - e^{\gamma L/2}) \\ = -j\chi R e^{\gamma L/2} \quad (41b)$$

Eg (40c)  $\Rightarrow$

$$[\gamma + (\alpha - j\Delta\beta)] \frac{R e^{-\gamma L/2}}{e^{\gamma L} - e^{-\gamma L}}$$

$$= j\chi \frac{j e^{\gamma L/2} - e^{-\gamma L/2}}{e^{\gamma L} - e^{-\gamma L}}$$

$$-[\gamma + (\alpha - j\Delta\beta)] R e^{-\gamma L/2} \quad (41c)$$

$$= j\chi (j e^{\gamma L/2} - e^{-\gamma L/2})$$

Eg (40d)  $\Rightarrow$

$$[\gamma + (\alpha - j\Delta\beta)] \frac{R e^{\gamma L/2}}{e^{\gamma L} - e^{-\gamma L}} =$$

$$= j\chi \frac{je^{-jL/2} - e^{jL/2}}{e^{-jL} - e^{jL}}$$

added  
4/25

$$\begin{aligned} & -[\gamma + (\alpha - j\beta)] Re^{jL/2} \\ & = (je^{-jL/2} - e^{jL/2}) (41/d) \end{aligned}$$

(41a)  $\Rightarrow$

$$\begin{aligned} Q &= -\frac{1}{j\chi} [\gamma + (\alpha - j\beta)] \\ &\quad \times (je^{jL} - 1) \end{aligned} \quad (42a)$$

(41b)  $\Rightarrow$

$$\begin{aligned} -Q &= \frac{1}{j\chi} [\gamma + (\alpha - j\beta)] \\ &\quad \times (je^{-jL} - 1) \end{aligned} \quad (42b)$$

$$(42a) + (42b) = 0$$

$$0 = \frac{1}{j\chi} \left\{ j\gamma \underbrace{\left( e^{\gamma L} + e^{-\gamma L} \right)}_{2 \cosh \gamma L} \right.$$

$$\left. - \gamma (\alpha - j\beta) \underbrace{\left( e^{\gamma L} - e^{-\gamma L} \right)}_{2 \sinh \gamma L} \right)$$

$$-\gamma - (\alpha + j\beta) - \gamma + (\alpha - j\beta) \}$$

$$2\gamma = \gamma (2 \cosh \gamma L$$

$$- 2 (\alpha - j\beta) \sinh \gamma L)$$

(43)

$$\boxed{J = \frac{\gamma}{\gamma \cosh \gamma L - (\alpha - j\beta) \sinh \gamma L}}$$

where

$$\gamma = \sqrt{\chi^2 + (\alpha - j\beta)^2}$$

Note:  $J = \infty$  if

$$\gamma \cosh \gamma L = (\alpha - j \Delta \beta) \\ \times \sinh(\gamma L)$$

in which characteristic  
affirmative  
eigentext for  
oscillator

or

$$(\alpha - j \Delta \beta) = \gamma \coth(\gamma L) \quad (44)$$

(compare to Eq(19) of K-S).

definition of oscillator -  
finite output w/ no  
input

light oscillator  $\rightarrow$  laser

Now, find an expression for  $R$ :

4(c)  $\Rightarrow$

$$j\chi J e^{\gamma L/2} = j\chi \bar{e}^{-\gamma L/2} - [\gamma + (\alpha - j\beta)] R \bar{e}^{-\gamma L/2} \quad (45a)$$

and 4(d)  $\Rightarrow$

$$j\chi J e^{-\gamma L/2} = j\chi e^{\gamma L/2} - [\gamma + (\alpha - j\beta)] R e^{\gamma L/2} \quad (45b)$$

$$-[\gamma + (\alpha - j\beta)] R e^{\gamma L/2}$$

(45a)  $\Rightarrow$

$$\begin{aligned} -j\chi J &= -j\chi \bar{e}^{-\gamma L} + [\gamma + (\alpha - j\beta)] \\ &\times R \bar{e}^{-\gamma L} \end{aligned} \quad (46a)$$

(45 b)  $\Rightarrow$

$$j\chi \mathcal{I} = j\chi e^{\gamma L} - [\gamma + (\alpha - j\beta)] \\ \times R e^{\gamma L} \quad (46b)$$

$$(46a) + (46b) \Rightarrow$$

$$0 = j\chi \left( e^{\gamma L} - e^{-\gamma L} \right)^{\cancel{2 \sinh}} \\ + R \gamma \left( e^{\gamma L} + e^{-\gamma L} \right)^{\cancel{2 \cosh}} \quad (47)$$

$$-R(\alpha - j\beta) \underbrace{\left( e^{\gamma L} - e^{-\gamma L} \right)}_{2 \sinh}$$

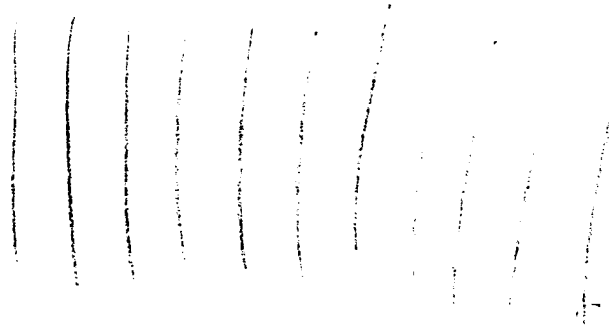
$$R \left\{ (\alpha - j\beta) \sinh(\gamma L) - \gamma \cosh(\gamma L) \right\}$$

$$= j\chi \sinh(\gamma L)$$

(48)

$$\rho = \frac{j\gamma}{(\alpha - j\Delta\beta) - \gamma \coth(\gamma L)} \quad (49)$$

So the structure



- acts as a distributed amplifier
- oscillates when

$$(\alpha - j\Delta\beta) = \gamma \coth(\gamma L)$$

Solve (49) for  $\tilde{E}$   
 (43) for

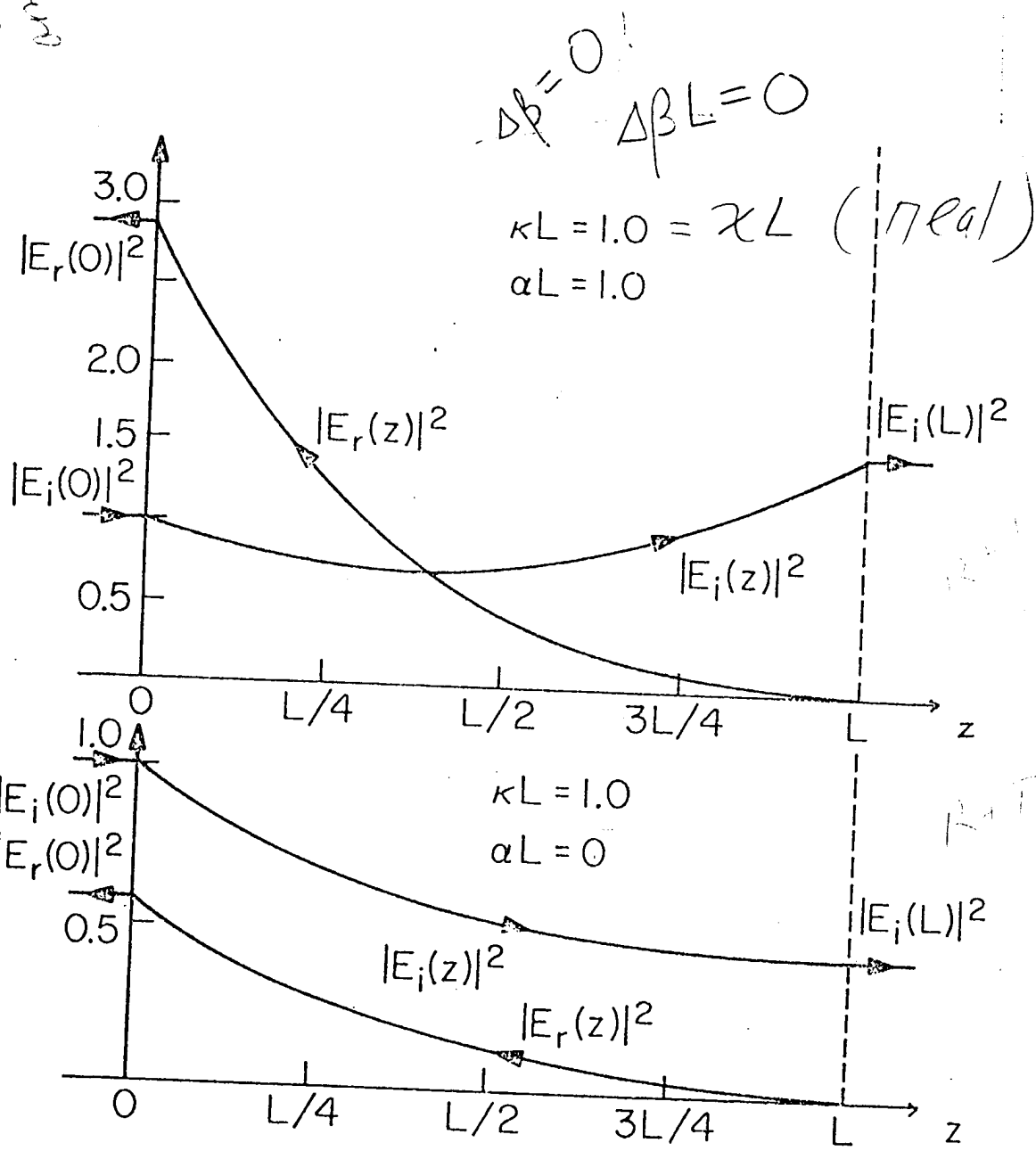


Fig. 3-3 The behavior of  $|E_i(z)|^2$  and  $|E_r(z)|^2$  in a periodic waveguide (a) with gain  $\alpha L = 1.0$  (b) without gain  $\alpha L = 0$ .

$$\alpha_L \left| \frac{E_r(0)}{E_i(0)} \right|^2 = |R|^2$$

$$\chi^2 = \chi^2 + (\alpha - j \Delta \beta)^2$$

see Fig 8, Fig 5

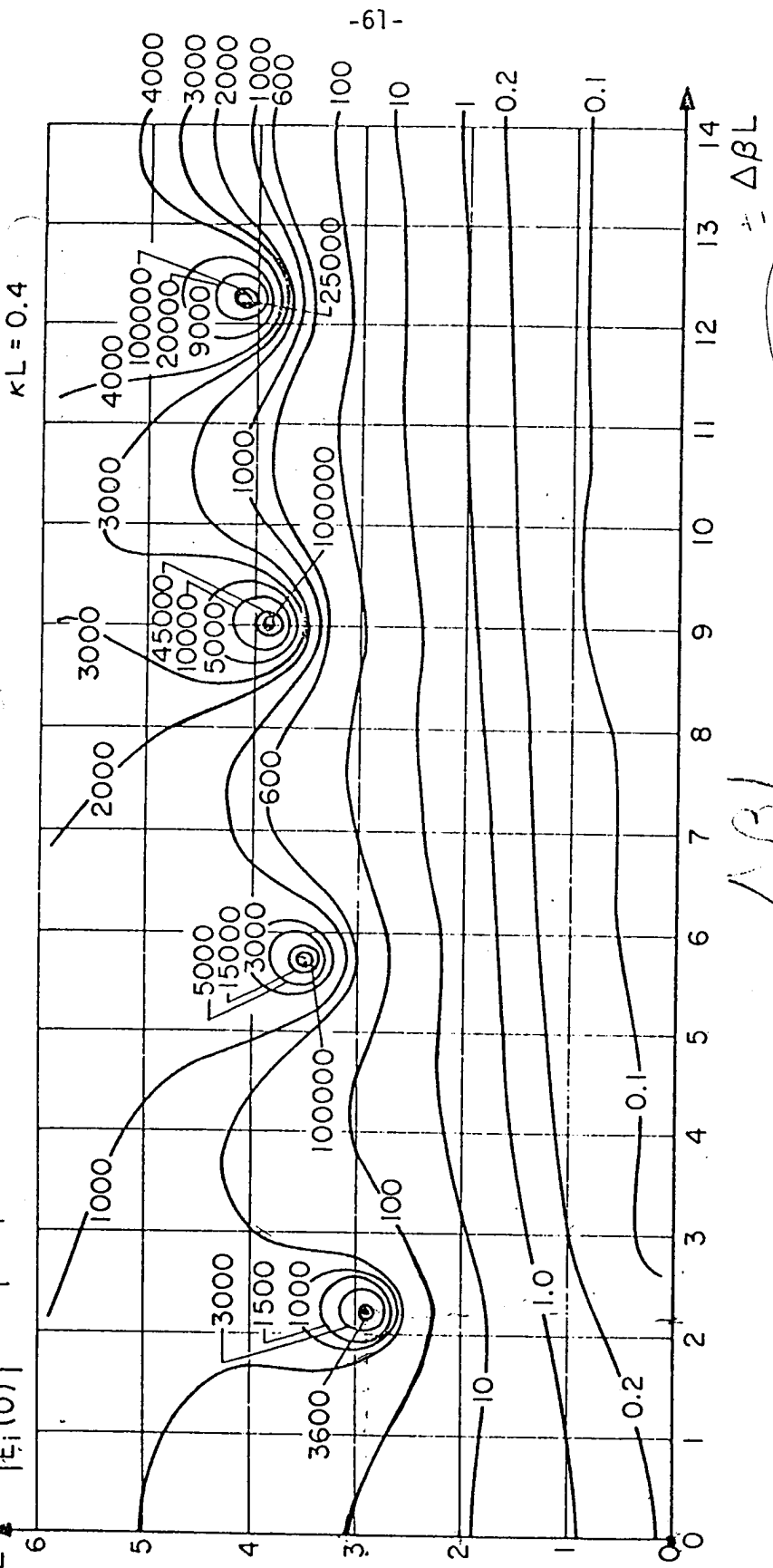


Fig. 3-4 The reflection gain as a function of  $\Delta BL$  and  $aL$  for  $kL = 0.4$ .

$$\zeta = \beta = \bar{v}, \lambda_{\beta} = \sqrt{\epsilon}, \frac{v}{\beta}$$

$$\frac{|E_1(L)|^2}{|E_1(O)|} = D^2 \left( -\frac{1}{2} \right)^2$$

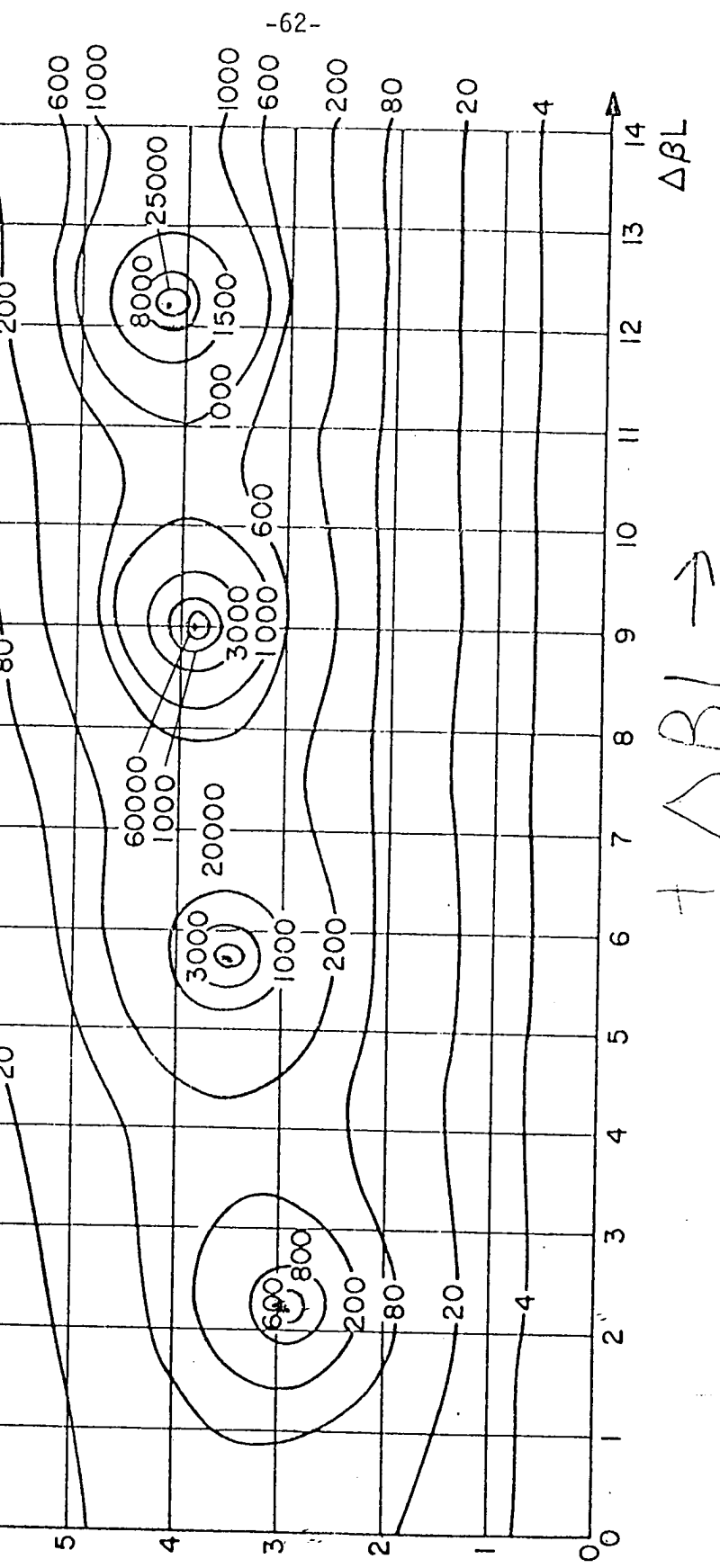


Fig. 3-5 The transmission gain as a function of  $\Delta BL$  and  $\alpha L$  for  $kL = 0.4$ .

Hassive Filter

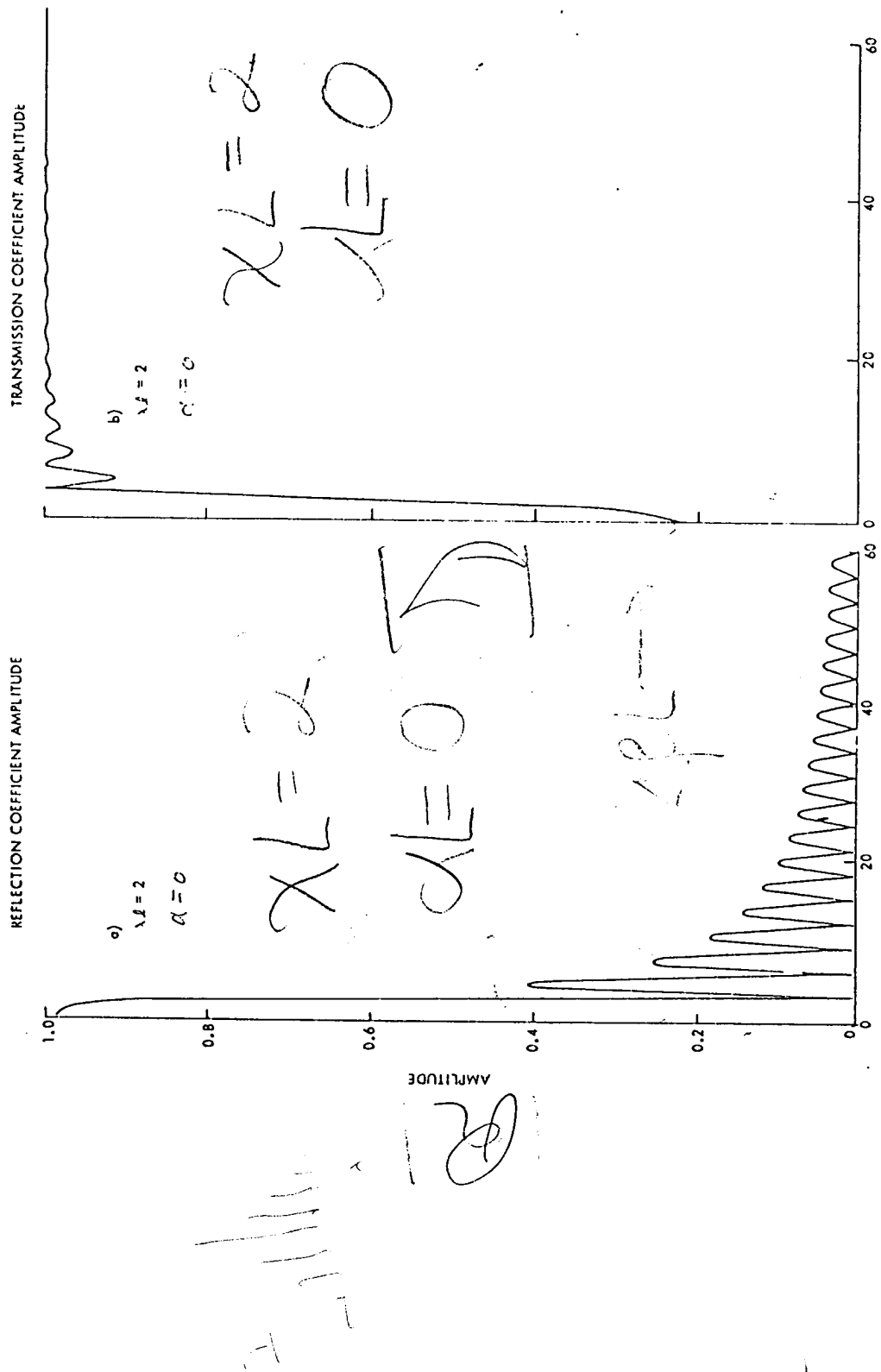


Fig. 6.4 Magnitude of reflection and transmission coefficients as a function of phase mismatch for fixed coupling. Boundary effects are neglected.

LB

# DFB Lasers

$$(\alpha - j\Delta\beta) = \gamma \coth(\gamma L)$$

Eg (44) of notes

Eg (19) of K-S (JAP, 43, 72)

Also,

$$\gamma = \sqrt{\chi^2 + (\alpha - j\Delta\beta)^2}$$

Eg (20) [4119, p③]

where  $\chi$  ( $\chi_L$ ) is  
the coupling coefficient

Case 1  $\chi$  is real

( $\Rightarrow$  index coupling )

In general, recall

$$\chi = \frac{\gamma \beta_0}{4} + j \frac{\gamma_i \beta_0}{4} = 0, \text{ case 1}$$

Eg (14) [4/19, p. 0]

If  $\chi_L$  is real, the solutions to (14)  
come in pairs

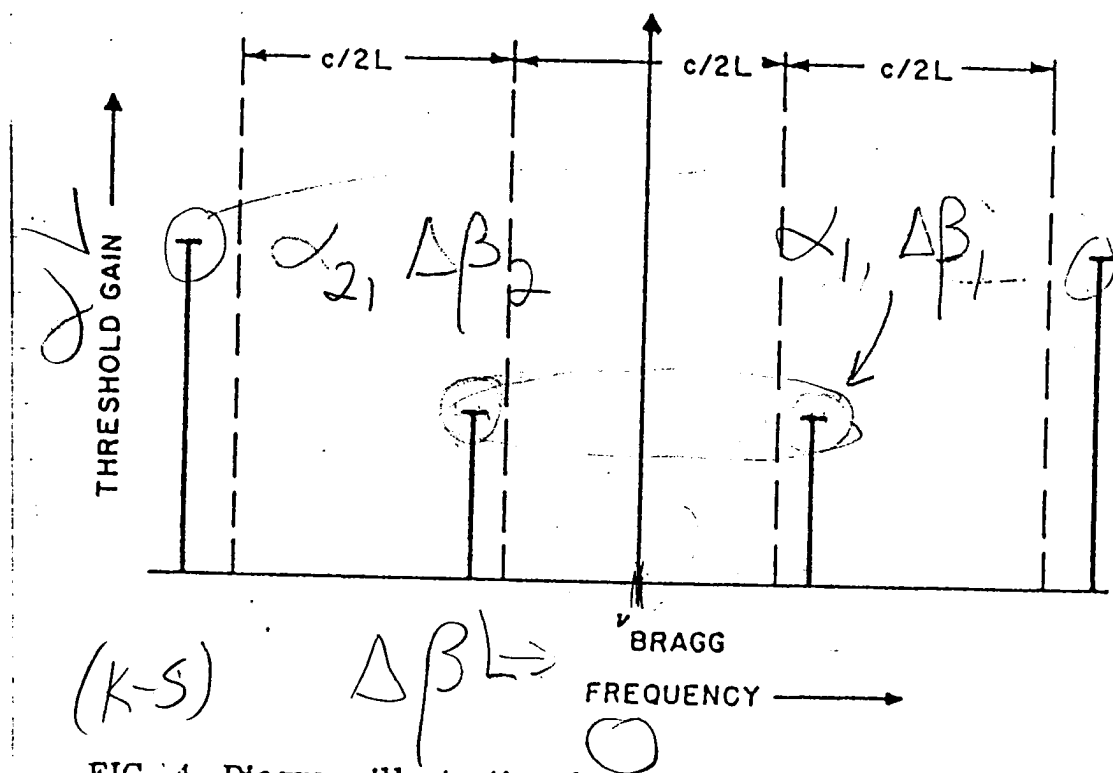
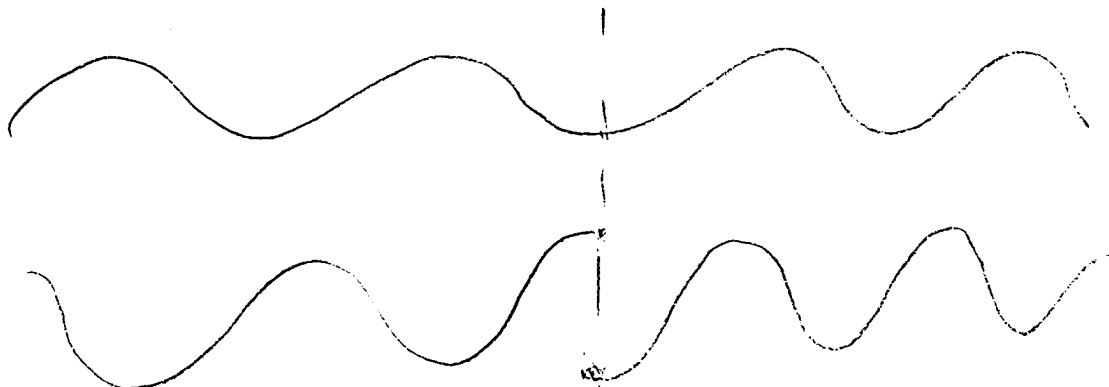


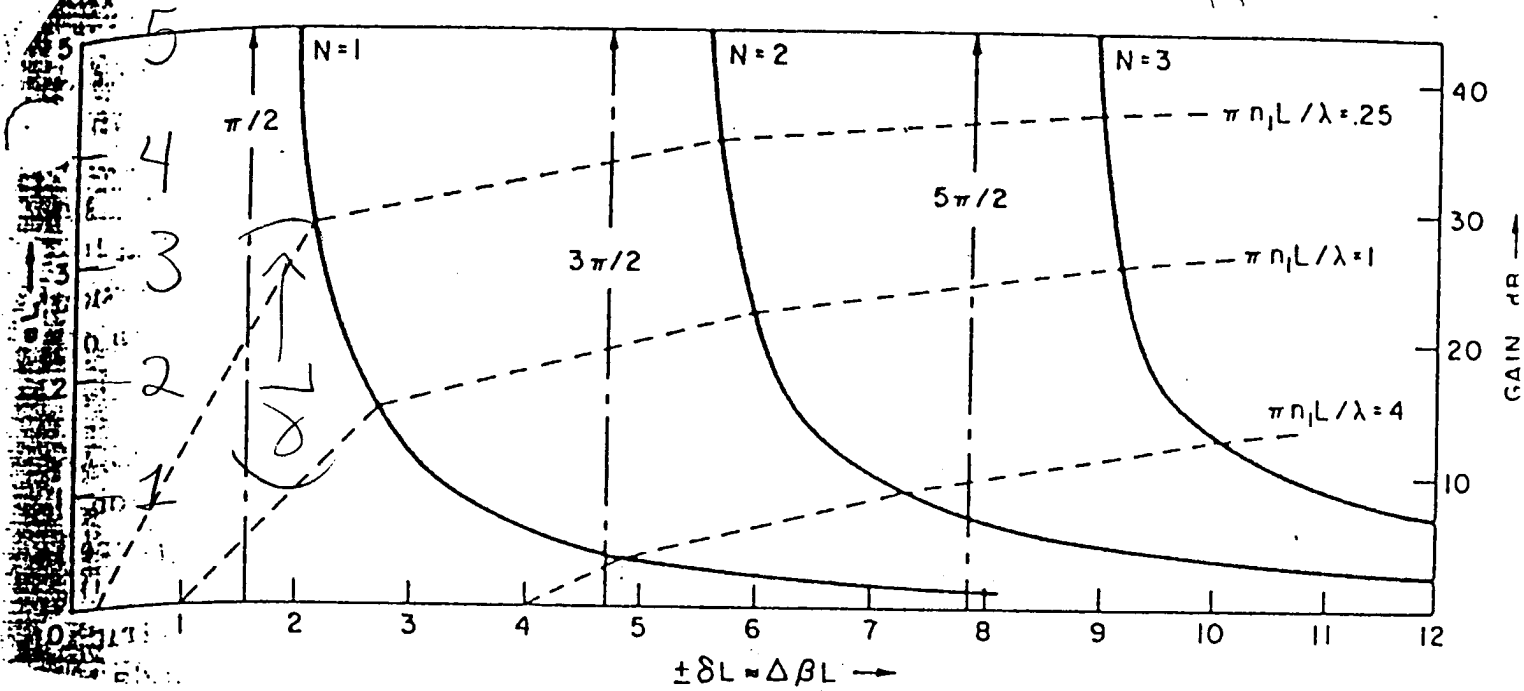
FIG. 4. Diagram illustrating the mode spectrum and required threshold gains for an index periodicity.

- no solution for  
 $\Delta\beta = 0$
- two modes with  
same threshold --  
spaced equally about  
 $\Delta\beta = 0$

Prefer "single mode"

- gain curve asymmetric
- phase at facet  $\rightarrow$
- other "tricks"



MODE SPECTRUM FOR INDEX COUPLING  $\chi = 5$ 

$$\Delta \beta L \rightarrow$$

- threshold  $\downarrow$  as  $\chi \uparrow$
- $\Delta \beta \uparrow$  as  $\chi \uparrow$

Case 2  $\chi$  is imaginary

$\Rightarrow$  gain coupling or periodic gain

$$\underline{\underline{\chi}} = \frac{n\beta_0^0}{4} + j \frac{n_i\beta_0}{4}$$

1st DFB laser was  
gain coupled

~~K~~ coherent



Kogelnik and Shank APL 18, p. 152  
1971 (ref 1 & 2) of K-S paper

- gain coupling forgot
- ~1980, Kunio Tada  
U of Tokyo, resurrected  
- demonstrated impressive  
results, ~1988-92
- Vertical cavity lasers  
renew interest ~1988

Why renewed interest?

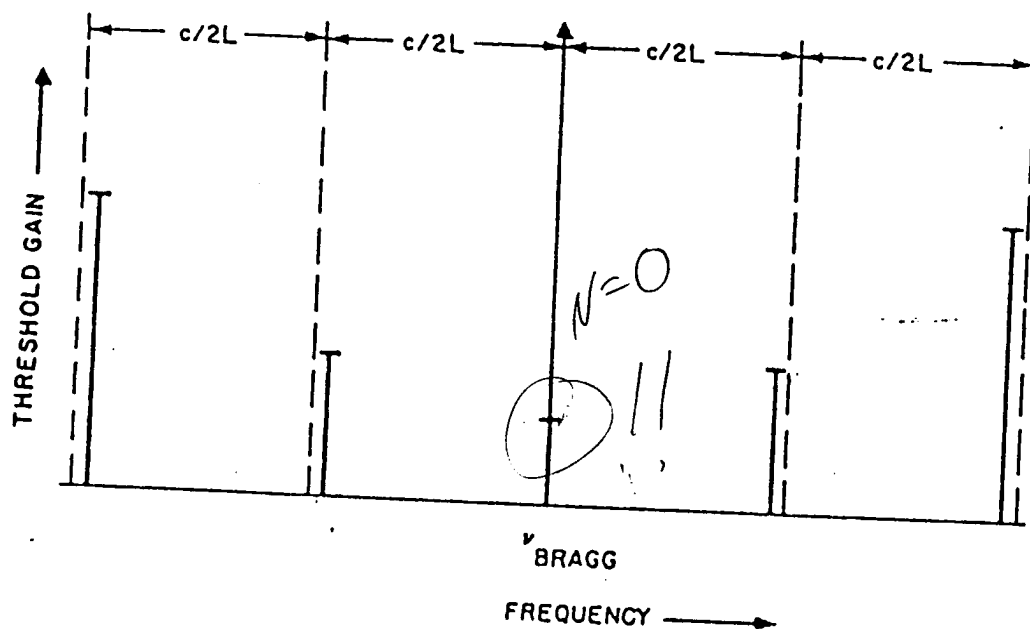


FIG. 6. Diagram illustrating the mode spectrum and required threshold gain for a gain periodicity

- only 1 lowest order mode ( $N=0$ )
- centered at  $\Delta\beta=0$
- stable mode with respect to reflections
- negative thresholds??

THRESHOLD FOR GAIN COUPLING

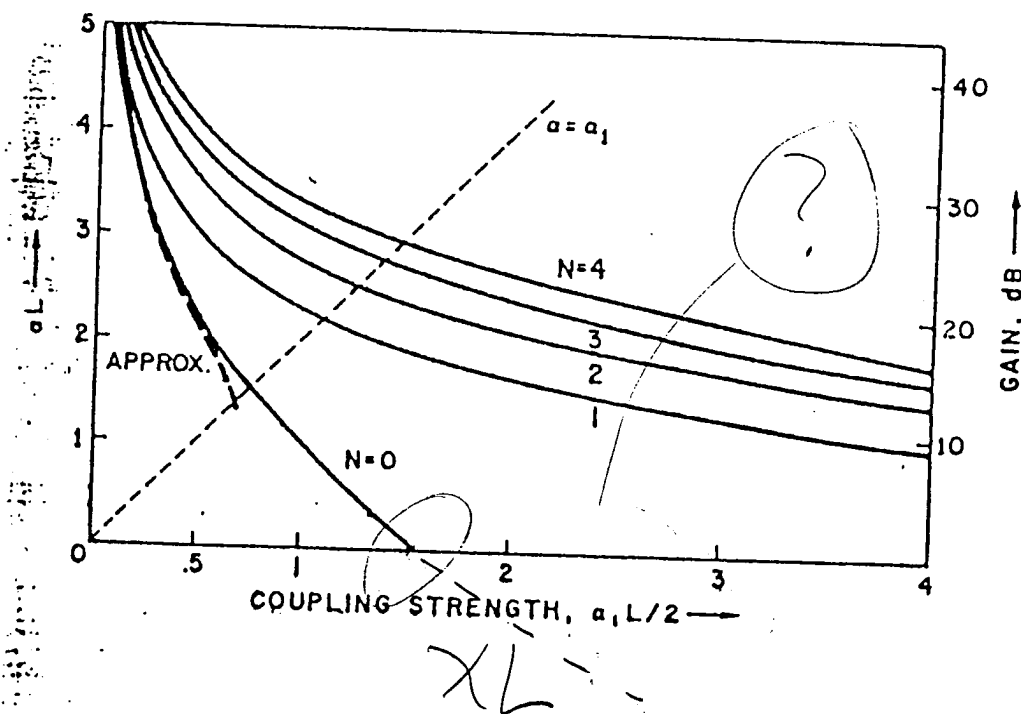


FIG. 8. Plot of the gain at threshold vs coupling strength for various modes. The  $N=0$  mode corresponds to a mode at the Bragg frequency. The numbers  $N>0$  correspond to a set of modes symmetrically placed about the Bragg frequency.

here

How can the threshold  
be negative?

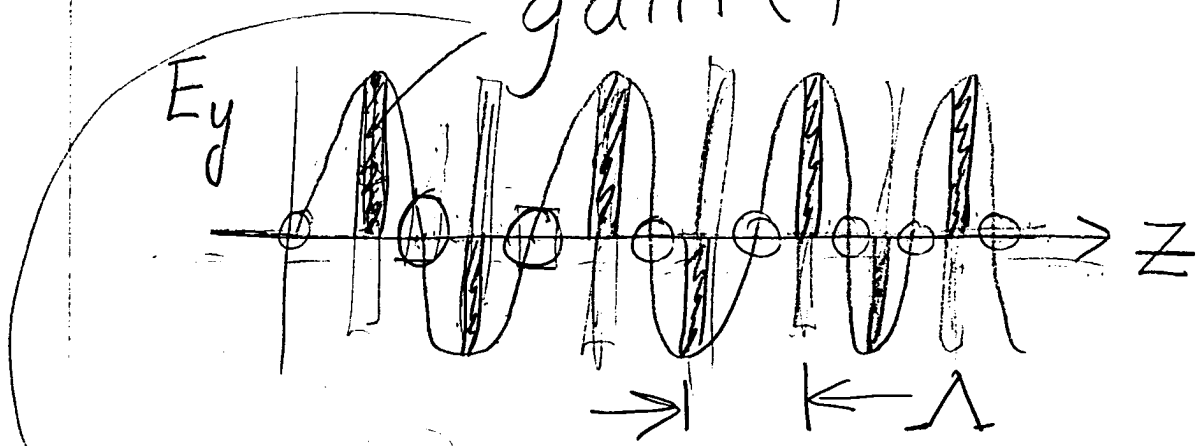
recall 4/19, p. 0, Eg(13):

$$\alpha = \frac{\epsilon_i k_0^2}{2\beta_0} = "dc" \text{ gain}$$

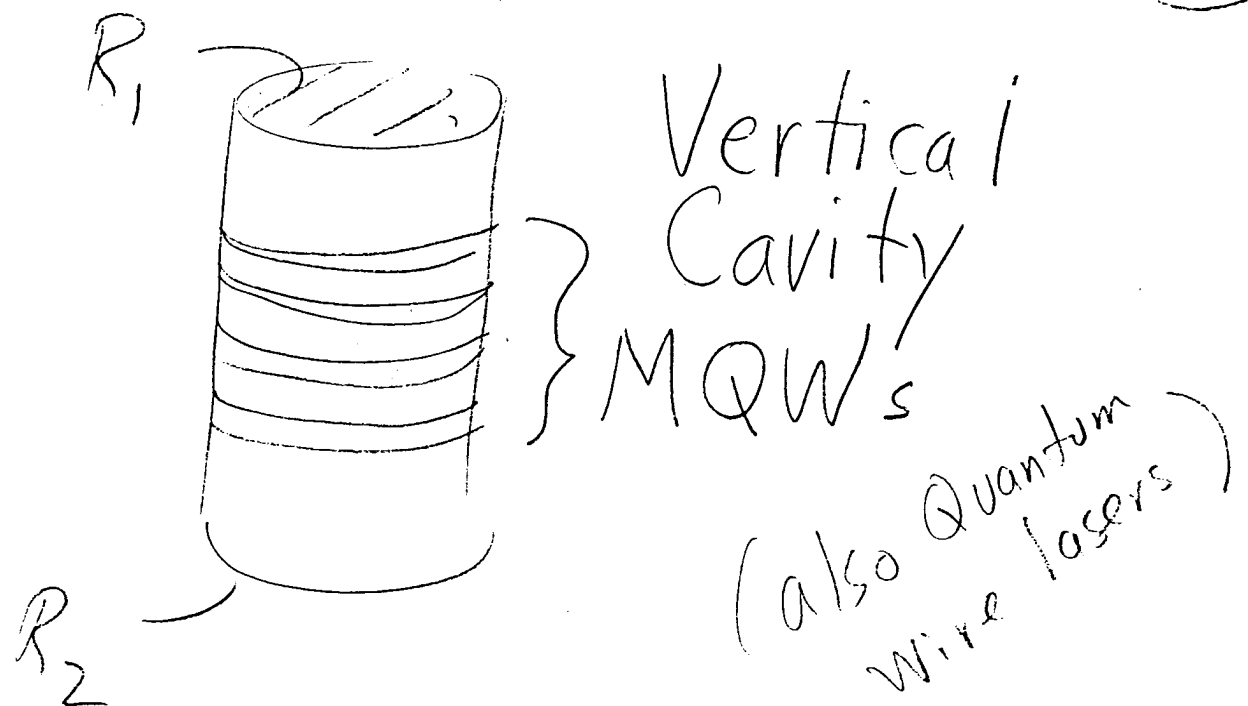
or loss

$\alpha < 0 \Rightarrow \epsilon_i < 0$  and the  
material is lossy

Consider gain (periodic)



$$X \sim \frac{\gamma_i \beta_0}{4} \cos(kz)$$



→ If place the multiple quantum wells correctly, have periodic gain

- most efficient use of gain (no gain where  $\vec{E} = 0$ )
- mode is very stable
- works for horizontal cavity
- periodic loss ok!

## Gain-Coupled DFB Laser Diode Using Novel Absorptive Conduction-Type-Inverted Grating

(2-5)

Y. LUO†, H.-L. CAO, M. DOBASHI†, H. HOSOMATSU†, Y. NAKANO, and K. TADA

*Dept. of Electronic Eng., University of Tokyo, Hongo, Bunkyo-ku, Tokyo 113*

*Phone: (03)3812-2111, Facsimile: (03)3818-5706*

*†Optical Measurement Technology Development Co., Ltd., Naka-cho, Musashino-shi, Tokyo 180*

*Phone: (0422)54-3336, Facsimile: (0422)55-8080*

**Abstract-** A gain-coupled DFB laser diode with an absorptive conduction-type-inverted grating has been fabricated. Low threshold current and linear operation are obtained by the conduction-type inversion. Moreover, ultralow chirping and narrow linewidth properties are demonstrated.

Using an absorptive grating to obtain a periodic change in net gain [1] is an effective way to incorporate the gain coupling mechanism into semiconductor lasers. However, the extra loss tends to increase threshold current as well as to cause nonlinear operation due to the saturable nature of the absorption. For high performance in gain-coupled DFB lasers with absorptive gratings, we propose a new structure, in which the conduction type of the absorptive grating region is inverted.

The cross-sectional layer structure is shown in Fig. 1. Guiding layers I and II are for canceling the index coupling produced by the absorptive grating. Since the n-GaAs absorptive region has the opposite conduction type against the surrounding layers, current flows more smoothly through the openings made by the grating formation. This structure might result in more efficient use of the injection current, thereby compensating the threshold increase due to the extra loss. Moreover, because the absorptive conduction-type-inverted regions become depleted and reverse-biased by the built-in potential, the carriers produced by optical absorption are quickly drawn away from these regions, thus preventing saturation of absorption.

Devices with a 3rd-order grating were made by two-step OMVPE. For comparison, those with a p-GaAs absorptive grating were also fabricated. The lasers, which had a 4  $\mu\text{m}$ -wide ridge waveguide, a cavity length of 200  $\mu\text{m}$ , and cleaved facets, were operated under cw condition. Average and minimum threshold currents were 20 mA and 15 mA. A typical I-L curve and a single-mode-oscillation spectrum with a side-

mode suppression ratio over 30 dB obtained from the same device are plotted in Fig. 2.

The average threshold current was examined for both the p-type and the n-type gratings. The results are plotted in Fig. 3. The average threshold current of the n-type lasers was about 10 mA lower than that of the p-type. A nonlinear I-L curve due to the saturable absorption was observed in the lasers with the p-type grating. By contrast, as shown in Fig. 2, the n-type grating resulted in a linear operation.

Dynamic behavior was investigated under gain switching conditions [2]. The widths of the chirped single-mode spectra and of the optical pulses of the same device versus dc bias current levels are shown in Fig. 4. With increasing dc bias, the width of the time-averaged spectra remains below 0.1 nm while the pulse width changes from 45 ps to 23 ps. These values of chirped spectrum width can be said as very small. Calculating the  $\alpha$  parameter using these data gives us values below 2.0.

In the device shown in Fig. 2, a minimum linewidth of 3.8 MHz was obtained at 10 mW output. Taking into account the cavity length of 200  $\mu\text{m}$  and the bulk active layer, this value seems to be excellent.

The authors express their gratitude to Prof. T. Kamiya and Dr. R. Takahashi for the chirping characteristics measurement. This work was supported in part by the Grant-in-Aid (#03505001) from the Ministry of Education, Science, and Culture, Japan.

[1] Y. Nakano et al., *Appl. Phys. Lett.* **55**, 1606 (1989).

[2] Y. Luo et al., *Appl. Phys. Lett.* **59**, 37 (1991).

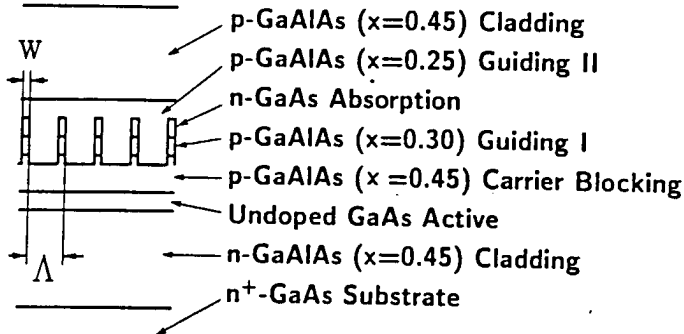


Figure 1 Layer structure of the GaAlAs/GaAs GC-DFB laser with an absorptive conduction-type-inverted grating.

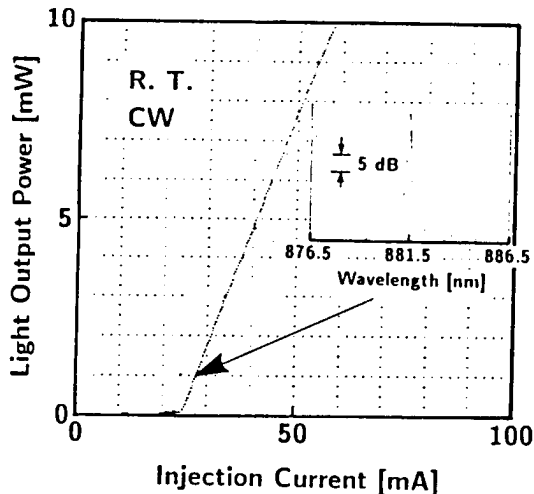


Figure 2 Light output versus injection current characteristics with a spectrum at the output power of 1 mW as an inset.

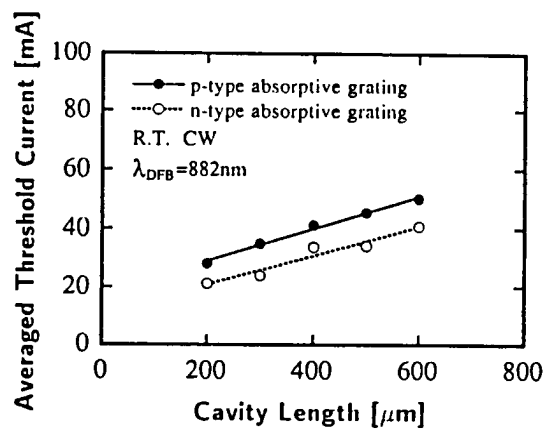


Figure 3 Average threshold current of the lasers with n-type (open circle) and p-type (closed circle) absorptive gratings.

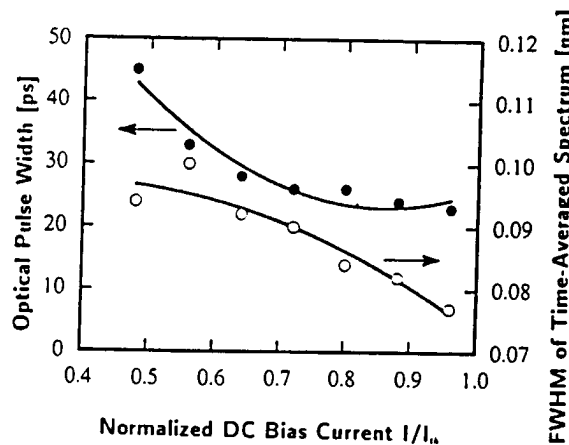


Figure 4 Widths of the optical pulse and the time-averaged single-mode spectrum versus normalized dc bias current levels.

led  
m-  
gs.  
age  
out  
lin-  
yone  
e 1  
ider  
the  
ical  
rent  
g dc  
ctr  
idht  
es of  
very  
these

num  
mW  
gth of  
value

Prof.  
shirp-  
work  
n-Aid  
at

, 1606  
1991).

(2/6)

## New Method to Reduce Effective Linewidth Enhancement Factor $\alpha_{eff}$ of DSM Lasers Using Optical Complex Coupling

-Koji Kudo, Shigehisa ARAI, and Kazuhiro KOMORI

*Department of Physical Electronics*

*Tokyo Institute of Technology*

2-12-1 O-okayama, Meguro-ku, Tokyo 152, Japan

Tel. +81(3)3726-1111 ext. 2512 Fax. +81(3)3729-0691

[1]

[2]

[3]

**Abstract:** We propose a new method to reduce effective linewidth enhancement factor  $\alpha_{eff}$  by using complex coupled (CC) structure with anti-phase combination. It is found that the introduction of CC structure into a distributed reflector (DR) laser leads to extremely low  $\alpha_{eff} (< 1)$ . It is also found that a CC-DFB laser has a possibility of low  $\alpha_{eff} (\sim 2)$  even with a bulk active layer.

Coherent and high bit rate optical communication systems require narrow linewidth and low chirp properties of dynamic single mode (DSM) lasers. Chirp and linewidth of DSM lasers are directly related with the effective linewidth enhancement factor  $\alpha_{eff}$  which is influenced by the laser structure and must be used instead of the material  $\alpha$  parameter. Until now, we have reported  $\alpha_{eff}$  reduction by detuning the Bragg wavelengths of corrugation<sup>[1]</sup>. Recently, we have found that complex coupled (CC) structure (gain coupling + index coupling) has a new reduction mechanism of  $\alpha_{eff}$ <sup>[2]</sup>, the reduction of  $\alpha_{eff}$  is expected in the case of Fig.1(a), namely anti-phase combination where the corrugation is composed that the higher gain region corresponds to the lower index region.

$\alpha_{eff}$  of DSM lasers including longitudinal distributions of laser parameters such as field intensity, material gain and so on, is expressed as

$$\alpha_{eff} = \frac{\sum_X \int \text{Im}\{C_{N,X}(z)\} \tau_{eff}(z) \bar{\xi}(z) v_g(z) g(z) I(z) dz}{\sum_X \int \text{Re}\{C_{N,X}(z)\} \tau_{eff}(z) \bar{\xi}(z) v_g(z) g(z) I(z) dz} \quad (1)$$

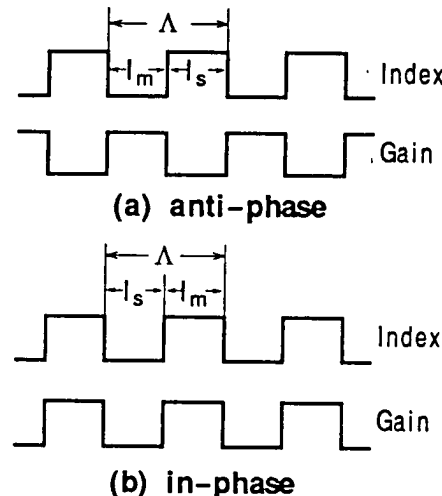
where  $\tau_{eff}(z)$ ,  $\bar{\xi}(z)$ ,  $v_g(z)$ ,  $g(z)$ , and  $I(z)$  are effective carrier life time, averaged optical confinement factor, group velocity, material gain, and photon density of longitudinal position  $z$ , respectively.  $C_{N,X}$  is the factor of weight function<sup>[3]</sup> with  $X = g$  : material gain,  $\beta$  : propagation constant,  $\kappa_i$  : index coupling coefficient, and  $\kappa_g$  : gain coupling coefficient.

Figure 2 shows the calculated  $\alpha_{eff}$  of CC-DFB lasers as a function of the ratio of  $\kappa_i$  to  $\kappa_g$ , and Fig.3 shows that as a function of material  $\alpha$ . The sign of  $\kappa_i/\kappa_g$  corresponds to the in-phase (positive) and the anti-phase (negative) combinations of a CC structure. When the refractive index and gain corrugation are arranged with the anti-phase combination,  $\alpha_{eff}$  is always reduced. Points indicated by a circle in Fig.2 mean minimum absolute value of  $\kappa_i/\kappa_g$  for arbitrary value of  $\kappa L$ . These points are determined by the fact that  $\kappa_g$  is automatically determined by the threshold gain of CC-DFB lasers with a specific value of  $\kappa_i$ . As can be seen in Fig.3,  $\alpha_{eff}$  of a CC-DFB laser with anti-phase combination of  $\kappa_i/\kappa_g = -2$  is reduced to almost the value of 2 even with the bulk active material of  $\alpha \sim 8$ . In Fig.4,  $\alpha_{eff}$  of a DR laser with normalized index coupling coefficient of passive region  $\kappa_{i,p} L_p = 3$  and normalized complex one of active region  $\kappa L_a = 0.5$  is plotted as a function of normalized detuning value  $\delta\beta_{ap}/\kappa_{i,p}$ . The dotted line and solid line correspond to the conventional index coupled (IC)

Effective Linewidth  
Enhancement Factor

DR laser and a CC-DR laser, respectively. With the detuning of  $\delta\beta_{ap}/\kappa_{i,p} \sim 1.5$  which is shown as the hatched region in Fig.4,  $\alpha_{eff}$  of  $\sim 0.2\alpha$  is obtained for a CC-DR laser. It means that the adoption of an anti-phase combination CC structure into a DR laser, which enhances the reduction of  $\alpha_{eff}$  due to the detuning of Bragg wavelengths, leads to the possibility of achieving extremely low  $\alpha_{eff}$  of less than 1 with quantum film active layer.

- [1] J. I. Shim et al., *IEEE J. Quantum Electron.*, vol.27, pp. 1736-1745, 1991.
- [2] K. Kudo et al., to be published in *IEEE Phot. Technol. Lett.*
- [3] B. Tromborg et al., *IEEE J. Quantum Electron.*, vol.27, pp. 178-192, 1991.



**Fig. 1** Schematic diagrams of complex coupled structures.  $\Lambda$ ,  $l_m$ , and  $l_s$  are corrugation pitch, length of region m, and that of region s, respectively.

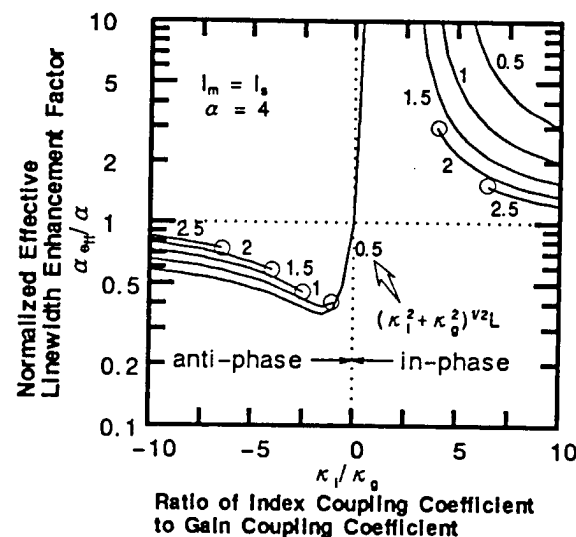


**Fig. 2** Calculated  $\alpha_{eff}$  of CC-DFB lasers normalized by the material  $\alpha$  as a function of the ratio of  $\kappa_i$  to  $\kappa_g$  for various coupling strength  $\kappa L = \sqrt{\kappa_i^2 + \kappa_g^2}L$ .

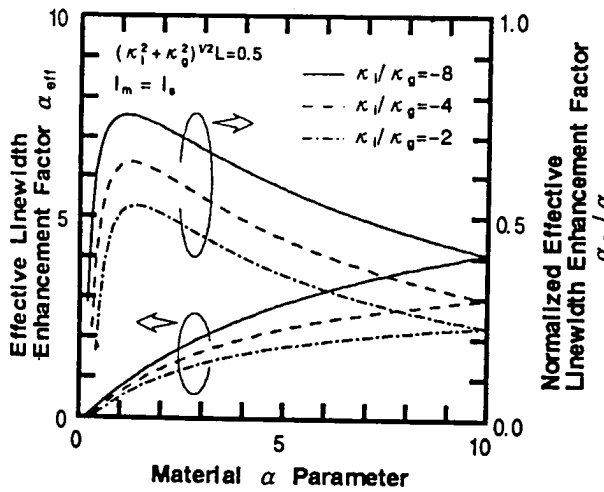


**Fig. 3** Calculated  $\alpha_{eff}$  of CC-DFB lasers as a function of the material  $\alpha$  for various ratio of  $\kappa_i$  to  $\kappa_g$ .

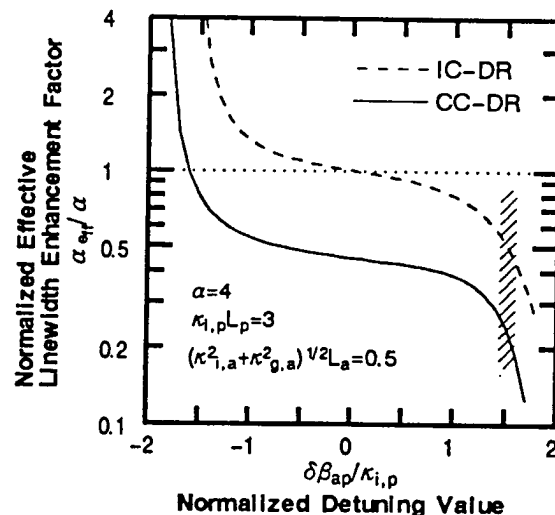


**Fig. 4** Calculated  $\alpha_{eff}$  of IC- and CC-DR lasers as a function of  $\delta\beta_{ap}/\kappa_{i,p}$ , where  $\delta\beta_{ap}$  means difference of propagation constant between active region and passive region.

35B RE  
 (1)  
 (2)  
 (3)

## Dynamic Characteristics of 1.55 $\mu\text{m}$ Gain-Coupled Distributed Feedback Laser

S. Nakajima, T. Inoue, Y. Luo, T. Oki, Y. Nakano\*, K. Tada\*, R. Takahashi\*, and T. Kamiya\*

*Optical Measurement Technology Development Co., Ltd.*

2-11-13, Naka-cho, Musashino-shi, Tokyo 180, Japan, Phone: (0422)54-3336 Facsimile: (0422)55-8080

\* Department of Electronic Engineering, University of Tokyo

7-3-1 Hongo, Bunkyo-ku, Tokyo 113, Japan, Phone: (03)3812-2111 Facsimile: (03)3818-5706

### ABSTRACT

A low wavelength chirp of 0.2 nm at -20 dB under 2.4 GHz modulation and a  $\Delta v \cdot \Delta t$  product of 0.55 which corresponds to an effective  $\alpha$  parameter as small as 0.76 under the gain switching operation were achieved.

We have reported 1.55  $\mu\text{m}$  InGaAsP/InP gain-coupled distributed feedback (GC-DFB) lasers, which are characterized by a low threshold current of 12 mA, a large side mode suppression ratio of 55 dB, a high single mode yields of 90 %, and a linewidth of 2.35 MHz that is very narrow enough for the bulk 600  $\mu\text{m}$ -long active layer<sup>(1)(2)</sup>. In GaAs based materials, excellent dynamic characteristics of GC-DFB lasers have already been reported<sup>(3)</sup>. As optical fibers have a minimum loss at 1.55  $\mu\text{m}$  wavelength, it is necessary to investigate dynamic characteristics of the InGaAsP/InP GC-DFB lasers.

Figure 1 shows the schematic view of our GC-DFB laser. The periodic perturbation in modal gain is produced by the thickness variation of the bulk active layer. A planer-buried-hetero structure (PBH) is adopted to confine the injection current. The device length is 250  $\mu\text{m}$ . No special technique for high-speed operation is introduced.

The optical short pulse generation and the wavelength chirping in the GC-DFB laser were tested by using a short electrical pulse pumped gain switching method. The electrical pumping pulses, produced by a comb generator, were of 130 ps width, about 15 V/50  $\Omega$  peak voltage, and at a 100 MHz repetition rate. The time-averaged spectra at different dc bias current levels are illustrated in Fig. 2. Minimum full width at half maximum (FWHM) of the spectrum was 0.148 nm with the dc bias being at threshold. Dynamic single mode oscillation was acquired at the higher dc biases. The spectrum width became narrower with increasing bias currents. These results suggest that the laser may operate in index-coupling at lower injection currents and in gain-coupling at higher injection currents. The minimum temporal FWHM of optical pulse was 27.7 ps at dc bias of 0.8 times threshold. From these data we obtain the minimum  $\Delta v \cdot \Delta t$  product of 0.554, which approaches the Fourier transform limit 0.441, corresponding effective  $\alpha$  parameter is calculated to be 0.76.

We also measured 20 dB down wavelength chirping under 2.4 GHz sinusoidal direct modulation. The rf power applied was 16 dBm. Figure 3 illustrates dc bias dependence of 20 dB down width of time averaged spectrum. The minimum value of 0.2 nm was obtained when the GC-DFB laser was biased at twice threshold (Fig. 4). Extremely low chirping nature of the GC-DFB laser is verified.

## REFERENCES

- (1) T. Inoue et al. : *IEEE Photonics Technology Letters*, vol. 3, no. 11, p. 958, 1991  
 (2) S. Nakajima et al. : *Conference on Fiber Communication (OFC '92)*, FB3, San Jose, Feb. 1992, p. 272  
 (3) Y. Luo et al. : *Applied Physics Letters*, vol. 59, no. 1, p. 37, 1991

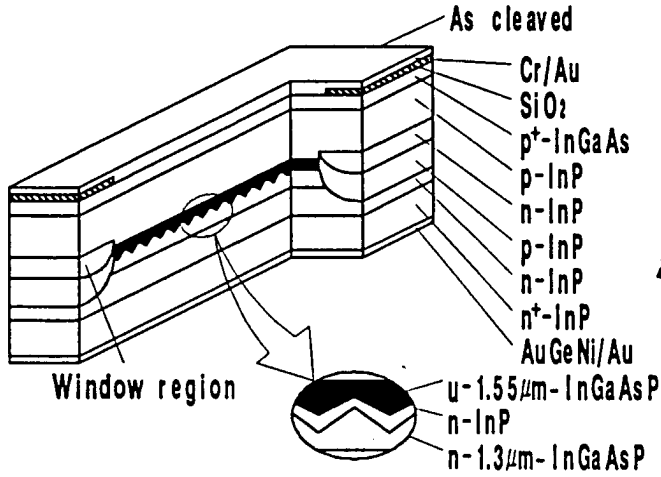


Fig. 1 Schematic view of the 1.55  $\mu\text{m}$  PBH-GC-DFB laser

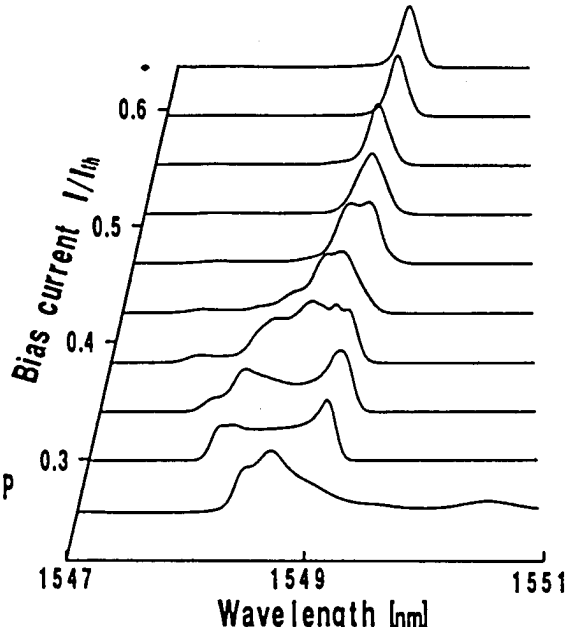


Fig. 2 Time-averaged spectra at different dc bias currents measured under the gain switching condition.

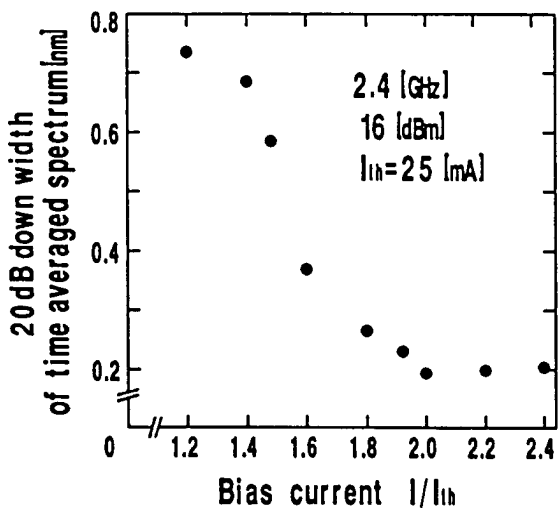


Fig. 3 20 dB down width of time-averaged spectrum vs. dc bias normalized by threshold current

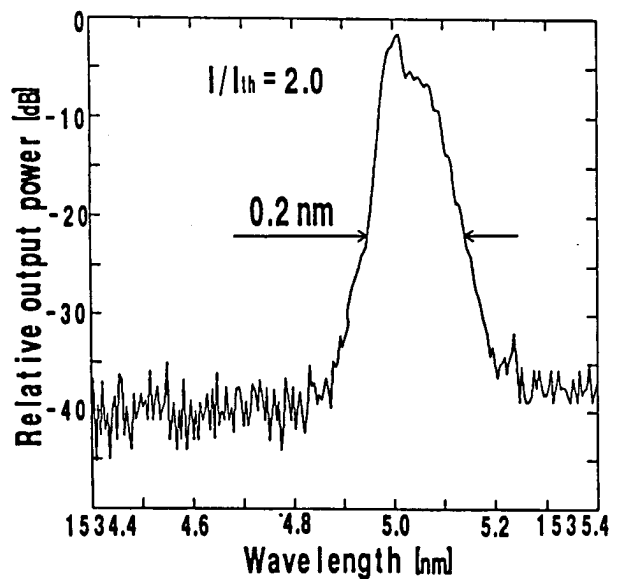
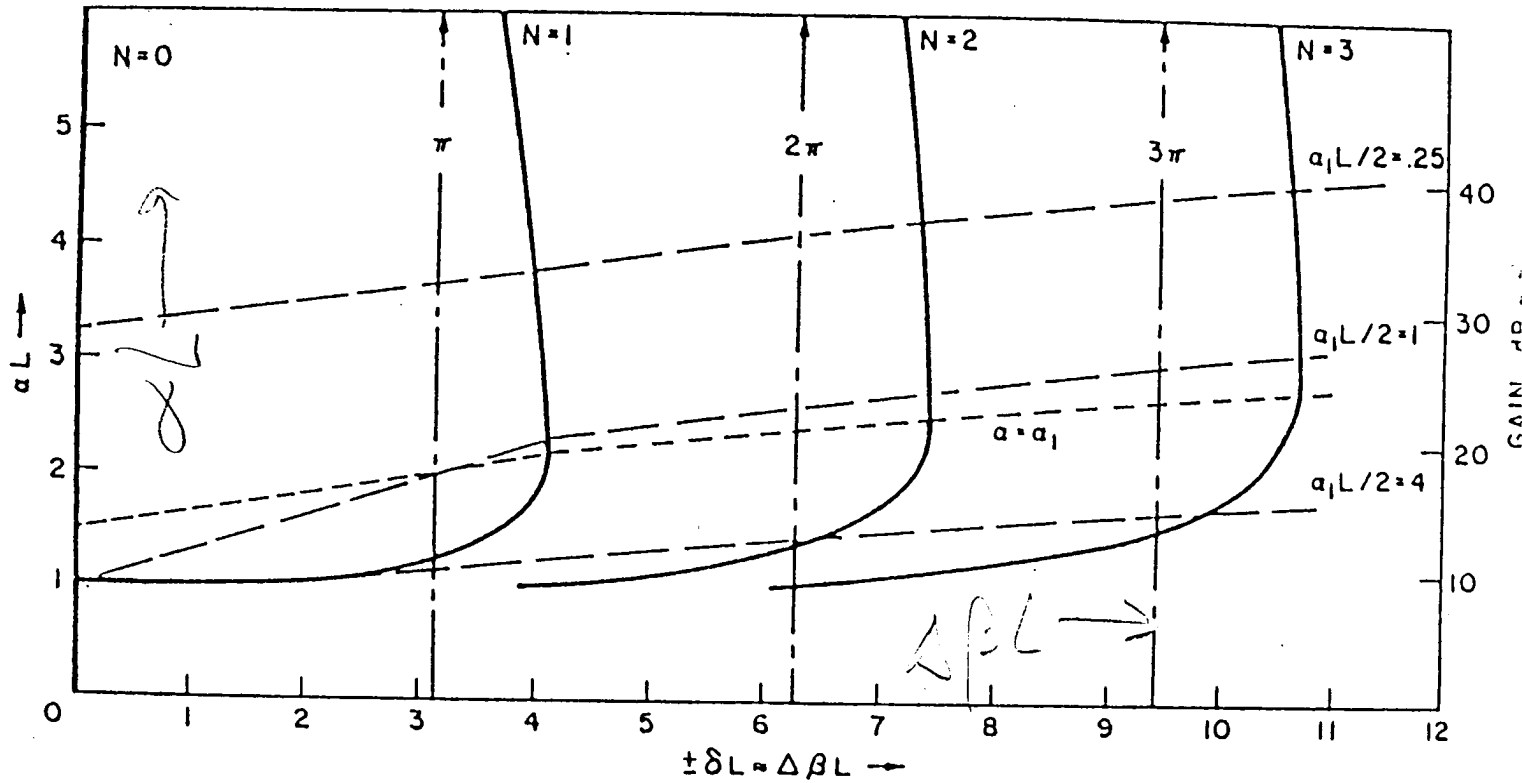


Fig. 4 Time-averaged spectrum showing 20 dB down width of 0.2 nm.

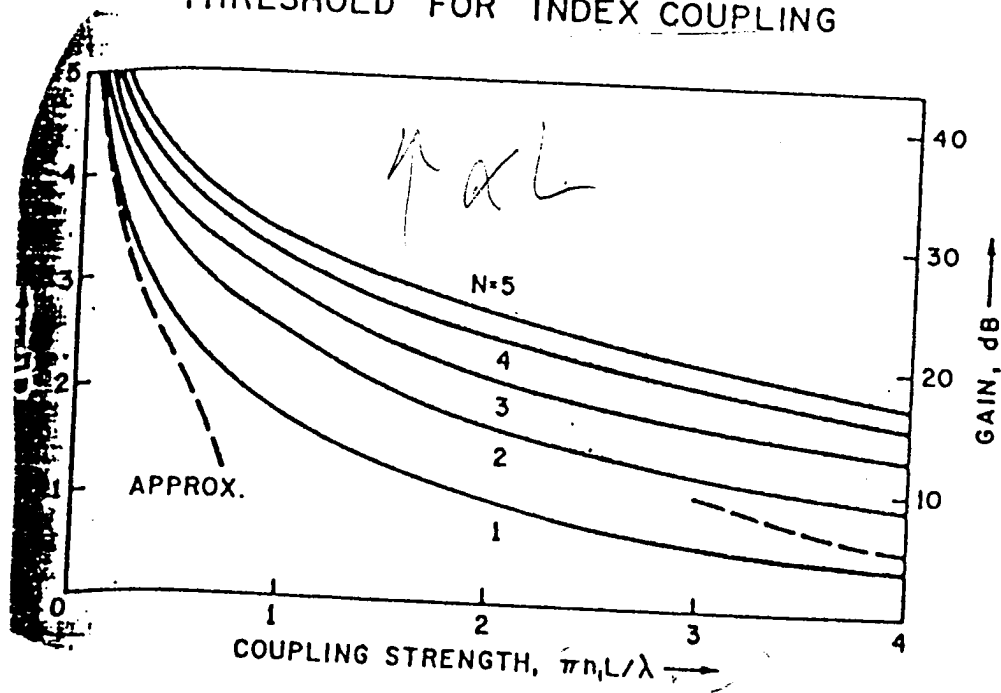
360

Other figs. from K-S:  
high  $\chi$ ?

### MODE SPECTRUM FOR GAIN COUPLING



### THRESHOLD FOR INDEX COUPLING



(36)

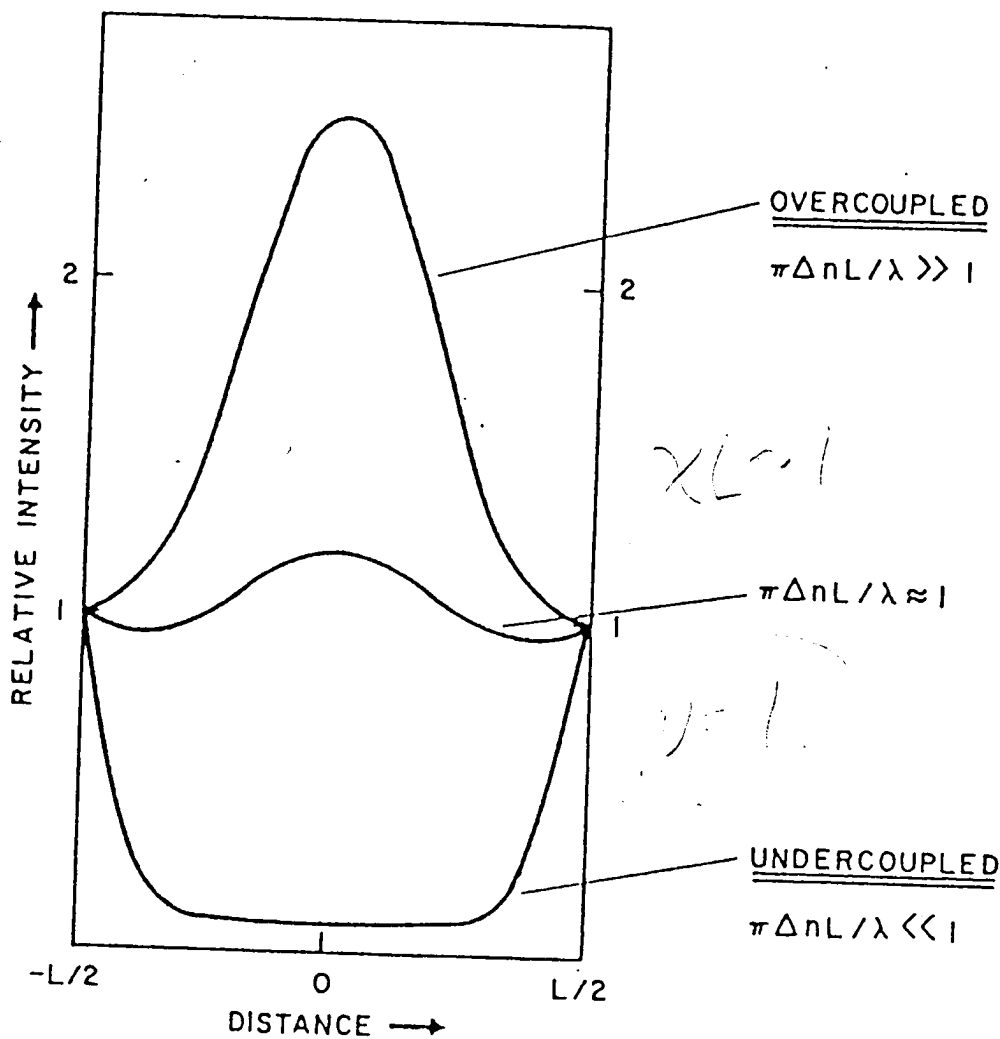
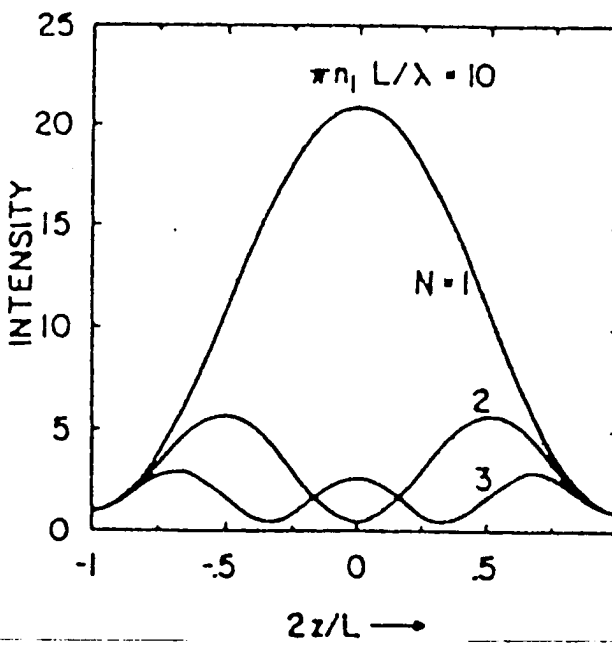
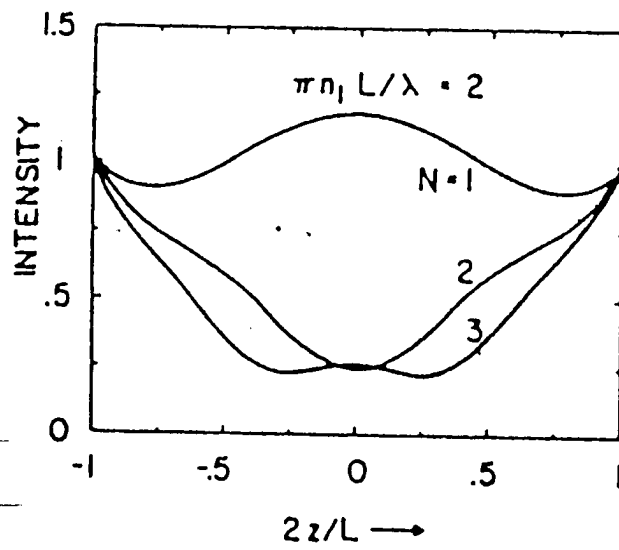
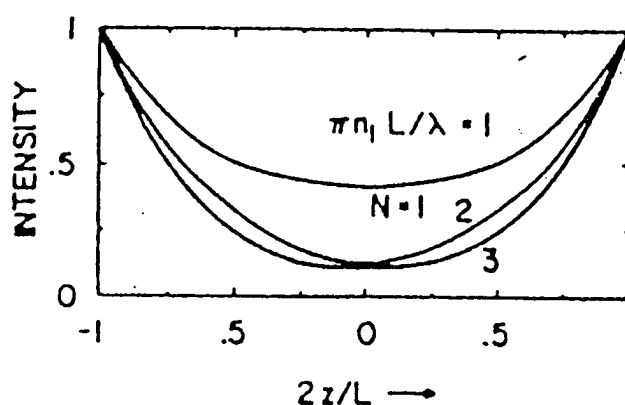
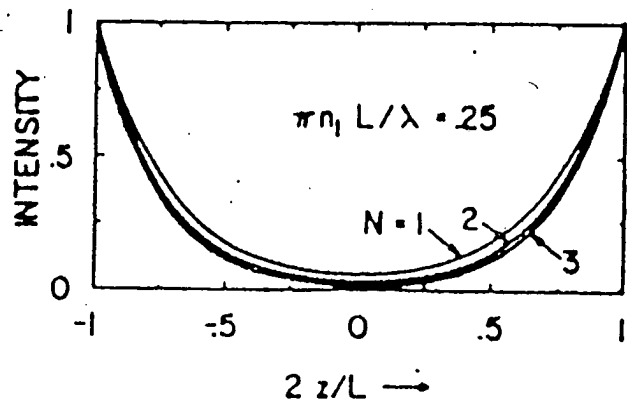


FIG. 10. Plot of the spatial intensity distribution of the lowest-order modes at various coupling levels.

- ①  $XL$  large, low output
- ②  $XL$  small, intensity @ ends
- ③  $XL \approx 1$  uniform intensity

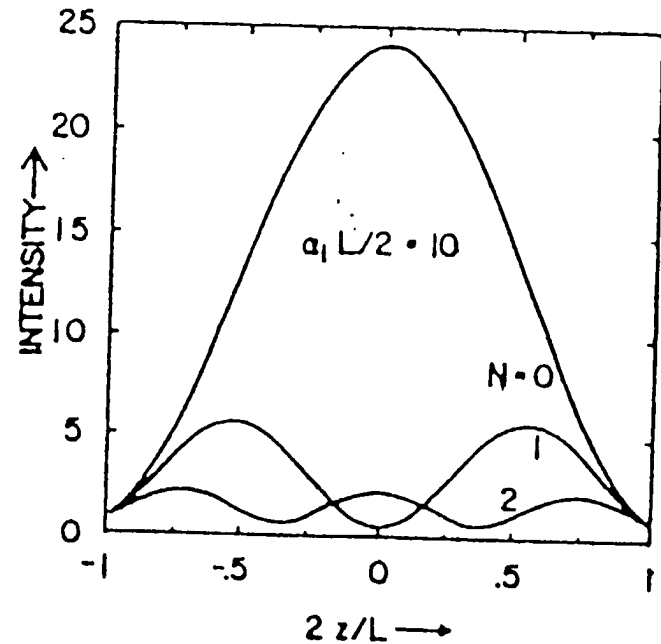
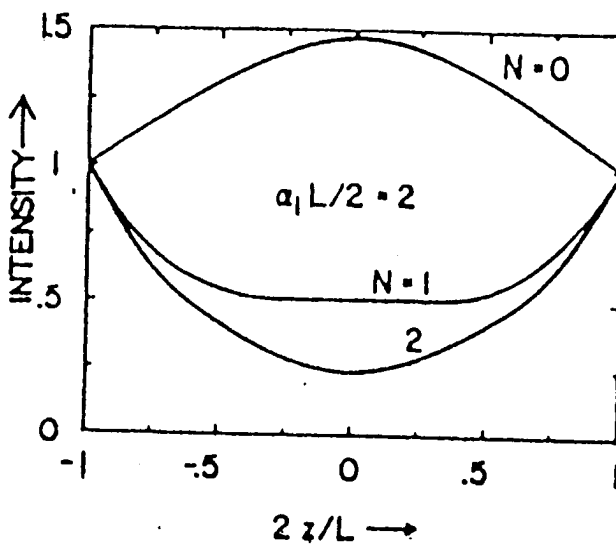
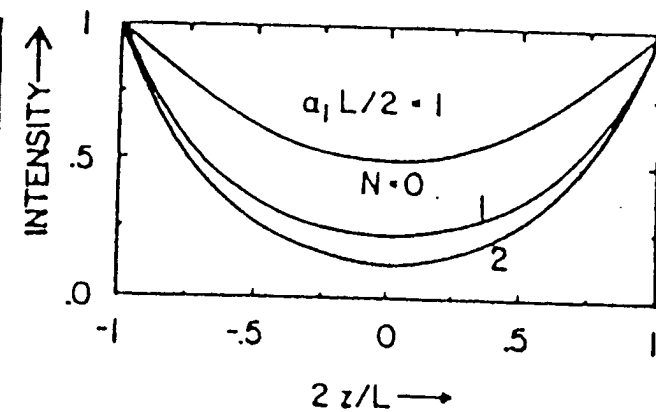
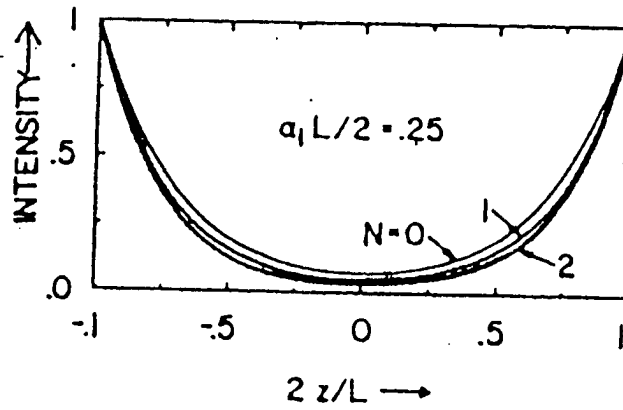
310

# 1st 3 Modes, XL real



(363)

# 1st 3 Modes, XL - Imaginary



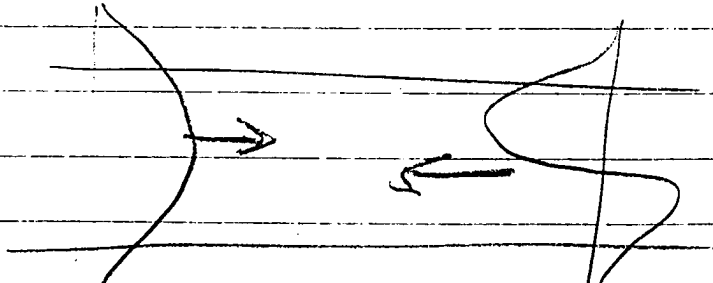
# Extension of Coupled Wave Theory to Waveguides

In unbounded media

$$R'(z) + (\alpha - j\Delta\beta) R(z) = j\chi S(z) \quad (2a)$$

$$S'(z) + (\alpha - j\Delta\beta) S(z) = j\chi R(z) \quad (2b)$$

Consider a dielectric which supports multiple modes  
 $\Rightarrow$  forward p-mode coupled to a backward q-mode



Now,

$$R_p(x, z) = a_p(x) d_p(z) \quad (1a)$$

$$S_q(x, z) = a_q(x) d_q(z) \quad (1b)$$

and the coupled wave equations look like

$$-d'_p(z) + [C_p \alpha - j \psi_p \omega] d_p(z) \\ = j \chi_{pq} d_q(z) \quad (2a)$$

$$d'_q(z) + [C_q \alpha - j \psi_q \omega] d_q(z) \\ = j \chi_{qp} d_p(z) \quad (2b)$$

(366)

where  $C_p$  and  $C_q$  are the effective gain (loss) coefficients for the  $p^{\text{th}}$  and  $q^{\text{th}}$  mode:

$$C_p = (C_{\text{eff}})_p \quad \text{and for a}$$

3-layer waveguide is given by [Eq. 20, 3/12 p(16)]:

$$C_p = \frac{\sqrt{\epsilon_2} k_0}{(\beta_{\text{re}})_p} \sqrt{\rho} \quad (3)$$

 $\epsilon_1$ 

$$\underline{\epsilon_2 + (j\epsilon_i)} \Rightarrow \infty$$

 $\epsilon_1$

Also,  $\Delta\beta_p = \beta_p - \beta_0$ ; since

$$\frac{d\beta}{dw} \approx \frac{\Delta\beta}{\Delta w} \Rightarrow \Delta\beta_p = \frac{d\beta_p}{dw} \Delta w$$

$$(v_g)_p = \frac{dw}{d\beta_p} \quad (\text{group velocity})$$

so we can write

$$\Delta\beta_p = \psi_p \Delta w \quad (4)$$

$$\Delta\beta_q = \psi_q \Delta w$$

and

$$E_y = R_p(x, z) e^{-j\beta_p z} + S_q(x, z) e^{j\beta_q z} \quad (5)$$

Eq (2a,b)  $\Rightarrow$

$$-d_p''(z) + \{(C_p - C_q)\alpha - j(\psi_p - \psi_q)sw\}$$

$$\times d_p'(z) + \{x_{pq}^2 + (C_q\alpha - j\psi_q sw)$$

$$\times (C_p\alpha - j\psi_q sw)\} d_p(z) = 0 \quad (6)$$

(6) is a homogeneous, 2<sup>nd</sup> order DEQ w/ constant coeffs:

$$y'' + by' + cy = 0 \Rightarrow$$

$$y = A e^{\gamma_1 x} + B e^{\gamma_2 x}$$

where  $\gamma_{1,2}$  solve  $\gamma^2 + b\gamma + c = 0$

(369)

Or

$$\gamma = \frac{-b}{2} \pm \frac{\sqrt{b^2 - 4c}}{2}$$

So

$$\gamma_{1,2} = \left( \frac{C_p - C_g}{2} \right) \alpha - j \left( \frac{\psi_p - \psi_g}{2} \right) \omega$$

$$\pm \sqrt{\chi_{pg}^2 + \left\{ \left( \frac{C_p + C_g}{2} \right) \alpha - j \left( \frac{\psi_p + \psi_g}{2} \right) \omega \right\}^2}$$

and

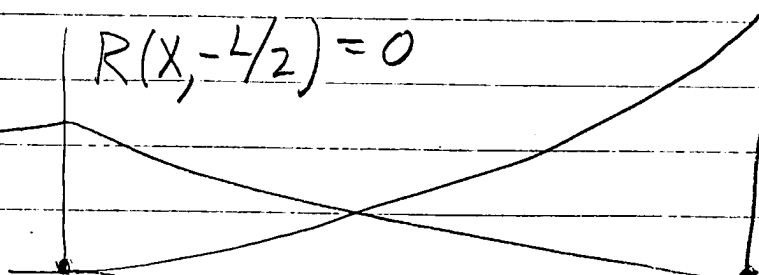
(7)

$$d_p(z) = r_1 e^{\gamma_1 z} + r_2 e^{\gamma_2 z} \quad (8a)$$

$$d_g(z) = s_1 e^{\gamma_1 z} + s_2 e^{\gamma_2 z} \quad (8b)$$

$$\leftarrow s \quad R(x, -L/2) = 0$$

$$R \rightarrow \quad S(x, L/2) = 0$$



- apply boundary conditions
- equate terms of exp<sup>i</sup>  
z dependence
- lots of algebra

↓

obtain transcendental equation: (9)

$$Y_{pq} = \sqrt{\chi_{pq}^2 + Y_{pq}^2} \coth \sqrt{\chi_{pq}^2 + Y_{pq}^2}$$

where

$$Y_{pq} = \left( \frac{C_p + C_q}{2} \right) \alpha - j \left( \frac{\psi_p + \psi_q}{2} \right) \Delta w \quad (10)$$

$$= \alpha_{\text{average}} - j \Delta \beta_{\text{average}}$$

(37)

To obtain the threshold gain  
and oscillation frequency:

$$\alpha = \frac{2}{C_p + C_q} \operatorname{Re} \{ Y_{pq} \} \quad (1a)$$

$$\Delta\omega = \frac{\pm 2}{\gamma_p + \gamma_q} \operatorname{Im} \{ Y_{pq} \} \quad (1b)$$

Note: if  $C_p = C_q = 1$ ,

$$\gamma_p = \gamma_q = \Delta\beta/\Delta\omega$$

(10)  $\rightarrow$

$$\alpha - j\Delta\beta = \gamma \coth(\gamma L)$$

Eq (19) of K-S

(372)

$$\gamma_1 = a_{pq} + b_{pq} \quad (12a)$$

$$\gamma_2 = a_{pq} - b_{pq} \quad (12b)$$

where

$$a_{pq} = \left( \frac{C_p - C_q}{2} \right) \alpha - j \left( \frac{\psi_p - \psi_q}{2} \right) \Delta w \quad (13a)$$

$$b_{pq} = \left[ \gamma_{pq}^2 + \left\{ \left( \frac{C_p + C_q}{2} \right) \alpha - j \left( \frac{\psi_p + \psi_q}{2} \right) \Delta w \right\}^2 \right]^{1/2} \quad (13b)$$

From the perturbation treatment of 3/12, p⑯

We can show

$$\psi_p = \frac{\Delta\beta_p}{\Delta\omega} = \frac{k_0}{\beta_p c} (\epsilon_2 A + \epsilon_1 B) \quad (14a)$$

where

$$A = \frac{sw + \sin^2(sw)}{1 + sw} \quad (14b)$$

and

$$B = \frac{\cos^2(sw)}{1 + sw} \quad (14c)$$

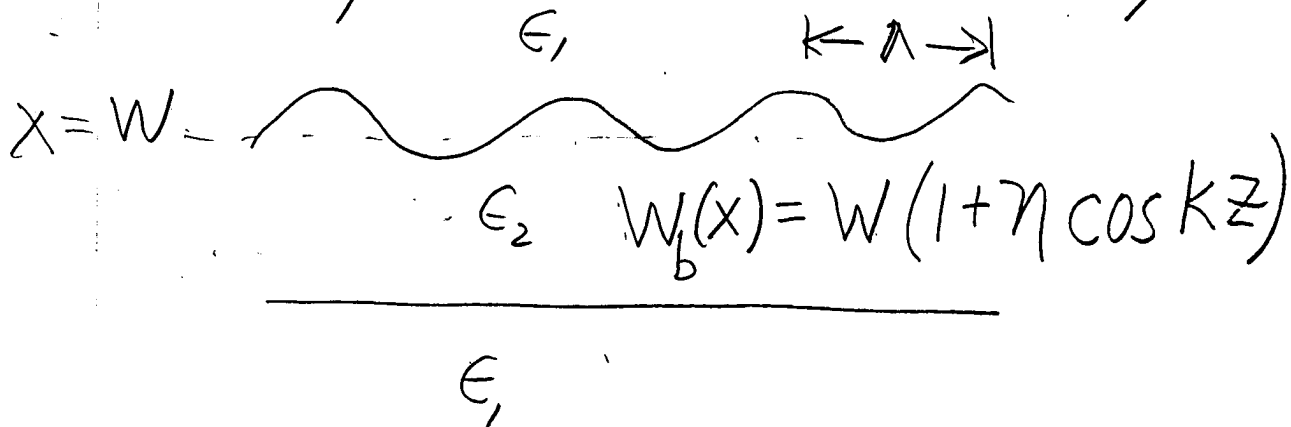
for even modes. For odd modes,  $\sin^2 \rightarrow \cos^2$  and  $\cos^2 \rightarrow \sin^2$

What about  $X_{pq}$ ?

The most common  
(at present) periodicity

to here  
4/28

IS a periodic boundary.



Approach: model a periodic boundary by a surface current:

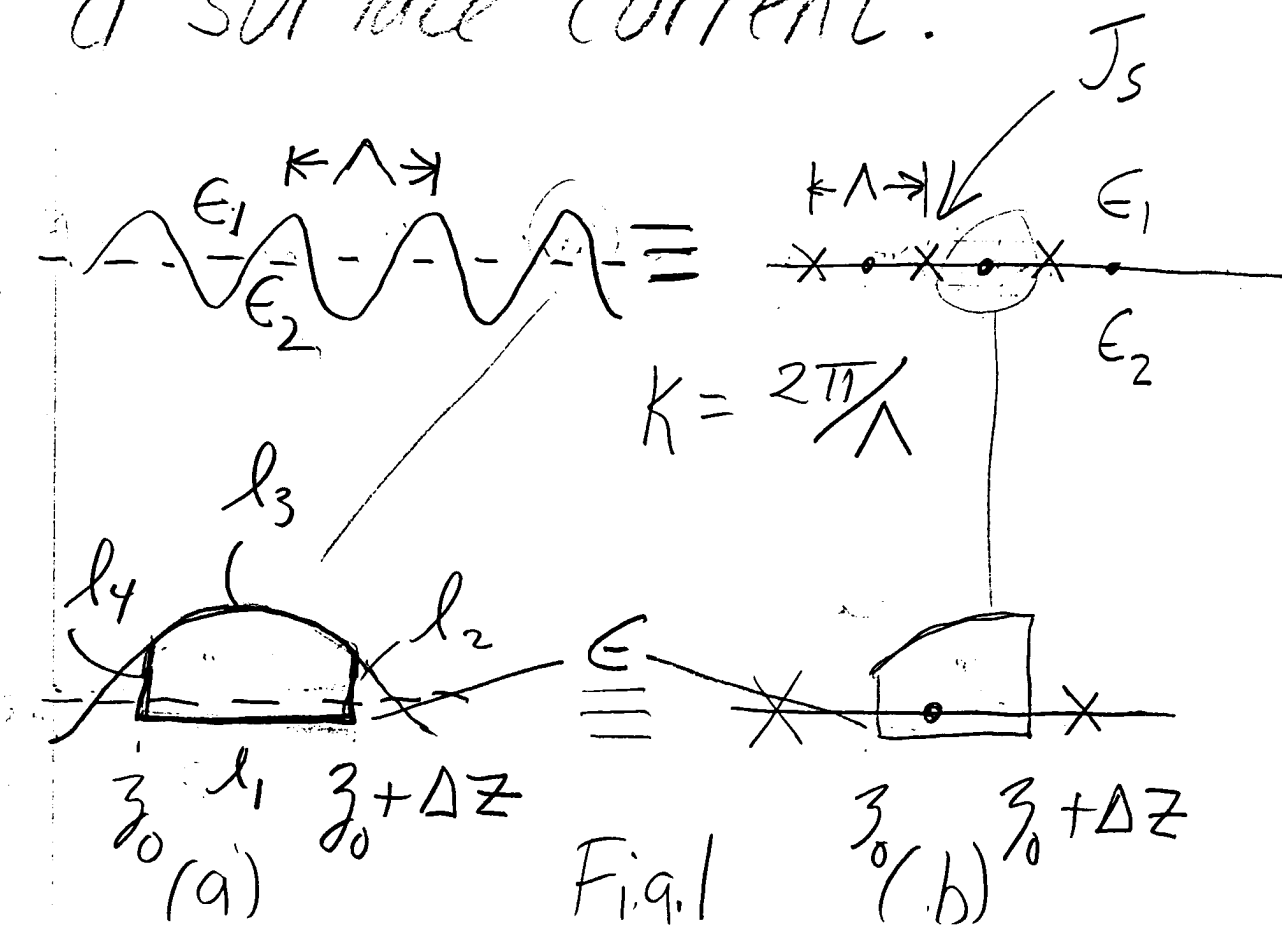


Fig. 1

In Fig (b),

$$\vec{J}_S = J_S(z) \delta(x-w) \hat{i}_y \quad (1)$$

From Maxwell's Equations:

$$\nabla \times \vec{H} = \vec{J} + \frac{\partial \vec{D}}{\partial t}$$

$$= \vec{J} + \epsilon_0 \epsilon_{\text{rel}} \frac{\partial \vec{E}}{\partial t} \quad (2)$$

$$= \vec{J} + j\omega \epsilon_0 \epsilon_{\text{rel}} \vec{E}$$

By Stokes Theorem:

$$\oint_D \vec{F} \cdot d\vec{l} = \int_S (\nabla \times \vec{F}) \cdot d\vec{S} \quad (3)$$

So,

$$\oint \vec{H} \cdot d\vec{l} = j\omega \epsilon_0 \epsilon_{rel} \int_S \vec{E} \cdot d\vec{s} + \int_S \vec{J} \cdot d\vec{s} \quad (4)$$

Applying (4) to Fig. 1a:

$$\oint_l \vec{H} \cdot d\vec{l} = j\omega \epsilon_0 \epsilon_2 \int_S \vec{E} \cdot d\vec{s} \quad (5)$$

Applying (4) to Fig. 1b:

$$\oint H \cdot dl = j\omega \epsilon_0 \epsilon_1 \int_S \vec{E} \cdot d\vec{s} \quad (6)$$

$$+ \int_S J(z) \delta(x-w) i_y d\vec{s}$$

Since 1a  $\equiv$  1b, Eq(5)  $\neq$  Eq(6)

$$\overline{J_s(z)} \Delta z = j\omega \epsilon_0 (\epsilon_2 - \epsilon_1)$$

$$\times \int_S \vec{E} \cdot d\vec{S} \quad (7)$$

Now

$$\int_S \vec{E} \cdot d\vec{S} \approx E(w, z) \Delta x \Delta z \quad (8)$$

$$\text{where } \Delta x = \eta w \cos k z$$

so

$$J(z) = j\omega \epsilon_0 (\epsilon_2 - \epsilon_1) \quad (9)$$

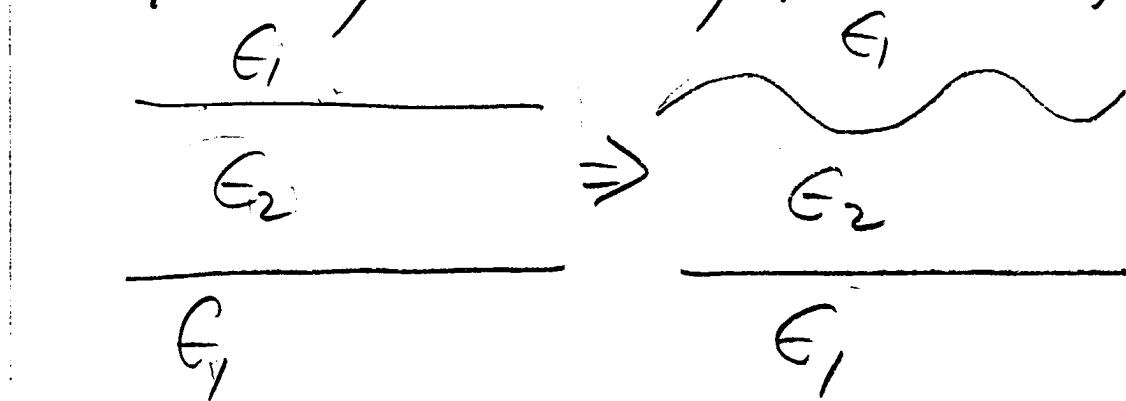
~~$$j\omega \epsilon_0 (\epsilon_2 - \epsilon_1) \times E(w, z) \eta w \cos(kz)$$~~

The boundary condition now becomes

$$\left. H_z \right|_{x=w^+} - \left. H_z \right|_{x=w^-} = J_s(z) \quad (10)$$

Tangential  $H$  is no longer continuous, but discontinuous by an amount equal to the surface current density  $J_s(z)$

Consider the simple 3-layer WG (symmetric, TE modes):



Treat periodic boundary  
as a perturbation

$$\hat{s}_p' \rightarrow \hat{s}_p + \Delta s_p \quad (11a)$$

$$s_p' \rightarrow s_p + \Delta s_p \quad (11b)$$

$$\beta_p' \rightarrow \beta_p + \Delta \beta_p \quad (11c)$$

where  $s_p$ ,  $\beta_p$  and  $\beta_p'$  are  
the unperturbed values  
and  $\Delta s_p$ ,  $\Delta \beta_p$ , and  $\Delta \beta_p'$   
are corrections

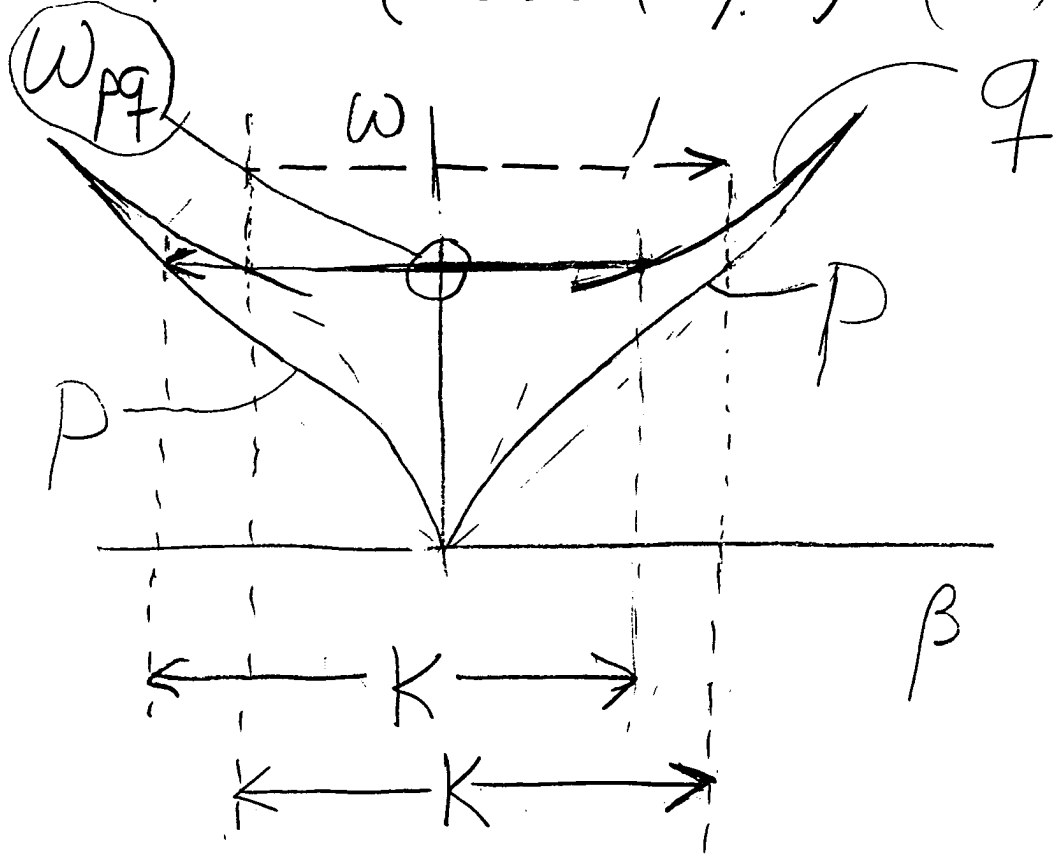
Recall:

$$\hat{s}_p^2 = \epsilon_2 k_b^2 - \beta_p^2 \quad (12a)$$

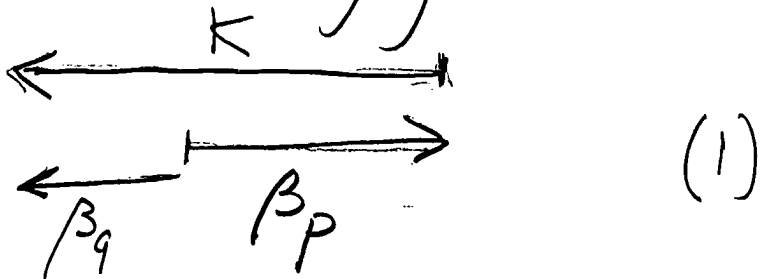
$$s_p^2 = -\epsilon_1 k_b^2 + \beta_p^2 \quad (12b)$$

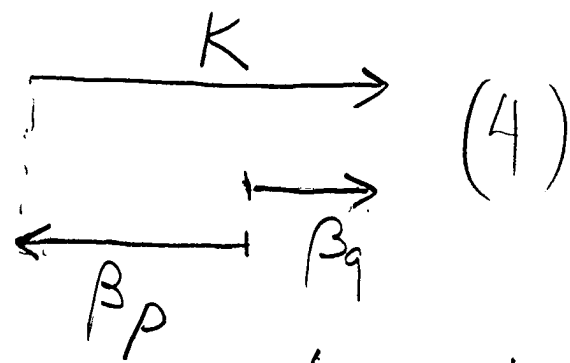
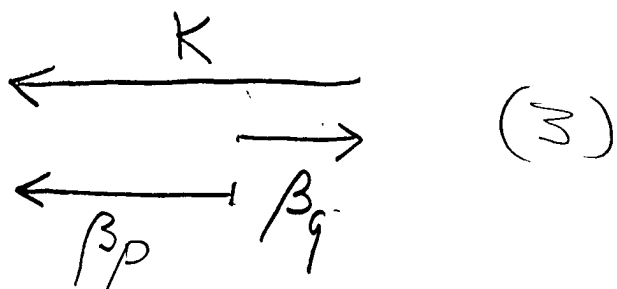
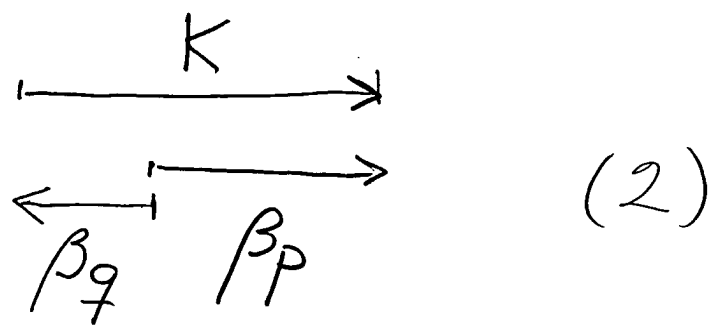
and (12c):

$$\delta_P = \delta_P \begin{cases} \tan(\delta_P w) & (\text{even}) \\ -\cot(\delta_P w) & (\text{odd}) \end{cases}$$



$\omega_{pq}$  is the radian frequency corresponding to the Bragg condition





Contra-directional  
wave coupling

Also can have  
co-directional wave-  
coupling:

$$\begin{array}{c} \beta_q \\ \longrightarrow \\ \beta_p \end{array} \quad K = \frac{2\pi}{\lambda}$$

contradirectional:

$$|\beta_p| + |\beta_q| = K \quad (13a)$$

codirectional:

$$|\beta_p| + K = |\beta_q| \quad (13b)$$

For the periodic boundary case, consider frequencies in the vicinity of the p-q stop band:

$$\omega = \omega_{pq} + \underline{\Delta\omega} \quad (14)$$

Note that from Eq (9) & (10) that a  $p^{\text{th}}$ -mode propagating in the perturbed waveguide gives rise to a surface current

$$J_s(z) = j\omega\epsilon_0(\epsilon_2 - \epsilon_1)d_p e^{-j\beta'_p z} \times \frac{\eta_W}{2}[e^{jkz} + e^{-jkz}] \quad (15)$$

$$= j\omega\epsilon_0\eta_W \left( \frac{\epsilon_2 - \epsilon_1}{2} \right) d_p \times \quad (16)$$

$$\textcircled{1} [e^{-j(\beta'_p - k)z} + e^{-j(\beta'_p + k)z}]$$

If  $K$  is chosen to provide contra directional mode coupling, we have (13a)

$$|\beta_p'| - K = -|\beta_q'|$$

so the surface current  $J_s$  has a term

$$(\sim) e^{j\beta_q' z}$$

which is the exact phase of a backward propagating  $q$  mode!

② If  $K$  is chosen to provide codirectional mode coupling, we have (136)

$$|\beta_p| + K = |\beta_q|$$

which is the phase for a

forward  $q$  mode.

The "surface current"  $J_s$  can be viewed as a source current (induced by the  $p^{\text{th}}$  mode) which excites (or causes) a  $q$  mode.

Consider the contradirectional case. ( $\Rightarrow \exp(\beta_p' + k)$  in (Eq 16)) is not effective in exciting a mode.

Also consider the symmetric 3-layer WG (TE modes) with the  $q^{\text{th}}$  mode

386

$$E_y^q(x, z) = d_q a_q(x) e^{j\beta_q' z} \quad (17)$$

from

$$\frac{\partial E_y}{\partial x} = -j\omega \mu_0 H_z$$

we have

$$H_z^q = \frac{j}{\omega \mu_0} \frac{\partial a_q(x)}{\partial x} d_q e^{j\beta_q' z}$$

$$= \frac{je^{j\beta_q' z}}{\omega \mu_0} d_q \begin{cases} \frac{s_q' \sin(s_q' x)}{\cos(s_q' w)} & (\text{even}) \\ \frac{\cos(s_q' x)}{\sin(s_q' w)} & (\text{odd}) \end{cases} \quad (18)$$

$|x| < w$

$$H_z = \frac{je^{j\beta_q' z}}{\omega M_0} d_f(-\delta_q') e^{j\delta_q' w - j\delta_q' |x|} \quad (19)$$

$$|X| > w$$

The boundary condition is:

$$H_z^+|_{(x,z)} - H_z^-|_{(x,z)} = J_S(z) \quad (20)$$

$$x = w^+ \quad x = w^-$$

which becomes:

$$\frac{j d_f}{\omega M_0} \left[ -\delta_q' + j \frac{1}{d_f} \left\{ \tan(j\delta_q' w) \right\} - \left\{ -\cot(j\delta_q' w) \right\} \right] e^{j\beta_q' z} \\ = j \omega \epsilon_0 \gamma W \left( \frac{\epsilon_2 - \epsilon_1}{2} \right) D_P e^{j\beta_q' z} \quad (21)$$

or

$$\left[ \zeta'_q \left\{ \tan(\lambda'_q w) - \zeta'_q \right\} d_q \right]_{\zeta'_q} = \omega^2 \mu_0 \epsilon_0 \eta_w \frac{(\epsilon_2 - \epsilon_1)}{2} d_p \quad (22)$$

## Important Result

- if  $\eta=0$ , we have the dispersion relation for the unperturbed (no grating) waveguide
- Eq (22) relates the amplitudes  $d_p$  and  $d_q$  in the presence of a periodic boundary

We treat the periodic boundary as a perturbation to the ideal case --

See Eq's (1) & (2):

- Eq (12a, b) are valid for  $\eta \neq 0$  (they were derived from the wave equation directly)
  - Eq (12c)  $\rightarrow$  Eq (22), if  $\eta \neq 0$
  - the unperfurbed wavevectors

$$S_p' \rightarrow S_p + \Delta S_p$$

$\equiv$  unperturbed

still satisfy (12c)

Plan:

- Insert  $(\{a, b\})$  into (22)
- Use Taylor series expansion:

$$f(x+\Delta x) = f(x) + \Delta x f'(x)$$

(22)  $\rightarrow$

$$\left[ \begin{array}{l} \left( S_g + \Delta S_g \right) \left\{ \tan(S_g W + \Delta S_g W) \right. \\ \left. - \cot(S_g W + \Delta S_g W) \right\} \\ - \left( S_f + \Delta S_f \right) \end{array} \right] d_q \quad (23)$$

$$= (\omega_{pq} + \Delta \omega)^2 \mu_0 \epsilon_0 \gamma W \left( \frac{\epsilon_2 - \epsilon_1}{2} \right) d_p$$

using:

$$\tan(S_q W + \Delta S_q W)$$

$$= \tan(S_q W) + \Delta S_q W \sec^2(S_q W) \\ + O((\Delta S_q)^2)$$

$$\cot(S_q W + \Delta S_q W)$$

$$= \cot(S_q W) - \Delta S_q W \csc^2(S_q W) \\ + O((\Delta S_q)^2)$$

and  $E_q(12c)$ , (23)  $\rightarrow$

$$(\Delta S_q [S_q W \{ \sec^2(S_q W) \\ \csc^2(S_q W) \} ] - \Delta S_q) d_q \quad (24)$$

$$+ \left[ \tan(S_q W) - \cot(S_q W) \right] d_q$$

$$= \omega_{pq}^2 \mu_0 \epsilon_0 \eta_W \frac{(\epsilon_1 - \epsilon_2)}{2} d_p$$

where we have neglected  
 $\eta_{SW}$  and higher order terms.

From expanding (12a,b)  
 using (11a,b,c), we have

$$\underline{\Delta S_p} = \frac{1}{S_p} (\epsilon_2 k SK - \beta S \beta) \quad (25)$$

$$\underline{\Delta S_p} = \frac{1}{S_p} (\beta S \beta - \epsilon_1 k SK) \quad (26)$$

so (24)  $\rightarrow$

(to here)

$$\left\{ \frac{1}{S_q} (\epsilon_2 k SK - \beta_q S \beta) \right. \left[ S_q W \right. \\ \times \left\{ \begin{array}{l} \sec^2(S_q W) \\ \csc^2(S_q W) \end{array} \right\} + \left\{ \begin{array}{l} \tan(S_q W) \\ -\cot(S_q W) \end{array} \right\} \left. \right] \\ \left. - \frac{1}{S_q} (\beta_q S \beta - \epsilon_1 k SK) \right\} d_q \equiv RHS$$

$$RHS = \frac{\omega_{pq}^2}{c^2} \eta W \frac{\epsilon_1 - \epsilon_2}{2} dP \quad (27)$$

with considerable algebra  
 (and using  $\tan^2 z + 1 = \sec^2 z$   
 $\cot^2 z + 1 = \csc^2 z$

$$(27) \rightarrow$$

$$\left[ -\frac{d\beta}{K} + \left( \frac{\beta_q}{K} \right) B_q \frac{\Delta W}{\omega_{pq}} \right] d_q \quad (28)$$

$$= \left( \frac{\omega_{pq}}{c} \right)^2 \eta \left( \frac{\epsilon_1 - \epsilon_2}{2} \right) \frac{\phi_{pq}}{\beta_q K} dP$$

where

$$\phi_{pq} = \delta_q W \frac{\cos^2(\delta_q W)}{1 + \delta_q W} \quad (29)$$

(39)

$$B_q = \left\{ \frac{\omega_{pq}^2}{C^2 \beta_q^2} \right\} \epsilon_2 \left\{ \begin{array}{l} \sin^2(\beta_q W) \\ \cos^2(\beta_q W) \end{array} \right\} + \epsilon_2 S_q W + \epsilon_1 \left\{ \begin{array}{l} \cos^2(\beta_q W) \\ \sin^2(\beta_q W) \end{array} \right\} \div (1 + S_q W) \quad (30)$$

Eq (28) was obtained by assuming a p-mode propagating in the WG which excites a q-mode

If we assume a q-mode is propagating, a p-mode

would be excited; the corresponding equation is

$$\left[ -\frac{\Delta \beta}{K} + \left( \frac{\beta_p}{K} \right) B_p \frac{\Delta \omega}{\omega_{pq}} \right] d_p = \\ = \left( \frac{\omega_{pq}}{c} \right)^2 \eta \left( \frac{\epsilon_2 - \epsilon_1}{2} \right) \frac{\phi_{pq}}{\beta_p K} d_q \quad (31)$$

for contradirectional mode coupling, assume

$$|\beta_p| = \beta_p ; |\beta_q| = -\beta_q$$

so Eqs (2.8) + (31)

become

$$\left[ -\frac{\Delta \beta}{K} - \frac{|\beta_q|}{K} B_q \frac{\Delta \omega}{\omega_{pq}} \right] d_q \\ = -\left( \frac{\omega_{pq}}{c} \right)^2 \eta \left( \frac{\epsilon_2 - \epsilon_1}{2} \right) \frac{\phi_{pq}}{|\beta_q| K} d_p \quad (32)$$

$$\left[ -\frac{\Delta \beta}{K} + \frac{|\beta_p|}{K} B_p \frac{\Delta \omega}{\omega_{pq}} \right] d_p \\ = \left( \frac{\omega_{pq}}{c} \right)^2 \eta \left( \frac{\epsilon_2 - \epsilon_1}{2} \right) \frac{\phi_{qp}}{|\beta_p| K} d_q \quad (33)$$

$$32 \Rightarrow a = b \quad \} \Rightarrow \\ 33 = c = d \quad \}$$

$$ac = bd \quad (34)$$

Or

$$\left(\frac{\Delta\beta}{K}\right)^2 = \left(\frac{|\beta_p|}{K} B_p \frac{\Delta\omega}{\omega_{pq}}\right) = b$$

$$- \frac{|\beta_q|}{K} B_q \frac{\Delta\omega}{\omega_{pq}} \frac{\Delta\beta}{K} \quad (34)$$

$$- \frac{|\beta_q| |\beta_p|}{K K} B_p B_q \left(\frac{K\omega}{\omega_{pq}}\right)^2 = c$$

$$+ \eta^2 \xi_{pq}^2 = 0$$

where

$$\xi_{pq} = \left(\frac{\omega_{pq}}{c}\right)^2 \left(\frac{\epsilon_2 - \epsilon_1}{2}\right) \left(\frac{\phi_{pq} \phi_{qp}}{|\beta_p||\beta_q|}\right)^{\frac{1}{2}} \frac{1}{K} \quad (35)$$

$$(34) \Rightarrow ax^2 + bx + c = 0$$

where  $a = 1$

$$\chi = -\frac{b}{2} \pm \frac{\sqrt{b^2 - 4ac}}{2a}$$

So

$$\frac{\Delta \beta}{K} = (\theta_p - \theta_q) \frac{\Delta \omega}{\omega_{pq}} \quad (36)$$

$$\pm \sqrt{(\theta_p + \theta_q)^2 \left( \frac{\Delta \omega}{\omega_{pq}} \right)^2 - \gamma^2 \zeta_{pq}^2}$$

where

$$\theta_i = \frac{|\beta_i|}{2K} B_i \quad (37)$$

Eq (36) is the desired result

- for  $P=Q$ ,  $\Delta\beta$  is pure real if

$$(\theta_P + \theta_Q)^2 \left( \frac{\Delta\omega}{\omega_{pq}} \right)^2 > \eta^2 \zeta_{pq}^2$$

- for  $P=Q$ ,  $\Delta\beta$  is pure imaginary ("stop band") if

$$(\theta_P + \theta_Q)^2 \left( \frac{\Delta\omega}{\omega_{pq}} \right)^2 < \eta^2 \zeta_{pq}^2$$

- The maximum imaginary component of  $\Delta\beta$  occurs at  $\Delta\omega=0$ , or

(399)

$$\chi_{pq} = i \sqrt{\eta^2 \xi_{pq}^2} \quad (38)$$

$$\chi_{pq} = \eta \left( \frac{E_2 - E_1}{2} \right) \left( \frac{\omega_{pq}}{c} \right)^2 \frac{\partial_{pq} \partial_{qp}}{1/\beta_p / 1/\beta_q}$$

Note that  $\chi_{pq} = \chi_{qp}$

- for  $p \neq q$ , and for

$$(\partial_p + \partial_q) \left( \frac{\omega}{\omega_{pq}} \right)^2 < \eta^2 \xi_{pq}$$

$\Delta\beta$  is not pure imaginary, but complex.

The real and imaginary part of  $\Delta\beta$  are

4/30

(400)

plotted in Fig 2.6 b

If we had assumed  
co-directional mode  
coupling, Eq (36)  $\rightarrow$

$$\frac{\Delta\beta}{K} = (\theta_p + \theta_q) \frac{\Delta\omega}{\omega_{pq}}$$

$$\pm \sqrt{(\theta_p - \theta_q) \left( \frac{\Delta\omega}{\omega_{pq}} \right)^2 + \gamma^2 \xi_{pq}^2}$$

and  $\Delta\beta$  is always real

(Fig 2.6 b)

4/30

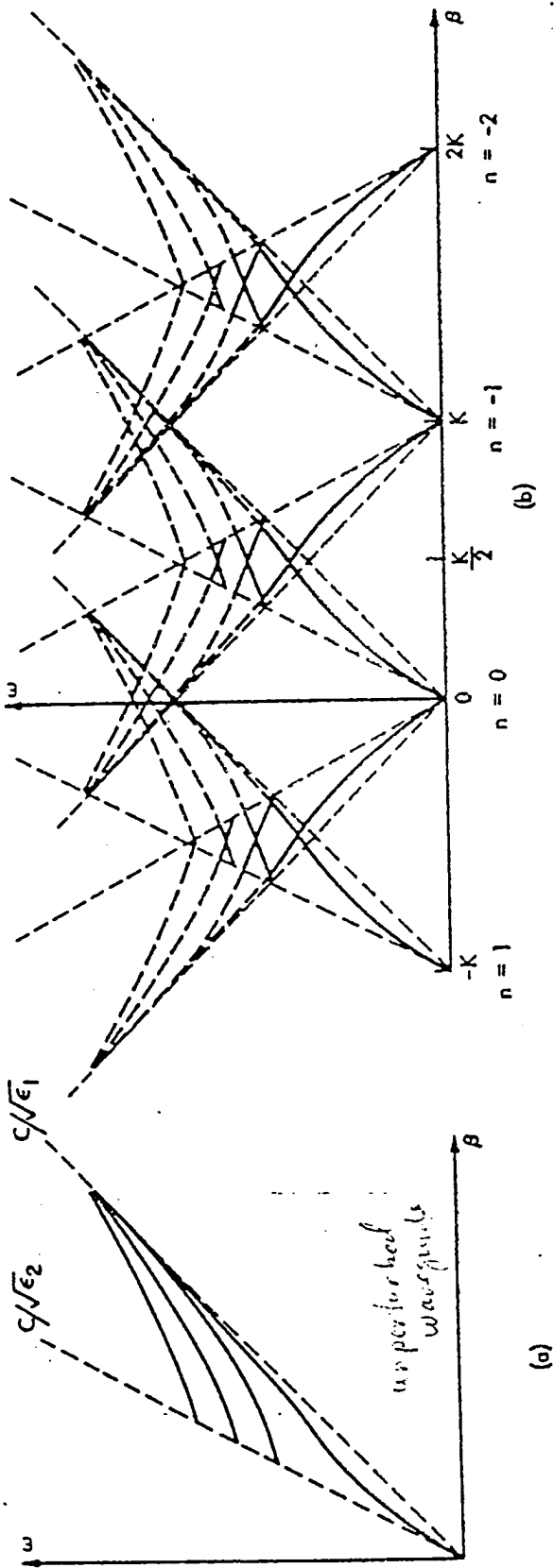


Fig. 2.5 (a)  $\omega$ - $\beta$  diagram (Brillouin diagram) for a typical dielectric waveguide. (b)  $\omega$ - $\beta$  diagram for a typical periodic dielectric waveguide.

periodicity.  $\alpha$  arises due to  $\epsilon_{\text{rel}}(z)$

$$\epsilon_{\text{rel}}(z) = \epsilon_1 (1 + \eta \cos k z), \quad \forall z$$

$$w(z) = W (1 + \eta \cos k z)$$

$$\begin{aligned} \epsilon_{\text{rel}}(z) &= \frac{\epsilon_1}{\epsilon_2} \\ &= C_1 (\beta^2 + k^2) \end{aligned}$$

 $|X| \gg w$  $|X| \ll w$ 

20

"contradicional model  
coupling can occur between  
coupling (symmetric)  
wave mode (symmetric)  
wave modes (antisymmetric)

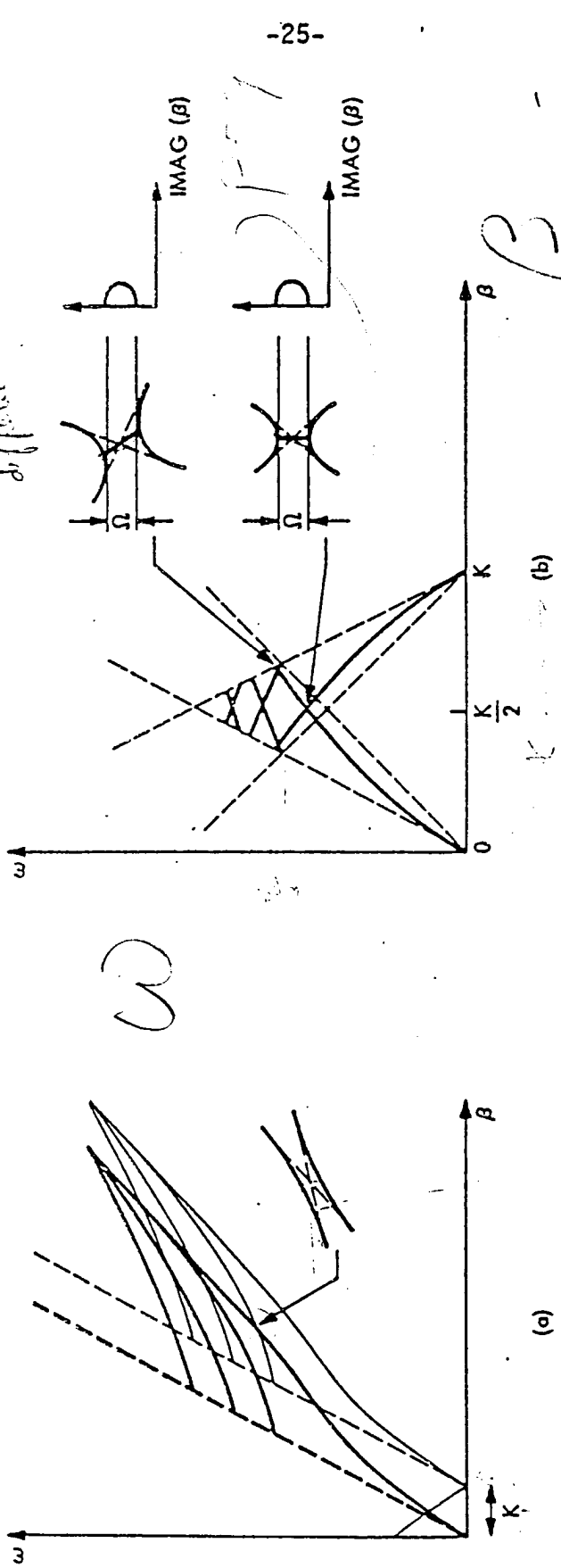


Fig. 2.6 Interaction regions between two space harmonics.  
(a) codirectional interaction, (b) contradiirectional  
symmetric and nonsymmetric interaction.

↳  $\omega_c$  for  
"codirectional"  
coupling

↳  $\omega_c$  for  
"contradiirectional"  
coupling

5/30 (21)

4/30 (22)

4/23

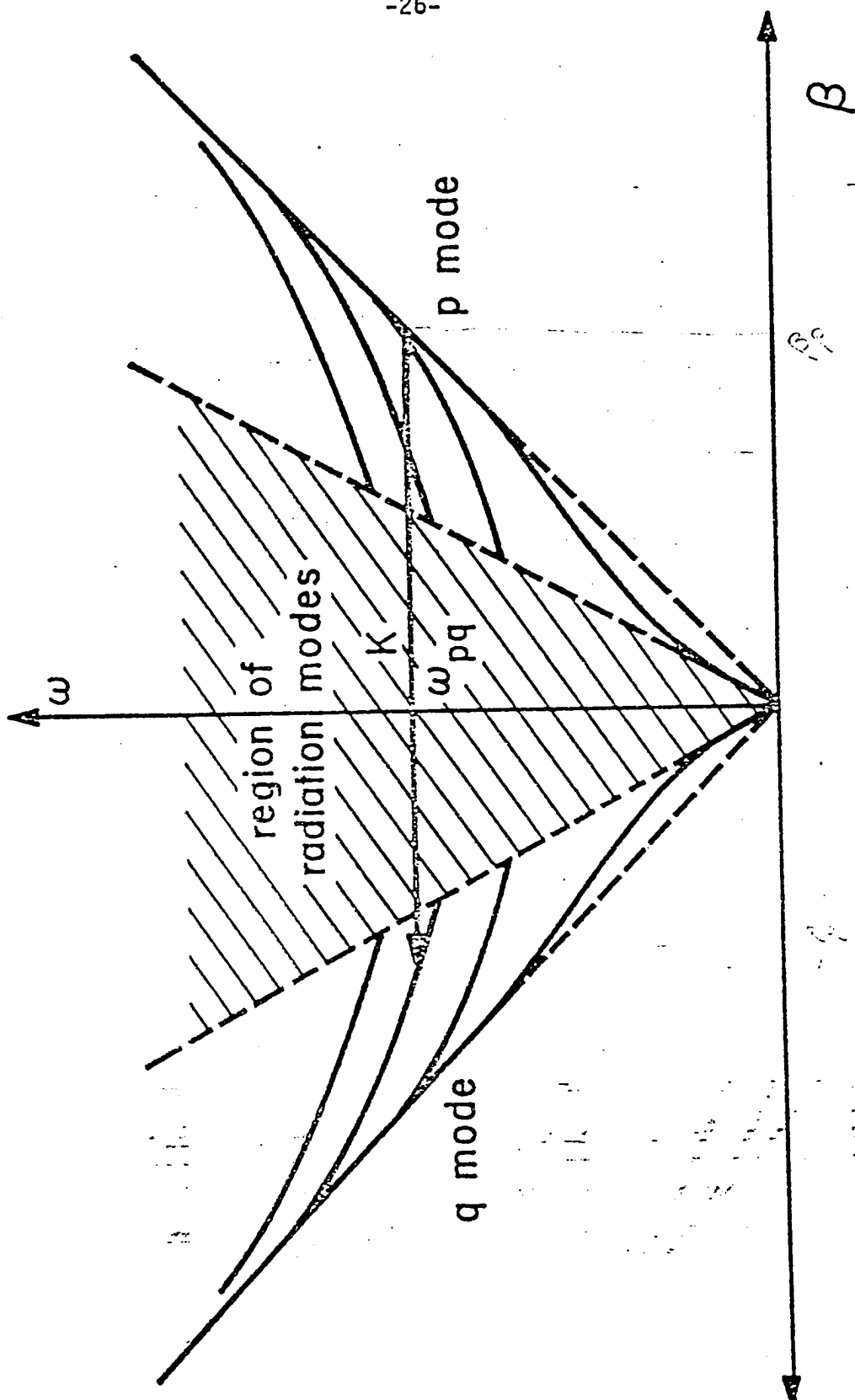


Fig. 2.7 A perturbation wave vector couples a forward p mode to a backward q mode.

4/30 (2B)  
404

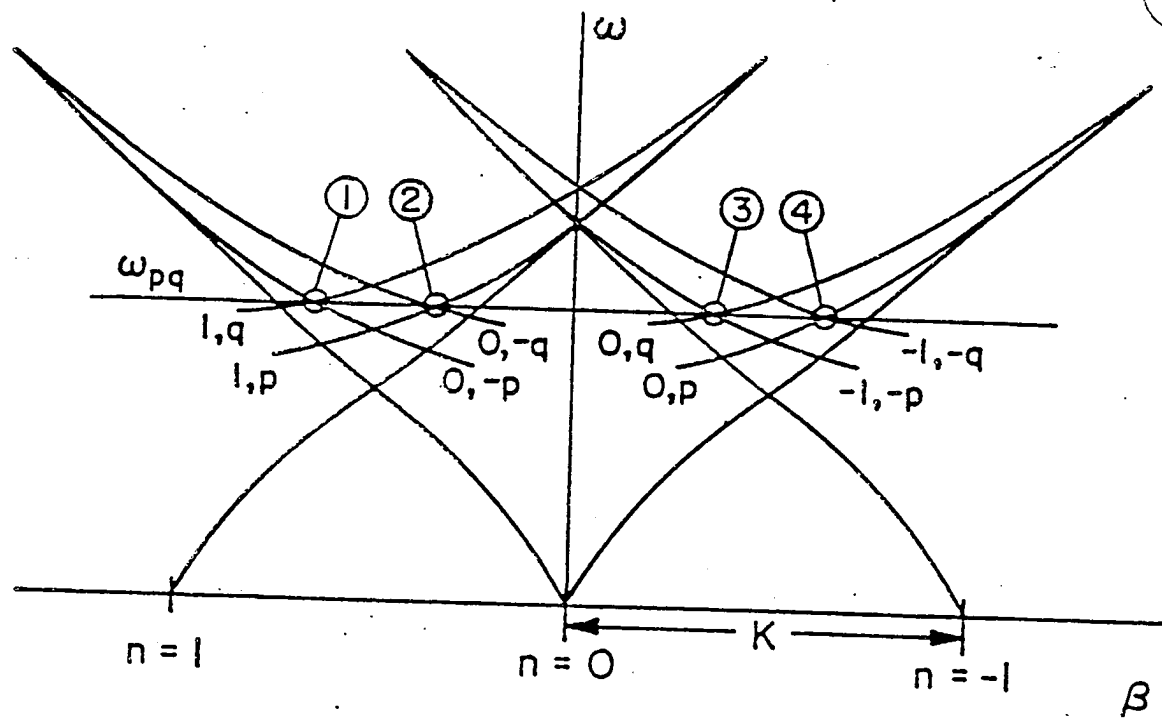


Fig. D.1 For the frequency  $\omega_{pq}$ , eight space harmonics have significant amplitudes.

relative amplitude

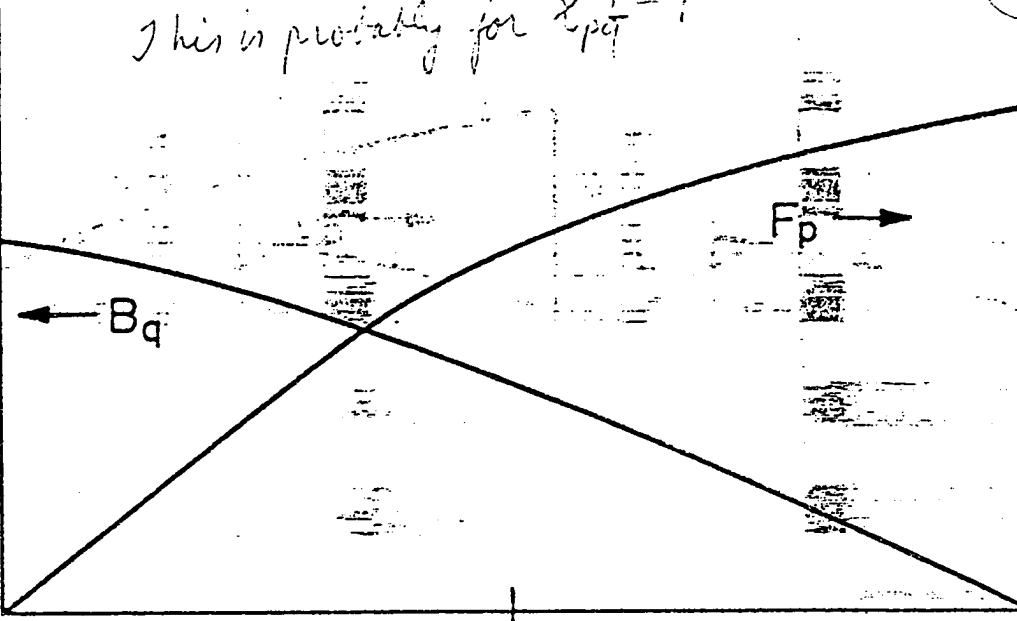
$-L/2$

0

$L/2$

distance  $Z \rightarrow$

This is probably for  $\chi_{pq}^{-1} = 1$



405

Fig. 2.8 Sketch of the amplitudes of the left traveling wave  $B_q$  and the right traveling wave  $F_p$  versus distance.

# Appendices

- homework assignments
  - project #1 (spring 93)
  - project #2 (spring 93)
  - M<sup>2</sup> Application Note

assignment #1 (due Fri, 11/29) 11/22/93

Homework problems (also read ch 1)

- ① Using Stokes Theorem,

$$\oint \vec{A} \cdot d\vec{l} = \iint_S (\nabla \times \vec{A}) \cdot d\vec{S},$$

derive the integral form of  
Faraday's Law and Ampere's Law  
starting with the differential forms

- ② Using the Divergence Theorem,

$$\iint_S \vec{A} \cdot d\vec{S} = \iiint_V (\nabla \cdot \vec{A}) dV,$$

derive the integral forms of Gauss'  
Laws (for the magnetic + electric field)  
starting with the differential forms

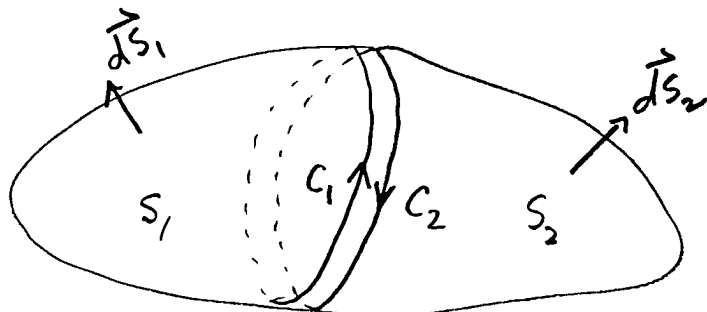
- ③ a Use the Stokes + Divergence theorem  
to show that (for any vector field  $\vec{A}$ )

$$\nabla \cdot \nabla \times \vec{A} = 0$$

1/22/93

(3, cont'd)

by considering the volume:



and starting from

$$\int_V (\nabla \cdot \nabla \times \vec{A}) dV = \oint_{S_1 + S_2} (\nabla \times \vec{A}) \cdot d\vec{S}$$

③b Show by direct substitution

$(\vec{A} = A_x \hat{i}_x + A_y \hat{i}_y + A_z \hat{i}_z)$  that

$$\nabla \cdot \nabla \times \vec{A} = 0$$

Assignment #2, due Fri, Feb 5  
 (hand in to Pam, EE dept)

① Derive a wave equation for  $\vec{H}$   
 using the same assumptions that  
 resulted in Eq(9), page 3 of 1/22

② Why is the "function"

(see notes page ⑬ of 1/27)

not a physical solution of the  
 wave equation?

③ For time harmonic fields ( $e^{j(\omega t - \beta z)}$ )  
 dependence), show that if the tangential  
 components of the electric + magnetic  
 fields satisfy the boundary conditions,  
 then the normal components of the  
 same fields automatically satisfy their  
 appropriate boundary conditions.

(#3-1) 2/5/93

## Assignment #3 (due 2/12/93)

Problem #1 Derive the dispersion relations for a symmetric 3 layer waveguide for the TM modes. That is, find the equations equivalent to (9) and (10) on page 10 of 1/29.

Problem #2 Show that the equation similar to Eq (16),  $P(\theta)$  of 2/3 is (or is close to)

$$\tan(ST) = \frac{\epsilon_1 ST \cdot \epsilon_3 \{ST\}}{\epsilon_2 \epsilon_1 (ST)^2 - \epsilon_2^2 (ST)\{ST\}}$$

for TM modes

#3-2 2/5/93

Assignment #3, cont'd

Problem #4 For the AlGaAs waveguide problem (p. 9 - p. 13, 2/13) find:  $s_1, s_2, s_3, s_4;$   
 $\delta_1, \delta_2, \delta_3, \delta_4; \xi_1, \xi_2, \xi_3, \xi_4;$   
 $\beta_1, \beta_2, \beta_3, \beta_4.$

Write expressions for  $E_y, H_x,$  and  $H_z$  for all 4 allowed modes of the waveguide. Roughly sketch the modes.

Problem #5 Use the computer program handed out in class (or your own) to analyze the AlGaAs waveguide in problem #4. The effective index  $n_{eff} = \beta/k_0.$

#3-3 2/5/93

Problem #5, cont'd:

Does the  $N_{eff}$  calculated by the computer program agree with that found from Problem #4? Do the plots agree?

Problem #6 What is the maximum thickness that a glass slide (or slab) must be to support only one TE mode?

Assume  $n_{glass} = 1.5$  and that the glass slide is surrounded by air with  $n_{air} = 1$ . Assume the waveguide is for the light from a He Ne laser ( $\lambda = 0.6328 \mu m$ )

Problem #7

What thickness range should be chosen for the

# 3-4 2/5/93

GaAs region for the  
AlGaAs waveguide in Problem  
4 and 5 if we want to  
support only one (1) TE  
mode?

2/2/93 (4-1)

## Assignment #4 (due 2/19/93)

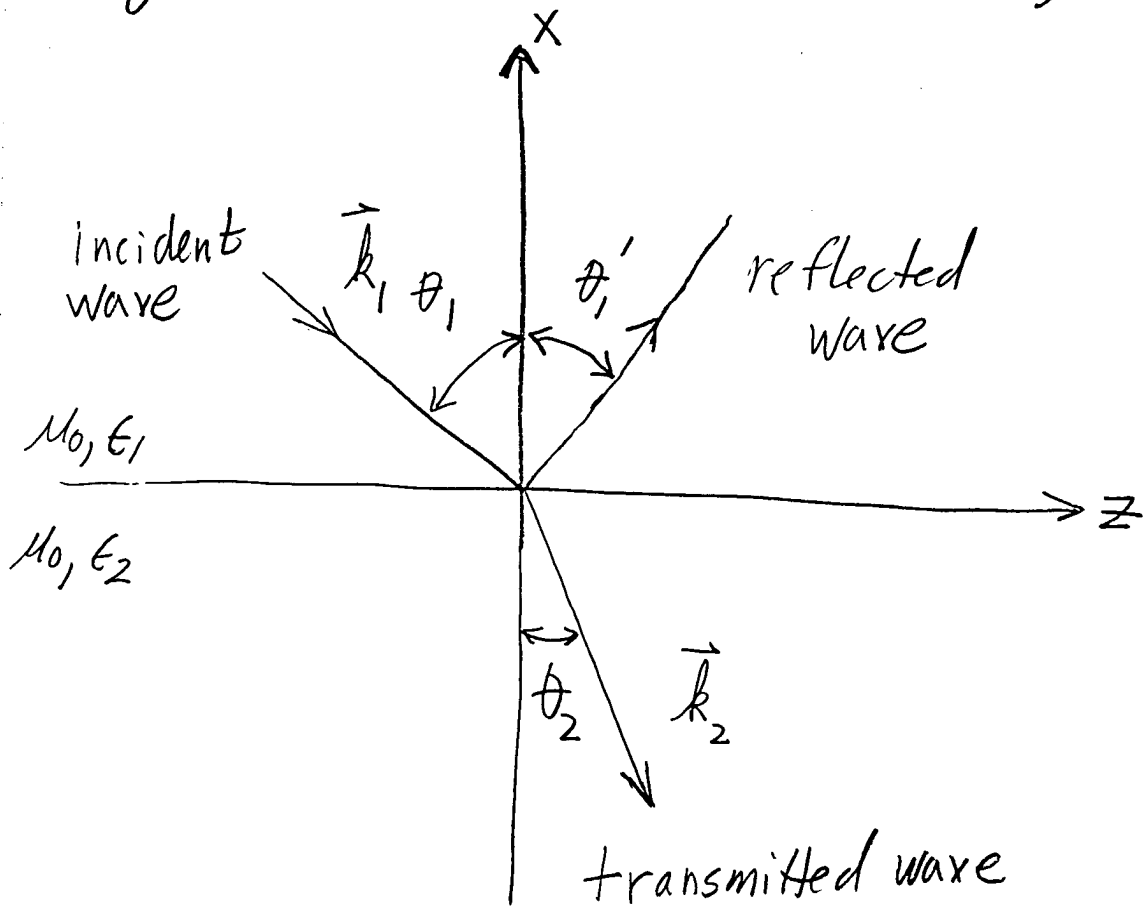


Fig 4-1.

Consider the 2 basic cases in Fig 4.1

- The  $\vec{E}$  field of the incident wave is  $\perp$  (perpendicular) to the  $x-z$  plane
- The  $\vec{E}$  field is  $\parallel$  (parallel) to the  $x-z$  plane

2/12/93

(4-2)

① Consider case (a), where

$$\vec{E}_i = \hat{i}_y E_0 \exp(-j\vec{k}_i \cdot \vec{r})$$

② show that

$$\vec{H}_i = -\left(\frac{E_0}{\eta_i}\right) [\hat{i}_x \sin \theta_i + \hat{i}_z \cos \theta_i] e^{-j\vec{k}_i \cdot \vec{r}}$$

where

$$\vec{r} = x \hat{i}_x + y \hat{i}_y + z \hat{i}_z$$

$$\eta = \sqrt{\frac{\mu}{\epsilon}}, \quad \eta_i = \sqrt{\frac{\mu_0}{G_i}}$$

③ show that the reflected fields  
are given by

$$\vec{E}_r = \hat{i}_y E'_0 e^{-j\vec{k}'_i \cdot \vec{r}}$$

$$\vec{H}_r = \left(\frac{E'_0}{\eta'_i}\right) [-\hat{i}_y \sin \theta' + \hat{i}_z \cos \theta'] \\ \times e^{-j\vec{k}'_i \cdot \vec{r}}$$

④ show that the transmitted fields  
are given by

7/12/93 (4-3)

$$\vec{E}_t = \hat{i}_y E_0'' e^{-jk_2 \vec{k}_2 \cdot \vec{r}}$$

$$\vec{H}_t = -\left(\frac{E_0''}{\eta_2}\right) [\hat{i}_x \sin \theta_2 + \hat{i}_z \cos \theta_2] e^{jk_2 \vec{k}_2 \cdot \vec{r}}$$

d) Apply the boundary conditions requiring tangential  $\vec{E}$  and  $\vec{H}$  to be continuous:

$$(\vec{E}_i + \vec{E}_r)_y = (\vec{E}_t)_y \quad (1)$$

$$(\vec{H}_i + \vec{H}_r)_y = (\vec{H}_t)_y \quad (2)$$

and show that eq (1) & (2) require

$$i) \theta_i = \theta_i' \quad (\angle \text{ of incidence} = \angle \text{ of refl}) \quad (3)$$

$$ii) k_1 \sin \theta_i = k_2 \sin \theta_2 \quad (\text{Snell's Law}) \quad (4)$$

$$iii) E_0 + E_0' = E_0'' \quad (5)$$

$$iv) \left(\frac{E_0}{\eta_1}\right) \cos \theta_i - \left(\frac{E_0'}{\eta_1}\right) \cos \theta_i' = \left(\frac{E_0''}{\eta_2}\right) \cos \theta_2 \quad (6)$$

② From Eq (5), (6) of problem ①,  
show that ③

$$1 + \rho = \tau \quad (7)$$

$$\left[ (\cos \theta_1) / \eta_1 \right] (1 - \rho) = \left[ (\cos \theta_2) / \eta_2 \right] \tau \quad (8)$$

where  $\rho = \frac{E_0'}{E_0}$ ,  $\tau = \frac{E_0''}{E_0}$

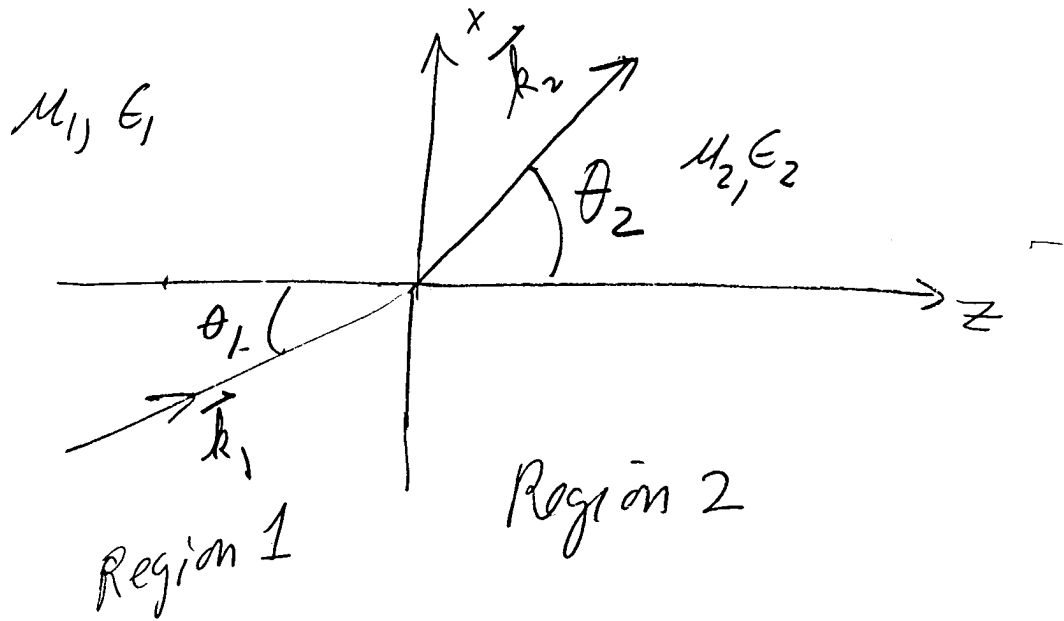
are the field (amplitude) reflection  
and transmission coefficients, respectively.

⑥ Show that (for  $\perp$  polarization)

$$\rho_{\perp} = \frac{\eta_2 / (\cos \theta_2) - \eta_1 / (\cos \theta_1)}{\eta_2 / (\cos \theta_2) + \eta_1 / (\cos \theta_1)} \quad (9)$$

$$\tau_{\perp} = 2 \frac{\eta_2 / (\cos \theta_2)}{\eta_2 / (\cos \theta_2) + \eta_1 / (\cos \theta_1)} \quad (10)$$

⑥ Show by geometrical arguments (for the sketch on P.D of 2/10):



that

$$\frac{\gamma_1}{\cos \theta_1} = -\frac{\gamma_0 k_0}{\beta} = z_1^\perp \quad (11)$$

$$\frac{\gamma_2}{\cos \theta_2} = -\frac{\gamma_0 k_0}{\sqrt{k_0^2 - \beta^2}} = z_2^\perp \quad (12)$$

(4-6)

note that you have shown  
that

$$\rho^\perp = \frac{Z_2^\perp - Z_1^\perp}{Z_2^\perp + Z_1^\perp} \quad (13)$$

$$T_{12}^\perp = \frac{2 Z_2^\perp}{Z_2^\perp + Z_1^\perp} \quad (14)$$

which was the starting point p(0) of  $z^2/10$ .

③ Show that the power reflection coefficient  $R = \rho^2$  is

$$R_\perp = \frac{|n_1 \cos\theta_1 - (n_2^2 - n_1^2 \sin^2\theta_1)^{1/2}|^2}{|n_1 \cos\theta_1 + (n_2^2 - n_1^2 \sin^2\theta_1)^{1/2}|^2}$$

For extra credit, do probs ①-③  
for case ⑥ of p. 4-1 -- (the  
 $\vec{E}$  field  $\parallel$  to the  $x-z$  plane.)

3/5 ①

## Assignment (due March 29)

① Show that  $\frac{P_2}{1+P_2}$

(eq. 18, p⑬, 3/12) is

equivalent to  $P_2 = \frac{A}{1+A}$

where A is defined  
on page ⑮, 3/12

⑥ show that  $P_2$  can  
be expressed as

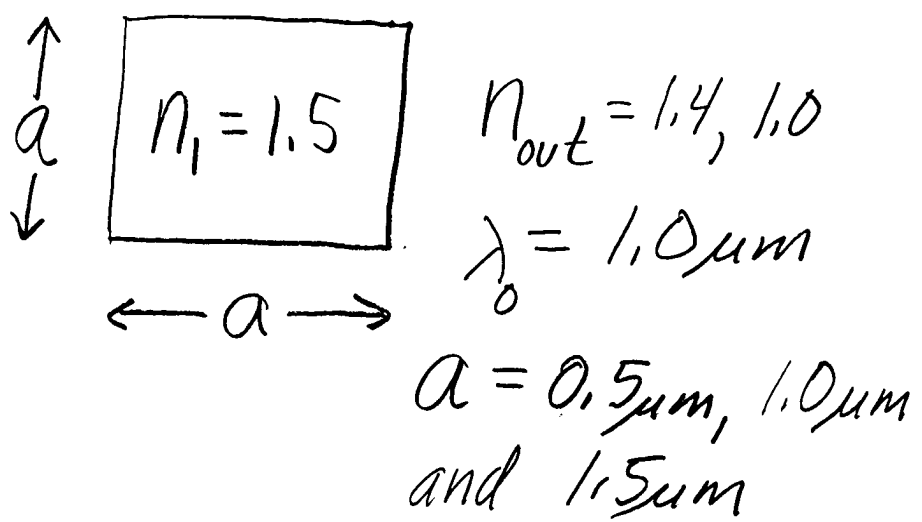
$$P_2 = \begin{cases} \tan^2(\Delta_{\text{re}}W) \left[ 1 + \frac{2\Delta_{\text{re}}W}{\sin(2\Delta_{\text{re}}W)} \right] & (\text{even}) \\ -\cot^2(\Delta_{\text{re}}W) \left[ 1 - \frac{2\Delta_{\text{re}}W}{\sin(2\Delta_{\text{re}}W)} \right] & (\text{odd}) \end{cases}$$

3/5 (2)

- ② For the commercial LDI structure,
- determine how much p-clad should remain outside the ridge region to have a lateral index step of  $8 \times 10^{-3}$ .
  - for a lateral index step of  $8 \times 10^{-3}$ , plot the lateral beam divergence (FWHP) as a function of ridge width (between 1 and  $10 \mu\text{m}$ ).
  - plot the near- and far fields, both I and II, for a ridge width of  $3 \mu\text{m}$ .

3/15 (3)

③ For the square dielectric waveguide, the effective index method gives a more accurate value of  $\beta$ . However, the field distribution is not symmetric if the effective index method is used. Plot the fields for the following structure using both methods:



## Mini Project #1 EE 6392, Spring 1993

### Background

Attached is a sheet from Laser Diode, Inc which shows the layers used in one of their commercial semiconductor laser diodes. Some applications of this device are pumping solid state lasers and optical fusing. Optical fusing involves coupling the laser light into an optical fiber and using the light exiting the fiber to initiate a powder similar to gunpowder. The DOE first started investigating optical fuses to replace electrical fuses in atomic weapons. The electrical fuses are susceptible to EMI or EMP. However, there could be mass markets for optical fuses, such as air bags in automobiles.

To couple light into a fiber efficiently (we will look at this problem later this semester), we would like a narrow beam divergence. Also, optical system designers prefer a narrow, low aspect ratio (perpendicular to parallel beam divergence) to simplify the optical system design.

Figure 1 is a sketch of the AlAs mole fraction in the present device. Figure 2 is a sketch of the index of refraction of the present device. The present beam divergences for this device are  $32^\circ \pm 4^\circ$  (perpendicular) and  $8^\circ \pm 3^\circ$  (parallel). This device has a low threshold current and high efficiency, which is related to the quantum well confinement factor (defined by Fig. 3). Assume that the wavelength of operation is  $0.808 \mu\text{m}$ .

### The Assignment

Design a waveguide structure that has similar performance (threshold and efficiency) to the present commercial device, but with a narrower perpendicular beam divergence (try for  $\sim 20^\circ$ , say).

### Suggested approach:

- 1) calculate the quantum well confinement factor and perpendicular beam divergence for the existing structure.
- 2) try modified waveguide structures as suggested in Fig. 4. Assume that the performance of the new device will be acceptable if the QW confinement factor is within 25% of the value found in 1).

**Comments:**

- 1) Ms. Wang who is auditing this course is familiar with running the program MODEIG, if you choose to use it.
- 2) MODEIG mainly runs on the MacIntosh, but I do have an IBM PC version that I have not tested. The source code used in the MAC version was converted to run on an IBM compatible by Mark Felisky at the Oregon Graduate Institute (503-690-1148).

**To use Modeig:**

The following references are helpful. The Modeig/II Manual and the Modeig Users Manual will be on the same computer disk as the program:

- 1) R. B. Smith and G. L. Mitchell, "Calculation of Complex Propagating Modes in Arbitrary, Plane-Layered, Complex Dielectric Structures. I. Analytic Formulation. II. Fortran Program MODEIG", EE Technical Report No. 206, University of Washington, Seattle, WN, 1977.
- 2) V. J. Masin, G. A. Evans, "Modeig Users Manual", unpublished.
- 3) P. L. Demers, "Modeig/II Manual", unpublished.

7-29-1993 18:24

FROM LASER DIODE INC.

IU

12147883883 P.01

LASER DIODE

MP (3)

LASER DIODE, INC.  
 1130 SOMERSET ST.  
 NEW BRUNSWICK, NJ 08901  
 (908) 249-7000  
 (FAX) 908-249-9165

FACSIMILE LEAD PAGEDATE: 1/29/93NUMBER OF PAGES: 1  
(INCLUDING THIS ONE)DELIVER TO: Dr. Gary EvansPHONE EXT.: (908)-249-7000COMPANY: SMIREF: Ext. 219FACSIMILE TELEPHONE: #: (214)-768-3883

SUBJ: \_\_\_\_\_

FROM: Jim Pooladdej

$$\theta_L = 32 \pm 4^\circ; \theta_H = 8 \pm 3^\circ$$

Gary;  
 I wrote forward to hearing from  
 you w.r.t. tapered amplifier/  
 oscillator. Regards Jim/

Layer	Material	Mole Fraction (Al)	Thickness (μm)	Free Carrier Density (cm <sup>-3</sup> ) by C.V (cm <sup>-3</sup> )	N <sub>b</sub> N <sub>d</sub>	Type	Dopant
7	GaAs		0.5±0.1		>3.0 E+19	p	Zn
6	AlGaAs	0.6±0.05	1.2±0.2		1.2±0.2E+18	p	Zn
5	AlGaAs	0.3->0.6	0.15±0.03		-	U/D	
4	AlGaAs		.007±.001		-	U/D	
3	AlGaAs	0.6->0.3	0.15±.03		-	U/D	
2	AlGaAs	0.6±0.5	1.3±0.2		1.2±0.2E+18	n	Si
1	GaAs		0.8±0.04		2±0.5 E+18	n	Si
	GaAs			see below			

(MP-4)

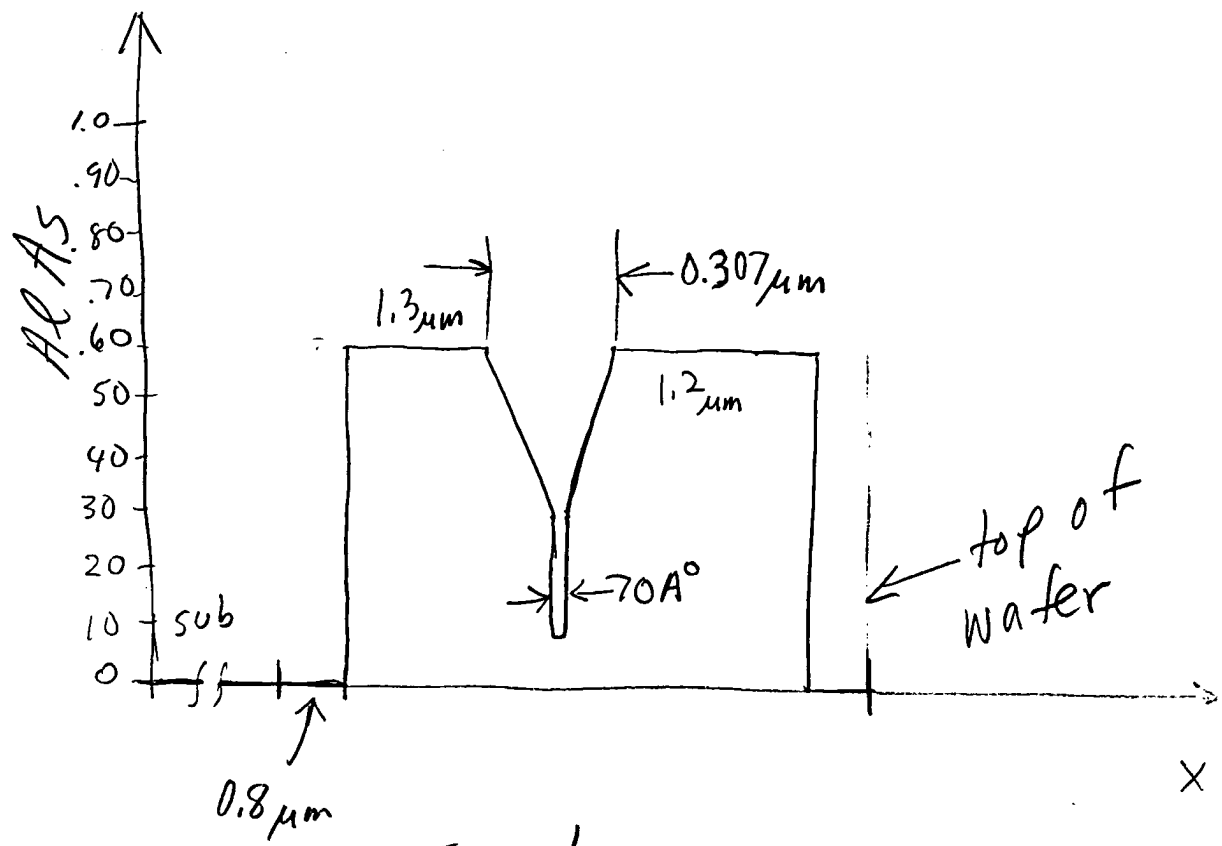


Fig 1

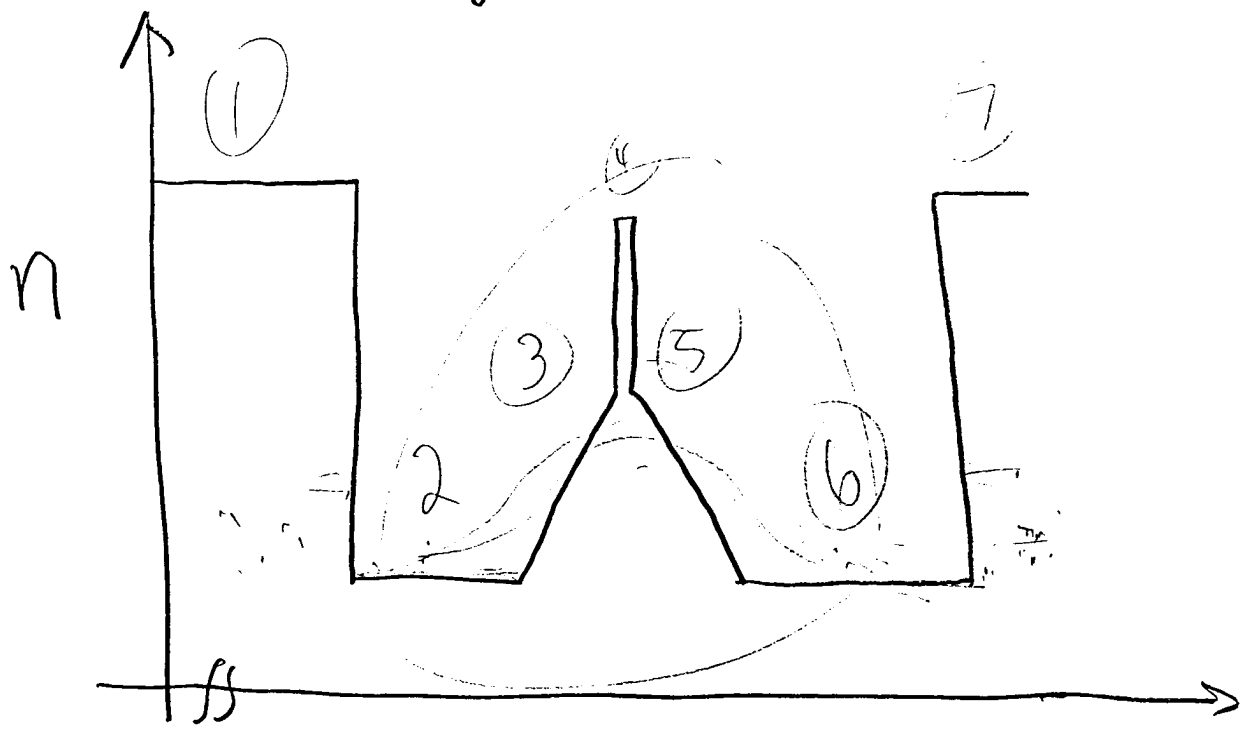
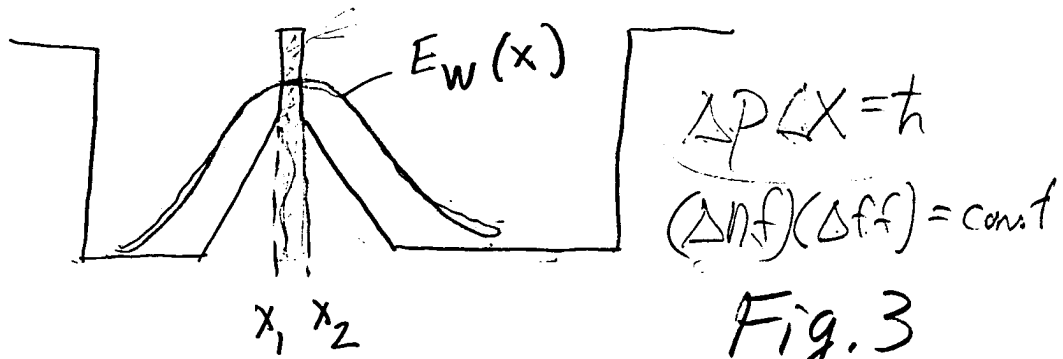


Fig 2



$$\Gamma_{QW} = \int_{x_1}^{x_2} |E_w(x)|^2 dx / \int_{-\infty}^{\infty} |E_w(x)|^2 dx$$

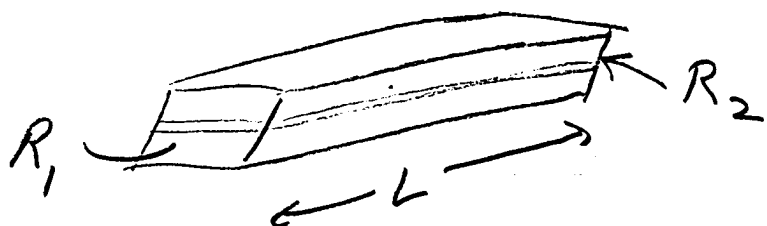
$$J_{th} \propto g_{th} = \frac{1}{\Gamma_{QW}} \left( \alpha_{int} + \frac{1}{L} \ln(R_1 R_2) \right)$$

$g_{th}$  = modal threshold gain

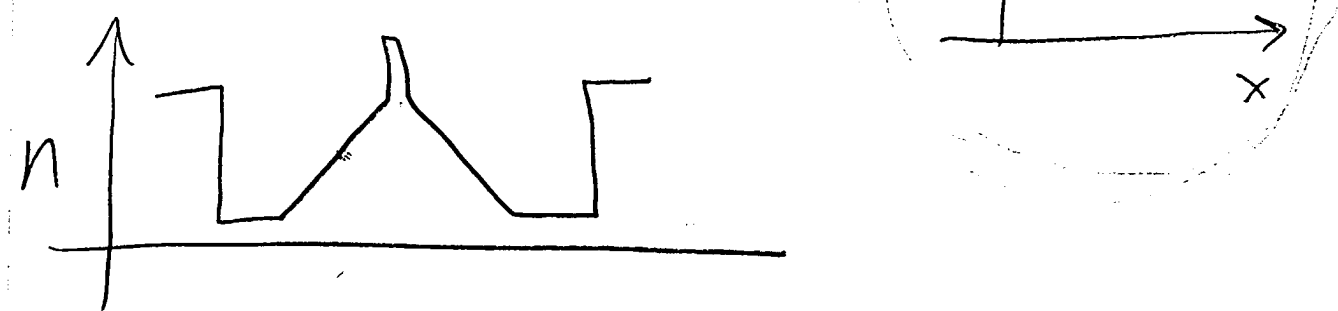
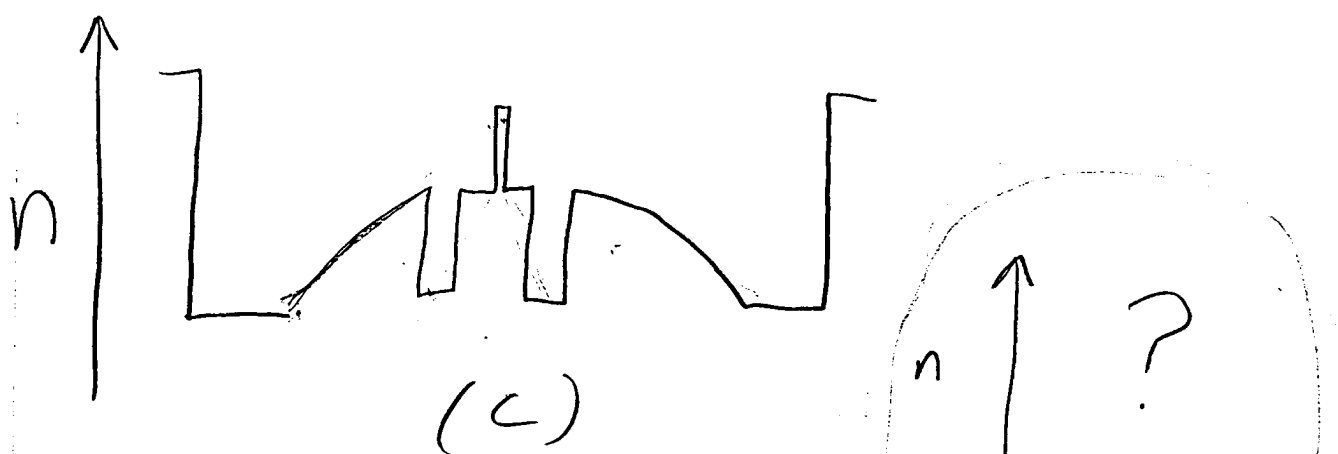
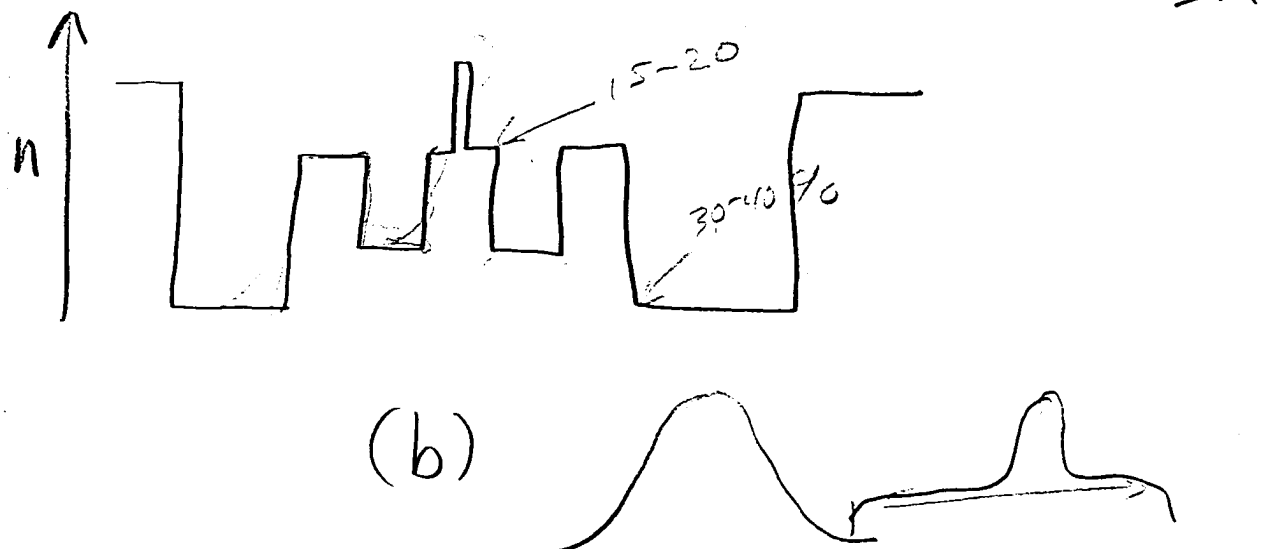
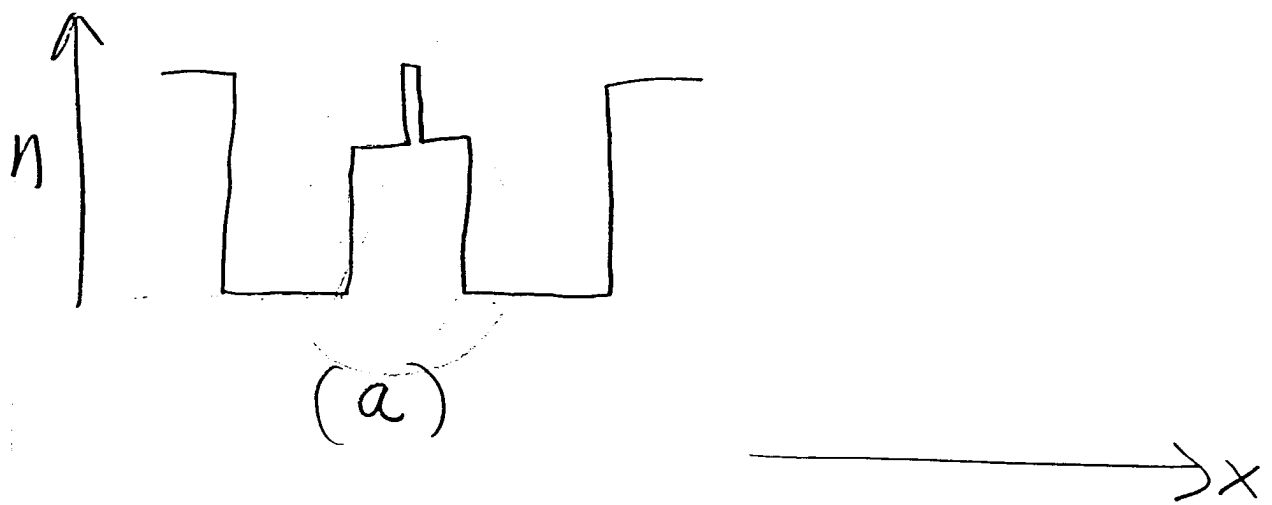
$\alpha_{int}$  = internal waveguide loss

$L$  = length of the laser

$R_i$  = power reflectivity of each facet



MP-6



2/23" b

Comments on (4) Outlines  
for Mini Project #1

1. The problem is not to rederive what we did in class. If you want to rederive the waveguide equations and far-field pattern (for your own benefit), you can put the derivations in an appendix. In the report, you can reference textbooks, journal articles, or class notes.
2. The problem is to find a waveguide structure that has a quantum well confinement factor of  $\geq 1.7\%$  and a target beam divergence of  $20^\circ$ . A beam divergence of less than  $20^\circ$  would be fine, if the quantum well confinement factor remains  $\geq 1.7\%$ . Perhaps some of you will design a structure with a beam divergence of  $25^\circ$  and maintain a quantum well beam divergence  $\geq 1.7\%$ . That is ok.
3. Suggestion: Analyze the present commercial LDI structure (we did most of this in class, and the input file is on your Mac version of MODEIG.) Try some variations of the LDI structure with MODEIG. Plot the trends. What do the curves suggest? Try ideas for index profiles that the trends suggest, or even ideas that come out of the blue. Look at all your data, and decide on a structure that meets (or comes close) to the requirements in the problem statement.
4. The version of MODEIG that you have does not give you threshold current density or efficiency. Do not worry about the length of the laser ( $L$ ) or the mirror reflectivities ( $R_1$  and  $R_2$ ). You can assume that the threshold current and efficiency will be okay as long as the quantum well confinement factor is  $\geq 1.7\%$ .
5. Most of the report should concentrate on item 3. I want to know what thought processes lead you to your final design.

"2/23" -1

Case # 1

This is the file 63921di with MODOUT = 1

```
CASE KASE=MINIPROJECT(1)
CASE EPS1=1E-7 GAMEPS=1E-3 QZMR=11.0206
CASE PRINTF=0 INITGS=0 AUTOQW=0 NFPLT=1 QZMI=0.0
      FFPLT=1
```

```
MODCON KPOL=1 APB1=0.25 APB2=0.25
```

```
STRUCT NQW=.364 WVL=.808
STRUCT GRW=.15 QW=.0070
STRUCT ALPERC1=.6 ALPERC2=0.3
```

```
→ LAYER ALPERC=.00 !GaAs substr
    LAYER ALPERC=^1 TL=1.3 ! n-Clad
    LAYER ALPERC=^1 ! 1st (n)GRINSCH
    LAYER NSLC=10 !
    LAYER ALPERC=^2 !"
    LAYER QWS=1 !QW GaAs-LAYER
    LAYER ALPERC=^2 !2nd (p)GRINSCH
    LAYER NSLC=10 !
    LAYER ALPERC=^1 !
    LAYER ALPERC=^1 TL=1.2 !2nd p-Clad
    LAYER ALPERC=.00 TL=0.5 !GaAs Cap
    LAYER NREAL=1 !Air
```

```
OUTPUT PHMO=1 GAMMAO=1 WZRO=1 QZIO=1 QZRO=1 QZIO=0
OUTPUT FWHPNO=1 FWHPFO=1 KMO=1 ITO=1
OUTPUT SPLTFI=1 MODOUT=1 LYROUT=1
GAMOUT LAYGAM=14 COMPGAM=0 GAMALL=0
```

```
!LOOPX1 ILX='TL' FINV=0.0 XINC=-0.05 LAYCH=30
!LOOPZ1 ILZ='GRW' FINV=.4 ZINC=.01
!LOOPZ2 ILZ='WVL' FINV=0.955 ZINC=-0.005
```

```
!LOOPZ1 ILZ='QZMR' FINV=10.9 ZINC=-.1!THIS LOOPS TO FIND INITIAL GUESS
!LOOPZ1 ILZ='GRW' FINV=.202 ZINC=.001
!LOOPZ1 ILZ='ALPERC1' FINV=.401 ZINC=.0005
```

2/23 (1.2)  
2/23 (1.2)

```
!LOOPX1    ILX="TL'      FINV=.15      XINC=.01      LAYCH=33
!LOOPX1    ILX="TL'      FINV=.0       XINC=-.01     LAYCH=34
END
```

This is the beginning of the output that is produced when the flag MODOUT = 1

To find this output, open the file 6392di\_OUTPUT\_

```
***** MODEIG ***** PROGRAM MODEIG *****
***** CALCULATION OF GENERAL COMPLEX*16 EIGEN-WAVES IN LAYERED STRUCTURES ****
*****
```

MODEIG/II  
version 1.4  
Revised: October 2, 1991

CASE NO. 0.1

SUMMARY OF LAYERED STRUCTURE, POLARIZATION, AND BOUNDARY CONDITIONS /  
IMPLIED UNIT OF LENGTH XU=0.10000D-05 METERS (BUT NOT USED EXPLICITLY). ALL QUANTITIES NORMALIZED.  
NOMINAL WAVELENGTH WVLL= .80800 XU, AND FREE-SPACE KO= 2PI/WVLL= 7.77622 RAD/XU.  
COMPLEX FREQUENCY FACTOR KC=( 1.00000, .00000). EFFECTIVE-KO= KC\*KO=( 7.77622, .00000).  
ALL PROPAGATION COEFFICIENTS ARE NORMALIZED TO EFFECTIVE-KO. (WAVE AND MATERIAL REFRACTIVE INDIC  
UNITY)  
(WAVE ADMITTANCE(TE) AND IMPEDANCE(TM), YX AND YZ, ARE NORMALIZED TO THAT OF FREE SPACE.  
NORMALIZED FREQUENCY KF=( 1.00000, .00000)= FREQ/C\*EFF.KO.

POLARIZATION, KPOL=1 (=1 TE CASE, =2 TM CASE)  
TRANSVERSE ELECTRIC CASE. EX=HY=EZ=0. TANGENTIAL FY=+EY, FZ=+HZ. TRANSVERSE FX=-HX, FY=+EY. LONGIT  
FZ=+HZ.  
YX=FZ/FY=+HZ/EY, AND YZ=FX/FY=-HX/EY, ARE WAVE ADMITTANCES. (IN THE POS X, Z, OR WAVE DIRECTION).

LAYERED STRUCTURE. 27 LAYERS TOTAL. 26 BOUNDARIES. 25 FINITE LAYERS.

PE=( 13.49305, .00000) PM=( 1.00000, .00000)

L 1 SEMI-INFINITE QN=( 13.49305, .00000) YN=( -1.00000, .00000)  $\Rightarrow$  Top A  
 L1= 1---BOUNDRAY FOR FIRST BOUNDARY CONDITION-----  
 -L 1---XL= .00000  
 PE=( 10.68918, .00000) PM=( 1.00000, .00000)  
 L 2 TL=.130000 QN=( 10.68918, .00000) YN=( 1.00000, .00000)  
 ( 1.60891WVL) RN=( 3.26943, .00000) PH0=( 33.05095, .00000)  
 -L 2---XL= 1.30000  
 PE=( 10.68918, .00000) PM=( 1.00000, .00000)  
 L 3 TL=.00750 QN=( 10.68918, .00000) YN=( 1.00000, .00000)  
 ( .00928WVL) RN=( 3.26943, .00000) PH0=( .19068, .00000)  
 -L 3---XL= 1.30750  
 PE=( 10.80564, .00000) PM=( 1.00000, .00000)  
 L 4 TL=.01500 QN=( 10.80564, .00000) YN=( 1.00000, .00000)  
 ( .01856WVL) RN=( 3.28719, .00000) PH0=( .38343, .00000)  
 -L 4---XL= 1.32250  
 PE=( 10.92273, .00000) PM=( 1.00000, .00000)  
 L 5 TL=.01500 QN=( 10.92273, .00000) YN=( 1.00000, .00000)  
 ( .01856WVL) RN=( 3.30496, .00000) PH0=( .38550, .00000)  
 -L 5---XL= 1.33750  
 PE=( 11.04045, .00000) PM=( 1.00000, .00000)  
 L 6 TL=.01500 QN=( 11.04045, .00000) YN=( 1.00000, .00000)  
 ( .01856WVL) RN=( 3.32272, .00000) PH0=( .38757, .00000)  
 -L 6---XL= 1.35250  
 PE=( 11.15881, .00000) PM=( 1.00000, .00000)  
 L 7 TL=.01500 QN=( 11.15881, .00000) YN=( 1.00000, .00000)  
 ( .01856WVL) RN=( 3.34048, .00000) PH0=( .38964, .00000)  
 -L 7---XL= 1.36750  
 PE=( 11.27779, .00000) PM=( 1.00000, .00000)  
 L 8 TL=.01500 QN=( 11.27779, .00000) YN=( 1.00000, .00000)  
 ( .01856WVL) RN=( 3.35824, .00000) PH0=( .39172, .00000)  
 -L 8---XL= 1.38250  
 PE=( 11.39741, .00000) PM=( 1.00000, .00000)  
 L 9 TL=.01500 QN=( 11.39741, .00000) YN=( 1.00000, .00000)  
 ( .01856WVL) RN=( 3.37601, .00000) PH0=( .39379, .00000)  
 -L 9---XL= 1.39750  
 PE=( 11.51766, .00000) PM=( 1.00000, .00000)  
 L 10 TL=.01500 QN=( 11.51766, .00000) YN=( 1.00000, .00000)  
 ( .01856WVL) RN=( 3.39377, .00000) PH0=( .39586, .00000)

2/23 - 4

-L 10--XL= 1.41250 PE=( 11.63854, .00000) PM=( 1.00000, .00000)  
L 11 TL=.01500 QN=( 11.63854, .00000) YN=( 1.00000, .00000)  
( .01856WVL) RN=( 3.41153, .00000) PH0=( .39793, .00000)  
-L 11--XL= 1.42750  
PE=( 11.76005, .00000) PM=( 1.00000, .00000)  
L 12 TL=.01500 QN=( 11.76005, .00000) YN=( 1.00000, .00000)  
( .01856WVL) RN=( 3.42929, .00000) PH0=( .40000, .00000)  
-L 12--XL= 1.44250  
PE=( 11.88219, .00000) PM=( 1.00000, .00000)  
L 13 TL=.00750 QN=( 11.88219, .00000) YN=( 1.00000, .00000)  
( .00928WVL) RN=( 3.44705, .00000) PH0=( .20104, .00000)  
-L 13--XL= 1.45000  
PE=( 13.24960, .00000) PM=( 1.00000, .00000)  
L 14 TL=.00700 QN=( 13.24960, .00000) YN=( 1.00000, .00000)  
( .00866WVL) RN=( 3.64000, .00000) PH0=( .19814, .00000)  
-L 14--XL= 1.45700  
PE=( 11.88219, .00000) PM=( 1.00000, .00000)  
L 15 TL=.00750 QN=( 11.88219, .00000) YN=( 1.00000, .00000)  
( .00928WVL) RN=( 3.44705, .00000) PH0=( .20104, .00000)  
-L 15--XL= 1.46450  
PE=( 11.76005, .00000) PM=( 1.00000, .00000)  
L 16 TL=.01500 QN=( 11.76005, .00000) YN=( 1.00000, .00000)  
( .01856WVL) RN=( 3.42929, .00000) PH0=( .40000, .00000)  
-L 16--XL= 1.47950  
PE=( 11.63854, .00000) PM=( 1.00000, .00000)  
L 17 TL=.01500 QN=( 11.63854, .00000) YN=( 1.00000, .00000)  
( .01856WVL) RN=( 3.41153, .00000) PH0=( .39793, .00000)  
-L 17--XL= 1.49450  
PE=( 11.51766, .00000) PM=( 1.00000, .00000)  
L 18 TL=.01500 QN=( 11.51766, .00000) YN=( 1.00000, .00000)  
( .01856WVL) RN=( 3.39377, .00000) PH0=( .39586, .00000)  
-L 18--XL= 1.50950  
PE=( 11.39741, .00000) PM=( 1.00000, .00000)  
L 19 TL=.01500 QN=( 11.39741, .00000) YN=( 1.00000, .00000)  
( .01856WVL) RN=( 3.37601, .00000) PH0=( .39379, .00000)  
-L 19--XL= 1.52450  
PE=( 11.27779, .00000) PM=( 1.00000, .00000)  
L 20 TL=.01500 QN=( 11.27779, .00000) YN=( 1.00000, .00000)

L 20 PE=( .01856WVL) RN=( 3.35824, .00000) PH0=( .39172, .00000)  
 -L 20---XL= 1.53950-----  
 PE=( 11.15881, .00000) PM=( 1.00000, .00000)  
 L 21 TL= .01500 QN=( 11.15881, .00000) YN=( 1.00000, .00000)  
 ( .01856WVL) RN=( 3.34048, .00000) PH0=( .38964, .00000)  
 -L 21---XL= 1.55450-----  
 PE=( 11.04045, .00000) PM=( 1.00000, .00000)  
 L 22 TL= .01500 QN=( 11.04045, .00000) YN=( 1.00000, .00000)  
 ( .01856WVL) RN=( 3.32272, .00000) PH0=( .38757, .00000)  
 -L 22---XL= 1.56950-----  
 PE=( 10.92273, .00000) PM=( 1.00000, .00000)  
 L 23 TL= .01500 QN=( 10.92273, .00000) YN=( 1.00000, .00000)  
 ( .01856WVL) RN=( 3.30496, .00000) PH0=( .38550, .00000)  
 -L 23---XL= 1.58450-----  
 PE=( 10.80564, .00000) PM=( 1.00000, .00000)  
 L 24 TL= .01500 QN=( 10.80564, .00000) YN=( 1.00000, .00000)  
 ( .01856WVL) RN=( 3.28719, .00000) PH0=( .38343, .00000)  
 -L 24---XL= 1.59950-----  
 PE=( 10.68918, .00000) PM=( 1.00000, .00000)  
 L 25 TL= .00750 QN=( 10.68918, .00000) YN=( 1.00000, .00000)  
 ( .00928WVL) RN=( 3.26943, .00000) PH0=( .19068, .00000)  
 -L 25---XL= 1.60700-----  
 PE=( 10.68918, .00000) PM=( 1.00000, .00000)  
 L 26 TL= 1.20000 QN=( 10.68918, .00000) YN=( 1.00000, .00000)  
 ( 1.48515WVL) RN=( 3.26943, .00000) PH0=( 30.50857, .00000)  
 -L 26---XL= 2.80700-----  
 L2=26---BOUNDRY FOR SECOND BOUNDARY CONDITION-----  
 PE=( 13.49305, .00000) PM=( 1.00000, .00000)  
 L 27 SEMI-INFINITE QN= 13.49305, .00000 YN=( 1.00000, .00000)  $\Rightarrow$  GA AS  
 RN=( 3.67329, .00000)

1-1  
1-2  
This is the file 63921da (air is the outer boundaries)  
with MODOUT = 1

Case #2

```
CASE KASE=MINIPROJECT (1)
CASE EPS1=1E-7 GAMEPS=1E-3 QZMR=11.0206
CASE PRINTF=0 INITGS=0 AUTOQW=0 NFPLT=1 QZMI=0.0
FFPLT=1

MODCON KPOL=1 APB1=0.25 APB2=0.25
```

```
STRUCT NQW=3.64 WVLL=808
STRUCT GRW=.15 QW=.0070
STRUCT ALPERC1=.6 ALPERC2=0.3
```

```
→ LAYER NREAL=1 !Air
LAYER ALPERC=.00 TL=0.5 !GaAs substr
LAYER ALPERC=^1 TL=1.3 !n-Clad
LAYER ALPERC=^1 !1st (n)GRINSCH
LAYER NSLC=10 !
LAYER ALPERC=^2 !
LAYER QWS=1 !QW GaAs-LAYER
LAYER ALPERC=^2 !2nd (p)GRINSCH
LAYER NSLC=10 !
LAYER ALPERC=^1 TL=1.2 !!
LAYER ALPERC=^1 TL=1.2 !2nd p-Clad
LAYER ALPERC=.00 TL=0.5 !GaAs Cap
LAYER NREAL=1 !Air
```

```
OUTPUT PHMO=1 GAMMAAO=1 WZRO=1 QZRO=1 QZIO=0
OUTPUT FWHFPNO=1 FWHRFO=1 KMO=1 ITO=1
OUTPUT SPLTFL=1 MODOUT=1 LYROUT=1
GAMOUT LAYGAM=15 COMPGAM=0 GAMALL=0
```

```
!LOOPX1 ILX="TL" FINV=0.0 XINC=-0.05 LAYCH=30
!LOOPZ1 ILZ="GRW" FINV=.4 ZINC=.01
!LOOPZ2 ILZ="WVL" FINV=0.955 ZINC=-0.005
```

1,0

2

1,0

2

1,0

2

```

!LOOPZ1 ILZ='QZMR' FINV=10.9 ZINC=-.1!THIS LOOPS TO FIND INITIAL GUESS
!LOOPZ1 ILZ='GRW' FINV=.202 ZINC=.001
!LOOPZ1 ILZ='ALPERCI' FINV=.401 ZINC=.0005
!LOOPX1 ILX='TL' FINV=.15 XINC=.01 LAYCH=.33
!LOOPX1 ILX='TL' FINV=.0 XINC=.01 LAYCH=.34
END

```

This is the beginning of the output that is produced when the flag MODOUT = 1

To find this output, open the file `6392lda_OUTPUT`

MODEIG/II  
version 1.4  
Revised: October 2, 1991

CASE NO. 01

SUMMARY OF LAYERED STRUCTURE, POLARIZATION, AND BOUNDARY CONDITIONS./  
 IMPLIED UNIT OF LENGTH XU= 0.10000D-05 METERS (BUT NOT USED EXPLICITLY). ALL QUANTITIES NORMALIZED.  
 NOMINAL WAVELENGTH WVL= 80800 XU, AND FREE-SPACE KO= 2PI/WVL= 7.77622 RAD/XU.  
 COMPLEX FREQUENCY FACTOR KC=( 1.00000, .00000). EFFECTIVE-KO= KC\*KO= ( 7.77622, .00000).  
 ALL PROPAGATION COEFFICIENTS ARE NORMALIZED TO EFFECTIVE-KO. (WAVE AND MATERIAL REFRACTIVE INDIC  
 UITY)  
 (WAVE ADMITTANCE(TE) AND IMPEDANCE(TM), YX AND YZ, ARE NORMALIZED TO THAT OF FREE SPACE.  
 NORMALIZED FREQUENCY KF=( 1.00000, .00000)= FREQ/C\*EFFEKO

POLARIZATION, KPOL=1 (=1 TE CASE, =2 TM CASE)  
 TRANSVERSE ELECTRIC CASE. EX=HY=EZ=0. TANGENTIAL FY=+EY, FZ=+HZ. TRANSVERSE FX=-HX, FY=+EY. LONGIT  
 $FZ=+HZ$ .  
 $YX=FZ/EY=HZ/EY$ . AND  $YZ=FX/FY=-HX/EY$  ARE WAVE ADMITTANCES  
 IN THE DIRECTION OF PROPAGATION.

LAYERED STRUCTURE. 29 LAYERS TOTAL. 28 BOUNDARIES. 27 FINITE LAYERS.

PE=( 1.00000, .00000) PM=( 1.00000, .00000)  
 L 1 SEMI-INFINITE QN=( 1.00000, .00000) YN=( 1.00000, .00000)  
 RN=( 1.00000, .00000)

---

**L1=1---BOUNDARY FOR FIRST BOUNDARY CONDITION**  
 -L 1---XL=.00000  
 PE=( 13.49305, .00000) PM=( 1.00000, .00000)  
 L 2 TL=.50000 QN=( 13.49305, .00000) YN=( 1.00000, .00000)  
 ( .61881WVL) RN=( 3.67329, .00000) PH0=( 14.28215, .00000)  
 -L 2---XL=.50000  
 PE=( 10.68918, .00000) PM=( 1.00000, .00000)  
 L 3 TL= 1.30000 QN=( 10.68918, .00000) YN=( 1.00000, .00000)  
 ( 1.60891WVL) RN=( 3.26943, .00000) PH0=( 33.05095, .00000)  
 -L 3---XL= 1.80000  
 PE=( 10.68918, .00000) PM=( 1.00000, .00000)  
 L 4 TL=.00750 QN=( 10.68918, .00000) YN=( 1.00000, .00000)  
 ( .00928WVL) RN=( 3.26943, .00000) PH0=( 19.068, .00000)  
 -L 4---XL= 1.80750  
 PE=( 10.80564, .00000) PM=( 1.00000, .00000)  
 L 5 TL=.01500 QN=( 10.80564, .00000) YN=( 1.00000, .00000)  
 ( .01856WVL) RN=( 3.28719, .00000) PH0=( .38343, .00000)  
 -L 5---XL= 1.82250  
 PE=( 10.92273, .00000) PM=( 1.00000, .00000)  
 L 6 TL=.01500 QN=( 10.92273, .00000) YN=( 1.00000, .00000)  
 ( .01856WVL) RN=( 3.30496, .00000) PH0=( .38550, .00000)  
 -L 6---XL= 1.83750  
 PE=( 11.04045, .00000) PM=( 1.00000, .00000)  
 L 7 TL=.01500 QN=( 11.04045, .00000) YN=( 1.00000, .00000)  
 ( .01856WVL) RN=( 3.32272, .00000) PH0=( .38757, .00000)  
 -L 7---XL= 1.85250  
 PE=( 11.15881, .00000) PM=( 1.00000, .00000)  
 L 8 TL=.01500 QN=( 11.15881, .00000) YN=( 1.00000, .00000)  
 ( .01856WVL) RN=( 3.34048, .00000) PH0=( .38964, .00000)  
 -L 8---XL= 1.86750  
 PE=( 11.27779, .00000) PM=( 1.00000, .00000)  
 L 9 TL=.01500 QN=( 11.27779, .00000) YN=( 1.00000, .00000)  
 ( .01856WVL) RN=( 3.35824, .00000) PH0=( .39172, .00000)  
 -L 9---XL= 1.88250  
 PE=( 11.39741, .00000) PM=( 1.00000, .00000)  
 L 10 TL=.01500 QN=( 11.39741, .00000) YN=( 1.00000, .00000)

11 2/2 3

5-4

( .01856WVL) RN=( 3.37601, .00000) PH0=( .39379, .00000)  
-L 10---XL= 1.89750 PE=( 11.51766, .00000) PM=( 1.00000, .00000)  
L 11 TL=.01500 QN=( 11.51766, .00000) YN=( 1.00000, .00000)  
( .01856WVL) RN=( 3.39377, .00000) PH0=( .39586, .00000)  
-L 11---XL= 1.91250 PE=( 11.63854, .00000) PM=( 1.00000, .00000)  
L 12 TL=.01500 QN=( 11.63854, .00000) YN=( 1.00000, .00000)  
( .01856WVL) RN=( 3.41153, .00000) PH0=( .39793, .00000)  
-L 12---XL= 1.92750 PE=( 11.76005, .00000) PM=( 1.00000, .00000)  
L 13 TL=.01500 QN=( 11.76005, .00000) YN=( 1.00000, .00000)  
( .01856WVL) RN=( 3.42929, .00000) PH0=( .40000, .00000)  
-L 13---XL= 1.94250 PE=( 11.88219, .00000) PM=( 1.00000, .00000)  
L 14 TL=.00750 QN=( 11.88219, .00000) YN=( 1.00000, .00000)  
( .00928WVL) RN=( 3.44705, .00000) PH0=( .20104, .00000)  
-L 14---XL= 1.95000 PE=( 13.24960, .00000) PM=( 1.00000, .00000)  
L 15 TL=.00700 QN=( 13.24960, .00000) YN=( 1.00000, .00000)  
( .00866WVL) RN=( 3.64000, .00000) PH0=( .19814, .00000)  
-L 15---XL= 1.95700 PE=( 11.88219, .00000) PM=( 1.00000, .00000)  
L 16 TL=.00750 QN=( 11.88219, .00000) YN=( 1.00000, .00000)  
( .00928WVL) RN=( 3.44705, .00000) PH0=( .20104, .00000)  
-L 16---XL= 1.96450 PE=( 11.76005, .00000) PM=( 1.00000, .00000)  
L 17 TL=.01500 QN=( 11.76005, .00000) YN=( 1.00000, .00000)  
( .01856WVL) RN=( 3.42929, .00000) PH0=( .40000, .00000)  
-L 17---XL= 1.97950 PE=( 11.63854, .00000) PM=( 1.00000, .00000)  
L 18 TL=.01500 QN=( 11.63854, .00000) YN=( 1.00000, .00000)  
( .01856WVL) RN=( 3.41153, .00000) PH0=( .39793, .00000)  
-L 18---XL= 1.99450 PE=( 11.51766, .00000) PM=( 1.00000, .00000)  
L 19 TL=.01500 QN=( 11.51766, .00000) YN=( 1.00000, .00000)  
( .01856WVL) RN=( 3.39377, .00000) PH0=( .39586, .00000)  
-L 19---XL= 2.00950 PE=( 11.39741, .00000) PM=( 1.00000, .00000)

L 20 TL=.01500 QN=( 11.39741, .00000) YN=( 1.00000, .00000)  
 ( .01856WVL) RN=( 3.37601, .00000) PH0=( .39379, .00000)  
 -L 20---XL= 2.02450-----  
 PE=( 11.27779, .00000) PM=( 1.00000, .00000)  
 L 21 TL=.01500 QN=( 11.27779, .00000) YN=( 1.00000, .00000)  
 ( .01856WVL) RN=( 3.35824, .00000) PH0=( .39172, .00000)  
 -L 21---XL= 2.03950-----  
 PE=( 11.15881, .00000) PM=( 1.00000, .00000)  
 L 22 TL=.01500 QN=( 11.15881, .00000) YN=( 1.00000, .00000)  
 ( .01856WVL) RN=( 3.34048, .00000) PH0=( .38964, .00000)  
 -L 22---XL= 2.05450-----  
 PE=( 11.04045, .00000) PM=( 1.00000, .00000)  
 L 23 TL=.01500 QN=( 11.04045, .00000) YN=( 1.00000, .00000)  
 ( .01856WVL) RN=( 3.32272, .00000) PH0=( .38757, .00000)  
 -L 23---XL= 2.06950-----  
 PE=( 10.92273, .00000) PM=( 1.00000, .00000)  
 L 24 TL=.01500 QN=( 10.92273, .00000) YN=( 1.00000, .00000)  
 ( .01856WVL) RN=( 3.30496, .00000) PH0=( .38550, .00000)  
 -L 24---XL= 2.08450-----  
 PE=( 10.80564, .00000) PM=( 1.00000, .00000)  
 L 25 TL=.01500 QN=( 10.80564, .00000) YN=( 1.00000, .00000)  
 ( .01856WVL) RN=( 3.28719, .00000) PH0=( .38343, .00000)  
 -L 25---XL= 2.09950-----  
 PE=( 10.68918, .00000) PM=( 1.00000, .00000)  
 L 26 TL=.00750 QN=( 10.68918, .00000) YN=( 1.00000, .00000)  
 ( .00928WVL) RN=( 3.26943, .00000) PH0=( .19068, .00000)  
 -L 26---XL= 2.10700-----  
 PE=( 10.68918, .00000) PM=( 1.00000, .00000)  
 L 27 TL= 1.20000 QN=( 10.68918, .00000) YN=( 1.00000, .00000)  
 ( 1.48515WVL) RN=( 3.26943, .00000) PH0=( 30.50857, .00000)  
 -L 27---XL= 3.30700-----  
 PE=( 13.49305, .00000) PM=( 1.00000, .00000)  
 L 28 TL=.50000 QN=( 13.49305, .00000) YN=( 1.00000, .00000)  
 ( .61881WVL) RN=( 3.67329, .00000) PH0=( 14.28215, .00000)  
 -L 28---XL= 3.80700-----  
 L 28---BOUNDRY FOR SECOND BOUNDARY CONDITION  
 PE=( 1.00000, .00000) PM=( 1.00000, .00000)  
 L 29 SEMI-INFINITE QN=( 1.00000, .00000) YN=( 1.00000, .00000)  
 RN=( 1.00000, .00000)

✓ ✓ ✓

2/23 (-6)

FIRST BOUNDARY CONDITION. L1= 1, KBC1= 1, KBD1= 2.

OPEN BOUNDARY, SEMI-INFINITE ADJACENT LAYER.  
PRINCIPAL BRANCH SPECIFICATION FOR WX. ANGLE APB=.250 PI, VECTOR VPB=( .707, .707), (WX\*DOT\*VPB.GE.0).  
EIGEN CONDITION. OUTWARD WAVE SOLUTION ONLY. (DIRECTION OF DECAY IF IM(WX).GT.0, OF PHASE PROPAGATI  
RE(WX).GT.0.)

SECOND BOUNDARY CONDITION. L2=28, KBC1= 1, KBD2= 2.

This is the file 63921d3 with MODOUT = 1  
 (The outer layers are 60% AlAs)

```
CASE KASE=MINIPROJECT(1)
CASE EPS1=1E-7 GAMEPS=1E-3 QZMR=11.0206
CASE PRINTF=0 INITGS=0 AUTOQW=0 NFPLT=1 QZMI=0.0
CASE PRPLT=1
```

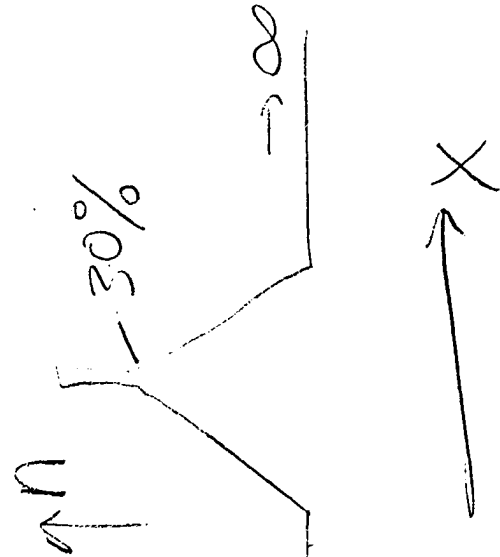
```
MODCON KPOL=1 APB1=0.25 APB2=0.25
```

```
STRUCT NQW=3.64 WVL=.808
STRUCT GRW=.15 QW=.0070
STRUCT ALPERC1=.6 ALPERC2=0.3
```

```
!LAYER NREAL=1
!LAYER ALPERC=.00 TL=0.5
!LAYER ALPERC=.1 !n-Clad
!LAYER NSLC=10 !1st (n)GRINSCH
!LAYER ALPERC=.2 !" !QW GaAs-LAYER
!LAYER QWS=1 !2nd (p)GRINSCH
!LAYER ALPERC=.2
!LAYER NSLC=10 !
!LAYER ALPERC=.1 TL=1.2 !2nd p-Clad
!LAYER ALPERC=.00 TL=0.5 !GaAs Cap
!LAYER NREAL=1 !Air
```

```
OUTPUT PHMO=1 GAMMAO=1 WZRO=1 QZIO=1 QZIO=0
OUTPUT FWHPNO=1 FWHPFO=1 KMO=1 ITO=1
OUTPUT SPLTFI=1 MODOUT=1 LYROUT=1
GAMOUT LAYGAM=13 COMPGAM=0 GAMALL=0
!LOOPX1 LX=TL FINV=0.0 XINC=-0.05 LAYCH=30
!LOOPZ1 LZ='GRW FINV=.4 ZINC=.01
!LOOPZ2 LZ='WVL FINV=0.955 ZINC=-0.005
```

```
!LOOPZ1 LZ='QZMR' FINV=10.9 ZINC=-.1!THIS LOOPS TO FIND INITIAL GUESS
```



2/23/91  
3/2/91

```
!LOOPZ1    ILZ='GRW'    FINV=.202      ZINC=.001
!LOOPZ1    ILZ='ALPERC1' FINV=.401      ZINC=.0005
!LOOPX1    ILX='TL'     FINV=.15       XINC=.01
!LOOPX1    ILX='TL'     FINV=.0       XINC=-.01   LAYCH=34
END
```

This is the beginning of the output that is produced when the flag MODOUT = 1

To find this output, open the file 63921d3\_OUTPUT\_

```
***** CALCULATION OF GENERAL COMPLEX*16 EIGEN-WAVES IN LAYERED STRUCTURES ****
* * * * * PROGRAM MODEIG ****
*****
```

MODEIG/I

version 1.4

Revised: October 2, 1991

CASE NO. 0.1

SUMMARY OF LAYERED STRUCTURE, POLARIZATION, AND BOUNDARY CONDITIONS./  
IMPLIED UNIT OF LENGTH XU=0.10000D-05 METERS (BUT NOT USED EXPLICITLY). ALL QUANTITIES NORMALIZED.  
NOMINAL WAVELENGTH WVL=.80800 XU, AND FREE-SPACE KO= 2PI/WVL= 7.77622 RAD/XU.  
COMPLEX FREQUENCY FACTOR KC=( 1.00000, .00000). EFFECTIVE-KO= KC\*KO=( 7.77622, .00000).  
ALL PROPAGATION COEFFICIENTS ARE NORMALIZED TO EFFECTIVE-KO. (WAVE AND MATERIAL REFRACTIVE INDIC  
UNITY)  
(WAVE ADMITTANCE(TE) AND IMPEDANCE(TM), YX AND YZ, ARE NORMALIZED TO THAT OF FREE SPACE.  
NORMALIZED FREQUENCY KF=( 1.00000, .00000)= FREQ/C\*EFF.KO.

POLARIZATION, KPOL=1 (=1 TE CASE, =2 TM CASE)  
TRANSVERSE ELECTRIC CASE. EX=HY=HZ=0. TANGENTIAL FY=+EY, FZ=+HZ. TRANSVERSE FX=-HX, FY=+EY. LONGIT  
FZ=+HZ.  
YX=FZ/FY=+HZ/EY, AND YZ=FX/FY=-HX/EY, ARE WAVE ADMITTANCES. (IN THE POS X, Z, OR WAVE DIRECTION).

LAYERED STRUCTURE. 25 LAYERS TOTAL. 24 BOUNDARIES. 23 FINITE LAYERS.

PE=( 10.68918, .00000) PM=( 1.00000, .00000)

L 1 SEMI-INFINITE QN=(-10.68918, .00000) YN=( 1.00000, .00000)  $\Rightarrow$  60% AlAs  
 L1= 1---BOUNDARY FOR FIRST BOUNDARY CONDITION-----  
 -L 1---XL=.00000 PE=(-10.68918, .00000) PM=(-1.00000, .00000)  
 L 2 TL=.00750 QN=(-10.68918, .00000) YN=(-1.00000, .00000)  
 (.00928WVL) RN=(-3.26943, .00000) PH0=(-1.9068, .00000)  
 -L 2---XL=.00750 PE=(-10.80564, .00000) PM=(-1.00000, .00000)  
 L 3 TL=.01500 QN=(-10.80564, .00000) YN=(-1.00000, .00000)  
 (.01856WVL) RN=(-3.28719, .00000) PH0=(-.38343, .00000)  
 -L 3---XL=.02250 PE=(-10.92273, .00000) PM=(-1.00000, .00000)  
 L 4 TL=.01500 QN=(-10.92273, .00000) YN=(-1.00000, .00000)  
 (.01856WVL) RN=(-3.30496, .00000) PH0=(-.38550, .00000)  
 -L 4---XL=.03750 PE=(-11.04045, .00000) PM=(-1.00000, .00000)  
 L 5 TL=.01500 QN=(-11.04045, .00000) YN=(-1.00000, .00000)  
 (.01856WVL) RN=(-3.32272, .00000) PH0=(-.38757, .00000)  
 -L 5---XL=.05250 PE=(-11.15881, .00000) PM=(-1.00000, .00000)  
 L 6 TL=.01500 QN=(-11.15881, .00000) YN=(-1.00000, .00000)  
 (.01856WVL) RN=(-3.34048, .00000) PH0=(-.38964, .00000)  
 -L 6---XL=.06750 PE=(-11.27779, .00000) PM=(-1.00000, .00000)  
 L 7 TL=.01500 QN=(-11.27779, .00000) YN=(-1.00000, .00000)  
 (.01856WVL) RN=(-3.35824, .00000) PH0=(-.39172, .00000)  
 -L 7---XL=.08250 PE=(-11.39741, .00000) PM=(-1.00000, .00000)  
 L 8 TL=.01500 QN=(-11.39741, .00000) YN=(-1.00000, .00000)  
 (.01856WVL) RN=(-3.37601, .00000) PH0=(-.39379, .00000)  
 -L 8---XL=.09750 PE=(-11.51766, .00000) PM=(-1.00000, .00000)  
 L 9 TL=.01500 QN=(-11.51766, .00000) YN=(-1.00000, .00000)  
 (.01856WVL) RN=(-3.39377, .00000) PH0=(-.39586, .00000)  
 -L 9---XL=.11250 PE=(-11.63854, .00000) PM=(-1.00000, .00000)  
 L 10 TL=.01500 QN=(-11.63854, .00000) YN=(-1.00000, .00000)  
 (.01856WVL) RN=(-3.41153, .00000) PH0=(-.39793, .00000)

"2/23"

"2-7D"

-L 10---XL=.12750  
PE=( 11.76005, .00000) PM=(- 1.00000, .00000)  
L 11 TL=.01500 QN=( 11.76005, .00000) YN=(- 1.00000, .00000)  
( .01856WVL) RN=( 3.42929, .00000) PH0=(- .40000, .00000)  
-L 11---XL=.14250  
PE=( 11.88219, .00000) PM=(- 1.00000, .00000)  
L 12 TL=.00750 QN=( 11.88219, .00000) YN=(- 1.00000, .00000)  
( .00928WVL) RN=( 3.44705, .00000) PH0=(- .20104, .00000)  
-L 12---XL=.15000  
PE=( 13.24960, .00000) PM=(- 1.00000, .00000)  
L 13 TL=.00700 QN=( 13.24960, .00000) YN=(- 1.00000, .00000)  
( .00866WVL) RN=( 3.64000, .00000) PH0=(- .19814, .00000)  
-L 13---XL=.15700  
PE=( 11.88219, .00000) PM=(- 1.00000, .00000)  
L 14 TL=.00750 QN=( 11.88219, .00000) YN=(- 1.00000, .00000)  
( .00928WVL) RN=( 3.44705, .00000) PH0=(- .20104, .00000)  
-L 14---XL=.16450  
PE=( 11.76005, .00000) PM=(- 1.00000, .00000)  
L 15 TL=.01500 QN=( 11.76005, .00000) YN=(- 1.00000, .00000)  
( .01856WVL) RN=( 3.42929, .00000) PH0=(- .40000, .00000)  
-L 15---XL=.17950  
PE=( 11.63854, .00000) PM=(- 1.00000, .00000)  
L 16 TL=.01500 QN=( 11.63854, .00000) YN=(- 1.00000, .00000)  
( .01856WVL) RN=( 3.41153, .00000) PH0=(- .39793, .00000)  
-L 16---XL=.19450  
PE=( 11.51766, .00000) PM=(- 1.00000, .00000)  
L 17 TL=.01500 QN=( 11.51766, .00000) YN=(- 1.00000, .00000)  
( .01856WVL) RN=( 3.39377, .00000) PH0=(- .39586, .00000)  
-L 17---XL=.20950  
PE=( 11.39741, .00000) PM=(- 1.00000, .00000)  
L 18 TL=.01500 QN=( 11.39741, .00000) YN=(- 1.00000, .00000)  
( .01856WVL) RN=( 3.37601, .00000) PH0=(- .39379, .00000)  
-L 18---XL=.22450  
PE=( 11.27779, .00000) PM=(- 1.00000, .00000)  
L 19 TL=.01500 QN=( 11.27779, .00000) YN=(- 1.00000, .00000)  
( .01856WVL) RN=( 3.35824, .00000) PH0=(- .39172, .00000)  
-L 19---XL=.23950  
PE=( 11.15881, .00000) PM=(- 1.00000, .00000)  
L 20 TL=.01500 QN=( 11.15881, .00000) YN=(- 1.00000, .00000)

```

( .01856WVL) RN=( 3.34048, .00000) PH0=( .38964, .00000)
-L 20---XL=.25450-----PE=( 11.04045, .00000) PM=( 1.00000, .00000)
L 21 TL=.01500 QN=( 11.04045, .00000) YN=( 1.00000, .00000)
( .01856WVL) RN=( 3.32272, .00000) PH0=( .38757, .00000)
-L 21---XL=.26950-----PE=( 10.92273, .00000) PM=( 1.00000, .00000)
L 22 TL=.01500 QN=( 10.92273, .00000) YN=( 1.00000, .00000)
( .01856WVL) RN=( 3.30496, .00000) PH0=( .38550, .00000)
-L 22---XL=.28450-----PE=( 10.80564, .00000) PM=( 1.00000, .00000)
L 23 TL=.01500 QN=( 10.80564, .00000) YN=( 1.00000, .00000)
( .01856WVL) RN=( 3.28719, .00000) PH0=( .38343, .00000)
-L 23---XL=.29950-----PE=( 10.68918, .00000) PM=( 1.00000, .00000)
L 24 TL=.00750 QN=( 10.68918, .00000) YN=( 1.00000, .00000)
( .00928WVL) RN=( 3.26943, .00000) PH0=( .19068, .00000)
-L 24---XL=.30700-----PE=( 10.68918, .00000) PM=( 1.00000, .00000)
L2=24---BOUNDARY FOR SECOND BOUNDARY CONDITION
L 25 SEMI-INFINITE QN=( 10.68918, .00000) PM=( 1.00000, .00000)
( RN=( 3.26943, .00000) YN=( 1.00000, .00000)

```

FIRST BOUNDARY CONDITION. L1= 1, KBC1= 1, KBD1= 2.

OPEN BOUNDARY, SEMI-INFINITE ADJACENT LAYER.  
 PRINCIPAL BRANCH SPECIFICATION FOR WX. ANGLE APB=.250 PI, VECTOR VPB=( .707, .707), (WX\*DOT\*VPB.GE.0).  
 EIGEN CONDITION. OUTWARD WAVE SOLUTION ONLY. (DIRECTION OF DECAY IF IM(WX).GT.0, OF PHASE PROPAGATI  
 RE(WX).GT.0.)

$\Rightarrow 60\% \text{ of } A_2$

### CASE 1

This is the DBASE file for input file 6392ldi (outer layers are semi-infinite GaAs layers)

*	PHM	GAMMA(14)	WZR	WZI	QZR	FWHPN	FWHPF	KM	IT
*	3.561981E-01	2.246067E-02	3.319740E+00	5.538958E-07	1.102067E+01	2.615820E-01	3.946414E+01	7	2

### CASE 2

This is the DBASE file for input file 6392lda (outer layers are semi-infinite air layers)

*	PHM	GAMMA(15)	WZR	WZI	QZR	FWHPN	FWHPF	KM	IT
*	4.248209E+00	2.246367E-02	3.319740E+00	-0.000000E-01	1.102067E+01	2.571319E-01	3.941710E+01	6	2

(note: phm is > 1 in the second case--- because there are numerous zero crossings of the field amplitude in the finite outer GaAs layers)

### CASE 3

This is the DBASE file for input file 6392ld3 (outer layers are semi-infinite and contain 60% AlAs layers)

*	PHM	GAMMA(13)	WZR	WZI	QZR	FWHPN	FWHPF	KM	IT
*	3.561746E-01	2.245564E-02	3.319740E+00	-0.000000E-01	1.102067E+01	2.571334E-01	4.284460E+01	6	1

### SUMMARY:

	WZR	$\Gamma_{qW}$	FWHPN	FWHPF	PHM
#1:	3.319740E+00	2.246067E-02	2.615820E-01	3.946414E+01	3.561981E-01
#2:	3.319740E+00	2.246367E-02	2.571319E-01	3.941710E+01	4.248209E+00
#3:	3.319740E+00	2.245564E-02	2.571334E-01	4.284460E+01	3.561746E-01

## M<sup>2</sup>, WHAT IS IT AND WHY DO I CARE?

by  
 Carlos B. Roundy, Ph.D.,  
 President  
 Spiricon, Inc.

### I. INTRODUCTION

Most laser engineers and scientists are familiar with today's standard methods of characterizing a laser beam. Parameters such as beam width, position, divergence angle, Gaussian fit, etc. have sufficed for many users in a large number of applications.

M<sup>2</sup> is one more parameter that can enable a user to quantitatively evaluate the performance of his laser. The primary advantage of M<sup>2</sup> is that it predicts the focusability of the laser beam in a way that is more precise than other laser parameters. For all laser users to whom the properties of the focused beam are important, M<sup>2</sup> is a very useful number to measure. Once measured, it is very easy to use in predicting focused spot properties.

### II. WHAT IS M<sup>2</sup> \* (and k\*\*) ?

M<sup>2</sup>, or k ( $k = 1/M^2$ ) is a measure of the quality of a laser beam. M<sup>2</sup> and k define how close an actual beam is to a perfect Gaussian single mode beam. A perfect beam has M<sup>2</sup> = k = 1, whereas an imperfect beam will have M<sup>2</sup> greater than 1 and k less than 1. M<sup>2</sup> and k definitions are an attempt by the international community, through the ISO committee, to arrive at a quantitative standard by which the relative quality of all laser beams can be determined. The ISO committee has generated preliminary definitions of M<sup>2</sup> and k, and how they are to be measured. This ISO definition is expected to become an international standard for the measurement and comparison of laser quality.

### III. WHY IS M<sup>2</sup> (and k) IMPORTANT?

A pure Gaussian beam with M<sup>2</sup> = 1 is typically considered a "perfect" laser beam. When M<sup>2</sup> is greater than one, this tells the user how far his beam is from the ideal, and that it contains modes in addition to the fundamental. On occasion the multimode beam can appear Gaussian when observed visually, even though it contains significant percentages of higher order modes. Thus, a measure of M<sup>2</sup> can often tell a user more than a Gaussian fit or visual observation.

\*M<sup>2</sup> is formally defined as the "times diffraction limit" factor  
 \*\*k is defined as the "beam propagation factor"

A "good" laser beam with minor distortion typically has an M<sup>2</sup> between 1.1 and 1.4. Higher mode content beams have M<sup>2</sup> ranging from 2 to 5, and even higher.

Typically, when laser modes other than the fundamental Gaussian are present, the beam does not focus as sharply as if it were a pure Gaussian beam. For example, when focusing an ideal beam through an ideal lens of a given focal length, the expected waist size or focal spot size is predictable by the equation:

$$d_0 = 2\lambda f/A$$

where d<sub>0</sub> = diameter of the focused spot,  $\lambda$  = wavelength, f = focal length of the lens, and A = the lens aperture that contains 99% of the input beam. This is shown in Figure 1. Notice that the larger the input beam to the lens, the smaller the focused spot size will be.

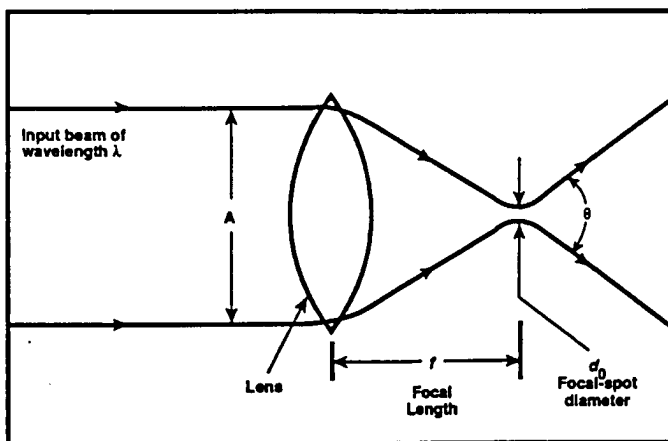


Figure 1. The diffraction-limited spot size at the focus of a lens for a pure Gaussian beam with M<sup>2</sup>=1.

However, if the beam contains modes other than the fundamental Gaussian, then the spot size becomes:

$$d_1 = M^2 \lambda f / A$$

which is M times larger than would be obtained with a fundamental mode Gaussian beam of the same input size. This is

illustrated in Figure 2. Note that the intensity density at the beam waist becomes  $M^2$  lower than expected for a pure Gaussian beam. Another measure of laser quality, the divergence angle of the beam in the far field, is also affected by  $M^2$ . This angle is  $\Theta = M\theta$ , where  $\Theta$  = the real divergence angle, and  $\theta$  = divergence angle of the fundamental mode. Thus the laser beam diverges  $M$  times faster than the fundamental mode, and the intensity density is  $M^2$  less than otherwise. This increased divergence is also shown in Figure 2.

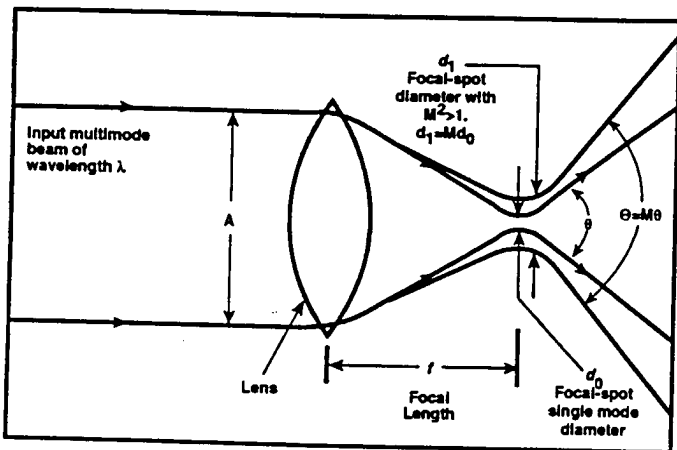


Figure 2. The diffraction-limited spot size at the focus of a lens for a beam with  $M^2$  greater than 1.

#### IV. WHAT IS THE EFFECT OF $M^2$ ON A PARTICULAR APPLICATION?

There are many applications wherein the laser is focused to a small spot. These include industrial, cutting, welding, drilling, and marking, etc. They also include scientific applications wherein the high intensity light is focused to interact with matter. Many lasers also use a pump laser that is focused into another material. This can provide doubling or tripling of the laser frequency, optical parametric oscillators, generation of multiple wavelengths through dyes, and many other such applications.

Depending on the  $M^2$  of the laser, the spot may not focus as tight as expected, and the intensity density will be  $M^2$  less than expected. In the case of industrial cutting applications, the holes may be larger than desired, and may not penetrate as deeply as would be the case with a pure beam. In scientific applications, the experiment often depends upon the intensity squared or cubed. The actual intensity being  $M^2$  less than the ideal would create an error of  $M^4$  or  $M^6$  in the expected results. Thus an  $M^2$  of 1.5 could create an error greater than 3.37 X, or 237%. Another application might be laser range finding. In this case the laser beam would diverge  $M$  times faster than a pure Gaussian, and provide an  $M^2$  lower intensity at the target.

#### V. WHY NOT MEASURE THE FOCUSED BEAM WIDTH AND INTENSITY DIRECTLY, AND NOT BOTHER WITH $M^2$ ?

First of all, the focused spot may be too small to measure with any convenient instrumentation. Also, the focused spot may not be readily accessible to measurement instrumentation.

Finally, the greatest need for the measurement of  $M^2$  is that once this parameter is measured, a person is able to predict what the beam will do in many other situations. For example, if the focal length of the lens is changed, one can scale the effect and predict the change in the focused spot size and intensity.

#### VI. HOW IS $M^2$ MEASURED?

$M^2$  is measured on real beams by focusing the beam with a lens of known focal length, and then measuring the characteristics of the artificially created beam waist and divergence. These measurements are then projected back to the laser properties through equations that take into account the focusing lens. The important characteristics to be measured are:

1. Size of the focused spot
2. The divergence angle of the beam beyond focus
3. The position of the focused spot relative to the lens
4. The beam size at the focal length of the lens

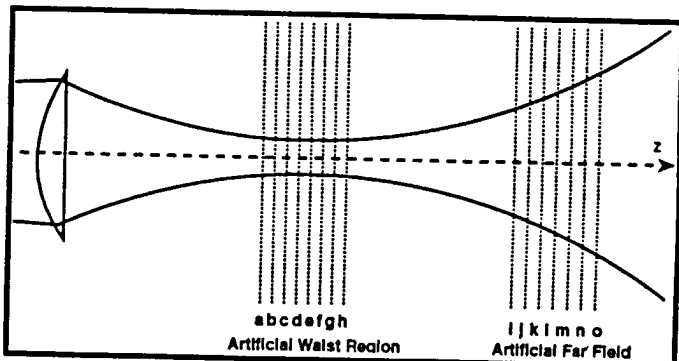


Figure 3. Multiple beam width measurements made by  $M^2$ -101.

To provide an accurate calculation of  $M^2$  it is valuable to make a number of measurements in the focused beam waist region, and a number of measurements in the far field. These measurements are illustrated in Figure 3. The multiple measurements ensure that the minimum beam width is found. In addition, the multiple measurements enable a "curve fit" that improves the accuracy of the calculations by minimizing measurement error at any single point. An accurate calculation of  $M^2$  and other laser characteristics can be made by using the data from the multiple beam width measurements, coupled with the known characteristics of the focusing lens.

## VII. WHAT ARE SOURCES OF ERROR IN M<sup>2</sup> MEASUREMENTS?

If a measurement and calculation of the laser M<sup>2</sup> is to be useful, it must be measured accurately. There are a number of sources of potential error in this measurement. These sources are described, and an explanation is given of how Spiricon engineers have gone to great lengths to minimize these errors.

One of the greatest errors in measuring M<sup>2</sup> comes from measurements of the beam widths. The ISO committee has defined a "second moment" method as the most theoretically correct definition of beam width. However, the "second moment" is not practical to measure in real situations, and the current consensus is that using a "knife-edge" method is the most practical. It can be related back to the "second moment" method. Spiricon's LBA-100A employs the knife-edge method using software algorithms on the data taken from a CCD camera. These measurements are performed in both the X and Y axes of the beam to enable characterization of non-symmetrical beams.

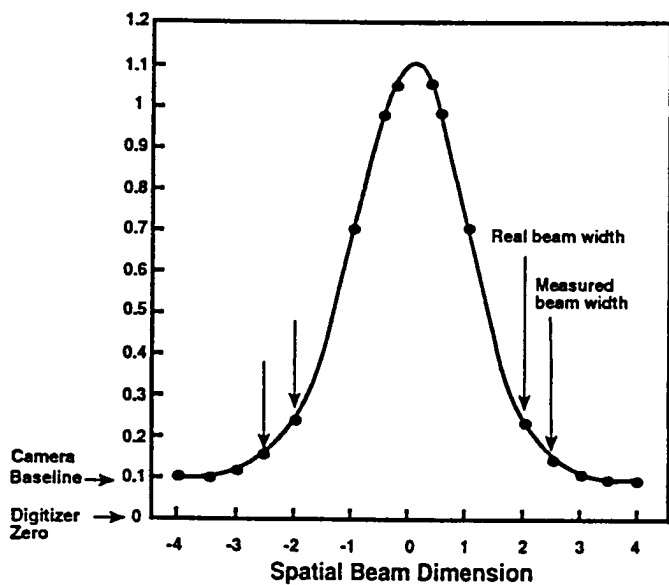


Figure 4. Beam width measurement errors with positive baseline offset.

The knife-edge beam width measurement method is, however, prone to significant errors if the "background" or "baseline" of the CCD camera is not adjusted correctly. For example, if the baseline is set too high, as in Figure 4, the measured beam width will be much larger than the actual beam width. Spiricon's LBA-100A uses a very sophisticated (patent pending) "Autocalibrate" method to ensure that background errors do not contribute to beam width measurement errors. This "Autocalibrate" is extremely important because at the beam focus, or waist, the beam may cover only a few pixels of the CCD camera. A slight error in

background over the many non-illuminated pixels could generate a response equal to, or greater than the real signal, and create significant error.

A second potential source of error can come from inaccuracies in the measurement of the Z axial distances from the lens. Accurate calibration of the sample point location and repeatability are essential features of the M<sup>2</sup>-101. Special calibration fixtures are used to accurately align and measure the path distances. A precision lead screw and stepper motor are employed to yield accurate and repeatable translation steps.

Another possible source of error can occur if the laser beam is truncated by an aperture. The resulting diffraction of the laser beam will alter the M<sup>2</sup> results. The effects can range from slight, rather significant, and even to M<sup>2</sup> values that may be less than 1. Beams that contain even small amounts of aperture induced diffraction are difficult to measure accurately. The user should be mindful of this effect and weigh the results accordingly.

Finally, the ISO method of M<sup>2</sup> measurement specifies that a lens should be placed at a fixed position in the beam path, and then the measurements made at specified distances from the lens. Some commercial M<sup>2</sup> measuring instruments employ a fixed position detector, and then move the lens in the beam. In some cases this gives a result similar to a fixed position lens. However, in many cases the laser beam is diverging or changing in some other way over the travel range of the lens. When this happens the reported M<sup>2</sup> value and other results can be significantly compromised. Also, depending upon where the instrument is placed in the beam, it may yield significantly different results. Spiricon uses a fixed position lens to eliminate this potential error source.

## VIII. HOW DO SPIRICON'S M<sup>2</sup>-101 AND LBA-100A MEASURE M<sup>2</sup>?

Spiricon has implemented the ISO recommended procedure for the measurement of M<sup>2</sup>. It uses a fixed position lens, and a method to effectively translate the camera through the beam waist and through the far field. It also uses "knife-edge" beam width measurement algorithms in X and Y axes to approximate the "second moment" beam width. Spiricon's M<sup>2</sup>-101 instrument implements the translation required to make the multiple position measurements in a unique way. On the M<sup>2</sup>-101 both the lens and the CCD camera are mounted at fixed positions on one end of the instrument housing. Inside the instrument is a table on which mirrors are mounted that direct the focused beam onto the camera. The table is connected to a very precise lead screw that is driven by a stepper motor. By translating the table in preset increments, a series of beam width measurements is obtained along the path of the focused beam as illustrated in Figure 3.

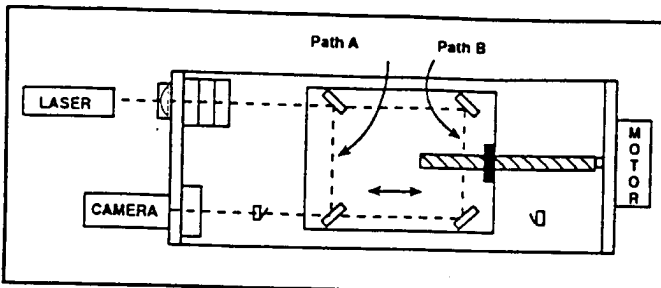


Figure 5. Dual path mirrors inside M<sup>2</sup>-101 for measurement of beam waist, Path A, and far field, Path B.

There are two sets of mirrors mounted on the translation table. One set, close to the input lens labeled "path A" in Figure 5, enables measurements in the "beam waist" region. These mirrors are then automatically removed from the beam path, which enables measurements in the far field over "path B" in Figure 5. All of these measurements are automatically controlled by software in the LBA-100A. As mentioned earlier, the accurate measurement of beam width is a critical part of M<sup>2</sup> measurement. Spiricon's very sophisticated "Autocalibrate" algorithm makes these measurements as accurately as today's technology permits.

Spiricon uses a CCD camera in these measurements, because it allows simultaneous measurements of the entire beam. This enables the M<sup>2</sup>-101 to characterize the M<sup>2</sup> on both CW and pulsed beams. (Other commercial instruments measure the width using an actual moving knife-edge, and thus cannot measure pulsed beams.) Besides using "Autocalibrate", Spiricon has implemented other sophisticated methods to ensure accurate measurements. These include automatic "PAN" and "ZOOM" of the camera to the ideal measurement location, automatic attenuation of the beam for optimum intensity measurements, and use of apertures around the beam to exclude extraneous noise and stray scattered light from other sources.

Once the multiple beam widths are acquired from the translation table, a curve fitting algorithm is used to determine the parameters of the beam propagation equation per the ISO procedure. Figure 6 shows the LBA-100A screen printout, wherein the upper right corner illustrates the measured points and the curve fit to the points. The M<sup>2</sup> values are calculated based upon the curve fit. By displaying the individual points along with the curve fit, the user can be alerted to any potential discrepancies. For example, if the laser changed characteristics (such as mode hopping), during the measurement, the changes would be displayed on the screen, and the operator could take appropriate action.

One might ask why Spiricon's M<sup>2</sup>-101 instrument is so large. The reason for this is that the instrument was designed to achieve the maximum possible accuracy and reliability consistent with CCD camera technology. A relatively long focal length lens, typically 400mm, was chosen so that the beam waist would be large enough to be accurately measured with a CCD camera. The steering

mirrors of Figure 5 are high quality front surface mirrors that direct the beam path with no distortion. No optical components are used to compress the beam path that would potentially distort the measurement. Using a dual set of mirrors, the instrument implements an equivalent straight rail length of 1270mm in a housing 720mm long. There has been no compromise of accuracy in the M<sup>2</sup>-101 for any other potentially desirable feature.

## IX. WHAT OTHER MEASUREMENTS ARE PROVIDED BY THE M<sup>2</sup>-101 BESIDES M<sup>2</sup>?

The measurement of M<sup>2</sup> simultaneously enables the measurement of other useful laser parameters. Shown in Figure 6 on the left side of the screen display are the measurements made by the LBA-100A, in combination with the M<sup>2</sup>-101. Under the section titled "Artificial Waist Region" are listed the results of measurements actually made inside the M<sup>2</sup>-101. Under the section titled "Laser Properties" are the computed characteristics of the laser under test. These are arrived at by mathematically translating the focused beam propagation results back across the lens to the real laser propagation parameters.

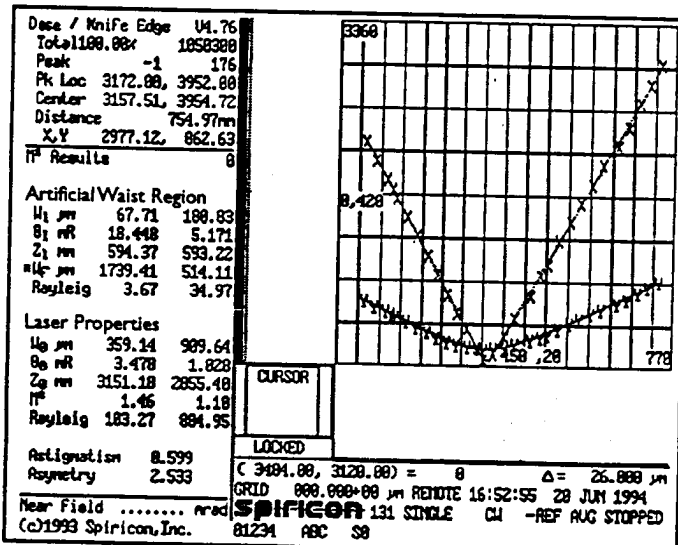


Figure 6. Display of M<sup>2</sup> measurement points and curve fit (upper right) and M<sup>2</sup> calculations (lower left) of a laser diode.

In the "Artificial Waist Region" section the following results are displayed.

1. W<sub>1</sub> are the X and Y waist widths derived from the curve fit.
2. θ<sub>1</sub> are the X and Y full divergence angles of the beam in milliradians, derived from the curve fit.
3. Z<sub>1</sub> is the distance in mm from the lens to the X and Y beam waist, derived from the curve fit.
4. W<sub>f</sub> are the X and Y beam widths at the focal length of the lens. These values can be either directly measured or computed from the resulting curve fit.
5. Rayleigh is the Rayleigh range of the artificial waist region.

Under "Laser Properties" the following displayed results are given for the laser under test, i.e. before being focused by the lens of the M<sup>2</sup>-101 instrument. These are calculated from the characteristics of the focusing lens and the measurements made inside the M<sup>2</sup>-101.

1. W<sub>0</sub> are the X and Y widths of the laser beam at its natural beam waist.
2. θ<sub>0</sub> are the X and Y divergence angles in milliradians of the laser beam.
3. Z<sub>0</sub> is the location of the laser beam waist in mm, measured either from the laser face plate or from the M<sup>2</sup>-101 input face plate.
4. M<sup>2</sup> is the X and Y axis M<sup>2</sup> of the laser beam, computed from the curve fit of the artificial beam.
5. Rayleigh is the Rayleigh range of the laser beam in mm. The Rayleigh range is the distance from the original beam waist to the point where the diameter increases to  $\sqrt{2}$  times the diameter of the waist.
6. Astigmatism is a value that relates how closely the X and Y beam waist widths coincide. Values near 0 indicate that the X and Y waists are located at approximately the same location. A value near 1 indicates that the beam waists are separated by about 1 Rayleigh range.
7. Asymmetry is a ratio of the X and Y beam waists dimensions. A value near 1 suggests that the beam is nearly circular. Values greater than 1 imply an elliptical beam geometry.

## X. WHAT DOES SPIRICON CONTRIBUTE WITH ITS M<sup>2</sup> LASER BEAM ANALYSIS?

Laser beam diagnostics can be divided into two basic functions; visual and quantitative. Spiricon has been the technology leader in providing highly illuminating visual displays of laser beams. These real-time displays combine to give a user the most effective way to visualize his beam and take whatever action these visual displays may dictate. Spiricon has also been the leader in providing quantitative measurements with great precision. Measurements of beam width, position, divergence angle, Gaussian fit, Top Hat characteristics, and statistics have sufficed for many users in a large number of applications.

In addition to the above measurements, the measurement of M<sup>2</sup> enables a user to quantitatively evaluate the "focussability" of the laser beam in a way that is more precise than other laser parameters. Spiricon is providing the instrumentation to accurately measure this parameter.

Spiricon, however, does not stop at just the measurement of M<sup>2</sup>. In addition, a user can view each individual measured frame through the waist and into the far field, in 2D or 3D display. This feature allows the user to "see" exactly what his beam is doing as it goes through focus. This feature can be most crucial, since a visual view of the beam can tell a user more than the single M<sup>2</sup> quantitative number. This is demonstrated for a diode laser, in Figure 7.

Spiricon's implementation of the M<sup>2</sup> measurement overcomes many of the objections of earlier M<sup>2</sup> instrumentation, and adds some highly illuminating new features. These include:

1. M<sup>2</sup> can be measured on pulsed, as well as CW lasers.
2. The M<sup>2</sup>-101 uses a fixed position lens to give reliable, consistent measurements.
3. The measured points are plotted on a large, easy to read graph, along with the curve fit, that allows easy visual interpretation of the results.
4. A user can step through the saved measurement points, and display the precise X and Y beam widths measured at each point along the focused beam path.

Knowledge of the M<sup>2</sup> value of your laser will facilitate the system designer's ability to predict how his laser and optical system will perform prior to fabricating expensive optical components. The visual displays from the M<sup>2</sup>-101 and LBA-100A will tell what the beam will look like in the "real world" conditions, but scaled in size by the actual focal length of the lens used. Thus, Spiricon continues its tradition of providing precise and useful instrumentation for the characterization of laser beams.

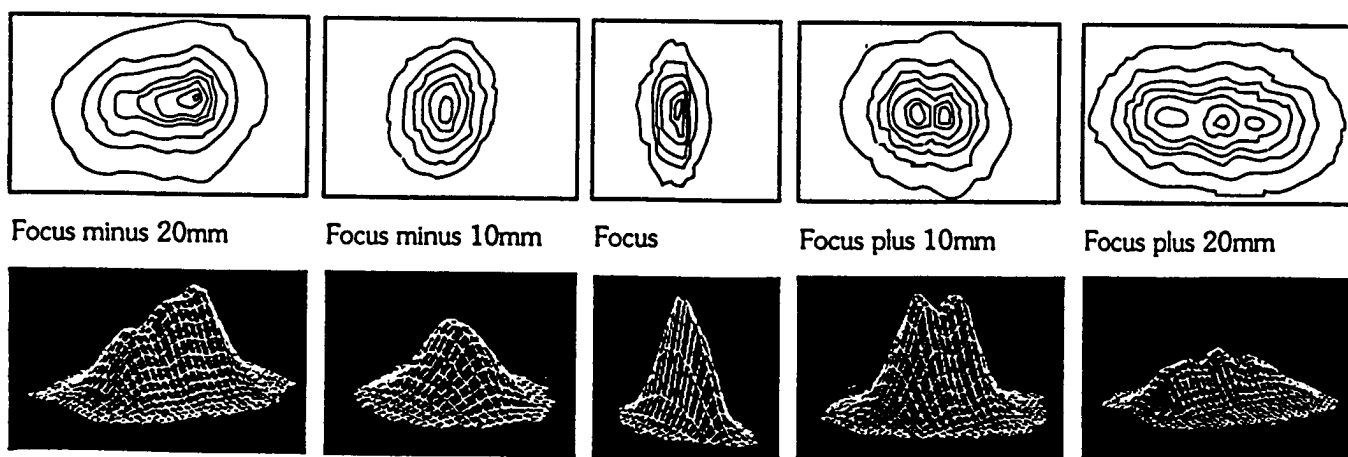


Figure 7. Display of beam profile patterns of diode laser through beam waist area. Upper: 2D displays. Lower: 3D displays.

## BIBLIOGRAPHY

1. International Organization for Standardization. (1993, November). Test methods for laser beam parameters: Beam widths, divergence angle and beam propagation factor. Document ISO/TC 172/SC 9/WG 1 N 56.
2. Johnston, Jr., T.F. (1990, May).  $M^2$  concept characterizes beam quality. Laser Focus World. pp. 173-183.
3. Jones, R.D., & Scott, T.R. (1994). Error propagation in laser beam spatial parameters. Optical and Quantum Electronics. 26, pp. 25-34.
4. Lawrence, G.N. (1994, July). Proposed international standard for laser-beam quality falls short. Laser Focus World. pp. 109-114.
5. Roundy, C.B., Slobodzian, G.E., Jensen, K. & Ririe, D. (1993, October). Digital imaging produces fast and accurate beam diagnosis. Laser Focus World. pp. 117-125.
6. Siegman, A.E., (1986). Lasers. University Science Books. Chapter 17.
7. Siegman, A.E., Sasnett, M.W. & Johnston, Jr. T.F. (1991, April). Choice of clip level for beam width measurements using knife-edge techniques. IEEE Journal of Quantum Electronics. Vol. 27, No. 4.



Spiricon, Inc. • 2600 North Main • Logan, Utah 84341 (801)753-3729 • FAX (801) 753-5231

© Copyright October, 1994, Spiricon, Inc., Logan, Utah • All Rights Reserved. Printed in the USA 10/94

*"2/23"* a

## ENGINEERING STUDENTS

### UNDERGRADUATES AND GRADUATES:

Meet **Dr. Ivan P. Kaminow**, AT&T Bell Laboratories (Friday's Spring Seminar Speaker) at **11:00 am in Studio 1** (Room 125 Caruth) before his 2:00 pm talk in Hughes-Trigg

Dr. Kaminow is meeting with the EE 6392 (photonic waveguides) class from 11:00 to 11:50 on Friday, February 26 for informal discussions. Come and ask one of the pioneering researchers in the fields of lasers and electrooptics his views on the future.

- will careers be different?
- are there any jobs out there?
- where/what are the opportunities?

(For information see Gary Evans, x83032, room 319 or any EE 6392 student)



## S M U - S E A S SPRING SEMINAR SERIES

February 26, 1993  
Hughes-Trigg Forum  
2:00 pm

### *Gigabit/s Lightwave Networks*

Ivan P. Kaminow  
AT&T Bell Laboratories  
Holmdel, New Jersey 07733

#### ABSTRACT

Lightwave technology employing optical fiber transmission lines is widely deployed in the US and throughout the world to provide high bit-rate telecommunications. Optical Frequency Division Multiplexing (OFDM) is an attractive new approach to high-speed networks that exploits the multi-terahertz bandwidth available in optical fibers. Novel photonic devices are required to realize a network that provides local, regional and backbone coverage via optical frequency routing. Many of the required components have already been demonstrated and others are being studied. These include fast tunable lasers, filters and receivers; integrated star couplers and frequency routers; and optical frequency translators and frequency division switches, using both silica-on-silicon and InGaAsP waveguides.

After discussing current lightwave applications for terrestrial and undersea transmission, I will describe our research on OFDM networks and components.

#### BIOGRAPHY

IVAN P. KAMINOW was born in Union City, N.J. on March 3, 1930. He received the B.S.E.E. degree from Union College (1952), the M.S.E. degree from the University of California, Los Angeles (1954), and the A.M. and Ph.D. degrees in Applied Physics from Harvard University (1957 and 1960). He was a Hughes Fellow at UCLA (1952-1954) and a Bell Laboratories CDTP Fellow at Harvard (1956-1960).

From 1952 to 1954 he worked on Microwave antennas at Hughes Aircraft Company, Culver City, California. Since 1954 he has been at AT&T Bell Laboratories in Whippany and Holmdel, New Jersey, and has done research on antenna arrays, ferrite devices, electrooptic modulators, ferroelectrics, non-linear optics, Raman scattering, integrated optics, semiconductor lasers, optical fibers, and lightwave networks. He was appointed Head of the Photonic Networks and Components Research Department in 1984. He has been a Visiting Lecturer at Princeton University, the University of California Berkeley, and Adjunct Professor at Columbia University, and Visiting Professor at Tokyo University. He has published 200 papers and received 37 patents. He is the author of *An Introduction to Electrooptic Devices* (1974), co-editor (with A. E. Siegman) of the IEEE Press book *Laser Devices and Applications* (1972) and co-editor (with S. E. Miller) of *Optical Fiber Telecommunications II* (1988).

Dr. Kaminow is a Fellow of the IEEE, the American Physical Society and the Optical Society of America. He is recipient of the Bell Labs Distinguished Member of Technical Staff Award and the IEEE Quantum Electronics Award. He is a member of the National Academy of Engineering and a Diplomate of the American Board of Laser Surgery.